PROCEEDINGS

VETERINARY PATHOLOGY SERVICE
WEDNESDAY SLIDE CONFERENCE
2011-2012

JOINT PATHOLOGY CENTER
SILVER SPRING, MD 20910
2012

ML2012

JOINT PATHOLOGY CENTER
VETERINARY PATHOLOGY SERVICE

WEDNESDAY SLIDE CONFERENCE
2011-2012

100 Cases

JOINT PATHOLOGY CENTER
SILVER SPRING, MD 20910
2012

ML2012

PREFACE

The Veterinary Pathology Service of the Joint Pathology Center (JPC), formerly known as the Armed Forces Institute of Pathology, has conducted a weekly slide conference during the resident training year since 12 November 1953. This ever-changing educational endeavor has evolved into the annual Wednesday Slide Conference program in which cases are presented on 25 Wednesdays throughout the academic year and distributed to 135 contributing military and civilian institutions from around the world. Many of these institutions provide structured veterinary pathology resident training programs. During the course of the training year, histopathology slides, digital images, and histories from selected cases are distributed to the participating institutions and to the JPC Veterinary Pathology Service. Following the conferences, the case diagnoses, comments, and reference listings are posted online to all participants.

This study set has been assembled in an effort to make Wednesday Slide Conference materials available to a wider circle of interested pathologists and scientists, and to further the education of veterinary pathologists and residents-in-training. The number of histopathology slides that can be reproduced from smaller lesions requires us to limit the number of participating institutions.

For their participation and permission to use their cases in this study set, we wish to thank each institution, and especially the individuals who prepared and submitted the selected cases.

A special note of appreciation is extended to the reviewers who helped edit and review this year's individual case summaries:

A final note of thanks goes to the moderators, who unselfishly gave of their time and expertise to help make each conference both enjoyable and educational.

Gross images and photomicrographs were submitted by contributing institutions where indicated.

Joint Pathology Center
WEDNESDAY SLIDE CONFERENCE 2011-2012
Table of Contents

WSC 2011-2012 Table of Contents

Joint Pathology Center
Veterinary Pathology Services

WEDNESDAY SLIDE CONFERENCE 2011-2012

Conference 1

07 September 2011

CASE I: 60226 (JPC 3103342).

Signalment: 3-week-old domestic shorthair cat (*Felis domesticus*).

History: This kitten had upper respiratory signs for several days, then became dyspneic and died en route to the emergency clinic.

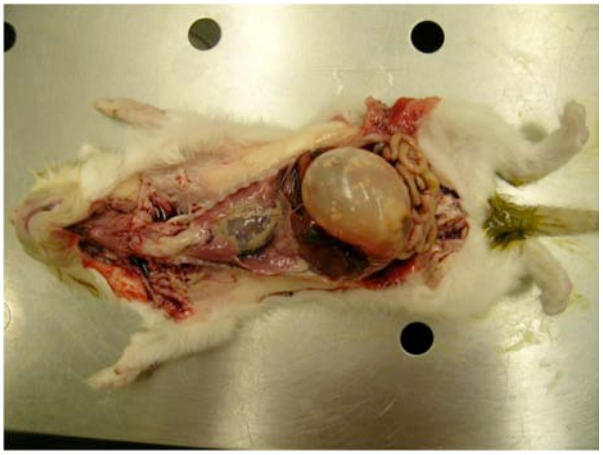

1-1. Lungs, esophagus, stomach, kitten. The lungs fail to collapse and are mottled tan and red, and the stomach is distended with air (aerophagia). Photograph courtesy of Department of Molecular and Comparative Pathobiology, Johns Hopkins University School of Medicine, www.hopkinsmedicine.org/mcp .

Gross Pathology: The lungs failed to collapse when the thoracic cavity was opened, and were mottled tan and pink, with a firm, rubbery texture. The esophagus and stomach were distended with air.

Histopathologic Description: Lung: Over 80% of the lung parenchyma is affected by severe inflammation, necrosis and perivascular and intra-alveolar edema. There are multifocal to coalescing areas of alveolar wall necrosis and replacement by dense infiltrates of macrophages and lymphocytes, mixed with abundant fibrin and cellular debris. At the periphery of the necrotic areas, alveolar septae are expanded by lymphocytes and macrophages. Pneumocytes are variably denuded or hypertrophic, protruding into the alveolar space (type II pneumocyte hyperplasia). Occasionally, there is a layer of fibrin adherent to the alveolar septa. Bronchioles and bronchi are lined by a thick layer of fibrin mixed with sloughed epithelial cells. Bronchial glands are hyperplastic. Multifocally, pneumocyte and glandular epithelial cell nuclei contain round, eosinophilic, 4-7 µm inclusion bodies that displace chromatin to the periphery. Airways and alveolar spaces contain fibrillar eosinophilic material (fibrin), sloughed pneumocytes, red blood cells and/or large foamy macrophages. Blood vessels are congested and perivascular spaces are expanded (edema). At the periphery of the lobe, alveolar spaces are dilated with occasional alveolar wall rupture and clubbing of septae (emphysematous change). Mesothelial cells along the

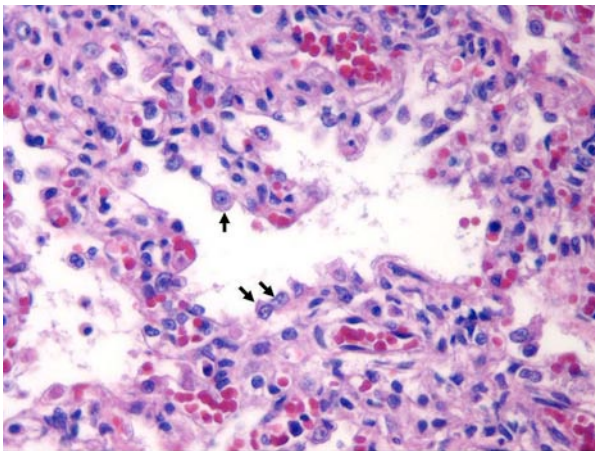

1-2. Lung, kitten. Alveolar septa are expanded by lymphocytes and macrophages. There is patchy type II pneumocyte hyperplasia (arrows). Photograph courtesy of Department of Molecular and Comparative Pathobiology, Johns Hopkins University School of Medicine, www.hopkinsmedicine.org/mcp. (HE 400X)

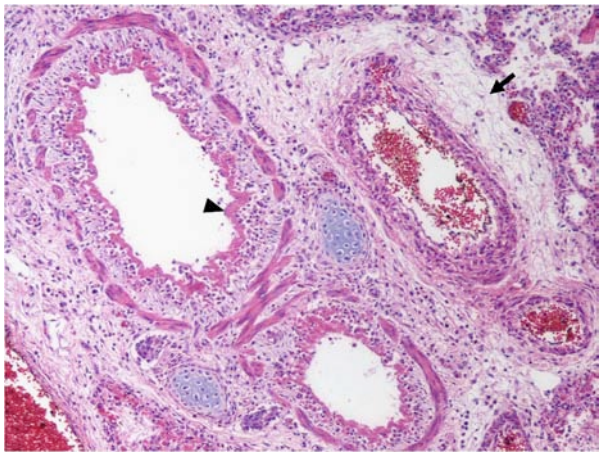

1-4. Lung, kitten. Perivascular spaces are markedly expanded by edema (arrow). Bronchial epithelium is necrotic and covered by a layer of fibrin (arrowhead). Photograph courtesy of Department of Molecular and Comparative Pathobiology, Johns Hopkins University School of Medicine, www.hopkinsmedicine.org/mcp. (HE 100X)

pleural surface of the lung are multifocally hypertrophic.

Contributor's Morphologic Diagnosis: Lung: Bronchointerstitial pneumonia, acute, necrotizing and fibrinous, multifocal to coalescing, severe, with perivascular edema, type II pneumocyte hyperplasia, reactive mesothelial cells, and intranuclear inclusion bodies.

Contributor's Comment: While upper respiratory tract infection in cats is very common, pneumonia is relatively rare. Infectious causes of feline pneumonia include bacteria (*Bordetella bronchiseptica*, *Pasteurella multocida*, *Eschericia coli*, *Pseudomonas spp*., *Staphylococcus spp*., and *Streptococcus spp*.), fungi (*Histoplasma capsulatum*), protozoa (*Toxoplasma gondii*), parasites (*Capillaria aerophila, Paragonimus kellicotti and Aelurostrongylus*

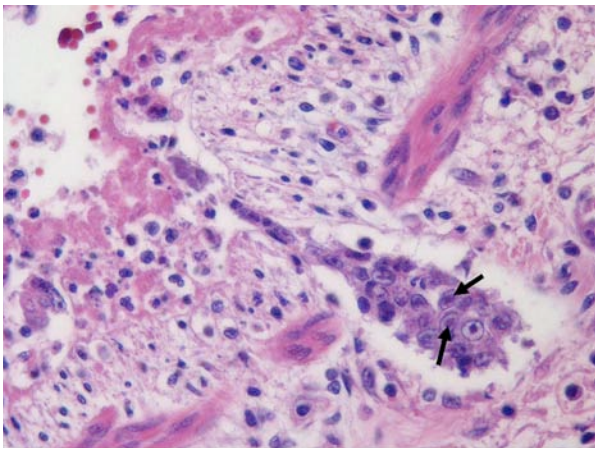

1-3. Lung, kitten. Bronchial glandular epithelial cells often contain 4-7 µm eosinophilic intranuclear inclusion bodies that peripheralize chromatin (arrows). Photograph courtesy of Department of Molecular and Comparative Pathobiology, Johns Hopkins University School of Medicine, www.hopkinsmedicine.org/mcp. (HE 400X)

abstrusus) and viruses (feline herpesvirus-1, feline calicivirus and feline infectious peritonitis virus). In this case, the intranuclear inclusion bodies and necrosis are most consistent with a feline herpesvirus-1 infection.

Feline herpesvirus-1 (FHV-1) is an alphaherpesvirus (genus Varicellovirus) that infects members of the family Felidae. The virus is antigenically and genetically similar to canine herpesvirus-1 and phocine herpesvirus-1. Infection is typically the result of direct contact, but environmental transmission is also reported. Although experimental studies have produced transplacental infection of kittens, natural *in utero* transmission has not been documented. Viral replication primarily occurs in the nasal cavity, tonsils, and pharynx. Viremia is rare, presumably because the virus replicates best at low body temperatures. The virus typically infects respiratory epithelial cells and causes necrosis, fibrin exudation and neutrophilic infiltration. Intranuclear inclusion bodies are commonly seen during the acute phase of infection.

FHV-1 causes upper respiratory tract disease, characterized by sneezing, inappetence, fever, conjunctivitis, ocular and nasal discharge. Primary FHV-1 pneumonia is uncommon, and usually seen only in young or debilitated animals. Neurological signs, abortion, osteolytic lesions in the nasal turbinates and skin ulcers, particularly in cheetahs[3] have also been reported with FHV-1 infections. Following acute disease, the virus can enter a latent phase, most likely in the trigeminal ganglion,[4] with periodic reactivation in times of stress.

Feline calicivirus (FCV) is another important cause of respiratory disease in cats. Like FHV-1, FCV can cause pneumonia, but is more commonly associated

with upper respiratory tract disease. FCV infected cats are more likely to have oral ulceration, and less likely to have ocular lesions, compared to FHV-1 infected cats. Co-infections with FHV-1 and FCV are not uncommon. In a study of cats from eight animal shelters, the prevalence of FCV ranged from 13 to 26% and the prevalence of FHV-1 varied between 3 and 38%.[1] Recently, a FCV-associated virulent systemic disease (VSD) has been described, which, in addition to upper respiratory tract disease, is characterized by cutaneous edema, ulcerative dermatitis, and jaundice.[3]

JPC Diagnosis: Lung: Pneumonia, bronchointerstitial, necrotizing, acute, diffuse, severe, with eosinophilic intranuclear inclusions, etiology consistent with feline herpesvirus-1.

Conference Comment: Pulmonary inflammation is classified in distinct morphologic categories based on distribution and pattern. Identification of a particular pattern often leads to the determination of other useful information, such as etiology, route of exposure, and pathogenesis. Morphologic categories in common usage are bronchitis/bronchiolitis, bronchopneumonia, interstitial and bronchointerstitial pneumonia, and embolic or hematogenous pneumonia.

This particular case is an example of a bronchointerstitial pneumonia because of the presence of bronchiolar epithelial necrosis as well as alveolar damage. Common causes of bronchointerstitial pneumonia are airborne viruses or toxin that damage both Clara cells and type II pneumocytes. Bronchointerstitial pneumonia is a form of interstitial pneumonia characterized by inflammation of alveolar or interlobular septa. In contrast, bronchitis and bronchiolitis involve only the airways, and bronchopneumonia is characterized by leukocytic exudates which fill bronchioles and alveoli but lacking significant bronchiolar or alveolar septal involvement.[2] Feline herpesvirus-1, an alphaherpesvirus, causes significant necrosis, neutrophilic inflammation and the elaboration of fibrin.

Bronchial glands are prominent in the cat lung but absent in most other domestic species. Microscopic evaluation of the lungs of felids should always include scrutiny of the bronchial glands because glandular epithelial necrosis and herpesviral inclusions are often readily apparent in these structures.

Contributor: Department of Molecular and Comparative Pathobiology, Johns Hopkins University School of Medicine, 733 N. Broadway, Baltimore, MD 21205
www.hopkinsmedicine.org/mcp

References:

1. Bannasch MJ, Foley JE. Epidemiologic evaluation of multiple respiratory pathogens in cats in animal shelters, *J Feline Med Surg.* 2005;7:109-119.
2. Caswell JL, Williams KJ. Respiratory system. In: Maxie MG, ed. *Jubb, Kennedy, Palmer's Pathology of Domestic Animals.* 5th ed. Vol. 2. Philadelphia, PA: Elsevier; 2007:561-7.
3. Munson L, Wack R, Duncan M, et al. Chronic eosinophilic dermatitis associated with persistent feline herpes virus infection in cheetahs (Acinonyx jubatus). *Vet Pathol.* 2004;41:170-176.
4. Pesavento PA, MacLachlan NJ, Dillard-Telm L, et al. Pathologic, immunohistochemical, and electron microscopic findings in naturally occurring virulent systemic feline calicivirus infection in cats. *Vet Pathol.* 2004;41(3):257-63.
5. Townsend WM, Stiles J, Guptill-Yoran L, et al. Development of a reverse transcriptase-polymerase chain reaction assay to detect feline herpesvirus-1 latency-associated transcripts in the trigeminal ganglia and corneas of cats that did not have clinical signs of ocular disease. *Am J Vet Res.* 2004;65:314-319.

CASE II: A09-650 (JPC 3136045).

Signalment: 13-year-old female Thoroughbred horse (*Equus caballus).*

History: This horse was presented for exercise intolerance. The radiographic appearance of the lungs was consistent with equine multinodular pulmonary fibrosis. The horse was euthanized and necropsied by the referring veterinarian, who submitted lung, liver and spleen for histologic examination and microbiologic tests.

Gross Pathology: Irregularly shaped, but well-demarcated, coalescing nodules (2 to >10 cm in diameter) of firm, pale tan tissue were distributed through all lobes of the lung.

Laboratory Results: Equine herpesvirus 5 was identified antemortem in bronchoalveolar lavage fluid by PCR. Herpesvirus was isolated from the lung postmortem and also identified as equine herpesvirus 5 by PCR.

Histopathologic Description: Lung: The pulmonary nodules are well-demarcated from unaffected lung and are the result of interstitial fibrosis. Within the nodules, -alveolar septa are thickened up to 100 µm or more by fibrous tissue composed of birefringent, orderly collagen fibers with low to moderate cellularity (well-differentiated fibroblasts) and light infiltration by lymphocytes, plasma cells and fewer neutrophils. Alveolar spaces are lined by cuboidal epithelial cells with pale vacuolated cytoplasm, and are partially filled with macrophages, neutrophils, exfoliated epithelial cells, and debris. Intranuclear eosinophilic to amphophilic inclusion bodies are easiest to find in alveolar macrophages. Bronchi and bronchioles within the nodules are filled with similar exudate and surrounded by increased fibrous tissue.

Contributor's Morphologic Diagnosis: Fibrosing alveolitis with eosinophilic intranuclear inclusions in macrophages.

Contributor's Comment: Histologic findings resemble those described in equine multinodular pulmonary fibrosis, attributed to infection with equine herpesvirus 5 (EHV-5). Infection with this gammaherpesvirus is reportedly fairly common in Europe, parts of South America, Australia and New Zealand, but association of EHV-5 infection with multinodular pulmonary fibrosis was first described in the United States in 2007[1] and then again in 2008.[2] Twenty-four adult horses with multinodular pulmonary fibrosis, 4-28 years of age (mean, 14.5 yr) and with nearly equal gender distribution, were evaluated in the first article.[1] Sixteen of the horses were

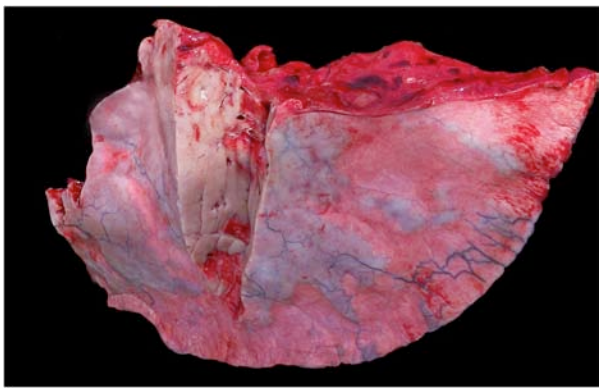

2-1. Lung, horse. Irregularly shaped, but well-demarcated, coalescing nodules (2 to >10 cm in diameter) of firm, pale tan tissue were distributed through all lobes of the lung. Photograph courtesy of Purdue University, Animal Disease Diagnostic Laboratory, http://www.addl.purdue.edu/.

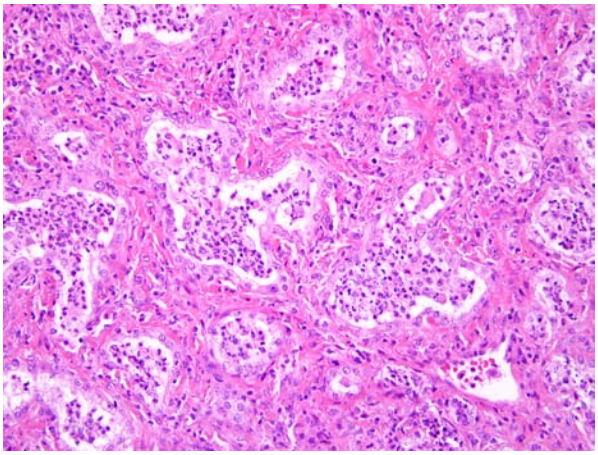

2-2. Lung, horse. Interalveolar septa are expanded by abundant collagen fibers. Alveoli are often filled with an exudate of alveolar macrophages, neutrophils and necrotic debris, and are lined by hypertrophied Type II pneumocytes. (HE 200X)

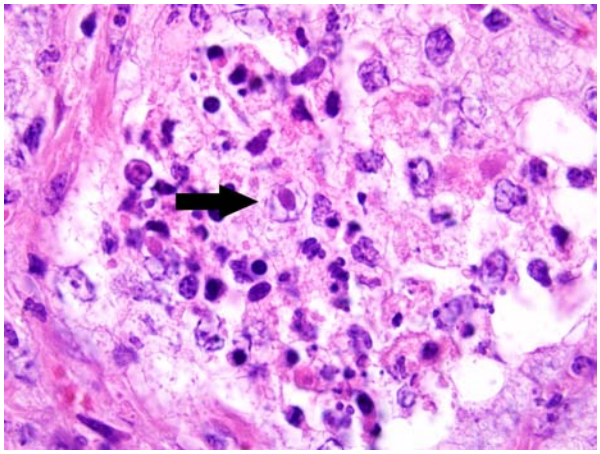

2-3. Alveolar macrophages occasionally contain an eosinophilic intranuclear inclusion body that marginates chromatin (arrow). (HE 1000X)

Thoroughbreds. Salient gross lesions were restricted to the lungs and bronchial lymph nodes, and usually appeared as numerous coalescing fibrotic nodules that involved most of the lung. A less common macroscopic presentation was as multiple discrete and larger fibrotic nodules, separated by unaffected pulmonary parenchyma.

Histologically, well-organized, mature fibrous tissue expand the interalveolar septa with preservation of alveolar architecture.[1] Lymphocytes infiltrate the fibrotic interstitium. Alveolar spaces are lined by cuboidal cells, and contain neutrophils and macrophages. A few of the alveolar macrophages have eosinophilic intranuclear inclusions.

Multinodular pulmonary fibrosis is histologically distinct from the pulmonary interstitial fibrosis of silicate pneumoconiosis, which is associated with granulomatous inflammation, and from idiopathic pulmonary fibrosis, which more commonly affects foals than adults and is attributed to diffuse alveolar damage.

In the second report, equine multinodular pulmonary fibrosis was tentatively diagnosed antemortem, as in this case, on the basis of clinical presentation and radiologic findings (nodular pulmonary interstitial pattern) with supportive PCR detection of EHV-5 from bronchoalveolar lavage specimens. Inappetance, weight loss, fever, cough, and respiratory distress were common to all 5 cases in that study.[2]

To date, Koch's postulates have not been fulfilled to establish EHV-5 as the definitive cause of equine multinodular pulmonary fibrosis. However, the virus is consistently associated with this unique pulmonary lesion, so pathologic findings of nodular pulmonary fibrosis with herpetiform inclusions and supportive PCR analysis should prompt consideration of EMPF in adult horses with respiratory distress and nodular interstitial pneumonia.

JPC Diagnosis: Lung: Pneumonia, interstitial, fibrosing, focally extensive, severe, with marked type II pneumocyte hyperplasia, neutrophilic and histiocytic alveolitis, and rare intrahistiocytic eosinophilic intranuclear inclusions.

Conference Comment: It is worth noting that EMPF presents grossly in two distinct manifestations: the more common diffuse to coalescing form with little unaffected lung parenchyma, and a discrete nodular form in which fibrotic nodules are separated by grossly unaffected lung. There is marked lymphadenomegaly of the bronchial lymph nodes resulting from lymphoid hyperplasia with sinus histiocytosis.

An interstitial pneumonia of donkeys has been reported which is associated with asinine herpesvirus.[1] This disease differs from EMPF in that it is a diffuse inflammatory disease with syncytial cell formation without viral inclusions; interstitial fibrosis is considered a secondary component.

Conference participants noted that pleural arteries were often hypertrophied and surrounded by abundant collagen. This is likely due to increased intrapulmonary blood pressure due to the diffuse fibrosis, which inhibits adequate blood flow through large portions of the affected lung.

Conference participants also discussed a differential diagnosis that included paraquat and diquat toxicosis, which causes fulminant pulmonary fibrosis, although due to the dwindling availability of these compounds, this differential is becoming exceedingly rare. Another possibility is exercise-induced pulmonary hemorrhage, which also has large areas of pulmonary fibrosis, but is characterized by numerous hemosiderophages, and lacks intranuclear inclusion bodies.

Alveolitis, a term commonly used in human respiratory pathology, was used in our morphologic diagnosis because of the striking inflammation centered on alveolar lumens as separate from the fibrosing interstitial pneumonia, which is characteristic of EMPF. This histologic finding is expected with interstitial pneumonias in which there is abundant protein exudation, as well as viral-induced leukocyte chemotaxis. A common feature of EMPF is the preservation of an "alveolar-like" architecture,[2] which are often filled with neutrophils and macrophages; hence the designation of alveolitis in addition to fibrosing interstitial pneumonia.

Contributor: Purdue University, Animal Disease Diagnostic Laboratory, 406 S. University Street Purdue University, West Lafayette, IN 47907, Animal Disease Diagnostic Laboratory: www.addl.purdue.edu/ Department of Comparative Pathobiology: www.vet.purdue.edu/cpb/

References:

1. Kleiboeker SB, Schommer SK, Johnson PJ, et al. Association of two newly recognized herpesviruses with interstitial pneumonia in donkeys (Equus asinus). *J Vet Diagn Invest.* 2002;14:273–280.
2. Williams KJ, Maes R, Del Piero F, et al. Equine multinodular pulmonary fibrosis: a newly recognized herpesvirus-associated fibrotic lung disease. *Vet Pathol*. 2007;44:849-862.
3. Wong DM, Belgrave RL, Williams KJ, et al. Multinodular pulmonary fibrosis in five horses. *J Am Vet Med Assoc.* 2008;232:898-905.

CASE III: C6352-11 (JPC 4002424).

Signalment: 9-year-old intact male beagle dog (*Canis familiaris*).

History: This dog, submitted by a Humane Society that had received several complaints from residents that the dog was neglected and left outdoors during the winter, was found dead and frozen in an outdoor enclosure.

Gross Pathology: The dog was thin (body condition score = 2/5) with easily palpable ribs and only a small amount of subcutaneous fat. There were small amounts of visceral fat and no evidence of serous fat atrophy in the bone marrow. The lungs had dark red mottling with lobes on the right side appearing darker than those on the left. Additionally, there were multifocal to coalescing tan-white areas (~10% of overall lung volume) that were firmer than the surrounding lung tissue and were slightly collapsed. These areas were mainly distributed along the margins of the lung with the largest area (2 cm X 2 cm) having a dark red center. The stomach was filled with food and had a roughly 2 X 3 cm area of congestion on the serosal and mucosal surfaces. The liver was dark reddish-brown and the gall bladder was mildly distended with bile. Two, roughly 0.5 cm diameter, raised, dark red nodules were noticed on opposite poles of the spleen (consistent with nodular hyperplasia). The kidneys appeared bilaterally dark red.

Laboratory Results: Scant growth of mixed flora including *Bacillus* sp. was found on lung tissue culture.

Histopathologic Description: Lung: The firm areas in the lungs correspond histologically to regions with diffuse alveolar fibrosis and infiltration of small to moderate numbers of predominately lymphocytes and plasma cells. Additionally, almost all of the alveolar spaces and many of the airways in this region are filled with aggregates of amorphous, relatively homogeneous (hyalinized) amphophilic material forming laminated bodies. These bodies are often surrounded by macrophages and occasional multinucleated giant cells. The material is uniformly PAS-positive and portions of the material, particularly at the margins, are birefringent under polarized light. The surrounding lung parenchyma is often mildly atelectatic and often markedly congested. In regions further away from the affected areas there is mild patchy congestion of the alveolar interstitium and infiltrates of small to moderate numbers of predominately macrophages within alveolar spaces.

Contributor's Morphologic Diagnosis: Lung: Pneumonia, interstitial, lymphoplasmacytic, histiocytic and fibrosing, multifocal, chronic, severe with intra-alveolar hyaline material (pulmonary hyalinosis).

Contributor's Comment: The lung lesions are characteristic of a condition known as pulmonary hyalinosis of dogs.[1-3] Pulmonary hyalinosis is a type of alveolar filling disorder, which is characterized by accumulations of abnormal material in airways. Other disorders in this group include endogenous lipid pneumonia, alveolar proteinosis and alveolar phospholipidosis and alveolar microlithiasis.[1]

The cause of pulmonary hyalinosis is unknown. Some pathologists consider it an incidental finding in older dogs[3], while others postulate that it is a response to inhalation of dust or pneumotoxicants such as silica in uranium ore dust[1] or to non-specific aspirated material.[2] This dog did not have any evidence of aspiration and it is unknown whether the unusual material in the lung was also present in the enclosure or environmental surroundings.

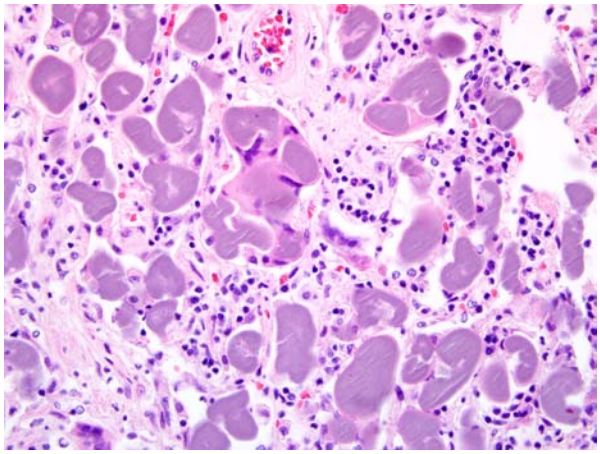

3-1. Alveolar spaces are filled by homogenous, amphophilic material that is within multinucleated macrophages. (HE 200X)

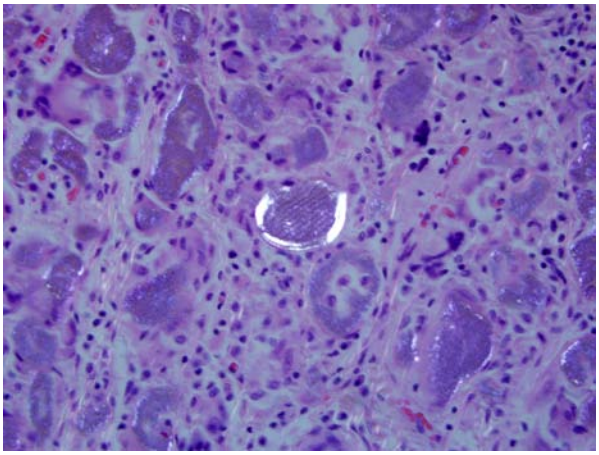

3-2. The material is birefringent under polarized light.

Unfortunately, the definitive cause of death in this dog remained inconclusive. The most significant findings were changes found in the lungs and kidneys and the overall poor body condition. The pulmonary lesions involved only a relatively small portion of the overall volume of lung (about 10%), however where the lesions were present, the normal architecture was completely obliterated. Additionally a moderate, chronic, multifocal-segmental, membranoproliferative glomerulonephritis was detected microscopically. Although no biochemical testing of renal function and urinalysis were done in this dog, there was no evidence of uremic lesions at necropsy, which could have indicated uremia or renal failure. However, as glomerular disease can cause protein loss, this lesion could have potentially contributed to the poor body condition of this dog.

Although the dog was thin at the time of death, it was not emaciated, as visceral and marrow fat stores were still present, and there was no histologic evidence of hepatocyte or pancreatic atrophy. Abundant foodstuffs were present in the stomach, however the long-term food consumption and therefore energy intake of this dog was unknown. Increased food energy is required in animals living in a cold environment to maintain adequate body temperature, so inadequate food intake would also have to be considered as a possible contributing factor to this dog being very thin.

JPC Diagnosis: Lung: Pneumonia, interstitial, granulomatous, chronic, focally extensive, severe, with abundant intra-alveolar hyaline material.

Conference Comment: This unusual canine condition was originally considered a result of aspiration pneumonia and analogous to a condition in humans known as pulmonary nodular granulomatosis, which was often found in nursing home patients with impaired swallowing abilities who were fed soft, legume-based diets. Hyaline rings were experimentally produced in animal lungs by injecting broth of lentils.[4] Lentils consist of grains of starch within honeycomb-like cotyledons; the cotyledons, which are composed of cellulose, incited the hyaline rings. The resulting lesion was termed ‘‘lentil pulse pneumonia.’’

In 1972, Dr. Leonard Billups of the Armed Forces Institute of Pathology reported that the canine condition now known as pulmonary hyalinosis was not composed of plant material as in pulse pneumonias; the hyaline bodies in dogs (known colloquially as “Billups bodies”) did not stain with silver impregnation stains as leguminous cotyledons do.[2]

Pulmonary hyalinosis may be differentiated from other conditions based upon histologic and staining features. The hyaline bodies are intracellular in macrophages and multinucleated giant cells, occasionally calcify, are birefringent, positive for periodic acid-Schiff (PAS), crystal violet and oil red 0, and ultrastructurally consist of a whorled arrangement of lamellar membranes suggestive of degenerate cells.[1,5] Corpora amylacea are rounded, basophilic hyaline masses that are often concentrically laminated. Corpora amylacea are not birefringent, do not calcify, and are weakly PAS positive. Pulmonary microliths are often distributed throughout the lung, and the calcospherites that compose this lesion are concentrically laminated, have radial striations, are calcified, and are intensely positive with PAS and colloidal iron stains, and unlike pulmonary hyalinosis, the material is extracellular.[6]

Contributor: Atlantic Veterinary College, University of Prince Edward Island
http://www.upei.ca/avc

References:

1. Dagle GE, Filipy RE, Adee RR, et al. Pulmonary hyalinosis in dogs. *Vet Pathol.* 1976;13:138-42.
2. Billups LH, Liu SK, Kelley DF, et al. Pulmonary granulomas associated with PAS-positive bodies in brachycephalic dogs. *Vet Pathol.* 1972;9:294-300.
3. Caswell JL, Williams KJ. Respiratory system. In: Maxie MG, ed. *Jubb, Kennedy and Palmer's Pathology of Domestic Animals.* 5th ed. Vol. 2. Philadelphia, PA: Elsevier-Saunders; 2007:572-573.
4. Knoblich R. Pulmonary granulomatosis caused by vegetable particles: so called lentil pulse pneumonia. *Am Rev Respir Dis.* 1969;99:380–389.
5. Harrison JD, Martin IC. Oral vegetable granuloma: ultrastructural and histological study. *J Oral Pathol.* 1986;15:322–326.
6. Rhee DD, Wu ML. Pulse granulomas detected in gallbladder, fallopian tube, and skin. *Arch Pathol Lab Med.* 2006;130:1839–1842.

CASE IV: 10A780 (JPC 4002925).

Signalment: 8-year-old male Indian rhesus macaque (*Macaca mulatta*).

History: This animal had a significant swelling in the left lower jaw with some drainage. The left mandible was very mobile with manual palpation. Radiographs indicated the left mandible was displaced by a large mass. The animal was not responsive to antibiotic treatment. Euthanasia was elected due to the poor prognosis.

Gross Pathology: This animal had normal body condition with adequate subcutaneous and abdominal adipose tissues. Expanding and effacing the left mandible, and displacing molar teeth was a solid, soft, white, 9x6x7 cm mass. The left mandibular lymph node was x3 enlarged. There was a focal gingival ulcer at the lower left jaw.

Laboratory Results: Bacterial culture from gingival ulcer: Normal flora Immunohistochemisty of pan-cytokeratin: odontogenic epithelial cells: +++ Immunohistochemistry of vimentin: mesenchymal cells: +++.

Histopathologic Description: Left mandible: Compressing, disrupting and infiltrating the alveolar bone, and extending into the cut borders is a partially encapsulated, well circumscribed neoplasm composed of islands, cords and strands of odontogenic epithelium separated by a large amount of edematous connective tissue. The islands and cords are often lined by 1-2 layers of distinct peripheral palisading, tightly packed, tall columnar epithelial cells with apical nuclei and basal cytoplasmic clearing. The centers of islands are loosely arranged by small spindle to stellate cells (stellate reticulum) with prominent intercellular spaces on a pale myxomatous matrix. The odontogenic epithelial cells have distinct cell borders, moderate amounts of pale eosinophilic fibrillar cytoplasm, a pale, oval to elongate, basillar nucleus, with finely stippled chromatin, and 1-2 distinct nucleoli. The neoplastic stellate cells have distinct cell borders, scant eosinophilic fibrillar cytoplasm, and an oval to elongate nucleus, with finely stippled chromatin and a variably distinct nucleolus. Occasionally, islands are surrounded by a variably thick layer of hyaline material. Surrounding the odontogenic epithelial cells are large amounts of primitive connective tissue comprised of loose, collagen-poor primitive stroma, with abundant extracellular matrix containing plump fibroblasts, sometimes with a stellate appearance, with dendritic branches resembling the dental papilla. Mitoses are rare in all cell populations. There are many microcyst formations in the epithelial and ectomesenchymal components. Fibrosis is also noted in multiple areas between the alveolar bone and neoplasm. There are multifocal areas of osteonecrosis and new bone formation. Dental hard tissue formation is not observed.

The odontogenic epithelial cells are strongly positive for cytokeratin, and ectomesenchymal tissue is strongly positive for vimentin by immunohistochemistry.

Contributor's Morphologic Diagnosis: Left mandible: Ameloblastic fibroma.

Contributor's Comment: Submitted are neoplastic tissues from two paraffin blocks. Our description is based on the tissue containing alveolar bone. The other tissue does not have adjacent alveolar bone, but major neoplastic lesions are present.

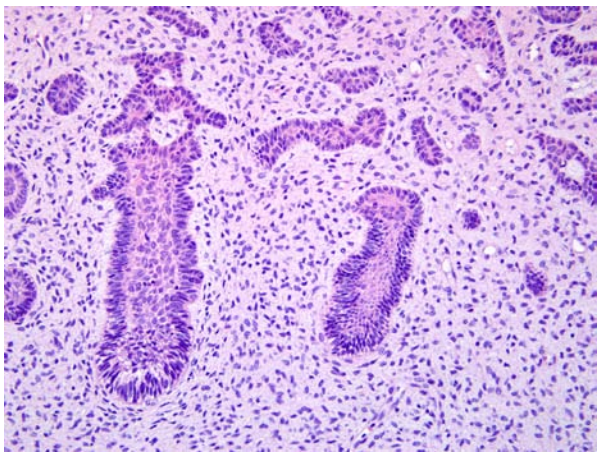

4-1. The neoplasm is composed of islands and cords of odontogenic epithelium on an abundant fibrous stroma with stellate cells in loose streams. (HE 200X)

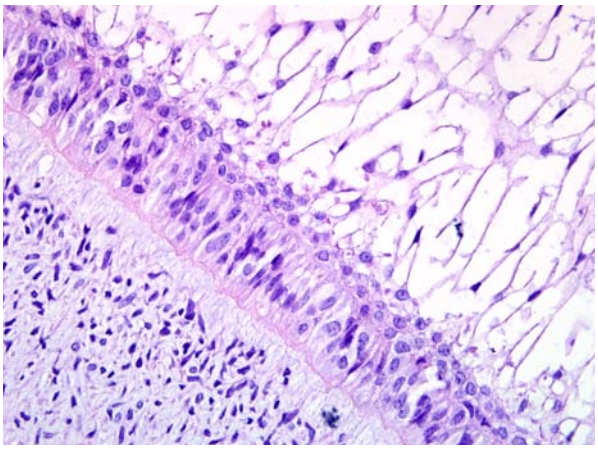

4-2. Islands of odontogenic epithelium have a peripheral palisading layer of columnar cells with anti-basilar nuclei and clearing of the basilar pole. Internal cells (upper right) are connected by long intercellular bridges. (HE 400X).

In humans, ameloblastic fibroma (AF) belongs to a family of tumors with mixed proliferating odontogenic epithelium and a cellular mesenchymal component that resembles dental papilla. Members of this family include AF, ameloblastic fibroscarcoma (ameloblastic sarcoma), ameloblastic fibro-odontoma, odontoameloblastoma and odontoma, with or without dental hard tissue formation.[1,7,8] AF is generally intraosseous, mostly in young patients, more male than female.[3,6] The mandible is the predominant site of occurrence and the posterior mandible is affected more commonly than the maxilla.[6]

Grossly, AF occurs as solid, soft tissue mass with or without a capsule. Histologically, epithelial cells are forming anastomosing cords and/or islands. The cells at the periphery of the epithelial islands are columnar cells, with palisading nuclei and reverse nuclear polarity, similar to ameloblasts. The cells in the center of the epithelial islands had a stellate reticulum-like appearance, similar to the stellate reticulum of the enamel organ. The ectomesenchymal component comprised loose connective tissue, with abundant extracellular matrix containing young, plump fibroblasts, sometimes with a stellate appearance, with dendritic branches resembling the dental papilla. Microcyst formation is rarely seen. If there is dentin formation, the lesion should be diagnosed as ameloblastic fibrodentinoma; if there is also enamel formation, it should be diagnosed as ameloblastic fibro-odontoma.[1]

AF is a rare tumor in animals and has been reported in young horses and dogs, but it is the most common odontogenic tumor in cattle. This neoplasm is similar to the lesions in humans and primarily composed of loose, collagen-poor primitive stroma resembling dental pulp. Odontogenic epithelial cells form cords and sheets, resembling enamel organ epithelium.[4]

AF must be distinguished from ameloblastomas, particularly those with desmoplastic changes. Distinct from AF, odontogenic epithelial cells in ameloblastoma are surrounded by mature fibrous connective tissue rather than primitive mesenchymal stroma.[4,7] Differentiation of ameloblastic fibrosarcoma from AF is also critical. Ameloblastic fibrosarcoma is the malignant counterpart of AF characterized by marked cytologic atypia, increased cellularity with diminution of the epithelial component, high numbers of mitoses and aggressive behavior.[10] Ameloblastic fibro-odontoma has features of AF, but, in addition, they have enamel and dentin deposition.[4]

Anti-pan-cytokeratin antibody is suggested to detect odontogenic epithelial cells. Odontogenic epithelial cells are positive for cytokeratin, but negative to vimentin by immunohistochemistry. The mesenchymal component is positive for vimentin.[2]

JPC Diagnosis: Mandible (per contributor): Ameloblastic fibroma.

Conference Comment: Understanding the normal process of the development of tooth structures and the interaction of epithelial and mesenchymal elements is helpful in understanding the various odontogenic tumors and their classifications. The tooth bud is an aggregation of cells that are derived from the ectoderm of the first branchial arch and the ectomesenchyme of the neural crest and is organized into the enamel organ, the dental papilla and the dental follicle.

The enamel organ is composed of the outer enamel epithelium, inner enamel epithelium, stellate reticulum and stratum intermedium, which give rise to ameloblasts that produce enamel.

The dental papilla contains cells that develop into dentin-forming odontoblasts, and mesenchymal cells within are responsible for formation of tooth pulp.

Tooth development is commonly divided into the following stages: the bud stage, the cap, the bell, and maturation. The bud stage is characterized by the appearance of a tooth bud without a clear arrangement of cells. The tooth bud itself is the group of cells at the end of the dental lamina, and is formed when cells of the oral ectoderm proliferate faster than cells of other areas, and is best described as an in-growth of oral ectoderm. This dividing tissue is surrounded and stimulated by ectomesenchymal growth. When it is present, the dental lamina connects the developing tooth bud to the epithelium of the oral cavity. Eventually, the dental lamina disintegrates into small clusters of epithelium and is resorbed. This invagination of ectodermal tissues is the progenitor to the later ameloblasts and enamel while the ectomesenchyme is responsible for the dental papilla and later odontoblasts.[8]

The first signs of an arrangement of cells in the tooth bud occur in the cap stage. A small group of ectomesenchymal cells stops producing extracellular substances, which results in an aggregation of these cells into the dental papilla. The tooth bud grows around the ectomesenchymal aggregation, taking on the appearance of a cap, and becomes the enamel organ. A condensation of ectomesenchymal cells called the dental follicle surrounds the enamel organ and limits the dental papilla, and later forms the surrounding alveolar bone and periodontal ligament.[5]

The dental organ is bell-shaped during the bell stage, and the majority of its cells are stellate reticulum.

Cells on the periphery of the enamel organ separate into three layers. Cuboidal cells on the periphery of the dental organ are the outer enamel epithelium, the columnar cells of the enamel organ adjacent to the dental papilla are the inner enamel epithelium, and the cells between the inner enamel epithelium and the stellate reticulum form the stratum intermedium. The rim of the dental organ where the outer and inner enamel epithelium joins is called the cervical loop. In summary, the layers in order of innermost to outermost consist of dentin, enamel, which is formed by inner enamel epithelium, or ameloblasts, as they move outwards and upwards, inner enamel epithelium and stratum intermedium, which are the specialized stratified cells that support the synthetic activity of the inner enamel epithelium.[5]

Hard tissues, including enamel and dentin, develop during the next stage of tooth development, which is the crown, or maturation stage. Mitosis stops during the crown stage at the location where the cusps of the teeth form, and the first mineralized hard tissues form at this location. At the same time, the inner enamel epithelial cells change in shape from cuboidal to columnar. The nuclei of these cells move closer to the stratum intermedium and away from the dental papilla. The adjacent layer of cells in the dental papilla increases in size and differentiates into odontoblasts, and form dentin. The odontoblasts secrete an organic matrix into their immediate surrounding which contains the material needed for dentin formation. As odontoblasts deposit organic matrix, they migrate toward the center of the dental papilla. Thus, unlike enamel, dentin starts forming in the surface closest to the outside of the tooth and proceeds inward. Cytoplasmic extensions are left behind as the odontoblasts move inward, which form the unique, tubular microscopic appearance of dentin.[5]

After dentin formation begins, the cells of the inner enamel epithelium secrete an organic matrix against the dentin. This matrix immediately mineralizes and becomes the tooth enamel. Outside the dentin are ameloblasts, which continue the process of enamel formation; therefore, enamel formation moves outwards, adding new material to the outer surface of the developing tooth. Reciprocal induction governs the relationship between the formation of dentin and enamel; dentin formation must always occur before enamel formation. Generally, enamel formation occurs in two stages: the secretory and maturation stages. Proteins and an organic matrix form partially mineralized enamel in the secretory stage, and the maturation stage completes enamel mineralization.[5]

In the secretory stage, ameloblasts release enamel proteins that contribute to the enamel matrix, which is then partially mineralized by the enzyme alkaline phosphatase. Odontoblasts differentiate from cells of the dental papilla. They begin secreting an organic matrix around the area directly adjacent to the inner enamel epithelium, closest to the area of the future cusp of a tooth. The organic matrix contains collagen fibers with large diameters (0.1–0.2 μm). The odontoblasts begin to move toward the center of the tooth, forming an extension called the odontoblast process. Thus, dentin formation proceeds toward the inside of the tooth. The odontoblast process causes the secretion of hydroxyapatite crystals and mineralization of the matrix. This area of mineralization is known as mantle dentin.[5]

There was some confusion among conference participants between the diagnosis of ameloblastic fibroma and ameloblastoma. Ameloblastic fibromas are well demarcated and consist primarily of a loose, matrix-poor primitive mesenchyme and sheets or cords of poorly formed odontogenic epithelium. Those ameloblastic fibromas with more advanced dentinal differentiation i.e. deposition of dentin or enamel matrix, are categorized as ameloblastic fibro-odontomas or odontoameloblastomas.

Ameloblastomas are usually discrete tumors with irregular islands and strands of odontogenic epithelium and an abrupt transition to mature fibrous stroma. They can occur in the gingival soft tissue (peripheral ameloblastoma) or deep in the bone of the jaw (central ameloblastoma). Additionally, keratinization can occur and be abundant within the odontogenic epithelium.

Contributor: Department of Comparative Pathology, Tulane National Primate Research Center, 18703 Three Rivers Rd., Covington, LA 70433

References:

1. Barnes L, Eveson J, Reichart P, et al. *World Health Organization Classification of Tumours. Pathology and Genetics Head and Neck Tumours.* Lyon: IARC Press; 2005.
2. Cardona A, Madewell BR, Naydan DK, et al. A comparison of six monoclonal antibodies for detection of cytokeratins in normal and neoplastic canine tissues. *J Vet Diagn Invest*. 1989;1:316-323.
3. Fernandes AM, Duarte EC, Pimenta FJ, et al. Odontogenic tumors: a study of 340 cases in a Brazilian population. *J Oral Pathol Med*. 2005;34:583-7.
4. Head KW, Cullen JM, Duielzig RR, et al. *Histological Classification of Tumors of the Alimentary System of Domestic Animals*. 2nd ed. Washington, DC: American Registry of Pathology/ AFIP; 1999:47-57.
5. McGeady TA, Quinn PJ, Fitzpatrick ES, et al. *Veterinary Embryology.* Oxford, England: Wiley-Blackwell; 2006:279-282.

6. Olgac V, Koseoglu BG, Aksakalli N. Odontogenic tumours in Istanbul: 527 cases. *Br J Oral Maxillofac Surg*. 2006;44:386-8.
7. Press SG. Odontogenic tumors of the maxillary sinus. *Curr Opin Otolaryngol Head Neck Surg*. 2008;16:47–54.
8. Reichart PA, Philipsen HP. Ameloblastic fibroma. In: *Odontogenic Tumors and Allied Lesions*, London, UK: Quintessence Publishing Co Ltd, 2004:121.
9. Sciubba JJ, Fantasia JE, Kahn LB. Development of the teeth and jaws. In: Rosai J, Sobin SH eds., *Atlas of Tumor Pathology, Tumors and Cysts of the Jaw.* 3rd ed. Washington, DC: American Registry of Pathology/ AFIP; 1994:1-5.
10. www.pathconsultddx.com. Ameloblastic fibrosarcoma.

WEDNESDAY SLIDE CONFERENCE 2011-2012

Conference 2

14 September 2011

CASE I: 10-5005 (JPC 4003270).

Signalment: 7-week-old male intact mixed breed dog (*Canis familiaris*).

History: The dog was part of a research colony affected with globoid cell leukodystrophy.

Gross Pathology: None provided.

Histopathologic Description: Brain, cerebrum: The white matter is multifocally expanded by large numbers of plump macrophages, which often surround blood vessels or infiltrate myelin sheaths. These cells contain abundant amounts of amphophilic to eosinophilic, fibrillar to flocculent cytoplasm, which often peripheralizes and compresses the nucleus (globoid cells). Multifocally, there are similar cells in the leptomeninges. Multifocally within the white matter, there are numerous dilated axons (spheroids) surrounded by dilated myelin sheaths. Capillaries are lined by plump reactive endothelial cells. There are multifocal aggregates of glial cells, predominantly at the grey-white matter junction.

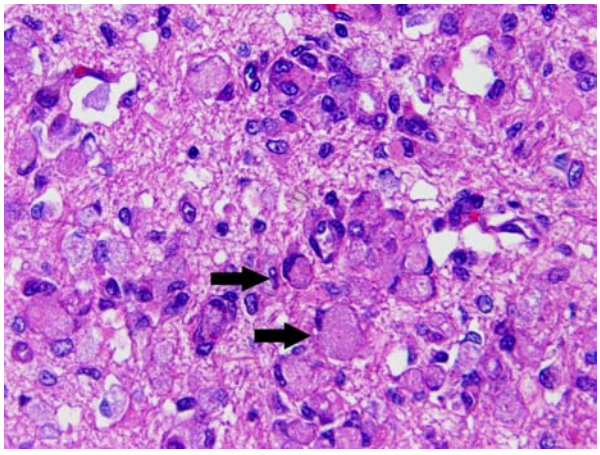

1-1. Cerebrum, dog. White matter is infiltrated by numerous "globoid cells" with abundant cytoplasm and crescentic nuclei.. (HE 400X)

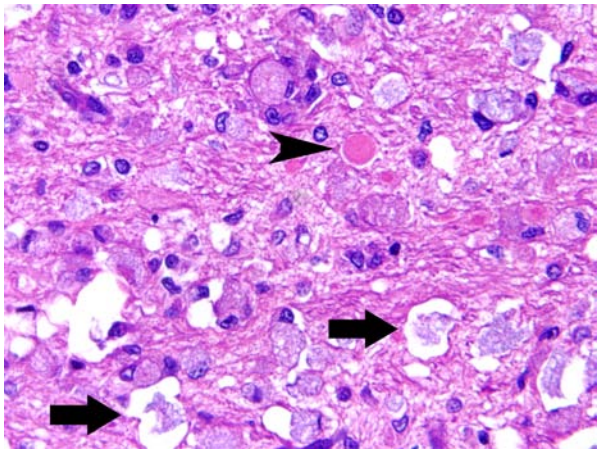

1-2. Cerebrum, dog. In affectedd white matter, globoid cells surround dilated axons (spheroids – arrowhead) and dlated empty myelin sheaths contain Gitter cells (arrows). (HE 400X)

Contributor's Morphologic Diagnosis: Cerebrum, white matter and leptomeninges: Histiocytosis, perivascular, moderate, multifocal, with abundant intracytoplasmic fibrillar material, and gliosis, mixed breed, canine.

Contributor's Comment: Similar histologic lesions are present in the cerebellum, medulla oblongata, and spinal cord. These lesions are consistent with globoid cell leukodystrophy (Krabbe's disease).

Globoid cell leukodystrophy, also known as galactocerebrosidosis, is an autosomal recessive disease caused by deficiency in the activity of lysosomal galactocerebrosidase (GALC).[1,2] Globoid cell leukodystrophy is part of the sphingolipidosis group of lysosomal storage diseases. The enzymatic deficit blocks the catabolism of galactocerebroside (galactosylceramide), a major component of myelin, and therefore the metabolic function of oligodendrocytes and Schwann cells is affected. The enzyme is also involved in the breakdown of other metabolites, including galactosylsphingosine (psychosine), normally synthesized by oligodendrocytes. This latter substance is cytotoxic to oligodendrocytes. Psychosine accumulation leads to oligodendrocyte degeneration and death, ceasing of myelination and degeneration of formed myelin.[1] Psychosine was sufficient to induce axonal defects and cell death in cultures of acutely isolated neurons in twitcher mice, a murine model of globoid cell leukodystrophy. Axonopathy in young twitcher mice occurred in the absence of demyelination and of neuronal apoptosis.[3]

Macrophages accumulate to ingest the degenerating myelin, but are unable to degrade galactocerebroside, and give rise to the distinctive, swollen, PAS positive "globoid cells". The cells are centered around blood vessels in the white matter, leptomeninges, and endoneurium of peripheral nerves. At the end stage of the disease there is diffuse demyelination, axonal loss, and dense astrogliosis.[1] On electron microscopy, cytoplasmic contents include myelin membranes in various states of degeneration, and aggregates of straight or arched tubules of galactosylceramide bound by a membrane.

Neurological signs in dogs typically appear in young animals (often between 3 and 6 months of age). Clinical signs associated with this disease are variable and may reflect the multifocal distribution of lesions.[2] Clinical signs include ataxia, hypermetria, tremors, and proprioceptive deficits. Progression leads to blindness, anorexia, muscular atrophy, and paraplegia. Death may occur before one year of age. The disease has been reported in a variety of canine breeds including: Cairn terrier, West Highland white terrier, miniature poodle, bluetick hound, basset hound, beagle[1], Pomeranian, Australian kelpie[4], Irish setter[5] and others. In addition to dogs, the disease is reported in domestic cats, polled Dorset sheep, rhesus macaques, and humans. There is a study model for the disease based on the twitcher mouse.[3] Up to date there are 33 distinct *GALC* mutant alleles reported in humans.[6]

JPC Diagnosis: Brain, cerebral cortex, white matter: Demyelination, diffuse, marked, with globoid cell infiltrates and axonal degeneration.

Conference Comment: The contributor has provided an excellent, concise review of this disease.

The conference moderator noted that gitter cells can resemble globoid cells on H&E stained sections and that both will have PAS positive cytoplasmic material; however, globoid cells are only found in the white matter and have a distinctly eccentric nucleus. Additionally, the presence of reactive endothelium can help to differentiate true pathologic findings from artifact or autolysis, and they may be the most noticeable pathologic change on subgross examination to indicate the presence of a microscopic lesion.

There was marked variation of anatomic location among the slides of conference participants. This should not detract from the diagnosis, but may reflect a difference in the histologic description compared to contributor slides.

Contributor: University of Pennsylvania
School of Veterinary Medicine
Department of Pathobiology
3900 Delancey St.
Philadelphia, PA 19104
www.vet.upenn.edu/departments/pathobiology/pathology

References:

1. Maxie MG, Youssef S. The nervous system. In: Maxie MG, ed. *Jubb, Kennedy and Palmer's Pathology of Domestic Animals*. 5th ed., vol. 1. Philadelphia, PA: Saunders Elsevier; 2007:381-382.
2. Braund KG. Storage disorders. In: Vite CH, Braund KG, eds. *Braund's Clinical Neurology in Small Animals: Localization, Diagnosis and Treatment*. Ithica, NY: International Veterinary Information Service, 2003: (www.ivis.org), A3219.0203.
3. Castelvetri LC, Givogri MI, Zhu H., et al. Axonopathy is a compounding factor in the pathogenesis of Krabbe disease. *Acta Neuropathol*. 2011;122(1):35-48.
4. Fletcher JL, Williamson P, Horan D., et al. Clinical signs and neuropathologic abnormalities in working Australian Kelpies with globoid cell leukodystrophy (Krabbe disease). *JAVMA*. 2010;237:6.

5. McGraw RA, Carmichael KP. Molecular basis of globoid cell leukodystrophy in Irish setters. *Vet J*. 2006;171(2):370-2.
6. Tappino B, Biancheri R, Mort M., et al. Identification and characterization of 15 novel GALC gene mutations causing Krabbe disease. *Hum Mutat*. 2010;12:E1894-914.

CASE II: 97-669-3 (JPC 4003037).

Signalment: 5-week-old male Yorkshire crossbred, *Sus scrofa domestica*, pig.

History: Three early-weaned piglets, each weighing approximately 9 kg, were submitted alive with listlessness and mostly hind limb ataxia and paresis of 4 days duration. One had been treated with dexamethasone and penicillin, with no results. Morbidity was qualified as moderate and mortality was not recorded at time of submission. No other clinical signs were reported. All other affected piglets recovered.

Gross Pathology: No significant gross lesions were seen (the whole CNS was examined in all piglets).

Laboratory Results: Enterovirus was isolated from a pool of fresh brainstem and spinal cord samples; it was not serogrouped.

Histopathologic Description: Spinal cord: There is an extensive, moderate nonsuppurative poliomyelitis involving mainly the ventral horns. It is characterized by mild to moderate lymphocytic perivascular cuffing, gliosis mostly in the form of glial nodules, and degeneration/ necrosis in large ventral horn (motor) neurons with neuronal loss and neuronophagia. The necrotic neurons' perikaryon is either swollen, markedly vacuolar and fibrillar or shrunken and hypereosinophilic; nuclei are either absent or pycnotic/ karyorrhectic. Microglial cells/macrophages can be seen around and within necrotic neurons (neuronophagia). Mostly in the dorsal funiculi there is Wallerian degeneration characterized by dilated myelin sheaths with axonal loss and occasional necrotic macrophages (myelinophage). Similar lesions were present in all sections of cervical, thoracic and lumbar spinal cord examined.

Brain (not provided): there were similar but milder lesions with minimal neuronal changes in the brain stem; a mild multifocal nonsuppurative leptomeningitis was also present.

Contributor's Morphologic Diagnosis: Moderate and extensive nonsuppurative poliomyelitis with marked neuronal necrosis and loss, and neuronophagia (ventral horns).

Contributor's Comment: No microscopic lesions were seen in other organs. Based on case history, microscopic lesions and isolation of enterovirus, a diagnosis of enteroviral polioencephalomyelitis, most consistent with Talfan disease, was given. Enteroviruses (genus *Enterovirus*, family Picornaviridae) are found in the enteric tract of humans and animals. Porcine enteroviruses (PEVs) were classified into 13 serotypes (PEV 1–13) that are antigenically related strains with variable virulence. These serotypes have further been grouped into groups I (PEV serotypes 1–7 and 11–13), II (PEV-8), and III (PEVs 9 and 10). Group I is now reclassified as Teschovirus.[7]

PEVs are ubiquitous and intestinal infection is frequent but most infections are asymptomatic. PEVs undergo local replication in the large intestine and ileum, mucosal lymphoid tissues and lymph nodes, followed by viremia that can lead to the central nervous system infection. The infrequent disease can appear in the postweaning period (generally 6 to 10-week-old pigs) secondary to mixing of pigs from different sources and decreased maternal immunity, and can result in mild to severe neurological disorders.[2] PEV serotype I is highly virulent and the causative agent of Teschen

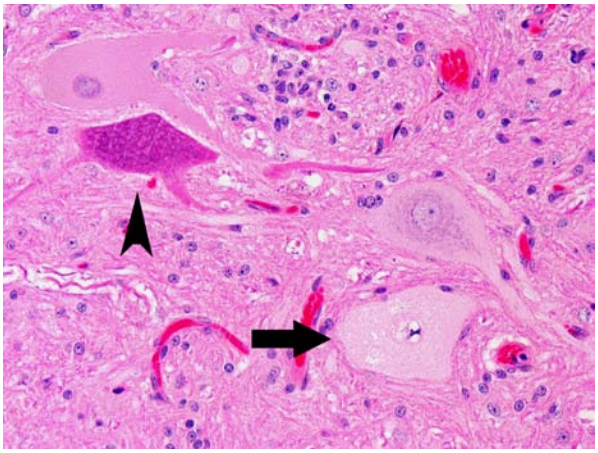

2-1, Spinal cord, gray matter, pig. Lower motor neurons of the ventral horns show a variety of degenerative changes, including marked cytoplasmic swelling with loss of Nissl substance (arrow) to an angular shape with eosinophilic cytoplasm (arrowhead). (HE 400X)

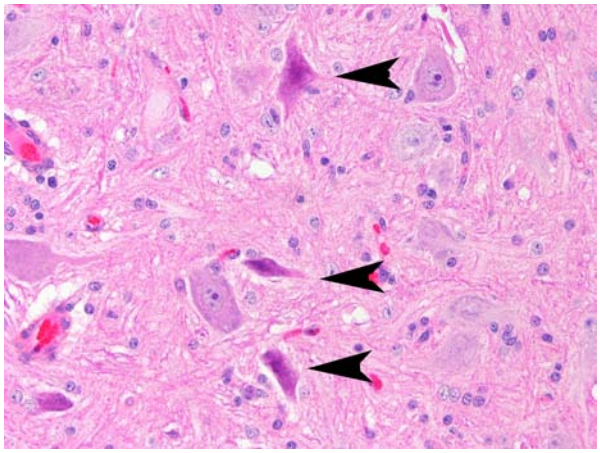

2.2 Spinal cord, gray matter, pig. Necrotic neurons are angular with dark eosinophilic cytoplasm. (HE 400X)

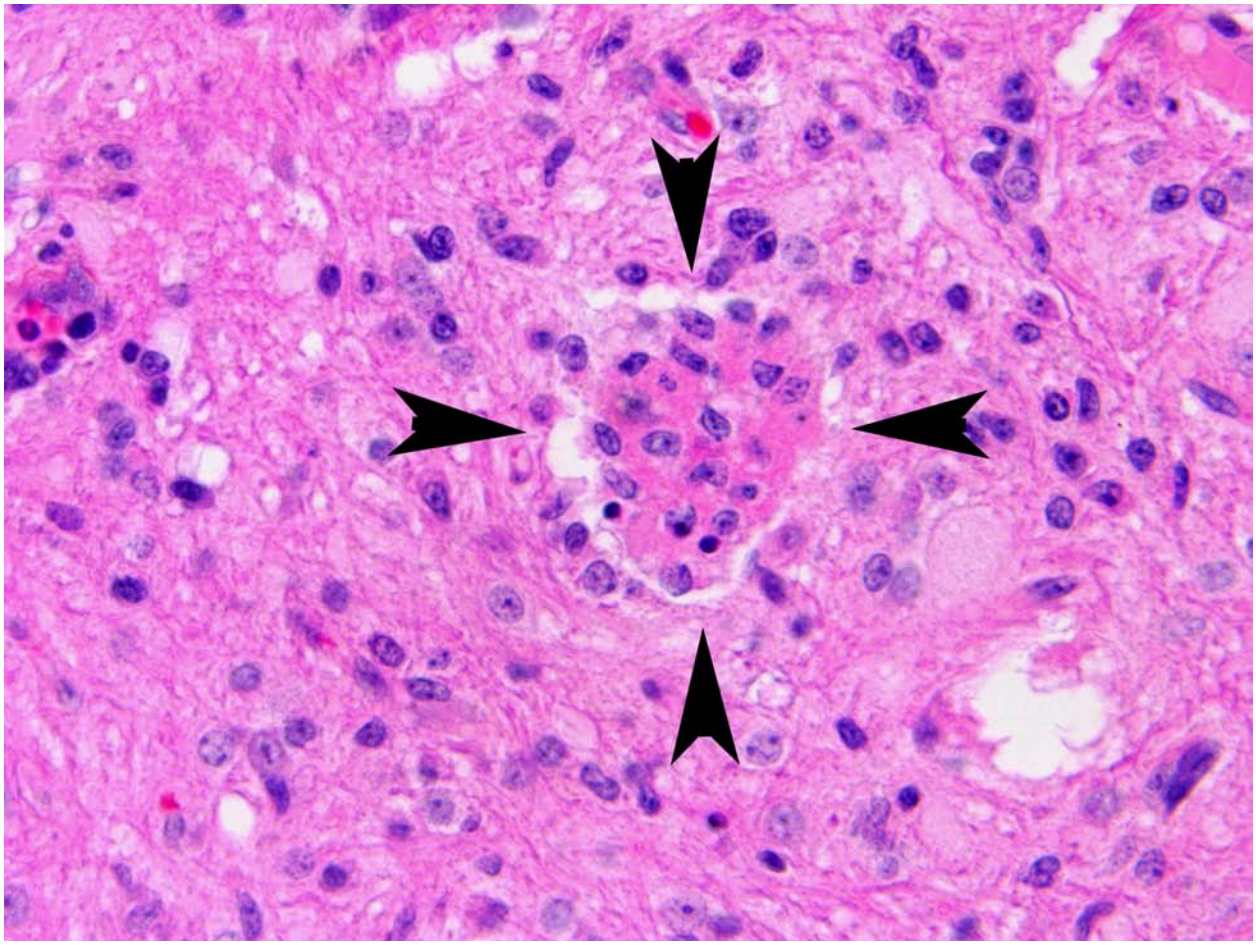

2-3. Spinal cord, gray matter, pig. Necrotic neurons are occasionally surrounded by numerous glial cells (satellitosis and neuronophagia). (HE 400X)

disease. Clinical signs are acute and include fever, ataxia, seizures, convulsions, opisthotonos, coma and death; mortality is high. Milder infections (also known as Talfan disease, poliomyelitis suum, benign enzootic paresis and Ontario encephalomyelitis) are linked to less virulent strains and clinical signs include ataxia, limb paresis, flaccid paraparesis or paraplegia; mortality is usually low and most pigs can recover.

There are no gross lesions in enteroviral polioencephalomyelitis. Microscopically, lesion distribution depends on the involved strain, but the cerebrospinal axis from the olfactory bulb to the lumbar cord is consistently involved.[3] As described above, there is progressive lymphocytic perivascular cuffing and infiltration of mononuclear cells (nonsuppurative polioencephalomyelitis) into the neuropil secondary to motor neuron degeneration in the ventral gray column. Neuronophagia and glial nodules, characteristic of CNS viral infections, are key features. Gray matter of the spinal cord and adjacent dorsal root ganglia (ganglioneuritis) are more involved than white matter, and changes in the dorsal horn are milder than in the ventral horn.[6] Other changes may be present, such as vacuolation at the periphery of the soma of neurons. There is relative sparing of the cerebral and cerebellar cortices, contrary to the deep substance of the cerebellum that is consistently and severely involved. Lesions can also be found in the pontine nuclei, medulla, thalamus and periaqueductal gray matter.[5] Leptomeningitis may be patchy and sometimes severe in the cerebellum in the older pigs in which the course is prolonged.[3]

Transmission electron microscopic examination reveals separation of ribosomes from the endoplasmic reticulum and loss of Nissl body clusters that provoke a progressive dilation of the endoplasmic reticulum.[5]

Survival is possible sometimes with sequelae. Extraintestinal infections are relatively transient, whereas the virus persists in the large intestine for several weeks.[2]

In this case, differential diagnoses included Teschen disease, Talfan disease and hemagglutinating encephalomyelitis virus (HEV) infection. To our knowledge, Teschen disease is not known to occur in

North America and is associated with high mortality rates. HEV was not isolated and would also have induced higher mortality rates. Porcine reproductive and respiratory syndrome (PRRS) should also be considered in cases with concomitant pulmonary lesions.

PEV are specific and are not zoonotic. Although PEV are different from the human enterovirus (poliovirus) that is responsible for acute flaccid paralysis called "polio", histological lesions induced by poliovirus are quite similar to those described above.[4]

Other enteroviruses are encountered in swine (Swine Vesicular Disease virus) and in mice (Theiler's murine encephalomyelitis virus infection). The virus causing avian encephalomyelitis, formerly classified as an enterovirus, has now been reclassified as a *hepatovirus*.[1]

JPC Diagnosis: Spinal cord, ventral horns: Neuronal necrosis, multifocal, marked, with gliosis, satellitosis, neuronophagia, and dorsal funiculi axonal degeneration.

Conference Comment: The contributor provided the most common examples of viruses that are typical rule outs for this disease. Other viral etiologies considered by conference participants were rabies virus, porcine herpesvirus 1 (pseudorabies), and Japanese encephalitis virus. With rabies virus infection, there is perivascular cuffing, focal gliosis, hemorrhage, neuronal degeneration, vacuolation of neurons and neuropil, and intracytoplasmic Negri bodies.[3] Pseudorabies presents histologically as a nonsuppurative meningoencephalitis with trigeminal ganglioneuritis, with marked neuronal degeneration and necrosis, and eosinophilic intranuclear inclusion bodies can be seen within numerous cells in the CNS.[8] Japanese encephalitis virus is often found in stillborn and neonatal piglets, and is histologically very similar to Teschen/Talfan disease. Gross lesions include hydrocephalus, cerebellar hypoplasia, hypomyelinogenesis, and anasarca.[3]

Another rule out that was regarded by conference participants was toxic poliomyelomalacia caused by selenium; however, this would present as a bilaterally symmetric malacia with distribution in the white and gray matter, with loss of neurons and endothelial and glial proliferation.[3]

This case provides wonderful examples of neuronophagia, neuronal necrosis, and satellitosis, which are characteristic of this and other cases of viral encephalitis. It is difficult to distinguish neurogenic viral etiologies by histology alone, and special diagnostic techniques are usually required.

There was some variation between slides in this case, most notably in the number of spinal nerves, some of which had perivascular inflammatory cells.

Contributor: University of Montreal
3200, Sicotte, St-Hyacinthe
Quebec, Canada, J2S 2M2

References:

1. Calnek, BW. Avian encephalomyelitis. In: Saif YM, Fadley AM, Glissen JR, McDougald LR, Nolan LK, Swayne DE, eds. *Diseases of Poultry*. 12th ed. Ames, Iowa: Wiley-Blackwell; 2008:430-441.
2. Derbyshire JB. Enterovirus. In: *Diseases of swine*. 8th ed. Ames, IA: Iowa State University Press; 1999:145-150.
3. Maxie MG, Youssef S. Nervous system. In: Maxie, MG ed. *Jubb, Kennedy, and Palmer's Pathology of Domestic Animals*. Vol. 1, 5th ed., Philadelphia, PA: Elsevier Saunders; 2007:281-457.
4. McAdam AJ, Sharpe AH. Infectious diseases. In: Kuma V, Abbas AK, Fausto N, eds. *Robbins and Cotran Pathologic Basis of Disease*. 8th ed. Philadelphia, PA: Elsevier Saunders; 2010:331-398.
5. Summers BA, Cummings JF, DeLahunta A. Inflammatory diseases of the central nervous system. In: *Veterinary neuropathology*. 1st ed. St. Louis, MO: Mosby; 1995:123-125.
6. Yamada M, Kozakura R, Nakamura K., et al. Pathological changes in pigs experimentally infected with porcine teschovirus. *J. Comp. Pathol*. 2009;141 (4):223-228.
7. Zell R, Dauber M, Krumbholz A., et al. Porcine Teschoviruses Comprise at Least Eleven Distinct Serotypes: Molecular and Evolutionary Aspects. *J. Virol*. 2001;75(4):1620-1631.
8. Zachary JF. Nervous system, mediastinum, and pleurae. In: McGavin MD, Zachary JF, eds. *Pathologic Basis of Veterinary Disease*. 5th ed. St. Louis, MO: Mosby; 2011:853.

CASE III: 02011 WSC CASE 2 0 0 (JPC 4003028).

Signalment: 10-week-old male Sprague-Dawley rat (*Rattus norvegicus*).

History: Tissue from a rat fed a high salt diet (8% NaCl) and infused with angiotensin II for 14 days.

Gross Pathology: None described.

Laboratory Results: Not available.

Histopathologic Description: Kidney: Multifocal glomeruli globally or segmentally have markedly thickened capillary loops and mesangial matrix expansion by homogeneous eosinophilic material (glomerular hyalinosis and sclerosis) resulting in glomerular tufts 50% to 100% larger than unaffected tufts. Multifocally, cells within affected glomerular tufts contain abundant hypereosinophilic cytoplasm and plump nuclei (hypertrophy) and some affected tufts contain pyknotic cellular debris (glomerulonecrosis). Other tufts contain cells with basophilic or vacuolated cytoplasm. Bowman's capsule parietal epithelium is hyperplastic with prominent, rounded nuclei and abundant slightly basophilic cytoplasm. Frequently, there is adhesion of the expanded glomerular tuft to the parietal epithelium (synechiae). Bowman's capsule basement membrane is variably thickened and surrounded by fibrous connective tissue (periglomerular fibrosis). The tunica media of small caliber vessels, particularly cortical and afferent and efferent juxtaglomerular arterioles and rarely arcuate and interlobar arteries, is multifocally expanded/ replaced by a homogenous, deeply eosinophilic material (fibrinoid necrosis) and occasionally contains basophilic cellular debris. Affected vessels in some areas are surrounded by concentric layers of loose fibrous connective tissue (fibrosis), small to moderate numbers of mononuclear leukocytes, and occasionally, extravasated erythrocytes (hemorrhage). Smooth muscle cells and endothelial cells are hypertrophic. Throughout the cortex are numerous regenerative tubules characterized by crowded tubular epithelial cells with basophilic (occasionally vacuolated) cytoplasm, deeply basophilic nuclei and rare mitotic figures. The tubular alteration is most prominent adjacent to affected glomeruli. Proximal tubules and collecting ducts frequently are ectatic and/or contain hypereosinophilic, homogenous proteinaceous fluid (proteinuria) or sloughed cells (cellular casts) and occasionally are lined by attenuated

Table 1. Selected rat models of systemic hypertension.

Rat Model	Hyper-tension Etiology	Hypertension Mechanism of Action	Age of Onset	Blood Pressure Elevation (Systolic)	Comments
Stroke-prone Spontaneously Hypertensive Rat (SHRSP)[2,9]	Primary, genetic	Renally related -- Transplanting a kidney from SHR to a normotensive Wistar rat increases blood pressure in the recipient	Begins at 6-7 weeks of age	200 mmHg	80% die from stroke
Spontaneously Hypertensive Rat (SHR)[2,9]	Primary, genetic	Renally related -- Transplanting a kidney from SHR to a normotensive Wistar rat increases blood pressure in the recipient	Begins at 5-6 weeks of age, maximal by 12 weeks	180-200 mmHg	30% develop heart failure at 4-5 months of age
Dahl Salt Sensitive Rat[9]	Primary, genetic and dietary	High dietary sodium content increases circulating sodium causing osmotic pull into vasculature, elevating pressure on vessel walls	4-6 weeks of age	Increased even on normal diet; Steeply elevated on high salt diet	30% develop heart failure at 18 months of age
Transgenic TGR (mRen2)27 Rat[4,9]	Primary, genetic	Overexpression of the mouse Ren-2 gene (increased renin activity)	Begins at 5 weeks and maximal by 10 weeks of age	Heterozygous: 240 mmHg; Homozygous: 300 mmHg (high mortality)	Mortality from heart failure at 10 weeks of age
Double Transgenic (dTG) Rat[11]	Primary, genetic	Expresses both human renin and angiotensinogen genes	Early	200-220 mmHg	50% mortality by 7-8 weeks of age
Deoxycorticosterone Acetate (DOCA) + High Salt Diet[2,7,9]	Secondary, endocrine/ dietary	Salt-dependent, mineralocorticoid (DOCA)-induced reabsorption of salt and water resulting in increased blood volume Also increased secretion of vasopressin = vasoconstriction + water retention	Hyper-tension begins 1-2 weeks after start of DOCA and high salt diet	200 mmHg	Mortality from brain, vascular, and renal lesions after 4-8 weeks of treatment
Ang II Infusion and High Salt Diet[10]	Secondary, endocrine	Daily infusion of angiotensin II via osmotic pump and high salt diet	Begins 1 day post infusion	130-200 mmHg	Mortality from renal glomerulosclerosis and vascular necrosis
Goldblatt Method: Two-Kidney One-Clip[2,9]	Secondary, renal	Clip on one renal artery increases circulating renin and angiotensin II	Develops 6 weeks post-surgery	160 - 190 mmHg	Mortality from renal failure and cardiovascular complications
Goldblatt Method: Two-Kidney Two-Clip[2]	Secondary, renal	Partial occlusion of both renal arteries (two stage surgery) increases circulating renin and aldosterone	Develops 4 weeks post-surgery	160 - 190 mmHg	
Godlblatt Method: One-Kidney One Clip[2]	Secondary, renal	Uninephrectomy and clip on renal artery of remaining kidney with rapid salt and water retention; Plasma renin activity is normal	Within hours of surgery	160 - 190 mmHg	
Renal Remnant[12]	Secondary, renal	Uninephrectomy and segmental 2/3 ablation of remaining kidney to 5/6 total renal mass	Within hours of surgery	170-190 mmHg	Mortality from renal failure with cardiovascular complications

epithelium. The interstitium is multifocally expanded by loose fibrous connective tissue and small numbers of mononuclear leukocytes.

Contributor's Morphologic Diagnosis: 1. Glomerulonephropathy, multifocal, chronic with glomerular hyalinosis and sclerosis and tubular degeneration/ regeneration, atrophy, ectasia and proteinuria.
2. Arteriolopathy, proliferative, chronic, multifocal with medial degeneration and fibrinoid necrosis.

Contributor's Comment: Hypertensive nephropathy is a common sequela to chronic high blood pressure in humans. One quarter of the US population is hypertensive and approximately 6% of affected individuals have chronic kidney disease with the risk of progression to end stage renal disease.[1] The relationship of hypertension and chronic renal disease is complex since hypertension is both a cause and consequence of renal disease.[6] In the human population, risk factors for hypertensive nephrosclerosis include African ancestry, severe and sustained hypertension, family history, microalbuminuria, diabetes mellitus, and left ventricular hypertrophy.[1] The morphological features of human hypertensive nephrosclerosis include vascular wall medial thickening with arteriolar hyaline deposits and intimal fibrosis as well as focal glomerular ischemic changes (retraction, wrinkling, and folding of the capillary walls) with basement membrane thickening, global or even segmental glomerulosclerosis and varying but subtotal foot process effacement (electron microscopy). Tubular atrophy and interstitial fibrosis also occur. This presentation of glomerular changes may be referred to as "focal segmental glomerulosclerosis" (FSGS) and may be attributed to hypertensive renal injury when accompanied by glomerular ischemic changes, periglomerular fibrosis, subtotal foot process effacement and disproportionate vascular sclerosis.[5] When diagnosing the human patient, clinical history is critical and hypertension typically precedes renal insufficiency and proteinuria.[5]

In experimental medicine, rats are the most popular hypertensive model and the spontaneous hypertensive rat (SHR) is the most common model utilized.[9] Impaired endothelium dependent relaxation, cardiac hypertrophy and/or heart failure, cerebral hemorrhage, nephropathy and/or renal failure are features of most models of rat hypertension, mimicking the human spectrum of disease. Hypertension in rats is defined as sustained systolic blood pressure of greater than 150 mmHg.[2] The submitted case illustrates microscopic features that developed after 14 days of hypertension induced by high salt diet and angiotensin II infusion.

Table 1 on the included chart compares selected systemic hypertensive rat models.

Angiotensin II has a wide array of biological effects including (from Kobori et. al[3]):

1. Arteriolar vasoconstriction (in the glomerulus, efferent > afferent)
2. Stimulation of aldosterone secretion (zona glomerulosa of the adrenal cortex)
   Acts on distal convoluted tubules and collecting ducts reabsorb sodium and water from urine (exchange for potassium which is excreted in urine) ↑blood volume ↑blood pressure
3. Secretion of anti-diuretic hormone from the pituitary
   a. Vasoconstriction
   b. Reabsorption of water in the kidneys
   c. Stimulation of thirst and salt appetite

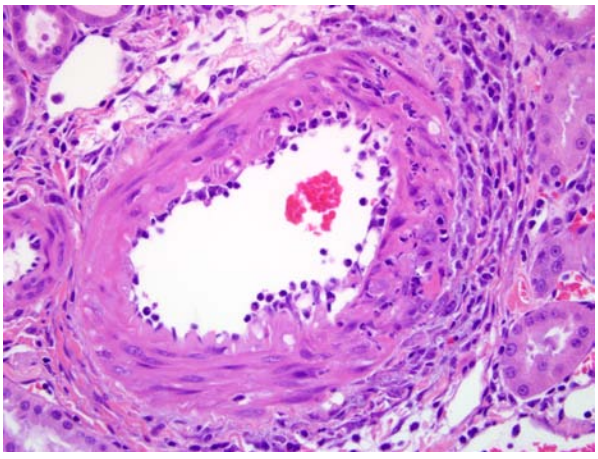

3-1. Kidney, Sprague-Dawley rat. The tunica media and adventitia of arterioles are expanded by eosinophilic protein and necrotic cellular debris (fibrinoid necrosis). (HE 400X)

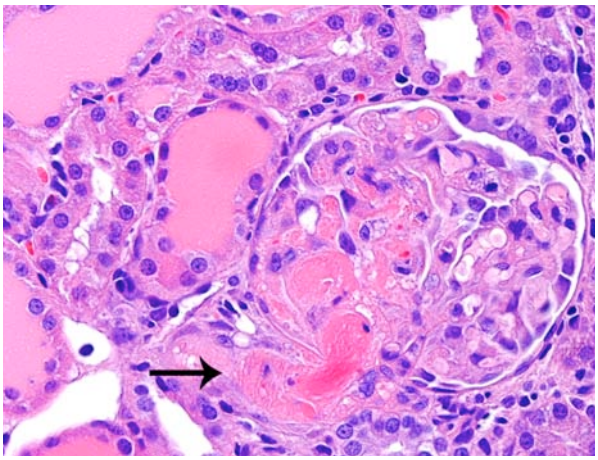

3-2. Kidney, Sprague-Dawley rat. Glomerular tuft with fibrinoid necrosis of the afferent arteriole (arrow) and hyalinosis of the tuft. (HE 400X)

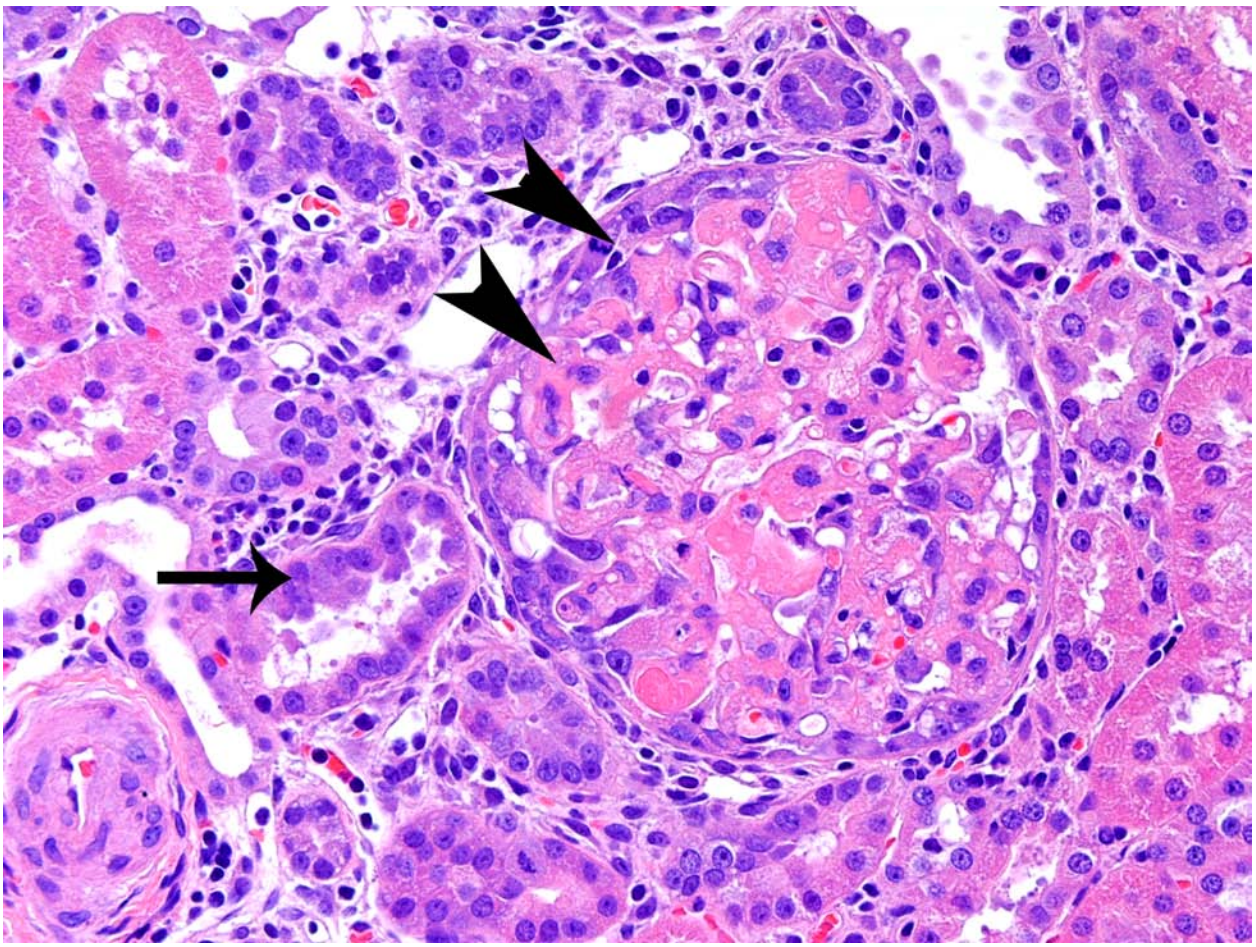

3-2. Kidney, Sprague-Dawley rat. Glomerular tufts frequently contain hypereosinophilic material (hyalinosis – arrowhead) and there is marked hyperplasia and hypertrophy of parietal epithelium. Tubular epithelium is often basophilic with vesicular nuclei and piling up (regeneration = arrow). (HE 400X)

4. Regulation of sodium transport by renal and intestinal epithelium
   In the kidney, stimulation of Na+/H+ exchange on proximal tubules, thick ascending limb of the loop of Henle, and collecting ducts increased sodium resorption
5. Hypertrophy of renal tubular epithelium
6. Release of prostaglandins counteracts renal vasoconstriction
7. Reduced renal medullary blood flow
8. Increases tubuloglomerular feedback sensitivity lower tubular perfusion (prevents excessive rise in glomerular filtration rate)
9. Other actions
   a. Enhanced cardiomyocyte growth and contractility
   b. Stimulation of release of catecholamines (norepinephrine from adrenal medulla)
   c. Increases sympathetic nervous system activity

JPC Diagnosis: 1. Kidney, arterioles: Arteriopathy, proliferative and necrotizing.
2. Glomerulosclerosis, multifocal, moderate, with tubular degeneration, regeneration, and protein casts.

Conference Comment: Differential diagnoses discussed during conference included chronic progressive nephropathy (CPN) and polyarteritis nodosa (PAN). CPN generally does not include a vascular component centered on small arterioles as in this case, and CPN typically has conspicuous basement membrane thickening, which is absent in this case. Polyarteritis nodosa tends to affect vessels of a larger caliber than is typical with hypertensive nephropathy and to affect vessels more randomly. As the name indicates, CPN becomes progressively more severe with age, and PAN is typically a disease of aged rats.

The contributor has provided an excellent comparative review of hypertensive nephropathy, a condition that is morphological similar in most affected species.

Contributor: Eli Lilly and Company
Department of Pathology and Toxicology
Indianapolis, IN 46285
www.lilly.com

References:

1. Barri YM. Hypertension and kidney disease: a deadly connection. *Curr Hypertens Rep*. 2008;10:39-45.
2. Doggrell SA, Brown L. Rat models of hypertension, cardiac hypertrophy and failure. *Cardiovasc Res*. 1998;39: 89-105.
3. Kobori H, Nangaku M, Navar LG., et al. The intrarenal renin-angiotensin system: from physiology to the pathobiology of hypertension and kidney disease. *Pharmacol Rev*. 2007;59:251-287.
4. Langheinrich M, Lee MA, Bohm M., et al. The hypertensive Ren-2 transgenic rat TGR (mREN2)27 in hypertension research. Characteristics and functional aspects. *Am J Hypertens*. 1996;9:506-512.
5. Marcantoni C, Fogo AB. A perspective on arterionephrosclerosis: from pathology to potential pathogenesis. *J Nephrol.* 2007;20:518-524.
6. Navar LG. The kidney in blood pressure regulation and development of hypertension. *Med Clin North Am*. 1997;81:1165-1198.
7. Park CG, Leenen FH. Effects of centrally administered losartan on deoxycorticosterone-salt hypertension rats. *J Korean Med Sci.* 2001;16:553-557.
8. Percy DH, Barthold SW. Pathology of Laboratory Rodents and Rabbits. 3rd ed., Ames, Iowa: Blackwell Publishing; 2007:161-4.
9. Pinto YM, Paul M, Ganten D. Lessons from rat models of hypertension: from Goldblatt to genetic engineering. *Cardiovasc Res*. 1998;39:77-88.
10. Rugale C, Delbosc S, Cristol JP., et al. Sodium restriction prevents cardiac hypertrophy and oxidative stress in angiotensin II hypertension. *Am J Physiol Heart Circ Physiol*. 2003;284:H1744-1750.
11. St-Jacques R, Toulmond S, Auger A., et al. Characterization of a stable, hypertensive rat model suitable for the consecutive evaluation of human renin inhibitors. *J Renin Angiotensin Aldosterone Syst*. 2011;12(3):133-45.
12. Sviglerova J, Kuncova J, Nalos L., et al. Cardiovascular parameters in rat model of chronic renal failure induced by subtotal nephrectomy. *Physiol Res.* 2010;59 Suppl 1:S81-88.

CASE IV: 08A747 (JPC 3134315).

Signalment: 12.7 yr female Indian rhesus monkey (Macaca mulatta).

History: This animal was inoculated with SIVB670 (clone12) six years prior to necropsy. It had a long history starting 2 years after inoculation of hair plucking that escalated to self-trauma. Epistaxis was noted from time to time. It was sacrificed due to new self-trauma, depression, and anorexia.

Gross Pathology: The surface of the left parietal region of the brain had a 1x2 cm darkened soft depression that extended to the subcortical white matter. Self-trauma to the foot and vegetative valvular endocarditis were noted.

Laboratory Results: Multiple clinical nasal swabs contained beta hemolytic coagulase positive staphylococcus. Bacterial culture of the brain was negative.

In situ hybridization of the kidney and brain demonstrates the presence of SV40 entire genomic nucleic acid (nick translation biotinylated probe, Enzo Life Sciences) in nuclei of renal tubule epithelium and oligodendrocytes.

Terminal CBC: 2.7 RBC, 5.5 Hgb, 19.8 Hct, 3.74 WBC, 65 Seg, 1 Eo, 3 Mno. 31 Lym, 150000 Plt, 6.4 Rtc

18 months prior CBC: 5.9 RBC, 14.3 Hgb, 43 Hct,3.8 WBC, 58 Seg, 6 Eo, 30.7 Lym
290000 Plt, 0 Rtc

Terminal Chem: 147 Na, 3.4 K, 111 Cl, 5.8 Pro, 2.1 Alb, 3.7 Glob, 0.6 A/G, 30.6 BUN, 85 Glu, 0.56 Crt

Histopathologic Description: Brain: Multiple zones of malacia and loss of neuropile are present in the cortical grey matter and, in some sections, extend into vacuolated white matter with increased numbers of glial cells. Malacic areas are infiltrated with plump granulated macrophages and smaller numbers of polymorphs. Gemistocytic astrocytes and oligodendrocyte cell bodies are swollen and hyalinized with marginated chromatin and poorly defined to distinct grainy amphophilic intranuclear inclusions. Scattered blood vessels in the surrounding parenchyma have modest cuffs of lymphoid cells or polymorphonuclear leukocytes in malacic areas. Meninges contain mild perivascular lymphoid infiltrates.

Contributor's Morphologic Diagnosis: Brain: Multifocal severe subacute meningoencephalitis with multifocal malacia, demyelination and gliosis, SV40.

Contributor's Comment: SV40 is an oncogenic DNA virus in the Papova virus family and the polyoma virus subfamily. SV40 produces large and small DNA-binding proteins (T antigens) which serve as DNA molecular chaperones with roles in viral replication (transcription and viron assembly) and tumorigenesis.[7] The rhesus monkey is the natural host, and SV40 persists as a clinically silent renal infection unless immunodeficiency due to Simian Immunodeficiency Virus (SIV) infection allows polyomal viral disease in the kidney, lung or brain. Human polyoma viruses, John Cunningham virus (JVC) and BKV are comparable, and subclinical renal infections can be associated with pregnancy, diabetes, or old age. In immunodeficiency, JVC infects oligodendrocytes and

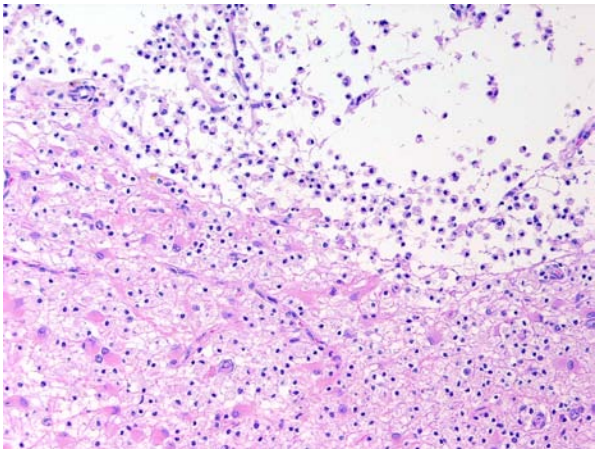

4-1. Cerebrum, white matter, rhesus macaque. Multifocally, the submeningeal white matter is necrotic, cavitated, and replaced by numerous Gitter cells (top) and adjacent tissue is infiltrated by many glial cells and large gemistocytic astrocytes. (HE 200X)

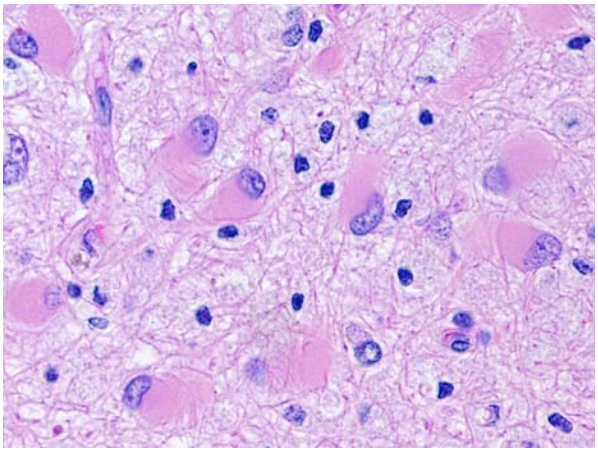

4-2. Cerebrum, white matter, rhesus macaque. Gemistocytic astrocytes with abundant eosinophilic cytoplasm and eccentric nuclei. (HE 600X)

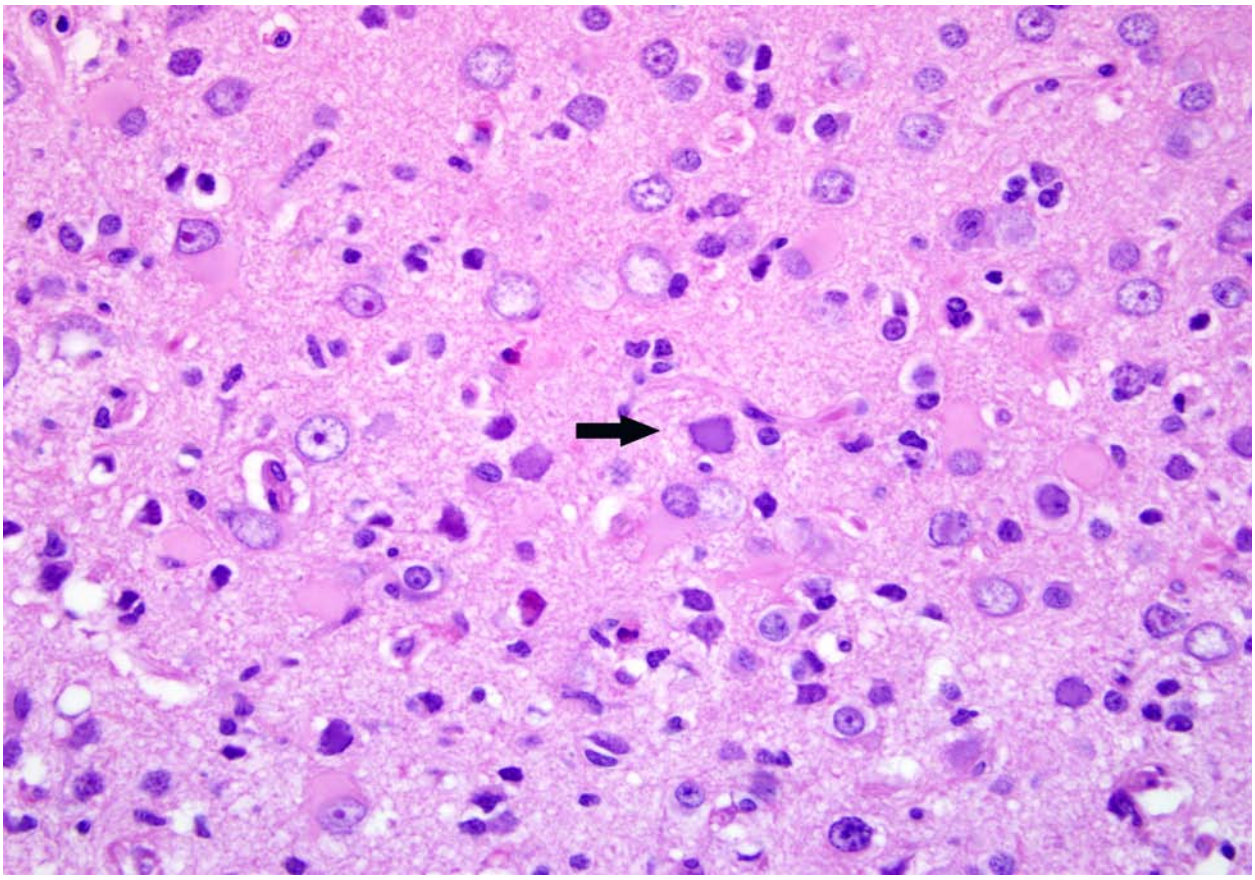

4-3. Cerebrum, white matter, rhesus macaque. Rarely astrocytes contain large amphophilic intranuclear viral inclusion bodies (arrow). (HE 400X)

causes progressive multifocal leukoencephalopathy (PML) while BKV-infected individuals develop fatal tubulointerstitial nephritis.[3] SIV-infected monkeys have two morphologic presentations of polyoma viral disease in the brain; 1) PML characterized by multifocal demyelination with inflammation and gitter cell accumumation[3] and 2) meningoencephalitis (ME) affecting grey matter without significant demyelination.[5] Both manifestations display gemistocytic astrocytes and swollen oligodendrocytes with intranuclear inclusions, microgliosis, and T lymphocyte infiltration. It has been suggested that, in monkeys, PML is associated with reactivation of a latent SV40 infection while ME is a manifestation of a primary SV40 infection in younger animals.[5] This case has the morphologic lesions of ME and the renal involvement consistent with a primary SV40 infection but the older age of the monkey, the long time duration between SIV inoculation and disease, and presence of demyelination previously linked with PML.

JPC Diagnosis: Brain: Polioencephalitis, necrotizing, multifocal, severe, with gemistocytes, axonal degeneration, and amphophilic intranuclear viral inclusions.

Conference Comment: Simian polyomavirus has historical significance, as it was first identified in 1960 in rhesus macaque renal cell cultures used to manufacture both Sabin and Salk polio vaccine, to which millions of inoculants were exposed. The virus is named for its propensity to produce vacuoles in infected cells, hence the name simian vacuolating virus 40.[2] SV40 suppresses p53 expression through the SV40 Large T-antigen and SV40 Small T-antigen, resulting in loss of transcription initiation.[7] SV40 can also play a role in development of tumors, most commonly sarcomas, and has been used in rats to develop a model for primitive neuroectodermal tumors (PNETs) and medulloblastomas.[1] Additionally, there is ongoing research into the potential of SV40 to cause cancer in humans, as SV40 has been detected in a variety of human cancers, although this topic remains controversial.[3]

Initially, MHC-I molecules cluster in caveolae and bind to SV40. SV40 then enters the host cell via endocytosis through caveolae, small uncoated invaginations in the host cell plasma membrane important for signal transduction and calcium regulation. Caveolins, membrane bound proteins important to the structure and function of caveolae,

associate with the virus membrane, facilitate budding of the virus-containing vesicle into the cell cytoplasm, and the subsequent transfer of virus to the endoplasmic reticulum.[6]

There is some variation among slides and, depending on the section, lesion distribution is either focal or multifocal.

Contributor: Department of Comparative Pathology
Tulane National Primate Research Center
Covington, LA 70433
www.tpc.tulane.edu

References:

1. Eibl RH, Kleihues P, Jat PS., et al. A model for primitive neuroectodermal tumors in transgenic neural transplants harboring the SV40 large T antigen. *Am J Pathol*. 1994;144(3):556-64.
2. Fiers W., et al. Complete nucleotide-sequence of SV40 DNA. *Nature*. 1978;273;113-120.
3. Horvath CJ, Simon MA, Bergsagel DJ., et al. Simian Virus 40-induced disease in rhesus monkeys with simian acquired immunodeficiency syndrome. *Am J Path*. 1992;140(6):1431-1440.
4. Rollison DEM, Page WF., et al. Case-control study of cancer among US army veterans exposed to simian virus 40-contaminated adenovirus vaccine. *American Journal of Epidemiology*. 2004;160(4):317-24.
5. Simon MA, Ilyinskii PO, Baskin GB., et al. Association of simian virus 40 with a central nervous system lesion distinct from progressive multifocal leukoencephalopathy in macaques with AIDS. *Am J Path*. 1999;145(2):437-446.
6. Stang E, Kartenbeck J, Parton RG. Major histocompatibility complex class I molecules mediate association of SV40 with caveolae. *Mol Biol Cell.* 1997;8(1):47-57.
7. Sullivan CS and Pipas JM. T antigens of simian virus 40: molecular chaperones for viral replication and tumorigenesis. *Microbiol Molec Biol Rev*. 2002;66 (2):179-202.

WEDNESDAY SLIDE CONFERENCE 2011-2012

Conference 3

21 September 2011

CASE I: 09.395.43 (JPC 3164204).

Signalment: 1-year-old male long-haired guinea pig (*Cavia porcellus*).

History: The patient presented at the Emergency Service of the Veterinary School of Alfort for a 10-day history of constipation, anorexia, and weight loss. An abdominal mass was found by palpation. Ultrasonography revealed multiple nodular masses in

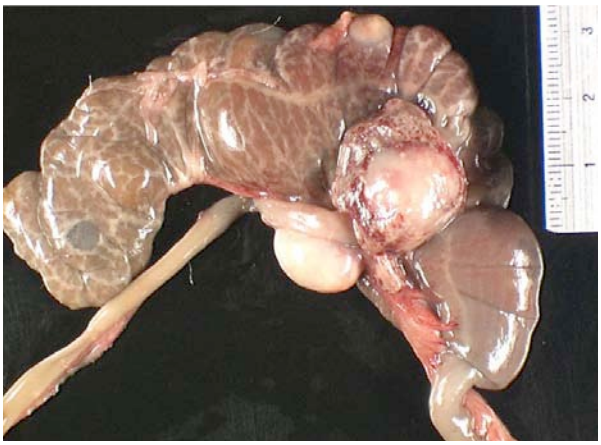

1-1, 1-2, 1-3. Liver, ileo-caecal junction, spleen, guinea pig. Multiple, soft, white, liquid filled nodules ranging from 3 to 15 mm were found in the liver, in the spleen, and at the ileo-caecal junction as well as on the caecal serosa. Photographs courtesy of Ecole Nationale Veterinaire D'Alfort, Unité d'Histologie et d'Anatomie Pathologique, Maisons-Alfort, France

the liver, spleen and abdominal lymph nodes. Lymphoma, tuberculosis and infection by pyogenic bacteria were suspected. The guinea pig was hospitalized but died within a week.

Gross Pathology: Multiple, soft, white nodules were found in the liver, in the spleen, at the ileo-caecal junction as well as on the caecal serosa. They ranged from 3 to 15 mm in diameter with a liquid center (multifocal suppurative hepatitis, splenitis, ileo-typhlitis and peritonitis).

Laboratory Results: Fine needle aspiration of an abdominal lymph node showed suppurative inflammation with high numbers of intracellular and extracellular bacteria with both coccoid and rod shapes. Repeated bacteriological analyses of samples from abdominal lymph nodes yielded mainly *Yersinia pseudotuberculosis* associated with a smaller population of *Escherichia coli.*

Histopathologic Description: Liver: Numerous, variable-sized nodules replace several portal tracts and compress the adjacent parenchyma. The largest nodules are 3 to 7 mm in diameter and are made of large colonies of coccobacilli embedded in large amounts of degenerate neutrophils, in turn surrounded by a fibrous and highly vascularized capsule rich in activated macrophages and lymphocytes (multiple hepatic abscesses). Numerous sections of biliary ducts are interspersed in the collagen bundles (biliary duct hyperplasia).

The smallest nodules are centered on colonies of coccobacilli admixed with degenerate neutrophils and necrotic, sometimes mineralized hepatocytes surrounded by activated macrophages, plasma cells, and lymphocytes. When visible, portal blood vessels are surrounded by lymphocytes and plasma cells or show invasion of their wall by macrophages and degenerate neutrophils with replacement of their media by a fibrillar eosinophilic material (fibrinoid necrosis).

In the remaining parenchyma, the cytoplasm of the hepatocytes is filled with variable-sized clear vacuoles consistent with lipid droplets (micro- and macrovacuolar steatosis). The central veins are congested. The coccobacilli do not stain with either Gram or Ziehl-Nielsen stains.

Spleen: The red and the white pulp is disrupted and compressed by multifocal, chronic, 0.5 cm-diameter abscesses and smaller pyogranulomas, with large colonies of intralesional coccobacilli. In the red pulp, siderophages are commonly seen (diffuse hemosiderosis, discrete).

Caecum: (autolysis) (absent from the slides).

In the submucosa, with extension to the musculosa and the serosa, there is a focal accumulation of degenerate neutrophils and variably mineralized cell debris around large coccobacilli colonies, surrounded by activated macrophages and fibrous tissue. The overlying mucosa is lost (focal ulcer). The remaining mucosa displays a diffuse, discrete infiltration of the lamina propria by lymphocytes and plasma cells.

Peritoneum surrounding the caecum: (absent from the slides).

Multifocally, coccobacilli-containing abscesses are centered on blood vessels with fibrinoid necrosis of their wall. Other vessels display only intraluminal thrombi or degeneration of the wall with infiltration by

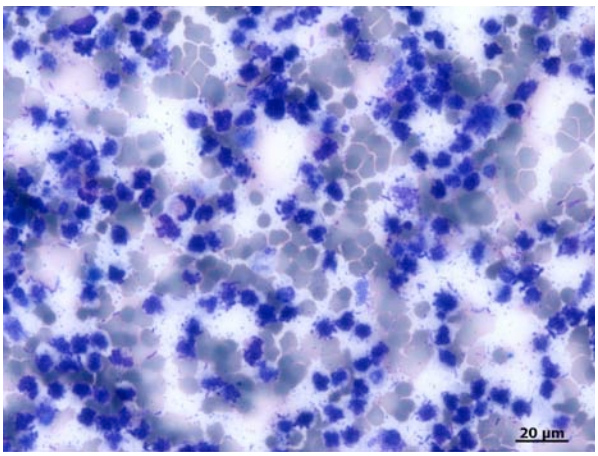

1-4. Fine needle aspirate, abdominal lymph node, guinea pig. Suppurative inflammation with many intracellular and extracellular bacterial rods and cocci. Photograph courtesy of Ecole Nationale Veterinaire D'Alfort, Unité d'Histologie et d'Anatomie Pathologique, Maisons-Alfort, France.

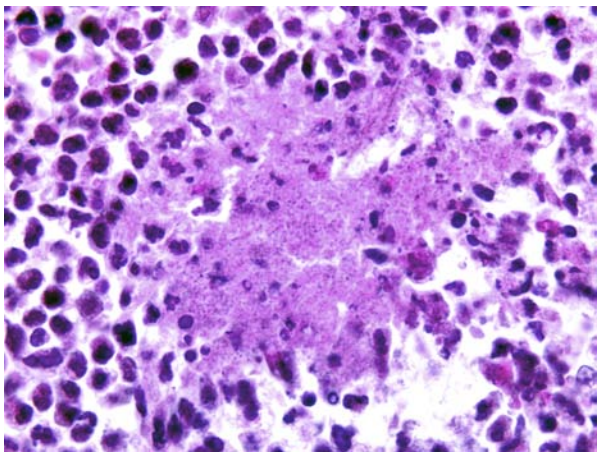

1-5. Liver, guinea pig. Abscesses have a central core of degenerate neutrophils, necrotic debris and are centered on large colonies of 2-4 µm bacilli, characteristic of Yersinia. (HE 1000X)

macrophages and degenerate neutrophils. There is an extensive deposit of fibrin and pus in the serosa.

Caeco-colic lymph nodes: (absent from the slides).

Two lymph nodes are almost entirely replaced by large abscesses surrounded by a rim of residual lymphoid tissue. There are numerous colonies of coccobacilli in the center of the abscesses. Another lymph node displays numerous macrophages in the subcapsular and medullary sinuses that are seldom binucleated with a large amount of granular cytoplasm (sinusal histiocytosis).

Contributor's Morphologic Diagnosis: Liver: Hepatitis, suppurative, multifocal, subacute, severe, with intralesional gram-negative coccobacilli colonies consistent with *Y. pseudotuberculosis.*
Steatosis, diffuse, severe.

Spleen: Splenitis, suppurative, multifocal, subacute, severe, with intralesional gram-negative coccobacilli colonies consistent with *Y. pseudotuberculosis.*

Caecum: Typhlitis, suppurative and ulcerative, transparietal, subacute, moderate with intralesional gram-negative coccobacilli colonies consistent with *Y. pseudotuberculosis.*

Peritoneum and caeco-colic lymph nodes: Peritonitis and lymphadenitis, suppurative, severe with intralesional gram-negative coccobacilli colonies consistent with *Y. pseudotuberculosis*.

Contributor's Comment: Multiple white friable foci in the liver, spleen, abdominal lymph nodes and intestines in a guinea pig may also be associated with the following bacterial diseases:
- *Salmonella* infection (*S. typhimurium, S. enteritidis, or S. dublin*): there is multifocal granulomatous to suppurative hepatitis, splenitis, lymphadenitis, and enteritis, characterized by paratyphic nodules;
- Tyzzer's disease (*Clostridium piliforme*): there is necrotizing hepatitis, ileitis and typhlitis, often with transmural involvement; the bacteria are intracellular bacilli that react positively with Warthin-Starry stain;
- *Streptococcus* infection with *S. zooepidemicus* or *S. pneumoniae*: these Gram-positive bacteria can be responsible for suppurative lymphadenitis (streptococcal lymphadenitis and pneumococcal infection), hepatitis and splenitis (streptococcal septicemia and pneumococcal infection).[7]
- Mycobacterial granulomas with Ziehl-Nielsen-positive bacteria.

Microscopically, the differential diagnosis for large plaque-like colonies of bacteria in H-E sections includes, following the « YACS » mnemonic method:
- *Yersinia* sp.
- *Actinomyces* sp., *Actinobacillus* sp., *Arcanobacter* sp.
- *Corynebacterium* sp., *Clostridium* sp.
- *Staphylococcus* sp., *Streptococcus* sp.

The morphology of the bacteria and the results of the Gram staining will further orientate the identification. In the present case, the bacteria were gram-negative cocco-bacilli; these characteristics were consistent with *Yersinia* sp.

Y. pseudotuberculosis and *Y. enterocolitica* are gram-negative coccobacilli that can survive and grow at low temperature (psychrophilia). The pathogenic strains of theses bacteria share several virulence factors, namely:
- the invasin: this adhesin binds to beta-integrins expressed on the surface of the intestinal M cells; it promotes uptake of the bacterium by these cells and triggers the production of chemotactic cytokines by epithelial cells;
- a plasmid-encoded type III secretion system that translocates *Yersinia* outer proteins (Yops) into the host cell;
- the Yops: these effector proteins allow the bacterium to remain extracellularly and evade phagocytosis and killing by neutrophils and macrophages; one mechanism can be an alteration of the actin cytoskeleton in the host cell as is the case with YopE.[4,8]

Y. pseudotuberculosis can also produce a superantigenic toxin termed *Y. pseudotuberculosis*-derived mitogen a (YPMa). Several pathogenic strains display on their chromosome a high-pathogenicity island (HPI), which carries genes of the yersiniabactin system involved in siderophore-mediated iron acquisition.[5]

Infection with *Y. pseudotuberculosis* is a zoonotic disease; yersiniosis can also occur in various domestic animals and non-human primates. Wild rodents and birds are the reservoir hosts. Transmission is fecal-oral.[2,4,6] After ingestion, *Y. pseudotuberculosis* or *Y. enterocolitica* invade Peyer's patches and lymphoid follicles. High numbers of neutrophils are recruited at the portal of entry. The lymphoid follicles and the overlying epithelium are subsequently replaced by suppurative foci. The bacterium then disseminates via lymphatics and hepatic portal veins to the draining lymph nodes and to the liver and the systemic circulation[4], as was the case in this guinea pig.

Y. pseudotuberculosis is considered to be an extracellular pathogen. It binds to the macrophages and survives attached to them. The immune response is humoral but also cellular. CD8+ T lymphocytes, considered to protect against intracellular pathogen, have been recently shown to restrict *Y. pseudotuberculosis* infection. The proposed model is that T cells could target host cells with extracellularly

attached *Y. pseudotuberculosis*, thus allowing the host cells and associated bacteria to be engulfed and removed by neighboring macrophages.[3]

Yersiniosis was one of the earliest bacterial diseases recognized in guinea pigs. Several types of clinical manifestation are recognized in this species:
- a peracute septicemic form;
- an acute form with miliary, cream-colored nodules in the intestinal wall and ulceration of ileum and caecum;
- chronic infection with caseous nodules in mesenteric lymph nodes, spleen, liver and lung, emaciation, and death;
- non-fatal infection with lesions of lymph nodes of the head and neck.

Inapparent carriage in healthy animals is also reported.[6,7] The lesions of *Y. pseudotuberculosis* and *Y. enterocolitica* cannot be differentiated either grossly or microscopically. In either case, characteristic microcolonies of coccobacilli are found in microabscesses through histological examination. Confirmation by bacterial isolation is needed.[4,7]

Yersinia pestis, the cause of plague in humans and animals, is a clone *of Yersinia pseudotuberculosis* that emerged 1,500 – 20,000 years ago.[1]

JPC Diagnosis: Liver: Abscesses, multiple, with large colonies of bacilli.

Conference Comment: Since guinea pigs digest much of their diet with the aid of hind-gut fermentation, the normal cecal flora is important for physiologic digestion. The cecum is the largest part of the digestive tract usually containing up to 65% of the gastrointestinal contents.[6]

Gut flora is primarily gram-positive bacteria with anaerobic lactobacilli. Coliforms, yeasts, and clostridia may be present in small numbers. A common cause of death in *Yersinia* infection is the result of the subsequent antibiotic treatment. Certain antibiotic therapies can induce a disruption of normal gut flora which are supplanted by pathogenic bacteria such as *Clostridium dificile* and *Escherichia coli* (dysbiosis). Altered microbial ecology in the gut may produce disease and dysfunction because of the intense metabolic activity or antigenicity of the inappropriate bacterial flora to include elaboration of bacterial enzymes which degrade pancreatic enzymes, damage the intestinal brush border, deconjugate and reduce bile acids and alter the intestinal milieu in numerous ways. It is usually the subsequent bacterial antigens and exotoxins that may cause death rather than the initial infection with *Yersinia* sp.[6]

Some conference participants interpreted perceived changes in the hepatic arteries as fibrinoid vascular necrosis, noting apparent hypereosinophilia and hyalinization in the vascular walls; however, the moderator believed this to be an artifact due to perceived staining differences, resulting from the use of saffron with standard hematoxylin and eosin.

Contributor: Ecole Nationale Veterinaire D'alfort
Unité d'Histologie et d'Anatomie Pathologique
7, avenue du Général De Gaulle
94704 Maisons-Alfort Cedex
France

References:

1. Achtman M, Zurth K, Morelli G, Torrea G, Guiyoule A, Carniel E. *Yersinia pestis*, the cause of plague, is a recently emerged clone of *Yersinia pseudotuberculosis*. *Proc. Natl. Acad. Sci.* 1999;96(24):14043-14048.
2. AFIP POLA notes, 2007.
3. Bergman MA, Loomis WP, Mecsas J, et al. CD8+ T cells restrict *Yersinia pseudotuberculosis* infection: bypass of anti-phagocytosis by targeting antigen-presenting cells. *PloS Pathog* 5(9): e1000573, doi: 10.1371/journal.ppat.1000573, 2009.
4. Brown CC, Baker DC, Barker IK. Alimentary system. In: Maxie MG, ed. *Jubb, Keneddy and Palmer's Pathology of Domestic Animals*. vol.2 ed. 5th ed. Philadelphia, PA: Elsevier Limited; 2007:204-205.
5. Fukushima H, Matsuda Y, Seki R, et al. Geographical heterogeneity between Far Eastern and Western countries in prevalence of the virulence plasmid, the superantigen *Yersinia pseudotuberculosis*-derived mitogen, and the high-pathogenicity island among *Yersinia pseudotuberculosis* strains. *J. Clin. Microbiol*. 2001;39(10):3541-3547.
6. Manning PJ, Wagner JE, Harkness JE. Biology and diseases of guinea pigs. In: Fox JG, Cohen BJ, Loew FM, eds. *Laboratory Animal Medicine*, London, UK: Academic Press; 1984;162-163.
7. Percy DH, Barthold SW. Guinea pigs. In: *Pathology of laboratory rodents and rabbits*. 3rd ed. Ames, Iowa: Blackwell Publishing; 2007:225-232.
8. Vlahou G, Schmidt O, Wagner B, et al. *Yersinia* outer protein YopE affects the actin cytoskeleton in *Dictyostelium discoideum* through targeting multiple Rho family GTPases. *BMC Microbiol.* 2009;(9):138.

CASE II: 09-2271-8 (JPC 3169272).

Signalment: 1-year-old (approximately) male mixed breed canine (*Canis familiaris*).

History: The dog was presented to its veterinarian with a history of consuming a white mushroom suspected to be of the *Amanita* genus. The dog began vomiting approximately 30 minutes after consumption and continued to vomit intermittently over the next 24 hours. Abdominal pain and distention, pallor, melena, and hematoma formation at venipuncture sites were noted on physical examination. The dog initially became severely lethargic then uncoordinated. Following one seizure episode the dog became obtunded. The dog remained hypoglycemic despite dextrose administration and died naturally less than 36 hours following consumption of the mushroom.

Gross Pathology: The peritoneal cavity contained approximately 600 ml of frank unclotted blood. The liver was diffusely pale and mottled with red foci throughout the parenchyma. All other organs and tissues including the heart and kidneys appeared diffusely pale. The heart had multifocal well-demarcated, slightly raised, dark red foci on the endocardial surface of the left ventricle. The serosal surface of the fundus and cardia of the stomach were dark red. The mucosal surface of the stomach appeared mildly thickened diffusely and had multifocal dark red areas. There were multifocal dark red areas on the serosal surface of the proximal duodenum. There was digested blood noted throughout the lumen of the gastrointestinal tract.

Laboratory Results: Severely elevated liver values (AST = 12,620; ALT = 7,540)
Coagulation times (PT/aPTT) were severely elevated (too high to measure)
Persistent and progressive hypoglycemia (initially 85 mg/dL, last measured value was 23 mg/dL)
Hypoproteinemia (Total protein = 2.5 g/dL; Albumin = 1.6 g/dL)
Acidemia (pH = 7.2)

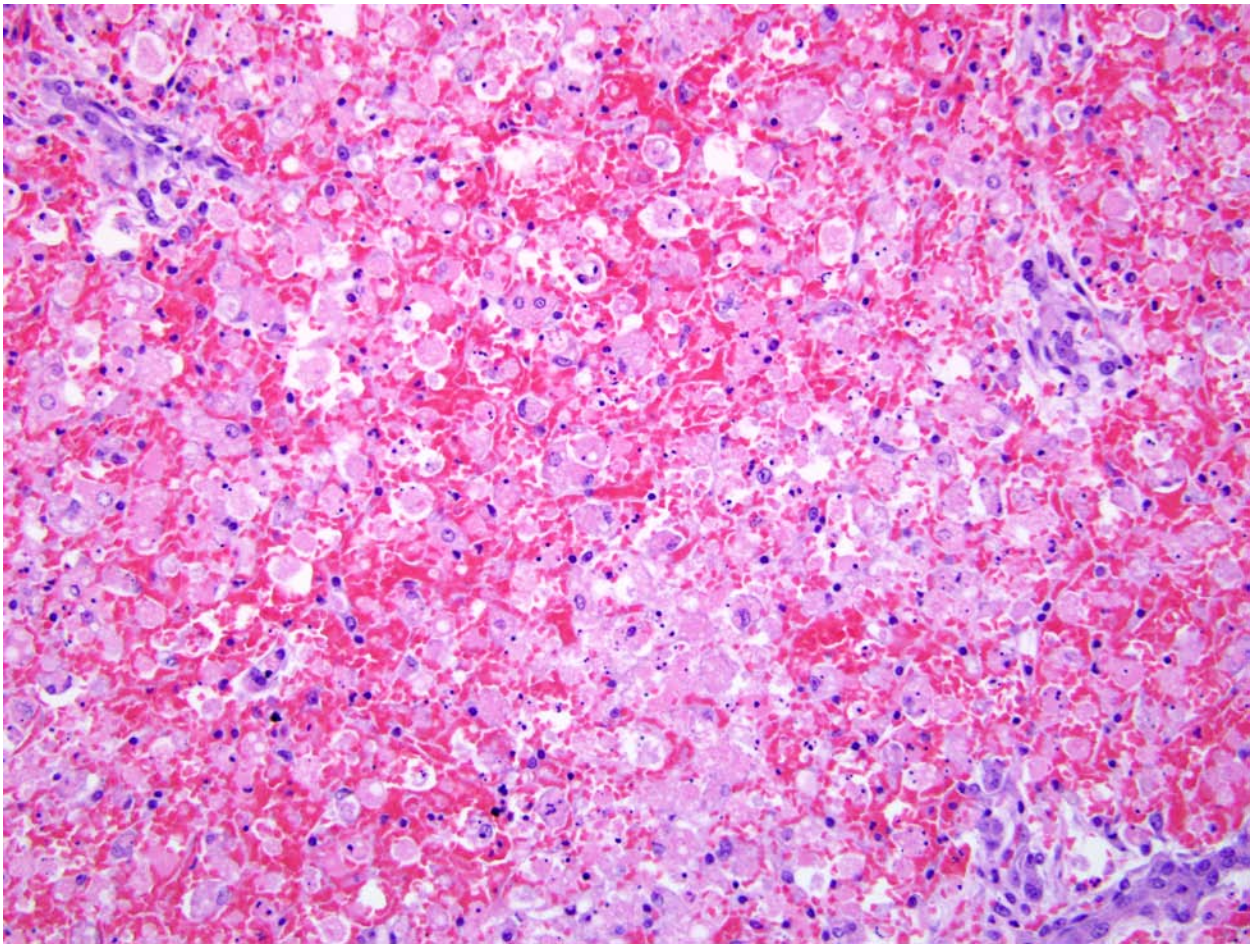

2-1. Liver, dog. There is massive necrosis of hepatocytes (necrosis of hepatocytes in all parts of the hepatic lobule) with loss of sinusoidal architecture, and diffuse hemorrhage. Portal areas are in close apposition without intervening central veins. (HE 100X)

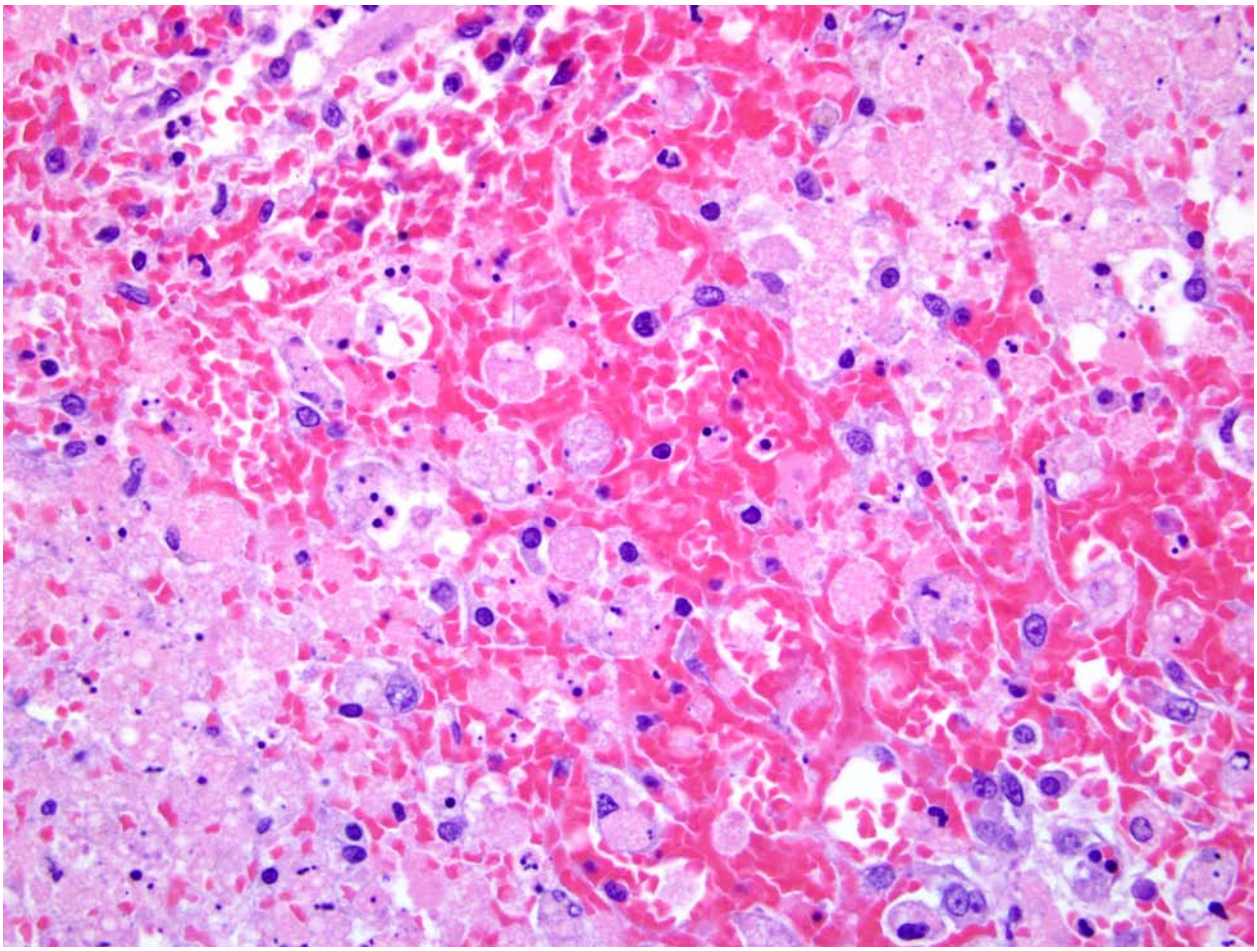

2-2. Liver, dog. Necrotic hepatocytes are disassociated, rounded up, with swollen or shrunken hypereosinophilic cytoplasm and pyknoti, or karyorrhectic nuclei. (HE 400X)

Histopathologic Description: Liver: Throughout the section there is a diffuse loss of hepatic lobular architectural organization with collapse of sinusoids in all zones, extending from central vein to portal triad. Hepatocytes are frequently individualized and either expanded with indistinct, vacuolated eosinophilic cytoplasm (hepatocellular vacuolar degeneration) or shrunken and hypereosinophilic with decreased differential nuclear staining (karyolysis) or deeply basophilic, fragmented nuclei (karyorrhexis) representing hepatocellular coagulation necrosis. Throughout the section are many large, round cells with eccentric oval nuclei and markedly vacuolated, foamy eosinophilic cytoplasm (activated macrophages). Hepatocytes in the periportal regions are separated by many erythrocytes (congestion).

Contributor's Morphologic Diagnosis: Liver: Severe panlobular acute hepatocellular coagulation necrosis.

Contributor's Comment: In the United States, *Amanita phalloides,* also known as "death cap" or "death angel" mushroom, is most commonly implicated in severe cases of mushroom hepatotoxicosis. *Amanita* species mushrooms contain a specific class of toxins referred to as amatoxins (bicyclic octapeptides).[2] Other hepatotoxic cyclopeptide-containing mushrooms include *Galerina*, and *Lepiota* species.[2] Classes of amanitin hepatotoxins include alpha, beta, gamma, and epsilon. The alpha and beta forms are the most toxic and account for over 90% of the amatoxin content of the mushroom. A 20g mushroom contains a potentially lethal dose of amatoxin (LD50 estimated at 0.5mg/kg).[3]

Amanitins bind eukaryotic DNA-dependant RNA Polymerase II and inhibit transcription and protein synthesis, resulting in cell death. Cells with a high metabolic rate are most susceptible (intestinal crypt cells, hepatocytes, proximal convoluted tubule cells). Amanitins also result in endocrine abnormalities.[4]

Reported clinical signs:
Phase 1 – Latency, the animal may appear normal for 8-12 hours following ingestion

Phase 2 – Severe GI signs due to gastroenteritis (nausea, vomiting, bloody diarrhea, abdominal pain)
Phase 3 – Apparent clinical improvement
Phase 4 – Multi-organ failure: Fulminant liver, often with coagulopathy and encephalopathy; Acute renal failure; Severe hypoglycemia, associated with the breakdown of liver glycogen.

Coma and death typically occurs 12-84 hours following ingestion of a lethal dose.[3]

JPC Diagnosis: Liver: Necrosis, massive, diffuse with biliary hyperplasia (ductal reaction type 3).

Conference Comment: The conference morphologic diagnosis parenthetically interprets the biliary hyperplasia as ductal reaction type 3. Prior to the conference, the moderator gave a wonderful presentation referencing a proposed new classification scheme by Desmet[1] for the reaction presently called biliary hyperplasia in veterinary medicine. The new classification scheme takes physiologic and embryologic responses by various cells in the liver to injury or insult into account. In summary, ductular reactions (DR) are categorized into three types based on the type of hepatic injury, the cells involved in the histologically viewed response, and their relationship to the formation of the embryonic ductal plate.

Embryonic biliary precursor cells form a periportal sheet called the ductal plate, which is progressively remodeled to generate intrahepatic bile ducts. A limited number of ductal plate cells participate in duct formation; those not involved in duct development are believed to involute by apoptosis. The ductal plate gives rise to cholangiocytes lining the intrahepatic bile ducts, including its most proximal segments. It also generates periportal hepatocytes and adult hepatic progenitor cells. During early embryogenesis, there is a single-layer ductal plate surrounding the portal vein and portal mesenchyme, followed by the formation of double layered plates. In normal development, extensive resorption of the primitive bile ducts leads to the final stage, in which a network of fine bile ducts surrounds the portal vein.

Ductular reactions generally form a structure similar to the ductal plate, and in the pathologic response, are termed mini-ductal plates. These mini-ductal plates are composed of a small central blood vessel surrounded by a small amount of mesenchyme derived from the original Disse space, and a double layer of small cholangiocyte-like cells lining a slit-like lumen with peripheral tubular dilatation.

This new system classifies DRs into type 1, in which pre-existing ducts and ductules proliferate as a result of cholestasis (and is the type most commonly referred to as "biliary hyperplasia" by veterinary pathologists); type 2A, which is ductular metaplasia induced by inflammation; type 2B, which is ductular metaplasia induced by hypoxia; and type 3, which is the activation and proliferation of liver progenitor cells (LPC) in response to massive hepatic parenchymal loss.

A central tenet which underlies these categorizations is the idea of differentiation and dedifferentiation of cells, specifically LPCs. An LPC differentiates into a mature hepatocyte by sequentially evolving from keratin 19-positive (K19+) hepatoblast, to K19+ K7+ intermediate hepatobiliary cells, then K7+ intermediate hepatocytes and finally to K7 negative mature hepatocytes. In cholangiocyte metaplasia, such as in the type 2 DRs, the mature hepatocytes dedifferentiate in a reverse fashion. Both pathways rely on Jagged1/ Notch signaling as well as a partnership with portal myofibroblasts, endothelial cells, and hepatic stellate cells, and the dedifferentiation of mature hepatocytes back to hepatoblasts recapitulates the embryonal ductal plate. It is hypothesized that the first layer of the mini-ductal plate is derived from this dedifferentiated K19+ hepatoblasts, and the second layer of the mini-ductal plate is from the activation of LPCs in the canal of Hering due to cholestasis or hypoxia.

Type 1 DR is the haphazard proliferation of pre-existing cholangiocytes due to severe cholestasis or interleukin-6 (IL-6) induction, which results in the activation of purinergic ATP receptors on cholangiocytes, which down-regulates NTPDase2 expressed on periductal portal fibroblasts that normally inhibit cholangiocyte proliferation. This physiologic response widens and elongates pre-existing ducts and ductules to accommodate the increase in toxic bile salts and reduce parenchymal damage in cholestasis or increased portal expansion by edema and inflammation. This type of structural adjustment, typically referred to as biliary hyperplasia, can be seen with the other categories of DR according to physiologic need.

Type 2A DR, which is generally periportal, is the "ductular metaplasia of hepatocytes" and formation of mini-ductal plates from LPCs, and results in the change of hepatocyte secretory polarity from horizontal as in canalicular to vertical as in cholangiocytes due to chronic cholestasis. This change in secretory polarity is due to the cytoplasmic keratin rearrangement from long-term exposure to bile salts, and also incites the dedifferentiation of mature hepatocytes to an intermediate K19+ K7+ hepatobiliary cell. This is accompanied by the activation of hepatic stellate cells located in the space of Disse into a myofibroblastic phenotype, which increases the production of connective tissue and the further induction of intermediate hepatobiliary cells

into K 7+ cholangiocytes. Both DR type 1 and 2A are reversible.

Type 2B DR generally occurs in centrilobular areas and is result of hypoxia. This reaction is microscopically similar to type 2A and is induced by hypoxia-inducible factor 1-alpha (HIF-1α). This in turn upregulates fibrotic and vasoactive mediators such as platelet-derived growth factor-A (PDGF-A), PDGFB and plasminogen activator inhibitor-1 (PAI-1). This activate HSCs and LPCs as described in DR type 2A, resulting in progressive centrolobular fibrosis and ductular metaplastic proliferation.

Finally, type 3 DR, which occurs in this case, occurs in massive parenchymal loss. This represents the traditional notion of progenitor cell-based regeneration, and results from the bipotential proliferation of remaining LPCs, resident in the remaining canals of Hering into hepatocytes and cholangiocytes. Following massive hepatic parenchymal loss, there is a massive influx of fibrous connective tissue, and this proliferation is as described in types 2A and 2B, with a tendency toward the cholangiocytic phenotype due to a preponderance of myofibroblasts.

This ductal reaction classification scheme is beginning to gain popularity in the human pathology realm, and has value due to the inherent pathogenic implication with each category. While there is a long way to go before this type of pathogenically descriptive scheme finds favor in veterinary pathology, if at all, a system like this can be very useful.

Contributor: Department of Veterinary Biosciences
College of Veterinary Medicine
The Ohio State University
1925 Coffey Road
Columbus, OH 43210
http://vet.osu.edu/biosciences.htm

References:

1. Desmet VJ. Ductal plates in hepatic ductular reactions. Hypothesis and implications. I. Types of ductular reaction reconsidered. *Virchows Arch*. 2011;458:251–259.
2. Puschner B, Rose, HH, Filigenzi MS. Diagnosis of *Amanita* toxicosis in a dog with acute hepatic necrosis. *J Vet Diagn Invest.* 2007;19:312-317.
3. Spoerke DG, Rumack BH. Handbook of mushroom poisoning: diagnosis and treatment. CRC Press, 1994.
4. Vetter J. Review. Toxins of Amanita phalloides. *Toxicon* 1998;36(1);13-24,1998.

CASE III: NTU08-968 (JPC 3138068).

Signalment: 4-year-old, male, Labrador retriever dog (*Canis familiaris*).

History: An outbreak of severe illness and death affected 181 dogs in an animal shelter starting in August 2008 and subsided in January 2009. Clinically, the dogs progressively developed signs of vomiting, anorexia, depression, icterus, ascites, melena, hematochezia or hematemesis, and eventually death. All dogs received vaccination and deworming for endo/ectoparasites. They were fed a commercialized dog food. PCR results for *Leptospira* sp., parvovirus, adenovirus, *Ehrlichia* sp., and *Babesia* sp. were all negative. Analysis for organic phosphorus and cyanide in intestinal contents was also negative. Based on the presentation and preliminary laboratory results intoxication was suspected by the clinicians.

Gross Pathology: The dog was severely icteric with marked yellow discoloration on mucous membranes, skin, sclera, and adipose tissue. The abdominal cavity contained approximately 970 ml of a yellow to dark orange, translucent, watery fluid (ascites). There were a few fibrin strings adherent to the intestinal serosa. The liver was slightly enlarged, diffusely yellow-tinged and firm with locally extensive white irregular, scar-like areas. The gall bladder wall was thickened with marked submucosal edema. There were multifocal to coalescing, red foci (hemorrhage) scattered on the gastrointestinal tract, urinary bladder, pancreas, and heart. The intestines contain small to moderate amounts of dark red, tarry contents. Aside from the hemorrhage, the urinary bladder was diffusely yellow. Lungs were diffusely reddened, wet and heavy. Bronchi were filled with frothy fluid. Both kidneys were slightly enlarged, and the medulla was yellowish on cut surfaces.

Laboratory Results: Aflatoxins were detected from the commercial canine food consumed by the affected dog. The concentration of aflatoxin B1 in this commercial canine food was over 150 ppb examined by Animal Health Research Institute and TÜV Rheinland Aimex Ltd. PCR results for *Leptospira* sp., parvovirus, adenovirus, *Ehrlichia* sp., and *Babesia* sp. were all negative. Analysis of intestinal contents for organic phosphorus and cyanide were also negative.

Histopathologic Description: Liver: The surface of the liver is irregular and the lobules become indistinct and irregular. The lobules are characterized by variable hepatocellular hydropic degeneration, lipidosis, and necrosis, biliary hyperplasia, and portal, periportal to bridging fibrosis. The remaining hepatocytes display cellular atypia and regeneration characterized by variably sized and shaped cells and nuclei. Scattered binucleated and multinucleated hepatocytes are also noted. Along with these changes, there is also diffuse moderate to severe inflammation characterized by locally extensive infiltration of macrophages, neutrophils, fewer plasma cells and lymphocytes accompanied with variable fibrosis. Mild to moderate bile stasis is diffusely present. Yellow to brown pigment-ladened macrophages and Kupffer cells are also frequently seen.

Contributor's Morphologic Diagnosis: Liver: Hepatocellular fatty change and regeneration, severe, with hepatitis, chronic-active, moderate; portal, periportal, and bridging fibrosis; bile duct hyperplasia; and cholestasis.

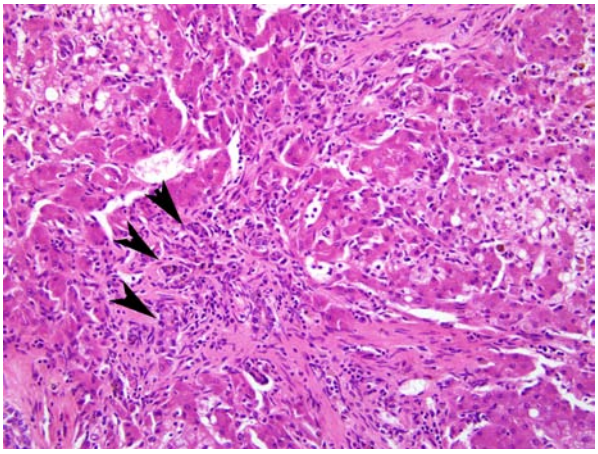

3-1. Liver, dog. Bridging fibrosis connects portal areas and there are numerous small biliary duct profiles (biliary hyperplasia (arrowheads). (HE 20X)

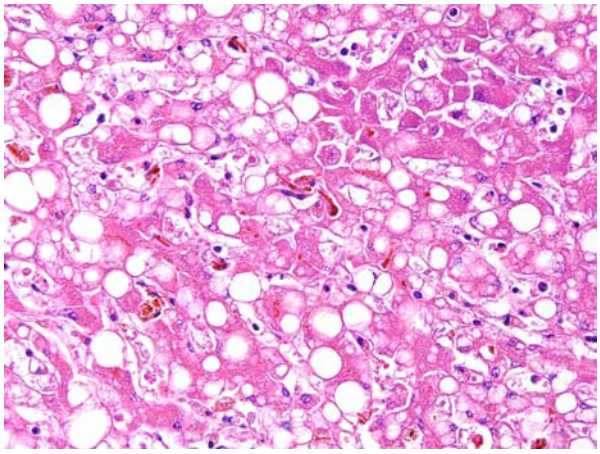

3-2. Liver, dog. Hepatocytes are swollen due to a combination of macro- and microvesicular steatosis; bile plugging (cholestasis) is prominent within these areas. (HE 400X)

Contributor's Comment: Aflatoxins are a group of related, natural, toxic byproducts of the fungi *Aspergillus flavus*, *Aspergillus parasiticus,* and a new select *Penicillium* spp. Aflatoxin B1 is the most hepatotoxic, and also can be immunosuppressive, nephrotoxic, and carcinogenic, and cause hemolytic anemia and coagulopathies.

Aflatoxins are liposoluble and readily absorbed from the gastrointestinal tract into the portal blood. They are then transported to the liver for metabolism. Toxicosis is a result of binding of essential enzymes, which blocks DNA polymerase and ribosomal translocase and leads to the formation of DNA adducts.

It has been suggested that the carcinogenic action of aflatoxin B1 in the rat results from a capacity to bind to DNA, a characteristic similar to that of actinomycin D. However, lethal doses of actinomycin D do not produce hepatic parenchymal cell necrosis. In all species studied, the organ most affected is the liver, although other organs, particularly the kidney, show signs of damage. The distribution of the hepatic lesion is not consistent from species to species, i.e., rat and duckling, periportal; guinea pig and swine, centrilobular; dog, periportal and centrilobular; and rabbit, mid-zonal. In contrast, most other hepatotoxins, such as carbon tetrachloride, regularly induce a centrilobular lesion in both rats and guinea pigs. There is a wide range in the acute LD dose of aflatoxin B1, varying from 0.3 mg/kg for ducklings to 16 mg/kg for mature female rats. In species for which data are available, the young appear to be more susceptible than mature animals. Although the Food and Drug Administration suggests a zero tolerance for aflatoxin in food, it lists a legal limit of 20 mg/kg (ppb) in feed. For dogs, the lethal dose, 50% (LD50) value is just 500 to 1,000 mg/kg (ppb), and, 60 mg/kg (ppb) is a toxic dose.

In the present cases from the Bali shelter, at necropsy the dogs fed commercial dog feed containing aflatoxic peanut meal were jaundiced with swelling and yellowish discoloration of the liver and edema of the gall bladder identical to that seen with crude or purified aflatoxin. The causes of death are believed mainly to be due to severe hepatic damage and the subsequent secondary coagulation defect. The insufficient production of coagulation factors due to severe hepatic injury induces hemorrhages in multiple organs and tissues, including heart, gastrointestinal tract, kidney, pancreas, and adipose tissue. The order of severity and histopathology are variable between different cases, because the varying rates of metabolism between different species, ages, nutritional status and hormone levels hinder assessment of exposure in animals. Additionally, the susceptibility of individual dogs can be affected by levels of sex hormones, age, dose, and/or degree of feed refusal.

JPC Diagnosis: Liver: Macronodular hepatocellular regeneration, diffuse, severe with microvesicular steatosis, necrosis, cholestasis, bridging portal fibrosis, and biliary hyperplasia (ductular reaction type 1.).

Conference Comment: Histologic features of prominent fatty degeneration, bridging fibrosis, and severe cholestasis, marked by bile pigment within hepatocyte cytoplasm (fig) are common features of a number of hepatotoxicities, including phenobarbitol intoxication, copper toxicosis, low-grade chronic microcystin toxicity, certain homeopathic herbal mixtures and chronic aflatoxicosis as in this case. Acute aflatoxicosis, by contrast, is characterized by hemorrhage, severe fatty change, and biliary hyperplasia.

Another important histologic feature is that many portal areas have diminutive portal veins or lack them altogether. This is presumably secondary to portal hypertension from the massive dissecting fibrosis, which prohibits adequate downstream perfusion of portal veins and venules.

Contributor: Division of Animal Medicine,
Animal Technology Institute Taiwan,
No. 52. Kedung 2rd, Ding-Pu Lii, Chunan, Miaoli, Taiwan 350

References:

1. Bingham AK, Huebner HJ, Phillips TD, et al. Identification and reduction of urinary aflatoxin metabolites in dogs. *Food Chem Toxicol*. 2004;42:1851-1858.
2. Newman SJ, Smith JR, Stenske KA, et al. Aflatoxicosis in nine dogs after exposure to contaminated commercial dog food. *J Vet Diagn Invest*. 2007;19:168-175.
3. Stanworth SJ, Hyde CJ, Murphy MF. Evidence for indications of fresh frozen plasma. *Transfus Clin Biol*. 2007;14:551-556.

CASE IV: P0802057 (JPC 3103210).

Signalment: 16-year-old bay Welsh-Pony stallion (*Equus caballus*).

History: The stallion showed reduced appetite and indolence for several weeks, accompanied by moderate to severe icterus, malodorous diarrhea and ataxic locomotion/ compulsive walking. Clinical symptoms were typical for severe hepatic failure with hepatic encephalopathy and the pony was euthanized. Other horses from the same stable, receiving the same diet, did not show any clinical signs of hepatic failure.

Gross Pathology: The stallion was moderately obese and showed intense yellow coloration of mucosal membranes and sclera as well as generalized subcutaneous edema. There was a moderate amount of free serous fluid in thorax and abdomen. The unpigmented skin between nostrils and on the upper and lower lip showed multifocal to coalescing moderate erythema with crusting, consistent with solar dermatitis. Several ulcers (2-3 cm in diameter) were present in the glandular mucosa of the stomach. The wall of the ascending colon showed severe diffuse subserosal edema. The greenish-brown liver had a diffusely thickened capsule with multifocal extensive filamentous proliferation (consistent with chronic parasitic perihepatitis), was very firm on cut surface and had an accentuated zonal/lobular pattern.

Laboratory Results: Blood parameters:

- Lymphocytes	7.7	(25-70 %)
- Granulocytes	88.7	(30-65 %)
- ALP	647	(97-269 U/l 37˚C)
- CPK	391	(<268 U/l 37˚C)
- Creatinine	197	(116-180 µmol/l)
- Total bilirubin	215	(<34 µmol/l)
- GOT	600	(22-488 U/l 37˚C)
- LDH	828	(162-412 U/l 37˚C)
- GGT	914	(16-56 U/l 37˚C)

Histopathologic Description: Liver: The architecture of the liver parenchyma is severely disturbed with marked portal fibrosis, often breaching the limiting plate and resulting in more diffuse parenchymal fibrosis, with prominent porto-portal and porto-central bridging and moderate to marked bile duct hyperplasia.

Predominantly in centrilobular regions, numerous hepatocytes show marked hepatocellular polyploidy and hepatocellular hypertrophy (megalocytosis) with marked nuclear pleomorphism often with cytoplasmic hypereosinophilia, foamy cytoplasm and multiple nuclei. Hepatocellular nuclei are often swollen, containing up to three large nucleoli and occasional mitotic figures and cytoplasmic inclusion. There are frequent intercellular bile plugs in bile canaliculi and

4-1. Sclera, horse. There is intense yellow coloration of the sclera (icterus). Photograph courtesy of University of Utrecht, Departement of Pathobiology, Utrecht, Netherlands, www.vet.uu.nl.

4-2. Skin, horse. The lightly pigmented skin of the muzzle shows multifocal to coalescing erythema with crusts (solar dermatitis). Photograph courtesy of University of Utrecht, Departement of Pathobiology, Utrecht, Netherlands, www.vet.uu.nl.

swelling and proliferation of Kupffer cells containing bile and lipofuscin pigment. Various amounts of bile and lipofuscin pigment are also present in the cytoplasm of hepatocytes.

There is multifocal, predominantly centrilobular, hyperemia with absence of hepatocytes, hepatocellular swelling and eosinophilia and karyopyknosis and karyorrhexis (hepatocellular necrosis) with associated infiltration of neutrophils, macrophages and swelling and proliferation of endothelial cells.

There are diffuse, randomly scattered islands of smaller hepatocytes arranged in broadened cords of liver cells (nodular hyperplasia), with hepatocytes frequently containing intracytoplasmatic vacuoles of varying size with sharp edges (hepatocellular lipidosis) and single apoptotic hepatocytes.

There is increased sinusoidal cellularity with infiltration of various numbers of neutrophils, histiocytes and lymphocytes.

The liver capsule shows moderate diffuse fibrosis and hypertrophic mesothelial cells and there is multifocal to coalescing mild lymphohistiocytic and neutrophilic sub-capsular infiltration.

Contributor's Morphologic Diagnosis: Hepatocellular degeneration and necrosis, centrilobular, mild, marked megalocytosis with marked portal bile duct hyperplasia, fibrosis, multifocal nodular hyperplasia and mild to moderate neutrophilic and lymphocytic inflammation (hepatitis).

Contributor's Comment: Microscopic investigation of the brain revealed subacute moderate hepatic encephalopathy, characterized by multifocal to coalescing clusters of Alzheimer type II astrocytes, predominantly in basal ganglia/ capsula interna and brainstem, multifocal mild to moderate perivascular and perineuronal edema, focally few perivascular lymphohistiocytic infiltrations and sparsely necrotizing neurons with satellitosis.

Widespread portal fibrosis, bile duct proliferation, and megalocytosis are often described as characteristic lesions observed in the liver of horses poisoned by plant-derived pyrrolizidine alkaloids (PA).[1,4,6,7] These chemicals have been found in various plant species widely distributed in the world, e.g. in genera *Senecio, Crotalaria, Heliotropium, Amsinckia, Cynoglossum, Echium, and Trichodesma.*[1,6] In The Netherlands, predominantly *Senecio* ssp. (e.g. "Jakobskruiskruid", *Senecio jacobaea*) from the *Asteraceae* family, are of increasing epidemiologic importance.[4] Ingested PAs are converted to pyrrolic esters by hepatic cytochrome p450 enzymes which mediates the N-oxidation of the esters. These esters are alkylating agents, which react with cytosolic and nuclear proteins and nucleic acids.[6] Dissociation of the alkylation products may result in the formation of new alkylating agents, which may cause cellular damage to persist after ingestion of the alkaloid has ceased.

Cytochrome p450 can also mediate a two-step hydroxylation of necine bases at C3 and C8 positions, which is followed by spontaneous dehydration to the highly reactive dehydro-pyrrolizidine (DHP). The toxic DHP metabolites are electrophilic and can bind to proteins and nucleic acids at guanine and adenine residues, and this DNA-binding activity is responsible for their genotoxicity.[6]

There are three common pathological expressions of PA poisoning[6]:

1. Acute periacinar zonal necrosis, occurs after ingestion of large amounts of PA (naturally occurring outbreaks are rare).
2. Hepatic atrophy with formation of regenerative nodules and characteristic pattern of hepatocellular megalocytosis, occurs after phasic (usually seasonal) repetitive exposure; this is the most common expression of field exposure to PAs.
3. Firm, atrophic livers without nodular regeneration, due to prolonged exposure.

Several studies on horses with experimental PA intoxication revealed that development of megalocytosis, as well as advanced fibrosis and bile duct proliferation, occurs in rather late/ chronic stages (up to 6 months) and/or due to prolonged low dose intoxications.[4,6] Furthermore, clinical signs of toxicosis generally do not appear until weeks to months after onset of plant consumption, and as soon

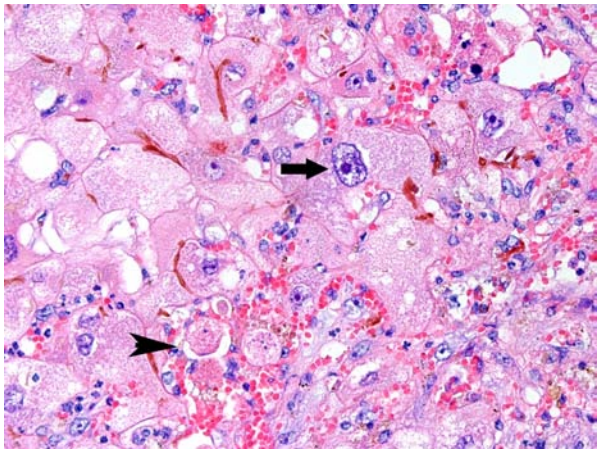

4-3. Liver, horse. Megalocytes (arrows) are characteristic findings in pyrollizidine intoxication of the horse. Hepatocytes are markedly swollen by numerous intracytoplasmic fat droplets, resulting in marked bile plugging (cholesteatosis). A cluster of necrotic hepatocytes is present (arrowhead). (HE 400X)

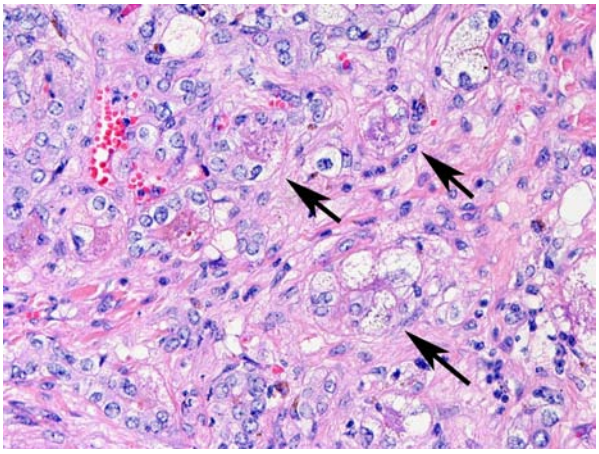

4-4. Liver, horse. Ductular reaction, type 2A is present adjacent to portal areas. In this type of ductular reaction, hepatocytes "de-differentiate", lostiong their characteristic morphology and forming lumina (arrows).

as marked clinical signs occur it was found that in most cases the pathological damage is irreversible.[2,4] The kinetics of conversion of alkaloids to pyrroles, and the chemical nature of these products, varies not only with plant species, but also with animal species, age and sex, and with the metabolic rate of the target cells.[4,6] For an individual PA, toxicity depends on the amount of alkaloid that can be converted to reactive metabolites, the rate of cytochrome p450-mediated generation of DHP, and the efficiency of the detoxification pathway.[6] Hence, the fact that in this case only one individual of the herd showed clinical symptoms of hepatic failure is feasible. In addition to this, estimating the onset of exposure to the toxin is very difficult.

One of the most characteristic effects of chronic exposure to toxic pyrroles is the induction of nuclear and cytoplasmic gigantism (megalocytosis). This effect is most likely due to an antimitotic effect with continued DNA synthesis.[6] Continued nucleoprotein synthesis, coupled with mitotic inhibition, probably accounts for the great increase in size of the nucleus and cytoplasm.[6] Some enlarged nuclei have cytoplasmic invaginations that can be misinterpreted as intranuclear inclusions.[6] Megalocytic cells can be up to 20 times normal size, however, many hepatocytes in an affected liver do not become megalocytic. Those that are completely inhibited do not replicate DNA at all, whereas those that are more resistant can replicate more normally and give rise to nodular populations of smaller, more normal hepatocytes. When hepatocytes are lost faster than they can be replaced, the liver can become atrophic, but the atrophy can be compensated to various degrees by megalocytosis and regenerative nodules.[6] Regenerative capacity might be, amongst others, due to species specific differences, because cattle more often show regenerative nodules than horses.[6]

Concurrently, there is usually fibroplasia and proliferation of the bile ducts. Proliferation of bile duct epithelial cells is largely explained by their unspecific propensity to respond to regenerative stimuli that prevail when liver mass is inadequate. The amount of fibroplasia varies with species and exposure, typically it is minimal in sheep, moderate in horses and may be marked in cattle.[6]

Horses are more likely to manifest signs of hepatic encephalopathy than other species, characterized by head pressing and compulsive walking, the latter of which also occurred in this patient. Although it could not be found in this case, pulmonary emphysema is described as an outstanding feature of pulmonary manifestation of certain PA intoxications in horses. The pulmonary lesions include severe vascular engorgement and edema, and diffuse fibrosis of alveolar and interlobular septa with patchy epithelialization.[6]

Other alkylating agents such as nitrosamine and aflatoxins can also result in portal fibrosis, bile duct proliferation and sometimes megalocytosis.[6,7] Due to lacking information about the quality of the patient's diet, chronic hepatic toxicosis from e.g. aflatoxins cannot be completely excluded. Although the histological lesions reveal characteristics of a chronic hepatitis, pathologists often do not include the term "hepatitis" in the morphological diagnosis of this toxic liver condition. This seems to reflect an inconsistency in the use of the term hepatitis in cases with primary liver cell necrosis due to a toxic insult resulting in an inflammatory reaction.

JPC Diagnosis: Liver: Fibrosis, portal and bridging, diffuse, moderate with hepatocellular anisocytosis and megalocytosis, necrosis, and cholestasis.

Conference Comment: Mesothelial hypertrophy was prominent in this case, and is likely the result of ascites secondary to severe hypoproteinemia. In horses, ascites is an uncommon finding as they usually manifest edema in the lower limbs. Also, the hepatocytes are frequently expanded and exhibit a "ground glass" appearance as a result of proliferation of smooth endoplastmic reticulum, likely due to induction of cytochrome P450 secondary to long term alkaloid exposure.

The moderator pointed out that in cases of hepatocellular nodular regeneration, regenerated hepatocytes develop compensatory enzymes to better accommodate repeat toxin exposure. This is recognized histologically in cases such as chronic copper toxicity, where regenerative nodules are often devoid of copper.

In this case, biliary hyperplasia can be characterized using the new scheme, as described in the previous case, as ductal reaction type 2A. The incipient metaplastic change in the bile ducts is the result of ductal formation by hepatocytes, which lose cytoplasmic eosinophilia and form lumens. Interestingly, the hepatocytes dedifferentiate to a more immature phenotype in response to chronic exposure to free bile acids secondary to severe cholestasis.[3]

Contributor: University of Utrecht
Departement of Pathobiology
Yalelaan 1,
NL-3508 TD Utrecht, The Netherlands
www.vet.uu.nl

References:

1. Cullen JM. Liver, biliary system, and exocrine pancreas. In: McGavin MD, Zachary JF, eds. Mosby *Pathologic Basis of Veterinary Disease*. 4th ed. St. Louis, MO: Elsevier; 2007;444-445.

2. Curran JM, Sutherland RJ, Peet RL. A screening test for subclinical liver disease in horses affected by pyrrolizidine alkaloid toxicosis. *Aust Vet J*. 1996;74:236-240.

3. Desmet VJ. Ductal plates in hepatic ductular reactions. Hypothesis and implications. I. Types of ductular reaction reconsidered. *Virchows Arch*. 2011;458:251–259.

4. Mendel VW, Witt MR, Gitchell BS, et al. Pyrrolizidine alkaloid-induced liver disease in horses: An early diagnosis. *Am J Vet Res*. 1988;49(4):572-578.

5. Olsman AFS, van Oldruitenborgh-Oosterbaan S. Primary liver diseases in horses [Article in Dutch]. *Tijdschr Diergeneeskd.* 2004;129:510-511.

6. Stalker MJ, Hayes MA. Liver and biliary system. In: Jubb KVF, Kennedy PG, and Palmer N, eds. *Pathology of Domestic Animals*. Volume 2, 5th ed. Toronto, Ontario: Saunders Elsevier; 2007:373-376.

7. Stegelmeier BL, Gardner DR, James LF et al. Pyrrole detection and the pathologic progression of Cynoglossum officinale (houndtongue) poisoning in horses. *J Vet Diagn Invest.* 1996;8:81-90.

Joint Pathology Center
Veterinary Pathology Services

WEDNESDAY SLIDE CONFERENCE 2011-2012

Conference 4

28 September 2011

CASE I: YN11-7424 (JPC 4006042).

Signalment: 21-year-old female sooty mangabey (*Cercocebus atys*).

History: This 21-year-old female mangabey was born at the Yerkes National Primate Research Center and had been maintained in a social colony in an indoor–outdoor compound since birth. No significant clinical signs were reported in this animal and she had been observed eating and acting normally, approximately one hour prior to being found deceased in the indoor housing area at the Primate Center.

Gross Pathology: At necropsy, she weighed 7.25 kilograms and was in a good body condition. A large amount of clotted blood filled the left pleural space around the lung lobes. The wall of the thoracic aorta was moderately thickened and focally perforated (~0.15 cm diameter). The perforation had smooth edges and clotted blood was adhering to the tunica intima and adventitia. The tunica intima also had

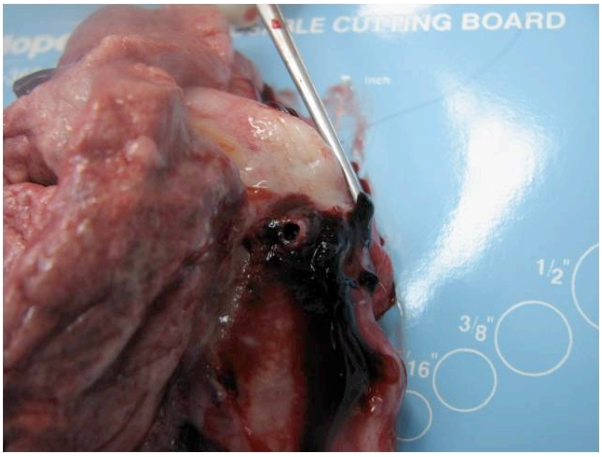

1-1. Aorta, sooty mangabey. The wall of the thoracic aorta is moderately thickened and focally perforated. Photograph courtesy of Yerkes National Primate Research Center, Atlanta, GA, www.yerkes.emory.edu/research/divisions/pathology.

1-2. Aorta, tunica intima, sooty mangabey. Within the tunica intima there are multiple firm yellow nodules. Photograph courtesy of Yerkes National Primate Research Center, Atlanta, GA, www.yerkes.emory.edu/research/divisions/pathology.

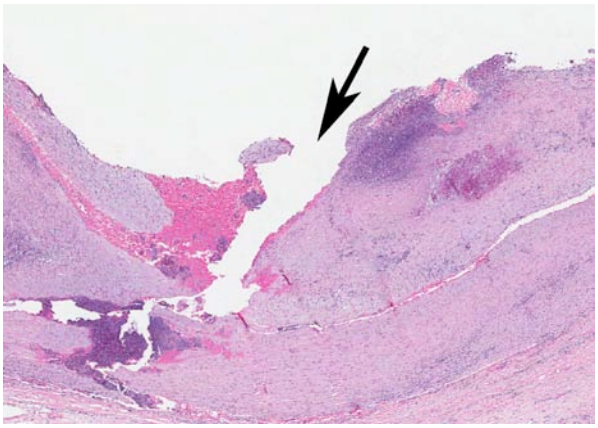

1-3. Aorta, sooty mangabey. The aortic wall is focally fractured and expanded by necrotic cellular debris. (HE 200X)

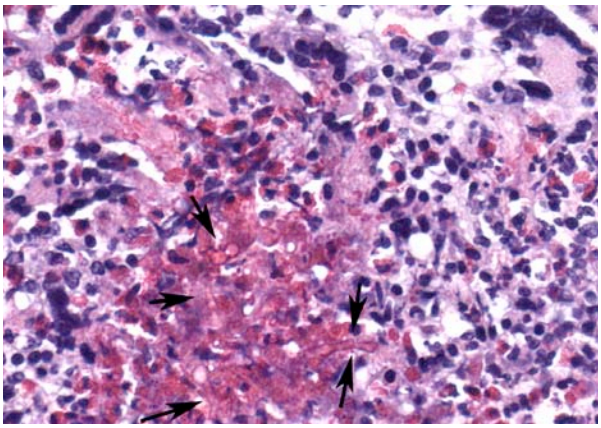

1-4. Aorta, sooty mangabey. Clusters of fungal hyphae with non-parallel walls and few septae incite a profound eosinophilic response. (arrow). In this case, silver stains for fungi were non-contributory. (HE 400X)

multiple, firm, pale yellow nodules (0.25cm-0.5 cm diameter).

Laboratory Results: PCR performed on the formalin-fixed paraffin-embedded aortic tissue confirmed *Basidiobolus* as the likely causative agent.

Histopathologic Description: Aorta: The aortic wall has moderate multifocal intimal fibrosis intermixed with necrosis and infiltrates of degenerate and viable eosinophils and neutrophils. The aortic intimal nodules contains pyogranulomatous inflammation intermixed with abundant eosinophils, necrosis, fibrin and broad, infrequently septate, thin-walled fungal hyphae, which occasionally show focal bulbous dilations and irregular branching. The immunohistochemistry for mucormycetes demonstrates fungal hyphae in areas of intense eosinophilic inflammation in the aortic intima. The inflammatory infiltrate often extends to the tunica media and occasionally to the tunica adventitia. No significant lesions or fungal hyphae were apparent in any other tissue.

Contributor's Morphologic Diagnosis: Aorta, severe multifocal pyogranulomatous to eosinophilic aortitis with intralesional fungal hyphae (*Basidiobolus* spp.)

Contributor's Comment: An aneurysm is a localized abnormal dilatation or outpouching of a thinned and weakened portion of a vessel, affecting usually large elastic arteries and hence can be fatal upon rupture.[8] Known causes of aneurysms in animals include copper deficiency in pigs, *Spirocerca lupi* infection in dogs and *Strongylus vulgaris* infection in horses.[8] In humans, aortic rupture can be spontaneous or a result of severe trauma, but in animals, physical trauma is a more common cause. Aortic rupture with dissecting aortic aneurysm has been studied in cattle due to similarities with Marfan syndrome in humans and it also occurs in ostrich, pigs, rats and turkeys.[8] Sudden rupture of the ascending aorta associated with marked exertion and excitement (due to breeding and racing) in horses has been associated with rapid death from cardiac tamponade.[8]

Aneurysm in the aortic arch associated with *Aspergillus* infection has been reported in a horse and fungal infections of the guttural pouch have been associated with ulceration of the internal carotid or maxillary artery resulting in their rupture and fatal hemorrhage in horses.[2,7] Though spontaneous aortic aneurysms have been described in NHPs along with dissecting aneurysms in monkeys used as experimental models of atherosclerosis[6], our case uniquely presents rupture of a spontaneous aortic aneurysm associated with entomophthoromycosis in a sooty mangabey. Immunohistochemistry detected a mucormycete infection in the aorta and the PCR further identified the fungus as *Basidiobolus* spp, a mucormycete.

Broadly, the term mucormycosis is the preferred name used to describe the angiotropic infection caused by a member of the subphylum *Mucoromycotina* or the subphylum *Entomophthoromycotina* (formerly Zygomycetes). Histopathology typically demonstrates angioinvasion with associated necrosis.[1] Medically important orders and genera include:

1. Mucorales, causing subcutaneous and systemic zygomycosis (Mucormycosis) - *Rhizopus, Lichtheimia (Absidia), Rhizomucor, Mucor, Cunninghamella, Saksenaea, Apophysomyces, Cokeromyces* and *Mortierella*
2. Entomophthorales, causing subcutaneous zygomycosis (Entomophthoromycosis) - *Conidiobolus* and *Basidiobolus.*[1]

Basidiobolus is a true pathogen, causing infections in immunocompetent and immunocompromised human

and animal hosts.[3] It occurs in decaying vegetation, soil, and as a saprobe in the intestinal contents of reptiles like lizards, chameleon, amphibians (toads) and mammals (bat).[3] The fungus is believed to enter the skin after insect bites, scratches and minor cuts. With the exception of *Basidiobolus ranarum,* the fungi in the Entomophthorales order, compared to those in Mucorales order, generally do not invade vascular tissue.[3] Tissue reaction to *Basidiobolus* infection may be acute with infiltrates of eosinophils, lymphocytes and plasma cells at the infected focus and/or a chronic granulomatous response with a predominance of eosinophils.

Finally, the aneurysm in the thoracic aorta of this sooty mangabey was a true aneurysm involving all the layers of the aortic wall and in the absence of any significant clinical signs and based on the gross and histologic lesions, the cause of death of this animal was an acute rupture of the aortic aneurysm associated with the fungal infection. The mucormycotic infection of the aorta was very severe and multifocal, but no evidence of a widespread infection of other organs was observed.

JPC Diagnosis: Aorta: Arteritis, proliferative, pyogranulomatous and eosinophilic, chronic-active, multifocal to coalescing, severe, with numerous fungal hyphae.

Conference Comment: Microscopically, aneurysms are either characterized by complete or partial rupture of the intima and media in the grossly stretched region, developing gradually with replacement by fibrous tissue, or, in the case dissecting or false aneurysms, fracture and necrosis in the media with dissection by blood. Neither of these lesions were present in the slide, so it is unclear if the aneurysm was caused by the fungal infection, or if it was merely secondarily colonized.[4]

Zygomycetes are ubiquitous, saprophytic, non-pigmented, 7-10 µm wide fungi with non-dichotomous branching and rare septa. The *Mucorales* order is more commonly pathogenic in warm-blooded animals, with angioinvasion being characteristic, while the *Entomophthorales* order, which usually infects arthropods, reptiles, and amphibians, is rarely pathogenic to warm-blooded animals. Recent taxonomic restructuring combines the previous four species of the genus *Basidiobolus* into the single species, *B. ranarum.* The typical mode of transmition of *Basidiobolus* and other *Entomophthorales* is via ingestion of insects, which carry the spores on their external bristles, by reptiles and amphibians, which then pass infective spores in their excreta.[11]

Differential diagnoses for these fungal hyphae should include *Pythium* and *Lagenidium,* members of the *Oomycetes* class.[11] Polymerase chain reaction is needed to definitively differentiate these three pathogens. Another differential diagnosis that should be considered is the proliferative arteriopathy associated with SIV infection. With SIV, large to medium vessels are typically affected, particularly pulmonary arteries. The intima and media are thickened, the internal elastic lamina is fragmented, and the endothelium can be hypertrophied or hyperplastic, or focally eroded with adherent thrombi. Eosinophilic and granulomatous inflammation, as seen in this case, is typically not seen.[5]

Some conference participants reported seeing Warthin-Finkeldey-type syncytial cells within germinal centers of the associated hyperplastic lymph node, which are occasionally seen in non-human primates infected with simian immunodeficiency virus (SIV) or measles virus, and represent the fusion of infected and uninfected CD4+ T lymphocytes. These cells have also seen in humans infected with HIV.[9] Attempts to characterize these syncitial cells through immunohistochemistry and electron microscopy have been unfruitful, but they may represent a multinucleated follicular dendritic cell.[10] While the presence of multinucleated cells was confirmed in the lymph node, the contributor confirmed that this sooty mangabey was seronegative for SIV.

Contributor: Yerkes National Primate Research Center
954 Gatewood Road
Atlanta, GA
http://www.yerkes.emory.edu/research/divisions/pathology/index.html

References:

1. Brown J. Zygomycosis: an emerging fungal infection. *Am J Health Syst Pharm*. 2005;62:2593-2596.
2. Ginn PE, Mansell, JEKL, Rakich PM. Skin and appendages. In: Maxie MG, ed. *Jubb, Kennedy, and Palmer's Pathology of Domestic Animals*. Philadelphia, PA: Elsevier Limited; 2007:707-608.
3. Gugnani HC. A review of zygomycosis due to Basidiobolus ranarum. *Eur J Epidemiol*. 1999:15:923-929.
4. Jones TC, Hunt RD, King NW. Cardiovascular system. In: Jones TC, Hunt RD, King NW, eds. *Veterinary Pathology*. 6th ed. Baltimore, MD: Williams & Wilkins; 1997:1001.
5. King NW. Simian Immunodeficiency Virus infections. In: Jones TC, Mohr U, Hunt RD, eds. *Nonhuman Primates I.* Berlin, Germany:Springer-Verlag; 1993:5-18.

6. Lowenstine LJ. A primer of primate pathology: lesions and nonlesions. *Toxicol Pathol*. 2003;(31 Suppl):92-102, 2003.
7. Okamoto M, Kamitani M, Tunoda N, et al. Mycotic aneurysm in the aortic arch of a horse associated with invasive aspergillosis. *Vet Rec*. 2007:160:268-270.
8. Robinson MGMaWF. Cardiovascular system. In: Maxie MG, ed. *Jubb, Kennedy and Palmer's Pathology of Domestic Animals*,. Philadelphia, PA: Elsevier Limited: 2007:62-63.
9. Rosenberg ES, Daskalakis DC. Impairment of HIV-specific immune effector cell function. In: ed. Badley AD. *Cell death during HIV infection*. Boca Raton, FL: CRC Press; 2006:195.
10. Sasseville et al. Induction of lymphocyte proliferation and severe gastrointestinal disease in macaques by a Nef gene variant of SIVmac238. *AJP*. 1996;149(1):163-176.
11. Songer JG, Post KW. Veterinary Microbiology: Bacterial and Fungal Agents of Animal Disease. St. Louis, MO: Elsevier Saunders; 2005:398-403.

CASE II: 10L2130 (JPC 4006056).

Signalment: Adult male Chukar partridge, *Alectoris chukar.*

History: Farm raised chukar, found dead.

Gross Pathology: Hepatic necrosis, multifocal, severe. Typhlitis, necrotizing, multifocal, severe. Nematodiasis, small intestine and cecae, severe.

Histopathologic Description: Liver: Multifocal, variably sized, random areas of coagulative and lytic necrosis replace hepatocytes throughout all lobules. Large numbers of macrophages, degenerative and intact heterophils intermixed with foreign body-type multinucleated giant cells are adjacent to areas of necrosis. Fewer lymphocytes and plasma cells surround these areas. Large numbers of macrophages and multinucleated giant cells contain myriads of intracytoplasmic, approximately 15 µm diameter, round, lightly eosinophilic protozoal trophozoites. Cecum: Similar trophozoites fill macrophages and multinucleated giant cells surrounded by degenerative heterophils, karyorrhectic debris and proteinaceous material cover the ulcerated lamina propria.

Contributor's Morphologic Diagnosis: Hepatocellular necrosis, lymphocytic-histiocytic hepatitis, with intracellular and intralesional trophozoites consistent with *Histomonas meleagridis.*

Typhlitis, necrotizing, multifocal, severe, and histiocytic, with intrahistiocytic and intralesional trophozoites consistent with *Histomonas meleagridis.*

Contributor's Comment: Histomoniasis is caused by a flagellated protozoan parasite, *Histomonas meleagridis*, that colonizes earthworms and the cecal nematode, *Heterakis gallinarum.*[1,2] Histomoniasis primarily affects gallinaceous birds (chickens, grouse, partridge, peafowl, pheasants, quail, turkeys); lesions are primarily found within the liver and cecum.[5,6] Turkeys, either wild or domestic, almost always develop severe disease following infection. Chukar partridge, peafowl and ruffed grouse also are prone to severe disease.[4.] Ring-necked pheasants, chickens and junglefowl rarely become sick; these species serve as carriers of the parasite. Bobwhites, guinea fowl and Hungarian partridge exhibit high morbidity, but intermediate mortality.

JPC Diagnosis: Liver: Hepatitis, necrotizing, multifocal to coalescing, severe, with numerous protozoal trophozoites.
Brain: No significant lesions.

Conference Comment: This historically important disease has caused more losses to the turkey industry than any other disease, and occurs especially in poults, as well as chickens and captive game birds. Although the disease is less severe in chickens, economic losses are often greater than in turkeys due to the frequency

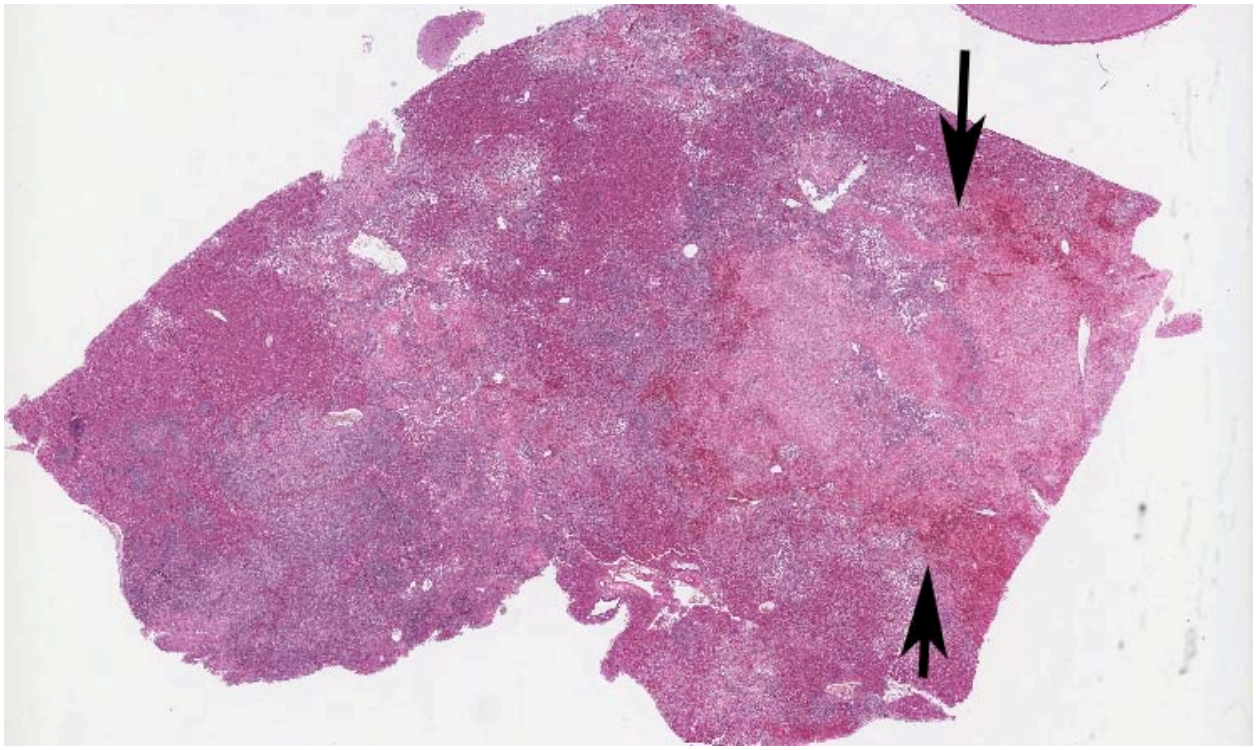

2-1. Liver, chukar partridge. There are coalescing areas of pallor (coagulative necrosis – arrows) and hemorrhage throughout the liver. (HE 63X)

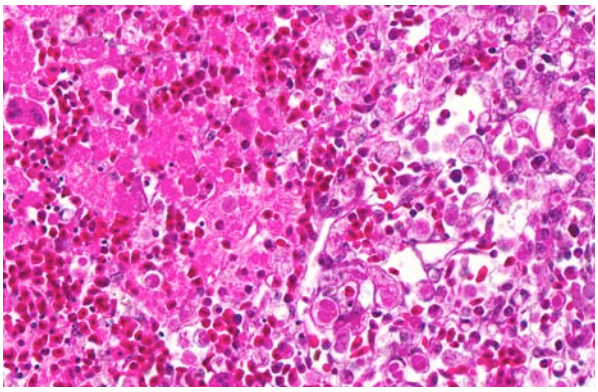

2-2. Liver, chukar partridge. Numerous extra- and intracellular trophozoites (arrows) populate areas of necrosis, with a sharply demarcated area of coagulative necrosis at left. (HE 200X)

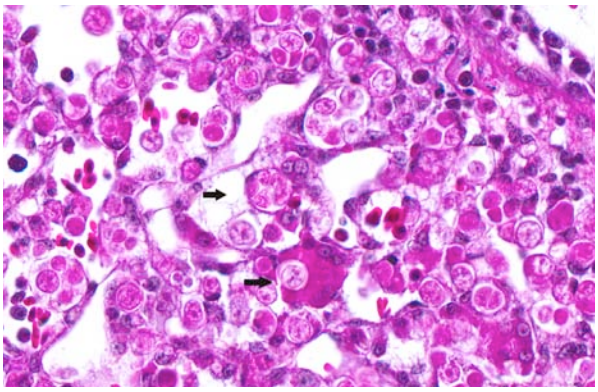

2-3. Liver, chukar partridge. Multinucleated giant cell macrophages containing trophozoites are scattered thoughout the section. (HE 400X)

of occurrence and greater number of birds affected.[7] *Histomonas* was originally classified as an amoeba, but was reclassified as a flagellated protozoan by Tyzzer in 1920 based on the presence of a flagellum when in the cecal lumen and absence of a cyst form.[6] Although histomoniasis is colloquially called "blackhead" for the development of cyanosis of the head, this inconsistent sign is not pathognomonic. The conversion of hemoglobin to methemoglobin in acute disease may also contribute to cyanosis.[7]

Transmission is by ingestion of 1) infected feces; 2) embryonated *Heterakis* eggs containing histomonads; or 3) an earthworm containing infected *Heterakis* larvae. Histomonads are released into the intestinal lumen when the *Heterakis* eggs hatch and then invade the cecal wall. Two to three days after cecal infection, the protozoa reach the liver via hepatic-portal circulation, and can also be found in the bursa of Fabricus, kidney, pancreas, and spleen.[7] In addition to vector-borne transmission, histomoniasis can spread directly through cloacal drinking, which is the retrograde peristalsis of urine and fecal contaminants from the vent into the bursa and ceca; this is important in rapid spread of the disease through turkey flocks.[6]

In addition to the gross lesions seen in this case, the ceca are often bilaterally enlarged and hyperemic with thickened walls, and may contain a central caseous, laminated core, necessitating differentiation from *Eimeria tenella* and *Salmonella* spp. The liver may have depressed targetoid lesions which often coalesce. *Histomonas* may be difficult to identify histologically in chronic lesions, and the presence of rounded empty spaces within a marked inflammatory response should raise the specter of histomoniasis, especially within the liver or ceca.[2]

Histomonas achieves its full virulent potential when *Escherichia coli*, *Clostridium perfringens*, or *Bacillus subtilis* is present in the cecum, and is avirulent in gnotobiotic poults. Conversely, *Histomonas* mitigates *Eimeria* infections in the cecum by creating an inhospitable environment for coccidia to flourish. In chickens with histomoniasis, coinfection with *Eimeria tenella* significantly increases the development of hepatic necrosis.[7]

Contributor: Utah Veterinary Diagnostic Laboratory
1400 N 950 E
Logan, UT 84341
http://www.usu.edu/uvdl/

References:

1. Callait-Cardinal M, Chauve C, Reynaud M, et al. Infectivity of *Histomonas meleagridis* in ducks. *Avian Pathology.* 2006;35:109-116.
2. Charlton BR. *Avian Disease Manual*. 4th ed. Atlanta, GA: American Association of Avian Pathologists; 2006:152-3.
3. Grabensteiner E, Hess M. PCR for the identification and differentiation of *Histomonas meleagridis*, *Tetratrichomonas gallinarum* and *Blastocystis* spp. *Vet Parasitol*. 2006;20:223-230.
4. Janildo L, Reis R, Beckstead C, et al. *Histomonas meleagridis* and Capillarid Infection in a Captive Chukar (*Alectoris chukar*). *Avian Diseases*. 2009;53:637-639.
5. McDougald L, Fuller L. Blackhead disease in turkeys: direct transmission of *Histomonas meleagridis* from bird to bird in a laboratory model. *Avian Diseases*. 2005;49:328-331.
6. McDougald L. Blackhead disease (histomoniasis) in poultry: a critical review. *Avian Diseases*. 2005;49:462-476.
7. McDougald LR. Histomoniasis (Blackhead) and Other Protozoan Diseases of the Intestinal Tract. In: Saif YM, ed., *Diseases of Poultry*. 12th ed. Ames, IA: Blackwell; 2008:1095-1100.

CASE III: 11-A-207 (JPC 4006289).

Signalment: 7 year and 346 day-old intact male rhesus macaque, *Macaca mulatta*.

History: This animal had a history of ill thrift and intermittent diarrhea. *Campylobacter coli and Campylobacter jejuni* were isolated on fecal culture several months prior to euthanasia. *Balantidium coli* and eggs of *Trichuris spp*. were identified on fecal parasitology screens at the same time. Supportive and therapeutic care was provided. Euthanasia was performed due to the poor prognosis for long-term resolution of diarrhea.

Gross Pathology: The animal was thin with no visible subcutaneous or visceral adipose tissue stores. The mesenteric lymph nodes were multifocally enlarged up to five times the normal size. The large intestine was markedly and uniformly dilated and contained green liquid fecal material admixed with gas. Numerous 2 cm long slender nematodes were present in the lumens that are consistent with *Trichuris* sp. The mucosa of the cecum, ascending colon and transverse colon was diffusely thickened, edematous and red.

Laboratory Results: Normal ranges are given in parentheses.

Albumin (g/dl):	2.4	(3.4 - 4.70)
Protein (g/dl):	5.5	(5.8 – 7.5)

Histopathologic Description: Colon: Diffusely, the colonic mucosa is thickened with a moderate inflammatory infiltrate composed of large numbers of neutrophils, plasma cells, lymphocytes and lesser numbers of eosinophils and macrophages that separate the crypts and often extend into the submucosa. Scattered within the mucosa are lesser numbers of large foamy macrophages measuring 8 - 20 µm in diameter and forming rare multinucleated giant cells containing up to 15 nuclei (muciphages). Crypt lumina multifocally contain intact and degenerate neutrophils admixed with cellular debris (crypt abscess) and affected crypts may be lined by attenuated epithelium. Occasionally the crypts are ruptured. Multifocally, there is mild loss of goblet cells. The remaining crypts are hypercellular and tall with moderate numbers of mitotic figures. The mucosal surface is multifocally eroded, irregular and attenuated with epithelial tags projecting into the lumen. Multifocally, the submucosal lymphatic vessels are dilated and contain eosinophilic flocculent fluid. Focally within the mucosa and within the lumen are 20-80 µm diameter protozoans with granular eosinophilic protoplasm containing variable numbers of vacuoles, a round to bean shaped nucleus, and a cell membrane covered with cilia. There are cross and tangential sections of nematodes with irregularly spaced projections on the cuticle, a stichosome surrounding the esophagus, a single prominent bacillary band, coelomyarian/ polymyarian musculature, pseudocoelom containing deeply eosinophilic fluid, digestive tract lined by uninucleate cells with a microvillous border, and ovary and uterus containing large numbers of thick shelled, oval unembryonated eggs with bipolar plugs. Multifocally, a wispy, basophilic mat of spirochetes is adhered to the microvillous border of the enteroocytes.

Contributor's Morphologic Diagnosis: Colon: Colitis, proliferative, neutrophilic, lymphoplasmacytic, eosinophilic, chronic-active, moderate, diffuse, with crypt abscesses, intralesional protozoa consistent with *Balantidium coli*, and intraluminal nematodes consistent with *Trichuris spp*.
Colon: Spirochetes, apical cytoplasm, moderate numbers, multifocal.
Microscopic findings of tissues not submitted:
Duodenum, jejunum and ileum: Enteritis, lymphoplasmacytic and eosinophilic, mild, multifocal with moderate deposits of amyloid in the lamina propria.
Spleen: Amyloid deposition, multifocal, mild.
Liver, space of Disse: Amyloid deposition, multifocal, minimal.
Adrenal gland, corticomedullary junction: Amyloid deposition, multifocal, minimal.

Contributor's Comment: The primary findings in this case are proliferative, neutrophilic, lymphoplasmacytic typhlocolitis with mesenteric lymphoid hyperplasia, and systemic amyloidosis. Chronic colitis in rhesus macaques is a complex syndrome with a prolonged clinical course of intermittent diarrhea, dehydration and poor growth rate. Juvenile to young animals are usually affected. The initiating and perpetuating cause of the chronic colitis is unknown and is most likely multifactorial. Microbial infection, stress, exposure to dietary antigens and inappropriate immune response are all thought to play a role in its pathogenesis.

Numerous enteric pathogens have been examined for their role in the development of chronic colitis. *C. coli* and *C. jejuni* were identified to be strongly associated with chronic colitis in rhesus macaques.[5] In a recent study, significant differences in the gastrointestinal tract microbial population have been reported between healthy animals and animals with chronic colitis.[5] In group housed colonies at ONPRC, *Campylobacter spp.* or *Shigella spp.* have been associated with initial episodes of diarrhea followed by presence of normal flora.[4] Virulent shiga toxin/eaeA intimin expressing *Escherichia coli, Balantidium coli, Giardia lamblia, Enterocytozoon bieneusi and Trichuris trichiura* have all been isolated in animals with and without diarrhea.[5]

Grossly, most of the animals with chronic idiopathic colitis are emaciated with no subcutaneous or visceral adipose tissue stores, and mild to severe thymic atrophy.[1] The large intestine may be dilated and contain liquid fecal material. The cecum, ascending colon, and transverse colon are consistently affected. In severe cases, most of the large intestine may be involved; however, the rectum is seldom affected. The affected mucosa is thickened and may have a rugose appearance[1] with or without erosions or ulcerations. The mesenteric lymph nodes, ileocecal lymph nodes and colonic lymph nodes are usually hyperplastic. In severely affected animals, serous atrophy of visceral adipose tissue may be seen. Gastritis is not a consistent finding in animals with chronic idiopathic colitis.[6]

Microscopically, the colonic mucosa is thickened variably with neutrophils, lymphocytes, plasma cells that often separate the crypts. Crypt abscesses and crypt ruptures are common in acute infections.[1] In chronic cases, the mucosa is proliferative; the crypts may be distorted, tortuous with karyomegaly, hyperchromicity, pseudostratification, frequent mitotic figures and presence of mitotic figures in the upper 1/3 of the mucosal glands. Goblet cell loss is common. The epithelial changes include micro-erosions, attenuation, irregularities of cell shape and size, disparity of nuclear size and hyperchromicity. Mucosal herniation into the submucosal lymphoid tissue is common. The ileum may be involved variably. Other associated histological changes include lymphoid hyperplasia of mesenteric lymph nodes, chronic cholecystitis, mild portal lymphocytic hepatitis and thymic atrophy.[1] Chronic inflammation is a risk factor for developing reactive amyloidosis and chronic colitis is a common underlying inflammatory condition leading to the development of amyloidosis in this species. Amyloid deposition may be present in the lamina propria of small intestine, spleen, liver, adrenal gland and kidney.[2]

This case exhibits all the classic gross and histologic features of chronic colitis in macaques but has some additional features. Numerous protozoa are present within the mucosa as well as in the lumen and the nematodes are present within the lumen. Additionally, moderate numbers of foamy macrophages (muciphages) and multinucleated giant cells are present. Their significance is unknown. (Acid fast stains were performed to rule out possible *Mycobacteria*. sp.) The filamentous spriochetes visible in some portions of the section are relatively uncommonly seen in macaques with chronic diarrhea but are typically found in animals with normal colons. Spirochetes in the large intestine of rhesus macaques have not been associated with disease processes and are generally considered benign. In addition, Congophilic amyloid deposits were present in the lamina propria of duodenum, jejunum and, ileum as well as spleen, liver and adrenal glands. The gross and microscopic findings suggest that the severity of chronic diarrhea in this animal could be multifactorial, i.e., the presence of chronic colitis, balantidiasis, trichuriasis and enteric amyloidosis. Enteric amyloid deposition leading to protein-losing enteropathy accounts for the laboratory finding of panhypoproteinemia.

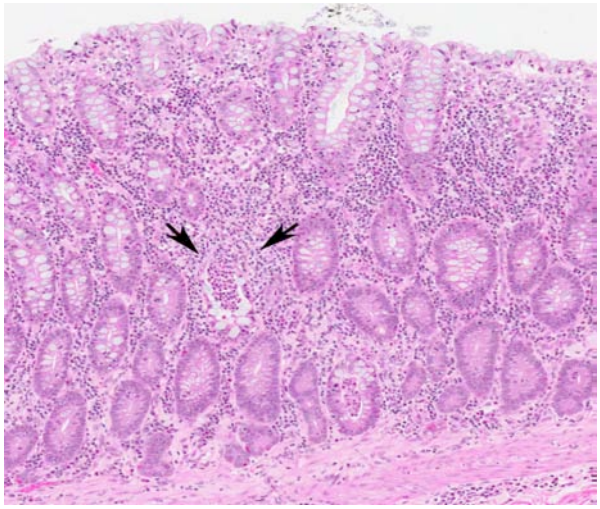

3-1. Colon, rhesus macaque. A profound lymphoplasmacytic inflammatory response in the colon separates and replaces colonic glands. There are numerous mitotic figures within the apical population, and a focal crypt abscess (arrows). "Crypt abscess" is a colloquial term for a dilated gland or crypt filled contain necrotic epithelial cells, neutrophils, and cellular debris. (HE 100X)

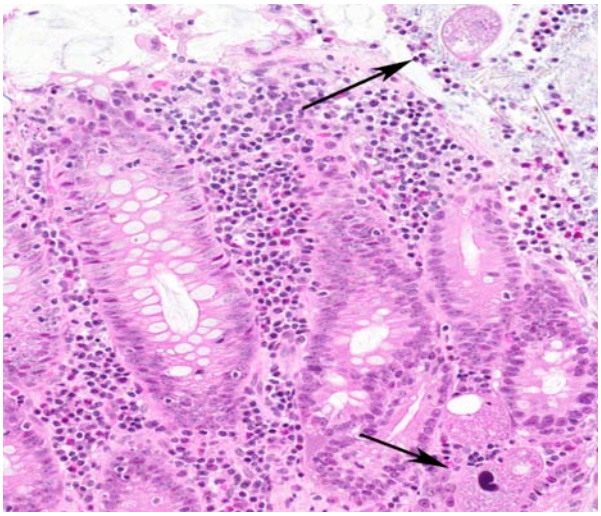

3-2. Colon, rhesus macaque. Luminal and invasive ciliates consistent with Balantidium coli. (HE 200X)

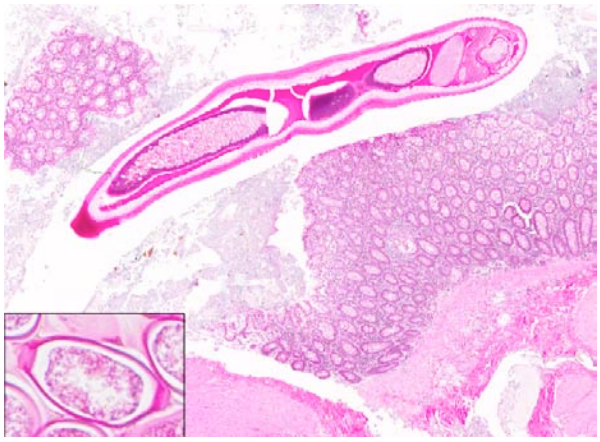

3-3. Colon, rhesus macaque. An adult nematode consistent with Trichuris trichiuria is present within colonic lumen. (HE 63X) The inset at lower left (400X) shows typical oval eggs with bipolar plugs.

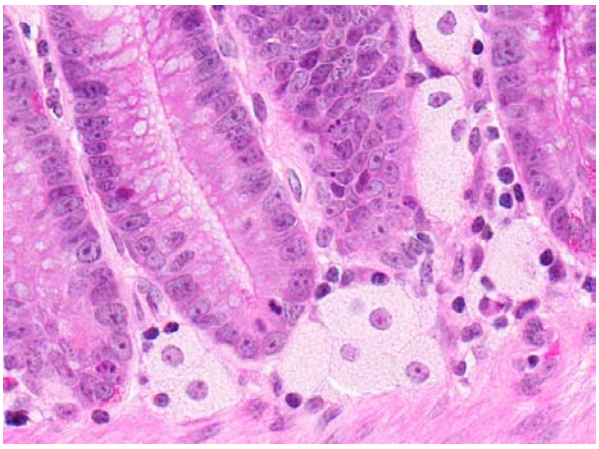

3-4. Colon, rhesus macaque. Large macrophages with abundant foamy cytoplasm (muciphages) are presnt at the base of the glands, and in lesser numbers at the villar tips. A proposed reason for their presence is damage to goblet cells. (HE 400X)

JPC Diagnosis: Colon: Colitis, proliferative, lymphoplasmacytic, chronic, diffuse, moderate, with crypt abscesses, luminal and intramucosal ciliates, and luminal adult aphasmid nematodes.

Conference Comment: The contributor has provided a comprehensive overview of chronic colitis in macaques. Chronic colitis of juvenile rhesus macaques, which typically occurs in animals from 10 months to three years of age, must be distinguished from chronic diarrhea from opportunistic infections associated with simian acquired immunodeficiency syndrome. Colonic neoplasia has not been associated with chronic colitis of juvenile rhesus macaques.[1] Conference participants also discussed the differential diagnosis of ulcerative cicatrizing colitis, which is also seen in rhesus macaques. In this disease, there is deep linear mucosal ulceration in the cecum and proximal colon, and resultant bands of reactive fibrosis cause colonic strictures.[4] This disease must be distinguished from colonic adenocarcinoma, a very common malignancy in older rhesus macaques, which often arises in the same location.

Muciphages are present in the superficial and deep mucosa and may be a response to damaged goblet cells. In the human, muciphages are seen in both normal and diseased large intestine and rectum, and are not considered predictive of disease.

The contributor mentioned the presence of mitotic figures in the upper 1/3 of the mucosal glands, and conference participants discussed this finding as a way to differentiate significant proliferative disease from normal mucosal epithelium turnover. Another helpful indicator of proliferative colitis is the relative paucity of goblet cells, as they are terminally differentiated cells and will not be present in newly regenerated epithelium. Chronic colitis of juvenile rhesus macaques differs from proliferative enteritides in other species in that severe ulceration and hematochezia, as well as the preneoplastic crypt mucosal dysplasia seen in the ulcerative diseases, are not present.

The spirochetes observed in some sections may be *Helicobacter cinaedi*, which has been associated with chronic colitis in a rhesus macaque, and has been shown to induce diarrhea and bacteremia in pigtail macaques.[3] There is superficial necrotizing colitis multifocally throughout this section, with neutrophilic and histiocytic inflammation, which is an indicator of active disease and is likely due to *Campylobacter jejuni* and *C. coli* overgrowth. These are usually seen in initial episodes, but *Campylobacter* and protozoans may be absent in subsequent episodes of the disease.[4]

Contributor: Oregon National Primate Research Center
Pathology Services Unit
Department of Animal Resources
505 NW 185th Avenue
Beaverton, OR 97006
http://onprc.ohsu.edu

References:

1. Alder RR, Moore PF, Scmucker DL, et al. Monographs on pathology of laboratory animals. In: Jones TC, Mohr U, Hunt RD, eds. *Nonhuman Primates II*. Berlin, Germany: Springer-Verlag;1993:81-86.
2. Blanchard JL, Baskin GB, Watson EA. Generalized amyloidosis in rhesus monkeys. *Vet Pathol*. 1986;23 (4):425-30.
3. Fox JG, et al. Isolation of *Helicobacter cinaedi* from the Colon, Liver, and Mesenteric Lymph Node of a Rhesus Monkey with Chronic Colitis and Hepatitis. *J Clin Microbiol.* 2001;39:1580-5.

4. Lewis AD, Colgin LMA. Pathology of noninfectious diseases of the laboratory primate. In: *The Laboratory Primate*. San Diego, CA: Elsevier; 2005:47–74.
5. McKenna P, Hoffmann C, Minkah N, et al. The macaque gut microbiome in health, lentiviral infection, and chronic enterocolitis. *PLoS Pathog*. 2008;4(2):e20.
6. Sonnenberg A, Melton SD, Genta RM, et al. Absence of focally enhanced gastritis in macaques with idiopathic colitis. *Inflamm Bowel Dis*. 2011;18. doi:10.1002/ibd.21696.

CASE IV: AFRRI Case 1 (JPC 4006476).

Signalment: 2-year-old spayed female domestic short hair cat.

History: On presentation the cat had a temperature of 105° F and was severely icteric.

Gross Pathology: Necropsy revealed minimal abdominal serocellular effusion, a pale swollen liver and shrunken, indented kidneys.

Laboratory Results:

Species	Breed	Sex	Pet Age	Reported
Feline	Domestic Short Hair	SF	1Y	4/23/11 1:51 PM

Test Requested	Results	Ref Range	Units
Superchem			
Total Protein	10.5 (HIGH)	5.2-8.8	g/dL
Albumin	LOW)	2.5-3.9	g/dL
Globulin	8.3 (HIGH)	2.3-5.3	g/dL
Albumin/ Globulin Ratio	0.3 (LOW)	0.35-1.5	Ratio
AST (SGOT)	44	10-100	U/L
ALT (SGPT)	52	10-100	U/L
Alk Phosphatase	51	6-102	U/L
GGTP	6	1-10	U/L
Total Bilirubin	0.5 (HIGH)	0.1-0.4	mg/dL
Urea Nitrogen	10 (LOW)	14-36	mg/dL
Creatinine	0.7	0.6-2.4	mg/dL
BUN/Creatinine Ratio	14	4-33	Ratio
Phosphorus	4.6	2.4-8.2	mg/dL
Glucose	110	64-170	mg/dL
Calcium	7.9 (LOW)	8.2-10.8	mg/dL
Magnesium	1.9	1.5-2.5	mEq/L
Sodium	142 (LOW)	145-158	mEq/L
Potassium	3.8	3.4-5.6	mEq/L
Na/K Ratio	37		
Chloride	111	104-128	mEq/L
Cholesterol	164	75-220	mg/dL
Triglycerides	77	25-160	mg/dL
Amylase	1017	100-1200	U/L
Lipase	42	0-205	U/L
CPK	157	56-529	U/L

CBC			
WBC	11.4	3.5-16.0	10^3/µL
RBC	6.77	5.92-9.93	10^6/µL
Hemoglobin	8.4 (LOW)	9.3-15.9	g/dL
Hematocrit	28.2 (LOW)	29-48	%
MCV	42	37-61	fL
MCH	12.4	11-21	pg
MCHC	29.8 (LOW)	30-38	g/dL
Platelet Count	139 (LOW)	200-500	10^3/µL
Platelet EST	Adequate	Adequate	

Platelet count reflects the minimum number due to platelet clumping.

Differential	Absolute	%	Ref Range	Units
Neutrophils	9348 (HIGH)	82	2500-8500	10^9/L
Bands	0	0	0-150	/µL
Lymphocytes	1596	14	1200-8000	
Monocytes	228	2	0-600	
Eosinophils	228	2	0-1000	
Basophils	0	0	0-150	

FeLV Antigen (ELISA)	Negative
FIV Antibody	**Positive**

Result verified.
May be due to infection, vaccination, or (in kittens) maternal antibody.

FCV (IFA)	
1:400	**Positive**
1:1600	**Positive**

A positive FCV titer indicates exposure to a coronavirus. It does not differentiate between FIP, feline enteric coronavirus exposure, or vaccination. Diagnosis of FIP should be based on history, physical examination, and other laboratory findings, including electrophoresis on effusions. FIP PCR testing on effusions, and/or FIP 7b ELISA testing on serum may be helpful in confirming FIP infection.

Toxoplasma IgG Antibody	Negative
Toxoplasma IgM Antibody	

**********FELINE**********

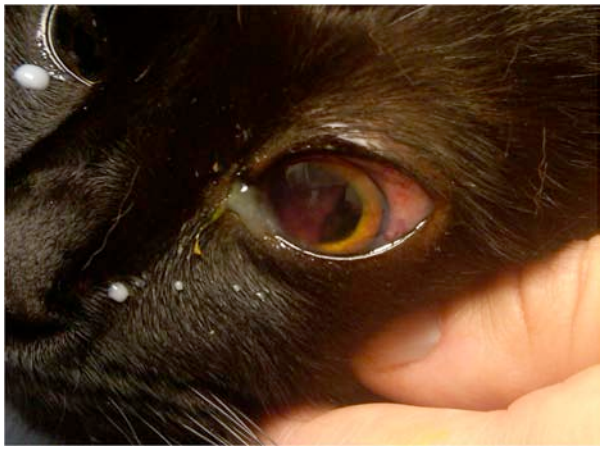

4-1. Eye, cat. The cat presented with anterior uveitis, hyphema, and a mucopurulent ocular discharge. Photograph courtesy of Armed Forces Radiobiology Research Institute, Bethesda, MD 20814-4712, http://www.usuhs.mil/afrri/.

IgM negative, IgG negative:
No serologic evidence of exposure to *Toxoplasma gondii*. However, some acutely infected cats are clinically ill prior to seroconversion. If clinical signs of toxoplasmosis are present, institute treatment and repeat serologic testing in 21 days to look for rising titers.

IgM 1:64 or greater, IgG negative or IgG 1:64 or greater:
Results are most consistent with recent exposure or active *Toxoplasma*
gondii infection. If clinical signs of Toxoplasmosis are present,

Urine Microalbumin (Feline)	Results	Ref Range	Units
Microalbuminuria	**12.2 (HIGH)**	**<2.5**	**mg/dL**

The MA is greater than 2.5 mg/dl and less than 30 mg/dl, indicating microalbuminuria.

institute treatment and repeat serologic testing in 21 days to look
for rising titers.

IgM>1:256, IgG negative or IgG 1:64 or greater:
Results are most consistent with active *Toxoplasma gondii* infection.

No serologic test documents clinical toxoplasmosis, but IgM titers >1:256 have almost exclusively been detected in clinically ill cats.

IgM negative, IgG 1:64 or greater:
Results are most consistent with chronic toxoplasmosis. However, IgM titers decrease rapidly in some infected cats. If clinical signs of Toxoplasmosis are present, institute treatment and repeat serologic testing in 21 days to look for rising titers.

Microalbuminuria (MA) usually indicates compromise of the glomerular barrier and is a significant finding when it is persistent (2 or more positive results obtained 2 or more weeks apart).

Persistent MA, in the majority of pets, is due to renal injury secondary to other systemic disease or primary renal disease. Systemic diseases associated with persistent MA include inflammatory disease, chronic infections, metabolic disease (e.g. hypertension, Cushing's Syndrome, diabetes mellitus, hyperthyroidism) and neoplasia. False positive results may occur with pyuria and gross hematuria. Suggestions for evaluating patients with microalbuminuria:

1. Check for and treat underlying diseases indicated above
2. Recheck MA in 2-4 weeks
3. In the absence of underlying disease, monitor for progression of MA and development of renal failure

Histopathologic Description: Eye and eyelid: Multifocal to coalescing, effacing and expanding 95%

Urinalysis	Results	Ref Range	Units
Collection Method	**Cystocentesis**		
Color	**Dark Yellow**		
Appearance	**Cloudy**	***Clear**	
Specific Gravity	**1.054**	**1.015-1.060**	
pH	**7.0**	**5.5-7.0**	
Protein	**2+ (HIGH)**	**Neg**	
Glucose	**Negative**	**Neg**	
Ketone	**Negative**	**Neg**	
Bilirubin	**2+ (HIGH)**	**Neg**	
Urine bilirubin verified by Ictotest.			
Blood	**Negative**	**Neg**	
WBC	**2-3**	**0-3**	**HPF**
RBC	**None**	**0-3**	**HPF**
Casts	**None Seen**		**LPF**
Struvite Crystals	**0-1**		**HPF**
Bacteria	**None Seen**	**None**	**HPF**
Squamous Epithelia	**0-1**	**0-3**	**HPF**

of the sclera and 75% of the ciliary body and iris are high numbers of neutrophils, macrophages, plasma cells and fewer lymphocytes, admixed with reactive fibroblasts, loose collagen, ectatic lymphatics with abundant pale eosinophilic proteinaceous material (edema), beaded to fibrillar material (fibrin), minimal hemorrhage and smaller amounts of eosinophilic cellular and karyorrhectic debris (necrosis). Frequently, histiocytes contain dark brown, intracytoplasmic pigment (melanin or hemosiderin). Frequently, throughout the affected tissue, the previously described inflammatory cells are centered upon and efface blood vessels. These are lined by reactive endothelium with frequent obliteration of the vascular wall (vasculitis). Expanding and filling the anterior chamber, posterior chamber and the vitreous is abundant previously described edema, fibrin, fewer inflammatory cells and moderate hemorrhage (hyphema). Diffusely the retina is detached and occasionally the underlying retinal pigment epithelial (RPE) cells are plump and individualized (hypertrophic or tombstoning), with occasional rupture of the RPE and extrusion of pyogranulomatous inflammation into the vitreous. The retina is diffusely disrupted by hemorrhage, fibrin and edema with segmental loss of ganglia, occasional fusion of the inner nuclear and outer nuclear layers, and mild infiltrates of the previously described inflammatory cells (retinitis). Multifocally, both the conjunctiva and orbital muscles

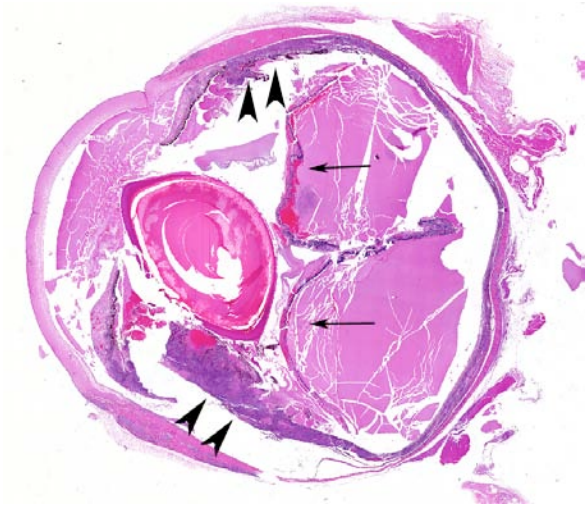

4-2. Eye, cat. A high-protein effusion fills the anterior and posterior segments, detaching the retina (arrows). There is a marked lymphoplasmacytic and histiocytic infiltrate within the uvea (arrowheads). (HE 63X)

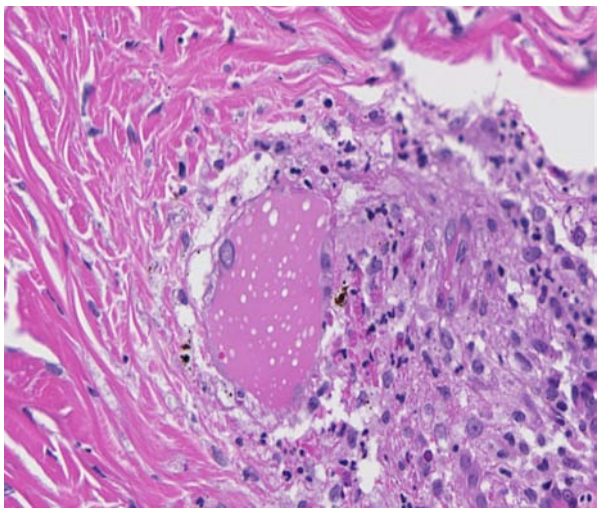

4-3. Eye, cat. Multifocally, areas of histiocytic and lymphoplasmacytic inflammation are centered on vessels. (HE 400X).

have perivascular infiltrates of lymphocytes, plasma cells, macrophages and neutrophils admixed with fibrin and edema. Multifocally, scattered rhabdomyocytes are undergoing degeneration; necrosis, characterized by contraction bands with hypereosinophilic fragmented sarcoplasm lacking cross-striations; or rarely are lost.

Contributor's Morphologic Diagnosis: Eye: Vasculitis, pyogranulomatous and lymphoplasmocytic, multifocal to coalescing, severe with hyphema, panuveitis, scleritis, retinal detachment, mild retinitis, and periocular, perivascular rhabodmyositis and conjunctivitis.

Contributor's Comment: This is a classic example of Feline Infectious Peritonitis Virus (FIP) affecting the eye of a cat. FIP is theorized to originate from mutated enteric coronavirus (FCoV) and can result in a systemic pyogranulomatous vasculitis dependant on the immune status of the affected animal. Feline coronavirus belongs to the family Coronaviridae of the order Nidovirales and, along with canine coronavirus and porcine transmissible gastroenteritis virus, are part of the group I coronaviruses.

While the genetic composition of the coronavirus affects the degree of virulence, the severity of disease is also directly linked to the genetic background of the affected animal. The literature describes a genetic predisposition which suggests that certain subsets of cats are at higher risk for clinical disease than other populations.[2] Evaluation of a large cohort of different cat breeds noted that Birman, Ragdoll, Bengal, Rex, Abyssinian, and Himalayan breeds may be predisposed.[1,8] Similar findings have been noted in cheetah populations which are at increased risk for FIP infection.[3,6,8]

Initial FIP viral replication occurs in the tonsils or intestinal tract, followed by incorporation into histiocytes and transmission to the regional lymph nodes where the virions replicate within macrophages, thereby disseminating the virus throughout the body. The severity of FIPV infection, once the virus is systemic, is determined by the host's immune response. A strong cell-mediated immune response can clear the infection and clinical feline infectious peritonitis will not develop; however, in cats with a poor cell-mediated immune response, antibodies develop which may facilitate macrophage uptake of virus and exacerbate the course of disease. Furthermore, the absence of CMI antigen-antibody complexes results in a type 3 hypersensitivity reaction with associated vasculitis and effusion into body cavities, to include the ocular chambers.[1,2,6]

While a variety of diagnostic modalities have been suggested, there is no gold standard for FIP diagnosis other than histopathology with accompanying immunohistochemistry.[3] However, CBC, blood chemistry, and serology can be highly suggestive of FIP infection and clinically ill cats with FIP may demonstrate the following abnormalities:

- Normocytic, normochromic, non-regenerative anemia
- Neutrophilic leukocytosis with lymphopenia, eosinopenia and monocytosis
- Hyperproteinemia with hyperglobulinemia
- Decreased Albumin:Globulin ratio (increased α2-, β- and γ-globulin concentrations)

Ocular pathology with panuveitis is a common finding with associated iridial changes in iris color, dyscoria or anisocoria secondary to iridocyclitis followed by a sudden loss of vision and clinically observable hyphema. Keratic precipitates colloquially known as 'mutton fat' deposits on the ventral corneal endothelium are reported. On ophthalmoscopic examination, chorioretinitis, fluffy perivascular cuffing (representing retinal vasculitis), dull perivascular puffy areas (pyogranulomatous chorio-retinitis), linear retinal detachment and fluid blistering under the retina may be observed and these findings mirror those seen microscopically.[1]

As a result of the unique anatomical and functional nature of the eye, pathology within one structure can have significant "bystander" effects on other tissues resulting in progressive destruction and a continuum of pathology from potential inflammation of one region, eventually progressing to complete destruction of the globe. Due to the probable type 3 hypersensitivity associated with the pathogenesis of FIPV in this case, with vasculitis concentrated in the uvea and the sclera, and the resultant effusion into the ocular chambers, the preferential morphological diagnosis defers to the vasculitis as the primary modifier and then identification of each ocular structure in turn affected by the progressive inflammatory process.

JPC Diagnosis: Eye: Panophthalmitis, lymphoplasmacytic and histiocytic, moderate to severe, with uveal vasculitis, anterior and posterior chamber effusions, and retinal detachment.

Conference Comment: Conference participants noted that some areas of the digitized slide were out of focus.

The diffuse uveitis associated with FIP is likely an immune-mediated reaction and, more specifically, a Type III hypersensitivity reaction. Type III hypersensitivity reactions result from the deposition of antigen-antibody complexes in vascular walls, serosa, and glomeruli and result in localized vasculitis from the activation of complement, the recruitment of neutrophils and monocytes, and subsequent damage from the liberation of free radicals and lysozymes. As the leukocyte adhesion cascade becomes activated, macrophages bind to the endothelium and release proinflammatory cytokines, resulting in an acute inflammatory response. Type III hypersensitivity occurs when there is a greater proportion of antigen to antibody, resulting in the formation of medium-sized immune complexes that do not fix complement and are not cleared from the circulation because macrophages are unable to bind them.[7]

Interestingly, FIP-induced ocular lesions are always bilateral. Although FIP typically results in pyogranulomatous inflammation of multiple organs, the inflammatory picture in the eye is unique. The anterior chamber is usually affected by a neutrophilic exudate, while lymphoplasmacytic inflammation is present in the uvea and choroid.[5] Also, in cats, there is no other known cause except FIP for the characteristic inflammation of the extra-ocular muscles combined with uveitis.

In this case, the drainage angle is open, which is to be expected in ocular FIP because the eye is one of the last organs to be infected in this disease, and the cat often dies of severe lesions elsewhere before there is time to develop glaucoma. There is also loss of the inner layers of the retina due to pressure necrosis from the exudate in the vitreous. The detachment of the retina is likely due to effusion in the choroid with leakage into the subretinal space, a process known as exudative retinal detachment.[5] Also present are collagen strands on the anterior surface of the iris, which represent pre-iridal fibrovascular membrane (rubeosis iridis in humans) formation. Pre-iridal fibrovascular membranes are initially composed of polymerized fibrin, hemorrhage, and high protein exudate in the anterior chamber, and are common in acute and chronic ophthalmitis in cats. Pre-iridal membranes originate as endothelial buds from the anterior iridal stroma and mature into fibrovascular membranes that can result in hyphema or glaucoma due to leaky interendothelial junctions of the new vessels resulting in occlusion of the filtration angle or the pupillary opening. This layer of granulation tissue then matures in typical fashion. Pre-iridal fibrovascular membranes are often difficult to identify due to the heavy pigmentation of the iris, and the severe concurrent inflammation that can accompany this phenomenon.[4]

Contributor: Armed Forces Radiobiology Research Institute
Veterinary Services Department
4301 Jones Bridge Road
Bethesda, MD 20814-4712
http://www.usuhs.mil/afrri/
Case Courtesy of Dr. Lynn Facemire

References:

1. Addie D, et al. Feline infectious peritonitis. ABCD guidelines on prevention and treatment. *J Feline Medicine and Surgery*. 2009;11(7):594-604.
2. Chang H, de Groot RJ, Egberink HF, et al. Feline infectious peritonitis: insights into feline coronavirus pathobiogenesis and epidemiology based on genetic analysis of the viral 3c gene. *Journal of General Virology*. 2010;91:415–420.
3. Diaz JV, Poma R. Diagnosis and clinical signs of feline infectious peritonitis in the central nervous system. *Can Vet J*. 2009;50(10):1091–1093.

4. Kumar V, Abbas AK, Fausto N, et al. Disease of the immune system. In: *Robbins and Cotran Pathologic Basis of Disease*. 8th ed. Philadelphia, PA: Saunders Elsevier; 2010:204-5.
5. Njaa BL, Wilcock BP. The eye and ear. In: Zachary JF, McGavin MD eds. *Pathologic Basis of Veterinary Disease*. 5th ed. St. Louis, MO: Elsevier Mosby; 2011:1208-1211, 1244.
6. Paltrinieri S, Grieco V, Comazzi S, et al. Laboratory profiles in cats with different pathological and immunohistochemical findings due to feline infectious peritonitis (FIP). *Journal of Feline Medicine and Surgery*. 2001;3:149–159.
7. Peiffer RL, Wilcock BP, Yin H. The Pathogenesis and Significance of Pre-iridal Fibrovascular Membrane in Domestic Animals. *Vet Pathol*. 1990;27(1):41-5.
8. Pesteanu-Somogyi LD, Radzai C, Pressler BM. Prevalence of feline infectious peritonitis in specific cat breeds. *J Feline Medicine and Surgery.* 2006;8:1-5.

Joint Pathology Center
Veterinary Pathology Services

WEDNESDAY SLIDE CONFERENCE 2011-2012

Conference 5

5 October 2011

CASE I: SDSU-2 (JPC 3105833).

Signalment: 12-month-old crossbred calf (*Bos taurus*).

History: Out of a group of 1200 from Canada, this was the 3rd calf to become ill and die after treatment. Calves were reported to be depressed and off feed and water. This calf presented to the field veterinarian "terminally ill in lateral recumbency" and was euthanized.

Gross Pathology: Necropsy findings noted by the field veterinarian included: esophagus contained non-hemorrhagic erosions. Small and large intestine contained multiple hemorrhagic ulcers.

Laboratory Results: Florescent antibody tests on lung, esophagus, and small intestine were positive for BVD virus. Cytopathic-BVD virus was isolated from lung and kidney. BVD ear notch ELISA test was positive on a fresh ear notch. Fecal flotation was negative for parasites.

Histopathologic Description: Within sections of small intestine, there is multifocal moderate to severe suppurative, mucohemorrhagic enteritis with attenuation and necrosis of crypt epithelium primarily confined to areas overlying Peyer's patches. Peyer's patches are severely depleted and their normal architecture has been destroyed; dilated crypts containing degenerate epithelial cell, neutrophils, mucous and hemorrhage are herniated into the submucosa previously occupied by Peyer's patches. Moderate infiltration of the lamina propria by lymphocytes and plasma cells is also present. Within mesenteric adipose tissue, there is mild accumulation of perivascular lymphocytes and plasma cells; vasculitis is not present.

Contributor's Morphologic Diagnosis: Small intestine: Enteritis, mucohemorrhagic, neutrophilic, acute to subacute, moderate to severe, with crypt epithelial necrosis and destruction of Peyer's patches due to BVD virus infection.

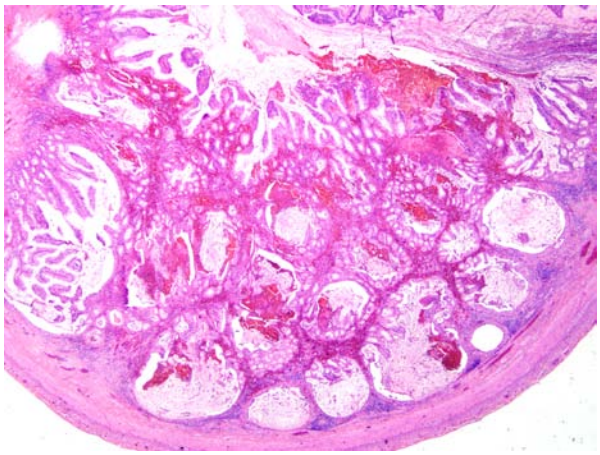

1-1. Small intestine, cow. Peyer's patches have collapsed with herniation of intestinal villi through the submucosa. The intestinal lumen is filled with mucin, cellular debris, and hemorrhage. (HE 20X)

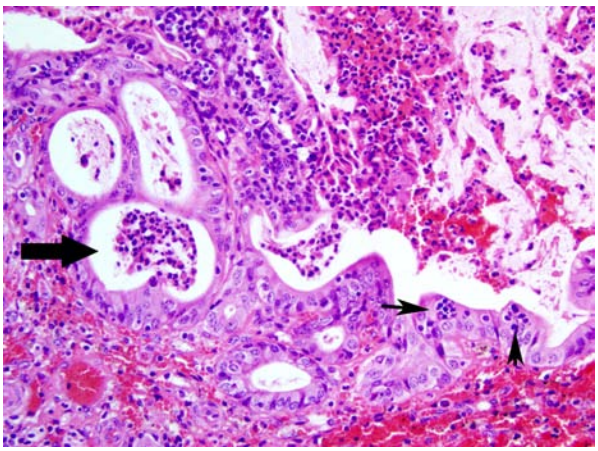

1-2. Small intestine, cow. Villi are markedly shortened and denuded of epithelium. Intestinal crypts are widely dilated, lined by attenuated epithelium and filled with degenerate neutrophils, necrotic epithelium, and cell debris (crypt abscesses). Multifocally mucosal epithelium is infiltrated by clusters of lymphocyte and neutrophils. (HE 200X)

Contributor's Comment: BVD virus is an RNA virus belonging to the genus *Pestivirus*. Infection of pregnant cattle can result in fetal abortion or birth of persistently-infected (PI) calves. PI calves typically are unthrifty and do not live beyond 2 years of age. PI calves can succumb to fatal mucosal disease if infected with cytopathic BVD virus (mutation of non-cytopathic BVD virus can also cause mucosal disease in these PI calves).[1]

Infection of healthy, immunocompetent, non-pregnant cattle by BVD virus usually results in only subclinical to mild clinical disease; however, primary infection by very virulent strains of BVD virus can result in severe clinical disease with mortality which cannot be differentiated from mucosal disease by clinical signs and necropsy findings.[1]

In this particular case, it is uncertain whether this calf was persistently infected and died as a result of mucosal disease, or if this was a healthy calf which became infected by a particularly virulent strain of BVD virus. The low morbidity, high mortality of the group suggests this was a PI calf, which died of fatal mucosal disease. Molecular characterization of the isolated virus may have aided in the differentiation of these two syndromes.

JPC Diagnosis: Small intestine: Enteritis, necrotizing, diffuse, moderate with focally extensive Peyer's patch necrosis and crypt herniation.

Conference Comment: Bovine viral diarrhea (BVD) is an acute, highly contagious disease of cattle with worldwide distribution that results in enteric disease, respiratory disease and reproductive loss. BVD virus can also infect sheep, goats and pigs and has been isolated in many wild and captive African species. BVD is separated into two biotypes, cytopathic (CP) and noncytopathic (NCP), based on cytopathic effects in vitro, and separated into two genotypes based on antigenic variation. NCP strains are associated with acute bovine virus diarrhea, BVD-induced thrombocytopenia, abortions, and are teratogenic, and CP strains produce mucosal disease. BVD is immunosuppressive and predisposes animals to secondary infections.[1,2]

Virus is shed in body fluids, and primary replication occurs in the tonsils and oropharyngeal lymphoid tissues. Virus then enters circulating monocytes and is transported to lymphoid tissues and the subepithelial connective tissue of the dermis and GI tract, where it spreads locally to overlying epithelial cells. In addition to the subclinical form in immunocompetent adults as mentioned by the contributor, BVD manifests in two other forms. Transplacental infections during days 50-100 of gestation result in fetal death, abortion, or mummification; infection at day 100-150 of gestation results in congenital defects such as microencephaly, cerebellar hypoplasia, hydranencephaly, hydrocephalus, microphthalmia, thymic aplasia, hypotrichosis, alopecia, brachygnathism, growth retardation, and pulmonary hypoplasia. If a calf survives infection prior to 125 days of gestation, it may develop immunotolerance and lifelong, subclinical infection, which is the most pervasive source of infection of other cattle. A second form is mucosal disease, which occurs when a calf is infected with a noncytopathic genotype prior to 125 days of gestation and becomes immunotolerant, and is then infected with a cytopathic strain. Mortality in calves with mucosal disease approaches 100%.[1,2,3]

Gross lesions with subclinical BVD are seen as mild erosions or shallow ulcerations of the oral cavity. Mucosal disease manifests with erosions and ulcerations of mouth, tongue, esophagus, oral and ruminal papillae, abomasum, cecum, and colon; linear esophageal ulcerations ("tiger-stripe"); swollen, necrohemorrhagic Peyer's patches with diphtheritic membranes; and erosive or ulcerative interdigital dermatitis and coronitis. The virus causes widespread vasculitis, epithelial necrosis, and lymphocytolysis.[1,2,3]

Contributor: South Dakota State University
Animal Disease Research and Diagnostic Laboratory
Brookings, SD 57007
http://vetsci.sdstate.edu

References:

1. Brown CC, Baker DC, Barker IK. Alimentary system. In: Maxie MG, ed. *Jubb, Kennedy, and Palmer's Pathology of Domestic Animals*. 5th ed. Edinburgh, Scotland: Saunders Elsevier; 2007:140-8.

2. Gelberg HB. Alimentary system and the peritoneum, omentum, mesentery, and peritoneal cavity. In: McGavin MD, Zachary JF, eds. *Pathologic Basis of Veterinary Disease*. 5th ed. St. Louis, MO: Mosby Elsevier; 2011:384.
3. Zachary JF. Mechanisms of microbial infections. In: McGavin MD, Zachary JF, eds. *Pathologic Basis of Veterinary Disease*. 5th ed. St. Louis, MO: Mosby Elsevier; 2011:206-7.

CASE II: 10L-0087 (JPC 3170668).

Signalment: 2-year-old male Thoroughbred horse (*Equus caballus*).

History: The colt initially presented with a short-term history of recurrent diarrhea and mild colic episodes. The animal had been losing weight for one month, appeared depressed and had a mildly elevated body temperature of 39°C. After initial treatment (prednisolone, worming with fenbendazole) but progressive deterioration it was referred. At referral it presented dull and depressed with a heart rate of 72bpm, a weak pulse, congested mucous membranes and normal gut sounds on auscultation. Rectal examination revealed a large fluid filled colon. Despite extensive fluid therapy the animal became acidotic (pH 7.21), hypoglycemic and failed to respond adequately to potassium supplementation and glucose/ insulin administration. The colt subsequently developed PU/PD, showed mild colic signs, which failed to respond to fluxinin and was euthanized two days after admission.

Gross Pathology: The animal was in good to moderate body condition with mild reduction of subcutaneous and mesenteric adipose tissue. Apart from mild ascites (1 litre), the cecum and colon were moderately filled with watery to viscous brown-green digesta and exhibited moderate to focally severe mucosal acute hemorrhages. Within the mucosa were large numbers of dark red to brown, 1 mm to 5 mm diameter, partly raised, centrally convex nodules containing small metazoan parasites (nematodes). Very few, red ~ 1 cm long nematodes were observed within the large intestinal content. A mild activation of cecal and colonic mesenteric lymph nodes was present.

Laboratory Results (clinical pathology, microbiology, PCR, ELISA, etc.)**:**
Clinical pathology:

PCV	48%
TP	56g/l
Albumin	21g/l
Globulin	35g/l
WBC	14.10 x 10^9
Lymphocytes	11%
Neutrophils	86%
Na	111 (126-146) mmol/l
K	1.2 (3.0-5.0) mmol/l

2-1. Colon, horse. The colon is filled with watery, brown ingesta. Similar fluid was seen in the cecum. Photograph courtesy of Veterinary Pathology, University of Liverpool, www.liv.ac.uk

2-2. Colon, horse. Numerous 1 mm to 5 mm dark red nodules containing small nematodes are present within the colonic mucosa. Photograph courtesy of Veterinary Pathology, University of Liverpool, www.liv.ac.uk

Parasitology: Colonic content was subjected to a parasitological worm egg screen examination. No eggs were detected.

Histopathologic Description: Colon, mucosa: There is focal erosion and ulceration of villus tips; enterocytes exhibit a mild goblet cell hyperplasia. Multifocally enterocytes contain 20-60 µm large, basophilic, PAS negative fine granular intracytoplasmic structures (goblet cell hyperplasia/ apicomplexan protozoa?). The lamina propria contains moderate to large numbers of metazoan parasites (nematode larval stages) consistent with small strongylid larvae.

Smallest larvae are 20 µm in diameter, up to 100 µm long and crescent shaped with pointed tail tips (L_3) with mild peripheral histiocytic infiltration. Fewer L_3 stages exhibit very mild or no inflammatory reaction (hypobiotic early third larval stages, EL_3).

A population of further matured up to 100 µm diameter nematode larvae with an eosinophilic, thick, smooth cuticle, vacuolated lateral cords, prominent

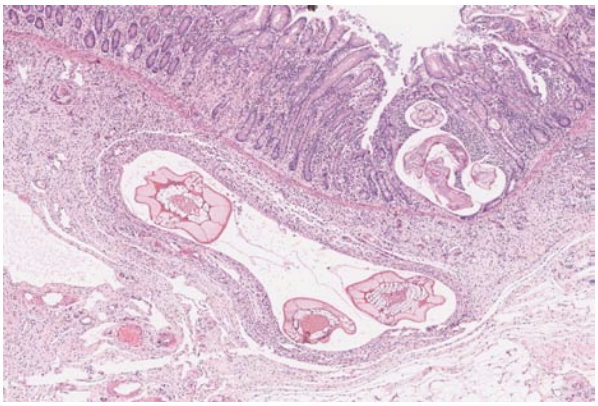

2-3. Colon, horse. Mucosal epithelium is eroded and there are numerous cyathostome larva of varying maturity within the lamina propria as well as the submucosa. (HE 40X)

platymyarian musculature and intestinal as well as genital tract is observed throughout the lamina propria mucosae (L_4). The intestine often exhibits prominent brush borders and these stages multifocally contain large amounts of dark red to dark brown pigment (iron pigment). The inflammatory response ranges from an acute, densely cellular neutrophilic and partly eosinophilic cuffing (emerging larvae?), to a capsule-like formation composed of macrophages and fibroblasts.

Few migrating L_4 stage larvae (not present in all sections) associated with superficial epithelial erosion and ulceration, acute haemorrhage and mild to moderate neutrophilic and eosinophilic infiltration is observed.

A mild to moderate diffuse infiltration by lymphocytes, plasma cells, lesser histiocytes and neutrophils and focal acute hemorrhages and few crypts containing cellular debris as well as neutrophils (crypt abscesses) is present in the mucosa.

Submucosa: Parasitic nematodes within the submucosa are much larger, 200 µm in diameter, with nematode specific external and nematode intestinal structures often containing erythrocytes, indicating blood uptake. A moderately dense histiocytic infiltration admixed with proliferating fibroblasts is surrounding the majority of these stages. The submucosa is generally expanded by clear spaces (moderate edema) as well as a multifocal to confluent mixed cellular (lymphocytes, plasma cells, macrophages, lesser neutrophils and occasional eosinophils) infiltrate.

Contributor's Morphologic Diagnosis: Moderate chronic ulcerative and hemorrhagic mixed cellular (histiocytic, lymphoplasmacellular, neutrophilic and eosinophilic) colitis with parasitic granuloma formation with intralesional, partly encapsulated nematode larval stages ($L_{3/4}$), consistent with small strongyles, "larval cyathostominosis", Thoroughbred horse (*Equus caballus*).

Contributor's Comment: Small strongyles (*Nematoda*, *Strongylida*), also known as cyathostomins, are extremely prevalent amongst the equine population worldwide and constitute frequent and highly pathogenic invaders of horses today.[5] Though horses can carry large worm burdens without displaying clinically significant symptoms, the clinical syndrome of larval cyathostominosis (cyathostomiasis), which occurs as a result of mass emergence of hypobiotic intestinal stages, can be associated with high fatality rates.[9]

More than 50 nematode species from subfamilies of *Cyathostominae* (~44 species), *Strongylinae* (minimum 11 species), and *Gyalocephalinae*, popularly known as trichonemes, cyathostomes or cyathostomins are embraced by the group 'small strongyles'.[10] Small strongyles range from 0.4 to 1.5 cm length in male animals and 0.5 to 2.0 cm length in female animals and are overall smaller than large strongyles, although some species may reach 2 cm to 3 cm in length.[9] Adults of some species inhabit the cecum or dorsal and ventral colon, with others inhabiting just one of these intestinal compartments. Adult small strongyles feed on enterocytes / enterocytic cellular debris or penetrate the epithelial barrier, open small vessels and digest blood.

In consistency with large strongyles, small strongyles have a direct life cycle with no intermediate hosts. Eggs are passed through the feces onto pasture. Depending on environmental conditions, eggs may hatch and develop from the first stage larvae (L_1) to infectious L_3 stages in as few as three days. Once ingested by the equine host, they continue to mature, and, in a rapid life cycle, new eggs may be passed onto the pasture in as few as 5-6 weeks. Larval development of most species takes place entirely in the mucosa of the cecum and colon, but few penetrate the muscularis mucosae and develop within the submucosa.[3]

In the present case, large nematode larvae containing ingested erythrocytes were observed in the submucosa. Due to their size and ingestion of blood, larval migration of large strongyle species has to be considered. It has been shown that L_3 of large strongyle species exsheath in the small intestine and penetrate the mucosa and submucosa of the small intestine, caecum and colon within 1–3 days where they moult to the fourth stage larvae (L_4) by about day 7.[4] Larval stages of different small and/or large

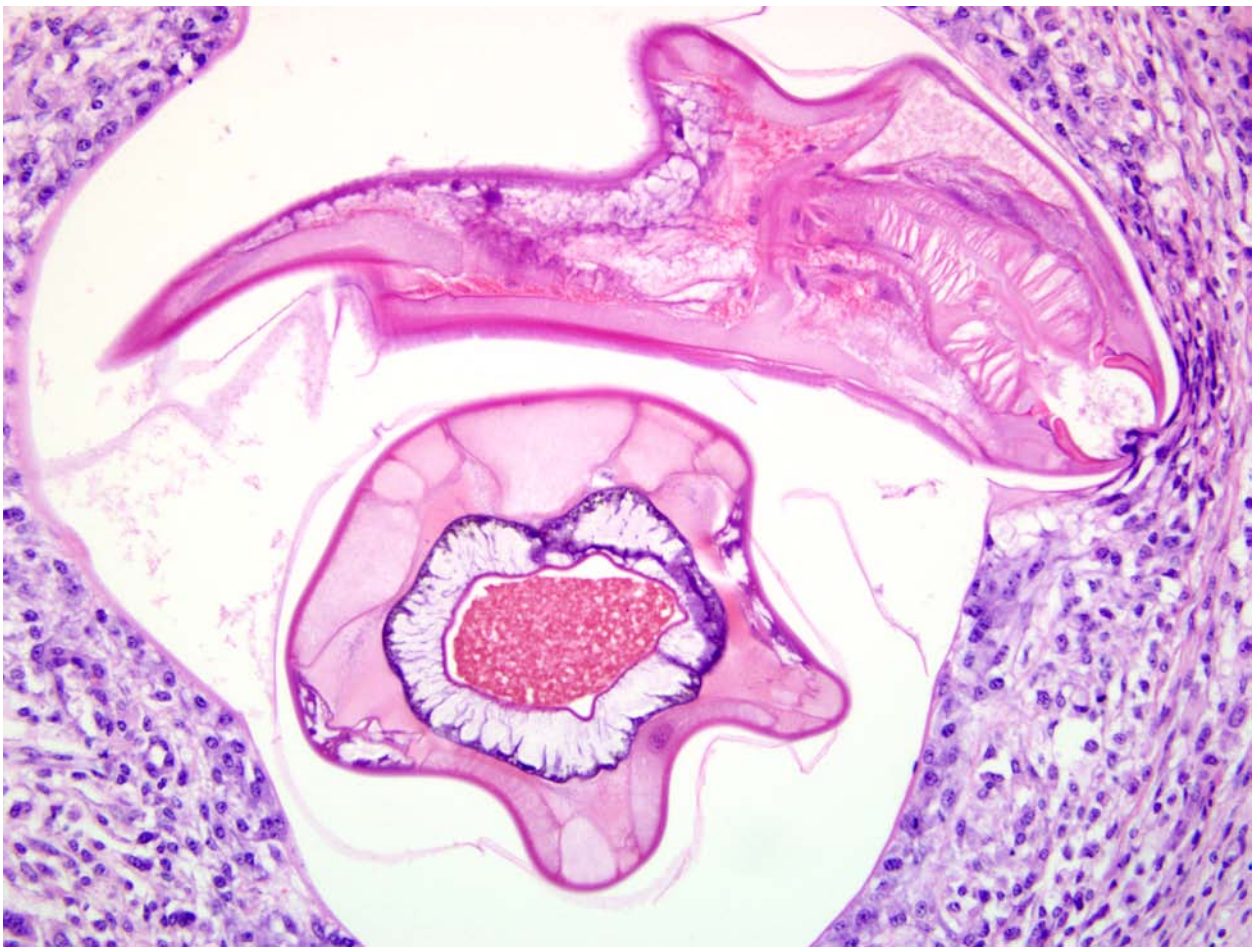

2-4. Colon, horse. Mature (L4) larval cyathostomes have an eosinophilic cuticle, vacuolated lateral chords, and a digestive tract containing blood. In longitudinal section (above) the chitinized buccal cavity and muscular esophagus are prominent. (HE 400X)

strongyle species are not distinguishable histologically and therefore, co-infection cannot be ruled out.

The entry of small strongyle larvae into tubular gland lumina generally provokes a chronic inflammatory response and marked goblet cell hyperplasia. Emergence of L_4 can be associated with an acute eosinophilic infiltration. Cyathostomins differ from other worm species in that the maturation of early third stage larvae (EL_3) can be arrested for prolonged periods of time (hypobiosis). After ingestion, L_3 exsheath and invade the large intestinal mucosa. Here, larvae protect themselves by becoming encysted and the host generally only reacts with a minimal inflammatory response to those stages. Up to 90% of an equine worm burden may become hypobiotic and EL_3 stages can remain within the intestinal walls for 4 months up to as long as 2 years.[3]

The majority of clinical signs associated with heavy infections in horses up to 2-3 years of age are unthriftiness, anemia and sometimes diarrhea. A typical clinical picture can include neutrophilia, hypoalbuminemia, hyperglobulinemia, low total serum protein as well as slightly high total protein, possibly due to dehydration, findings most consistent with protein-losing enteropathy.[7] Marked clinical signs are less common in older animals, though protective immunity never develops. However, the most significant damage can arise from simultaneous mass emergence of encysted L_4 larvae ('larval cyathosominosis') continuing their development to the adult stage in the intestinal lumen. Catarrhal and/ or hemorrhagic enteritis with severe diarrhea, potentially serious colic, leading to emaciation and in some cases death (mortality rate up to 50%) can be caused by severe damage to the gut wall. The climate is responsible for the occurrence of hypobiotic stages. In temperate climates larvae will accumulate during grazing season, encyst during the cooler months and re-emergence may occur en-masse as spring sets in. Reversed timing is observed in tropical climates where larval hypobiosis generally occurs during hot, stressful summer months with larval emergence in autumn.[1,7]

The antemortem diagnosis of larval cyathostominosis can, due to presentation of nonspecific clinical signs, be challenging. Depending on clinical findings, a variety of gastrointestinal diseases (e.g. salmonellosis, nonsteroidal anti-inflammatory drug-induced colitis, intestinal lymphosarcoma, inflammatory bowel disease, infections with *Lawsonia intracellularis* or *Clostridium* spp.) as well as other causes of ill-thrift and hypoproteinemia in nondiarrheic animals (e.g. renal disease, peritonitis, malnutrition) have to be considered as differential diagnoses.[8] Diagnosis in the live horse can be attempted by the fecal flotation method. However, this method can be unreliable because of variation in larval survival rates under certain culture conditions, is time-consuming and labor intensive and can be falsely negative or low because of the absence or paucity of adult nematodes. Therefore, definitive antemortem diagnosis is often not possible.

However, a presumptive diagnosis can be made based on signalment, clinical signs and exclusion of other possible causes. Post mortem diagnosis generally reveals strongly indicative findings. Additionally, transillumination is an easily employable method to detect intramucosal larvae and provides a fast and definitive diagnosis. Recently, investigations into internal transcribed and intergenic spacers of nuclear rDNA have been undertaken and these markers have proven to be useful for the identification of *Strongylinae* and *Cyathostominae* species. Importantly, the PCR-based methods developed using these markers can be sensitive and specific for diagnosis, and therefore might, via the detection of parasitic DNA extracted from intestinal biopsies, provide a useful diagnostic tool for *intra vitam* diagnosis of larval cyathostominosis.[4,6]

JPC Diagnosis: Colon: Colitis, granulomatous, with numerous mucosal and submucosal L_3 and L_4 stage larvae.

Conference Comment: The contributor mentioned large PAS-negative cells in the mucosal epithelium which contain fine intracytoplasmic granules. Conference participants attributed this to goblet cell hyperplasia. When we repeated the PAS stain at our institute, the cytoplasm of some of these cells was PAS positive, consistent with goblet cells. Conference participants also noted intimal bodies - irregular mineralized masses covered by endothelium which protrude into the lumen of small arteries and arterioles of horses, especially in the intestinal submucosa. These are considered to be normal findings.

The moderator discussed the importance of careful preparation and examination of the luminal surface of the affected intestine, because the characteristic gross appearance of cyathostomiasis with multiple red to black pinpoint nodules diffusely covering the mucosa can easily be missed if the digesta or feces is not carefully washed from the mucosal surface. Also, the mucosa and submucosa become very edematous and congested but not hemorrhagic, and will easily tear if palpated carelessly.

The process of massive emergence of hypobiotic larvae causing disease in otherwise clinically normal horses is similar to the phenomenon in cattle with "type II" disease as a result of *Ostertagia* spp. Ostertagiosis is the most important parasitic disease in grazing cattle and sheep in temperate climates, resulting in production loss and death. Lesions include severe abomasal mucous metaplasia, epithelial hyperplasia, and interstitial inflammation. This results in abomasal alkalosis, edema, and significant protein loss.[2]

Contributor: University of Liverpool
Veterinary Pathology
Crown Street
Liverpool
L69 7ZJ
www.liv.ac.uk

References:

1. Baudena MA, Chapman MR, French DD, et al. Seasonal development and survival of equine cyathostome larvae on pasture in south Louisiana. *Vet Parasitol.* 2000;88:51-60.
2. Brown CC, Baker DC, Barker IK. Alimentary system. In: Maxie MG, ed. *Jubb, Kennedy, and Palmer's Pathology of Domestic Animals*. 5th ed. Edinburgh, Scotland: Saunders Elsevier; 2007:233-4, 248-9.
3. Corning S. Equine cyathostomins: a review of biology, clinical significance and therapy. *Parasit Vectors*. 2009;2 (Suppl 2): S1.
4. Gasser RB, Hung GC, Chilton NB, et al. Advances in developing molecular-diagnostic tools for strongyloid nematodes of equids: fundamental and applied implications. *Mol Cell Probes.* 2004;18:3-16.
5. Lyons ET, Tolliver SC, Drudge JH. Historical perspective of cyathostomes: prevalence, treatment and control programs. *Vet Parasitol*. 1999;85: 97-111; discussion 111-112, 215-125.
6. Matthews JB, Johnson DR, Lazari O, et al. Identification of a LIM domain-containing gene in the Cyathostominae. *Vet Parasitol*. 2008;154:82-93.
7. McWilliam HEG, Nisbet AJ, Dowdall SMJ, et al. Identification and characterisation of an immunodiagnostic marker for cyathostomin developing stage larvae. *International Journal for Parasitology.* 2009;40:265-275.
8. Peregrine AS, McEwen B, Bienzle D, et al. Larval cyathostominosis in horses in Ontario: an emerging disease? *Can Vet J.* 2006;47:80-82.

9. Rommel M, Eckert J, Kutzer E, et al. Parasitosen der Einhufer. In: Buchverlag P, ed. *Veterinaermedizinische Parasitologie*. Berlin, Germany: Blackwell; 2000:367-395.
10. Taylor MA, Coop RL, Wall RL. Parasites of horses. In: *Veterinary Pathology*. 3rd ed. Hong-Kong: Wiley-Blackwell; 2007:272-273.

CASE III: SL-10-1298 (JPC 4002887).

Signalment: One male and one female, eight-month-old Holstein calves (*Bos taurus*).

History: Out of this herd of 100 animals, 25 are sick, and seven have died. Clinical signs include sudden onset of respiratory disease characterized by open mouth breathing and recumbency that occurred over a period of 24 hours. The affected animals all share a common feed bunk.

Gross Pathology: None provided.

Laboratory Results: PCR detected bovine respiratory syncytial virus RNA in pooled samples of lung. General bacterial cultures from each animal obtained many colonies of *Mannheimia hemolytica*.

Histopathologic Description: Lung: There is multifocal, segmental necrosis of bronchiolar epithelium and multifocal fibrinosuppurative bronchopneumonia. Multifocally affecting bronchioles is segmental to complete necrosis of bronchiolar epithelium with formation of respiratory epithelial syncytia. The syncytia are closely associated with the airway surface, present within the bronchiolar lumina, or occasionally found within adjacent alveoli. The syncytia rarely contain 5-8 micron in diameter, homogeneous, eosinophilic intracytoplasmic inclusion bodies. Airways contain sloughed cells and abundant necrotic cellular debris.

Affecting the pulmonary parenchyma is multifocal to coalescing, fibrinous and necrotizing bronchopneumonia. Alveoli contain variable amounts of viable and degenerate neutrophils, round "oat cells" with streaming nuclear contents, mats of fibrin, eosinophilic proteinaceous edema fluid, and intact alveolar macrophages. Occasional colonies of small coccobacilli are admixed with necrotic debris within alveoli. Alveolar septa are markedly expanded by fibrin, edema, and neutrophils. There are rare fibrin thrombi. The pleura and interlobular septa are markedly expanded by fibrin, edema, and suppurative infiltrates. Mats of fibrin, degenerate cellular debris, and viable and degenerate neutrophils line the pleural surface.

Contributor's Morphologic Diagnosis: Lung: 1) Marked, multifocal to coalescing, fibrinosuppurative bronchopneumonia.
Lung: 2) Marked, multifocal, necrotizing bronchiolitis with intralesional syncytia.

Contributor's Comment: Bovine respiratory disease complex (BRD), also known as shipping fever, is a common disease process in feedlot cattle and of major economic importance in North America. BRD is an infectious respiratory disease caused by numerous viral and bacterial agents. Viral agents include bovine herpes virus-1, bovine viral diarrhea virus, bovine respiratory syncytial virus (BRSV), and bovine parainfluenza virus-3 (PI-3), and are considered key elements in the pathogenesis of BRD.[7] Bacterial pathogens contributing to BRD include *Mannheimia haemolytica*, *Pasteurella multocida*, *Histophilus somni*, and *Mycoplasma bovis*.[7] *M. haemolytica* is considered to be the predominant bacterial pathogen associated with this disease complex, and it plays a more significant role in adult dairy cattle than in dairy calves.[6]

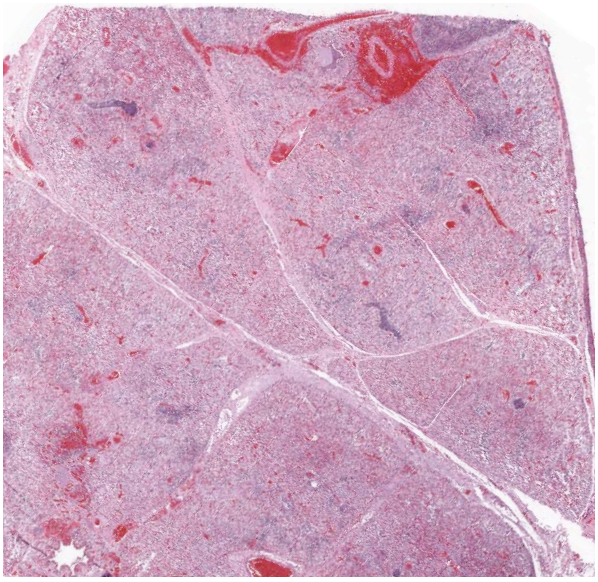

3-1. Lung, cow. At low magnification, there is marked lobular consolidation, outlines of airways with necrotic cellular debris, and expansion of interlobular septa with edema and emphysema. (HE 63X)

The classic presentation of BRD in beef animals is pneumonia affecting multiple calves three days to three weeks after shipment from the farm of origin to the feedlot.[5] Risk factors in this group include: mixing of naïve calves from various sources; stress due to weaning, transport, crowding, handling, vaccination, dehorning, and food/water deprivation; metabolic acidosis due to diet change; and exposure to adverse or rapidly changing environmental conditions. In one-to-four-month-old dairy and veal calves, cases may be sporadic, enzootic, or epizootic.[5] In this group, risk factors include: poor air quality due to indoor housing, crowding, poor ventilation, and high humidity; reduced defenses due to failure of passive transfer of immunoglobulin; exposure to viral or other pathogens from co-housing with adults; and stress due to concurrent diseases or weaning.[5,6] Clinical signs include depression, pyrexia, tachypnea, dyspnea, and anorexia. While animals may respond to early antimicrobial therapy, relapse is common.[5]

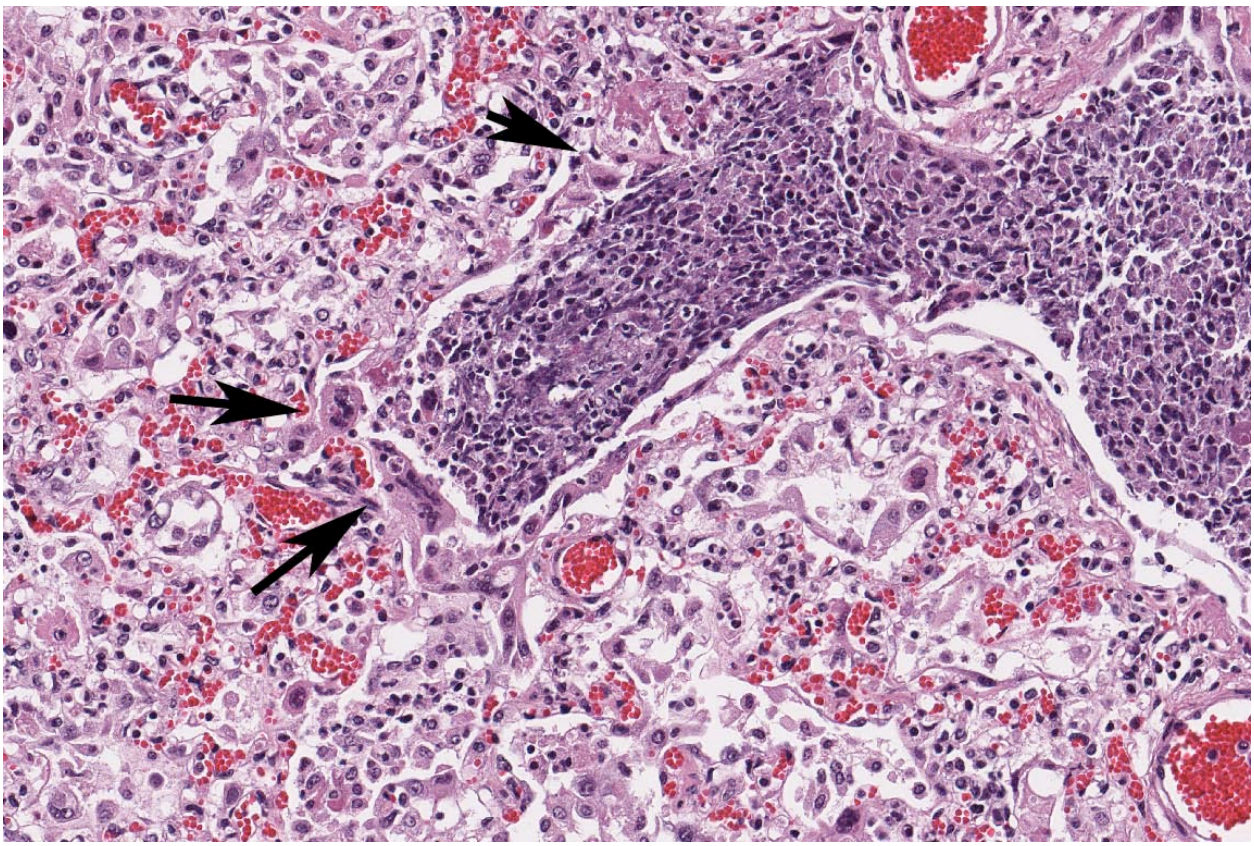

3.2. Lung, cow. Airways are filled with necrotic cellular debris. Alveolar walls are markedly thickened and alveolar lumens contain a fibrinocellular exudate with numerous macrophages and neutrophils. There are numerous multinucleated viral syncytia within remaining airway epithelium.

This case includes lung from one of two submitted eight-month-old Holstein calves that demonstrated open mouth breathing and acute onset of respiratory disease. The histologic features are consistent with a viral and bacterial etiology. Differentials for the bronchiolar epithelial necrosis and epithelial syncytia formation included BRSV and PI-3. Polymerase chain reaction detected BRSV nucleoprotein. The severe fibrinosuppurative bronchopneumonia, coagulative necrosis, and leukocyte necrosis ("oat cells") is suspicious for *Mannheimia haemolytica* or *Histophilus somni*. Many colonies of *M. haemolytica* were obtained via general bacterial cultures of lung.

Bovine respiratory syncytial virus (BRSV) is of the genus Pneumovirus in the family Paramyxoviridae. It is a major cause of respiratory disease and a major contributor to BRD.[1] The infection is common in North America and Europe, within both beef and dairy operations. The seroprevalence of BRSV in adult dairy and beef cattle ranges from 40-95%.[1,2] BRSV is an important cause of respiratory disease in two-week to five-month-old beef and dairy calves, and epidemics involving adult cattle have been reported.[3]

The severity of disease caused by BRSV depends on the age and immune status of the calf, route of infection, and strain of the virus.[3] Aerosol spread is the most common route of infection. The virus replicates in the epithelial cells of the upper respiratory tract, including the nasal cavity, pharynx, trachea, bronchi and bronchioli, and type II pneumocytes and alveolar macrophages. Significant effects include loss of cilia, necrosis of bronchial and bronchiolar epithelial cells, and depressed opsonization and phagocytosis by alveolar macrophages.[3] While specific serum and mucosal antibody responses occur in response to BRSV, the antibody is nonneutralizing and serum titers are poorly correlated with protection from disease.[2] A biphasic clinical course that is observed in some natural infections may represent a worsening of the disease following an immune response; however, the enhancement of the disease process by the immune system is controversial.[2] Viral shedding following experimental infection of naïve calves occurs between two and eight days post-infection. Viral antigen is most abundant in the cranioventral lung.

Most BRSV infections are subclinical. Mildly to severely affected dairy calves may demonstrate fever, cough, nasal/oral/ocular discharge, and tachypnea.[3] Severely affected animals may exhibit severe respiratory distress, including dyspnea, forced grunting upon expiration, and increased abdominal effort.

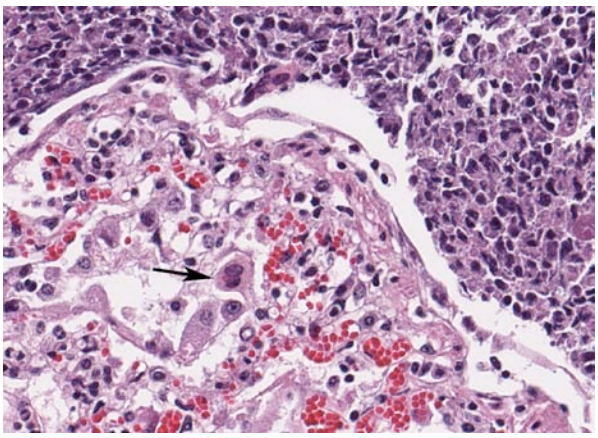

3-3. Lung, cow. Airways are filled with necrotic cellular debris, and remaining epithelium is flattened and attenuated. A multinucleated viral syncytia contains a prominent round eosinophilic viral inclusion (arrow). (HE 200X)

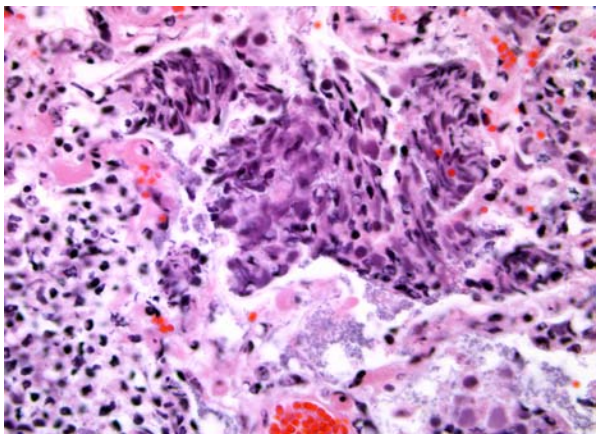

3-4. Areas of necrosis contain many degenerate neutrophils with streaming, often smudgy nuclei (oat cells). Numerous colonies of coccobacilli are admixed with necrotic cellular debris. (HE 400X)

Gross findings of BRSV infections differ between cranial and caudal portions of lung. The cranioventral lung is grossly deep red to mottled, atelectatic, collapsed, and rubbery in texture.[1,2] The caudodorsal lung may be heavy, edematous, or more firm than normal, with or without emphysema.[1,2] These gross lesions are widely variable, and may vary with concurrent bacterial bronchopneumonia. Lesions in other organs are not usually observed.[2]

Histologically, BRSV is characterized by necrotizing bronchiolitis, formation of bronchiolar epithelial syncytia, and exudative or proliferative alveolitis; these lesions are due to the cytopathic effects of the virus on epithelium, as previously described. Bronchioles are lined by attenuated epithelium, and multinucleated syncytial cells are frequently closely associated with these areas or found free in the lumina. Occasionally, alveoli may contain syncytia.[2] Bronchioles contain necrotic epithelial cells and neutrophils, and alveoli contain neutrophils and macrophages. Hyaline membranes may occur but are infrequent.[1,2] Intracytoplasmic eosinophilic inclusion bodies are occasionally present in syncytial cells.[2]

Differential diagnoses include bovine parainfluenza virus-3 (PI3) infection. In both diseases, syncytia with intracytoplasmic inclusion bodies occur. Generally, PI3 is associated with fewer syncytia located within the alveoli. Ancillary diagnostics are usually necessary for definitive diagnosis of BRSV, due to the confounding nature of multiple pathogens in the bovine respiratory disease complex. Diagnosis may be confirmed using fluorescent antibody tests, immunohistochemistry, antigen-detecting ELISA, or real time reverse transcriptase PCR(qRT-PCR).[1,2] qRT-PCR is considered the gold standard, based on its speed and sensitivity.[1]

Mannheimia haemolytica is a member of the Pasteurellaceae family. *M. haemolytica* is a small gram-negative coccobacillus that exists in the upper respiratory tract of healthy ruminants, primarily within the nasopharynx and tonsillar crypts.[4,5] Twelve serotypes exist, and serotypes A1 and A5 are known to colonize the upper respiratory tract of cattle and sheep as part of the normal commensal flora4. Serotype A1 quickly becomes the predominant organism once the commensal relationship is disrupted, and this serotype is also frequently isolated from pneumonic tissue.[4,5] Stress, exposure to cold, and concurrent viral illness and decreases in lung defenses are possible causes for the shift from a commensal relationship to pathologic one. The host response to the infection is the primary cause of clinical disease.[5] Virulence factors include leukotoxin, lipopolysaccharide, capsular polysaccharide, transferring-binding proteins A and B, O-sialogylcoprotease, neuraminidase, IgG1-specific protease, outer membrane proteins, and fimbriae.[5] These virulence factors allow *M. haemolytica* to evade clearance, avoid host defenses, and impair leukocyte function.[4,5] The result is massive recruitment of neutrophils into alveoli that are ineffective at killing bacteria but cause significant endothelial damage to capillaries and small vessels resulting in vascular leakage of protein, fluid, and fibrin into alveolar and interstitial spaces.[4,5,8]

Gross lesions caused by *M. haemolytica* include cranioventral lobar or lobular fibrinous bronchopneumonia, foci of coagulative necrosis, and variable fibrinous pleuritis.[5] Variable amounts of straw-colored thoracic fluid may be present.[4] On cut surface, the lung may be described as "meaty," being dark purple to red, heavy, firm or hard, and moist.[4,5]

Histopathologic findings of *M. haemolytica* pneumonia include fibrinous and suppurative bronchopneumonia

with necrosis of leukocytes.[5] Necrotic leukocytes, including neutrophils and macrophages, are lytic, and exhibit a streaming pattern of pale basophilic chromatin; as this pattern resembles oats, the term "oat cells" is commonly used.[5] Alveoli and airways contain variable amounts of viable and degenerate neutrophils and macrophages, fibrin, edema, erythrocytes, colonies of bacteria, and necrotic debris. Fibrin thrombi are frequently present, and interlobular septa are distended by fibrin, edema, and inflammation. Sharply demarcated regions of coagulative necrosis are often present.[5] Differential diagnoses for the gross and histopathologic lesions include *H. somni* and *P. multocida*. Evidence of bronchiolar necrosis is suggestive of an underlying viral infection; however, neutrophil-mediated damage may also cause such lesions.[5]

In the diagnostic setting, definitive diagnosis is determined by aerobic bacterial culture. However, prior treatment of the animal with antimicrobials frequently results in failure to culture bacterial agents. As well, opportunistic and secondary bacteria, including *Arcanobacterium pyogenes* and *Mycoplasma* species, may be present and confound the results.

JPC Diagnosis: 1. Lung: Bronchopneumonia, necrotizing, diffuse, moderate, with epithelial viral syncytia and intracytoplasmic viral inclusion bodies.
2. Lung: Bronchopneumonia, fibrinosuppurative, diffuse, moderate, with oat cells, numerous bacteria, and fibrinosuppurative pleuritis.

Conference Comment: The contributors provided an excellent synopsis of bovine respiratory disease complex, an economically important syndrome in cattle. The moderator emphasized that although the classic presentation of BRSV infection is with a gross appearance of cranioventral consolidation and caudoventral emphysema, as mentioned by the contributors, BRSV infection may also present as diffuse scattered edema and emphysema, without the typical gross demarcation. Additional differential diagnoses for enzootic pneumonia were discussed, such as bovine herpesvirus-1 and bovine adenovirus, which produce intranuclear viral inclusion bodies instead of inclusions in the cytoplasm.

The contributor mentioned leukotoxin, a primary virulence factor produced by *M. haemolytica*, which is a repeats in toxin (RTX) exotoxin. RTX is named for the presence of a tandemly-repeated nine-amino acid residue sequence in the protein, specifically glycine-rich nonapeptides, which bind Ca2+ on the C-terminal half of the protein. RTX toxins are pore-forming protein toxins produced by a wide range of pathogenic gram-negative bacteria that result in necrosis or apoptosis and are generally classified as hemolytic, cytotoxic or both. Other important RTX toxins in veterinary medicine include hemolysin produced by *Escherichia coli*, ApxI and ApxII produced by *Actinobacillus pleuropneumoniae*, leukotoxin produced by *Pasteurella multocida*, and adenylate cyclase toxin produced by *Bordetella bronchiseptica*.[2,5]

Contributor: Michigan State University
Diagnostic Center for Population and Animal Health
4125 Beaumont Rd.
Lansing, MI 48910-8104
www.animalhealth.msu.edu

References:

1. Brodersen BW. Bovine Respiratory Syncytial Virus. *Vet Clin North Am Food Anim Pract*. 2010;26(2): 323-33.
2. Caswell JL, Williams KJ. Respiratory System. In: Maxie MG, ed. *Jubb, Kennedy, and Palmer's Pathology of Domestic Animals*. 5th ed. Philadelphia, PA: Saunders Elsevier; 2007:596–598.
3. Vuuren MV. Bovine respiratory syncytial virus infection. In: Coetzer JAW, Tustin RC, eds. *Infectious Diseases of Livestock*. 2nd ed. Toronto, CA: Oxford University Press, 2004:677–679.
4. Griffin D, Chengappa MM, Kuszak J, et al. Bacterial Pathogens of the Bovine Respiratory Disease Complex. *Vet Clin North Am Food Anim Pract*. 2010;26(2):381–394.
5. Caswell JL, Williams KJ. Respiratory System. In: Maxie MG, ed. *Jubb, Kennedy, and Palmer's Pathology of Domestic Animals*. 5th ed. Philadelphia: Saunders Elsevier; 2007:587-8, 601–604.
6. Gorden PJ, Plummer J. Control, Management, and Prevention of Bovine Respiratory Disease in Dairy Calves and Cows. *Vet Clin North Am Food Anim Pract*. 2010;26(2):243–259.
7. Griffin D. Bovine Pasteurellosis and Other Bacterial Infections of the Respiratory Tract. *Vet Clin North Am Food Anim Pract*. 2010;26(2):57–71.
8. Ackermann MR, Brogden KA. Response of the ruminant respiratory tract to *Mannheimia* (*Pasteurella*) *haemolytica*. *Microbes Infect*. 2000;2:1079–1088.

CASE IV: TAMU-01 (JPC 4003049).

Signalment: 20-year-old American Paint mare (*Equus ferus caballus).*

History: This icteric horse presented with anemia, and renal failure and hemoglobinuria, were noted on clinicopathologic evaluation. Despite transfusion of eight liters of blood, supportive care, and diuresis, renal values continued to increase and the animal's clinical condition continued to decline. Twenty-four hours prior to euthanasia, the animal was anorectic and had no fecal output.

Gross Pathology: All tissues were discolored tan/yellow (icterus), with pallor of all organs (anemia). The kidneys were swollen and bulged on section (N11-296A, nephrosis). Compared to other pale organs, the kidneys were dark and brown urine was in the urinary bladder (hemoglobinuria).

Laboratory Results:
Hemogram
Leucocytosis with absolute mature neutrophilia (28975 {2260-8580})
Mild absolute monocytosis
Mild lymphoctosis
2+ eccentrocytes

Serum = 4+ hemolysis
Creatinine kinase 4683U/L (73-450)*
Aspartate aminotransferase 2246U/L (134-643)*
Total protein 11.6 g/dl (5.3-7.3)*
BUN 58mg/dl (7-28)
Creatinine 4.3mg/dl (1.1-2)
Total bilirubin 10.3mg/dl (<4.1)*
*** tests can be falsely elevated when hemolysis >2+**

Histopathologic Description: Kidney: Segmentally, proximal tubules are variably distended and lined by attenuated, pale, basophilic epithelium with variably sized nuclei that are large and vesiculate with a prominent nucleolus. Some tubule are lined by necrotic and apoptotic cells, a few tubules have proliferation of cells with many nuclei/cells, and a few scattered tubules are lined by a simple, tall/cuboidal epithelium with occasional mitoses (tubular degeneration, necrosis and regeneration). Many distended lumens contain granular casts (Perl's negative) that sometimes have admixed, smooth hyalinized foci and often contain degenerating neutrophils (heme pigment casts). Many less affected proximal tubules are lined by swollen epithelium and contain a pale eosinophilic acellular content. In these tubules the content stains pale blue with Fe stain (Perl's/Prussian –blue reaction), and the cells contain Fe-positive stippling. The interstitium and perivascular areas are pale and expanded (edema) with foci that are hyalinized and eosinophilic (fibrin, presumed) and large, reactive stromal cells. Many sloughed cells are in lower nephron tubules and collecting ducts with granular casts, fewer degenerating neutrophils and acid hematin (Perl's negative) clumping, and interstitial edema is obvious.

4-1. Kidney, horse. The kidneys are swollen, bulge on cut section, and are dark red. Photograph courtesy of Texas A&M University, Dept of Veterinary Pathobiology, College of Veterinary Medicine and Biomedical Sciences, http://vetmed.tamu.edu/vtpb.

4-2. A leaf from Acer rubrum, the red maple. Photograph courtesy of Texas A&M University, Dept of Veterinary Pathobiology, College of Veterinary Medicine and Biomedical Sciences, http://vetmed.tamu.edu/vtpb.

Contributor's Morphologic Diagnosis: Subacute, segmental tubular nephrosis with tubular degeneration necrosis and regeneration, karyomegaly, and granular casts with edema.

Contributor's Comment: This slide has most of the changes imaginable with tubular nephrosis, especially those of a nephrosis from hemoglobinemia. The horse had exposure to red maple limbs with leaves that had fallen after a wind storm over a week before presentation, and identifiable pieces of red maple leaves (N11-296B) were found in the colon.[1] Contact with wilted red maple (*Acer rubrum*) leaves and the presentation with hemolytic anemia, hemoglobinuria, icterus, Heinz bodies or eccentrocytes (methemoglobin) and some degree of renal failure are

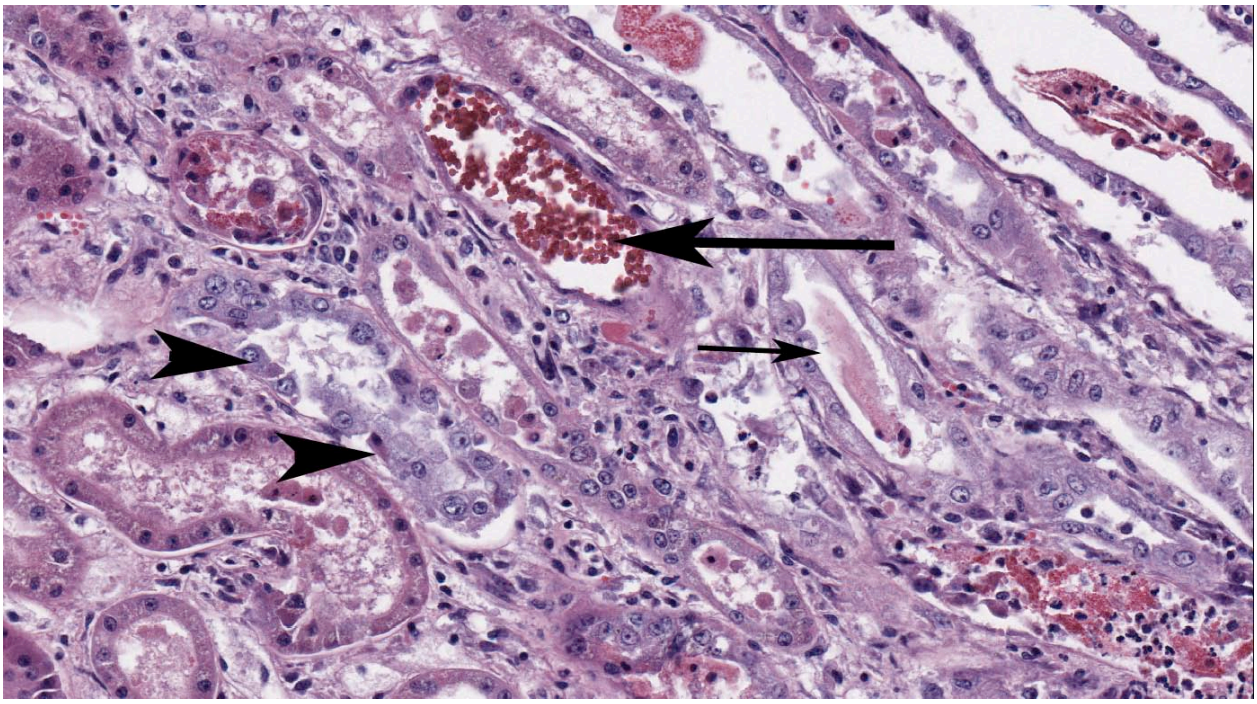

4-3. Kidney, horse. Necrotic tubules contain bright granular eosinophilic hemoglobin casts (large arrow) and protein casts (small arrow). Numerous tubules are lined by hypertrophic basophilic regenerative epithelium (arrowheads). (HE 200X)

characteristic.[1-14] Apparently, methemoglobin is not often quantitated to show defective oxygen carrying capacity, and our lab did not do new methylene blue staining, so Heinz bodies were not described. Many cases are published and most do reference renal failure, and although some report deaths, many horses survive (dose response, presumably). Our horse could not be stabilized and clinically was considered to be in renal failure. The renal lesion certainly is a joy for the pathologist. Features of interest to pathologists in red maple toxicity are:

- the kidney was/is remarkably preserved despite autolysis in other tissue
- note where the iron metal stains
- it is a segmental nephrosis
- the karyomegaly often is not emphasized.[6]

The toxic principle is in wilted leaves, and its identity is unknown. Gallic acid is one of the usual suspects as an oxidant, and Vitamin C (and steroids) is recommended for treatment.[1,8] The combination of intravascular hemolysis, hemoglobinemia and hypoxemia make the renal lesion. Reasonable differential diagnoses include: onion toxicity (we have cases of wild onion toxicity in horses but it is milder), nitrite intoxication (iatrogenic), equine infectious anemia (fever), babesiosis (fever and parasites visible) and immune mediated hemolytic anemia (agglutination positive). We have had cases associated with silver maple.

JPC Diagnosis: Kidney: Tubular degeneration, necrosis, and regeneration, diffuse, moderate with hemoglobin and cellular casts and scattered tubulorrhexis.

Conference Comment: This condition is only described in equids, and is probably due to their decreased capacity to reduce methemoglobin. Damage to the kidney results from acute tubular ischemic necrosis secondary to hemolysis. Neither hemoglobin nor myoglobin are nephrotoxic by themselves, and neither will cause injury when injected into a healthy kidney; however, in an ischemic kidney either may increase tubular necrosis. Gallic acid contributes to the oxidative stress of erythrocyte membranes resulting in Heinz body formation and subsequent anemia and methemoglobinemia. Heinz bodies are 1-2µm round protuberances on the erythrocyte membrane composed of denatured, precipitated hemoglobin.[1,3,5,7,13]

There are two forms of *A. rubrum* toxicosis: a peracute form that typically occurs late in the autumn and a hemolytic form which occurs in early autumn. The peracute form results in massive methemoglobinemia, tissue anoxia and sudden death. Gross lesions include brown discoloration of tissues and blood, and cyanotic mucous membranes. The hemolytic form causes Heinz body formation, and subsequent intra- and extravascular hemolysis, in combination with methemoglobinemia. Clinical signs include weakness, lethargy, depression, anemia, icterus, hemoglobinuria and hemoglobinemia. Gross lesions include icterus,

serosal petechia and ecchymosis, brown discoloration of the kidneys, splenomegaly, pulmonary congestion and edema, and mild to severe centrilobular hepatic degeneration and lipidosis.[5,7,13]

Differential diagnoses for hemolytic anemia in horses include *Leptospira bratislava*, *Babesia caballi* and *B. equi*, and wild onion (*Allium* sp.), which cause intravascular hemolysis; equine infectious anemia and *Anaplasma plasmaphagocytophilum* cause extravascular hemolysis. Other causes of methemoglobinemia include nitrate poisoning, chlorate toxicosis, and drugs such as phenacetin and acetanilide. Additional causes of Heinz body anemia include onion consumption in cattle, horses, dogs, and cats; rape, kale, and turnip consumption in cattle and sheep; chronic copper toxicosis in sheep, cattle, and swine; zinc toxicity in dogs; selenium deficiency; and the urinary acidifier methylene blue in cats. Heinz bodies can also occur spontaneously in cats.[5,7,13]

Contributor: Texas A&M University
Department of Veterinary Pathobiology
College of Veterinary Medicine and Biomedical Sciences
College Station, TX 77843-4467
http://vetmed.tamu.edu/vtpb

References:

1. Alward A, Corriher CA, Barton MH, et al. Red Maple (*Acer rubrum*) leaf toxicosis in horses: A retrospective study of 32 cases. *J Vet Intern Med.* 2006;20:1197-1201.
2. Brockus CW. Erythrocytes. In: Latimer KS, ed. *Duncan & Prasse's Veterinary Laboratory Medicine Clinical Pathology*, 5th ed. Ames, IA: John Wiley & Sons Inc; 2011:34-5.
3. Corriher CA, Gibbons DS, Parviainen, AKJ, et al. *Compend Cont Educ Prac Veter*. 1999;21:74-80.
4. Divers TJ, George LW, George JW. Hemolytic anemia in horses after the ingestion of Red Maple leaves. *JAVMA*. 1982;180:300-302.
5. Fry MM, McGavin MD. Bone marrow, blood cells, and lymphatic system. In: McGavin MD, Zachary JF, eds. *Pathologic Basis of Veterinary Disease*. 5th ed. St. Louis, MO: Mosby Elsevier; 2011:718.
6. George LW, Divers TJ, Mahaffey EA, et al. Heinz body anemia and methemoglobinemia in ponies given Red Maple (*Acer rubrum L.*) leaves. *Vet Pathol.* 1982;19:521-533.
7. Maxie MG, Newman SJ. Urinary system. In: Maxie MG, ed. *Jubb, Kennedy, and Palmer's Pathology of Domestic Animals*. 5th ed. St. Louis, MO: Saunders Elsevier; 2007:446-447.
8. McConnico RS, Brownie CF. The use of ascorbic acid in the treatment of 2 cases of Red Maple (*Acer rubrum*)-poisoned horses. *Cornell Vet*. 1982;82:293-300.
9. Plumlee KH. Red Maple toxicity in a horse. *Vet Hum Toxicol.* 1992;33:66-67.
10. Semrad SD. Acute hemolytic anemia from ingestion of Red Maple leaves. *Compend Cont Educ Pract Veter*. 1993;15:2, 261-264.
11. Stair EL, Edwards WC, Burrows GE, et al. Suspected Red Maple (*Acer rubrum*) Toxicosis with Abortion in Two Percheron Mares. *Vet Hum Toxicol*. 1993;35:229-230.
12. Tennant B, Dill SG, Glickman LT, et al. Acute Hemolytic Anemia, Methemoglobinemia, and Heinz Body Formation Associated with Ingestion of Red Maple leaves by Horses. *JAVMA*. 1981;179:143-150.
13. Valli VEO. The hematopoietic system. In: Maxie MG, ed. *Jubb, Kennedy, and Palmer's Pathology of Domestic Animals*. 5th ed. St. Louis, MO: Saunders Elsevier; 2007:254-255.
14. Warner AF. Methemoglobinemia and hemolytic anemia in a horse with acute renal failure. *Compend Cont Educ Pract Veter*. 1984;6:S465-8, S472.

WEDNESDAY SLIDE CONFERENCE 2011-2012

Conference 6

19 October 2011

CASE I: 08B1647 (JPC 3134348).

Signalment: 14-year-old female Dutch Warmblood horse (*Equus ferus caballus*).

History: The horse had a history of an approximately 1 cm mass within the lower left cheek that was excised 3 months prior to presentation and diagnosed as a trichoblastoma. The mass had recurred and was rapidly enlarging at the time of presentation. On palpation, a 5 x 3 x 2 cm, bilobed, firm mass was present within the left cheek at the level of the first three mandibular cheek teeth (307 to 309). The mass elevated both the intact overlying skin and underlying intact oral mucosa. Some pain appeared to be associated with the mass, and the horse was intermittently depressed. An initial incisional biopsy was followed by complete surgical excision 12 days after presentation.

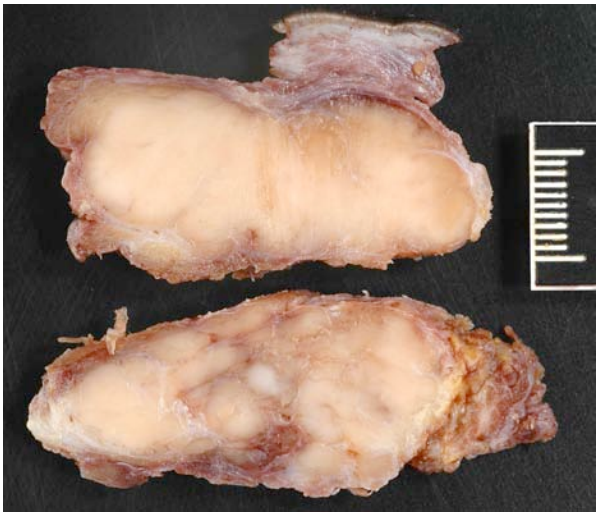

1-1. Fibrous connective tissue (cheek, per contributor), equine. Multilobulated fleshy neoplasm within subcutis and skeletal muscle. Photograph courtesy of Department of Pathology, Microbiology, and Immunology, School of Veterinary Medicine, University of California, Davis, http://www.vmth.ucdavis.edu, http://www.vetmed.ucdavis.edu/PMI.

Gross Pathology: A 5.5 x 3.0 cm by 2.5 cm thick section of skeletal muscle with an associated section of overlying skin was submitted. Within the subcutis and muscle on cut section, there was a multilobulated, pink, fleshy mass extending to the surgical margins.

Histopathologic Description: Mass, left cheek: Examined is an unencapsulated, poorly demarcated, multilobulated, densely cellular mass composed of lobules and tracts of neoplastic cells that infiltrate adjacent skeletal muscle and connective tissue and extend to the tissue margins. The cells within the bulk of the mass are arranged in sheets, cords, and packets within a moderately abundant fine fibrovascular stroma. Cells in these areas are polygonal with distinct cell borders, small amounts of wispy eosinophilic to clear cytoplasm, and large round central nuclei with finely stippled chromatin. In scattered areas (not present on every slide), the cells are pleomorphic, very large, lack distinct cell borders, and are often multinuceated and have bizarre nuclei and prominent

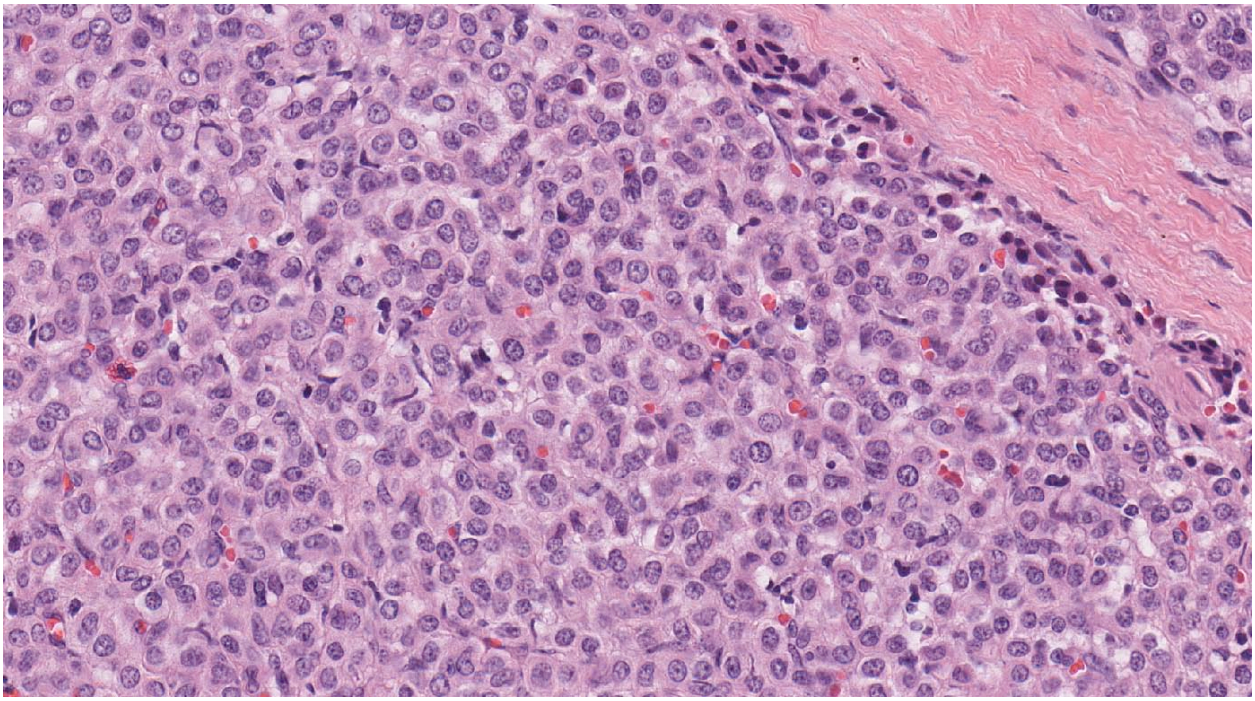

1-2. Fibrous connective tissue (cheek, per contributor), equine. A monomorphic population of polygonal cells are arranged in nests and packets on a fine fibrovascular stroma. (HE 320X)

nucleoli. There are 0-3 mitoses per 10 high power fields (8 per 50 high power fields) in all regions. Along the thick fibrous septae, neoplastic cells abut and bulge into large irregular, occasionally blood-filled, endothelial-lined clefts. Clusters of neoplastic cells are occasionally present within these vascular lumina.

Neoplastic cells exhibited strong cytoplasmic immunoreactivity for smooth muscle actin and vimentin and variable to strong cytoplasmic immunoreactivity for desmin. A well-defined basal lamina surrounding the individual tumor cells was demonstrated by positive immunoreactivity for laminin outlining the cytoplasmic border of each cell. Neoplastic cells were diffusely negative for pan-cytokeratin, cytokeratin 14, synaptophysin, CD11c, skeletal myosin, factor VIII-ra, and S100 α and β. With factor VIII-ra, a single layer of endothelium could be variably demonstrated separating the tumor from the lumina of vessels and clefts. With S100, several immunoreactive nerves were present within the tumor.

Contributor's Morphologic Diagnosis: Mass, left cheek: Malignant glomus tumor (glomangiosarcoma).

Contributor's Comment: Glomus tumors are thought to arise from modified smooth muscle cells of the glomus body, a type of arteriovenous anastomosis or shunt which is involved in regulating temperature.[6,10] Glomus bodies are composed of an afferent arteriole and small venules connected by a series of small channels (Sucquet-Hoyer canals), surrounded by dense collagenous tissue, and closely associated with small nerve branches. Within the walls of the anastomosing canals are epithelioid cells with ultrastructural and immunocytologic features similar to smooth muscle cells, called glomus cells, which are thought to be the cell of origin for glomus tumors.[4,10]

Glomus tumors have best been characterized in humans where their locations correspond to the most common sites for glomus bodies, i.e. subungual regions and skin of the extremities. Other reported sites of glomus tumors in humans include dermis, subcutis and soft tissues in other locations, as well as bone, nerve, stomach, colon, nasal cavity, and trachea.[6,10] Glomus tumors of the head and neck account for only approximately 6% of the cases in humans.[10] A similar distribution has been seen in dogs and cats, with most of the few reported cases occurring in the digits.[2,3,7,9] Of the 3 known cases of glomus tumors in horses, one occurred as an osteolytic lesion within the third phalanx deep to the hoof wall, a presentation very similar to that seen in humans,[1] while two others, this and another unpublished case from UC Davis, occurred in the cheek and skin of the neck, respectively. The distribution of normal glomus bodies in horses has not been well characterized, although they occur frequently in the skin of the mammary gland.[4]

A feature of glomus tumors of the subungual region in humans, and less commonly of these tumors in other

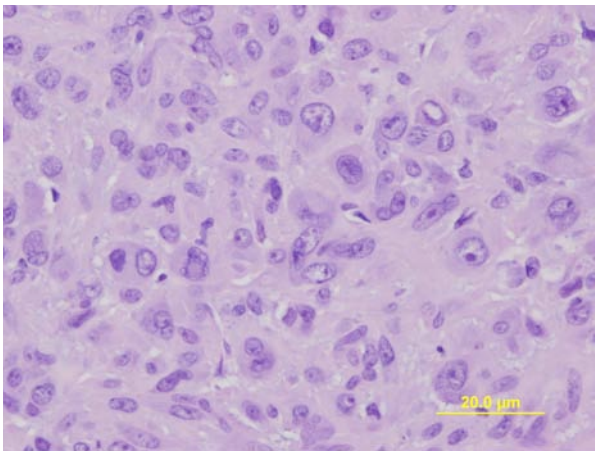

1-3. Fibrous connective tissue (cheek, per contributor), equine. Focus of cellular atypia with karyomegaly and prominent nucleoli. Photograph courtesy of Department of Pathology, Microbiology, and Immunology, School of Veterinary Medicine, University of California, Davis, http://www.vmth.ucdavis.edu, http://www.vetmed.ucdavis.edu/PMI (HE 400X).

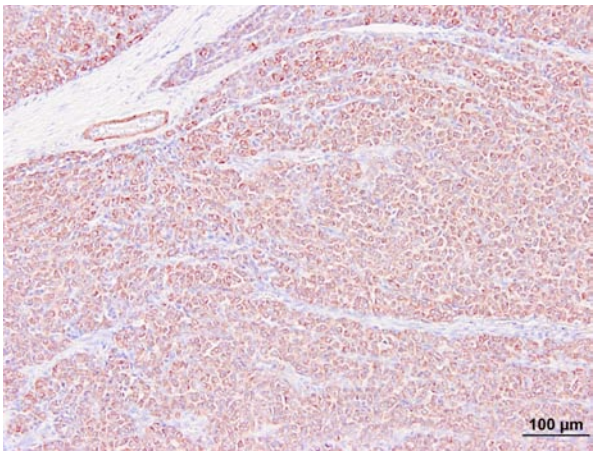

1-4. Fibrous connective tissue (cheek, per contributor), equine. Diffuse strong immunopositivity for smooth muscle actin. Photograph courtesy of Department of Pathology, Microbiology, and Immunology, School of Veterinary Medicine, University of California, Davis, http://www.vmth.ucdavis.edu, http://www.vetmed.ucdavis.edu/PMI.

sites, is associated intense pain, presumably a result of innervation with substance P-containing nerve fibers.[6,10] In human medicine, this feature is diagnostically useful as few types of skin tumors are painful. Some degree of "soreness" was thought to be associated with this tumor, which was immediately adjacent to the facial nerve grossly and included several nerve fibers histologically. Interestingly, the other equine glomus tumor in the UC Davis case files was removed because it appeared to be painful to the horse when touched.

Glomus tumors in humans can be classified as solid, angiomatous, or myxoid types.[6] Except for multiple angiomatous glomus tumors in the bladder of a cow,[5] glomus tumors in animals, including this case, have generally been of the solid type.[2,3,7,9] They have several characteristic features which were seen in this case, including an intimate relationship with blood vessels, which may only be evident at the periphery, a round or cuboidal "epithelioid" cell shape with a "punched out" round nucleus and eosinophilic cytoplasm, and a network of basement membranes around each cell.[6,10] Immunohistochemistry for laminin was used in this case to demonstrate the basal lamina surrounding the neoplastic cells. Primary differential diagnoses for this tumor included trichoblastoma (the initial diagnosis), other epithelial neoplasms, or a neuroendocrine tumor, all of which were ruled out with additional immunohistochemical stains. Typical of glomus tumors, the neoplastic cells were positive for smooth muscle actin and vimentin and negative for cytokeratins, synaptophysin, factor VIII, and S100. The cells were variably positive for desmin, which has occasionally been reported in human and canine glomus tumors.[10]

In humans, malignant glomus tumors (glomangiosarcomas) are very rare, but have been defined by being larger than 2 cm with a deep location, having atypical mitotic figures, or having marked nuclear atypia and mitoses >5 per 50 high power fields (hpf). The tumor in this horse was considered to be malignant based on recurrence and rapid growth, invasiveness of deep tissues, large size, and areas of marked cellular atypia. Mitotic figures were also 8 per 50 hpf. Although clusters of neoplastic cells appeared to be present within vascular channels, true intravascular invasion was difficult to assess because of the close association of the tumor with blood vessels. No metastases were evident at presentation. The horse was treated with intralesional injections of cisplatin every 2-4 weeks post-surgery, with a total of 4 treatments planned. However, the mass recurred prior to the final injection, and the horse was euthanized (necropsy not performed at our institution).

JPC Diagnosis: Left cheek, fibrovascular tissue: Glomus tumor.

Conference Comment: Despite the history of recurrence and rapid growth, conference participants felt the tumor was a benign entity based on the section presented in conference, and a discussion on the features of malignancy ensued. Cytomorphologic features mentioned by the contributor such as areas of cellular atypia, atypical mitoses, and local invasiveness were not seen by conference participants, who felt the tumor showed no overt signs of malignancy.

The differentiation between benignancy and malignancy is one of the most important roles of the pathologist, and tumors can sometimes defy typical classifications, so a best effort must be made on a

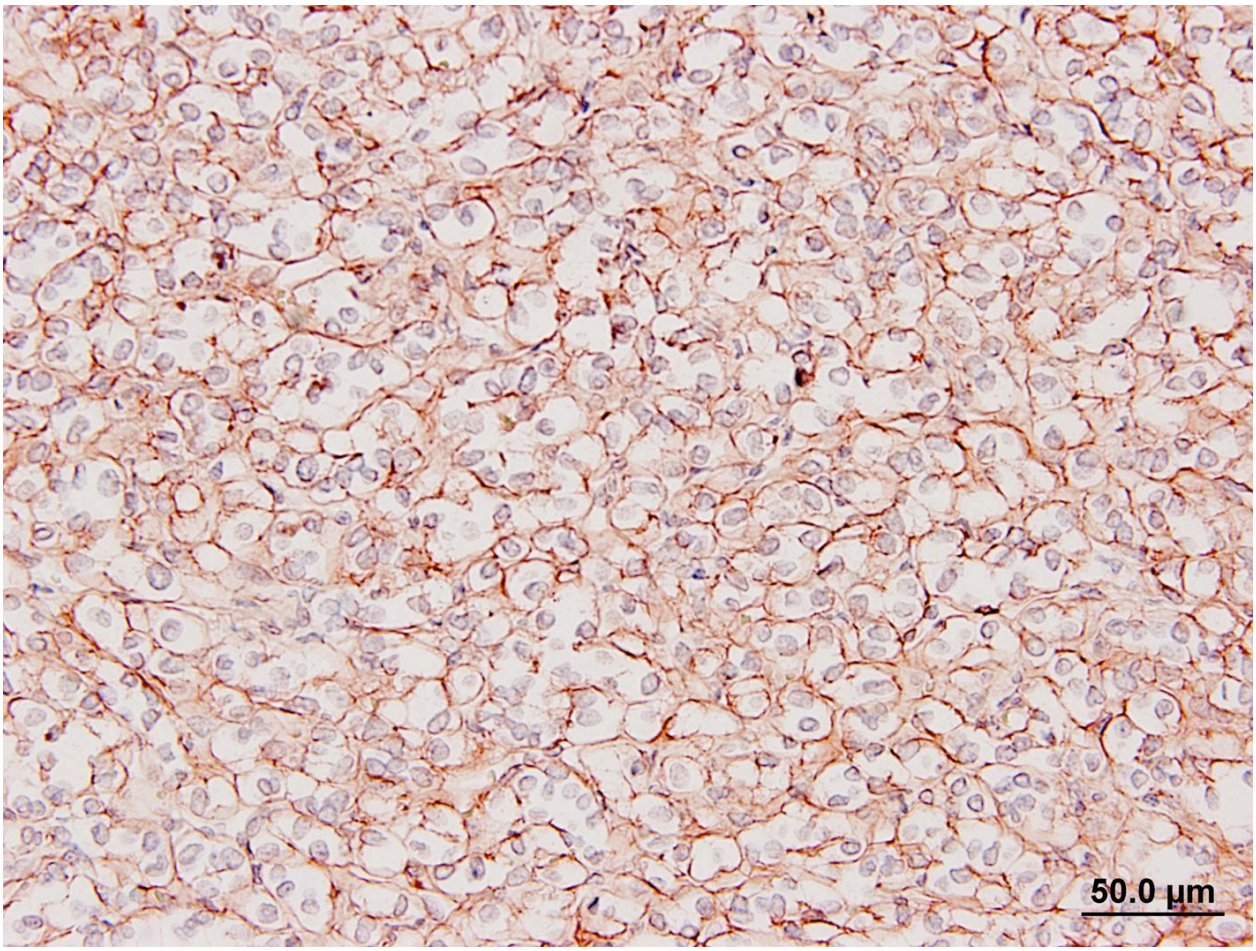

1-5. Fibrous connective tissue (cheek, per contributor), equine. Diffuse strong membrane immunopositivity for laminin. Photograph courtesy of Department of Pathology, Microbiology, and Immunology, School of Veterinary Medicine, University of California, Davis, http://www.vmth.ucdavis.edu, http://www.vetmed.ucdavis.edu/PMI.

diagnosis. Standard features to differentiate a benign tumor from its cancerous counterpart are the amount of differentiation or presence of anaplasia, the rate of growth, and the presence of local invasion and metastasis. The moderator commented that often with a surgical biopsy, which can be accompanied by a limited or no history as was the case with conference participants, the pathologist gets no information on metastasis, and local invasion may not be observed if no adjacent normal tissue is present.[8]

Differentiation is the degree to which neoplastic cells resemble the cell or tissue of origin, both in appearance and function. Anaplasia is when the tumor is poorly differentiated, and it is believed that the undifferentiated cells with immature "stem-cell-like" properties have loss of differentiation capacity. Anaplastic tumors may also exhibit lack of cell and nuclear uniformity, or pleomorphism; abnormal nuclear morphology with hyperchromasia, high nuclear-to-cytoplasmic ratio, irregular shape, and variable nucleoli; bizarre mitoses or a high mitotic rate; loss cellular polarity with haphazard organization; tumor giant cells; and large areas of ischemic necrosis. The rate of growth in malignant tumors is often erratic, ranging from slow to rapid, and this is a difficult parameter to measure and use for the evaluation of malignancy. The local aggressiveness of a tumor is a good indicator of malignancy, as benign tumors are often expansile, while malignant tumors invade or efface the surrounding normal tissue. Malignant tumors are often poorly demarcated and lack an obvious cleavage plane. Finally, the presence of metastasis is an indisputable marker of malignancy, as benign tumors by definition to do not metastasize. Metastasis is achieved through either the seeding of body cavities and surfaces, as in carcinomatosis, or hematogenous or lymphatic spread. While generally carcinomas spread via lymphatic routes and sarcomas spread via hematogenous routes, the interconnectedness of the two vascular systems often blurs these lines. In lymphatic spread, neoplastic cells follow the natural route of lymphatic drainage. In hematogenous spread, veins are more easily penetrated by neoplastic cells, and spread usually occurs in the closest capillary bed. However, pulmonary capillary

beds or primary pulmonary tumors allow easier access to arterial spread.[8]

Despite the history of recurrence and rapid growth, conference participants felt the tumor was a benign entity based on the section presented in conference; a discussion of malignancy features followed. Cytomorphologic features of malignancy, such as areas of cellular atypia, atypical mitoses, and local invasiveness, lack of cellular differentiation, and evidence of metastasis, were not appreciated by conference participants. The moderator commented that often with a surgical biopsy, limited or no history and the relatively small amount of tissue evaluated in a single histologic slide may make the differentiation between benign and malignant tumors elusive.

The moderator offered his approach to the characteristics of malignancy in order of most reliable to least as follows: By its very definition, evidence of metastasis means that a tumor is malignant. However, this information is often not present, and the next best feature to indicate metastasis is the presence of intravasation of the neoplasm, which underscores its aggressive nature. The next most reliable feature of malignancy is focal tissue invasion, characterized by neoplastic cells breaking through basement membranes, or inciting a desmoplastic response, inflammation or other features of host reaction. The least reliable criterion of malignancy is the cytologic appearance of neoplastic cells. When evaluating malignancy based on cellular features, evidence of cell behavior is more important that their appearance, such as the presence of bizarre mitotic figures; however, this can be difficult to completely ascertain based on the two-dimensional cut through a three-dimensional nucleus.

Glomus tumors are often difficult to characterize based on histomorphology alone, and this was an excellent example, having definitive features of a glomus tumor, including characteristic bulging into vascular channels.

Contributor: University of California, Davis
Anatomic Pathology Service
Veterinary Medical Teaching Hospital and Department of Pathology, Microbiology and Immunology
School of Veterinary Medicine
http://www.vmth.ucdavis.edu, http://www.vetmed.ucdavis.edu/PMI

References:

1. Brounts SH, Adams SB, Vemireddi V, et al. A malignant glomus tumour in the foot of a horse. *Equine Vet Educ*. 2008;20:24-27.
2. Dagli MLZ, Oloris SCS, Xavier JG, et al. Glomus tumour in the digit of a dog. *J Comp Path*. 2003;128:199-202.
3. Furuya Y, Uchida K, Tateyama S. A case of glomus tumor in a dog. *J Vet Med Sci*. 2006;68:1339-1341.
4. Ludewig T. Occurrence and importance of glomus organs (Hoyer-Grosser's organs) in the skin of the equine and bovine mammary gland. *Anat Histol Embryol*. 1998;27:155-159.
5. Roperto S, Borzacchiello G, Brun R, et al. Multiple glomus tumors of the urinary bladder in a cow associated with bovine papillomavirus type 2 (BPV-2) infection. *Vet Pathol*. 2008;45:39-42.
6. Rosai J. Soft tissues. In: *Surgical Pathology*. 9th ed. St. Louis, MO: Mosby; 2004:2288-2290.
7. Shinya K, Uchida K, Nomura K, et al. Glomus tumor in a dog. *J Vet Med Sci*. 1997;59: 949-950.
8. Stricker TP, Kumar V. Neoplasia. Neoplasia. In: Kumar V, Abbas AK, Fausto N, Aster JC, eds. *Robbins and Cotran Pathologic Basis of Disease*. 8th ed. Philadelphia, PA: Saunders Elsevier; 2010:262-271.
9. Uchida K, Yamaguchi R, Tateyama S. Glomus tumor in the digit of a cat. *Vet Pathol*. 2002;39:590-592.
10. Weiss SW, Goldblum JR. Perivascular tumors. In: *Soft Tissue Tumors*. 5th ed. St. Louis, MO: Mosby; 2008:751-757.

CASE II: H11.0882 (JPC 4003612).

Signalment: 8-year-old male castrate mixed breed domestic dog, canine (*Canis lupis familiaris*).

History: The animal was admitted to the Small Animal Clinic of the University of Zurich after a history of vomiting and diarrhea for two months. The animal had been operated on one year earlier because of a stenosis in the ileocecal region. The histology of the resected tissue revealed a lymphangitis and eosinophilic ileitis. Now, the small intestines were again severely dilated and congested with ingesta and a new stenosis in the mid jejunum was evident through ultrasound investigation. The animal was submitted to surgery for a second time; the stenotic intestine was resected and sent in for further histological investigation.

Gross Pathology: The wall of the jejunum and the attached mesenterium was severely thickened by firm connective tissue. Multifocal, small, round, soft, whitish nodules of up to 0,5cm in diameter could be seen between the longitudinal and circular muscle layers of the tunica muscularis. The lymphatic vessels on the mesenteric site of the intestine were severely congested with lymph.

Laboratory Results: The animal had a slightly distended abdomen with a small amount of free, accumulated fluid. The fluid was characterized by a specific gravity of 1.015, protein content of 10 g/L and nucleated cell count of 7475 Lc/µl. The leukocytes consisted mainly of viable neutrophils (95%), few lymphocytes (2%) and monocytes/macrophages (3%). No bacteria could be found within the fluid.

Histopathologic Description: Jejunum: The shortened villi are diffusely blunted and the crypts are often elongated and hypertrophied. The crypt to villus ratio is often 1:1. On the tips of the villi the enterocytes are often desquamated (autolysis). Within the lamina propria there is mild edema, slightly dilated lacteals (not visible on all slides) and on the tips of villi a mild infiltration of macrophages with foamy cytoplasm can be seen. In the mucosa, mildly increased numbers of neutrophils and eosinophils are found.

The entire wall of the small intestine is thickened by up to 3 times due to severely congested lymphatics and multifocal necrotic areas with a width of up to 0.5 cm and proliferation of granulation tissue in the lamina and tunica muscularis and the mesentery. The necrotic areas consist of a foamy, slightly granular, protein rich fluid in the center, surrounded by numerous lipid-laden macrophages (lipophages) with a foamy appearance in their cytoplasm. The periphery is marked by infiltration of moderate numbers of lymphocytes and plasma cells, few neutrophils and marked proliferations of fibroblasts with broad collagen bundles. The collagen bundles lay perpendicular to the many newly formed capillaries (granulation tissue).

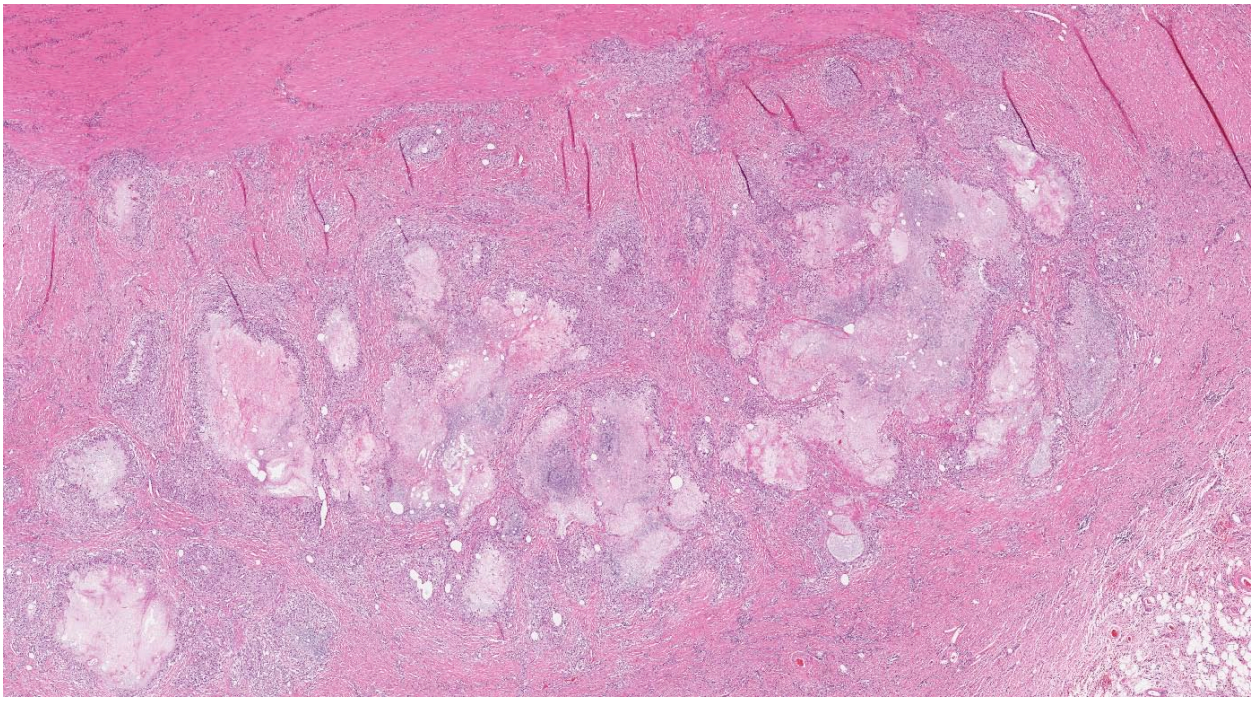

2-1. Intestine, dog. Granulomatous inflammation centered on lymphatic vessels which markedly expands the intestinal serosa. (HE 130X)

Contributor's Morphologic Diagnosis: Small intestine: Lymphangitis, lipogranulomatous, severe, multifocal with moderate granulation tissue formation. Jejunitis, neutrophilic and eosinophilic, mild diffuse.

Contributor's Comment: Protein-losing enteropathy is an idiopathic syndrome that occurs in dogs and to a lesser extent in species such as horses and cats and is characterized by weight loss, hypoproteinemia, and malabsorption. Multiple different diseases such as inflammatory infiltrates in the lamina propria, neoplasia, amyloidosis or lymphangiectasias eventually associated with villus atrophy are possible causes for this syndrome. Often a biopsy is necessary to formulate a final diagnosis.[3]

In our case, the lacteals within the villar tips are not the prominent feature, although the villi are shortened and the crypts elongated. The main feature of the lesion is the occurrence of numerous lipogranulomas in the mucosa and mesentery. These lipogranulomas occur adjacent to dilated mesenteric lymphatics, but are not usually a consistent feature of lymphangiectasia.[2,3,4,6] They are often considered as secondary lesions due to lymphatic hypertension and fat leakage and to subsequent granulomatous reponse.[3,4] Similar granulomas occurred in experimental chronic lymphatic obstruction in rats lacking in lymphatic recanalization.[4] Experimental ligation of lymph vessels in the dog did not cause an inflammatory reaction or granuloma formation.

The cause of lymphangiectasia is not always clear. Some cases appear to be acquired by a chronic inflammatory bowel disease, malignant lymphoma or granulomatous infiltrates, but in others, neither a congenital or acquired obstruction of the lymphatic system nor an increase in the inflammatory population of cells in the bowel wall can be seen. This suggests the etiology of the clinical syndrome might be more complex than simple obstruction of the lymphactics.[4]

In Basenjis and Soft Coated Wheaten Terriers (SCWT), a familial predisposition for both protein-losing enteropathy (PLE) and protein-losing nephropathy (PLN) is suspected. However, Basenjis differ from SCWT in their clinical presentation. In Basenjis, PLN was not seen separately without intestinal lesions, whereas PLN occurred alone in the SCWT.[2]

JPC Diagnosis: Small intestine and mesentery: Lymphangitis, lipogranulomatous, diffuse, severe, with mild villar blunting.

Conference Comment: Lymphangiectasia is usually caused by obstruction of lymphatic flow, most commonly due to inflammation.[5] Other underlying mechanisms include neoplastic infiltration, fibrosis, congenital malformation, or physiologic obstruction due to congestive heart failure. When the lymphatics become obstructed, Starling's law dictates the leakage of excess protein and lipid, which incites granulomatous inflammation. This exacerbates the obstruction of lymphatics, and the ensuing cycle may result in lipogranulomatous lymphangiectasia and lymphangitis as seen in this case.[1]

Clinical pathology abnormalities often associated with lymphangiectasia include panhypoproteinemia, which is seen in severe disease with failure of compensatory plasma protein production; lymphopenia, due to loss in lymphatic fluid or stress; hypocholesterolemia; and hypocalcemia. Hypocalcemia is attributed to hypoalbuminemia, and the majority of dogs have serum calcium levels in the normal reference range after correction for albumin[5]; however, some dogs develop ionized hypocalcemia, which may be the result of vitamin D malabsorption, seen commonly with lymphangiectasia.[1]
As mentioned by the contributor, the lesions in this case largely spare the mucosa and lack the dilation of lacteals classically described in lymphangiectasia-derived protein-losing enteropathy. As such, this case

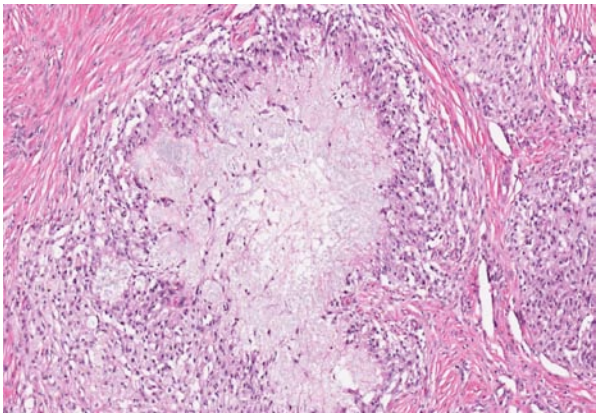

2-2. Intestine, dog. Closer view of occluded lymphatic withmineralized content, bounded by numerous epithelioid macrophages. (HE 360X)

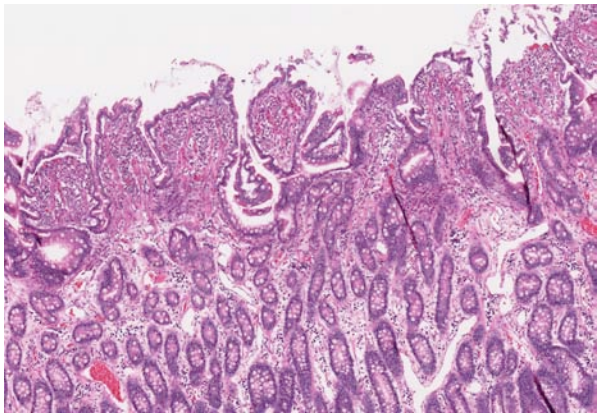

2-3. Intestine, dog. Marked villar blunting within the overlying mucosa; lymphatics are widely dilated due to downstream occlusion. (HE 200X)

illustrates a major limitation of surgical mucosal biopsy, which would have failed to sample the diagnostic lesions in the submucosa and outer tunics. The conference moderator emphasized the distinction between lipogranulomatous lymphangitis and lipogranulomas. In two-dimensional cross section, an inflamed lymphatic vessel may appear as a characteristic discrete granuloma with the four typical layers (i.e. central necrosis surrounded by histiocytes, fibrosis, and lymphocytes); however, since the inflammation is actually tracking lymphatics, the term "lipogranulomatous lymphangitis" may be preferable to "lipogranuloma."

Contributor: Institute of Veterinary Pathology
Vetsuisse Faculty Zurich
Winterthurerstrasse 268
CH-8057 Zurich
Switzerland
www.vetpathology.uzh.ch

References:

1. Hall EJ, German AJ. Diseases of the small intestine. In: Ettinger SJ, Feldman EC eds. *Textbook of Veterinary Internal Medicine*. 7th ed. St. Louis, MO: Saunders Elsevier; 2010:1076, 1566-7.
2. Littman MP, Dambach DM, Vaden SL, et al. Familial Protein-losing Enteropathy and Protein-losing Nephropathy in Soft Coated Wheaten Terriers: 222 Cases (1983-1997). *J Vet Intern Med*. 2000;14:68-80.
3. Brown CC, Baker DC, Barker IK. Alimentary system. In: Maxie MG, ed. *Jubb, Kennedy, and Palmer's Pathology of Domestic Animals.* 5th ed. vol. 2. London, UK: Saunders Elsevier; 1984;2007:102-104.
4. Suter MM, Palmer DG, Schenk H. Primary intestinal lymphangiectasia in three dogs: a morphological and immunopahtologial investigation. *Vet Pathol*. 1985;22:123-130.
5. Tarpley HL, Bounous DI. Digestive system. In: Latimer KS, ed. *Duncan & Prasse's Veterinary Laboratory Medicine Clinical Pathology*. 5th ed. Ames, IA: Wiley-Blackwell; 2011:242-5.
6. Van Kruiningen HJ, Lees GE, Hayden DW, et al. Lipogranulomatous lymphangitis in canine intestinal lymphangiectasia. *Vet Pathol*. 21:377-383.

CASE III: 1106976 (JPC 4002864).

Signalment: Tissue from yearling cattle (*Bos taurus*), breed and sex unknown.

History: Several livers were collected at slaughter from animals belonging to a single producer, and were submitted for diagnosis. The veterinarian reported that the animals had been given anthelminthics, which did not appear to be effective. There was further indication that these lesions had been seen in a few calves the previous year, but that more animals were affected this year.

Gross Pathology: Gross findings included the presence of multiple black, irregularly sized tracts throughout the parenchyma that occasionally contained trematode parasites. Fibrosis was apparent in a minority of lesions.

Laboratory Results: Parasites were identified by a veterinary parasitologist as *Fascioloides magna.*

Histopathologic Description: Liver: There is some variation between slides, with some containing more acute and others more chronic lesions. However, they are characterized by periportal fibrosis and inflammation together with much larger randomly distributed tracts that may contain mixed inflammation and hemorrhage, or inflammation and fibrosis. Eosinophils, plasma cells and lymphocytes dominate periportal infiltrates with more numerous macrophages, eosinophils and a few neutrophils in migratory tracts. Many macrophages contain small, isomorphic, birefringent granules of brown cytoplasmic pigment. Acutely, hemorrhage and eosinophils predominate. Stranded in the fibrosis of chronic lesions or in hemorrhage in acute lesions are scattered operculate ova, each with a well defined yellow-brown shell and a central developing embryo. Some ova are degenerate, with neutrophils or multinucleate phagocytes occur around them. Adult trematodes are present in acute migratory tracts surrounded by hemorrhage, and are not located in bile ducts. They are characterized by an external tegument and absence of a body cavity. Muscular, external suckers are present in some sections. The body is filled by loose, pale eosinophilic parenchyma and suspended within is the intestinal tract, containing brown pigment like that seen in tissue. Vitelline bodies are also sometimes apparent. Both male and female reproductive organs can be seen in some sections. A mixture of eosinophils and lymphocytes is present in peripheral hemorrhage and in the adventitia of portal triads. In areas of acute migration, hepatocytes have undergone localized necrosis without reference of their position in the lobule. Most inflamed portal areas contain increased bile duct profiles.

Contributor's Morphologic Diagnosis: Acute to chronic multifocal hepatitis, eosinophilic to granulomatous, with hemorrhage, fibrosis pigment deposition, adult trematodes, trematode ova, and eosinophilic cholangitis with bile duct proliferation.

Contributor's Comment: *Fascioloides magna* is the liver fluke of white tailed deer and undergoes aberrant migration in domestic ruminants. In cattle, adults are eventually encapsulated in fibrous tissue and cease migration at that time, but in small ruminants they continue to wander, causing extensive damage and eventual death.[1,4] In cattle, cysts containing the

3-1. Liver, ox. Numerous black tracts, some containing trematodes, traverse the liver. Racts are occasionally bordered by pale hepatic parenchyma suggesting fibrosis and/or hepatic necrosis and steatosis due to hypoxia. Photograph courtesy of Veterinary Medical Diagnostic Lab, University of Missouri, http://www.cvm.missouri.edu/vpbio/index.html.

3-2. Liver, ox. Adult trematode removed from one of the tracts. Photograph courtesy of Veterinary Medical Diagnostic Lab, Univerity of Missouri, http://www.cvm.missouri.edu/vpbio/index.html.

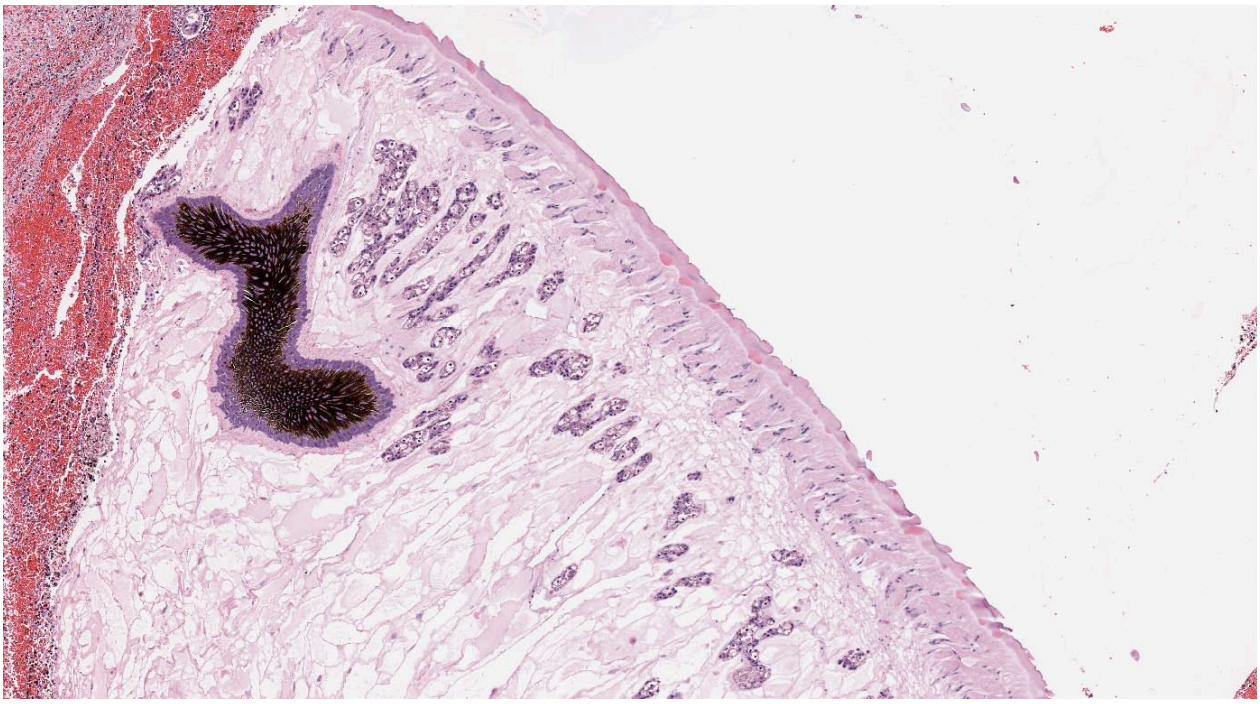

3-3. Liver, ox. Subgross view of section showing adult trematode in cross-section within a migration tract. (HE 100X)

parasite do not communicate with the biliary system and ova have no access to feces; hence the life cycle is incomplete. The black pigment associated with migratory tracts is iron-porphyrin.

Other species are occasionally infected with *Fascioloides magna*. A single case has been reported in a horse[2] and it is of increasing concern to European farmed cervids, particularly red and fallow deer.[3] Because of the need of a snail intermediate, *Fascioloides magna* is not commonly observed in Missouri, although two summers of heavy rain have probably increased a normally low level of parasitism on certain farms.

JPC Diagnosis: Liver: Necrosis and hemorrhage, focally extensive, with adult trematodes, granulomatous hepatitis, and eosinophilic portal hepatitis and cholangitis.

Conference Comment: As the contributor mentioned, there is marked variation between sections, with some characterized primarily by acute necrosis and hemorrhage associated with adult trematodes, and others with fibrosis from chronic migration tracts.

A primary differential in this case is *Fasciola hepatica*, which can be as large as *F. magna* and may appear similar histologically. In cattle, these two flukes can

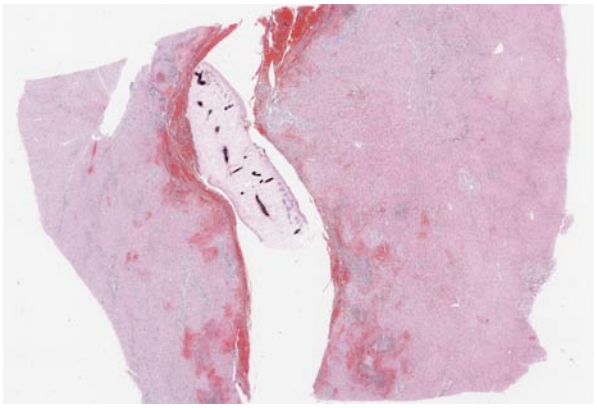

3-4. Liver, ox. On cut section, easily identifiable structures include (from exterior): thick eosinophilic tegument, somatic cell nuclei, spongy body cavity, multiple vittelarian glands, and cross section of a digestive tract with black hematin fluke pigment. (320X)

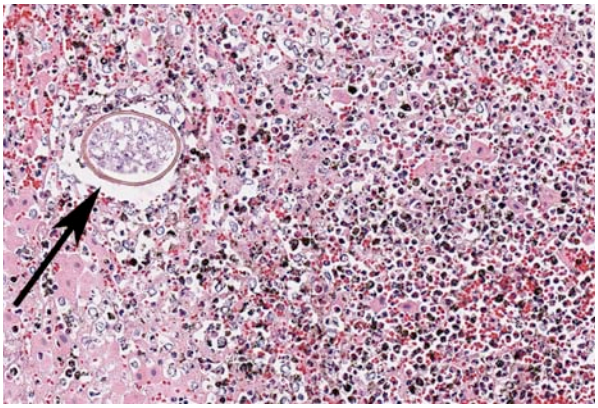

3-5. Liver, ox. Migration tracts are composed of necrotic hepatocytes, abundant necrotic debris, pigment laden macrophages, lesser numbers of neutrophils and eosinophils, and trematode eggs (arrow). (HE 400X)

be differentiated, though, by the location of the adult flukes the liver and the presence of considerable iron porphyrin pigment in *Fascioloides magna* infections. Adults of *F. hepatica* are present in bile ducts, while *F. magna* adults are distributed throughout the liver parenchyma. The migration tracts produced by larval *F. hepatica* do not generally cause sufficient damage to alter liver function in the host, as may be the case with *F. magna*. However, clinically important disease can be caused by *F. hepatica* in cattle and sheep when migrating larvae produce areas of local coagulative necrosis and lower hepatic oxygen tension. The areas of hypoxia create a favorable environment for the germination of *Clostridium noyvi* spores, resulting in a form of necrotizing hepatitis known as black disease. *C. noyvi* releases an alpha toxin and the necrotizing and hemolytic beta toxin, lecithinase. In Western and Eastern Europe, black disease may be incited by *Dicrocoelium dendriticum*. Bacillary hemoglobinuria, caused by the closely related *C. haemolyticum*, may also occur secondary to *F. hepatica* migration and has a similar pathogenesis to that of black disease.[4]

When *Fascioloides magna* encysts in the liver, the resulting 2-5 cm diameter encapsulated, pigmented cysts may grossly resemble melanocytic tumors.

Contributor: University of Missouri
Veterinary Medical Diagnostic Lab/ Department of Pathobiology
1100 East Rollins
Columbia, MO 65211
http://www.cvm.missouri.edu/vpbio/index.html

References:

1. Cullen JM. Liver, biliary system and exocrine pancreas. In: McGavin MD, Zachary JF, eds. *Pathologic Basis of Veterinary Disease*. 4th ed. St. Louis, MO: Mosby Elsevier; 2007:437.
2. McClanahan SL, Stromberg BE, Hayden DW. Natural infection of a horse with Fascioloides magna. *J Vet Diagn Invest*. 2005;17:382-385.
3. Novobilsky A, Horackova E, Hirtova L, et al. The giant liver fluke Fascioloides magna (Bassi 1875) in cervids in the Czech republic and potential of its spreading into Germany. *Parasitol Res*. 2007:100:549-553.
4. Stalker MJ, Hayes MA. Liver and biliary system. In: Maxie MG, ed. *Jubb, Kennedy and Palmer's Pathology of Domestic Animals*. 5th ed. vol. 2. Sanders Elsevier: St. Louis, MO; 2007:354-362.

CASE IV: N10-0920 (JPC 4003271).

Signalment: 7-week-old intact male Burmese cat.

History: The animal presented to the UW VMTH emergency service for acute respiratory distress following 5 days of lethargy, anorexia and decreased activity with occasional sneezing. On presentation the animal was quiet, alert and responsive, tachypnic at 92 breaths per minute, with increased respiratory effort, and harsh lung sounds bilaterally. He was tachycardic at 260 beats per minute. There was mild ocular discharge OU. Thoracic radiographs revealed a marked alveolar pattern in the cranioventral portion of the left and right-sided lung lobes, markedly dilated and cylindrical air bronchograms that failed to taper towards the periphery. He declined on overnight supportive oxygen and fluid therapy. Approximately forty minutes after initiation of mechanical ventilation he went into cardiac arrest. Cardiopulmonary resuscitation was unsuccessful and he was presented for necropsy.

Gross Pathology: Gross pathology is limited to the respiratory tract with no ocular discharge noted. A focal 2 x 2 x 1.5 cm region at the caudal tip of the right caudal lobe contains appreciable air. Remaining lung lobes are diffusely mottled and firm. The tracheobronchial lymph nodes are enlarged, with the left measuring 13 x 3 x 3 mm and the right measuring 9 x 6 x 3 mm.

Laboratory Results: Clinical tracheal wash cytology:

- Highly cellular, numerous nondegenerate neutrophils, few macrophages and rare well-differentiated anucleated squamous cells.

- Heterogenous population of extracellular bacteria, including diplococci, rods, small rods in chains, and possibly *Mycoplasma* organisms, is noted.

- Interpretation: Marked neutrophilic inflammation

Clinical tracheal wash culture: moderate mixed growth of oral flora

Blood chemistry:

- PCV/TP - 35%/7.4 g/dL
- Blood glucose - 89 mg/dL
- BUN (azo) 5-15

Post-mortem aerobic culture of lung tissue: heavy growth *Mycoplasma* sp. (not speciated)

Viral PCR on lung tissue:

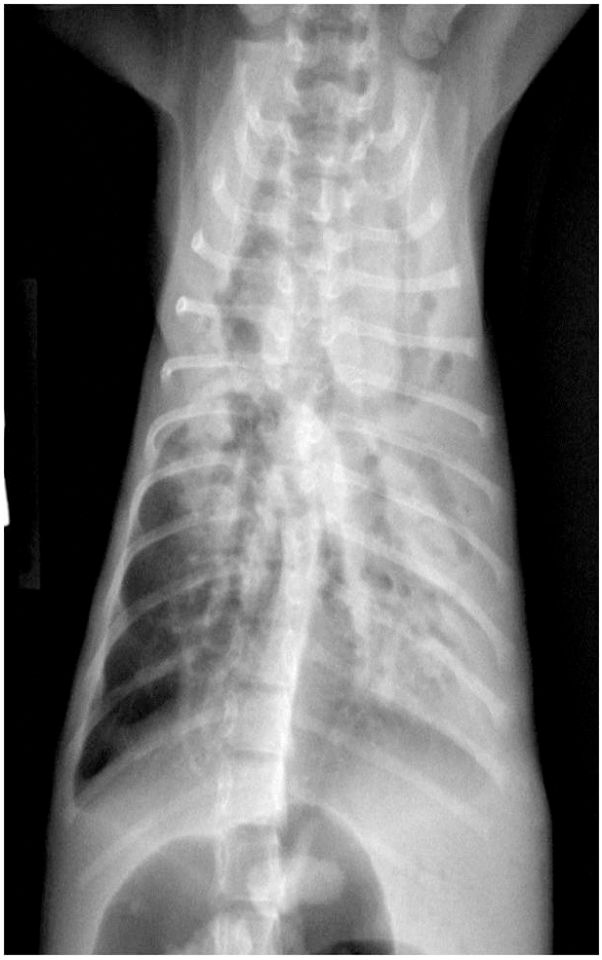

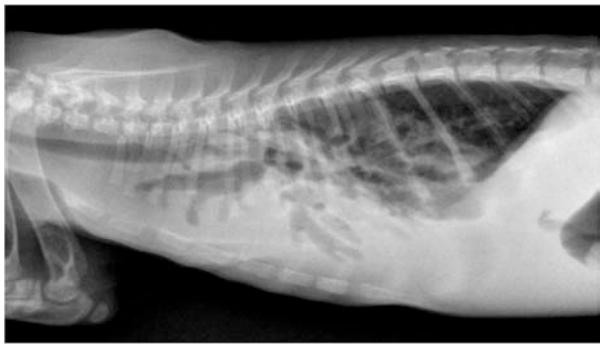

4-1, 4-2. Radiographs, lateral and dorsoventral views, cat. Both views show markedly ectatic airways against a marked bilateral alveolar pattern. Radiographs courtesy of the Department of Pathobiological Sciences, Univ. of Wisconsin School of Veterinary Medicine, http://www.vetmed.wisc.edu/home/.

- Negative for Chlamydia, feline herpes virus, influenza A
- Weakly positive for feline corona virus (CT value 29)
- Weakly positive for feline calici virus (CT value 38)

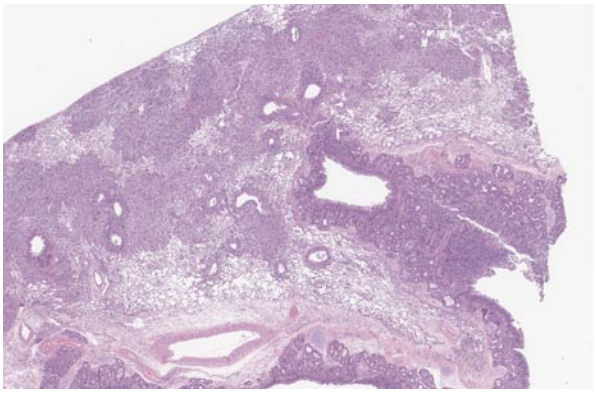

4-3. Lung, cat. The inflammation is centered upon airways throughout the section. (HE 15X)

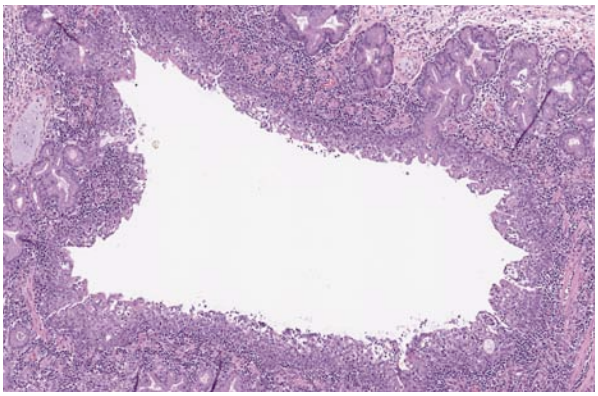

4-4. Lung, cat. Affected bronchiole is markedly ectatic, with profound hyperplasia of bronchiolar epithelium and an infiltrate of large numbers of lymphocytes, histiocytes, and neutrophils which througout all layers of the bronchiolar wall. (HE 300X)

Histopathologic Description: Lung: All lung lobes, with the exception of the caudal margin of the right caudal lung, are diffusely and severely affected. There is near complete effacement of alveolar spaces by neutrophils and macrophages with fewer lymphocytes and plasma cells. Alveolar septae are infiltrated and distended by macrophages and neutrophils and in some areas are completely obliterated. Some alveoli are lined by plump cuboidal epithelium (type II pneumocyte hyperplasia). A suppurative exudate fills distal airways making it difficult to distinguish lining epithelial cells. The larger airways are markedly dilated and filled with moderate amounts of neutrophils, macrophages and red blood cells. There is marked hyperplasia of the respiratory epithelium and exocytosis of intraepithelial neutrophils. There are minute, round, basophilic bacteria present on the cilia of bronchiolar epithelial cells (not present in all slides).

A moderate lymphoplasmacytic infiltrate is present in the submucosa of the bronchi and trachea, which is further expanded by edema. Multifocally there is erosion and ulceration of the epithelium covered by a thick layer of fibrin admixed with degenerate neutrophils.

Right caudal lobe (not submitted with case material): The section examined is nearly free of pathology with delicate alveolar walls and normal bronchioles. Multifocally there are small aggregates of neutrophils in alveolar and perivascular spaces. Scarce neutrophils and macrophages are present in alveolar spaces.

Tracheobronchial lymph node (slide 11, not present on all slides): Medullary sinuses and cords are expanded by numerous histiocytes. Multifocally there are discrete clear spaces containing tingible body macrophages. Numerous lymphocytes have pyknotic and fragmented nuclei (lymphocytolysis).

Contributor's Morphologic Diagnosis: Lung: bronchointerstitial pneumonia, pyogranulomatous, diffuse, subacute, severe, with bronchiectasis, localized necrosis and minute supraciliary bacteria.

Trachea: tracheitis, lymphoplasmacytic, necrosuppurative and ulcerative, diffuse, subacute, moderate.

Tracheobronchial lymph node: histiocytosis with lympholysis, diffuse, severe, subacute.

Contributor's Comment: Clinical signs in this case are attributed to co-infection with feline calicivirus and *Mycoplasma sp*. *Mycoplasma* species are common contributors to lower respiratory disease as single or contributory agents in pigs, cattle, and humans. In cats, *Mycoplasma* spp. are considered by many to be normal flora of the upper respiratory tract that can contribute to upper respiratory signs and ocular diseases. A single case report of a cat with primary, culminant pneumonia requiring mechanical ventilation is reported.[9] Three cats are included in a retrospective review of 17 cases of *Mycoplasma* respiratory infections in small animals at Colorado State.[5] In a retrospective study of lower respiratory infections in cats, 11 of 18 were attributed to primary *Mycoplasma* infection, another case was attributed to *Mycoplasma* and *Pasteurella multocida* coinfection, and the remaining 6 individual cases were attributed to various non- *Mycoplasma* bacterial, fungal and parasitic causes.[5]

Feline calicivirus is a common cause of both upper and lower respiratory disease in cats. Pneumonia is not uncommon and most cats recover. Classically described histologic lesions include hyaline membranes and neutrophilic and serofibrinous exudate in alveoli, not seen in this case. Additional gross findings including mucosal vesicles and ulceration

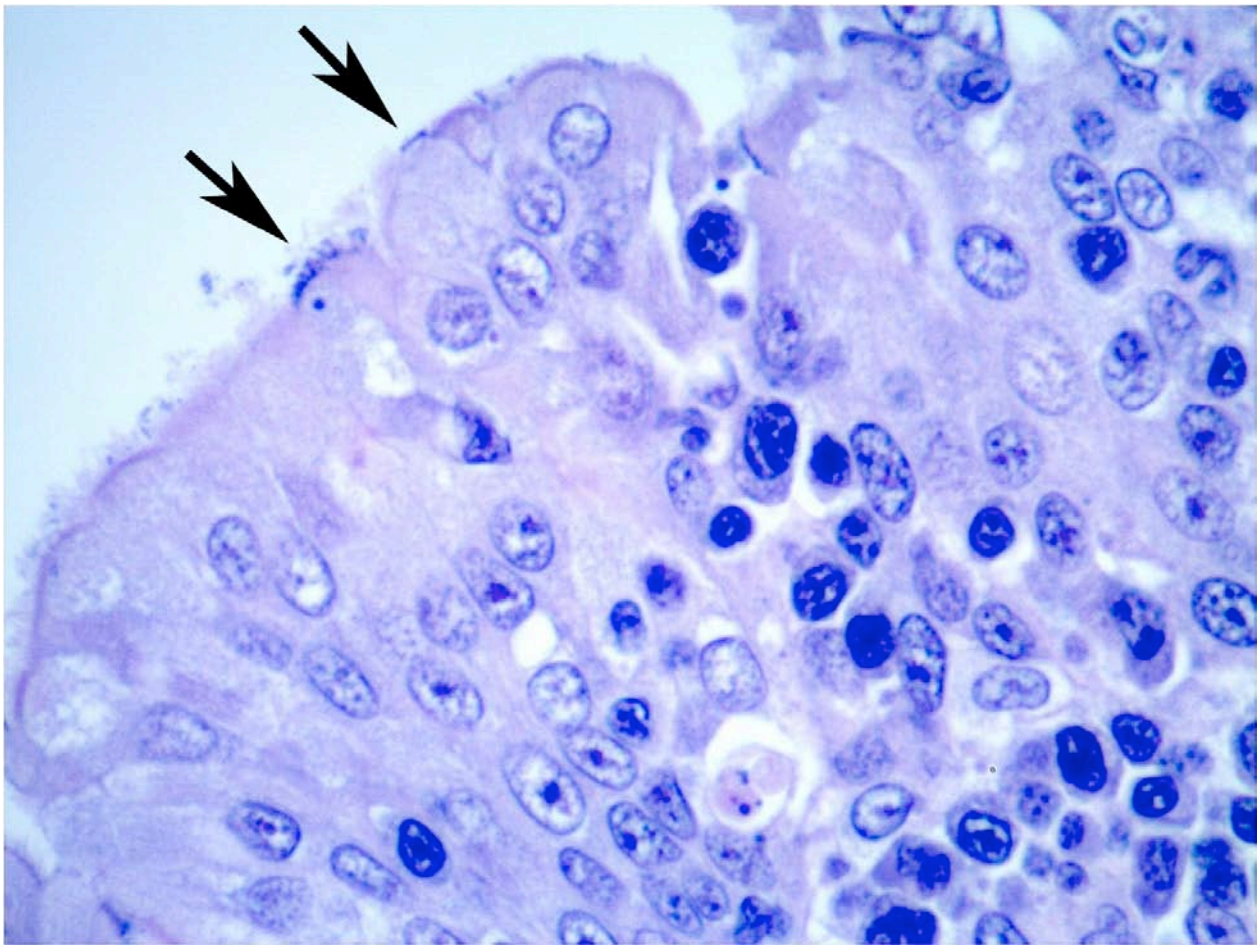

4-5. Lung cat. Small round basophilic bacilli within the cilia of bronchiolar epithelial cells. Photograph courtesy of the Department of Pathobiological Sciences, Univ. of Wisconsin School of Veterinary Medicine, http://www.vetmed.wisc.edu/home/.

were not seen in this case.[1] The vaccination status in this case is unclear, and the low CT value in this case could represent vaccine exposure rather than natural infection.

Bronchiectasis in cats is usually attributed to chronic bronchitis, bronchopneumonia, or pulmonary neoplasia.[2] A case series in 2000 reported chronic bronchitis and bronchiolitis, neoplasia, bronchopneumonia, endogenous lipid pneumonia and emphysema as the etiology in 12 adult cats.[7] The age of this cat could suggest a congenital ciliary dyskinesia. Diagnostic modality to examine ciliary function or ultrastructure are not routinely available as part of our diagnostic workup. In this case, the functional obstruction due to marked inflammatory infiltrate was interpreted as sufficient to explain the bronchiectasis.

Absent vascular or gastrointestinal lesions, the positive PCR finding for feline coronavirus is interpreted clinically insignificant.

Although this kitten was the only one of three kittens in the litter affected, a second kitten born to the same dam in a subsequent litter presented with similar clinical signs and gross pathology. In addition to similar lung findings, this 7-week-old male kitten presented a mediastinal, purulent abscess. Histology, microbiology and viral PCR on the second kitten are pending at the time of press.

JPC Diagnosis: 1. Lung: Pneumonia, bronchointerstitial and proliferative, neutrophilic and histiocytic, diffuse, marked with neutrophilic and lymphoplasmacytic bronchitis, bronchiolitis, bronchiectasis, and lymphoid hyperplasia.
2. Lymph node: Reactive hyperplasia, diffuse, moderate.

Conference Comment: This case demonstrates a combination of pneumonia patterns, which help elucidate the underlying etiologies. One pattern is centered on airways and is caused by *Mycoplasma sp.,* and the other is an interstitial pattern caused by feline calicicvirus. Mycoplasmas colonize the upper respiratory tract and are not thought to be a primary cause of disease; however, colonization of the respiratory epithelium results in degeneration of cilia

and ciliostasis, impedance of the mucocilary escalator and impaired clearance of microorganisms in the mucous blanket. Aerosolized feline calicivirus also causes upper respiratory disease as well as interstitial pneumonia and, in this case, impaired respiratory clearance secondary to mycoplasmal infection may have contributed to viral infection. Typically, acute infection with feline calicivirus results in type I pneumocyte lysis and the formation of hyaline membranes and, with chronicity, type II pneumocyte hyperplasia, fibrosis and increased numbers of lymphocytes and plasma cells within the alveolar interstitium, as is seen in this case.[1]

Mycoplasma cell membranes contain superantigens, which bind multiple T-cell receptors (TCR) and non-specifically stimulate the activation of large numbers of T-cells, resulting in lymphoid hyperplasia of the bronchiolar-associated lymphoid tissue (BALT), as is seen in this case. The subsequent massive immune response, which is not specific to any epitope, undermines the ability of the adaptive immune system to target antigens with a high degree of specificity. There is also a massive release of cytokines and resultant inflammatory response, resulting in further tissue damage.[8]

The moderator discussed how bronchiectasis, likely caused by inflammatory obstruction, predisposes the lung to secondary infections. Ectatic airways result in decreased airflow, which allows the settling of particulates and the deposition of microorganisms. Subsequent inflammation and hypoxia further exacerbates the bronchiectasis, continuing the cycle.

Conference participants also discussed the histologic difference between active bronchiolitis and the presence of a retrograde alveolar exudate. Active bronchiolitis is the observance of active inflammation at the level of the bronchiole, as well as corroborating evidence such as epithelial proliferation, inflammation in the adjacent interstium, and leukocyte transmigration. A retrograde alveolar exudate is simply the presence of an exudate within the bronchiole, likely an extension of an alveolar exudate, without any corroborating evidence of bronchiolar disease.

Some slides included sections of tracheobronchial lymph node with lymphocytolytic debris, likely caused either by stress or viral infection.

Contributor: University of Wisconsin – Madison
School of Veterinary Medicine
Department of Pathobiological Sciences
2015 Linden Drive West
Madison, WI 53706
http://www.vetmed.wisc.edu/home/

References:

1. Caswell J, Williams K. Infectious respiratory diseases of cats. In: Maxie M, ed. *Pathology of Domestic Animals*. 5th ed. vol 2. Philadelphia, PA: Elsevier Saunders, 2007:648-50.
2. Caswell J, Williams K. Bronchiectasis. In: Maxie M, ed. *Pathology of Domestic Animals*. 5th ed. vol 2. Philadelphia, PA: Elsevier Saunders; 2007:557-9.
3. Chandler J, Lappin M. Mycoplasmal respiratory infections in small animals: 17 Cases (1988-1999): *JAAHA*. 2002;38:111-119.
4. Foster S, Barr V, Martin P, et al. Pneumonia associated with Mycoplasma *spp* in three cats. *Aust Vet J.* 1998;76(7): 460-4.
5. Foster S, Martin P, Allan G, et al. Lower respiratory tract infections in cats: 21 cases (1995–2000): *J Feline Med Surg 6*:167–180, 2004.
6. Kumar V, Abbas AK, Fausto N. *Robbins and Cotran Pathologic Basis of Disease*. 7th ed. Philadelphia, PA: Elsevier Saunders; 2005.
7. Norris C, Samii V. Clinical, radiographic, and pathologic features of bronchiectasis in cats: 12 cases (1987–1999). *JAVMA*. 2000;216(4):530-534.
8. Stricker TP, Kumar V. Neoplasia. In: Kumar V, Abbas AK, Fausto N, Aster JC, eds. *Robbins and Cotran Pathologic Basis of Disease*. 8th ed. Philadelphia, PA: Saunders Elsevier; 2010:132.
9. Trow AV, Rozanski EA, Tidwell AS. Primary mycoplasma pneumonia associated with reversible respiratory failure in a cat. *J Feline Med Surg*. 2008;10:398-402.

Joint Pathology Center
Veterinary Pathology Services

WEDNESDAY SLIDE CONFERENCE 2011-2012

Conference 7

26 October 2011

CASE I: AFIP-3 (JPC 4004305).

Signalment: A 400 pound cross-bred calf (*Bos taurus*), age and gender unknown.

History: Lung and liver tissues of the calf have been submitted to the necropsy section of the ADRDL-SDSU with a history of respiratory signs ("Well vaccinated, small feedlot calves. Having trouble with *Mycoplasma* sp.?").

Gross Pathology: Gross necropsy results not reported.

Laboratory Results: *Mycoplasma* sp. and *H. somni* have been isolated from the lung.

The bovine virus isolation and the FA for BVD, IBR and BRSV results were negative.

Histopathologic Description: Lung: There is diffuse infiltration of neutrophils and accumulation of fibrin and edema fluid in the airways. There are multifocal pulmonary necrotic areas surrounded by a zone of the inflammatory cells, primarily neutrophils and fewer macrophages. In addition to that there is also diffuse infiltration of neutrophils and accumulation of fibrin in the pleura. The pulmonary blood vessels are congested.

Contributor's Morphologic Diagnosis: Bronchopneumonia, fibrino-suppurative, subacute, diffuse, severe, with multifocal areas of abscessation; diffuse fibrinosuppurative pleuritis.

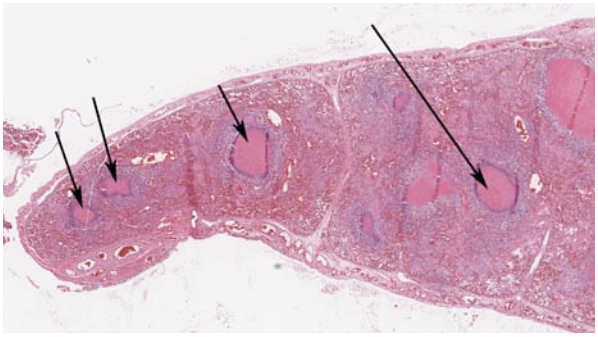

1-1. Lung, calf. Suppurative bronchiolitis and bronchiectasis at lobe margins in one section. (HE 40X)

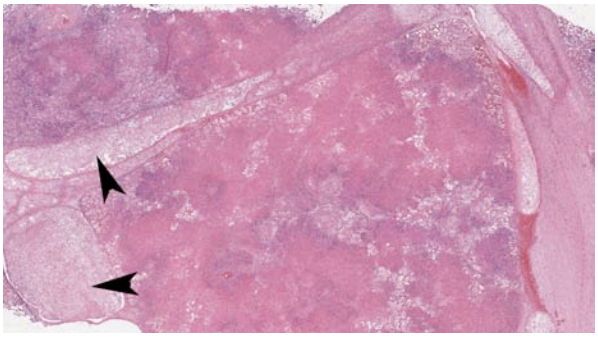

1-2. Lung, calf. Well-defined coalescing areas of coagulative necrosis are present throughout both sections; massive dilation of interstitial lymphatics by fibrin thrombi (arrowheads). (HE 40X)

Contributor's Comment: Calf pneumonia is one of the major problems in beef and dairy sectors. It is the most common post-mortem diagnosis in calves at 1-5 months of age. Although it is associated with low mortality, it is highly infectious in nature, affecting more than 50% of young calves. Affected calves suffer from low growth rate. It is a multifactorial disease including a number of bacterial, viral and fungal pathogens.

Calf pneumonia occurs due to a complex interaction between host, environment and pathogen. Young calves with low immunity are highly susceptible to this disease. Among various bacterial agents that cause pulmonary infections, *Mycoplasma* and Histophilus are most common.

Mycoplasma bovis was first reported in the United States in the 1970s. The high number of new cases was reported in the summer of 2000. After that, *M. bovis* has been found almost in every herd. A study conducted in 2006 revealed a 46% prevalence of *Mycoplasma bovis* in lungs of normal cattle.[3] Calves suffering from *Mycoplasma* pneumonia show low grade fever, tachycardia and mild depression.

H. somni is another important cause of bovine pneumonia.[1,4] *H. somni* is also associated with a wide variety of other cattle diseases including abortion, infertility and arthritis.[4] *H. somni* pneumonia is characterized grossly by grey to red consolidation of the cranio-ventral lung, involving from 5 to 80% of total lung volume.[1] Tracheobronchial and mediastinal lymph nodes are typically edematous, with fibrinous pleuritis seen irregularly.[1,3] Histologically, the suppurative necrotizing bronchopneumonia is the most common histopathologic identification of bacterial pulmonary infections.

Note: Multiple blocks were used for the slides submission; therefore not all the participants will get the same copy of the slides.

JPC Diagnosis: 1. Lung: Pleuropneumonia, fibrinosuppurative and necrotizing, diffuse, severe, with marked intralobular edema and lymphatic fibrin thrombi.
2. Lung: Bronchopneumonia, fibrinosuppurative and necrotizing, with marked suppurative bronchilitis and bronchiectasis.

Conference Comment: There was marked slide variation, and some slides did not contain both sections of lung. The two sections of lung demonstrated the distinctly different histomorphologies of each entity.

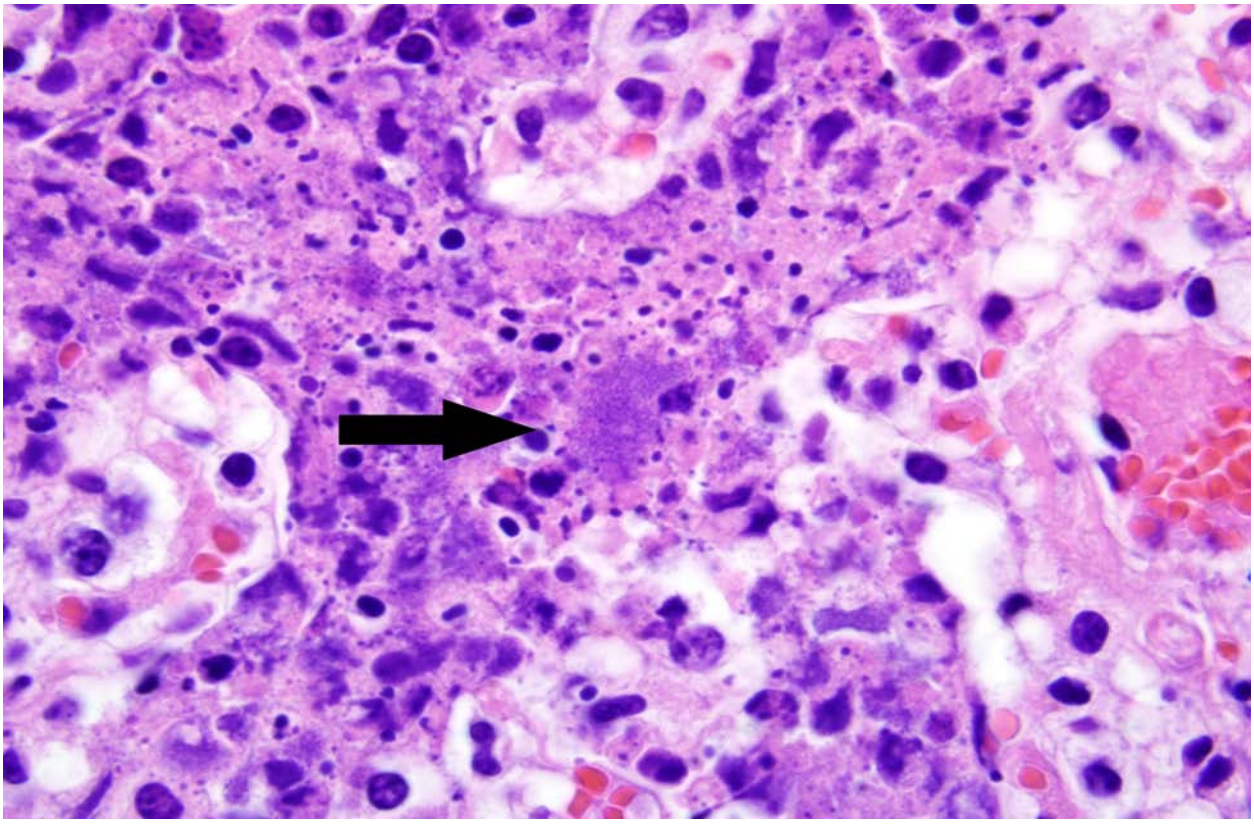

1-3. Lung, calf. Rare colonies of bacilli consistent with Histophilus somni are present within areas of necrosis (arrow). (HE 1000X)

One section contains multiple ectatic bronchioles filled with caseonecrotic material within areas of profound atelectasis characteristic of mycoplasmal pneumonia. Bronchiolar-associated lymphoid tissue (BALT) is depleted, which is characteristic of enzootic bovine pneumonia. Affected cattle often present with otitis media, as *Mycoplasma* preferentially colonize areas of the body lined by ciliated epithelium (such as airways).

The other section of lung exhibits necrosuppurative bronchopneumonia, which is more typical of gram-negative bacteria, such as *Mannheimia haemolytica or Histophilus somni.* In affected lungs, alveoli are filled with fibrin and leukocytes and larger areas of coagulative necrosis may become sequestra. Grossly, affected areas of lung will be sharply demarcated from adjacent lung, and the presence of large amounts of fibrin and cellular exudate will give it a firm feel.[2]

Contributor: ADRDL-Veterinary & Biomedical Sciences Department
South Dakota State University
Box 2175
North Campus Drive
Brookings, SD 57007-1396
http://www.sdstate.edu/vs/

References:

1. Andrews JJ, Anderson TD, Slife LN, et al. Microscopic lesions associated with the isolation of Haemophilus somnus from pneumonic bovine lungs. *Vet Pathol*. 1985;22:131-136.
2. Caswell JL, Williams KJ. Respiratory system. In: Maxie MG, ed. *Jubb, Kenedy, and Palmer's Pathology of Domestic Animals*. 5th ed. Philadelphia, PA: Saunders Elsevier; 2007:601-5, 610-5.
3. Gagea MI, Bateman KG, van Dreumel T, et al. Diseases and pathogens associated with mortality in Ontario beef feedlots. *J Vet Diagn Invest*. 2006;18:18-28.
4. Kwiecien JM, Little PB. Haemophilus somnus and reproductive disease in the cow: A review. *Can Vet J*. 1991;32: 595-601.

CASE II: NIAH-2 (JPC 3133973).

Signalment: 5-year 3-month-old female Japanese native breed goat, (*Capra aegagrus*).

History: A Japanese native breed goat showed respiratory symptoms including tachypnea and cough. Three months later, the goat developed mild carpal swelling. At the time, the serum was negative for caprine arthritis-encephalitis (CAE) virus. Two months later, many nodules resembling abscesses, up to 10 cm in diameter, developed in the mammary gland and lip. The goat was submitted for necropsy.

Gross Pathology: The goat was in poor body condition. The lung had distinctive pale firm lesions with ecchymosis throughout the lung. Both carpal joints had mild swelling. Many abscesses were seen in the mammary gland.

Histopathologic Description: Lung: The foci in the lung were demarcated from relatively unaffected areas. Distinctive cuffs consisting of lymphocytes and plasma cells were formed around blood vessels and airways. Alveolar septa were thickened with infiltrates of lymphocytes and the hyperplasia of type II pneumocytes. Alveoli were filled with eosinophilic fluid, small amounts of fibrin, neutrophils and macrophages. Occasionally, macrophages phagocytizing eosinophilic fluid were seen.

Both carpal joints had arthritis and periarthritis characterized by the villous proliferation of the synovial membrane, lymphoplasmacytic infiltration and necrosis of the tendon sheath.

In mammary glands, periductal infiltration of lymphocytes and many abscesses were observed. No lesion was found in the central nervous system.

Immunohistochemically, the eosinophilic materials in alveoli were positive for anti-surfactant protein A antibody (Chemicon). Furthermore, immnohistochemical examination with anti-CD3 (DAKO), anti-CD79a (DAKO), anti-CD68 (DAKO) antibodies showed that most of the lymphocytes around blood vessels and airways were T-lymphocytes that can relate to the cell-mediated immunity. *Pasteurella multocida* antigens were detected in the area of bronchopneumonia. Immunohistochemical detection of CAE virus antigens was not successful.

Contributor's Morphologic Diagnosis: Lung: Pneumonia, interstitial, lymphocytic, with perivascular and peribronchial lymphoplasmacytic infiltration, type

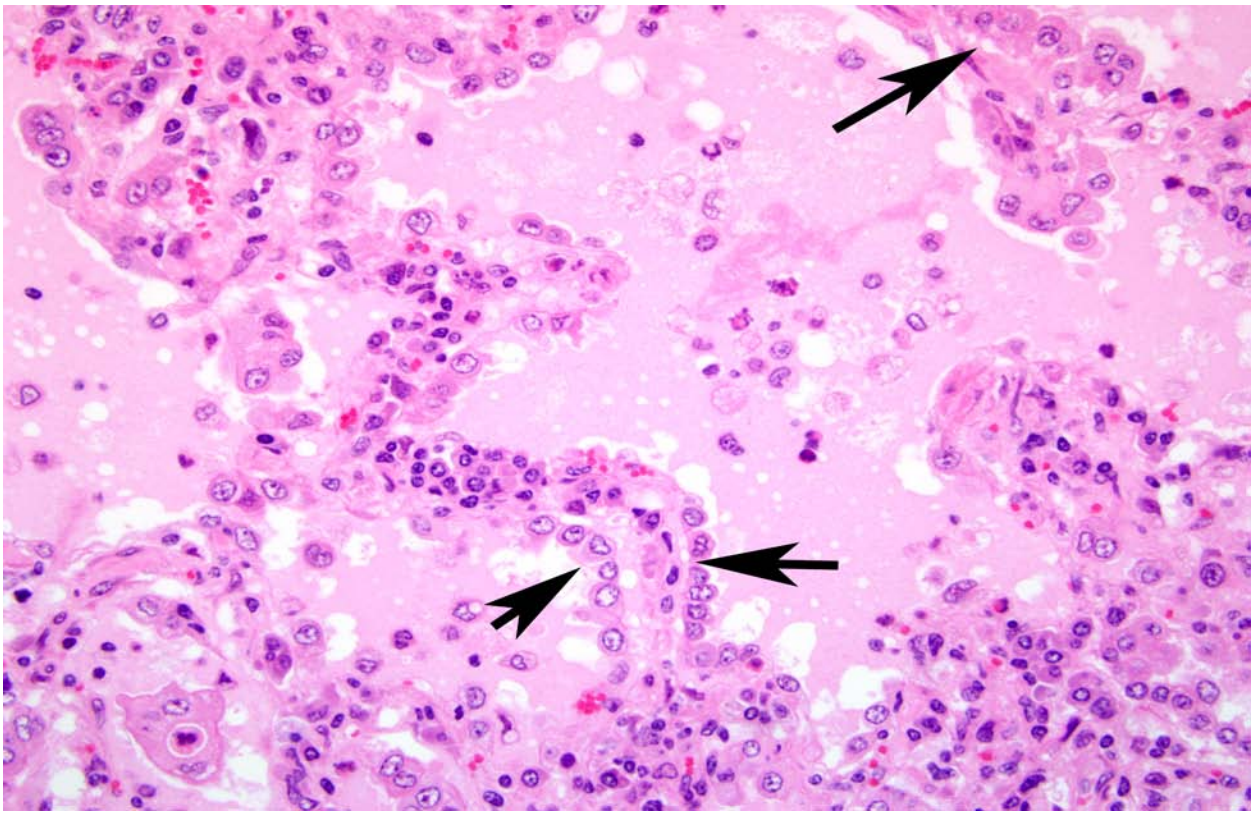

2-1. Lung, goat. Diffuse expansion of alveolar septa and type II pneumocyte hyperplasia (arrows); alveolar lumina are filled with abundant eosinophilic proteinaceous fluid (not just edema). (HE 400X)

II pneumocyte hyperplasia and intra-alveolar eosinophilic proteinaceous materials.
Etiology: CAE.

Contributor's Comment: CAE is a progressive disease of domestic goats caused by the CAE virus and belongs to Lentivirinae of the family Retroviridae. The first case was identified in USA in 1974. In Japan, the first case was identified in 2002.[2] Most infected goats develop subclinical disease. However, affected adult goats may develop the chronic arthritis and mastitis, occasionally leading to the pneumonia and encephalitis. World Organization for Animal Health recommends serological diagnosis like AGID test and ELISA.[7] In addition to these tests, histopathological diagnosis is definitive for CAE.

The lesions of the lung in the present case consisted of those of typical CAE which are characterized by the lymphoplasmacytic infiltration in septa with the type II pneumocyte hyperplasia, infiltration of lymphocytes around blood vessels, bronchi, and bronchioles, and eosinophilic exudates in alveoli.[1,4] Distinctive eosinophilic fluid is an important finding for differential diagnosis between CAE and maedi.[4]

The present case had lymphoplasmacytic arthritis and periarthritis with villous proliferation of the synovium, which are suggestive of CAE.[6] In the mammary gland, many abscesses and periductal cuffs consisting of lymphocytes were seen. Unlike abscesses caused by *Arcanobacterium pyogenes* infection, the infiltration of lymphocytes around ducts was a characteristic finding of the nonsuppurative mastitis caused by CAE virus.[5]

Although the serum was weakly positive for CAE virus antibody by AGID test, pathological findings in this case were identical to those of CAE virus infection. *Pasteurella multocida* infection of the lung might be a secondary infection to CAE.

JPC Diagnosis: Lung: Pneumonia, interstitial, lymphohistiocytic, diffuse, moderate, with marked pulmonary edema, peribronchial and perivascular lymphohistiocytic infiltrates, and type II pneumocyte hyperplasia.

Conference Comment: CAE is primarily transmitted through infected colostrum and milk, and manifests as either nonsuppurative leukoencephalomyelitis in kids or nonsuppurative arthritis and synovitis in adult goats. Pneumonia and mastitis are less frequently seen. There is B cell hyperplasia of BALT and marked tracheobronchial lymphadenomegaly.[4]

Conference participants discussed the primary differential diagnosis for nonsuppurative interstitial pneumonia in sheep and goats, and a primary consideration for many was ovine progressive pneumonia (OPP) - also known as "maedi", to which goats are also susceptible, and which is more common than the pneumonia form of CAE in the United States. One difference between OPP and CAE is that type II hyperplasia and eosinophilic alveolar fluid is not a prominent feature of OPP. Additionally, type II pneumocyte hyperplasia is not prominent in OPP because the type I pneumocytes remain uninjured.[4] Both have a typical gross appearance of heavy, rubbery, pale gray lungs that fail to collapse. Another consideration for the florid type II pneumocyte hyperplasia seen in this case is ovine pulmonary adenomatosis caused by ovine retrovirus (also known as "jaagsiekte sheep retrovirus - JSRV), which rarely affects goats.[1] An associated clinical sign of jaagsiekte is the drainage of fluid from the nose following elevation of the hind limbs. A final cause of lymphocytic interstitial pneumonia in sheep and goats is parasitic pneumonia caused by *Meullerius capillaris*.

The section of lung in this case demonstrates a typical histologic appearance of CAE and other lentiviruses affecting sheep and goats, with a sharp demarcation between affected and unaffected lung. The copious proteinaceous fluid filling the alveoli in this section is visually distinct from edema fluid, and is also very characteristic of this disease. The moderator pointed out that there was no corroborative evidence to attribute the prominent eosinophilic fluid to hydrostatic edema, such as dilated lymphatics and rarefaction around blood vessels. This fluid has been shown to contain pulmonary surfactant, which is consistent with the abundant type II pneumocyte hyperplasia. As the virus destroys type I pneumocytes, and type II pneumocytes proliferate, the local environment becomes hypoxic due to the thickening of the interstitium, which also fills with lymphocytes, plasma cells, and macrophages. As the diffusion capacity of the lung decreases, cells release hypoxia-induced factor-1α, which activates the transcription of vascular endothelial growth factor, increasing vascular permeability and the leakage of high protein plasma fluid.[3] The interstitial pneumonia seen with CAE results from infected macrophages expressing IL-8, which recruits additional inflammatory cells, perpetuating the inflammatory cycle.[8]

Contributor: National Institute of Animal Health
3-1-5 Kannondai
Tsukuba, Ibaraki
305-0856 Japan

References:

1. Caswell JL, Williams KJ. Lentiviral pneumonia: maedi-visna (ovine progressive pneumonia) and caprine arthritis-encephalitis viral pneumonia. In:

Maxie MG, ed. Pathology of Domestic Animals. 5th ed. vol. 2. Edinburgh, UK: Saunders; 2007:618-620.
2. Konishi M, Tsuduku S, Haritani M, et al. An epidemic of caprine atthritis-encephalitis in Japan: Isolation of the virus. *J Vet Med Sci*. 2004;66:911-917.
3. Kumar V, Abbas AK, Fauster N, et al. Cellular response to stress and toxic insults: adaptation, injury, and death. In: Kumar V, Abbas AK, Fauster N, Aster JC, eds. *Robbins and Cotran Pathologic Basis of Disease*. 8th ed. Philadelphia, PA: Saunders Elsevier; 2010:45.
4. López A. Respiratory system, mediastinum, and pleura. In: McGavin MD, Zachry JF, eds. *Pathologic Basis of Veterinary Disease*. 4th ed. St. Louis, MO: Mosby; 2011:517-18.
5. Phelps SL, Smith MC. Caprine arthritis-encephalitis virus infection. *J Am Vet Med Assoc*. 1993;203:1663-1666.
6. Thompson K. Viral arthritis. In: Maxie MG, ed. *Pathology of Domestic Animals*. 5th ed. vol. 1. 2007:170-171. Edinburgh, UK: Saunders.
7. World Organization for Animal Health: Caprine arthritis-encephalitis and Maedi-visna. In: OIE manual of diagnostic tests and vaccines for terrestrial animals 2008, Chapter 2.7.3/4. [cited 2009 Jun 1]. Available from http://www.oie.int/eng/normes/mmanual/2008/pdf/2.07.03-04_CAE_MV.pdf
8. Zachary JF. Mechanisms of microbial infections. In: McGavin MD, Zachry JF, eds. *Pathologic Basis of Veterinary Disease*. 4th ed. St. Louis, MO: Mosby; 2011:216.

CASE III: 08VD29987B (JPC 3134635).

Signalment: Porcine (*Sus domestica*), 50-60 lbs pigs (approximately 9 weeks of age), crossbreed (unknown), gender unknown (tissues were received for diagnostic evaluation).

History: Sudden death.

Gross Pathology: N/A (tissues were received for diagnostic evaluation).

Laboratory Results:
Bacteriology: *Streptococcus suis* and *Arcanobacterium pyogenes* were isolated from lung. Kidney was not cultured (only fixed renal tissue was received)
Mycoplasma hyopneumoniae PCR was negative (lung)

Virology: PRRSV PCR was negative (lung)
SIV PCR was negative (lung)
PCV2 IHC was **positive** (abundant staining, in kidney, spleen, and lymph node)

Histopathologic Description: Kidney: Renal interstitium is multifocally infiltrated by marked inflammatory cells and modest amounts of fibrous connective tissue that frequently coalesce and form linear streaks that extend from the capsule to the medulla. Lymphocytes, plasma cells, macrophages, lesser eosinophils, edema, and scant fibrin separate frequently dilated tubules, surround multifocal glomerular tufts, or cuff arterioles within the cortex and at the corticomedullary junction. Dilated tubules are lined by lost, flattened, swollen (degeneration), or necrotic epithelium that occasionally contain intracytoplasmic basophilic botryoid inclusion bodies ranging in size from 1-5 µm. Proteinic fluid, karyorrhectic cellular debris, and sloughed renal tubular epithelium containing cytoplasmic inclusion bodies are present within multifocal tubular lumens. Multifocally, there is complete loss of tubules (atrophy) or tubules are lined by crowded or stacked epithelium (regeneration). Corticomedullary arterioles are frequently accentuated by proliferation of the tunic intima and smooth muscle hypertrophy and hyperplasia of the tunic media. Blood vessels within the cortex are frequently congested and infrequently contain myriad 1µm coccoid bacteria, and there is mild multifocal hemorrhage. Glomerular tufts are multifocally congested, and mildly hypersegmented and hypercellular.

Contributor's Morphologic Diagnosis: 1. Kidney. Tubulointerstitial nephritis, lymphoplasmacytic and macrophagic, multifocal, severe, chronic with fibrosis and tubular loss, degeneration, necrosis, and regeneration, and botryoid intraepithelial cytoplasmic inclusions (etiology consistent with porcine circovirus type II infection).
2. Kidney. Arteritis, proliferative and perivascular, lymphocytic, multifocal, severe, chronic with intimal and tunic medial proliferation.
3. Kidney. Intravascular coccoid bacteria, multifocal, acute.

Contributor's Comment: In recent years, there has been a marked increase in the number of porcine circovirus associated disease (PCVAD) cases at the Iowa State Veterinary Diagnostic Laboratory. Affected pigs often have classical lesions of lymphoid depletion, interstitial pneumonia, and interstitial nephritis. The severity of these microscopic lesions depends greatly on the timing of viral infection. Interstitial nephritis typically begins with a perivascular accumulation of macrophages, lymphocytes, and fewer plasma cells adjacent to large vessels at the corticomedullary junction. In time, the mononuclear infiltrate extends to

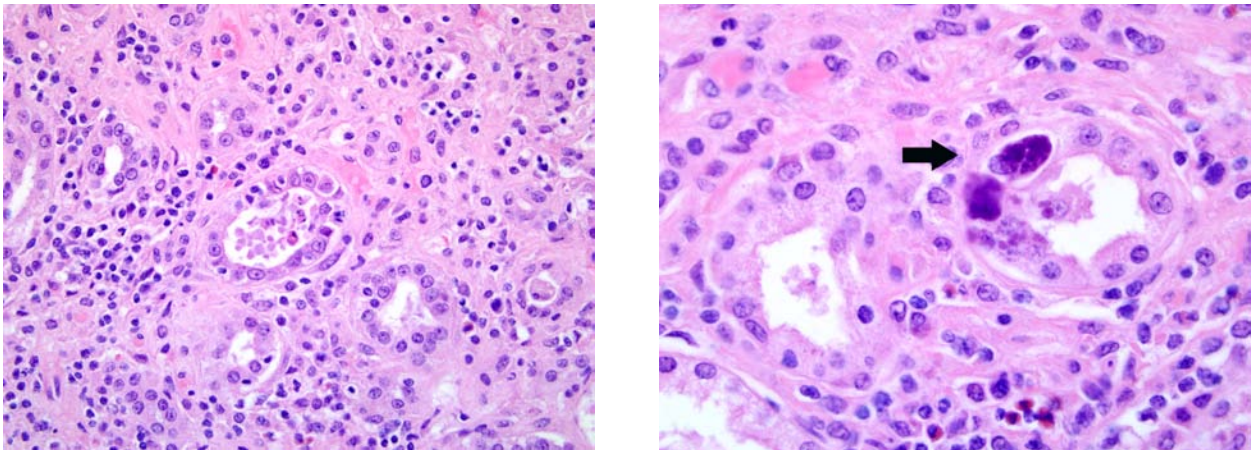

3-1, 3-2. Kidney, pig. Tubules are widely separated by interstitial fibrosis containing moderate numbers of lymphocytes and histiocytes. Multifocally, tubules are filled with necrotic tubular epithelium, or lined by more basophilic, closely spaced epithelial cells. Tubular epithelial cells occasionally contain basophilic, botryoid cytoplasmic inclusions (arrows). (HE 400X)

the cortical interstitium and to a lesser degree to the medulla. Inflammatory cells separate adjacent tubules and occasionally surround glomerular tufts. Renal tubular epithelium is frequently degenerative, sloughed, or regenerative and lumina can contain protein or cellular casts. Another feature that is occasionally seen (often depending on timing of viral infection) are basophilic intracytoplasmic botryoid inclusion bodies.[5] In this particular case, sudden death of the pig was likely due to bacterial septicemia which was predisposed by PCV2 infection. One can only speculate that PCV2 infection may have occurred 2-4 weeks prior to sudden death. Porcine circoviruses (PCV) are non-enveloped, single-stranded, circular DNA viruses of approximately 1.7kb classified in the *Ciroviridae* family, genus *Circovirus*. There are two known PCV species, porcine circovirus type 1 (PCV1) and porcine circovirus type 2 (PCV2). PCV1 was first described in 1974 as a non-cytopathic contaminate of a porcine kidney cell line, PK-15. Experimental studies later determined that PCV1 was non-pathogenic in swine. In contrast, PCV2 is pathogenic in swine and associated with multiple disease entities.

PCV2 is globally distributed and most herds are seropositive for anti-PCV2 antibodies.[7] PCV2 infection occurs as maternally derived antibodies wane in post-weaned pigs (7-15 weeks of age) and results in either subclinical infection or clinical disease. Clinical disease associated with PCV2 infection can have multiple manifestations which include the following: post-weaning multisystemic wasting syndrome (PMWS), respiratory disease, enteritis, porcine dermatitis and nephropathy syndrome (PDNS), myocarditis/vasculitis, and exudative dermatitis.[1,2] Porcine circovirus associated disease (PCVAD) is more common terminology used in North America to summarize the different clinical manifestations associated with PCV2 infection.[7]

Subclinical disease: PCV2 can be detected in normal, healthy pigs without signs of disease. Subclinical PCV2 infection can reduce growth performance, can cause increased susceptibility to other swine-associated pathogens, or result in decreased efficacy of commonly administered swine vaccines.[7] Quantification of PCV2 DNA in serum and tissue has been proposed as a

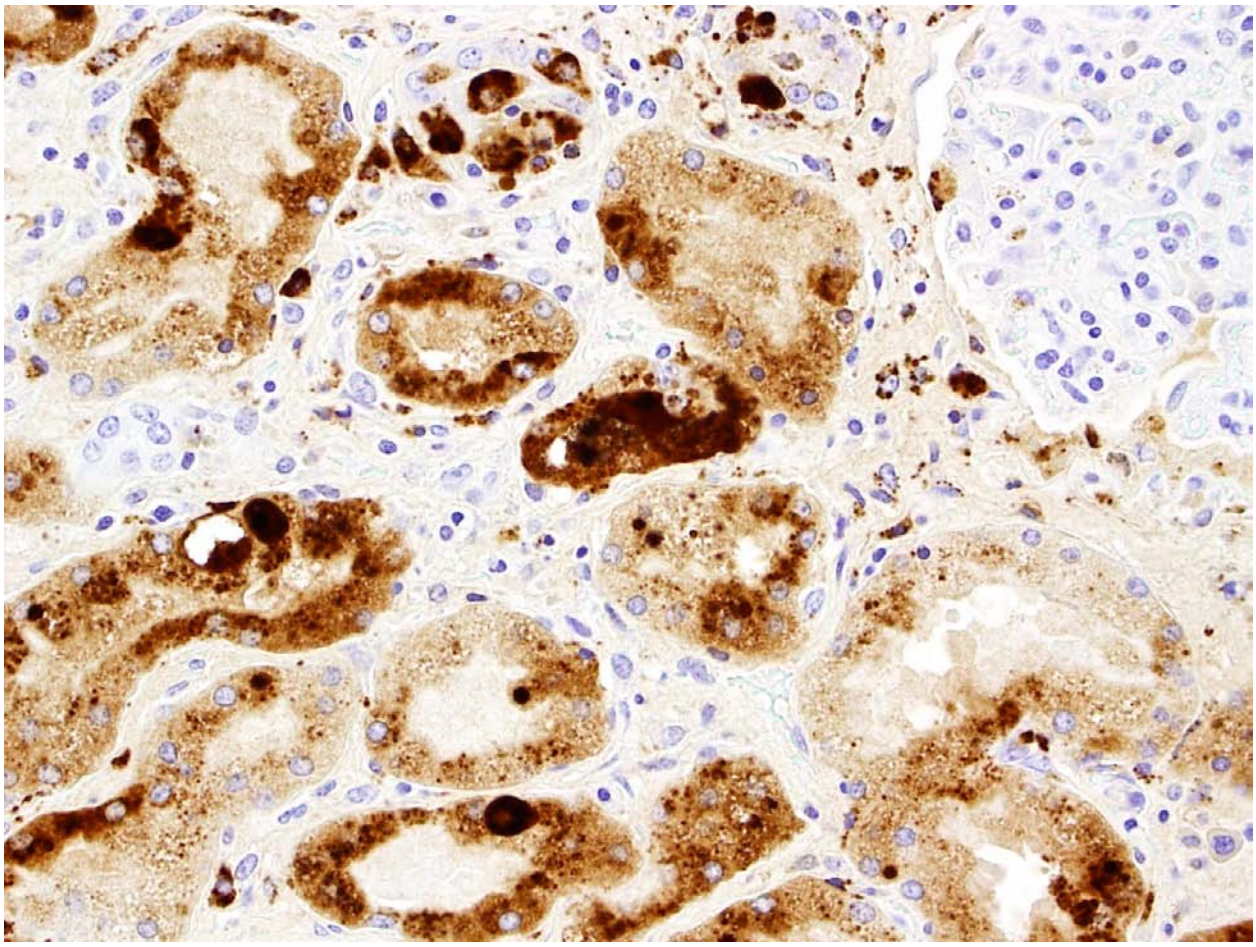

3-3. Kidney, pig. Renal tubular epithelium demonstrates positive cytoplasmic immunoreactivity for porcine circovirus 2 antigen. Photograph courtesy of Iowa State University College of Veterinary Medicine, Department of Veterinary Pathology, http://www.vetmed.iastate.edu/departments/vetpath/. (200X)

means of differentiating subclinical from clinically affected animals. Subclinically infected PCV2 pigs typically have lower amounts of DNA in serum and tissue ($\geq 10^7$ genomic copies per ml/serum or tissue).

Post-weaning multisystemic wasting syndrome (PMWS): PMWS is a multifactorial systemic disease and clinically manifests at 25-150 days of age with most cases occurring between 7 and 15 weeks. Six fundamental clinical signs are emphasized and include wasting, dyspnea, lymphadenopathy, diarrhea, pallor and jaundice. Coughing, pyrexia, gastric ulceration, and meningitis have also been reported, but are sporadic. Not all clinical signs have to be present in an individual pig, but all six fundamental signs can generally be observed among the population of pigs in affected herds over time.[4] Herd morbidity in PMWS herds is variable with 4-30% of the pigs affected. Mortality rates are often high (20%) with occasional reports of greater than 50% death loss within a group. The most consistent necropsy finding in PMWS pigs is generalized lymph node enlargement. Other macroscopic lesions can include mottled tan non-collapsing lungs and thymic atrophy. PMWS pigs are frequently coinfected with other common bacterial and viral pathogens, and coinfection often complicates gross findings.

Microscopic lesions in PMWS-affected pigs are consistently found in lymphoid tissues and characterized by loss (depletion) of lymphocytes and replacement by histiocytic/granulomatous inflammation. Lymphoid depletion can be associated with paracortical or follicular regions with the latter being more prevalent. Multinucleated giant cells (Langhans-type), epithelioid macrophages and macrophage-associated intracytoplasmic, botryoid-like, basophilic inclusions are also commonly seen in lymphoid tissues (lymph node, tonsil, and spleen). Focal parenchymal coagulative and apoptotic necrosis in lymphoid tissues has also been described. Microscopic lesions in non-lymphoid tissues are composed of lymphomacrophagic inflammation and include interstitial pneumonia, hepatitis, interstitial nephritis and enteritis/colitis.

Clinical signs along with macroscopic and microscopic lesions associated with PCV2 infection are suggestive, but not definitive for a PMWS diagnosis in an individual or group of pigs. A definitive diagnosis of PMWS is based on the following definition: (1) clinical signs of wasting, weight loss or failure to thrive that may or may not include respiratory distress and icterus, (2) microscopic lesions of lymphoid depletion and granulomatous inflammation, and (3) the presence of PCV2 antigen or nucleic acid associated with microscopic lesions.[8] Not all PMWS-affected pigs will have equal distribution of microscopic lymphoid lesions.

PCV2-associated respiratory disease: PCV2-associated respiratory disease can often overlap with PMWS or be a contributing factor in porcine respiratory disease complex (PRDC). In the first cases of PMWS, lymphomacrophagic interstitial pneumonia was a common microscopic lesion. Other hallmark microscopic lung lesions of PCV2 include type II pneumocyte hypertrophy and hyperplasia, peribronchiolar fibrosis, and associated lymphoid hyperplasia.[2]

PCV2-associated enteritis: The suspected major route of PCV2 transmission is fecal-oral, suggesting that the alimentary mucosa, intestinal M-cells, and gut-associated lymphoid tissue (GALT; Peyer's patches) are exposed to varying amounts of infectious virus. Peyer's patches can exhibit hallmark microscopic lesions of lymphoid depletion and granulomatous inflammation in both PCV2-associated enteritis and PMWS-affected pigs. The diagnosis of PCV2-associated enteritis is appropriate when (1) there is clinical diarrhea, (2) the hallmark microscopic lesions are present in Peyer's patches but not in other lymphoid tissues, and (3) PCV2 DNA or antigen can be demonstrated within the lesions.[2]

PCV2-associated enteritis may occur anytime in the grow-finish phase, and can be associated with the small or large intestine. Affected intestinal segments are sometimes thickened and necrotic resembling gross lesions of *Lawsonia intracellularis* infection and can be misdiagnosed as such. Microscopically, PCV2-associated enteritis has been described as having variable amounts of macrophages infiltrating the mucosa with PCV2 antigen present in crypt epithelium, the lamina propria, and submucosa. Villous atrophy and fusion along with multinucleated giant cells within the lamina propria have also been described.

Porcine dermatitis and nephropathy syndrome (PDNS): PDNS is a distinctive, acute clinical entity of growing swine that was first recognized in 1993 and is now globally distributed.[2] Affected pigs have circular to coalescing, red to purple macules or raised papules and plaques, occasionally with black centers, that originate on the skin of the hind legs and perineal region. Lesions may become exudative, crust-over, and eventually regress leaving dermal scars. Bilateral swollen kidneys with widely disseminated cortical petechial hemorrhages are common features of the syndrome. Increased mortality is seen in affected pigs older than three months of age, the syndrome is sporadic, and herd-outbreak mortality can range from 0.25 to > 20%.

The hallmark microscopic lesion in PDNS-affected pigs is necrotizing vasculitis and glomerulonephritis. Small to medium sized dermal and subcutaneous arterioles are cuffed by neutrophils, macrophages, lymphocytes, and plasma cells that are sometimes present within vascular walls. Arterioles are lined by plump endothelial cells, occasionally occluded by fibrin thrombi and walls can display multifocal hyalinization. The corresponding dermis is necrotic and hemorrhagic. Kidney sections are characterized by distension of urinary spaces by fibrin intermixed with necrotic cellular debris and hemorrhage, periglomerular and interstitial mononuclear cell infiltration, and distension of renal tubules that contain cellular and proteinaceous casts. Perirenal lymph nodes are sometimes depleted and hemorrhagic.

Skin and glomerular lesions are characteristic of a type III hypersensitivity reaction with deposition of antigen-antibody complexes (immune complexes). Immune complexes have been demonstrated in glomerular tufts. Multiple viral and bacterial pathogens have been implicated in PDNS, but PCV2 is considered a contributing factor. To date, PDNS has not been reproduced with PCV2 infection.

JPC Diagnosis: 1. Kidney: Nephritis, interstitial, lymphohistiocytic, diffuse, moderate, with tubular degeneration, necrosis, and regeneration, granular and cellular casts, intraepithelial intracytoplasmic botryoid inclusions, and proliferative, eosinophilic and histiocytic arteritis.
2. Kidney, glomeruli and vasa recta: Intravascular bacterial emboli.

Conference Comment: The contributor has provided an excellent and comprehensive overview of circovirus-associated disease in swine.

A central nervous system manifestation of PCV2 infection is cerebellar hemorrhage and edema from necrotizing and lymphohistiocytic vasculitis and thrombosis. Gross findings include multiple cerebellar petechiae and fibrinopurulent meningitis. PCV2 antigen has been demonstrated in macrophages and cerebellar endothelial cells in affected areas.[3]

A differential diagnosis discussed by conference participants is leptospirosis, which results in clinical illness in only a small portion of infected swine. The primary effect on swine is abortion and the birth of weak piglets, but leptospirosis may also result in interstitial nephritis and renal papillitis with infiltration by mononuclear cells and numerous bacteria in the medulla.[6]

Contributor: Iowa State University
College of Veterinary Medicine
Department of Veterinary Pathology
http://www.vetmed.iastate.edu/departments/vetpath/

References:
1. Chae C. Postweaning multisystemic wasting syndrome: a review of aetiology, diagnosis and pathology. *Vet J 168*. 2004;41-49.
2. Chae C. A review of porcine circovirus 2-associated syndromes and diseases. *Vet J*. 2005;169:326-336.
3. Correa AM, et al. Brain lesions pigs affected with postweaing multisystemic wasting syndrome. *J Vet Diagn Invest*. 2007;19:109-12.
4. Harding JC. The clinical expression and emergence of porcine circovirus 2. *Vet Microbiol*. 2004;98:131-135, 2-4.
5. Huang YY, Walther I, Martinson SA, et al. Porcine circovirus 2 inclusion bodies in pulmonary and renal epithelial cells. *Vet Pathol*. 2008;45:640-644.
6. Maxie MG, Newman SJ. Urinary system. In: Maxie MG, ed. *Jubb, Kenedy, and Palmer's Pathology of Domestic Animals*. 5th ed. Philadelphia, PA: Saunders Elsevier; 2007:487-9.
7. Opriessnig T, Meng XJ, Halbur PG. Porcine Circovirus Type 2 associated disease: Update on current terminology, clinical manifestations, pathogenesis, diagnosis, and intervention strategies. *J Vet Diagn Invest.* 2007;19:591-615.
8. Sorden SD. Update on porcine circovirus and postweaning multisystemic wasting syndrome (PMWS). *Swine Hlth Prod*. 2000;8:133-136.

CASE IV: IPTA Berne Case 1 (JPC 3164992).

Signalment: 4-month-old male calf (*Bos primigenius taurus*).

History: The animal is from a dairy farm and presented for necropsy in October 2009. Clinical signs included fever and bloody diarrhea. Antibiotic treatment was attempted but the animal died after two days from the onset of the clinical signs. Vaccination history was unknown and the animal tested negative for Bovine Viral Diarrhea virus as required by the eradication program (October 2009).

Gross Pathology: A general poor body condition was noted at necropsy. The small and large intestines contained a large amount of fibrino-hemorrhagic exudates. The mucosa was edematous and hyperemic with multifocal, pinpoint areas of necrosis more evident at the level of the Peyer's patches with occasional wider foci of ulceration.

Laboratory Results: Bacteriology for *Salmonella* spp. was negative. Virology for BVDV (Ag ELISA method) was negative.

Histopathologic Description: Small and large intestine sections: The lymphoid follicles at the level of the Peyer's patches contain large areas of necrosis characterized by hypereosinophilic cellular debris mixed with fibrinous exudate. Lymphocytolysis is evident in the more preserved lymphoid follicles. Numerous intranuclear, basophilic to amphophilic, completely or partially filling the nuclei, round to oval inclusion bodies are present in the endothelial cells of mucosal and submucosal small blood vessels. Multifocally, the mucosa shows loss of tissue architecture and cellular detail; replaced by hypereosinophilic cellular debris (coagulative necrosis) mixed with fibrin and extravasated erythrocytes (hemorrhage). Moderate edema is present in the submucosa adjacent to the lymphoid tissue. Multifocally, few crypts are markedly dilated and filled with necrotic epithelial cells, viable and degenerate neutrophils and, occasionally mucinous material (crypt abscesses). In some places this is associated with the herniation of the overlying mucosal glands into the necrotic lymphoid centers. Few foci of granulation tissue are present around some lacunar spaces filled with neutrophilic exudates in the submucosa (cecum). In the new-formed blood vessels of the granulation tissue are visible intranuclear inclusion bodies. Distended lymphatic vessels (edema) are scattered throughout the muscular layer. Bacterial colonies (not present in all sections) are associated with the necrotic mucosa and present within the inflamed herniated cystic glands.

Contributor's Morphologic Diagnosis: 1. Enterocolitis, multifocal, necrotizing and fibrino-hemorrhagic, severe, acute with severe Peyer's patch necrosis and intranuclear inclusion bodies (adenoviral type). 2. Colitis, multifocal, submucosal, neutrophilic, chronic moderate with granulation tissue formation and intralesional bacterial colonies.

Contributor's Comment: After human and fowl adenoviruses, bovine adenoviruses (BAdVs) present the third largest group of adenoviruses originating from one host species.[7] They have been classified into two separate genera: Atadenovirus (namely types 4-8) and Mastadenovirus (types 1-3 and 9). The most recently described, BAdV 10, is the cause of a well-defined disease in cattle, particularly in calves, characterized by acute severe fibrinous, necrotizing and hemorrhagic enterocolitis of worldwide occurrence.[1,6,7] Another uncommon characteristic of this virus is the variation in the genome size of various isolates, which justifies its classification as a separate BAdV species.[1,4] Electron microscopical examination showed the

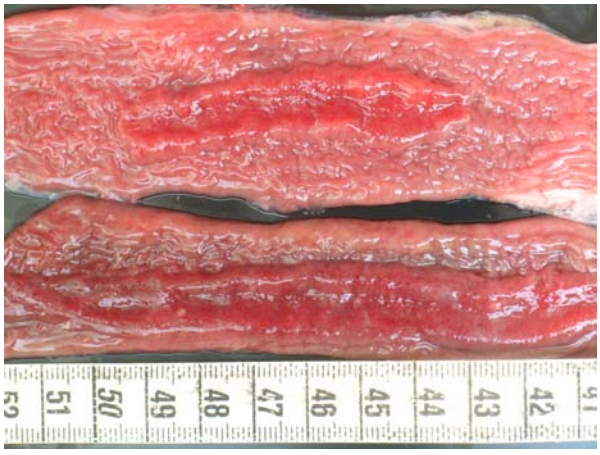

4-1, 4-2. Small and large intestine, Peyer's patches, cow. The mucosa is edematous and hyperemic and there is multifocal necrosis of lymphoid tissue. Photographs courtesy of University of Berne, Berne, Switzerland, http://www.itpa.vetsuisse.unibe.ch/html.

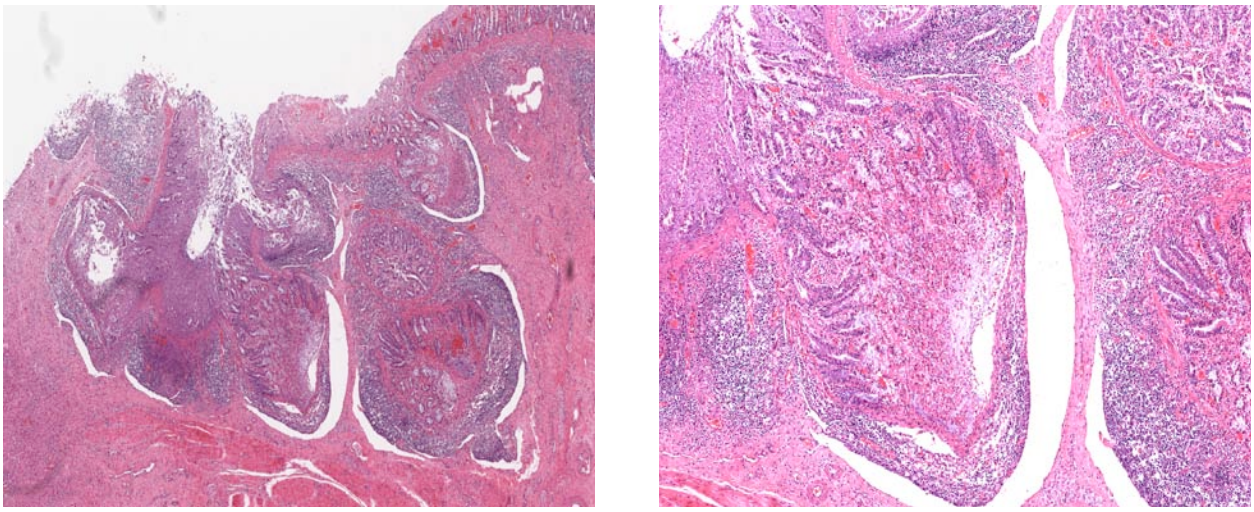

4-3, 4-4. Ileum, cow. Crypt herniation and necrosis happens over Peyer's patches. (HE 100X and 280X)

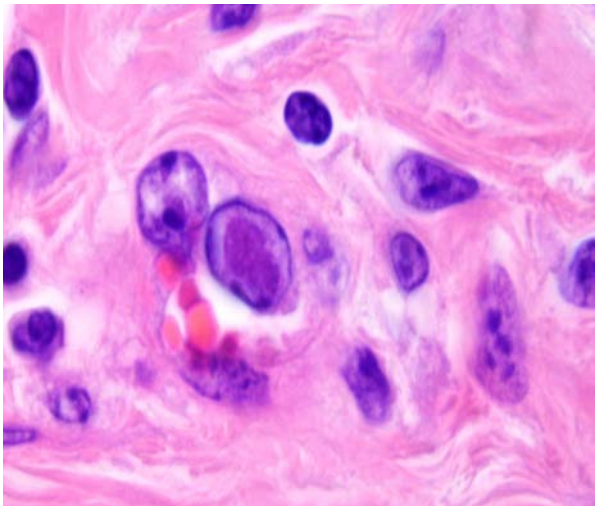

4-5. Arteriole, ileum,cow. Oblong basophilic intranuclear viral inclusions expand the nucleus and marginate chromati of endothelial cells throughout the section. (HE 1000X)

densely stained virus particles measured 70 to 75 nm in diameter.[1,6]

Microscopic lesions were found in the respiratory (bronchiolitis and bronchopneumonia) and intestinal tract (necrosis, fibrinous exudates, hemorrhage, mild infiltration with mononuclear cells and granulocytes) whereas the basophilic or amphophilic vascular inclusion bodies were identified in the lung, kidney, liver, abomasum, small intestine and colon.[2,4] Necrosis preferentially affected Peyer's patches with extension to the overlying mucosa. In the described cases the pathologic findings were related to the primary vascular damage produced by the virus, supported by the absence of other enteric pathogens.[3,4,5] Bacteria, when present, are considered secondary opportunists, but potential contributors to the ultimate pathologic process.[3] The vessels sometimes contained thrombi with many leukocytes and neutrophils present in the walls.[3] However, further experimental studies are needed to determine the virulence of BAdV and to establish if its presence in the vascular endothelium is a cause or a consequence of a co-existing enteric disease.[5]

In other domestic species like horses and pigs, enteric adenovirus infection targets the epithelial cells, yielding to villus atrophy, epithelial sloughing and mild diarrhea. This differs from what is seen in calves in which the intestinal pathology is associated with primary infection of blood vessels resulting in necrosis of the mucosa and lymphoid tissue.

The disease must be differentiated from common causes of fibrinous and hemorrhagic enterocolitis, including coccidiosis, bovine viral diarrhea, salmonellosis and bovine malignant catarrhal fever. There is very limited information available on the prevalence of BAdVs, particularly BAdV 10 infection within cattle populations.[5] At present, adenoviral infection of cattle with enteric disease is probably underdiagnosed especially because there is no test suitable for diagnosis of the disease in live animals and, second, because diagnostics require histopathologic or immunocytochemical examination of the intestine.[4,5] It has been speculated that the sporadic cases of fatal BAdV 10 infection can be the result of some type of immunological incompetence.[2] Further confirmation through electron microscopy, in situ hybridization, or virus isolation in tissue cell cultures was not possible at that time.

JPC Diagnosis: Small intestine: Enteritis, necrotizing, multifocal to coalescing, severe, with villar blunting, crypt herniation, lymphoid depletion, and endothelial intranuclear viral inclusions.

Conference Comment: The contributor does an excellent job of summarizing and describing the lesions associated with BAdV 10. Although difficult to reflect in the morphologic diagnosis, the lesions in this case are most severe within and directly overlaying the necrotic Peyer's patches. There are two different gross lesion presentations associated with BAdV 10 infection. The first includes hemorrhagic bands along the serosa, while the second is a more generalized hemorrhagic enteritis overlain by a fibrinous exudate and with associated Peyer's patch necrosis.[1,4] Other gross lesions occasionally associated with BAdV 10 infection include pulmonary edema and abomasal ulceration.[4]

The use of the term "crypt abscess" to describe the material filling the crypts is considered by some to be a misnomer as the material is often composed of necrotic epithelial and inflammatory cells within a crypt lumen, rather than suppurative inflammation of the crypt epithelium. The moderator prefers "cryptitis" as a more descriptively accurate term for the lesions in this case. Crypt abscess would more appropriately describe the lesions associated with ulcerative colitis where a suppurative inflammatory process of the epithelium predominates; however, the term "crypt abscess" is widely used by veterinary pathologists and is generally understood.

Contributor: University of Berne
Länggassstrasse 122 / Pf 8466
CH-3001 Berne, Switzerland
http://www.itpa.vetsuisse.unibe.ch/html

References:

1. Adair BM, McKillop ER, Smyth JA, et al. Bovine adenovirus type 10: properties of viruses isolated from cases of bovine haemorrhagic enterocolitis. *Vet Rec*. 1996;138: 250-252.
2. Lehmkuhl HD, Cutlip RC, DeBey BM. Isolation of a bovine adenovirus serotype 10 from a calf in the United States. *J Vet Diagn Invest*. 1999;11:485-490.
3. Orr JP. Necrotizing Enteritis in a calf infected with adenovirus. *Can Vet J*. 1984;25:72-74.
4. Smyth JA, Benkö M, Moffett DA, et al. Bovine Adenovirus Type 10 identified in fatal cases of adenovirus-associated enteric disease in cattle by in situ hybridization. *J Clin Microbiol*. 1996;34:1270-1274.
5. Smyth JA, Moffett DA, Garderen E, et al. Examination of adenovirus-types in intestinal vascular endothelial inclusions in fatal cases of enteric disease in cattle, by in situ hybridization. *Vet Microbiol*. 1999;70:1-6.
6. Thompson KG, Thomson GW, et al. Alimentary tract manifestations of bovine adenovirus infections. *Can Vet J*. 1981;22: 68-71.
7. Ursu K, Harrach B, Matiz K, et al. DNA sequencing and analysis of the right-hand part of the genome of the unique bovine adenovirus type 10. *J Gen Virol*. 2004;85:593-601.

Joint Pathology Center
Veterinary Pathology Services

WEDNESDAY SLIDE CONFERENCE 2011-2012

Conference 8

02 November 2011

CASE I: 1 (JPC 4002931).

Signalment: Greek tortoise male 6 years *Testudo graeca*.

History: This was a pet tortoise that awoke from hibernation with nasal and ocular discharge. At clinical examination the tortoise was dehydrated and had a severe intestinal parasitic infection (ascarids and oxyurids) diagnosed by the referring veterinarian. Despite antibiotic, antiparasite and rehydrating therapy, clinical signs including open mouthed breathing worsened and the tortoise died spontaneously.

Gross Pathology: A full necropsy was performed by the referring veterinarian who reported the presence of ulcerative glossitis and stomatitis with pannus formation and severe hyperaemia of lungs. Esophageal and tracheal mucosal linings were reported to be diffusely ulcerated. Heart, liver, kidney, spleen, testes, stomach and intestine were grossly normal.

Several organs, including the lungs, were formalin-fixed and sent for histopathology.

Contributor's Microscopic Description: Lung: Severe and diffuse inflammatory changes involving

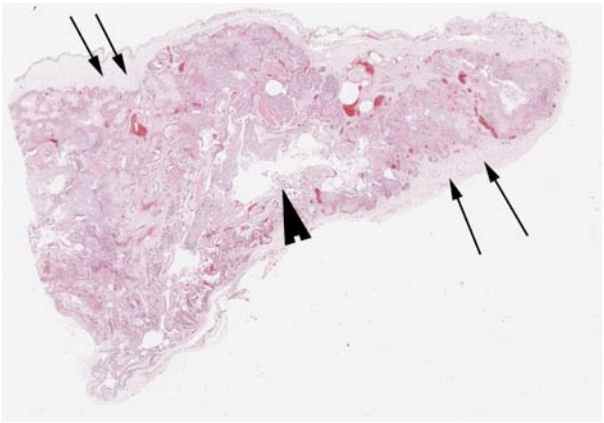

1-1. Lung, tortoise. There is general consolidation of faveoli throughout the lung; only the large bronchiole (arrowhead) is partially spared. Pleura (arrows) are markedly expanded by edema. (HE 63X)

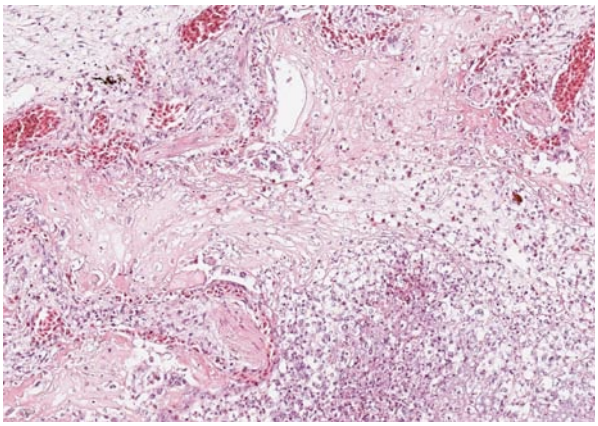

1-2. Lung, tortoise. Faveoli are markedly expanded and filled with abundant polymerized fibrin, heterophils, macrophages, and cellular debris. Congested capillaries and smooth muscle show the extent of the faveolar tissue in the photomicrograph. (HE 260X)

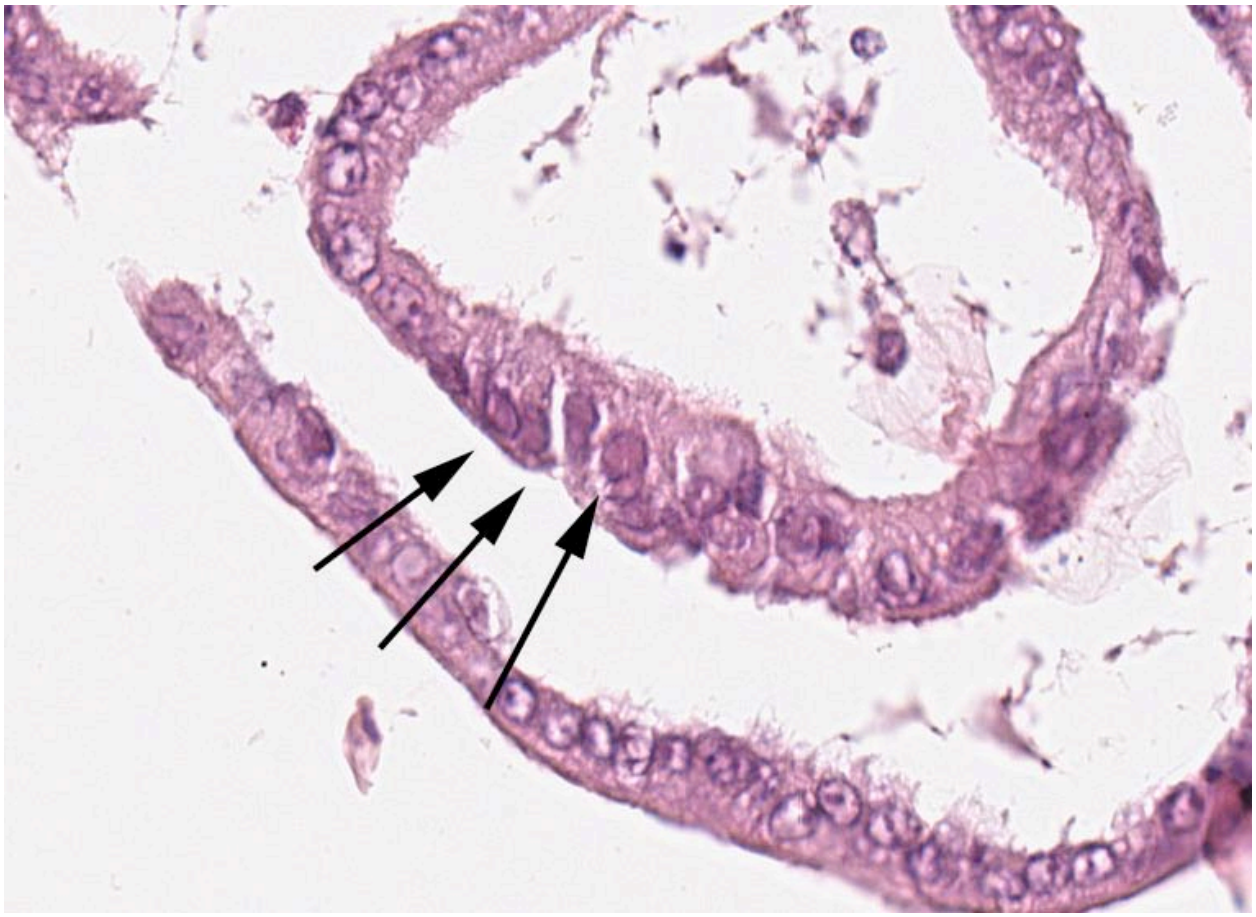

1-3. Lung, tortoise. Groups of contiguous faveolar pneumocytes contain nuclei which are expanded by smudgy amphophilic viral inclusions. (HE 400X)

80% of the pulmonary parenchyma are present in all sections. Upper and lower airways (ediculae) contain variably abundant luminal accumulation of mucus and fibrin admixed with numerous sloughed necrotic epithelial cells, moderate numbers of heterophils, viable or occasionally degenerated (karyolysis and karryorrhexis), and rare reactive macrophages. The epithelium lining larger airways and ediculae is multifocally eroded and ulcerated. In the epithelial cells (sloughed and viable), nuclei are multifocally characterized by chromatin margination and occasionally contain amphophilic, homogeneous variably sized and shaped inclusions bodies often filling the nucleus (consistent with herpesviral inclusions).

The pulmonary interstitium is moderately to severely and diffusely expanded by hyperaemia and edema, numerous heterophils and lesser numbers of lymphocytes and plasma cells. Pleura is severely, diffusely edematous and contains a small number of heterophils.

Contributor's Morphologic Diagnosis: Severe, diffuse, acute, necrotizing pneumonia with amphophilic intranuclear inclusions consistent with herpesvirus, Greek tortoise, *Testudo graeca*.

Etiology: Chelonid herpesvirus (most likely type 3).

Contributor's Comment: Herpesviruses are enveloped viruses with a double stranded DNA surrounded by icosahedrally arranged caspomeres. Herpesvirus infections are widespread and occur in most classes of vertebrates including fish, amphibians, and reptiles. Infection with herpesvirus has been reported in chelonians, lizards, snakes and in crocodilians. In chelonians, herpesviruses have been associated with several disease complexes, which are characterized by diphtheritic-necrotizing stomatitis, hepatitis, rhinitis, tracheitis, and pneumonia in tortoises.[8] Tortoises in the genus *Testudo* including Greek tortoise (*T. graeca*), Hermann's tortoise (*T. hermanni*), and Russian tortoise (*Agrionemys horsfieldi*) are particularly prone to infection with Chelonid herpesvirus (ChHV). ChHV infections have been associated with glossitis, stomatitis, enteritis, and meningoencephalitis in Hermann's tortoises (*Testudo hermanni*); with stomatitis and enteritis in Afghan tortoises (*Testudo horsfieldii*); with stomatitis,

tracheitis, and pneumonia in desert tortoises (*Gopherus agasizii*)[11]; and with stomatitis and encephalitis in spur-thighed tortoises (*Testudo graeca*).[8] Green turtles older than one year of age have also been susceptible to pneumonia, tracheitis and conjunctivitis ascribed to herpesvirus.[8]

Herpesviruses have also been associated with oral, respiratory, cutaneous, and genital lesions in Atlantic loggerhead sea turtles (*Caretta caretta*)[13] and skin diseases in sea turtles, such as gray patch disease and fibropapillomatosis in green turtles (*Chelonia mydas*).[1,7,12]

The exact route of transmission of herpesvirus in wild chelonids is still unknown. In captive animals, a major means of transmission is the exchange of pet tortoises between private collections.[8] It is very likely that direct contact between affected animals and unaffected tortoises represents the primary route of transmission. The finding of viral particles in testicular epithelium of Greek and Hermann's tortoises suggests the possibility of vertical transmission.[8]

Herpesviruses identified in various species of turtles and tortoises have been preliminarily named chelonid herpesviruses (ChHVs), but represent an up-to-now unassigned species in the herpesvirus family. Classification of ChHVs is mainly based on putative differences in the host spectrum and 4 variants have been recognized. ChHV-1 was first described in association with gray patch disease in captive green sea turtles (*Chelonia mydas*) in the West Indies.[12] This disease is characterized by patchy gray areas of hyperkeratotic and necrotic papules that occur over the head, neck, and flippers. ChHV-2 was seen in two Pacific pond turtles (*Clemmys marmorata*) with fatal hepatic necrosis. A similar disease has been seen in painted turtles (*Chrysemys picta*) and in map turtles (*Graptemys pseudogeographica*) in association with herpesvirus-like particles.

These viruses have been preliminarily named ChHV-3.[6] ChHV-4 was seen in tissues of Argentinian tortoises (*Geochelone chilensis*) with necrotizing stomatitis or mouth rot. Interestingly, red-footed tortoises (*Geochelone carbonaria*) kept together with the diseased Argentinian tortoises remained clinically healthy.[4] Epizootics of chronic seromucous rhinitis (running nose syndrome) were described in large populations of captive *T. graeca.* This outbreak was part of a series of epidemic ChHV infections that have occurred in Europe during the last decade. In most cases, outbreaks follow shared housing of different tortoise species after addition of new animals. In all of these cases, presumed carrier species, especially *T. graeca,* remained healthy, whereas other, presumably less resistant species, became sick or died.

Clinical signs in tortoises include nasal serous to mucopurulent discharge, open mouth breathing, wheezing, dyspnea, lethargy, anorexia, weight loss and ataxia. Radiographs, magnetic resonance, CT scans, bronchoscopy, and cytology have been used for clinical diagnosis.[8]

Pathological findings in most chelonids with respiratory disease include necrotizing caseous stomatitis that extends in the oral cavity and nares and necrotizing glossitis with presence of diphtheritic plaques. Lower airways can be involved resulting in necrotizing pneumonia and emphysema. Enteritis and hepatomegaly have been also reported.[8] In tortoises, eosinophilic intranuclear inclusions are commonly seen in epithelial cells of affected tissues stained with haematoxylin and eosin and are associated with syncytial cells.[8] Secondary bacterial complications are associated with development of multiple bacterial granulomas. Intranuclear inclusions have also been reported in lung and trachea of green turtles (*Chelonia mydas*) with respiratory disease[5] and in cutaneous fibropapillomas.[7] Using TEM, virions can be detected in the nucleus and cytoplasm of infected cells of the tongue, trachea, bronchi and alveoli, endothelial cells of glomerular capillaries and within neurons and glial cells of the medulla oblongata and diencephalon.[8]

Tests that have been developed to diagnose chelonid herpesvirus include enzyme-linked immunosorbent assay (ELISA) for the detection of herpesvirus antibodies in plasma samples of Mediterranean tortoises.[9] Indirect and direct immunoperoxidase assay have been used either for assessing the presence of anti-herpesvirus antibody in tortoise plasma or for detecting herpesvirus antigen in tissues.[10]

ChHV DNA has been demonstrated in a broad range of formalin fixed and paraffin embedded tissues in tortoises suffering from stomatitis–rhinitis complex by in situ hybridization and PCR. The ISH signal colocalizes to the same areas and cell types that contain intranuclear inclusions in haematoxylin and eosin stained tissue sections from tortoises of different geographic provenances. Nuclear hybridization signals have been detected in epithelial cells of the lingual mucosa and glands, in tracheal epithelium, pneumocytes, hepatocytes, the renal tubular epithelium, cerebral glial cells and neurons, intramural intestinal ganglia and in endothelial cells of many organs.[14]

JPC Diagnosis: Lung: Pneumonia, bronchointerstitial, fibrosing, heterophilic and histiocytic, subacute, diffuse, severe, with type II pneumocyte hypertrophy and exfoliation with numerous epithelial intranuclear viral inclusions.

Conference Comment: The differential diagnosis discussed by conference participants included adenovirus, ranavirus, and fibropapillomavirus. Previous reports of chelonian adenoviruses include an atAdenovirus in a leopard tortoise (*Geocehlone pardalis*) and a Siadenovirus in Sulawesi tortoises (*Indotestudo forsteni*).[15] Reported gross lesions include hepatosplenomegaly, fibrinonecrotic membranes in the lumen of the colon, oronasal fistulae, and ulceration of the tongue and oral mucosa. The histologic appearance of adenovirus is very similar to herpesvirus, including epithelial, endothelial and myeloid necrosis with basophilic to amphophilic intranuclear viral inclusions in many tissues.[3,14]

Ranavirus is in the family Iridovirus, with gross lesions including hepatic necrosis, ulcerative tracheitis, pneumonia, and ulcerative pharyngitis and esophagitis. Histopathologic findings include basophilic intracytoplasmic viral inclusions in hepatocytes and epithelial cell, and fibrinoid vasculitis in multiple organs. Reptiles are thought to aquire ranavirus from amphibians.[3]

Fibropapillomatosis is found in all species of sea turtles except for the leatherback, and is caused by a herpesvirus. Fibropapilloma-associated turtle herpesvirus causes a debilitating disease characterized by large numbers fibropapillomas which result in decreased mobility and occasional blindness when located near the eyes. These are often accompanied by anemia and immunosuppression. Histology of the masses is that of a typical fibropapilloma, and intranuclear viral inclusions are rarely seen. Fibropapillomas can also be seen on the viscera, with the kidney and lung being primary target tissues.[16]

Contributor: Sezione Anatomia Patologica e Patologia Aviare
Dipartimento di Patologia Animale, Igiene e Sanita' Pubblica
Facolta' di Medicina Veterinaria
Via Celoria 10
20133 Milano – Italy
http://www.anapatvet.unimi.it/

References:

1. Coberley SS, Herbst LH, Brown DR, et al. Detection of antibodies to a disease-associated herpesvirus of the green turtle, *Chelonia mydas*. *J Clin Microbiol*. 2001;39:3572-3577.
2. Herbst LH, Jacobson ER, Klein PA, et al. Comparative pathology and pathogenesis of spontaneous and experimentally induced fibropapillomas of green turtles (*Chelonia mydas*). *Vet Pathol*. 1999;36:551-564.
3. Jacobson ER. Viruses and viral diseases of reptiles. In: Jacobson ER, ed. *Infectious Diseases and Pathology of Reptiles*. Boca Raton, FL: CRC Press; 2007:396-405.
4. Jacobson ER, Clubb S, Gaskin JM, et al. Herpesvirus-like infection in Argentine tortoises. *J Am Vet Med Assoc*. 1985;187:1227–1229.
5. Jacobson ER, Gaskin JM, Roelke M, et al. Conjunctivitis, tracheitis, and pneumonia associated with herpesvirus infection in green sea turtles. *J Am Vet Med Assoc*. 1986;189:1020-1031.
6. Jacobson ER, Gaskin JM, Wahlquist H. Herpesvirus-like infection in map turtles. *J Am Vet Med Assoc.* 1982;181:1322–1324.
7. Jacobson ER, Mansell JL, Sundberg JP, et al. Cutaneous fibropapillomas of green turtles (*Chelonia mydas*). *J Comp Pathol.* 1989;101:39–52.
8. Origgi FC, Jacobson ER. Diseases of the respiratory tract of chelonians. *Vet Clin North Am Exot Anim Pract.* 2000;3:37-549.
9. Origgi FC, Klein PA, Mathes K, et al. Enzyme-linked immunosorbent assay for detecting herpesvirus exposure in Mediterranean tortoises (spur-thighed tortoise [*Testudo graeca*] and Hermann's tortoise [*Testudo hermanni*]). *J Clin Microbiol*. 2001;39:3156-3163.
10. Origgi FC, Klein PA, Tucker SJ, et al. Application of immunoperoxidase-based techniques to detect herpesvirus infection in tortoises. *J Vet Diagn Invest*. 2003;15:133-140.
11. Peitan-Brewer KCB, Drew ML, Ramsay E, et al. Herpesvirus Particles Associated With Oral and Respiratory Lesions in a California Desert Tortoise *(Gopherus agassizi*). *J Wildlife Dis.* 1996;32:521-526.
12. Rebell G, Rywlin A, Haines H. A herpesvirus-type agent associated with skin lesions of green sea turtles in aquaculture. *Am J Vet Res*. 1975;36:1221–1224.
13. Stacy BA, Wellehan JF, Foley AM, et al. Two herpesviruses associated with disease in wild Atlantic loggerhead sea turtles (*Caretta caretta*). *Vet Microbiol*. 2008;126:63-73.
14. Teifke JP, Lo HR CV, Marschang RE, et al. Detection of Chelonid Herpesvirus DNA by Nonradioactive In Situ Hybridization in Tissues from Tortoises Suffering from Stomatitis–Rhinitis Complex in Europe and North America. *Vet Pathol*. 2000;37:377–385.
15. Rivera S, et al. Systemic adenovirus infection in Sulawesi tortoises (*Indotestudo forsteni*) caused by a novel siadenovirus. *J Vet Diagn Invest.* 2009;21(4): 415-26.
16. Wyneken J, Mader DR, Weber III ES, et al. Medical care of seaturtles. In: Mader DR, ed. *Reptile Medicine and Surgery*. 2nd ed. St. Louis, MO: Saunders Elsevier; 2006:986-91.

CASE II: 11-03780 (JPC 4003460).

Signalment: An approximately 1-year-old male *Boa constrictor*.

History: Three boid snakes were purchased from a breeder and incorporated into a private reptile collection. Although apparently normal at the time of purchase, within a few days this snake developed sluggish behavior with twisting, ataxia, and opisthotonus. Clinical signs persisted for a week prior to death.

Gross Pathology: The body of an 823 g, 129 cm male boa was in thin body condition with decreased fat stores and mildly atrophied skeletal muscle. A moderate pericardial effusion consisting of 2-3 ml of serous to faintly serosanguinous fluid was present as well as serous atrophy of epicardial fat. Excessive clear mucus was present in the mouth, and the stomach was empty. The kidneys appeared somewhat pale and ureters were prominent and filled with uric acid.

Laboratory Results: Routine fecal flotation revealed no parasite eggs or oocysts.

Contributor's Microscopic Description: Liver: There is widespread hepatocellular necrosis associated with large, amorphic, amphophilic to basophilic intranuclear inclusion bodies resulting in karyomegaly and margination of nuclear chromatin. Occasional hepatocytes and numerous biliary epithelial cells contain one or more rounded, brightly eosinophilic intracytoplasmic inclusion bodies. Loose fibrin thrombi, high numbers of heterophils and scattered lymphocytes are present within sinusoids throughout the liver.

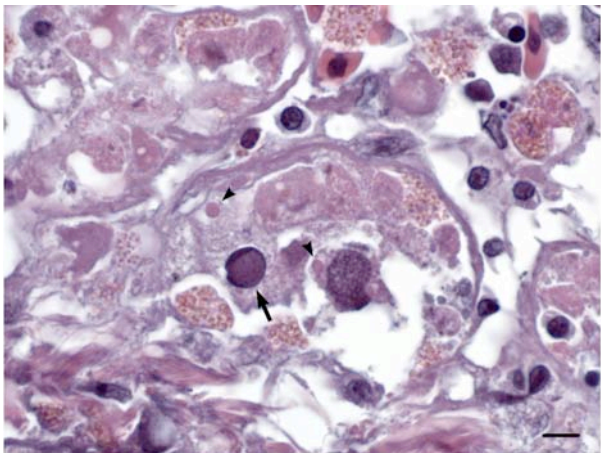

2-1. Liver, snake. A hepatocyte nucleus is markedly expanded by a darkly basophilic cytoplasmic adenoviral inclusion (small arrow). A necrotic hepatocyte is present (large arrow). The remaining hepatocytes are atrophic and numerous heterophils are present within sinusoids. Remaining viable hepatocytes contain brightly eosinophilic round protein inclusions characteristic of boid inclusion disease. (HE 1000X) Photograph courtesy of the Veterinary Diagnostic Laboratory, College of Veterinary Medicine, Oregon State University, Magruder Hall 134, Corvallis, OR 97331 http://oregonstate.edu/vetmed/diagnostic

Stomach: Numerous mucosal epithelial cells contain rounded, brightly eosinophilic intracytoplasmic inclusion bodies. Occasional epithelial cells contain amphophilic intranuclear inclusion bodies. Additional lesions not included on the slide include brightly eosinophilic intracytoplasmic inclusion bodies within neurons and glial cells in the brain (occasionally associated with gliosis); within epithelial cells of the adrenal gland, thyroid follicles, bronchi, renal tubules, acinar pancreatic cells, and intestinal enterocytes; within lymphocytes in the spleen; and occasionally within cardiomyocytes. Low numbers of intestinal enterocytes also contain amphophilic intranuclear inclusion bodies.

Contributor's Morphologic Diagnosis: Liver: Severe, diffuse acute necrotizing hepatitis with intralesional inclusion bodies.
Stomach: Intracytoplasmic and intranuclear inclusion bodies.

Contributor's Comment: Death in this case was determined to be due to dual viral infection with histologic lesions consistent with concurrent inclusion body disease and adenovirus infection, although confirmation of the latter infection by virus isolation was not attempted. In the absence of ancillary testing, herpesviral infection could not be ruled out as a cause of hepatic necrosis.

Inclusion body disease is an important infection in boid snakes, having emerged during the last 30 years on several continents.[13] Although snakes may remain chronic carriers of the disease, once clinical signs develop, the disease is fatal within weeks or months.[2,13] Clinical signs are variable and can include neurologic, digestive or respiratory systems.[6,12,13] Antemortem diagnosis can be achieved by biopsy of the liver, esophageal tonsil, gastric mucosa or skin; or by detection of typical cytoplasmic inclusion bodies within peripheral blood leukocytes, although this method yields higher false positives and false negatives.[2,3] Histologically, there are large, brightly eosinophilic intracytoplasmic inclusion bodies within a wide range of tissues (particularly in the liver and pancreas), often in the absence of a tissue or cellular response.[1,2,6,14]

Retroviruses have been isolated from boids with inclusion body disease; however, Koch's postulates have yet to be completely fulfilled.[5,13,16] The bloodsucking snake mite, *Ophionyssus natricis*, may act as a vector.[13] Concurrent infectious disease is common, possibly due to lymphoid depletion and resultant immunosuppression.[6] Pneumonia, ulcerative

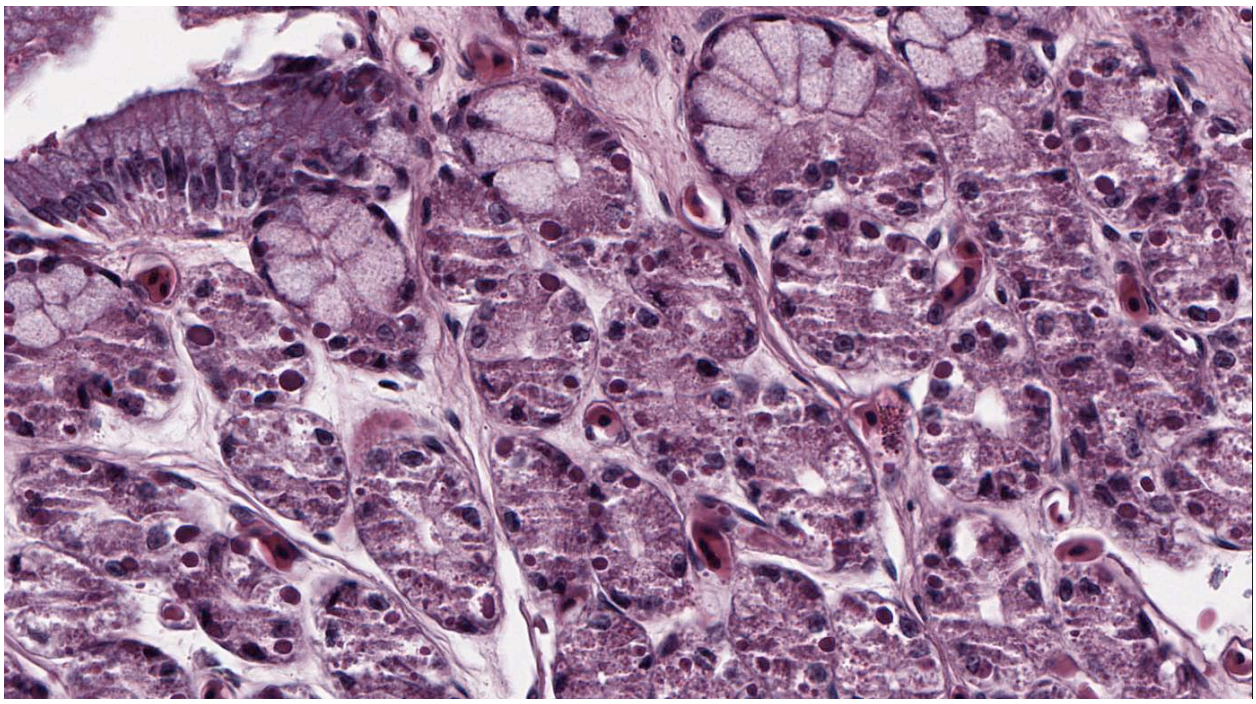

2-2. Stomach, snake. Numerous chief cells contain brightly eosinophilic round protein inclusions characteristic of boid inclusion disease. Chief cells are shrunken and lack zymogen granules (atrophy). (HE 400X)

stomatitis[6], entamoebic colitis[10], and neoplastic diseases such as lymphoma[11] have been reported in conjunction with inclusion body disease.

Adenoviral hepatitis has previously been described in boid snakes, and is characterized by severe necrotizing hepatitis with basophilic to eosinophilic intranuclear inclusions within hepatocytes, accompanied by heterophils and small mononuclear cells.[4,8,13] Other lesions previously attributed to adenovirus or adenoviral-like infection in snakes include enteritis, splenitis, nephritis, pneumonia and encephalopathy.[7] The ability for latent adenoviral infections to induce clinical disease following immunosuppression has been demonstrated in species other than snakes[15], and in the case presented here it is tempting to speculate that inclusion body disease was involved in that respect.

Major viral diseases in boid snakes

Agent	Typical lesions	Inclusions
Adenovirus	Necrotizing hepatitis	Amphophilic (occasionally eosinophilic), intranuclear
Herpesvirus	Necrotizing hepatitis, glomerulonephritis	Eosinophilic to amphophilic intranuclear inclusions
Inclusion body disease virus (suspected retrovirus)	Inclusions in the absence of a tissue or cellular response	Eosinophilic, intracytoplasmic
Paramyxovirus	Hemorrhagic to necrotizing pneumonia, pancreatitis, occasionally CNS disease	Occasional, eosinophilic, intranuclear or cytoplasmic
Adenovirus, parvovirus, picornavirus, herpesvirus	Viral-associated gastrointestinal disease - causal relationship not established	

JPC Diagnosis: 1. Liver: Hepatic atrophy, diffuse, severe.
2. Liver: Necrosis, hepatocellular, multifocal, with rare intranuclear viral inclusions.
3. All cell types: Intracytoplasmic inclusions.
4. Stomach: Diffuse loss of parietal cell granules.

Conference Comment: The moderator attributed the hepatic atrophy and gastric parietal cell granular degeneration to the poor nutritional status of the animal, which is a common finding in inclusion body disease. The rare intranuclear inclusions in hepatocytes are likely due to the concurrent adenoviral infection. The conference moderator also noted the presence of melanin pigment within the liver, which is normal in reptiles.

The moderator discussed the composition of the inclusions seen in inclusion body disease, which remains controversial. The inclusion material was initially thought to result from the associated retrovirus, but recent research suggests that this condition may be a storage disease, similar to the transmissible spongiform encephalopathies. The intracytoplasmic inclusions, which ultrastructurally are either non-membrane limited aggregates of granular

electron-dense material, or membrane-bound aggregates of electron-dense material with membrane-like fragments, are composed of a distinct 68-kd protein, and typically cause no inflammatory response, as opposed to necrosis and inflammation associated with viral infections. Nonviral inclusions have been demonstrated in cells infected with other retroviruses, such as avian leukosis virus, visna virus, and simian immunodeficiency virus.

Boid inclusions stain with PTAH and toluidine blue, and are eosinophilic with H&E, suggesting protein composition; they do not stain with Congo red or thioflaven-T, suggesting that the material in not amyloid. Boid inclusions have a similar staining pattern to Mallory bodies, non-viral inclusions composed of cytokeratin filaments. The inclusions may also be overproduced or poorly degraded components of the virus that accumulates in the host cell cytoplasm.[16]

As this is one of the most important viral diseases of boas and pythons with no known treatment, diagnosis of IBD is imperative. Antemortem diagnosis is often easily obtained through biopsy, since the inclusions are present in all tissues. Preferring the liver, the moderator discussed various high-yield biopsy locations. The skin is a poorer option because inclusions are more widely distributed, necessitating multiple biopsies to decrease false positive results. Cytology is another option, but the slides must be stained with H&E in order to differentiate the inclusions from other structures, such as lipid or intracellular parasites. Currently, immunohistochemical staining is available for frozen tissue, which may lead to a serologic test in the future.

Contributor: Oregon State University
Veterinary Diagnostic Laboratory
College of Veterinary Medicine
Magruder Hall 134
Corvallis, OR 97331
http://oregonstate.edu/vetmed/diagnostic

References:

1. Carlisle-Nowak MS, Sullivan N, Carrigan M, et al. Inclusion body disease in two captive Australian pythons (*Morelia spilota variegata* and *Morelia spilota spilota*). *Aust Vet J*. 1998;76:98-100.
2. Chang LW, Jacobson ER. Inclusion body disease, a worldwide disease of boid snakes: A review. *J Exotic Pet Med*. 2010;19:216-225.
3. Garner MM. Methods for diagnosing inclusion body disease in snakes. In: Small animal and exotics. Proceedings of the North American Veterinary Conference. 2005;19:1283-1284.
4. Jacobson ER, Gaskin JM, Gardiner CH. Adenovirus-like infection in a boa constrictor. *JAVMA*. 1985;187:1226-1227.
5. Jacobson ER, Orós J, Tucker SJ, et al. Partial characterization of retroviruses from boid snakes with inclusion body disease. *AJVR*. 2001;62:217-224.
6. Orós J, Tucker S, Jacobson ER. Inclusion body disease in two captive boas in the Canary Islands. *Vet Rec*. 1998;143:283-285.
7. Perkins LEL, Campagnoli RP, Harmon BG, et al. Detection and confirmation of reptilian adenovirus infection by in situ hybridization. *J Vet Diagn Invest*. 2001;13:365-368.
8. Ramis A, Fernández-Bellon H, Majó N, et al. Adenovirus hepatitis in a boa constrictor (*Boa constrictor*). *J Vet Diagn Invest*. 2000;12:573-576.
9. Raymond JT, Lamm M, Nordhausen R, et al. Degenerative encephalopathy in a coastal mountain kingsnake (*Lampropeltis zonata multifasciata*) due to adenoviral-like infection. *J Wild Dis*. 2003;39:431-436.
10. Richter B, Kübber-Heiss A, Weissenböck H. Diphtheroid colitis in a *Boa constrictor* infected with amphibian *Entamoeba* sp. *Vet. Parasit*. 2008;153:164-167.
11. Schilliger L, Selleri P, Frye FL. Lymphoblastic lymphoma and leukemic blood profile in a red-tail boa (*Boa constrictor*) with concurrent inclusion body disease. *J Vet Diagn Invest*. 2011;23:159-162.
12. Schumacher J, Jacobson ER, Burns R, et al. Adenovirus-like infection in two rosy boas (*Lichanura trivirgata*). *J Zoo Wild Med.* 1994;25:461-465.
13. Schumacher J, Jacobson ER, Homer BL, et al. Inclusion body disease in boid snakes. *J Zoo Wild Med*. 1994;25:511-524.
14. Vancraeynest D, Pasmans F, Martel A, et al. Inclusion body disease in snakes: a review and description of three cases in boa constrictors in Belgium. *Vet Rec*. 2006;158:757-761.
15. Ward JM, Young DM. Latent adenoviral infection of rats: intranuclear inclusions induced by treatment with a cancer chemotherapeutic agent. *JAVMA*. 1976;169:952-953.
16. Wozniak E, McBride J, DeNardo D, et al. Isolation and characterization of antigenically distinct 68-kd protein from nonviral intracytoplasmic inclusions in boa constrictors chronically infected with the inclusion body disease virus (IBDV: *Retroviridae*). *Vet Pathol.* 2000;37:449-459.

CASE III: 08120419 (JPC 3136279).

Signalment: 3-year-old female red kangaroo (*Macropus rufus*).

History: This kangaroo died acutely with no observed clinical signs. Four animals died at this private zoo over the past 3 months, also without any clinical signs. This zoo has a large feral cat population.

Gross Pathology: The animal was in a mild state of decomposition. Gross examination revealed the animal was in good nutritional condition. The lungs failed to collapse upon opening the thoracic cavity. There were hundreds of firm, 1-2 mm in diameter, white to tan, slightly raised foci disseminated throughout the pulmonary parenchyma. Mediastinal and tracheobronchial lymph nodes were enlarged and on section were hemorrhagic. Multiple white radiating streaks were identified on the epicardial surface extending into the myocardium.

Laboratory Results: Immunohistochemical stains for *Toxoplasma* on lung tissue were positive. Fluorescent antibody staining for CAV-1 on lung tissue was negative.

Contributor's Microscopic Description: Lung: The normal architecture of the lung is disrupted by interstitial and alveolar inflammation, necrosis, fibrin deposition, edema, and intralesional protozoa. Expanding and occasionally forming nodular aggregates within the alveolar interstitium and alveoli are a large number of macrophages, lymphocytes, and plasma cells. Rare degenerate neutrophils are observed. Often the alveolar interstitium contains abundant amounts of fibrin. There is marked necrosis within the sections, characterized by eosinophilic cellular debris and basophilic nuclear debris. Admixed within the inflammation are 1-2µm, oval to round organisms arranged individually (tachyzoites) or grouped together into packets or cysts (bradyzoites) 20-25 µm in diameter. There is a mild amount of pulmonary edema. Alveolar interstitium are markedly congested. [*Organisms are present in all slides; conspicuous in some, inconspicuous in others*]

Contributor's Morphologic Diagnosis: Lung: Necrotizing interstitial pneumonia, lymphohistiocytic, diffuse, acute, severe, with multifocal necrosis and intralesional *Toxoplasma gondii* protozoa.

Contributor's Comment: Toxoplasmosis is caused by *Toxoplasma gondii*, an obligate intracellular coccidian parasite. *Toxoplasma gondii* has a broad intermediate host range and the only known definitive hosts for *T. gondii* are domestic cats and other felidae.[2] Infection with *T. gondii* within the cat is dependent on enteroepithelial or extraintestinal life cycle. In kangaroos, similar to other intermediate hosts, infection is dependent on the extraintestinal life cycle. *Toxoplasma gondii* has a worldwide distribution and causes high morbidity and mortality in Australian marsupials, particularly macropods.[1]

Kangaroos are herbivores and presumably acquire *T. gondii* by ingestion of oocysts from their environment. In this case, it was difficult to determine whether there was contamination of the foods, grazing areas, or water, or if oocysts were ingested during grooming activities. However, it was likely that feral cats defecated in the enclosure area, resulting in contamination of the ground or feeding stations

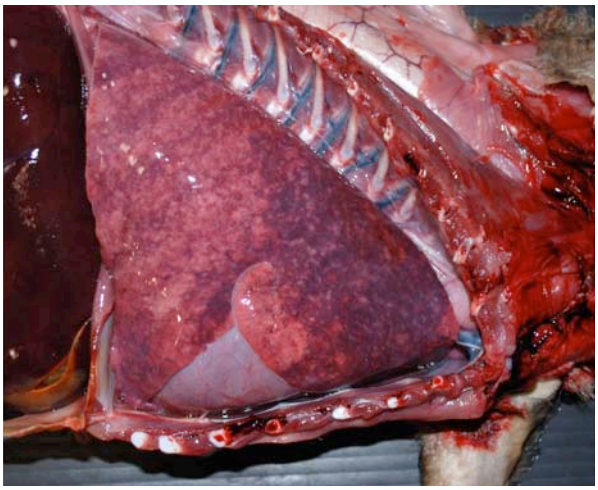

3-1. Lung, kangaroo. Disseminated throughout the non-collapsing lungs were hundreds of firm 1-2 mm in diameter, white to tan, slightly raised foci. Photograph courtesy of Oklahoma State University, Department of Veterinary Pathobiology, 250 McElroy Hall, Stillwater, OK 74078. www.cvm.okstate.edu

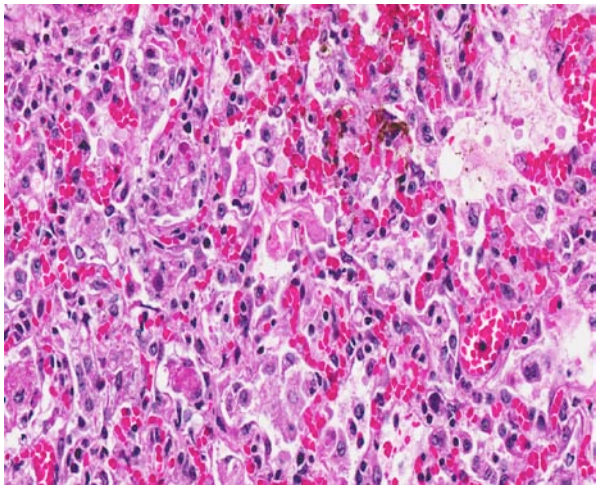

3.2. Lung, kangaroo. Alveolar septa are markedly expanded by fibrin and edema, and occasionally type I pneumocytes are necrotic. Alveoli are filled with polymerized fibrin, foamy alveolar macrophages, neutrophils, and small amounts of cellular debris. (HE 400X)

potentially exposing these animals to infectious oocysts.

At necropsy, kangaroos with toxoplasmosis have gross lesions similar to other domestic animal species; including pulmonary congestion and edema, pulmonary consolidation, pale myocardial streaks and hemorrhage, a miliary pattern of white pulmonary foci, lymphadenomegaly, and splenomegaly. In addition to the lung lesion, this patient exhibited inflammatory lesions with *Toxoplasma* organisms in the brain, heart, liver and kidney. Similarly, disseminated toxoplasmosis was confirmed in the other four kangaroos that had died previously.

JPC Diagnosis: Lung: Pneumonia, interstitial, necrotizing, diffuse, moderate, with rare intrahistiocytic apicomplexan cysts and free zoites.

Conference Comment: A characteristic finding of toxoplasmosis is necrosis, which is caused both by rupture of infected cell membranes by rapidly dividing tachyzoites, and by ischemia secondary to vasculitis. The moderator emphasized that the most susceptible captive zoo species are the squirrel monkey, macropods, lemurs, and the Thomson's gazelle, that protozoal cysts are most readily found in skeletal muscle and the central nervous system, and that pulmonary infection is the most common cause of death. Characteristic gross findings in the lung include pulmonary consolidation with multifocal to coalescing green foci; lymphadenomegaly, and hemorrhage and necrosis of the lymph nodes are also commonly noted. The moderator also discussed the serious problem that toxoplasmosis causes in zoos, with the parasite reservoirs being feral cats, opossums, rats, and cockroaches.

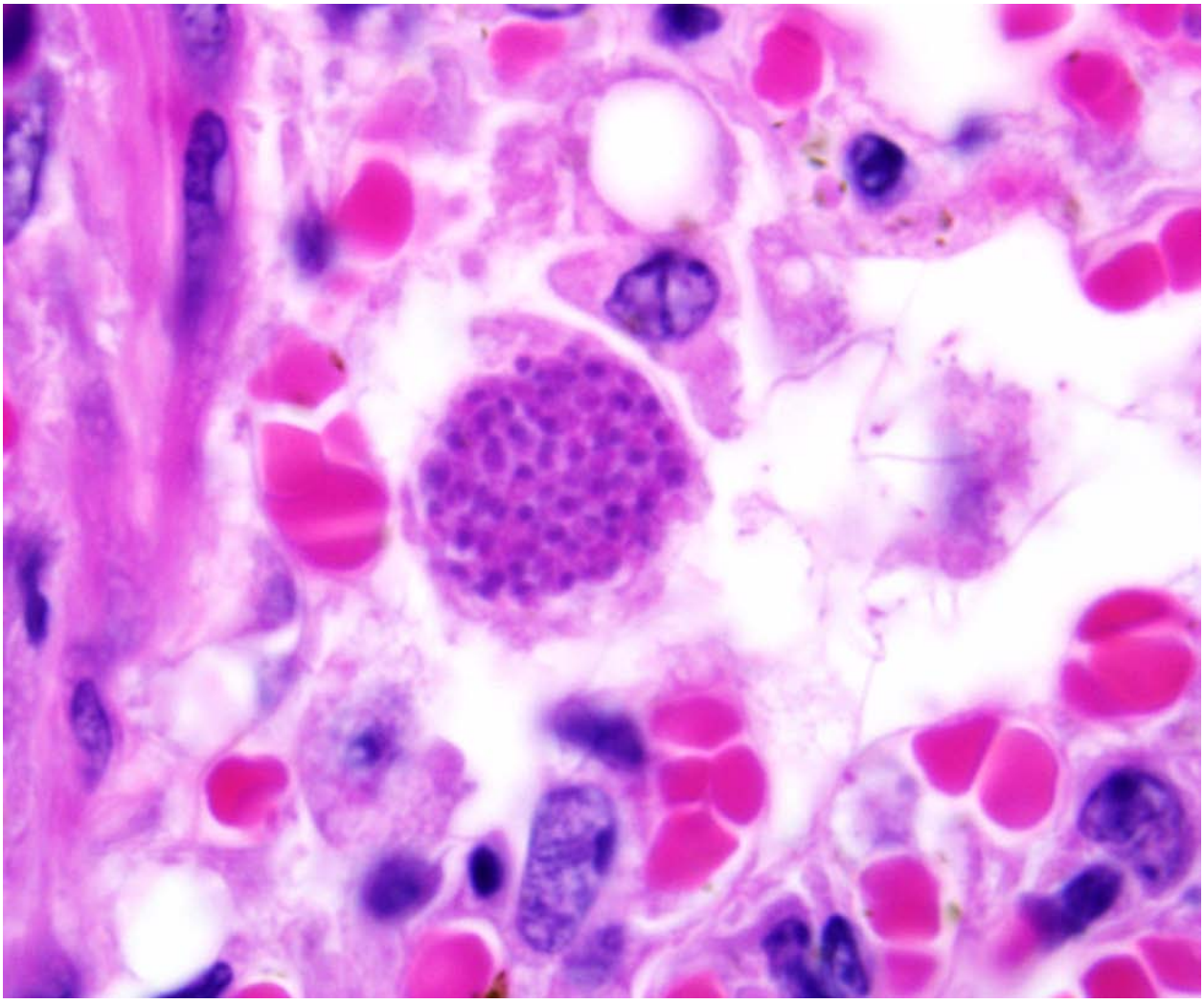

3-3. Lung, kangaroo. Alveolar macrophage containing numerous rutracytoplasmic zoites consistent with Toxoplasma gondi. (HE 1000X)

Contributor: Oklahoma State University
Department of Veterinary Pathobiology
250 McElroy Hall
Stillwater, OK 74078
www.cvm.okstate.edu

References:

1. Canfield P, Hartley W, Dubey P. Lesions of toxoplasmosis in Australian marsupials. *J Comp Path*. 1990;103:157-167.
2. Dubey J, Lappin M. Toxoplasmosis and Neosporosis In: Green CE, ed. *Infectious Diseases of the Dog and Cat* Saunders Elsevier, St. Louis, MO, 2006:754-775.
3. Schlafer DH, Miller RB. Female genital system. In: Maxie MG, ed. *Jubb, Kennedy, and Palmer's Pathology of domestic* Animals. 5th ed. Edinburgh, Scotland: Saunders Elsevier; 2007:513-4.

CASE IV: N-0811520 (JPC 3134355).

Signalment: 1-year-old male giant elephant shrew (*Rhynchocyon petersi*).

History: A 1-year-old male captive-bred giant elephant shrew (*Rhynchocyon petersi*) presented with lameness of the right hind limb. The shrew had been pair housed with a male littermate in a 75 sq. ft. indoor enclosure since arriving 3 months earlier from the Smithsonian National Zoological Park. Empirical daily therapy with oral meloxicam (0.1 mg/kg) and a ten-day course of cefdinir (10 mg/kg) resulted in minimal improvement. Physical exam and radiographs revealed no remarkable findings. Three weeks later, the fifth digit of the left forelimb exhibited marked swelling. Further, a mass measuring 2 x 2 x 0.5 cm was palpated at the medial and lateral aspect of the right stifle. Subsequent, repeat radiographs of the affected digit (5th phalanges) and right stifle (distal femur and proximal tibia) revealed bone lysis and soft tissue swelling. Two weeks after limited success with oral antimycobacterial therapy using rifabutin (20 mg/kg) and azithromycin (15 mg/kg), the shrew became ataxic, lethargic and anorexic. Shortly after transport to an intensive care unit for supportive care, the shrew was found tachypneic in right lateral recumbency, and due to its deteriorating condition and poor prognosis, the elephant shrew was humanely euthanized and submitted for necropsy.

Gross Pathology: On gross examination, there was enlargement of the right femorotibial (stifle) joint with multiple, coalescing foci of purulent material (abscesses) within a 2 cm x 2 cm x 1.5 cm area of the quadriceps and a 3 cm x 2 cm area of the hamstring muscles. Crepitus suggestive of a fracture was present on palpation of the stifle joint. The fifth digit on the left front lateral toe was swollen. Numerous pinpoint to 0.2 cm white foci were found disseminated throughout all lung lobes and diffuse, pinpoint, white foci were frequently observed on liver surfaces. Approximately 2 ml of serous sanguineous fluid was observed in the abdominal cavity.

Laboratory Results:
Microbiology Culture:
Right stifle joint and lung: *Mycobacterium spp*.
PCR:
A 100% identity for *Mycobacterium intracellulare*

Contributor's Microscopic Description: Lung: Within ~25% of the lung lobes, there are multiple individual to coalescing irregular granulomas composed centrally of necrosis with a peripheral rim of degenerative neutrophils, which in turn is surrounded by numerous macrophages, scattered multinucleated giant cells and occasional lymphocytes and plasma cells. Some granulomas encompass airways and vasculature with extension of inflammatory cells into the surrounding tissue. The pulmonary interstitium is also multifocally mildly to severely expanded by macrophages and neutrophils spatially distinct from granulomas. There are also multifocal areas within the airways that contain macrophages with multifocal loss of airway epithelium. Review of acid fast bacteria (AFB)-stained sections of lung and stifle joint revealed numerous AF-positive bacteria.

Contributor's Morphologic Diagnosis: Lung: Pneumonia, pyogranulomatous, severe, chronic active, multifocal.

Contributor's Comment: The giant elephant-shrew (*Rhynchocyon petersi*) is a small insectivorous mammal of the family *Macroscelididae*, widely distributed across central and southern Africa. Their traditional common English name comes from a resemblance between their long noses and trunk of an elephant, and an assumed relationship with the true shrews (family *Soricidae*) in the order Insectivora. Phylogentically, elephant shrews are closely related to aardvarks, golden moles and tenrecs. Currently, there are 15 known species in this strictly African mammal group, three of which are referred to as "giant" elephant shrews belonging to the genus *Rhynchocyon*. All three *Rhynchocyon* species are considered threatened due to habitat destruction and fragmentation.

Mycobacterium avium complexes (MAC) are a group of nontuberculous mycobacteria characterized as gram-positive, aerobic, non-motile, acid-fast rods. *M. avium* and *M. intracellulare* are the most notable species within the group.[30] Because *M. avium ssp. avium* and *M. intracellulare* are difficult to distinguish on the basis of phenotypic characteristics, the term *M. avium* complex is used when referred to these organisms. The mycobacterium now designated as *M. intracellulare* was first cultured in 1969 from the sputum of tuberculosis patients in the Battey State Hospital of Rome, Georgia and was originally referred to as "Battey bacillus".[25] In 1971, the nontuberculosis mycobacteria were divided into three groups; based on their association with human disease, production of yellow or orange pigment, and their rate of growth. The photochromogens contain 3 species that develop yellow or orange pigment when exposed to light. Examples include *M. kansasii*, *M. marinu, and M. simiae*. The scotochromogens, including *M. gordonae, M. szulgai* and *M. scrofulaceum,* form orange-yellow pigment in the dark. The unpigmented *M. avium* complex (MAC)*, M. xenopi,* and *M. malmoense* have been classified as nonphotochromogens.[25] Based on glycolipid typing MAC has been further subdivided

into 28 serotypes.[28] Serotypes 1 to 6 and 8 belong to *M. avium* and serotypes 7, 12, 14, 16, and 18 to *M. intracellulare.*

Rodents, insectivores, domestic animals and humans can be a reservoir of mycobacteria. The occurrence of mycobacteria in rodents was first reported by Wells and Oxon[5], with a prevalence of 9 to 31% of *Mycobacterium microti* in rodents. Mycobacteriosis in shrews was also demonstrated by the isolation of the organism from tuberculous pathomorphological changes in the lungs, spleen, liver, kidneys and lymph nodes in 8 of 500 common shrews (*Sorex araneus*) caught in 1946 in Great Britain.[5] Mycobacteria are found in the feed and bedding, as well as the droppings of livestock.[9]. Insectivores and small rodents commonly come into contact with mycobacteria via plants, animal foods, watery environments or contact with birds or humans infected with MAC. At the same time, shrews can easily get inside human or livestock housing and contaminate the environment with their droppings. *Mycobacterium avium-intracellulare* is a common cause of disseminated disease among patients with human immunodeficiency virus (HIV) infection.[3] In a recent study, Voles (*Microtus pennsylvanicus*) infected with *M. bovis* were capable of disseminating the organism via their feces. Both *M. intracellulare* and *M. avium* are capable of gastric transit in animals without destruction due to their resistance to acid. In this way they can be spread over long distances with the migration of the animal.[6] Also, there are several other possible routes of mycobacterial transmission: a) through direct contact with rodent excreta, b) ingestion of food or water contaminated with rodent excreta, c) ingestion of the animal itself, d) inhaling aerosolized rodent excreta, or e) rodent bites, or through ectoparasites.[9]

Depending on the route of infection, affected mammals can present with local cutaneous disease or systemic signs related to the alimentary, and/or respiratory tracts. Typically, disseminated MAC disease begins as a localized process that progress rapidly to include numerous organ systems (i.e. pulmonary, central nervous system, lymphatic, gastrointestinal, and musculoskeletal system).[2-4,7,9-12,14,16-19,21-22,24] The common clinical signs of a MAC infection in immune compromised humans are respiratory distress[19,26], anemia, chronic diarrhea, weight-loss[14], lymphadenitis[19,23], lethargy, hepatosplenomegaly, and arthritis.[29,31]

MAC infections must be differentiated from *M. tuberculosis* or *M. bovis*, and other nontuberculous mycobacterial infections, as well as histoplasmosis, cryptococcosis, coccidioidomycosis, and blastomycosis. The rapid speciation and prevalence estimation of these infecting organisms is desirable because of the public health concerns associated with *M. avium intracellulare*, *M. bovis*, and *M. tuberculosis* infections.[27] Thus, laboratory diagnoses by culture, PCR, and /or histopathology are the traditional methods of testing. A positive culture of MAC from normally sterile sites (blood, bone marrow, lymph node, or liver biopsies), should be considered diagnostic of disseminated disease.[21]

4-1. Giant elephant shrew at necropsy – note swelling on the fifth digit on the left front foot. Photograph courtesy of the Section of Comparative Medicine, Yale Medical School 123 LSOG, http://medicine.yale.edu/compmed/

4-2. Quadriceps muscles, giant elephant shrew at necropsy. There are multiple, coalescing foci of purulent material (abscesses) within the quadriceps and hamstring muscles. Photograph courtesy of the Section of Comparative Medicine, Yale Medical School 123 LSOG, http://medicine.yale.edu/compmed/

4-3. Lungs, giant elephant shrew. Multiple granulomatous foci are scattered throughout the lung. Photograph courtesy of the Section of Comparative Medicine, Yale Medical School 123 LSOG, http://medicine.yale.edu/compmed/

In this case, one of three possible mechanisms probably explains the occurrence of disseminated MAC. The first possibility is that MAC was introduced directly into the tissue via direct inoculation, then disseminating to various organs over a period of time. Secondly, MAC is ubiquitous in the environment, including water sources, and can contaminate drinking water.[18] Water distribution systems have been reported as a possible source of infection in hospitals, homes, and commercial buildings.[1] Because MAC grows slowly, a six month lag between inoculation and clinical presentation, as seen in humans, is biologically plausible.[13] The third possibility is that the shrew had undiagnosed disseminated MAC at the time of arrival, and underwent a period of stress, which suppressed the immune system. Stress of any kind can tip the scale in the direction of the mycobacteria and produce fulminant infection. Systemic mycobacterial infection is an important differential diagnosis for an acute onset of lameness in insectivores.

JPC Diagnosis: Lung: Pneumonia, granulomatous and caseating, multifocal to coalescing, moderate, with numerous intracellular bacilli.

Conference Comment: This case does not have discrete granulomas, but manifests rather as nodular aggregates of granulomatous inflammation that appear to spread from alveolus to alveolus. Caseous necrosis is not typical in granulomatous disease without the formation of discrete granulomas; however, conference participants felt that the morphology of the lesions in this case of MAC-induced nontuberculous mycobacteriosis supported granulomatous as a more descriptive and appropriate term.

In contrast to nontuberculous mycobacterial infections such as MAC, *Mycobacterium tuberculosis* is the prototypical etiologic agent resulting in granulomas

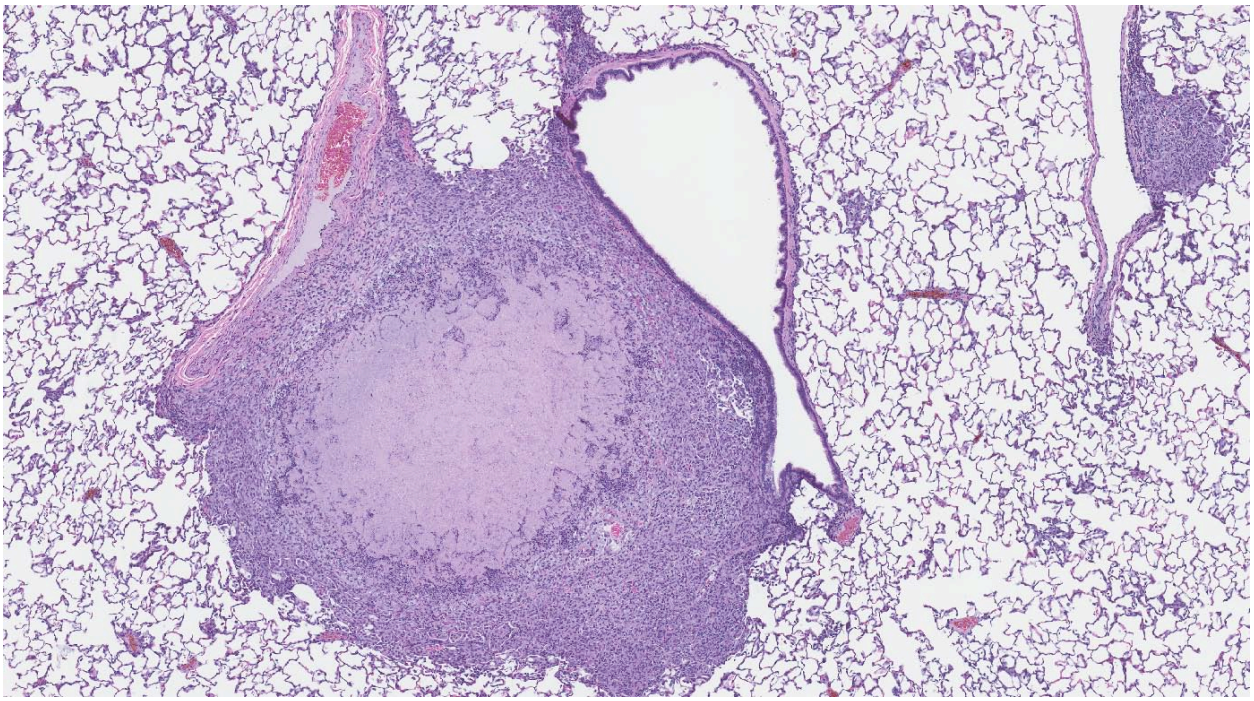

4-4. Lung, giant elephant shrew. Multiple foci of granulomatous inflammation with necrotic centers are present throughout the section. (HE 120X)

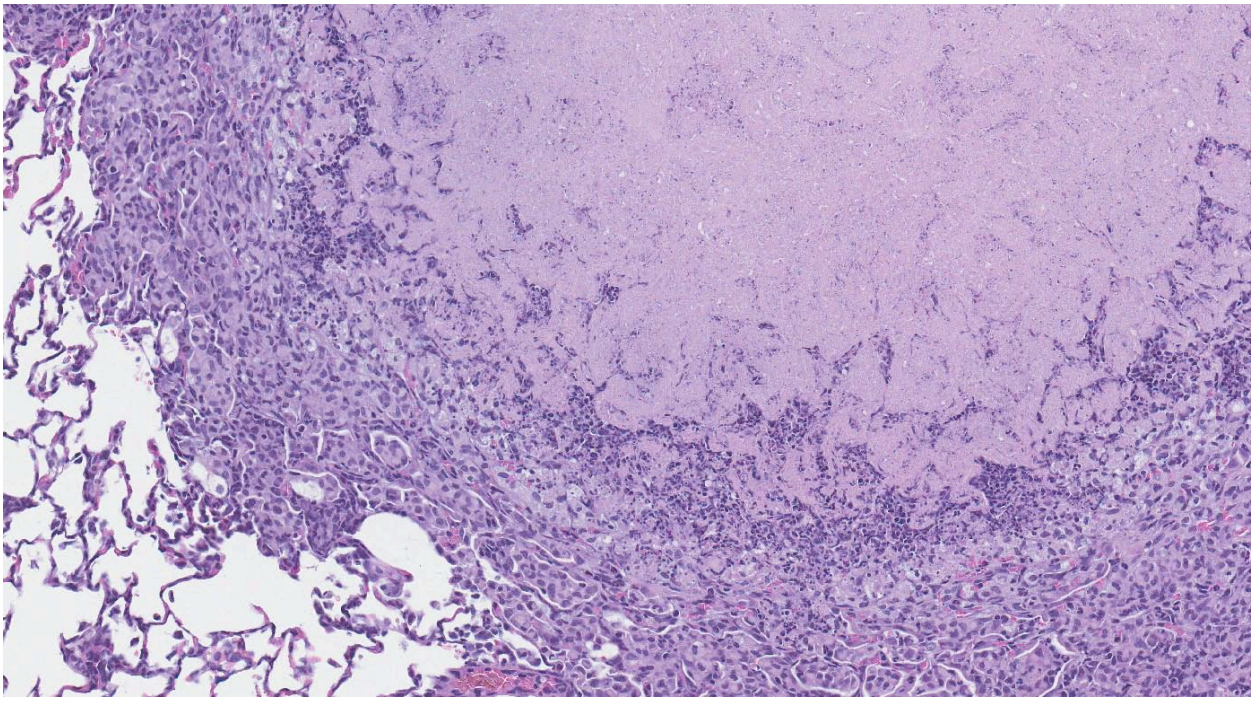

4-5. Lung, giant elephant shrew. The advancing edge of the inflammatory nodule is composed of aggregates of epithelioid macrophages which fill alveoli. The characteristic structure of a granuloma, a fibrous wall, is not present in this case, hence the morphologic diagnosis of granuloma is not appropriate in this case. (HE 280X)

and subsequent tubercle formation. Tubercles form when granulomas develop and coalesce. The center of a tubercle typically consist of white, friable material (caseous necrotic debris) derived from lysed cells and bound by epithelioid macrophages, multinucleated giant macrophages, lymphocytes, plasma cells, fibroblasts and collagen. With time, tubercles may become calcified.

Generally speaking, granulomas form as the result of cell-mediated immunity to a poorly degradable entity such as *Mycobacteria*. Initially, antigen presenting cells (APC), such as alveolar macrophages, present phagocytized mycobacterial antigen and MHC class II proteins to naïve T-cells. Binding of the T-cell receptor with mycobacterial antigen and exposure to the cytokine IL-12 released by the APC promotes differentiation from naïve CD4+ TH1 lymphocytes to activated T-helper 1 lymphocytes producing IL-2, which, in turn, activates additional T cells, tumor necrosis factor, and interferon-γ. Interferon-γ is an important factor in the differentiation of monocytes to epithelioid macrophages and multinucleated giant cells.[17]

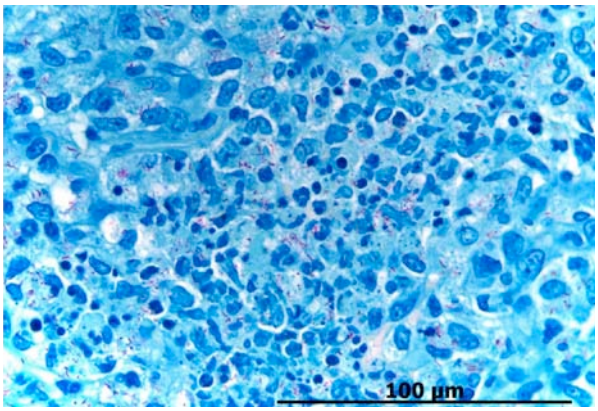

4-6. Lung, giant elephant shrew. Epithelioid macrophages contain few to moderate numbers of acid-fast bacilli. (Ziehl-Nielsen, 400X)

Contributor: Yale Medical School 123 LSOG
Section of Comparative Medicine
http://medicine.yale.edu/compmed/

References:

1. Alvarez J, Garcia IG, Aranaz A, et al. Genetic diversity of mycobacterium avium isolates recovered from clinical samples and from the environment: Molecular characterization for diagnostic purposes. *J. Clin. Microbiol*. 2008;46:1246-1251.
2. Appelberg R. Pathogenesis of mycobacterium avium infection: Typical responses to an atypical mycobacterium? *Immunol. Res.* 2006;35:179-190.
3. Biet F, Boschiroli ML, Thorel MF, et al. Zoonotic aspects of mycobacterium bovis and mycobacterium avium-intracellulare complex (MAC). *Vet. Res*. 2005;36:411-436.
4. Bruijnesteijn van Coppenraet LE, de Haas PE, Lindeboom JA, Kuijper EJ, et al. Lymphadenitis in children is caused by mycobacterium avium

hominissuis and not related to 'bird tuberculosis'. *Eur. J. Clin. Microbiol. Infect. Dis*. 2008;27:293-299.
5. Cavanagh R, Begon M, Bennett M, et al. Mycobacterium microti infection (vole tuberculosis) in wild rodent populations. *J. Clin. Microbiol*. 2002;40:3281-3285.
6. Clarke KA, Fitzgerald SD, Zwick LS, et al. Experimental inoculation of meadow voles (microtus pennsylvanicus), house mice (mus musculus), and norway rats (rattus norvegicus) with mycobacterium bovis. *J. Wildl. Dis.* 2007;43:353-365.
7. Cvetnic Z, Spicic S, Benic M, et al. Mycobacterial infection of pigs in croatia. *Acta Vet. Hung*. 2007;55:1-9.
8. Desimone JA, Jr, Babinchak TJ, Kaulback KR, et al. Treatment of mycobacterium avium complex immune reconstitution disease in HIV-1-infected individuals. *AIDS Patient Care STDS*. 2003;17:617-622.
9. Durnez L, Eddyani M, Mgode GF, et al. First detection of mycobacteria in African rodents and insectivores, using stratified pool screening. *Appl. Environ. Microbiol*. 2008;74:768-773.
10. Fox LE, Kunkle GA, Homer BL, et al. Disseminated subcutaneous mycobacterium fortuitum infection in a dog. J. Am. Vet. Med. Assoc. 1995;206:53-55.
11. Gow AG, Gow DJ. Disseminated mycobacterium avium complex infection in a dog. *Vet. Rec*. 2008;162:594-595.
12. Hibiya K, Higa F, Tateyama M, et al. Mycobacteriosis as zoonotic disease--comparative pathological study on mycobacterium avium complex infection. Kekkaku. 2007;82:539-550.
13. Hoffman GS, Myers RL, Stark FR, et al. Septic arthritis associated with mycobacterium avium: A case report and literature review. *J. Rheumatol*. 1978;5:199-209.
14. Horn B, Forshaw D, Cousins D, et al. Disseminated mycobacterium avium infection in a dog with chronic diarrhoea. *Aust. Vet. J*. 2000;78:320-325.
15. Kasperbauer SH, Daley CL. Diagnosis and treatment of infections due to mycobacterium avium complex. *Semin. Respir. Crit. Care. Med*. 2008;29:569-576.
16. Koh WJ, Kim YH, Kwon OJ, et al. Surgical treatment of pulmonary diseases due to nontuberculous mycobacteria. *J. Korean Med. Sci*. 2008;23:397-401.
17. Kumar V, Abbas AK, Fausto N, et al. Cellular responses to stress and toxic insults: Adaptation, injury, and death. In: Kumar V, Abbas AK, Fausto N, Aster JC, eds. *Robbins and Cotran Pathologic Basis of Disease*. 8th ed. Philadelphia, PA: Saunders Elsevier; 2010:16,74.
18. Marinho A, Fernandes G, Carvalho T, et al. Nontuberculous mycobacteria in non-AIDS patients. *Rev. Port. Pneumol*. 2008;14:323-337.
19. Miller MA, Greene CE, Brix AE. Disseminated mycobacterium avium--intracellulare complex infection in a miniature schnauzer. *J. Am. Anim. Hosp. Assoc*. 1995;31:213-216.
20. Murdoch DM, McDonald JR. Mycobacterium avium-intracellulare cellulitis occurring with septic arthritis after joint injection: A case report. *BMC Infect. Dis*. 2007;7:9.
21. Naughton JF, Mealey KL, Wardrop KJ, et al. Systemic mycobacterium avium infection in a dog diagnosed by polymerase chain reaction analysis of buffy coat. *J. Am. Anim. Hosp. Assoc*. 2005;41:128-132.
22. Ogawa E, Murata M, Ohnishi H, et al. AIDS-related mycobacterium avium infection dissemination in a patient with endobronchial lesions associated with immune reconstitution inflammatory syndrome. *Kansenshogaku Zasshi*. 2008;82:341-346.
23. Oloya J, Opuda-Asibo J, Kazwala R, et al. Mycobacteria causing human cervical lymphadenitis in pastoral communities in the Karamoja region of Uganda. *Epidemiol. Infect*. 2008;136:636-643.
24. Rubin DS, Rahal JJ. Mycobacterium-avium complex. *Infect. Dis. Clin. North Am*. 1994;8:413-426.
25. Runyon EH. Whence mycobacteria and mycobacterioses? *Ann. Intern. Med*. 1971;75:467-468.
26. Steiger K, Ellenberger C, Schuppel KF, et al. Uncommon mycobacterial infections in domestic and zoo animals: Four cases with special emphasis on pathology. *Dtsch. Tierarztl. Wochenschr.* 2003;110:382-388.
27. Thorel MF, Huchzermeyer HF, Michel AL. Mycobacterium avium and mycobacterium intracellulare infection in mammals. *Rev. Sci. Tech*. 2001;20:204-218.
28. Tsang AY, Denner JC, Brennan PJ, et al. Clinical and epidemiological importance of typing of mycobacterium avium complex isolates. *J. Clin. Microbiol*. 1992;30:479-484.
29. Wolinsky E. Nontuberculous mycobacteria and associated diseases. *Am. Rev. Respir. Dis*. 1979;119:107-159.
30. Wolinsky E. Mycobacterial diseases other than tuberculosis. *Clin. Infect. Dis*. 1992;15:1-10.
31. Wong NM, Sun LK, Lau PY. Spinal infection caused by mycobacterium avium complex in a patient with no acquired immune deficiency syndrome: A case report. *J. Orthop. Surg*. (Hong Kong). 2008;16:359-363.

Joint Pathology Center
Veterinary Pathology Services

WEDNESDAY SLIDE CONFERENCE 2011-2012

Conference 9

09 November 2011

CASE I: HSRL-425/00724637 (JPC 4002934).

Signalment: 4-year-old intact female German shepherd canine (*Canis lupus familiaris*).

History: The animal was presented after she fell down the steps in the house a few weeks ago. Owner noted that after the fall she has been wobbling and weak. One week before referral, the owner also reported some bloody vaginal discharge. The referring veterinarian described the patient as bright, alert, responsive, and calm. The dog was reported to have been in heat two months ago. The oral mucosa was pink with a normal capillary refill time; temperature was 101.6 º F (38.6 º C). The animal weighed 37 kg; a loss of 2 kg since last visit.

Ultrasound revealed a distended bladder; the uterus was distended with fluid in both horns. Pyometra was considered but hemogram and serum biochemical analyses were normal, except for a mild serum globulin concentration. Radiographs showed no pulmonary involvement.

Clinical pathology findings at this time:

Low positive Lyme titer. CBC profile: HTC 40.3 (37-55 %); WBC 14.38 (6.5-15.90 th/ul); & neutrophils 80, lm 5%, mono 12 % eos 3 %. Mild moderate platelet clumping.
BUN creatitine within normal limits.
Total protein 8.6 (5.2-8.2)
Albumin 2.9 (2.5-4)
Globulin 5.7 (2.5-4.5)

Two days after the animal's initial visit she was walking sideways, not defecating, and falling down. The animal had a mild head tilt to the left, walked in circles, and bilateral nystagmus. Vestibular disease, Lyme disease and Leptospirosis were included in the differential diagnosis. The dog was treated with tetracycline. The owner wanted an ovariohystorectomy performed on the animal. Cytology performed during surgery revealed numerous degenerated neutrophils and long thin septated fungal hyphae. The animal started fluconazol therapy. The owner was advised of the cytology findings and the owner decided on euthanasia 3 days after surgery. The animal collapsed just before arriving to the clinic and arrived unconscious. The animal was euthanized.

Gross Pathology: The postmortem examination performed by the local veterinarian revealed multifocal, white- gray well demarcated lesions in the liver, heart and kidney. Heart, uterus, and kidney were submitted for histopathology. No brain samples were submitted.

Laboratory Results:
Uterine content were submitted for microbiology: *Bulbithecium spp.* (closely related to *Bulbithecium hyalosporium*) was isolated. The anomorph of this fungus is *Acremonium spp.*

Contributor's Microscopic Description: Uterus: There is a marked thickening of the endometrial wall with severe proliferation of the endometrial glands and lining epithelial cells, partially or completely occluding the uterine lumen. The abundant hyperplastic endometrium forms variable sized cystic dilations filled with eosinophilic acellular granular proteinaceous material admixed with variable numbers and combinations of neutrophils mixed with numerous fungal hyphae. The hyphae are thin (2-4 µm), long (100-200 µm), septate, and occasionally branch out, suggestive of *Acremonium* spp. The inflammatory reaction extends to the myometrium and to the serosal surface.

Contributor's Morphologic Diagnosis: Uterus: Severe, transmural neutrophilic subacute endometritis with intralesional fungal hyphae and marked severe endometrial cystic hyperplasia.

Contributor's Comment: Mycotic uterine infections in dogs are very rare and have been associated with systemic fungal infection rather than exclusive uterine infections. Young German shepherds (GS) have been over represented in cases of systemic aspergillosis or acremoniosis.[4,10,12] It has been described that GS have an immunologic disorder that makes them predisposed for these type of invasions with saprophytic organisms.[6] This case described a mycotic systemic infection due to *Bulbithecium* spp., the anamorph phase of *Acremonium*. Unfortunately in this case no nervous tissue was submitted for histopathology to confirm that the systematic involvement explains the entire clinical presentation. The multifocal, well delimitated white nodules in the heart and the kidney are the classic findings in these systemic mycotic infections. GMS stain done on the uterus sections were positive and not necessary since the fungal hyphae and typical morphology can be seen in the H&E sections submitted for the conference.

The classification of *Acremonium spp.* has *changed*; previously it was described as hypomycetes, and currently it is classified as one of the two members under the group *Dykara* in the sub group A*scomycotas*. It is still classified as Imperfect fungi (Deuteromycota), and nondematiaceous (not pigmented), but the term hyphomycetes is obsolete.

Pyometra is inflammation of the uterus that has variable symptomology from genitourinary disease to non-specific systemic disease. In the dog, pyometra is associated with cystic endometrial hyperplasia predisposed for by luteal activity (progesterone). During this phase, progesterone inhibits the intrauterine leukocyte response, decreases muscle contractibility and stimulates development and secretion of endometrial glands.[2,8] Clinically, pyometra

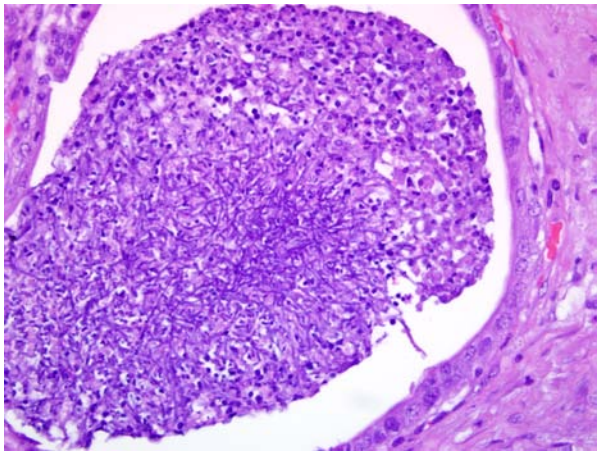

1-1. Uterus, dog. Ectatic endometrial glands are filled with tangles of fungal hyphae enmeshed with abundant cellular debris. (HE 400X)

can be associated with or without vaginal discharge depending on whether the cervix is closed or open. If the cervix is closed, the prognosis is more serious since the possibility of septic or uterine peritonitis exists.[2,9]

Fungi are a very variable group of eukaryotic organisms that belong to the fungi kingdom.[7] The old classification was based on morphologic microscopic features that classified the kingdom in 6 phyla. Classification of fungi is confusing and based on several criteria including formation of hyphae, pseudohyphae, or yeast forms. Another feature important in classification is the presence of a sexual stage of reproduction (teleomorph stage) or the absence of sexual reproduction (anamorphous stage). Biochemical and physical properties can be used to distinguish different species. However, more recently, molecular genetics and DNA analysis have played a role in taxonomy.[7]

Unfortunately, at the present time, there are no agreements on specific rules for an international system to facilitate the fungal nomenclature. There are some efforts to create an organized fungal classification scheme.[7]

The kingdom of Fungi is classified in 7 or 8 phyla or subdivisions.[5]

Infections by hyalohyphomycosis with nondematiaceous or not pigmented fungi have been described in other species such as horse, reptiles, and humans.[6]

JPC Diagnosis: Uterus: Endometritis, necrotizing, diffuse, severe, with marked cystic endometrial hyperplasia and numerous fungal hyphae.

Conference Comment: The contributor mentioned the predisposition of German shepherd dogs to

disseminated infection with saprophytic fungi, and conference participants discussed *Aspergillus terreus* as the most common culprit, with reported lesions including pneumonia, myositis, myocarditis, endometritis, encephalitis, nephritis, splenitis, osteomyelitis, and lymphadenitis due to hematogenous spread of the fungal aleurospores.[3] In addition to bacterial and rare fungal and viral causes of endometritis in dogs, a differential diagnosis should include other non-infectious etiologies such as pseudopregnancy, caused by retained corpora lutea which can contribute to cystic endometrial hyperplasia-pyometra complex, and placental sub-involution, which manifests as necrosis and hemorrhage of the endometrium with invasion of trophoblasts into adjacent myometrium and blood vessels, producing a hemorrhagic vaginal discharge.[11]

In mares, a reported fungal cause of abortion is fescue grass toxicity caused by *Neotyphodium* (formerly *Acremonium) coenophialum.* This fungal endophyte infects grass and produces the ergot alkaloid ergovaline, which causes dysmaturation of foals and infrequent abortion. Ergovaline, in addition to its well known alpha-2 adrenergic agonistic effects causing vasoconstriction seen in fescue foot in cattle, is a potent dopamine D_2 receptor agonist which blocks prolactin, which is important in maintaining the corpus luteum and mammary gland growth and milk production. The lack of prolactin with decreased progesterone and increased estradiol in the mare during pregnancy can lead to fetal death. Fetal death also occurs from suffocation due to a thick edematous placenta that does not rupture at the cervical star. The mares are also agalactic with minimal colostrum, and if the foal survives to term, they often die due to failure of passive transfer.

Contributor: Western University of Health Sciences
College of Veterinary Medicine
309 E. Second street
Pomona, California
http://www.westernu.edu/xp/edu/veterinary/about.xml

References:

1. Blodgett DJ. Fescue toxicosis. In: Gupta RC, ed. *Veterinary Toxicology Basic and Clinical Principles*. New York, NY: Academic Press; 2007:907-13.
2. Bonagura JD, Kirk RW. *Kirk's Current Veterinary Therapy XII, Small Animal Practice.* W.B. Saunders Co; 1995.
3. Bruchim Y, Elad D, Klainbart S. Disseminated aspergillosis in two dogs in Israel. *Mycoses*. 2006;49 (2):130-3.
4. Day MJ, Eger CE, Shaw SE, Penhale WJ. Immunologic study of systemic aspergillosis in German shepherd dogs. *Veterinary Immunology and Immunopathology.* 1985;9(4):335-347.
5. Deacon, JW. *Modern Mycology 3rd ed.* Oxford, UK: Blackwell Science; 1997.
6. Foley JE, Norris CR, Jang SS. Paecilomycosis in Dogs and Horses and a Review of the Literature. *Journal of Veterinary Internal Medicine.* 2002;16(3): 238-243.
7. Hibbett DS, et al. A higher level phylogenetic classification of the Fungi. *Mycological Research*. 2007;111(5):509–47.
8. McGavin DM. *Pathologic Basis of Veterinary Disease 4th ed*. Mosby/Elsevier; 2007.
9. Noakes DE, Dhaliwal GK, England GC. Cystic endometrial hyperplasia/pyometra in dogs: a review of the causes and pathogenesis. *J Reprod Fertil.* 2001;57 (Suppl):395-406.
10. Pedersen NC. A review of immunologic diseases of the dog. *Veterinary Immunology and Immunopathology.* 1999;69 (2-4):251-342.
11. Schlafer DH, Miller RB. Female genital system. In: Maxie MG, ed. *Jubb, Kennedy, and Palmer's Pathology of Domestic Animals*. 5th ed. Vol 3. Philadelphia, PA: Saunders Elsevier; 2007:537-8.
12. Simpson KW, Khan KN, Podell M, et al. Systemic mycosis caused by Acremonium sp in a dog. *J Am Vet Med Assoc*. 1993;203(9):1296-9.

CASE II: 8-456-11 (JPC 4003080).

Signalment: Adult cow bison, *Bison bison.*

History: Placenta submitted from a bison cow that recently aborted in a capture facility in Yellowstone National Park.

Gross Pathology: The non-cotyledonary regions of the chorioallantois were diffusely opaque, edematous and white/pink. The cotyledons were tan and had scattered hemorrhage.

Laboratory Results: *Brucella abortus* biovar 1 was isolated from the placenta.

Contributor's Microscopic Description: Placenta: Multifocally, the cotyledons of the chorioallantois are necrotic as characterized by loss of distinct villar architecture with replacement by a granular to fibrillar eosinophilic material containing karyorrhectic debris including necrotic leucocytes. Intracytoplasmic bacteria occur within trophoblasts. The deeper connective tissue is edematous with scattered infiltrates of neutrophils and fewer macrophages.

Contributor's Morphologic Diagnosis: Placentitis, necrotizing, acute, multifocal, severe, with intracytoplasmic bacteria and severe edema, chorioallantois, placenta.

2-1, 2-2. Fetus and placenta, bison. The cotyledons are tan with multifocal hemorrhages and the intercotyledonary portions of the placenta are opaque and edematous. Photographs courtesy of Montana Veterinary Diagnostic Laboratory http://liv.mt.gov/liv/lab/index.asp.

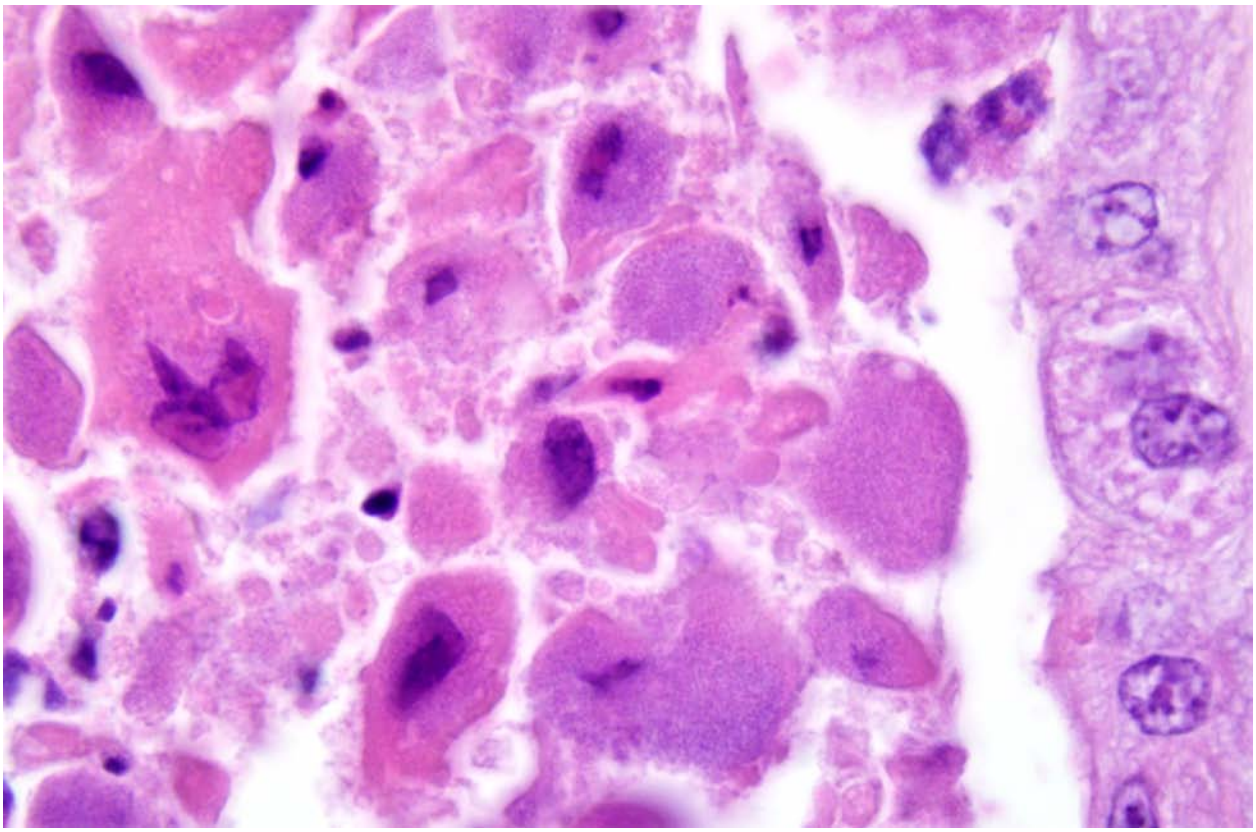

2-3. Placenta, bison. Trophoblasts are shrunken and hypereosinophilic (necrosis) and often contain many lightly basophilic intracytoplasmic coccobacilli. (HE 1000X)

Contributor's Comment: The primary consequences of brucellosis in domestic animal populations are economic losses due to decreased production. Infections also occur in wild populations and in the United States; bison and elk in the Greater Yellowstone Area (GYA) and wild/feral swine in other areas of the US are natural reservoirs hosts. The recent *Brucella abortus* outbreaks in cattle within the GYA are considered to be the result of transmission from infected elk herds. Disease management practices in bison herds of Yellowstone National Park have been controversial and polarizing for several decades. Permanent solutions for disease control or population management in the bison and elk herds of this region will be difficult to implement because of a multitude of factors including the following: large wild animal populations within a large geographic area; differing jurisdictional boundaries of governmental agencies; differing state and federal agency missions and mandates; naïve understanding and exaggerated fears of the disease by various groups and entities; the urbanization of the populace; and financial interests. Although brucellosis has been eradicated in domestic herds in some advanced countries, the disease is still significant in animals and humans throughout most of the world. The agent's zoonotic potential also lead to the propagation and incorporation of the agent into national bio-warfare arsenals.

Brucellosis is caused by small gram-negative bacilli of the genus *Brucella*; these bacteria are facultative intracellular organisms. The organism lacks many of the typical virulence factors of pathogenic bacteria and how the organism resists phagocytic degradation and is able to replicate within professional and non-professional phagocytes is poorly understood. There are multiple species within the genus and include: *B. abortus* biovars 1-9 (cattle), *B. suis* biovars 1-5 (swine), *B. ovis* (sheep), *B. melitensis* biovars 1-3 (sheep and goats), *B. canis* (dog), *B. neotomae* (rodents), and species that infect pinnipeds and cetaceans. *B. abortus, B. suis* and *B. melitensis* are further subdivided into biovars but contrary to the species name, these organisms can also cause disease in numerous other domestic and wild animal hosts and these are the common species infecting man. *B. canis* and marine *Brucella* species have also rarely been associated with disease in man, whereas *B. ovis* and *B. neotomae* are recognized to only infect sheep and rodents, respectively.

Brucellosis in animals is characterized by third trimester abortion with necrotizing placentitis, retained placentas and metritis, weak calves, mastitis, arthritis/

hygromas/bursitis, and in males, orchitis/epididymitis and seminal vesiculitis. The disease in susceptible domestic animal populations has significant economic consequences due to calf loss, infertility, decreased milk production and disease regulatory consequences. Infected animals can eventually become resistant but could still act as intermittent shedders that serve as a reservoir of infection within the herd. Transmission is usually through ingestion or contamination of mucous membranes after exposure to infected fetuses, fetal membranes or contaminated body fluids. Venereal transmission occurs with *B. suis, B. ovis* and *B.canis* but is uncommon with *B. abortus* or *B. melintensis*. Abortions also can occur after vaccination of pregnant females with live vaccine strains.

Brucellosis in man has multiple synonyms such as undulant fever and Malta fever. In countries where the disease is common, infection in man is normally acquired by ingestion of contaminated dairy products or exposure to infected animal reproductive tissues and fluids. Infection can result from exposure to the agent after ingestion, inhalation, through open wounds, accidental injection when vaccinating animals, and congenitally from infected mothers. Effective animal disease control programs and pasteurization of dairy products are major contributors in the low rates of human infections in modern societies. Laboratory personnel, veterinarians and agricultural and slaughterhouse workers are at higher risk for acquiring infections. Laboratory personnel are extremely vulnerable and can readily be exposed if safety precautions are not utilized. Centers for Disease Control and Prevention Biosafety in Microbiological and Biomedical Laboratories (CDC BMBL) recommends strict adherence to BSL-3 safety practices in conjunction with sound laboratory techniques when culturing the organism. The infectious dose for man varies depending on the species. In man, only 1-10 CFU of *B. melitensis* can cause disease. Reported infectious doses for immune-competent people with the following species are: *B. suis* (1000-10,000 CFU), *B. abortus* (100,000 CFU) and *B. canis* (greater that 1,000,000 CFU).

Acute disease in man usually results in incapacitating flu-like illness, cyclic fevers, gastrointestinal upsets, epididymitis/orchitis, and in severe cases, CNS or endocardial disease. Chronic infections can manifest as chronic fatigue-like syndromes, depression, arthritis, endocarditis, hepatitis, cholecystitis, meningitis, uveitis, and osteomyelitis. Mortality rate is less than 5%. Treatment involves long term antibiotic therapy and currently, there is no human vaccine.

JPC Diagnosis: Chorioallantois: Placentitis, necrotizing, multifocal to coalescing, moderate, with marked edema, diffuse vasculitis, and with numerous intratrophoblastic bacilli.

Conference Comment: Transmission of brucellosis is by contact with infected tissues, secretions or excretions, such as milk, urine, and fetal and placental tissues. The bacteria penetrate the mucosa and migrate to local and regional lymph nodes after being engulfed by local macrophages or dendritic cells, within which the bacteria grow and replicate. The bacteria kill the phagocytes and incite a pyogranulomatous lymphadenitis due to the lipopolysaccharide composition of the bacterial cell wall. The bacteria are systemically disseminated via leukocyte trafficking, enabling them to infect the mammary glands, reproductive organs, placenta and fetus. Chorionic epithelial cells naturally produce erythritol around the fifth month of gestation, which is a carbohydrate growth promoter for *Brucella abortus*, and the bacteria multiply in the rough endoplasmic reticulum of chorionic trophoblasts. Other intratrophoblastic bacterial agents causing abortion include *Leptospira interrogans*, *Coxiella burnetti*, *Listeria monocytogenes*, *Campylobacter fetus* and *C. jejuni*, and *Chlamydophila abortus* and *C. pecorum*; intratrophoblastic protozoa include *Toxoplasma gondii*, *Neospora caninum*, and *Sarcocystis* spp., although protozoal cysts are more commonly found in other tissues, especially in the central nervous system.[11]

Fetal death and abortion are attributed to placental disruption and endotoxemia; fibrinous bronchopneumonia, pleuritis and pericarditis are seen in the fetus. In addition to *Arcanobacterium pyogenes*, *B. abortus* is the most common cause of bacterial fetal pneumonia. The bacterial infection induces hypoxia through placental inflammation, and this disruption of the placenta induces a breathing response in the fetus, and death is due to aspiration of the amniotic fluid.[3,5,14] Typical gross placental lesions include extensive cotyledonary necrosis; intercotyledonary edema with a tough, yellow to gray, leathery surface; necrosis and inflammation of the placental arcades; and inflammation of the maternal septa, leading to placental interlocking and retained placenta.[5] *Brucella abortus* is also commonly associated with bursitis in horses, known colloquially as poll evil and fistulous withers.[13]

Contributor: Montana Veterinary Diagnostic Lab
PO Box 997, 19th and Lincoln
Bozeman, Montana 59715
Corvallis, OR 97331
http://liv.mt.gov/liv/lab/index.asp

References:

1. August K, Rovid-Spickler A, et al. Brucellosis. Available at http://www.cfsph.iastate.edu/Factsheets/pdfs/brucellosis.pdf. 2009

2. Beja-Pereira A, Bricker B, et al. DNA genotyping suggests that recent brucellosis outbreak in Greater Yellowstone Area originated from elk. *J Wild Dis*. 2009;45:1174-1177.
3. Foster RA. Female reproductive system and mammary gland. In: Zachary JF, McGavin MD, eds. *Pathologic Basis for Veterinary Disease*. 5th ed. St. Louis, MO: Elsevier Mosby; 2011:531.
4. Kreeger TJ, Cook WE, et al. Brucellosis in captive Rocky Mountain bighorn sheep (*Ovis* canadensis) caused by *Brucella abortus* biovar 4. *J Wild Dis*. 2004;40:311-315.
5. Lopez A. Respiratory system, mediastinum, and pleurae. In: Zachary JF, McGavin MD, eds. *Pathologic Basis for Veterinary Disease*. 5th ed. St. Louis, MO: Elsevier Mosby; 2011:1113.
6. Meyer M, Meagher M. Brucellosis in free ranging bison (*Bison bison*) in Yellowstone, Grand Teton and Wood Buffalo National Parks: a review. Letter to editor. *J Wild Dis*. 1997;31:579-598.
7. Olsen SC, Holland SD. Safety of revaccination of pregnant bison with *Brucella abortus* strain RB51. *J Wild Dis*. 2003;39:824-829.
8. Rhyan JC, Gidlewski T, et al. Pathology of brucellosis in bison from Yellowstone National Park. *J Wild Dis*. 2001;37:101-109.
9. Rhyan JC, Holland SD, et al. Seminal vesiculitis and orchitis caused by *Brucella abortus* biovar 1 in young bison bulls from South Dakota. *J Vet Diagn Invest*. 1997;9:368-374.
10. Rhyan JC, Quinn WJ, et al. Abortion caused by *Brucella abortus* biovar 1 in free ranging bison (*Bison bison*) from Yellowstone National Park. *J Wild Dis*. 1994;30:445-446.
11. Schlafer DH, Miller RB. Female genital system. In: Maxie MG, ed. *Jubb, Kennedy, and Palmer's Pathology of Domestic Animals*. 5th ed. Vol 3. Philadelphia, PA: Saunders Elsevier; 2007:484-9, 490-516.
12. Tessaro SV, Forbes LB. Experimental *Brucella abortus* infection in wolves. *J Wild Dis*. 2004;40:60-65.
13. Thompson K. Bones and joints. In: Maxie MG, ed. *Jubb, Kennedy, and Palmer's Pathology of Domestic Animals*. 5th ed. Vol 1. Philadelphia, PA: Saunders Elsevier; 2007:172-3.
14. Zachary JF. Mechanisms of microbial infection. In: Zachary JF, McGavin MD, eds. *Pathologic Basis for Veterinary Disease*. 5th ed. St. Louis, MO: Elsevier Mosby; 2011:189-90, 198.

CASE III: NF-08-747 (JPC 3134538).

Signalment: Term fetus female Alpine dairy goat, (*Capra hircus).*

History: Twin female American Alpine dairy goat fetuses were submitted for determination of the cause of abortion. These were from a newly assembled dairy goat herd which had experienced multiple abortions over the last week.

Gross Pathology: On physical exam, the fetuses were moderately autolytic, and contained serosanguinous fluid within their pleural cavities. No other gross lesions were detected in the fetuses or their accompanying placentas. All samples were taken from the larger of the two fetuses.

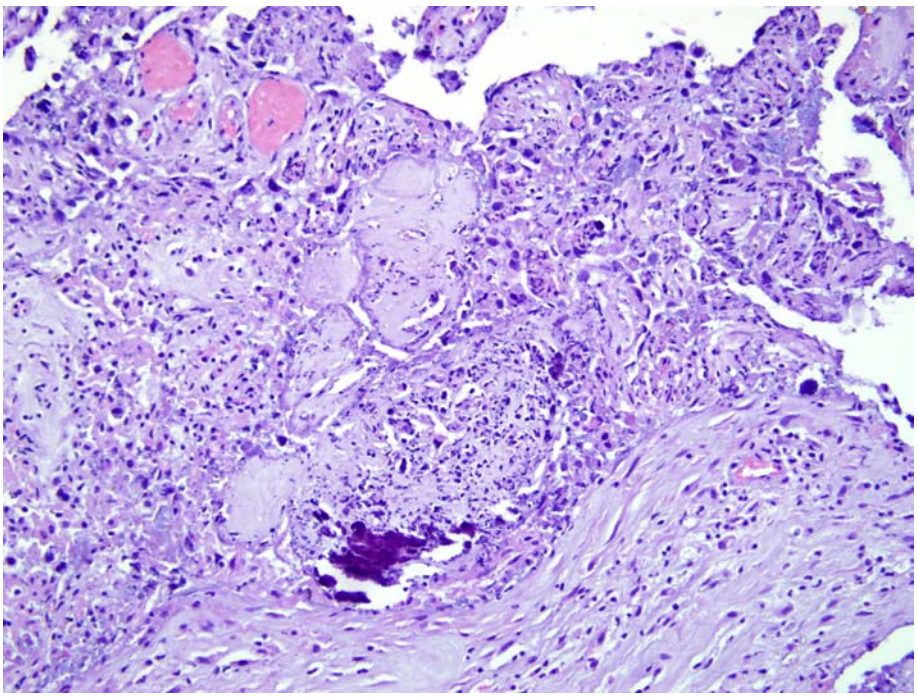

3-1. Placenta, goat. Chorionic villi are collapsed and largely replaced by necrotic cellular debris, degenerate neutrophils and multifocal mineralization. (HE 200X)

Laboratory Results: PCR for *Coxiella burnetii* was positive on placenta; PCR for *Chlamydophila* sp. was negative. Mixed coliforms and *Streptococcus* sp. were isolated from the placenta. Cultures of lung, liver, and stomach contents were negative.

Contributor's Microscopic Description: Slides contain sections of chorioallantois. Chorionic villi are necrotic, and the surface has adherent necrotic cellular debris and degenerate neutrophils. A mixed infiltrate of neutrophils, lymphocytes, plasma cells, and histiocytes extends throughout the interstitium of the chorioallantois. Numerous trophoblasts are distended by intracellular colonies of palely basophilic bacteria. Gram stains of the chorionallantois demonstrate these colonies consist of gram-negative short bacilli. Depending on the section, there is variable partial mineralization of the epithelium.

Immunohistochemistry using a generic antibody against *Coxiella burnetii* was strongly immunopositive for the intracytoplasmic bacterial colonies.

Contributor's Morphologic Diagnosis: Chorioallantois: Severe acute necrotizing placentitis with intracellular bacterial colonies.

Contributor's Comment: *Coxiella burnetii* is a member of the Rickettsiaceae family, which are small,

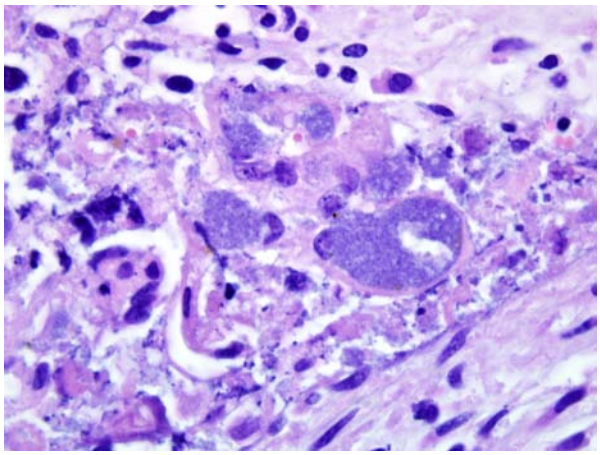

3-2. Placenta, goat. Trophoblasts are distended by numerous intracytoplasmic basophilic coccobacilli. (HE 1000X)

non-motile gram-negative bacteria that replicate only within host cells. Infection with *Coxiella burnetii* is relatively common in domestic cattle, sheep and goats, which serve as the reservoir hosts. Infection is persistent, and shedding of the organism through urine, feces, milk and placental fluids contaminates the environment. Acute infection in domestic ruminants may manifest itself as late third trimester abortions, stillbirths, delivery of weak neonates, retained placentas, endometritis and infertility. When the placenta is infected, the obligate intracellular bacteria are encountered within the cytoplasm of trophoblasts. Gross lesions in the placenta (not noted in this case)

include thickened and leathery appearance, and off-white exudates which are most prominent in the intercotyledonary regions of the chorioallantois. However, histologically, the predominantly necrotizing and suppurative placentitis frequently extends into cotyledonary regions as well. The principal differential for *C. burnetii* in the placenta is *Chlamydophila* infection, which produces a similar placentitis with intracytoplasmic colonies.

In humans, *C. burnetii* results in the zoonotic condition known as Q fever. Acute infection may include mild flu-like symptoms, pneumonia, or hepatitis. The organism infects monocytes and macrophages which internalize the organism into phagolysosomes. In the environment, the organism survives as the highly resistant extracellular small cell variant. But once inside monocytes or macrophages, the organism switches to the large cell variant. The more debilitating chronic form of the disease in humans is characterized by endocarditis, hepatitis, and chronic fatigue syndrome. Due to *C. burnetii*'s resistance to environmental conditions of heat and pressure, and its highly infectious nature, it is classified as a "Category B" biological warfare agent.

JPC Diagnosis: Chorioallantois: Placentitis, necrotizing, multifocal to coalescing, marked, with numerous intratrophoblastic bacilli.

Conference Comment: *Coxiella burnetii* is transmitted by most tick species and can be acquired by aerosolization and direct contact. Although infection occasionally causes abortions in cattle, abortion is a more common result in small ruminants and typically presents as isolated abortions rather than as an abortion storm. Unless infection is overwhelming, as in this case, the organisms may not be visible with hematoxylin and eosin (H&E) staining, but silver stains and immunohistochemistry are useful.[3] Because of concerns for safety of laboratory personnel, the organism should only be cultured within a biosafety level-3 laboratory.

Brucella abortus, another differential for this case, also causes cotyledonary and intercotyledonary necrosis, but the fetus usually has bronchopneumonia, which helps differentiate infection with this organism from *Coxiella*. Other differential causes for necrotizing placentitis are *Chlamydophila abortus*, which commonly also causes vasculitis, and *Toxoplasma gondii*, which primarily affects the cotyledons and spares the intercotyledonary areas.[3] Multifocal epithelial mineralization around blood vessels in small ruminant placentas can be a normal physiologic process and contributes to ossification of the fetal skeleton.

Contributor: Michigan State University
Diagnostic Center for Population and Animal Health
4125 Beaumont Rd
Lansing, MI 48910
www.animalhealth.msu.edu

References:

1. Kazar J. *Coxiella burnetii* infection. Ann NY *Acad Sci*. 2005;1063:105-114.
2. Sanchez J, Souriau A, Buendia AJ, et al. Experimental *Coxiella burnetii* infection in pregnant goats: a histopathological and immunohistochemical study. *J Comp Path*. 2006;135:108-115.
3. Schlafer DH, Miller RB. Female genital system. In: Maxie MG, ed. *Jubb, Kennedy, and Palmer's Pathology of Domestic Animals*. 5th ed. Vol 3. Philadelphia, PA: Saunders Elsevier; 2007:484, 502, 505, 513.

CASE IV: 648-11 (JPC 4003704).

Signalment: 8-day-old female Aberdeen Angus *(Bos taurus),* bovine.

History: This calf was from a cow-calf herd with 55 suckler cows. The herd had suffered from increased morbidity and mortality of suckling calves aged 1-9 days old. Clinical signs of this calf included diarrhea, petechiae on the conjunctival and buccal membranes, fever and generalized weakness.

Gross Pathology: Weight 39 kg, moderate post mortem changes, moderate fat stores, and severely dehydrated. All visible lymph nodes were swollen. The umbilical arteries were swollen and deep red. The spleen was moderately enlarged. The liver contained multiple disseminated 2-3 mm pale yellow spots all over the parenchyma. The abomasum contained 1 liter of coagulated milk, mucosa was moderately red and swollen. The distal parts of the jejunal and the ileal serosa and mucosa were red, and ileal lymph nodes were severely swollen and reddish gray. Pale purulent exudate covered the meninges of the brain stem. Fibrinous pale exudate was detected in the joint cavities of the legs.

Laboratory Results: *Listeria monocytogenes* was isolated in pure growth from the spleen, liver, lung, ileal lymph node and brain. *Salmonella* was not detected.

Contributor's Microscopic Description: Liver: Multifocal, disseminated, random, variable sized foci of deeply eosinophilic (coagulation necrosis) hepatocytes, infiltrated with variable, usually moderate, numbers of degenerating neutrophils and a few macrophages. Brown-Benn staining showed multiple gram-positive short rod shape bacteria in these foci. In other tissues (samples not submitted), a suppurative synovitis and meningitis, and a necrotizing lymphadenitis and enteritis were detected.

Contributor's Morphologic Diagnosis: Liver: Multifocal moderate subacute necrotizing hepatitis.

Contributor's Comment: The genus *Listeria* includes 6 species, of which two, *L. monocytogenes* and *L. ivanovii,* are known to cause disease in animals. *L. ivanovii* has been detected causing abortions in ruminants. *L. monocytogenes* is ubiquitous in the environment, in the soil, plants and feces of animals. It

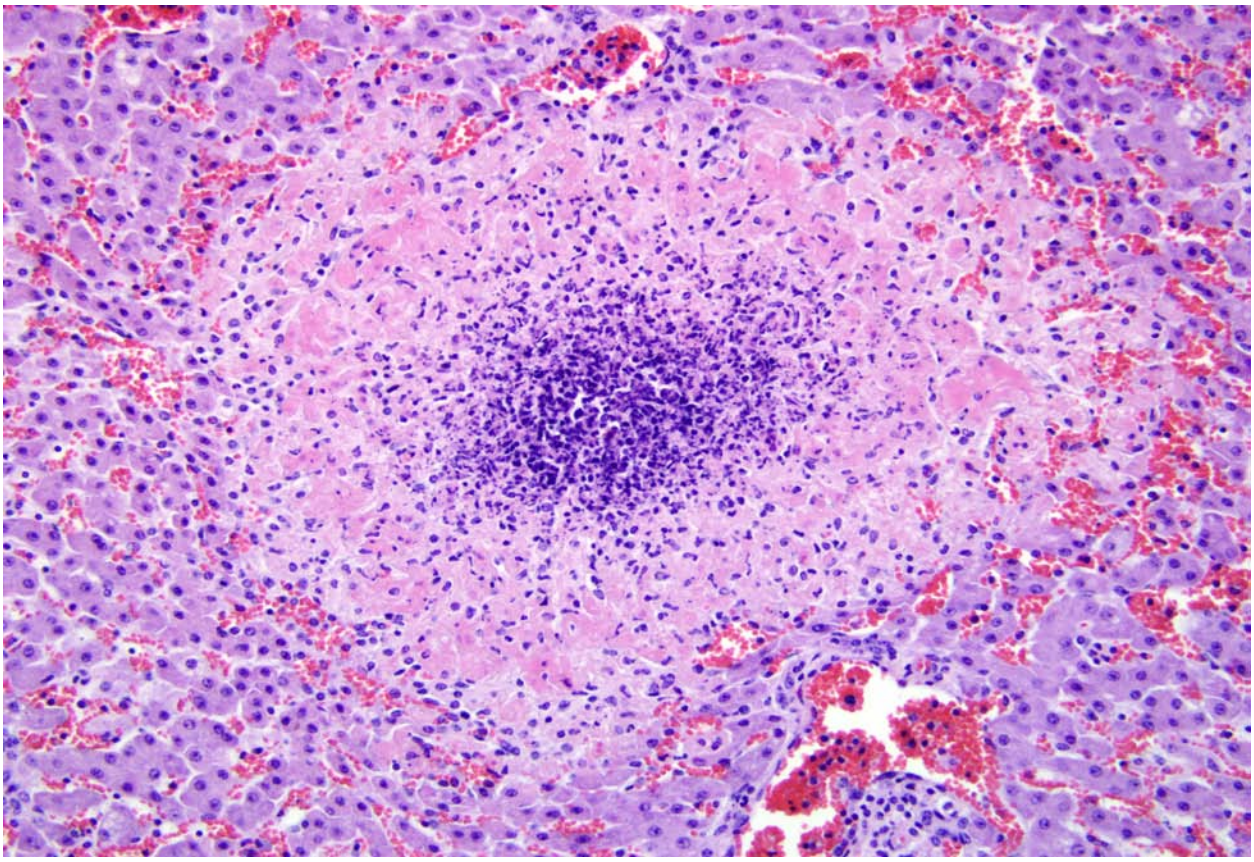

4-1. Liver, calf. There are numerous randomly distributed foci of lytic necrosis bordered by a rimof hepatocytes undergoing coagulative necrosis. (HE 200X)

is a gram-positive short non-spore forming rod capable of growing from 1° C to 45° C and pH 4.5-9.6. *L. monocytogenes* is an opportunistic pathogen and causes disease in several animal species including mammals, birds and fish. Of the domestic species, most commonly ruminants are affected, rarely also foals or pigs.[2,6] Feeding of poorly fermented silage with pH over 5 has commonly been associated with occurrence of the disease in ruminants. Listeriosis is a zoonosis.

The three main types of disease caused by *Listeria* are meningoencephalitis, abortions and septicemia. Meningoencephalitis is the most common form of the disease and occurs mainly in adult ruminants. Abortions in the last third of the pregnancy or stillbirths are most often detected in sheep, goats and cattle. Septicemia occurs in young ruminants and neonate monogastric animals. Less common forms of the disease are conjunctivitis, keratitis or uveitis in ruminants and horses[1]; mastitis, endocarditis, meningitis in young animals; spinal myelitis in sheep; and enteritis in adult sheep. Recently, a fatal mesenteric lymphadenitis was described in adult cattle.[5] Also, skin infections have been described in veterinarians. *L. monocytogenes* septicemia occurs also in rabbits, chinchillas, hares, and has been described in semi-domesticated reindeer calves associated with silage feeding.[3] The disease is often sporadic but small epidemics occur.

Infection occurs via ingestion, from the contaminated feed or udder, via milk or umbilical cord, or in the uterus. The bacteria penetrate the intestinal mucosa and cause a subclinical bacteremia. Encephalitis in ruminants has a different pathogenesis and is probably acquired via cranial nerves from oral mucosal abrasions or an infected tooth cavity. In these cases the bacteria reach the brain stem by using axonal transport. This is supported by the special distribution of the lesions in the brain stem. The incubation period varies from 2 days to several weeks. Only a small proportion of infected animals develop clinical disease. The predisposing factors include stress, pregnancy, parturition, poor nutritional state, large dose and failure of passive transfer. In humans the infection is usually foodborne and pregnant women, elderly and immunocompromised individuals are predisposed.

Listeria is a facultative intracellular parasite and invades cells, macrophages, monocytes, neutrophils and epithelial cells by using a special surface protein, internalin.[2] In the cell, bacteria escape from the phagosomes by producing a haemolysin called listeriolysin O and phospholipases. The bacteria are motile and have a special cell to cell movement system. Cell-mediated immunity has a role in causing tissue damage. Gross pathological findings in septicemic forms of the disease consist of multiple random pale necrotic foci or microabscesses, most commonly in the liver and spleen.
Histologically, in the septicemic form, multiple necrotic foci or microabscesses with variable numbers of neutrophils and macrophages are seen in the liver, and are often also in the spleen or other tissues.

The differential diagnoses for necrotic hepatitis include S*almonella*, *Bacillus piliformis* (Tyzzer's disease), *Yersinia pseudotuberculosis,* and in rodents also *Toxoplasma gondii*.

JPC Diagnosis: Liver: Hepatitis, necrotizing, multifocal and random, moderate.

Conference Comment: Glycogen vacuoles present in the liver suggest this is a young animal. Because infection occurs following ingestion, *Listeria* causes individual abortions rather than an abortion storm. It also causes placentitis with cotyledonary necrosis and vasculitis of the chorioallantois but not the amnion. Necrotizing hepatitis and enteritis may also be prominent features in the aborted bovine fetus. With early third trimester infection and following abortion, the placenta is often retained due to mild metritis; however, the dam usually does not suffer severe illness. Conversely, if infected near term, the dam often suffers from dystocia, severe metritis and septicemia.[4] Neutrophils are the primary inflammatory cell in listeriosis, due in part to *Listeria* infected endothelial cells expressing P- and E-selectin, intracellular adhesion molecule-1 (ICAM-1), and vascular cell-adhesion molecule-1 (VCAM-1), which activate the neutrophil adhesion cascade and neutrophil binding.[7]

Contributor: Finnish Food Safe Authority Evira
Production Animal and Wildlife Research Unit
Elektroniikkatie 3, 90590 Oulu, Finland

References:

1. Evans K, Smith M, McDonough P, et al. Eye infections due to Listeria monocytogenes in three cows and one horse. *J Vet Diagn Invest*. 2004;16:464-9.
2. Maxie MG, Youssef S. Nervous system. In: Maxie MG, ed. *Jubb, Kennedy and Palmer's Pathology of Domestic Animals*. 5th ed. Vol 1. Philadelphia, PA: Saunders Elsevier; 2007:405-8.
3. Nyyssönen T, Hirvelä-Koski V, Norberg H, et al. Septicaemic listeriosis in reindeer calves- a case report. *Rangifer*. 2006;26:25-28.
4. Schlafer DH, Miller RB. Female genital system. In: Maxie MG, ed. *Jubb, Kennedy, and Palmer's Pathology of Domestic Animals*. 5th ed. Vol 3. Philadelphia, PA: Saunders Elsevier; 2007:492-3.

5. Thompson H, Taylor DJ, Philbey AW. Fatal mesenteric lymphadenitis in cattle caused by Listeria monocytogenes. *Vet Rec*. 2009;164:17-18.
6. Wilkins PA, Marsh PS, Acland H, et al. Listeria monocytogenes septicaemia in a thoroughbred foal. *J Vet Diagn Invest*. 2000;12:173-176.
7. Zachary JF. Mechanisms of microbial infection. In: Zachary JF, McGavin MD, eds. *Pathologic Basis for Veterinary Disease*. 5th ed. St. Louis, MO: Elsevier Mosby; 2011:195.

Joint Pathology Center
Veterinary Pathology Services

WEDNESDAY SLIDE CONFERENCE 2011-2012

Conference 10

16 November 2011

CASE I: CS-1 (JPC 4002461).

Signalment: A 5-year-old spayed female Rhodesian Ridgeback dog (*Canis familiaris*).

History: The dog was presented for a large (approximately 7 cm diameter), subcutaneous moveable mass over the left shoulder. Two weeks after surgical excision, the dog presented with neurologic signs and blindness. Euthanasia was elected because of poor prognosis.

Gross Pathology: There is a 14 cm diameter, fluid-filled, ulcerated subcutaneous mass present over the left shoulder (seroma). The abdominal lymph nodes are enlarged (2x2x2 to 2x3x1.5 cm diameter). On cut section, the architecture of lymph nodes is effaced by

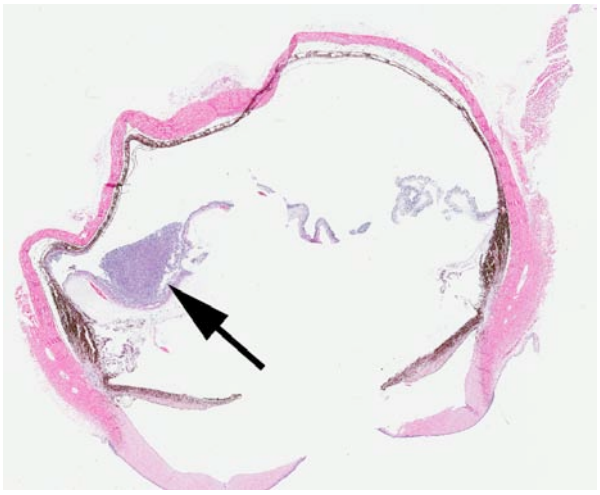

1-1. Eye, dog. The retina is elevated and detached from the underlying choroid by a fibrinocellular exudate (arrow). (HE 63X)

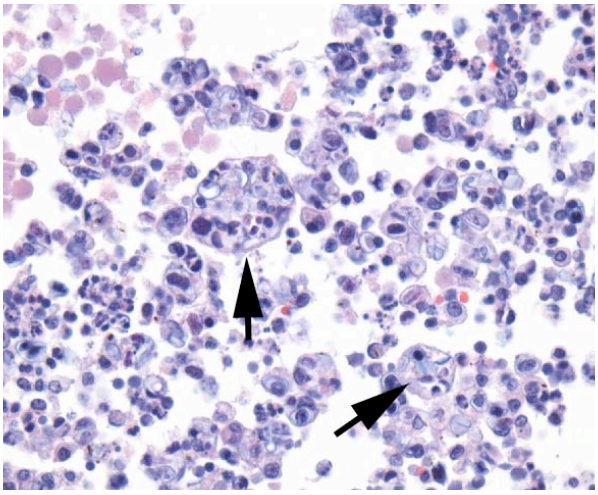

1-2. Eye, dog. Within the subretinal space, numerous macrophages, lymphocytes and few degenerate and intact neutrophils mixed with numerous intrahistiocytic (arrow) and extracellular algae consistent with Protheca spp. (H&E, X400). Photograph courtesy of the Cummings School of Veterinary Medicine at Tufts University (http://www.tufts.edu/vet/dbs/pathology.html)

white-tan tissue with no clear distinction of cortex and medulla.

Laboratory Results: The cytology smears from the left shoulder mass contain few macrophages and medium sized lymphocytes mixed with small numbers of organisms found both extracellularly and within neutrophils or macrophages. These organisms are reniform to oval and are approximately 15 microns in length and 5 microns in width with a clear capsule. The cytoplasm contains basophilic granules and clear vacuoles without discrete nuclei. The cerebrospinal fluid collected at the time of necropsy shows pleocytosis (nucleated cell count-17,600/microliter) and increased protein levels (516 mg/dL).

Contributor's Histopathologic Description: Eye. The subretinal space is diffusely expanded by large numbers of histiocytes, lymphocytes, degenerate and intact neutrophils, mixed with eosiniophilic cellular and karyorrhectic debris, fibrin and numerous extracellular and intrahistiocytic algae. The algae are round to oval, 15-25 microns in diameter, with a 2-3 micron thick cell wall and a basophilic round nucleus. Occasionally, algae contain 2-3 wedge shaped 5-10 micron diameter, round to oval, basophilic endospores. Multifocally, the above-mentioned inflammatory cells extend to the posterior choroid, retina and occlude the trabecular meshwork. A segment of the tapetal retina shows marked hypertrophy (tomb-stoning) of the RPE. The ganglion cells are mostly absent and the inner and outer nuclear layers are attenuated and coalesce. Moderate amounts of eosinophilic fibrillar material (fibrin) are present in the vitreous mixed with few neutrophils, lymphocytes, and plasma cells that adhere to the inner plexiform layer of the retina. Predominantly near the papillary border, the anterior surface of the iris is covered by a single layer of spindle cells (pre-iridal fibrous membrane). The posterior iris epithelium is hyperplastic.

Contributor's Morphologic Diagnosis: Eye: Diffuse, severe, granulomatous endophthalmitis with retinal detachment and numerous extracellular and intrahistiocytic algae.

Contributor's Comment: The dog had widespread granulomatous inflammation affecting skin, lymph nodes, brain, lung, kidney, ileum, and colon. The histomorphologic features of the algae are consistent with *Prototheca* spp. and were confirmed by culture of CSF and urine. Protothecosis is a rare disease caused by *Prototheca* spp., a saprophytic achlorophyllous alga affecting a wide range of species.[1] Two pathogenic species of *Protheca* has been recognized- *P. zopfi* and *P. wickerhamii*. The disease has been identified in Europe, Asia, Africa, Australia, islands of the Pacific Ocean, and North America. The organism is ubiquitous and commonly found in raw and treated sewage, slime flux of trees, and animal wastes. Despite the abundance of this organism in nature, the incidence of disease is rare. The disease primarily develops when the host's immune resistance is suppressed or altered, often by a preexisting or

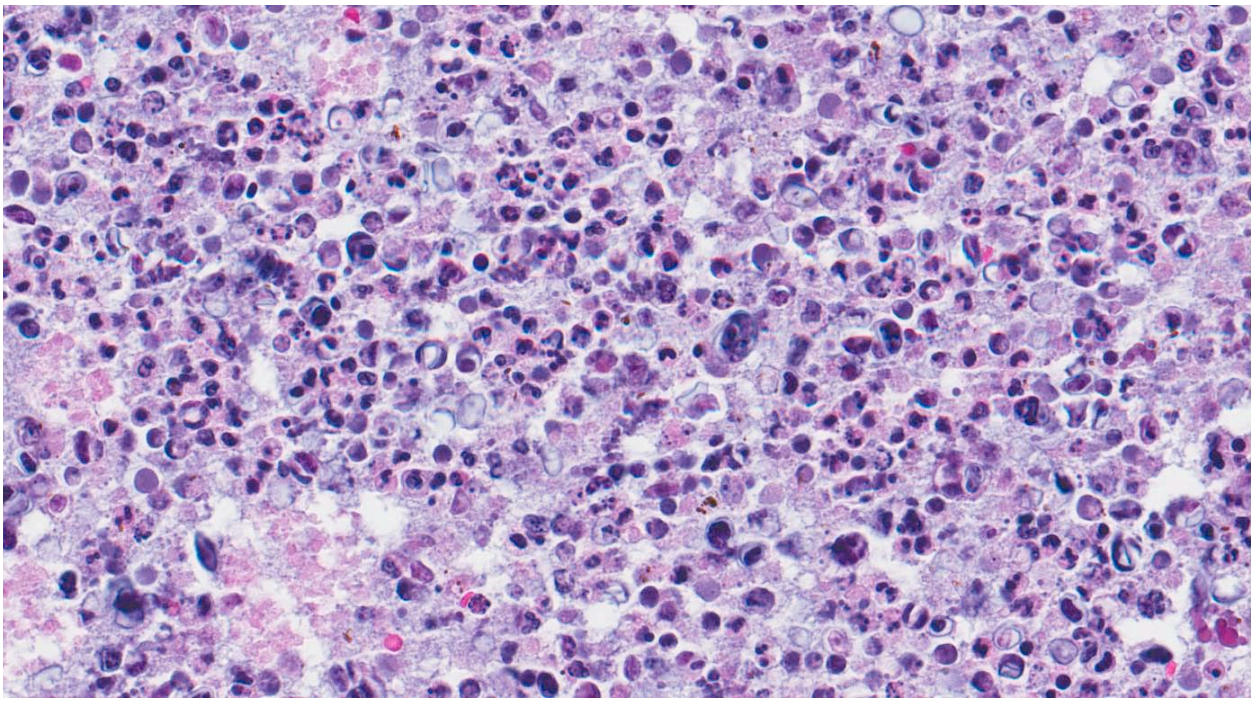

1-3. Eye dog. The subretinal exudate contains numerous algae, some endosporulating (arrowhead), and some collapsed cell walls (arrow). (HE 400X)

concurrent disease. No preexisting inflammatory, neoplastic or metabolic disease was detected in this dog.

Protothecosis can present either as systemic or localized cutaneous infection. In the alimentary tract, *Prototheca* is thought to be an opportunistic invader of existing mucosal lesions. Skin infections are thought to result from traumatic inoculation.[2] In the present case, the dog was initially presented for dermatitis rather than diarrhea and therefore skin was considered to be the primary site of infection in this dog. Cattle, horses, and wild pigs may pass *Prototheca* in the feces without apparent clinical disease.

The intestine and the eye are the most common sites in protothecosis of dogs. *P. zopfii* is almost always isolated from dogs with systemic infections and *P. wickerhamii* has been isolated from dogs and cats with cutaneous infections. Grossly, white to tan, 0.2-2 mm diameter, granulomatous lesions can be seen within the affected organs. There is mild inflammation with few macrophages, lymphocytes, plasma cells, and neutrophils mixed with large numbers of algal organisms.[2,3]

Protothecal organisms can be identified on rectal or colonic scrapings if the large intestine is involved. *Prototheca* sp. are round, oval or angular cells that are 8-20 micron diameter, have a refractile wall and contain granular cytoplasm. The organism reproduces by endosporulation and can be identified histologically as morula of 2-20 daughter cells within a single organism. *Prototheca* and *Chlorella* spp. are morphologically indistinguishable in tissues stained with H&E. *Chlorella* spp. contain periodic acid-Schiff-positive cytoplasmic starch granules that are PAS-negative following diastase digestion, but *Prototheca* spp. do not contain these granules. Ultrastructurally, chloroplasts consist of a highly organized, twisted lamellar component associated with amorphous, electron dense vacuolated material (starch). *Prototheca* spp. may contain visible starch granules (plastids) on electron microscopy, but these are not associated with a lamellar component. *Prototheca* organisms must be differentiated from other organisms that undergo endosporulation, such as *Coccidioides immitis* and *Rhinosporidium seeberi*. *Rhinosporidium* spp. have large sporangia, filled with uniformly round, 2-10 micron endospores. *Coccidioidomyces* spp. have spherules that measure up to 50 micron in diameter containing small, round endospores.

Molecular characterization and speciation of the *Protheca* spp. can be performed by 18S rDNA sequencing, genotype-specific PCR, restriction fragment length polymorphism, or qPCR followed by DNA Resolution Melting Analysis.[4]

JPC Diagnosis: Eye: Endopthalmitis, pyogranulomatous, diffuse, severe with numerous algae -- etiology consistent with *Prototheca* sp.

Conference Comment: Ocular protothecosis is only described as part of a systemic infection and never as a primary, solitary lesion. In the eye, it presents as a bilateral granulomatous panuveitis. The primary differential in this case is mycotic endophthalmitis, caused either by *Cryptococcus* or *Blastomyces*, which produce similar histologic lesions. Conference participants discussed the likely route of infection in this dog being hematogenous, and the necessity of the algae to overcome the blood-ocular barrier via induction of inflammatory cytokines.[2] The blood-ocular barrier is composed of the blood-aqueous barrier (which consists of tight junctions in the ciliary body and iridal capillaries and the phagocytic function of the ciliary epithelium) and the blood-retinal barrier (formed by tight junctions in the non-fenestrated capillary endothelium and between the retinal pigment epithelial cells).

Contributor: Cummings School of Veterinary Medicine at Tufts University
Section of Pathology
200 Westboro Rd
North Grafton, MA 01536
http://www.tufts.edu/vet/dbs/pathology.html

References:

1. Greene CE. *Infectious Diseases of the Dog and Cat*. 3rd ed. St. Louis, MO: Saunders-Elsevier; 2006: 656-662.
2. Wilcock BP. The eye and ear. In: Maxie MG, ed. *Jubb, Kennedy, and Palmer's Pathology of Domestic Animals*. 5th ed. vol 1. Philadelphia, PA: Elsevier Saunders; 2007:503-504.
3. Brown CC, et al. Alimentary System. In: Maxie MG, ed. *Jubb, Kennedy, and Palmer's Pathology of Domestic Animals*. 5th ed. vol 1. Philadelphia PA, Elsevier Saunders; 2007:231-232.
4. Ricchi M, et al. A rapid real-time PCR/DNA resolution melting method to identify *Prototheca* species. *J Appl Micro*. 2010;110(1):27-34.

CASE II: PV 1650/10 (JPC 4003047).

Signalment: Common kestrel, (*Falco tinnunculus*).

History: The wild bird was treated in a center of wildlife rehabilitation because of the presence of periocular swelling and exophthalmos. No additional history was available.

Gross Pathology: Swelling around the eye.

Contributor's Histopathologic Description: In the retrobulbar space, there is an irregular unencapsulated tumor, composed of tissue types arising from all three primordial germ cell lines. There are numerous cystic areas containing pale basophilic material, surrounded by solid areas of cartilage, bone, neural and adipose tissue. The cysts vary in size, up to 3 mm in diameter, and are lined by cuboidal to columnar epithelial cells, multifocally ciliated or with distended vacuolated cytoplasm (goblet cells), (respiratory epithelium, endoderm). Peripheral to these cysts are occasional, much smaller cysts, filled with concentrically laminated keratin, with a wall of keratinizing squamous epithelium (ectoderm).

2-1. Retrobulbar space, common kestrel. An unencapsulated neoplasm composed of tissues from three cell lines (ectodermal, mesodermal, and endodermal) compresses the globe (upper portion of image) and the brain (lower right). (HE 63X)

Multifocally, solid areas are composed of moderately cellular neoplastic neural tissue with neurons and glial cells embedded in neuropil (ectoderm). There are multifocal areas of formation of bone with marrow and cartilage (mesoderm). In a few of the sections, there are small lobules of zymogen-filled acini, resembling pancreas (endoderm). Mitoses in all cell populations are not prominent (fewer than 1 per HPF). In the small area of eye present, there is evidence of retinal detachment, hypertrophy of the retinal pigment epithelium, and retinal degeneration.

Contributor's Morphologic Diagnosis: Retrobulbar mass: Teratoma.

Contributor's Comment: Teratomas are defined as germ cell origin neoplasms composed of at least two, and often three, germinal layers.[7]

They are uncommon in domestic animals, but have been reported mostly in the bitch, sow, mare and cow; their most common localization is the gonads.[7,11] In avian species, involvement of the testes appears to be more common than the ovary[9] and they are most commonly observed in chickens.[6,10]

There are two reports of retrobulbar teratomas in wild birds.[6,10] One of the tumors was poorly differentiated and interpreted as malignant.[6] Incidentally, old literature reports describe experimental induction of teratomas in testicles of fowl by local injection of metal ions (zinc) in young animals [2,3,9], which was initially intended as a method of chemical castration.[2,3]

Teratomas in animals, in contrast to those in humans, are almost always benign.[7] In humans, classification of a teratoma as benign or malignant is based largely on the identification of primitive, undifferentiated cells and tissues within the tumor.[1] In general, the presence of a germ cell component worsens the prognosis, and teratomas with incompletely differentiated tissues

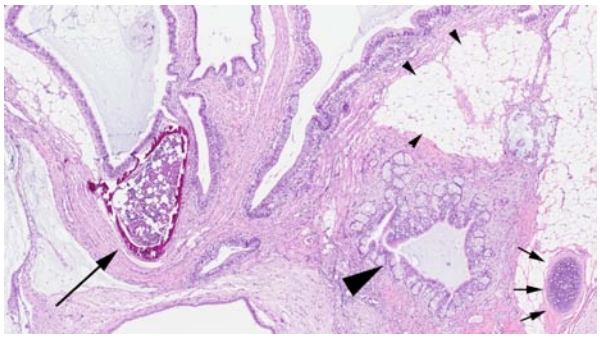

2-2. Retrobulbar space, common kestrel. A variety of well-differentiated tissues are present within the neoplasm, including numerous tortuous cysts lined by columnar epithelium which are occasionally surrounded by glands composed of goblet cells (large arrowhead) ,bone with marrow (large arrow), cartilage (small arrows), and fat (small arrowheads). (HE 160X)

should be considered potentially malignant.[1,5]

In this particular case, the eye was submitted as an enucleation and the kestrel was presumed alive at the time of biopsy. Unfortunately, follow-up evaluation was not available.

JPC Diagnosis: Eye: Retrobulbar teratoma.

Conference Comment: Teratomas, like dysgerminomas, are germ cell neoplasms; they usually originate from totipotent cells, such as those normally present in the ovary and testis (and sometimes abnormally present in sequestered midline embryonic rests). Such cells have the capacity to differentiate into any of the cell types found in the adult body.[12] Most extragonadal teratomas affect juvenile or young adult animals, develop from germinal elements, and occur along the migration pathway of the germ cells along the body midline, in the mediastinum, or in the central neuraxis. The sacrococcygeal region is the most frequent extragonadal location; other sites include the mediastinum and retroperitoneum.[6]

Several conference participants were unable to identify ectodermal differentiation to haired skin due to slide variability; however, this does not affect the diagnosis of teratoma, since only 2 germ cell lines are required to make the diagnosis. Although most reports define teratomas as having at least 2 of the 3 germ cell lines, rare variants (in humans) have only 1 line (monodermal variant).

Contributor: Weizmann Institute
Department of Veterinary Resources
Rehovot 76100
Israel
http://www.weizmann.ac.il/vet/

References:

1. Crum CP. The female genital tract. Germ cell tumors. In: Cotran RS, Kumar V, Collins T, eds. *Robbins Pathologic Basis of Disease*. 6th ed. Philadelphia, PA:Saunders;1999;1073-1075.
2. Guthrie J**.** Specificity of the metallic ion in the experimental induction of teratomas in fowl. *Br J Cancer*. 1967;21:619-22.
3. Guthrie J. Zinc induction of testicular teratomas in Japanese quail (*Coturnix coturnix Japonica*) after photoperiodic stimulation of testis. *Br J Cancer*. 1971;25:311-4.
4. Hooper CC. Teratoma in the cerebrum of a fantail pigeon. *Avian Pathol*. 2008;37:141-3.
5. Klein MK. Tumors of the female reproductive system. Germ cell tumors. In: Withrow SJ, MacEwen EG, eds. *Small Animal Clinical Oncology*. 3rd edition. St. Louis, MO: Saunders; 2001:446.
6. López RM, Múrcia DB. First description of malignant retrobulbar and intracranial teratoma in a lesser kestrel (*Falco naumanni*). *Avian Pathol*. 2008;37:413-4.
7. MacLachlan NJ, Kennedy PC. Tumors of the genital systems, Teratoma. In: Meuten DJ ed. *Tumors in Domestic Animals.* 4th ed. Ames, Iowa: Iowa State University Press, 2002:554.
8. Petrak ML, Gilmore CE. Neoplasms. In: Petrak ML, ed. *Diseases of Caged and Aviary Birds*. 2nd ed. Philadelphia, PA: Lea and Febiger; 1982:606-637.
9. Reece RL. Tumors of unknown etiology. In: Calnek BW, ed. *Disease of Poultry*. 10th ed. Ames, Iowa: Iowa State University Press, 1997:496-497.
10. Schelling SH. Retrobulbar teratoma in a great blue heron (*Ardea herodias*). *J Vet Diagn Invest*. 1994;6:514-6.
11. Shlafer DH, Miller RB. Female genital system. In: Maxie MG, ed. *Jubb, Kennedy, and Palmer's Pathology of Domestic Animals*. 5th ed. vol 3. St. Louis, MO; Saunders Elsevier; 2007:453-454.
12. Stricker TP, Kumar V. Neoplasia. In: Kumar V, Abbas AK, Fausto N, Aster JC, eds. *Robbins and Cotran Pathologic Basis of Disease*. 8th ed. Philadelphia, PA: Saunders Elsevier; 2010:261-2.

CASE III: 18124-09 (JPC 3164804).

Signalment: 5-year-old spayed female domestic shorthair cat, *Felis domesticus*, feline.

History: Five-year-old spayed female cat whose pupils began to dilate and ears to twitch after application of "Bio Spot for cats" on 05/27/2009. Cat returned to clinic with bilateral enlarged eyeballs with normal tonometry on 7/7/09. Conjunctiva slightly enlarged and oozy. Treated with antimicrobial eye ointment and dexamethasone. 7/23/09 and began treatment with metacam, doxycyclin, prednisone, antirobe, and strongid. Vaccination status unknown. Lesions progressively worsened over next few months. Animal euthanized and submitted for necropsy 09/08/09.

Additional History after diagnosis was made:

The owner moved into her present premises several months ago. The previous owner used one of the stalls in the barn as a chicken coop. Owner reported that all her animals (horses, dogs, and cats) began to lose weight with no response to deworming attempts. All other animals, except this cat, appeared to slowly recover on their own. At time of euthanasia all other animals were in good condition, even the other cats which had been treated with "Bio Spot for cats".

Gross Pathology: The cat is extremely cachectic. All bones can be easily palpated and the skin moves easily over the bones due to a scant amount of subcutaneous adipose tissue. There is no fat around the kidney, in the mesentery, or in the coronary groove. The eyes bulge forward. A portion of the cloudy cornea can be seen on the left eye. The sclera of both eyes is composed of bulging proliferative white tissue. Similar tissue is found in the frontal sinus, bulging through the calvarium at the bridge of the nose and extending down, around, and behind both eyes.

Laboratory Results: 07/23/09: CBC, Chemistry: WNL; FeLV/FIV negative. *Toxoplasmosa* negative. *Hemobartonella* positive.

Contributor's Histopathologic Description: Cross sections of the eyes reveal that all layers of the globe, including the iris, portions of the cornea, and portions of the eyelids are effaced by sheets of macrophages distended with *Histoplasma capsulatum* and necrotic debris. The tissue removed from the nasal cavity and frontal sinus are found to be distorted in a histologically similar manner.

Contributor's Morphologic Diagnosis: Chronic, severe, bilateral granulomatous panophthalmitis and blepharitis with intracellular *Histoplasma capsulatum*, feline.

3-1. Eye, cat. 5-year-old cachectic female cat with bilateral exophthalmos, bulging corneas and scleras, and corneal opacity. Photograph courtesy of C.E. Kord Animal Disease Diagnostic Laboratory, Dept. of Agriculture, Ellington Agricultural Center, 440 Hogan Road, Nashville, TN 37220. http://www.tennessee.gov/agriculture/regulatory/kord.html

3.2. Eye, cat. Closer view of head showing the degree of infiltration of the sclera and overlying conjunctiva bilaterally. Photograph courtesy of C.E. Kord Animal Disease Diagnostic Laboratory, Dept. of Agriculture, Ellington Agricultural Center, 440 Hogan Road, Nashville, TN 37220. http://www.tennessee.gov/agriculture/regulatory/kord.html

Contributor's Comment: Dogs are very susceptible hosts for histoplasmosis and they are considered sentinel animals.[3,4] However, while cats appear less susceptible to the disease, ocular manifestations of histoplasmosis are more commonly encountered in the cat.[4,5] *Histoplasma capsulatum* is a soil-borne dimorphic fungus.[2] It grows best in moist soil containing nitrogen-rich organic matter such as bird or bat feces. The fungus can grow in moist soil associated with house plants, so even indoor-only cats can be at risk. Similar to blastomycosis, the disease is acquired by inhalation of fungal microconidia. The incubation period is 12 to 16 days. The microconidia in the lung convert to the yeast form which is

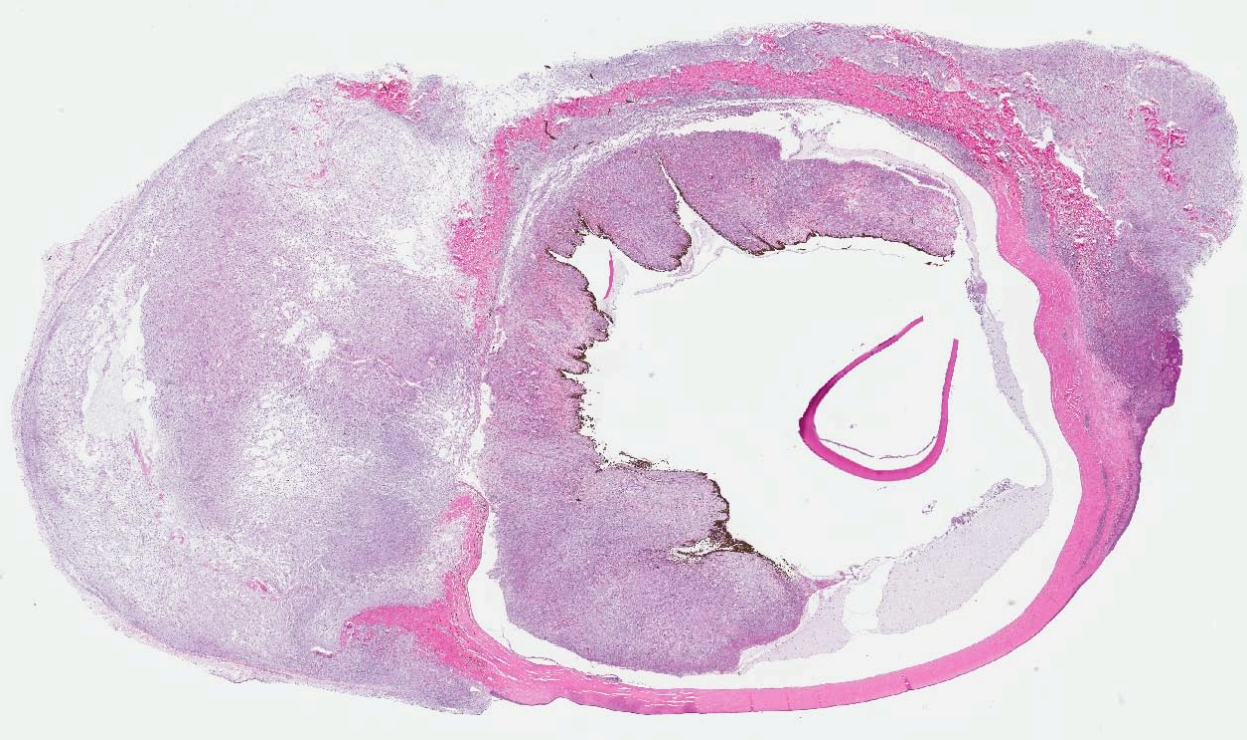

3-3. Eye, cat. This sagittal section of the globe shows a marked cellular exudate that expands and effaces the sclera and choroid. (HE 63X)

phagocytized by macrophages, where they undergo further intracellular replication. The organism is then disseminated via the lymphatic and circulatory system. Occasionally, histoplasmosis infects the eye causing conjunctivitis, granulomatous blepharitis, granulomatous chorioretinitis, retinal detachment, and optic neuritis.

Histoplasmosis is an important zoonotic disease. People do not contract the disease from animals, but may contract the disease if they are exposed to the same environmental source; consequently, anyone in the household experiencing respiratory disease or nonspecific clinical symptoms should consult a physician as soon as possible. Laboratory workers can also contract the disease from fungal cultures containing mycelial growth of *Histoplasmosis capsulatum*.

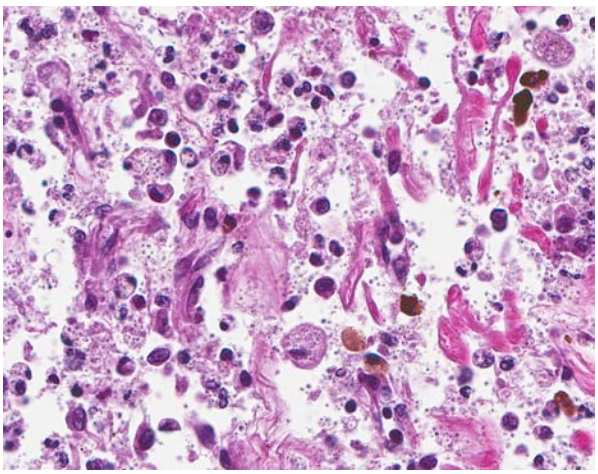

3-4. Eye, cat. The pyogranulomatous infiltrate is composed of numerous histiocytes and neutrophils with fewer lymphocytes and macrophages which dissect between scleral collagen fibers. Large numbers of 2-4 µm round yeasts are present both within macrophages and neutrophils, as well as extracellularly. (HE 400X)

JPC Diagnosis: Eye: Panophthalmitis, pyogranulomatous, focally extensive, severe, with numerous intrahistiocytic and extracellular yeasts consistent with *Histoplasma capsulatum*.

Conference Comment: Other common systemic mycoses in animals in North America can typically be readily differentiated from histoplasmosis in tissue section. *Blastomyces dermatitidis*, the most frequently reported cause of intraocular mycosis in dogs[6], appear as in tissue as 5-15 µm round nonencapsulated yeast with a 1 µm thick wall and broad-based budding. Yeasts of *Cryptococcus neoformans* have a thick capsule and often form a "soap bubble" appearance, frequently extend from brain infection via the optic nerves and generally cause little tissue reaction. Spherules of *Coccidioides immitis* and *C. posadasii,* which are generally the most destructive and the most limited in geographical distribution, range from 20-200 µm in diameter and contain endospores.[1] Protozoal endophthalmitis caused by *Toxoplasma gondii, Encephalitozoon* spp., *Neospora* spp., or *Leishmania*

spp. is more difficult to differentiate histologically and may require additional diagnostic modalities such as immunohistochemistry and electron microscopy.[6] *Toxoplasma gondii* causes necrotizing granulomatous or lymphoplasmacytic ophthalmitis with tachyzoites in intracellular pseudocysts or cysts. *Neospora caninum* may or may not reside in a parasitophorous vacuole and requires EM to distinguish it from *Toxoplasma*. The amastigote stage of *Leishmania* spp. are present in macrophages and are 2-4 µm in diameter with a rod-shaped kinetoplast that is perpendicular to the nucleus. *Encephalitozoon cuniculi* are intracellular, gram-positive, 1-2 µm protozoa present in large (up to 120 µm) pseudocysts and may induce periarteritis within the uvea and retina. Of these protozoal conditions, only *Toxoplasma gondii* and *Neospora caninum* specifically cause intraocular lesions and should be considered in the differential diagnosis for this case.[6]

Contributor: C.E. Kord Animal Disease Diagnostic Laboratory
Dept. of Agriculture
Ellington Agricultural Center
440 Hogan Road
Nashville, TN 37220
http://www.tennessee.gov/agriculture/regulatory/kord.html

References:

1. Caswell JL, Williams KJ. Respiratory system. In: Maxie MG, ed. *Jubb, Kennedy, and Palmer's Pathology of Domestic Animals* 5th ed. vol. 1, Philadelphia, PA: Saunders Elsevier; 2007:642.
2. Green CE. Histoplasmosis. In: Greene CE, ed. *Infectious Diseases of the Dog and Cat*. ,3rd ed. St. Louis, MO: Elsevier Saunders; 2006;577-584.
3. Gwin RM, Makley TA, Wyman M, et al. Multifocal ocular histoplasmosis in a dog and a cat. *J Am Vet Med Assoc.* 1980;176:638-642.
4. Percy DH. Feline histoplasmosis with ocular involvement. *Vet Pathol*. 1981;18:163-169.
5. Stiles J. Ocular Infections. In Infectious Diseases of the Dog and Cat, , 3rd ed., pp. 974-991. Elsevier Saunders, St. Louis, Missouri, 2006.
6. Wilcock BP. Eye and ear. In: Greene CE, Maxie MG, eds. *Jubb, Kennedy, and Palmer's Pathology of Domestic Animals.* 5th ed. vol. 1. Philadelphia, PA: Saunders Elsevier; 2007:502-3.

CASE IV: 1009-235 (JPC 4002756).

Signalment: 8-year-old intact female Golden Retriever dog, *Canis familiaris.*

History: A female, golden retriever dog presented for abnormality in the left eye. The intraocular proliferative lesion was confirmed by ultrasonography. No other symptoms were found at clinical examination. Because tumor lesion was suspected in globe, left eye enucleation was performed.

Gross Pathology: The left eye was swollen and approximately 2.5 cm in diameter. The lesion was mainly located in the anterior and posterior uvea and was gray-white or black in color. The lens was dislocated in the globe. The optic nerve had no remarkable change.

Contributor's Histopathologic Description: The neoplastic tissue effaced the iris and choroid in the globe and was composed of large pleomorphic mononuclear cells and multinucleated giant cells. In addition, some lesions include spindle cell forms, which resemble spindle cell sarcomas such as malignant melanoma. The tumor cells were loosely arranged in sheets, and were partially dispersed. Neutrophils multifocally infiltrated the neoplasm, and there were areas of necrosis and hemorrhage. Tumor cells were predominantly mononuclear cells with marked pleomorphism. The cytoplasm was eosinophilic and varied from scant to abundant. Cytoplasmic vacuolation was frequently encountered. Nuclei were ovoid, indented or folded and extremely variable in size. The chromatin pattern was coarsely granular. Nucleoli were large and frequently multiple. The mitotic index was high and bizarre mitotic figures were frequently shown. Tumor cells often engulfed erythrocytes, melanin granules, nutrophils and mononuclear cells such as lymphocytes. These tumor cells were moderately immunoreactive with Iba-1, lysozyme, MHC-class II and vimentin. However, tumor cells were negative for cytokeratin AE1/AE3, CD3, CD18, CD20, CD79cy, E-cadherin, Melan-A, neurofilament, and S-100 protein. In electron microscopy, the predominant large irregular cells with abundant cytoplasm had no discernable junctional complexes or basal lamina. The cytoplasm contained numerous organelles, including rough endoplasmic reticulum, and a prominent Golgi apparatus. Mitochondria varied in size and shape. However, the number of lysosomes was small, and phagolysosomes and secondary lysosomes were sometimes seen. Tumor cells also contained small lipid droplets.

Contributor's Morphologic Diagnosis: Eye: Histiocytic sarcoma.

4-1. Eye, dog – The left eye was swollen to approximately 2.5 cm in diameter. The anterior and posterior uvea contained a grey to black neoplasm with dislocation of the lens. The sclera and the lens were dislocated in globe. The optic nerve and sclera had no gross changes. Optic nerve had no remarkable change. Photo courtesy of: Department of Pathology, Faculty of Pharmaceutical Science, Setsunan University, 45-1 Nagaotohge-cho, Hirakata, Osaka 573-0101, Japan ozaki@pharm.setsunan.ac.jp

Contributor's Comment: The initial presentation of our case is an intraocular lesion. The first presenting sign is an ocular abnormality with no other apparent proliferative lesions in clinical examination. After one month, a contralateral globe lesion and disseminated cutaneous masses, which are also diagnosed as histiocytic sarcoma, are identified. Because histiocytic sarcoma is capable of widespread metastasis, it is not always possible to differentiate true multicentric origin as malignant histiocytosis from widespread metastasis of disseminated histiocytic sarcoma. However, as the lesions of eye and cutis do not occur simultaneously and the ocular neoplasm is firstly recognized, our case can be regarded as disseminated histiocytic sarcoma likely to be intraocular in origin.

Histiocytic sarcoma, which is identified as a single lesion of histiocytic neoplasia, is due to proliferation of dendritic antigen presenting cells (DC). The majority occurs in the subcutis, but other primary locations have been observed. Disseminated histiocytic sarcoma, which spreads to distant sites beyond the local lymph nodes, is an aggressive multisystem disease characterized by presence of multiple tumor masses in several organ systems. Primary sites are spleen, lung, and bone marrow. Secondly, lesions are observed in lymph nodes and liver, and subsequently other organs can be affected. When histiocytic neoplasia occurs in multiple sites simultaneously, the disease is termed malignant histiocytosis.[1]

Histiocytic sarcoma is an uncommon primary intraocular neoplasm, whereas life expectancy following diagnosis is very short compared to other ocular tumors. It is important that malignant melanoma, irido-ciliary epithelial tumor, and malignant

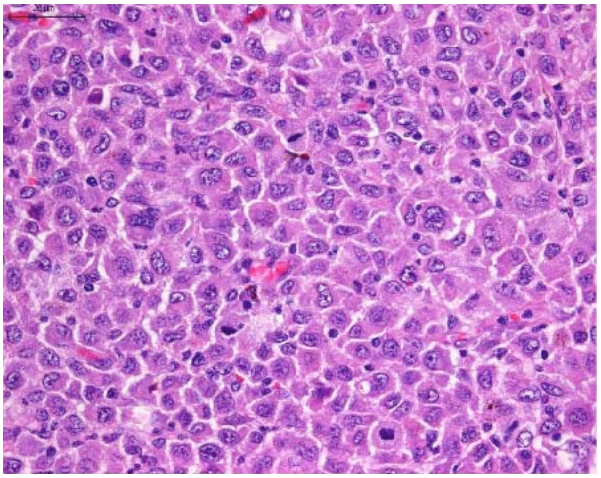

4-2. Eye, dog – Histiocytic neoplastic cells within the iris and choroid are moderately pleomorphic, occasionally multinucleated and have a high mitotic rate. (HE 400X) Photo courtesy of: Department of Pathology, Faculty of Pharmaceutical Science, Setsunan University, 45-1 Nagaotohge-cho, Hirakata, Osaka 573-0101, Japan ozaki@pharm.setsunan.ac.jp

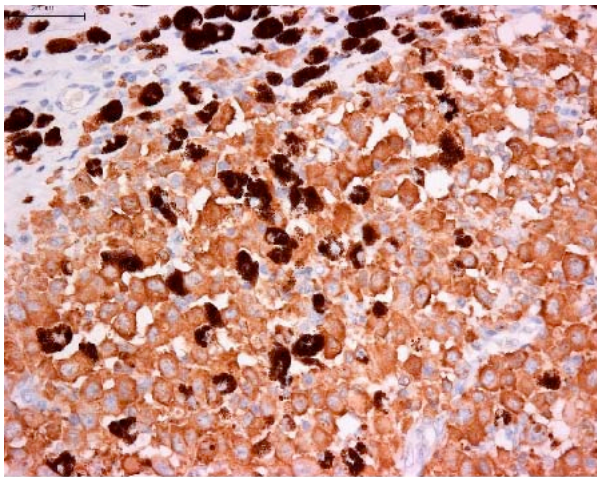

4-3. Eye, dog – Histiocytic neoplastic cells are diffusely and variably immunopositive for Iba-1, a marker for activated macrophages and microglia. Photo courtesy of: Department of Pathology, Faculty of Pharmaceutical Science, Setsunan University, 45-1 Nagaotohge-cho, Hirakata, Osaka 573-0101, Japan ozaki@pharm.setsunan.ac.jp

lymphoma were eliminated from the differential diagnosis by histomorphologic examination. Melanocytic tumors arising from the uvea are the most commonly detected ocular tumors in dogs, and approximately 20% of these tumors are malignant melanoma. Irido-ciliary epithelial tumor is the second-most-common primary uveal tumor in dogs, accounting 12.5% of canine ocular tumors. Primary malignant lymphoma is the third-most-common intraocular tumor in dogs, representing 3.3% of canine ocular tumors.[9]

Primary intraocular histiocytic sarcoma has a strong breed association. Approximately 70% of these tumors occur in Retriever breeds accounting for Golden Retrievers and Labrador Retrievers.[9] Among other breeds Rottweilers are the third-most-common breed. On the other hand, histiocytic sarcoma and malignant histiocytosis is best recognized in the Bernese mountain dog, in which a familial association is apparent.[5] Other breeds are predisposed to histiocytic sarcoma and include Rottweilers, Golden Retrievers, and Flat-coated Retrievers. Because histiocytic sarcoma is characterized by rapid dissemination, it should be listed in differential diagnoses of intraocular tumors of Retriever breeds, especially Golden Retrievers and Labrador Retrievers.

Histiocytes differentiate from CD34+ myeloid stem cells into monocyte/macrophages and several dendritic antigen presenting cells (DC) lineages, which include epithelial DC or Langerhans cells, interstitial DC, plasmacytoid DC, and interdigitating DC of the paracortical area of the lymph node. Histiocytic sarcomas express leukocyte surface molecules characteristic of DC such as CD1, CD11c and MHC II.[1]

Diffuse expression of E-cadherin, CD4 and Thy-1 has not been observed in histiocytic sarcoma. On the other hand, the phenotype of histiocytoma, which is a benign tumor of non-activated Langerhans cells, is quite similar to that of histiocytic sarcoma except for the expression of E-cadherin, which occurs in histiocytoma especially in the cellular infiltrate immediately adjacent to the epidermis. Reactive histiocytosis, which is a proliferative disease of activated interstitial DC, consistently expresses CD4 and Thy-1.[1]

CD1, CD11c and CD4 antibodies could not be used on formalin fixed paraffin embedded specimens. So, we need to use the antibody panel for CD3 (T cells), CD20 (B cells), CD79cy (B cells), CD18 (macrophage, lymphocyte, granulocyte), MHC-II, Iba-1 (macrophage, microglia). MHC-II, Iba-1 and lysozyme expression with the absence of CD3, CD20 and CD79cy is evidence of macrophage and DC differentiation. Macrophages, which are specialized scavengers, have more numerous lysosomes than dendritic antigen presenting cell (DC). In the present case, the neoplastic cells have small numbers of lysosomes under electron microscopic examination. Thus, these neoplastic cells are regarded as DC rather than macrophages. In addition, neoplastic cells are negative for E-cadherin, which intra-epithelial DC such as Langerhans cells express. The exact sublineages of histiocytes and dendritic cells involved in HS have not been determined in most instances, but our present case is highly suggestive of interstitial DC origin.

JPC Diagnosis: Eye: Histiocytic sarcoma.

Conference Comment: The contributor provides an excellent overview of histiocytic proliferative diseases. Curiously, this neoplasm is negative for CD18, a β_2-integrin subunit expressed by all leukocytes including histiocytes, dendritic cells, lymphocytes and granulocytes. In a recent article differentiating ocular histiocytic sarcoma from melanocytic neoplasms[10], all neoplasms considered to be histiocytic sarcoma were either Melan A and/or S-100 protein negative and/or CD18 positive. Additionally, this neoplasm demonstrates immunoreactivity for MHCII and Iba-1, an ionized calcium-binding adaptor specific for macrophages and microglia. Via electron microscopy, only a few lysosomes and phagosomes were identified, suggesting this neoplasm is possibly of myeloid dendritic cell origin rather than macrophage. The immunophenotyping of cells throughout the spectrum of histiocytic diseases varies based on the reference text or journal consulted, and reflects the continuous information explosion in this very active field of research. The following list outlines the most consistent and commonly cited immunophenotypes[1-8]:

Cell of origin	**Disease(s)**	**Immunohistochemistry**	
		Positive	**Negative**
Epidermal dendritic (Langerhans) cell	Cutaneous histiocytoma; Feline PCLH (**Birbeck's granules** on EM)	**E-cadherin**, CD1a, CD14, CD11c, CD18, MHC II, ICAM-1, langerin	Thy-1, CD4
Interstitial dendritic cell	Reactive histiocytosis	**Thy-1**, **CD4**, CD1c, CD11b/c, MHC II, CD18	ICAM-1, E-cadherin
Myeloid dendritic cell	Histiocytic sarcoma	**ICAM-1**, CD1, CD11c, MHC II, ± CD90	CD4, E-cadherin
Macrophage	Hemophagocytic histiocytic sarcoma	**CD11d (β_2-integrin)**, MHC II, ± CD11c/ CD18, CD1c	CD1c/CD11c

Contributor: Setsunan University
Department of Pathology
Faculty of Pharmaceutical Science
45-1 Nagaotohge-cho, Hirakata
Osaka 573-0101, JAPAN

References:

1. Affolter V, Moore PF. Localized and disseminated histiocytic sarcoma of dendritic cell origin in dogs. *Veterinary Pathology.* 2002;39:74.
2. Affolter VK, Moore PF. Canine cutaneous and systemic histiocytosis. *Am J Dermatopathol.* 2000;22:40-48.
3. Baines SJ, McInnes EF, McConnell I. E-cadherin expression in canine cutaneous histiocytomas. *Vet Rec.* 2008;162(16):509-513.
4. Coomer AR, Liptak JM. Canine histiocytic diseases. *Compend Contin Educ Vet.* 2008;30(4):202-204.
5. Dubielzig RR, Ketring KL, McLellan GJ, et al. Uveal neoplasia. *Veterinary ocular pathology*. Philadelphia, PA: Saunders; 2010:282-309.
6. Fernandez NJ, West KH, Jackson ML, et al. Immunohistochemical and histochemical stains for differentiating canine cutaneous round cell tumors. *Vet Pathol.* 2005;42(4):437-445.
7. Ginn PE, Mansell JEKL, Rakich PM. Skin and appendages. In: Maxie MG, ed. *Jubb, Kennedy, and Palmer's Pathology of Domestic Animals* 5th ed. vol. 1. Philadelphia, PA: Saunders Elsevier; 2007:768-769.
8. Goldschmidt MH, Hendrick MJ. Tumors of the skin and soft tissues. In: Meuten DJ, ed. *Tumors in Domestic Animals*. 4th ed. Ames, IA: Iowa State Press; 2002:109-111.
9. Moore PF, Rosin A. Malignant histiocytosis of Bernese mountain dogs. *Vet Pathol.* 1986:23:1-10.
10. Naranjo C, Dubielzig RR, Friedrichs KR. Canine ocular histiocytic sarcoma. *Vet Ophthalmol*. 2007 May-Jun;10(3):179-85.

Joint Pathology Center
Veterinary Pathology Services

WEDNESDAY SLIDE CONFERENCE 2011-2012

Conference 11

14 December 2011

CASE I: 08108 (JPC 3134302).

Signalment: 15-year-old, female, rhesus macaque (*Macaca mulatta*).

History: This single-housed animal had a long-standing history of seizures induced by ketamine sedation. One day, care staff noted blood in the cage, but no external injuries were noted. Clinical staff suspected epistaxis. However, closer observation revealed she was not eating or drinking. A physical examination at that point revealed traumatic amputation of the rostral third of the tongue. The veterinary staff and primary investigator elected for euthanasia.

Gross Pathology: Examined was a 5.5 kg, intact, female rhesus macaque. The serosa covering 2 cm of the proximal colon was irregularly thickened and rough with prominent blood vessels and was covered by several bright red, multifocal to coalescing, raised lesions admixed with dark red fibrillar material (fibrin and hemorrhage). The corresponding mucosa was also rough and thickened in this area. An 8 mm x 6 mm x 5 mm, oval, grey-brown nodule was present adjacent to the left ovary. The left oviduct is tortuous and thickened, and numerous small, coalescing, white to tan plaques cover the diaphragm and abdominal wall. The head of the pancreas was replaced by a 2.5 cm x 1.5 cm x 1.5 cm firm, yellow-brown mass with prominent, tortuous vessels and was attached to the stomach, duodenum and body wall by fibrous adhesions. Multiple brown-red foci ranging in size from 1mm to 5 mm diameter were present in the peripancreatic and mesenteric adipose. The urinary bladder was adhered to the uterus, also by a fibrous adhesion.

Laboratory Results: Blood work revealed BUN 39 mg/dl (21-31), creatinine 1.3 mg/dl (0.8-1.0), creatine kinase 3914 U/L (1-2692) and AST 120 U/L (28-58). The elevated BUN and creatinine levels are consistent

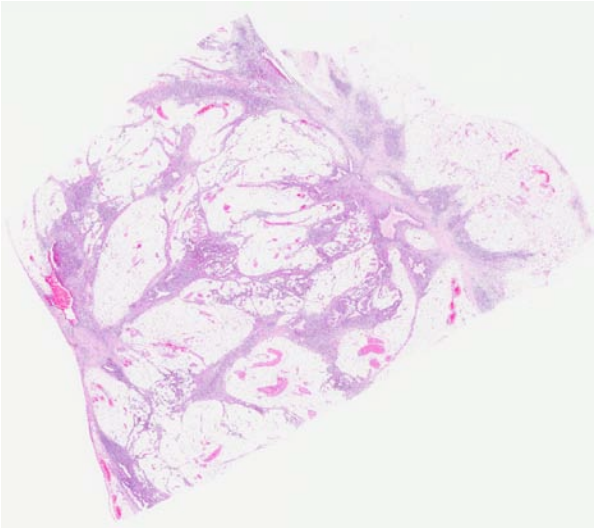

1-1. Mesentery, rhesus macaque. The mesentery is subdividedby dense bands of fibrous connective tissue which contain tortuous endometrial glands and stroma. (HE 4X)

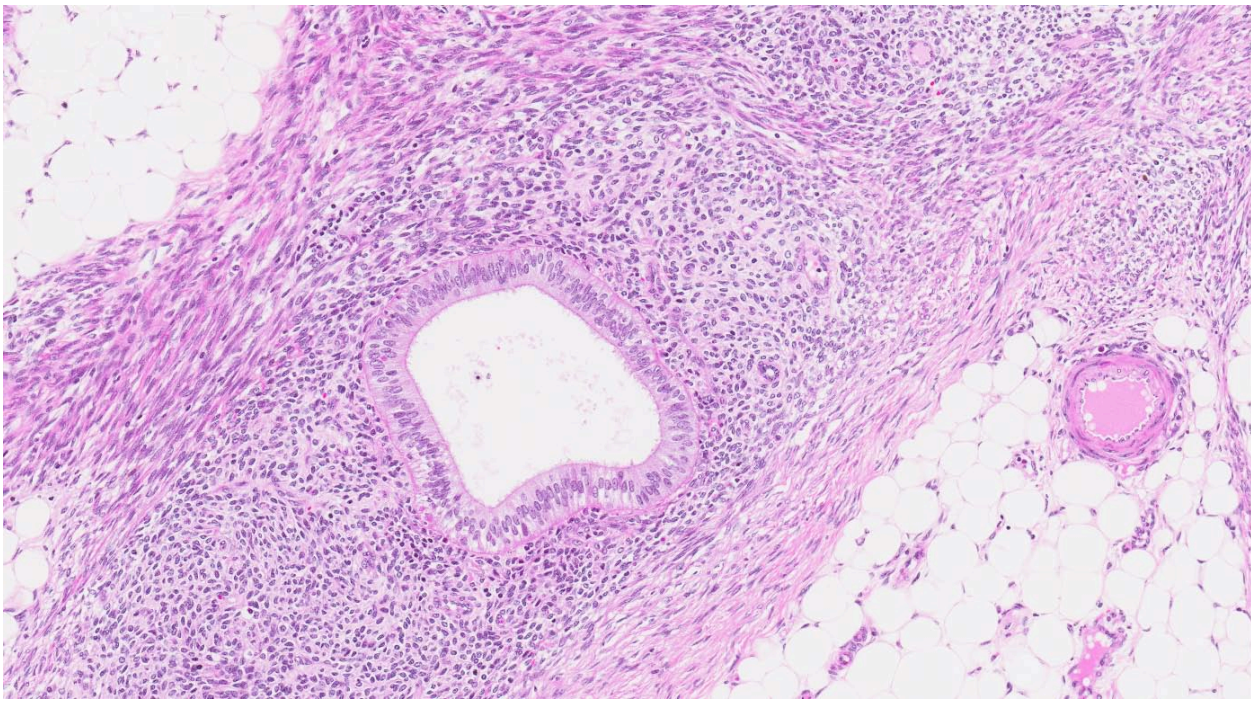

1-2. Mesentery, rhesus macaque. Higher magnification image ofan endometrial gland lined by tall columnar ciliated epithelium and surrounded by dense endometrial stroma. (HE 100X)

with mild dehydration resulting from the reduced oral intake of food and fluids. The traumatic tongue injury explains the rise in serum creatine kinase and AST as both of these enzymes have a muscle isozyme that is released when muscle is injured.

Contributor's Histopathologic Description: A section of mesenteric adipose is infiltrated by dissecting and intersecting streams of eosinophilic fibrillar material and elongated cells with scant deeply eosinophilic cytoplasm, indistinct cell borders and elongated, deeply basophilic nuclei with tapered ends (fibroblasts and fibrous connective tissue). These streams frequently contain groups of oval to polyhedral cells with pale eosinophilic cytoplasm and central, deeply basophilic nuclei often with perinuclear clearing (endometrial stromal cells). Abundant well-differentiated glands are present among the stromal cells which are lined by pseudo-stratified, ciliated, columnar epithelium punctuated by occasional clear cells. The glands contain dense amorphous to mildly granular eosinophilic or pale wispy eosinophilic material. Lymphocytes are scattered throughout the stroma along with fewer macrophages and neutrophils and rare eosinophils. Occasionally, lymphocytes and macrophages form aggregates within the stromal cells, and rarely small hemorrhages surrounded by macrophages containing greenish-brown pigment (hemosiderin) are noted in the stroma.

Contributor's Morphologic Diagnosis: Ovary, oviduct, diaphragm, intestinal serosa, and mesenteric adipose tissue: Endometriosis, multifocal, subacute to chronic, moderate to marked with marked fibroplasia.

Contributor's Comment: Developed in 1950 by Te Linde and Scott, the rhesus macaque was the first animal model for endometriosis. Presently the baboon model is utilized more frequently due to the ability to non-invasively monitor their menstrual cycle, continuous breeding in captivity, adequate volumes of spontaneous peritoneal fluid production and ease of vaginal transcervical uterine access.[4,6]

Endometriosis is an estrogen-dependent, chronic disease that occurs in menstruating species; which include human and non-human primates, the elephant shrew (*Elephantulus myuras jamesoni*) and one species of bat (*Glossophaga soricina*). Spontaneous endometriosis has only been reported in women and female non-human primates and the pathogenesis is not completely understood. It may be induced in other species through intra-peritoneal injection of viable endometrial tissue. Rodent models of the disease have been created in this manner. By definition, it is the presence of viable, ectopic, extra-uterine, functional endometrial glands with stroma in various sites throughout the pelvis and peritoneal cavity.[5,7]

The most widely accepted explanation of the pathogenesis is Sampson's three-fold transplantation: retrograde menstruation occurs, viable endometrial cells must be present, and adherence and implantation into structures in the peritoneum must successfully

occur. Retrograde menstruation alone is not enough for the condition to occur. In some baboon studies, retrograde menstruation has been reported in over 83% of animals. Endometrial cells have been reported in the peritoneal fluid of 59-79% of women during menses. However, endometriosis is not clinically present at these rates and is estimated to affect only 15-20% of women during their reproductive lives. Other theories include vascular and lymphatic dissemination, *in-situ* development from Wolffian or Müllerian duct remnants, and the development of metaplastic ovarian or peritoneal tissue. An alternate theory suggests induction and differentiation of mesenchymal cells that are affected by substances released by degenerating endometrial tissue following reflux into the peritoneal cavity. While the retrograde menstruation and transplantation theory is the most widely accepted, the cellular and molecular mechanisms that lead to the development of the disease are controversial.[2,4,7]

Angiogenesis, immune suppression (cytotoxic T-cells, NK cells), mesothelial lining injury and pro-inflammatory cytokines, matrix metalloproteinases, adhesion molecules, toxin (dioxin) exposure and genetic polymorphisms are all among the multitude of candidate factors in the creation of the proper peritoneal environment that must exist for successful survival, adhesion and implantation to occur. In women, an autoimmune component has also been proposed due to the demonstration of auto-antibodies and an association with other autoimmune diseases and immune mediated abortion. In humans, there is a 6-9 fold increase in prevalence among first-degree relatives.[2,4,7]

Briefly, an abnormal or "permissive" peritoneal environment in the face of endometrial reflux is thought to be central cause for this chronic inflammatory condition. Conditions that favor tubal reflux (e.g., cervical stenosis) in addition to increased sloughing and retrograde flow may increase tubal reflux and overwhelm peritoneal macrophage's ability to eliminate the sloughed endometrial material. However, it should be noted that conditions such as cervical stenosis are not present in all cases.[5,7]

Chronic inflammation and the release of certain cytokines in this inflammatory stage (TNF-alpha, IL-1, IL-6 and IL-8) may alter innate immunity and permit the viable cells to persist through decreased peritoneal macrophage, natural killer cell and cytotoxic T-cell activity. However, the decreased NK cell activity has also been described as constitutive rather than a result of cytokine or hormone induced immune suppression and secretory ICAM (sICAM) expression by endometrial tissue may bind LFA-1 and help prevent NK-cell recognition of endometrial implants.[2,5,7]

Endometrial cells from women with endometriosis have decreased rates of apoptosis, insensitivity to macrophage cytolysis, and enhanced gene expression of the anti-apoptotic gene Bcl-2, secretory ICAM (intercellular adhesion molecule), vascular endothelial growth factor (VEGF), and various matrix metalloproteinases which suggests increased intra-peritoneal viability, and ability to adhere and invade peritoneal membranes and tissues.[2,5,7]

JPC Diagnosis: Mesentery: Endometriosis.

Conference Comment: The contributor provided an excellent review on endometriosis, which is the extrauterine growth and proliferation of endometrial glandular and stromal cells in menstruating animals, most commonly in Old World primates. Three histologic features of endometriosis are the presence of endometrial glands, endometrial stroma, and hemosiderophages; at least two of these features are required for a diagnosis of endometriosis. Endometriosis presents grossly as blood-filled "chocolate cysts" which progress to fibrotic scar tissue in chronic cases. While implantation generally occurs in the pelvic and extrapelvic abdominal cavity, endometriosis has also been reported in the thoracic cavity, lungs, and brain. There are also rare reports of endometriosis in men undergoing estrogen therapy for prostate cancer and in premenstrual girls. As the first tenet of Sampson's threefold transplantation theory (retrograde menstruation) is clearly lacking in these cases, it is possible that another of the proposed pathogeneses for endometriosis (*in-situ* development from Wolffian or Müllerian duct remnants or development of metaplastic ovarian or peritoneal tissue) may still be reasonable theories in some individuals.[1]

Conference participants also discussed various risk factors in non-human primates which predispose them to endometriosis. These include low numbers of pregnancies, with increased numbers of menstruations throughout life, resulting in increased endometrial turnover compared to multiparous primates. Non-laproscopic abdominal surgical procedures, including hysterectomy and estradiol therapy are also implicated, as well as genetic predisposition and age. Aged non-human primates are more likely to develop endometriosis than older women because unlike human females, menstruation continues indefinitely due to lack of menopause.[3]

Contributor: Wake Forest University Health Sciences
Animal Resources Program
Medical Center Boulevard
Winston-Salem, NC 27157
http://www1.wfubmc.edu/compmed/faculty/kock.htm

References:

1. Assaf BT, Miller AD. Pleural Endometriosis in an Aged Rhesus Macaque (*Macaca mulatta*): A Histopathologic and Immunohistochemical Study. *Vet Pathol.* 2011 Apr 26. (Epub ahead of print).

2. D'Hooghe, TMD, Kyama CM, Chai D, et al. Nonhuman primate models for translational research in endometriosis. *Reproductive Sciences.2009;*16(2): 152-161.

3. Fazleabas AT, Brudney A, Gurates B, et al. A modified baboon model for endometriosis. *Ann N Y Acad Sci*. 2002;955:308-17; discussion 340-2, 396-406.

4. Hadfield RM, Yudkin PL, Coe CL, et al. Risk factors for endometriosis is the rhesus monkey *(Macaca mulatta)*: a case-control study. *Human Reproduction Update*. 1997;3(2):190-115.

5. Matarese G, De Placido G, Nikas Y, et al. Pathogenesis of endometriosis: natural immunity dysfunction or autoimmune disease? *Trends in Molecular Medicine*. 2003;9(5):223-228.

6. Mwenda JM, Kyama CM, Chai DC, et al. The baboon as an appropriate model for the study of multifactorial aspects of human endometriosis. *The Laboratory Primate*. 1st ed. Academic Press; 2005:Chapter 33.

7. Van der Linden PJQ. Theories on the pathogenesis of endometriosis. *Human Reproduction.* 1996;11(3): 53-65.

CASE II: 43121 (JPC 3165086).

Signalment: 6-year-old, male, domestic rabbit (*Oryctolagus cuniculus*).

History: A male, sexually intact pet rabbit presented for enlargement of the left testicle in the scrotum. No other symptoms were found at clinical examination. Bilateral orchiectomy was performed.

Gross Pathology: The enlarged left testicle was firm and globular, in contrast to the elongated right one, and approximately 1.7 cm in diameter. The cut surface was flat, smooth and gray-white in color.

Contributor's Histopathologic Description: The left testicle was almost entirely replaced by tumoral tissue. The tumoral tissue consisted of discrete tubular structures separated by a fibrous stroma. Tubular structures were composed of an intermixture of large round cells similar to germ cells and spindle cells with elongated nuclei similar to Sertoli or granulosa cells. The spindle cells mainly located at the periphery of tubular structures formed a palisade surrounded by basement membrane (coronal pattern). Spindle cells sometimes surround an isolated or collected large round cell similar to a germ cell and took an appearance like follicular epithelium surrounding the ovum of the primary follicle (follicular pattern). Arrangement of a microfollicular pattern containing eosinophilic amorphous material (Call-Exner-like pattern) was also seen. The central eosinophilic amorphous material was PAS-positive. The large round cells (germ cell components) had abundant clear cytoplasm and round, vesicular nuclei with prominent nucleoli. The spindle cells (sex cord components) had scant clear cytoplasm and small oval or elongated nuclei with indiscernible nucleoli. Mitotic figures were occasionally observed in the germ cell components, but were not detected in the sex cord components. Aggregates of Leydig cells were present within the intertubular stroma. These cells were non-neoplastic and lacked crystals of Reinke. Immunohistochemically, the germ cell components were positive for c-kit and placental alkaline phosphatase (PLAP). The sex cord components stained for vimentin and Wilms tumor-1 (WT-1). Electron microscopic examination revealed that the germ cell components had abundant cytoplasm within a few organelles and large round nuclei with dispersed chromatin and prominent nucleoli in the neoplastic lesion. The sex cord components had many organelles composed predominantly of mitochondria in the primarily scant cytoplasm. The nuclei of cells of the sex cord components were irregular or oval shaped and contained few or modest nucleoli. Amorphous materials surrounded by sex cord components consisted of duplicated basal laminae.

2-1. Testis, rabbit. The enlarged left testicle was firm and globular in contrast to elongated right one and approximately 1.7 cm in diameter. The cut surface was flat, smooth and gray-white in color. Photograph courtesy of Department of Pathology, Faculty of Pharmaceutical Science, Setsunan University, 45-1 Nagaotohge-cho, Hirakata, Osaka, 5730101, Japan

Contributor's Morphologic Diagnosis: Testicle: Gonadoblastoma.

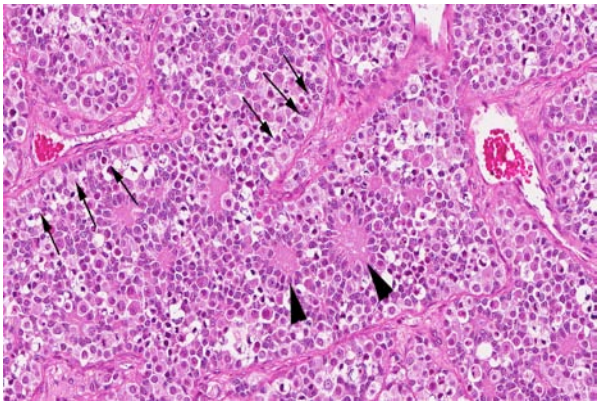

2-2. Testis, rabbit. Two distinct morphologies are present within neoplastic cells. The germ-cell phenotype are large round cells present in sheets, which resembles a seminoma. The second phenotype is a spindle cell which forms rosettes (arrowheads) and often palisades along the basement membrane (arrows). (HE 200X)

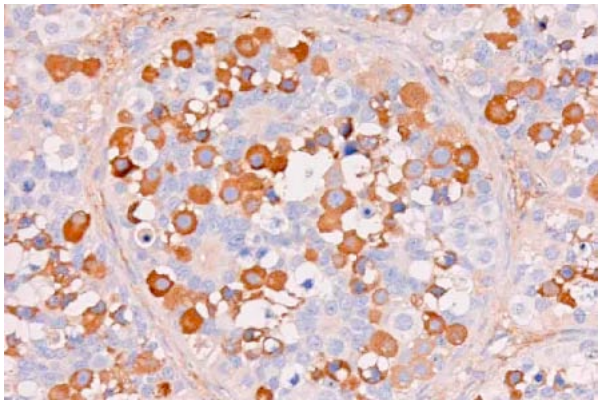

2-3. Germ cells show diffuse strong cytoplasmic immunoreactivity for Wilms tumor -1 antigen. Photograph courtesy of Department of Pathology, Faculty of Pharmaceutical Science, Setsunan University, 45-1 Nagaotohge-cho, Hirakata, Osaka, 5730101, Japan

Contributor's Comment: Tumors arising in testis of rabbits have rarely been reported. In domestic rabbits, one of the most common testicular tumors is the interstitial (Leydig) cell tumor.[3] Gonadoblastoma rarely develops, almost exclusively in dysgenetic gonads, or in those with an intersex syndrome in humans.[5] On the other hand, gonadoblastomas can be found in apparently normal ovaries and testes.[6] In animals, gonadoblastomas have only been reported in two dogs.[4,7]

Gonadoblastoma is histomorphologically defined as a tumor composed of two principal cell types: germ cell components similar to those of seminoma and sex cord components similar to Sertoli cells. In this case, immunohistochemical examination revealed both the germ cell derivative of the large round cells (c-kit and PLAP positivity) and the sex cord nature of the spindle cells (vimentin and WT-1 positivity) in addition to characteristic morphological features. Furthermore, the ultrastructural pattern of eosinophilic amorphous bodies that are comprised of whorled laminae is already verified in canines[6] and those of human gonadoblastomas.

The differential diagnosis includes mixed germ cell-sex cord-stromal tumor (MGSST) and sex cord tumor with annular tubules (STAT). MGSST generally lacks the discrete tubular structures seen in gonadoblastoma, and usually shows proliferative activity in the sex cord component, because unlike in gonadoblastoma, germ cells in MGSST are thought to be non-neoplastic and entrapped by neoplastic sex cord-stromal tumor. The histomorphological features showing characteristic three typical patterns (i.e. coronal, follicular, and Call-Exner-like) of sex cord elements within the discrete tubules is most characteristic and diagnostic for gonadoblastoma. In a gonadoblastoma, more than one pattern is usually found in an individual tubule.[6] The presence of these patterns supports the diagnosis of gonadoblastoma in this case. STAT has a growth pattern similar to gonadoblastoma and contains eosinophilic amorphous bodies and frequently calcified material, but lacks a germ cell component. Our case is conclusively distinguished from these diagnoses.

Gonadoblastoma typically occurs within dysgenic gonads in children or young adults. Approximately 80% of cases occur in phenotypic females, and most of the remaining 20% are in phenotypic male pseudohermaphrodites.[6] In more than 90% of patients with gonadoblastoma, a Y chromosome or fragment can be identified.[6] However, it has been found in the testes of normal men.[2] Our rabbit has no clinical symptoms such as alopecia, feminization, or cryptorchidism. Our case was apparently sexually intact judging from the intact right testis and normal development of genital organs, and has no dysgenic gonads. However, it remains unclear whether this rabbit had Y chromosome fragments or not, because karyotypic analysis was not done.

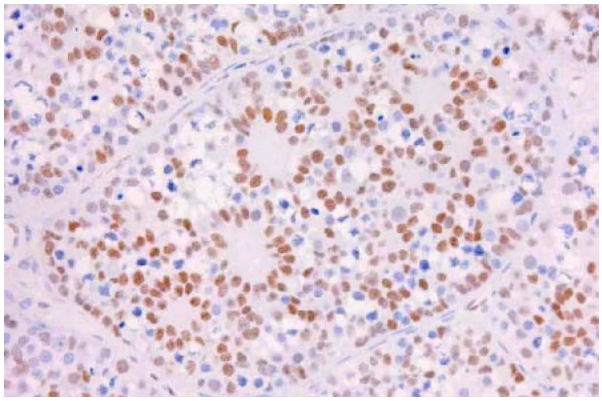

2-4. Testis, rabbit. Sex cord-like cells show diffuse strong nuclear immunoreactivity for c-kit. Photograph courtesy of Department of Pathology, Faculty of Pharmaceutical Science, Setsunan University, 45-1 Nagaotohge-cho, Hirakata, Osaka, 5730101, Japan

JPC Diagnosis: Gonad: Gonadoblastoma.

Conference Comment: This neoplasm was considered benign because the tumor showed no evidence of invasive germ cells. It is postulated that gonadoblastomas result from abnormal proliferation of germ cells, which induce the sex cord mesenchymal cells around the germ cells to differentiate into granulosa-Sertoli-like cells.[8] A Call–Exner body surrounded by sex cord stromal cells indicates areas of the collection of degenerate and necrotic debris, similar to the phagocytosis of apoptotic spermatogenic cells by Sertoli cells in normal testicles, suggesting that sex cord components may have a tendency to assemble in the area of cell dissolution.[9]

Placental alkaline phosphatase (PLAP) only stains neoplastic germ cells, in addition to rare somatic epithelial malignancies, and not normal germ cells, which is useful in distinguishing this neoplasm from a mixed germ cell-sex cord-stromal tumor.[11] The transcription factor Wilms' tumor-1 (WT-1) protein, in addition to staining nephroblastomas, is a marker of Müllerian epithelial origin, and regulates the k-ras oncogene, which plays an important role in tumor suppression. Loss of WT-1 drives cells expressing oncogenic k-ras toward a senescence program, and inhibits the progression of certain types of neoplasia.[10] Sex cord stromal tumors are among several neoplasms in veterinary medicine that co-express vimentin and cytokeratin (AE1/AE3); others include canine prostatic carcinoma, feline bronchogenic adenocarcinoma, synovial cell sarcoma, ciliary body adenoma, renal carcinoma, amelanotic melanoma, meningioma, mesothelioma, and anaplastic carcinoma. However, due to the growing list of neoplasms that can express

both cytokeratin and vimentin, the diagnostic utility of vimentin is increasingly coming into question.[1]

Contributor: Setsunan University
Department of Pathology
Fuculty of Pharmaceutical Science
45-1 Nagaotohge-cho
Hirakata, Osaka, 5730101, Japan

References:

1. Burgess HJ, Kerr ME. Cytokeratin and vimentin co-expression in 21 canine primary pulmonary epithelial neoplasm. *J Vet Diagn Invest*. 2009;21(6):815-20.
2. Chapman WH, Plymyer MR, Dresner ML. Gonadoblastoma in an anatomically normal man: a case report and literature review. *J Urol*. 1990;144:1472-1474.
3. Maratea KA, Ramos-Vara JA, Corriveau LA, et al. Testicular interstitial cell tumor and gynecomastia in a rabbit. *Vet Pathol*. 2007;44:513-517.
4. Reis-Filho JS, Ricardo S, Gärtner F, et al. Bilateral gonadoblastomas in a dog with mixed gonadal dysgenesis. *J Comp Pathol.* 2004;130:229-233.
5. Scully RE. Gonadoblastoma. A review of 74 cases. *Cancer*. 1970;25:1340-56.
6. Talerman A, Roth LM. Recent advances in the pathology and classification of gonadal neoplasms composed of germ cells and sex cord derivatives. *Int J Gynecol Pathol*. 2007;26:313-321.
7. Turk JR, Turk MA, Gallina AM. A canine testicular tumor resembling gonadoblastoma. *Vet Pathol*. 1981;18:201-7.
8. Hou-Jensen K, Kempson RL. The ultrastructure of gonadoblastoma and dysgerminoma. *Human Pathol.* 1974;5(1):79-91.
9. Suzuki M, et al. Testicular gonadoblastoma in two pet domestic rabbits (*Oryctolagus cuniculus domesticus*). *J Vet Diag Invest.* 2011;23(5):1028-32.
10. Vincent S, et al. Wilms' tumor 1 (WT1) regulate KRAS-driven oncogenesis and senescence in mouse and human models. *J Clin Invest.* 2010;120(11): 3940-52.
11. Wick MR. Immunohistology of melanocytic neoplasms. In: Dabbs DJ. *Diagnostic Immunohistochemistry, Theranostic and Genomic Applications*. 3rd ed. Philadelphia, PA: Saunders Elsevier; 2010:191.

CASE III: Case 1 (JPC 4002497).

Signalment: Adult female dog, *Canis familiaris.*

History: This dog was euthanized due to clinical signs of depression, diarrhea, anorexia, and vomiting.

Gross Pathology: Gross findings included pelvic dilatation in the left kidney; multiple brown foci in the right kidney; bloody, opaque fluid in the uterus; multifocal dark red foci on the lungs; and petechia on the serosa of all sections of the intestine.

Contriubutor's Histopathologic Description: Uterus: The endometrium is diffusely expanded by an infiltrate of large numbers of lymphocytes, plasma cells, and fewer macrophages and neutrophils which surround and separate, and replace ectatic glands and numerous congested vessels. Ectatic glands are often filled with varying combinations and concentrations of degenerate and non-degenerate neutrophils, foamy macrophages, necrotic debris, and brightly eosinophilic proteinaceous secretory materials. Glands are often lined by tall columnar epithelium (attenuated to cuboidal in dilated glands) with abundant eosinophilic foamy cytoplasm and vesiculate nuclei (progestational epithelium). Multifocally, within all layers of the uterine wall, there are extensive areas of lytic necrosis containing large numbers of viable and degenerate neutrophils, necrotic debris, hemorrhage, fibrin, and edema. Additionally within all layers, vessels (both veins and lymphatics) are markedly dilated and often contain fibrin thrombi which are composed of abundant polymerized fibrin and numerous neutrophils, often with mural effacement and numerous viable and degenerate neutrophils, bright pink protein, and cellular debris within the vessel wall (vasculitis). Hemorrhage, edema, fibrin, and numerous viable and degenerate neutrophils expand the submucosa and muscularis, markedly separating submucosal collagen fibers and smooth muscle fibers. Smooth muscle fibers are often swollen, brightly eosinophilic, and fragmented, with pyknotic or lytic nuclei, and low numbers of infiltrating neutrophils (degeneration and necrosis). The adjacent broad ligament is infiltrated with low to moderate numbers of neutrophils and there is abundant hemorrhage.

Contributor's Morphologic Diagnosis: Uterus: Cystic hyperplasia, endometrial, moderate.
Uterus: Necrosuppurative and lymphoplasmacytic endometritis, marked, with hemorrhage.
Uterus, myometrium: Vasculitis, necrosuppurative, with thrombus formation, marked.

Contributor's Comment: Although numerous findings were present in other organs, the primary cause of moribundity was considered to be septicemia arising from the uterus. In addition to bacteria being observed in the kidney at sites of necrosis, other tissues including peritoneal fat, heart, and lungs had necrosuppurative or hemorrhagic lesions arranged in an embolic pattern characteristic of septicemia. The source of the thromboemboli appeared to be the uterus, where there was marked necrosuppurative vasculitis in the myometrium. The cause of the uterine vasculitis was not determined but was likely a sequela to the cystic endometrial hyperplasia (CEH) and observed pyometra.

CEH most commonly occurs in intact bitches (most frequency in those animals that have not undergone pregnancies) and its pathogenesis is related to estrogen stimulation of the uterus followed by prolonged exposure to progesterone during diestrus. Progesterone acts to stimulate endometrial glandular secretion and to suppress contractions of the uterus, thus creating a uterine environment predisposed to bacterial growth.[11] Although CEH has long been thought to be a necessary predisposing factor for pyometra and certainly they are often observed together as in this case, each can occur independently

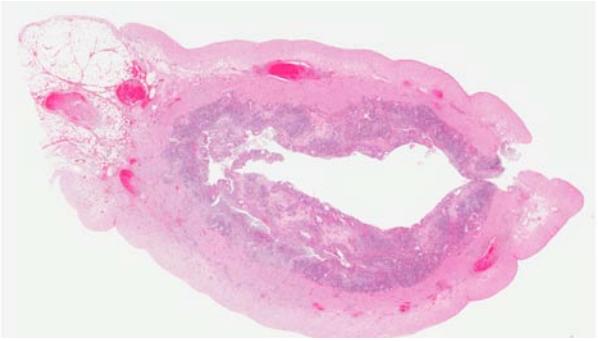

3-1. Uterus, dog. Cross section of the uterus of a dog showing a markedly thickened and inflamed endometrium.(HE 4X)

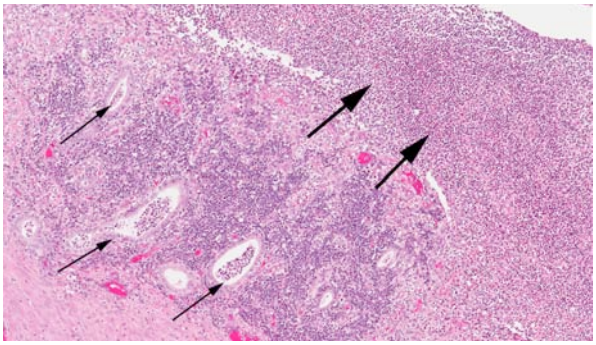

3.2. Uterus, dog. At higher magnification, the lumen contains numerous viable and degenerate neutrophils (large arrows), and the endometrium is expanded by large numbers of lymphocytes, macrophages, and neutrophils. Remaining endometrial glands are often ectatic (small arrows) and contain neutrophils and sloughed endometrial epithelial cells. (HE 200X)

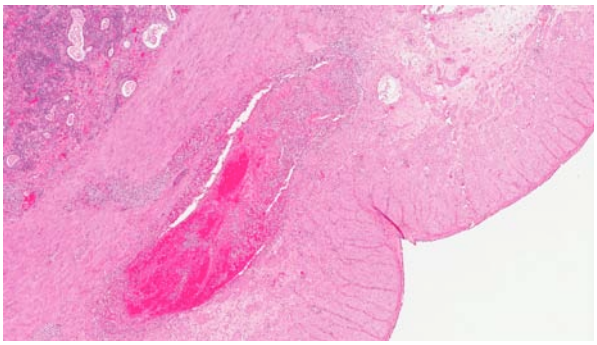

3-3. Uterus, dog. Vessels throughout the muscular layers of the uterine body as well as the broad ligament exhibit vasculitis and partially occlusive fibrinocellular thrombi. (HE 120X)

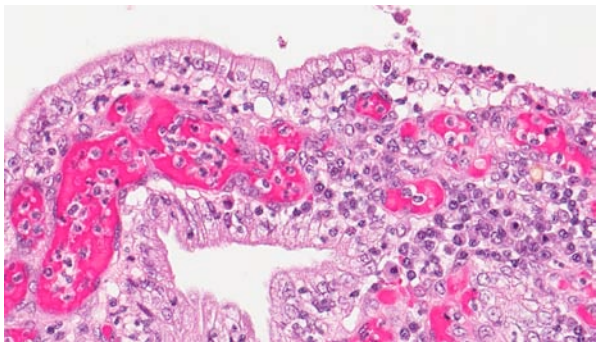

3-4. Uterus dog. Endometrial endothelium is tall columnar and vacuolated under the influence of progesterone. (HE 400X)

of the other. New evidence suggests that pyometra should be considered a separate entity from CEH since CEH relies entirely on a hormone pathogenesis while pyometra is ultimately triggered by bacterial infection.[4,11] The most common bacterium isolated in canine pyometra is *Escherichia coli*, which is isolated in 59-96% of cases.[4] Endotoxin derived from the etiologic agent (which is most often a gram-negative bacteria) often results in sepsis, manifested by numerous cardiovascular, gastrointestinal, and overwhelming systemic inflammatory findings. In the absence of surgical intervention, death is common.[4]

The typical clinical presentation of pyometra is inappetance, depression, polydipsia, lethargy, abdominal distension due to an enlarged uterus, +/- vaginal discharge. Marked leukocytosis is the most common hematologic finding, although anemia, hyperglobulinemia, hypoalbuminemia, and elevation of markers of intrahepatic cholestasis are also often observed.[4,11] The incidence of pyometra in a colony of intact female beagles >4 years of age was 15%, and incidence increased with age.[5] Despite its bacterial component, antibiotic treatment is rarely effective. Ovariohysterectomy is the most reliable and successful treatment for canine pyometra.[5]

JPC Diagnosis: Uterus: Endometritis, chronic-active and suppurative, diffuse, severe, with mild chronic endometrial hyperplasia, vasculitis, and thrombosis.

Conference Comment: Progestational changes cause the endometrial epithelium to be enlarged, columnar, and vacuolated with pyknosis, as well as undergo pseudostratification or papillary proliferation, which are seen in this case. The underlying cause of endotoxin-derived polyuria/polydipsia, a consistent clinical finding with pyometra and associated septicemia, is a decreased response to antidiuretic hormone, glomerular dysfunction due to membranoproliferative glomerulonephropathy from immune-complex deposition, and renal tubular cell damage.[7]

The contributor mentioned the clinicopathologic finding of intrahepatic cholestasis, which is increased alkaline phosphatase, bilirubin, and cholesterol with an ALT within normal limits, which differentiates the findings from hepatocellular necrosis.[3]

Death from pyometra is often due to systemic inflammatory response syndrome (SIRS), resulting in the release of inflammatory mediators and the activation of neutrophils and platelets, resulting in multiple organs dysfunction syndrome and shock. Clinical criteria for diagnosing SIRS in dogs are at least two of the following: heart rate greater than 160 beats per minute, body temperature greater than 103.5°F or less than 100°F, respiratory rate of greater than 20 breaths per minute, pCO2 of less than 32, or a leukocyte count of greater than 12,000 or less than 4,000 or greater than 10% bands.[9]

SIRS caused by the lipopolysaccharide (LPS) endotoxin, as in this case, causes tachycardia and tachypnea in lower doses, and hemorrhagic diarrhea, vomiting, myocardial failure, and death in high doses. LPS binds lipopolysaccaride binding protein (LBP) in serum which in turn binds cell surface pattern-recognition receptor CD14. This activates clotting factor XII (Hageman factor), and induces toll-like receptor (TLR) 4. Also, the endothelium is activated, and the anticoagulant tissue factor production inhibitor (TFPI) and thrombomodulin are inhibited. Monocytes and macrophages are activated, releasing tumor necrosis factor alpha (TNF), IL-1, IL-6, IL-8, and other chemokines, which induces further inflammation and incites the release of acute phase proteins from the liver, such as LBP, mannose-binding protein, fibrinogen, C-reactive protein, serum amyloid A (SAA), hepatoglobin, hepcidin, C3 and C4, alpha-1 antitrypsin and alpha-1 acid glycoprotein. Many of the acute phase proteins bind bacterial components, such as the cell wall, and act as opsonins and fix complement. Some proteins that are reduced, also known as negative acute phase proteins, are transferrin,

albumin, pre-albumin, antithrombin, and alpha-2 macroglobulin (in cattle). Also, the complement cascade is directly activated, generating C3a and C5a.[6,7,8]

Animals that survive SIRS are predisposed to compensatory anti-inflammatory response syndrome (CARS), leading to decreased macrophage activity, T cell anergy, and apoptosis of lymphocytes.[2]

Conference participants also discussed some causes of endometrial hyperplasia, such as prolonged hyperestrogenism due to subterranean and red clover in ewes, which causes reduced fertility, dystocia, uterine prolapse due to hypotonicity, endometrial gland development in the cervix, and mammary gland engorgement. Sows develop endometrial cysts due to zearalenone mycotoxicosis, and cows develop cystic follicles and granulosa cell tumors from prolonged plant estrogen ingestion.[10]

Contributor: Novartis Institutes for BioMedical Research
One Health Plaza
East Hanover NJ 07836-1080
www.novartis.com

References:

1. Ackermann MR. Inflammation and healing. In: Zachary JF, McGavin MD, eds. *Pathologic Basis of Veterinary Disease.* 5th ed. St. Louis, MO: Elsevier; 2012:135.
2. Adib-Conquy M, Cavaillon JM. Compensatory anti-inflammatory response syndrome. *Thromb Haemostat.* 2009;101(1):36-47.
3. Bain PJ. Liver. In: Latimer KS, ed. *Duncan & Prasse's Veterinary Laboratory Medicine: Clinical Pathology.* Ames, IA: Wiley-Blackwell; 2011:212, 218.
4. Fransson BA, Ragle CA. Canine Pyometra: An Update on Pathogenesis and Treatment. *Compendium*. 2003;25:602-612.
5. Fukuda S. Incidence of Pyometra in Colony-raised Beagle Dogs. *Exp. Anim*. 2001;50:325-329.
6. Joles JA, Malnix JA. Polydipsia and polyuria. In: Kirk RW ed. *Current Veterinary Therapy*. Vol. 6 Philadelphia, PA: Saunders; 1977.
7. Kumar V, Abbas AK, Fausto N, et al. Acute and chronic inflammation. In: Kumar V, Abbas AK, Fausto N, Aster JC, eds. *Robbins and Cotran Pathologic Basis of Disease*. 8th ed. Philadelphia, PA: Saunders Elsevier; 2010:45-75.
8. Mitchell RN. Hemodynamic disorders, thromboembolic disease, and shock. In: Kumar V, Abbas AK, Fausto N, Aster JC, eds. *Robbins and Cotran Pathologic Basis of Disease*. 8th ed. Philadelphia, PA: Saunders Elsevier; 2010:111-32.
9. Purvis D, Kirby R. Systemic inflammatory response syndrome: septic shock. *Vet Clin North Am*. 1994;24 (6):1225–1247.
10. Schlaefer DH, Gifford AT. Cystic endometrial hyperplasia, pseudo-placentation endometrial hyperplasia, and other cystic conditions of the canine and feline uterus. *Theriogenology.* 2008;70(3):349-58.
11. Smith FO. Canine pyometra. *Theriogenology*. 2006;66:610-612.

CASE IV: 112D (JPC 4003045).

Signalment: 18-month-old male mini-mule (donkey (*Equus asinus*) x minihorse (*Equus caballus*, subtype miniature) hybrid)

History: A 100kg mini-mule was presented for elective castration.

Gross Pathology: None.

Contributor's Histopathologic Description: Testis (cross-section): This ~2.5 x 2 cm (hypoplastic) testis is bounded by a thick tunica albuginea with two focally extensive (iatrogenic) disruptions of the capsule. Subjacent to one of the areas of capsular discontinuity is a large area of extravasated red blood cells (hemorrhage) within the interstitium; at the margin of this area and under the second area of capsular discontinuity, there is extensive interstitial pallor with separation of collagen fibers (edema). This acute hemorrhage and edema is interpreted as artifactual from the castration procedure.

The number of seminiferous tubules is decreased (testicular hypoplasia); a variable amount of fibrous stroma separates the tubules. There are prominent fibrous septae with many plump oval fibroblast nuclei and pigmented macrophages with pale gray-blue non-polarizing granular cytoplasm (lipochrome, lipofuscin, ceroid). Interstitial (Leydig) cells are difficult to discern, and are therefore less populous than expected. Seminiferous tubules are diffusely hypocellular (hypoplasia) with diameters estimated at 120-130 m. All tubules contain Sertoli cells, often with marked apical micro- and macrovacuolation (degeneration), creating a wispy cytoplasmic appearance. Approximately 95% of seminiferous tubules contain at least one spermatogonium within the basal compartment; mitotic figures are occasionally noted. Meiotic figures are rare, and only a small fraction of the expected number of spermatocytes is identified; many have swollen clear cytoplasm with vacuolated nuclei (degeneration) or are individuated with hypereosinophilic cytoplasm and round condensed or fragmented nuclei (apoptosis). Neither elongating nor mature spermatids are identified. Rare multinucleated syncytial (degenerate) spermatocytes or spermatids are noted; some are apoptotic (may not be present in all sections). Approximately 5% of the seminiferous tubules contain only Sertoli cells with frothy, vacuolated apical cytoplasm. There are multiple small to moderately sized perivascular interstitial aggregates of mature lymphocytes. Clusters of seminiferous tubules without apparent lumina are noted (cause and significance not apparent).

Contributor's Morphologic Diagnosis: Testis: Severe spermatocyte degeneration with testicular hypoplasia and Leydig cell atrophy.

Contributor's Comment: A typical hypoplastic mule testis is examined. Testicular hypoplasia in mules is believed to result from the failure of autosomal

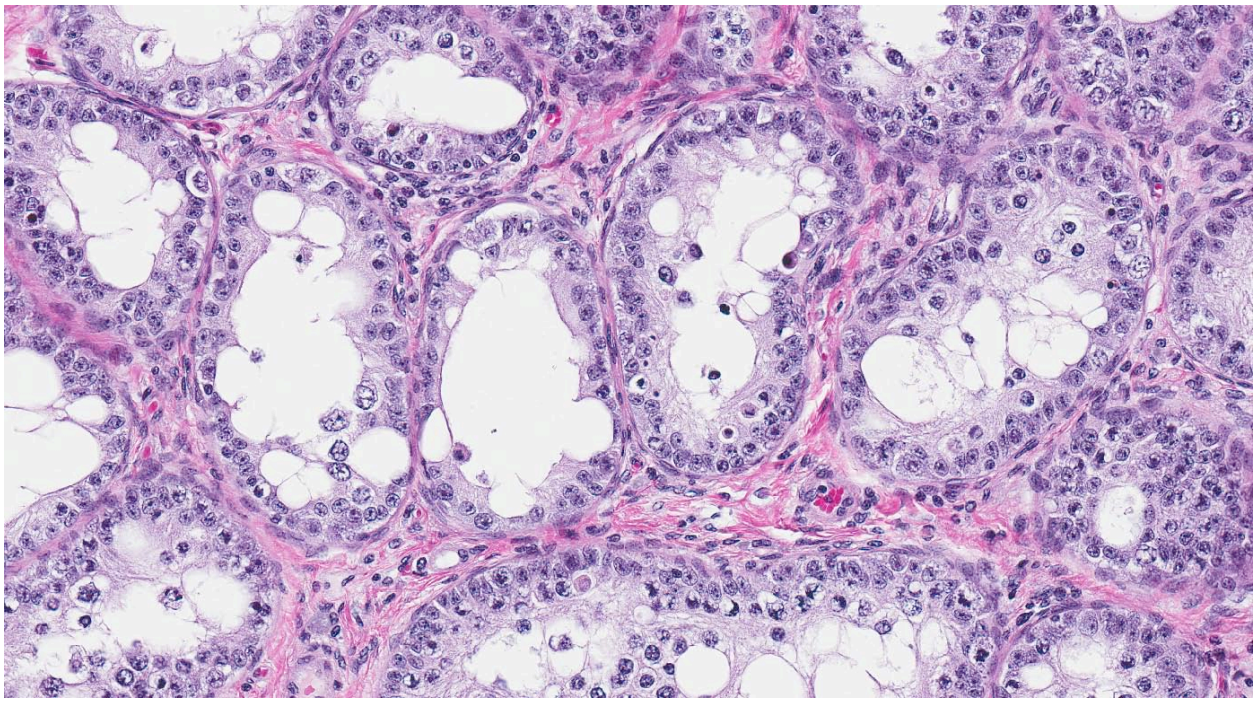

4-1. Testis, minimule – Diffusely, seminiferous tubules are largely devoid of spermatogonia and lined by a single layer of Sertoli cells. Remaining spermatogonia are shrunken (degenerate). Note: also the absence of interstitial cells. (HE 192X)

chromosomal pairing in meiosis;[5] donkeys have a diploid chromosome number of 62, horses have 64, and mules have 63.[2] Donkeys also have more metacentric chromosomes and fewer acrocentric chromosomes than horses, making meiotic pairing physically difficult in mules.[2]

Because the size and development of the mule testis is entirely controlled by the donkey sire (which supplies the male mule's Y chromosome), it is more relevant to compare mule testes with donkey testes, but, as limited information is available for the jack, the stallion can also serve as a reference. The Y chromosome carries the Sry gene, which controls the development and differentiation of the testis, as well as the number of Sertoli cells and the length of the spermatogenic cycle.[5] The donkey Sry gene is significantly divergent from that of the stallion, and may be only partially successful in inducing and supporting testicular development in mules.[7] This is supported by the finding of a skewed sex ratio in mule foals (44 male:56 female) compared to horse foals (52.5 male:47.5 female)[(reviewed in 7)].

This testis has three features of hypoplasia: 1) it is small; 2) it has fewer seminiferous tubules than expected; and 3) the luminal diameter of the seminiferous tubules is decreased. The testis examined is about the size of that of a medium-sized dog, and is much smaller than expected for a 100kg animal. The average mule testis weighs 350g, while that of a jack weighs 750g, and that of a stallion weighs 900g.[4] Only a portion of the testis was submitted, thus the weight of this mini-mules testis was not measured. There is also a decrease in the number of tubules in this testis, possibly causing an apparent increase in the interstitial tissue. Mule testes are reported to have 73% fewer seminiferous tubules than jack testes, and the total length of mule seminiferous tubules is calculated to be only 57% of the total length of seminiferous tubules in jacks.[5] Finally, the average width of seminiferous tubules in mules is decreased; it was estimated at 120-130µm in this mini-mule. Previous quantitative reports suggest that the average width of seminiferous tubules in mules is 127µm and in jacks is 222µm.[5] It is 146µm in stallions.[3]

The number of Leydig cells is decreased in this testis, as is expected with fewer differentiating germ cells failing to provide sufficient crosstalk to support an appropriate number of Leydig cells. Mules have approximately 67% of the number of Leydig cells identified in jacks, and about 40% of the number seen in stallions,[4] but mule Leydig cells are ultrastructurally normal and identical to those of jacks and stallions.[4,5,6] The smaller number of Leydig cells in mule testes is believed to reflect the failure of spermatogenesis, rather than be the cause of it. This is supported by anecdotal evidence that mules have very high libido among equids, presumably due to high levels of testosterone synthesized by the Leydig cells. Mules also typically demonstrate normal epididymal duct epithelium (a steroid-dependent phenotype).[1]

The number of Sertoli cells in this case is likely within normal limits, as is Sertoli cell function. Although the seminiferous tubular diameter is decreased compared to that seen in jacks, there is no waviness or buckling of the basement membrane, suggesting that the number of Sertoli cells is appropriate. Other references have shown that the number of Sertoli cells is equal in donkeys and mules,[5] and that they are ultrastructurally identical.[6] Additionally, lanthanum exclusion studies have shown that the blood-testis barrier is intact in mule testis.[6]

Failure of chromosomal pairing in the zygotene stage of meiotic prophase I leads to deletion of nascent germ cells by apoptosis. Apoptosis in the testis of mammals is a normal process, and is mediated by Fas on germ cells and FasL on Sertoli cells.[3] The number of germ cells undergoing apoptosis is increased after any insult, regardless of cause. It is also increased in testis with maturation arrest, as is present in mule testes.[3] Degeneration of seminiferous tubules in stallions frequently elicits a lymphocytic interstitial orchitis,[3] and that is the likely inciting cause of the inflammation seen in this case. Equine testes also commonly exhibit prominent fibrous tissue septa,[3] and the amount of interstitium in this testis may be within normal limits.

JPC Diagnosis: 1. Testis, seminiferous tubules: Hypoplasia, diffuse, severe.
2. Testis: Hemorrhage, focally extensive, severe.

Conference Comment: Conference participants felt the perception of decreased Leydig cells may be related to the relative decrease in tubules compared to the remaining stroma and interstitial cells. Participants also discussed a recent ultrastructural study of mule testicles which concluded that Sertoli and Leydig cell structure and steroidogenic capacity in mules is normal and not affected by chromosomal abnormality, as they are somatic in origin. The study also concludes that mule seminiferous tubules are able to sustain complete spermatogenesis and, the lack of complete spermatogenesis in mules is due mainly to the failure of homologous chromosomes to pair.[6]

Contributor: University of Wisconsin-Madison
Research Animal Resources Center
School of Veterinary Medicine
1710 University Avenue, Madison, WI 53726
http://www.rarc.wisc.edu/

References:

1. Arrighi S, Romanello M, Domeneghini C. Morphological examination of epididymal epithelium in the mule (E. hinnu) in comparison with parental species (E. asinus and E. caballus). *Histol Histopathol*. 1991;6:325-337.

2. Benirschke K, Brownhill L, Beath, M. Somatic chromosomes of the horse, the donkey, and their hybrids, the mule and the hinny. *J Reprod Fert*. 1962;4:319-326.

3. Foster R, Ladds P. Male Genital System. In: Maxie MG, ed. Jubb, Kennedy, and Palmer's Pathology of Domestic Animals. 5th ed., vol. 3, St. Louis, MO: .Elsevier Limited; 2007: 566, 572-3, 580, 585.

4. Hernandez-Jauregui P, Monter H. Fine structure of mule testes: light and electron microscopy study. *Am J Vet Res*. 1977;38:443-447.

5. Neves E, Chiarini-Garcia H, Franca L. Comparative testis morphometry and seminiferous epithelium cycle length in donkeys and mules. *Biol Reprod*. 2002;67:247-255.

6. Neves E, Chiarini-Garcia H, Franca L. Ultrastructural observation of the mule testis indicates normal function of somatic cells. *Anim Reprod*. 2005;2:263-271.

7. Short R. An introduction to mammalian interspecific hybrids. *J Hered*. 1997;88:355-357.

Joint Pathology Center
Veterinary Pathology Services

WEDNESDAY SLIDE CONFERENCE 2011-2012

Conference 12

11 January 2012

CASE I: CRL-1 (JPC 3167482).

Signalment: 16-week-old female nude (NU-Foxn1nu) mouse (*Mus musculus*).

History: Submitted for routine health monitoring.

Gross Pathology: The liver was enlarged, with rounded margins and adhesions to the pancreas, intestines and right kidney.

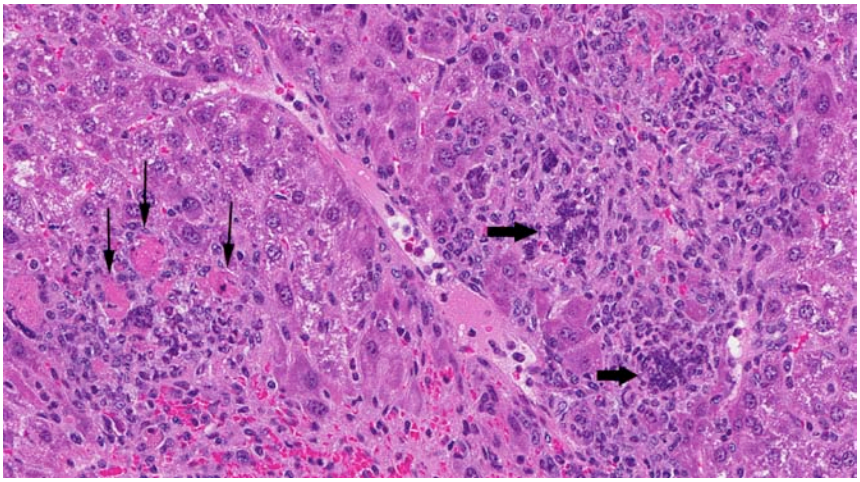

1-1. Liver, mouse. Multifocally and randomly there are small foci of necrotic hepatocytes (thin arrows) admixed with infiltrating neutrophils, and histiocytes. There are also multinucleated giant cells (viral syncitia). (HE 320X)

Laboratory Results: MFIA and IFA positive for mouse hepatitis virus and murine norovirus (serology performed on an immunocompetent cagemate).

Contributor's Histopathologic Description: The liver has multiple foci of degeneration/necrosis and hemorrhage, with inflammatory cell infiltrates comprising neutrophils, histiocytes and lymphocytes. There are many syncytial cells characterized by large degenerate cells at the periphery of foci of necrosis which contain multiple deeply basophilic nuclei and nuclear remnants. There is multifocal extramedullary hematopoiesis. Depending on the section, there is variable capsular fibrosis and inflammation, with some fibrin admixed, and adhesions to the pancreas, with chronic suppurative dochitis and syncytial cells.

Contributor's Morphologic Diagnosis: Liver: Hepatitis, chronic, necrosuppurative, multifocal, marked, with syncytial cells.

Etiology: Mouse hepatitis virus.

Contributor's Comment: Mouse hepatitis virus (MHV) is a coronavirus that infects mice, although the virus shares

antigenic cross reactivity with Group 2 coronaviruses, including rat coronavirus and bovine coronavirus.[5] Infant rats can be experimentally infected.[1] Susceptibility to MHV varies with host and viral factors, such as genotype, age, strain of virus, route of inoculation, immune status, diet, and concurrent infections. MHV can be loosely classified into two groups according to the primary target organ; enterotropic and respiratory strains. Enterotropic strains selectively infect intestinal mucosa with little, if any, dissemination to other tissues in immunocompetent mice. Respiratory strains are considered polytropic, replicating in the nasal mucosa followed by secondary dissemination to multiple organs. Although improved husbandry has markedly reduced the prevalence of MHV in laboratory mice, the rate of MHV seropositive samples received at a major commercial rodent diagnostic laboratory was reported to be 1.6% (commercial vendor mice excluded).[6] Diagnosis of MHV infection is typically accomplished with serology and histopathology on sick animals.

The pathogenesis of infection with a respiratory MHV strain begins with replication in the nasal epithelium, followed by dissemination via the blood stream to other tissues including liver, vascular endothelium, lymphoreticular tissues and brain, depending on host susceptibility. Pulmonary involvement is restricted to vascular endothelium and does not involve respiratory mucosa. The route of dissemination of infection to the brain is age-dependent. In adult mice, infection tends to occur by extension of virus along the olfactory neural pathway. Microscopic findings are multifocal necrosis with syncytia in multiple organs, commonly including liver, spleen, lymph nodes and other lymphoid tissue.[5] Hallmark syncytia of MHV infection are characterized by large degenerating cells at the periphery of necrotic foci, containing dense basophilic nuclei and nuclear remnants. Syncytia are more common and more well-developed in immunocompromised mice, as in this case.

Endemic infections are usually subclinical, sustained by continued arrival of naive susceptible animals (newborns), as there is generally no carrier state.[1]

Immunocompromised mice infected with either respiratory or enterotropic strains of MHV may develop progressively fatal, multi-systemic infections with severe necrotizing lesions in nasal epithelium, vascular endothelium, brain, liver, bone marrow, lymphoid tissue and other sites.[2] Virulent MHV strains kill these mice rapidly, but disease can be chronic with wasting in mice exposed to natural, avirulent strains of virus. Immunocompromised mice with only B cell defects infected with enterotropic MHV may develop enteric infections which are chronic but may not manifest overt clinical disease.[2] High morbidity and mortality can develop with enterotropic MHV infection in neonatal mice in naive mouse colonies.[5]

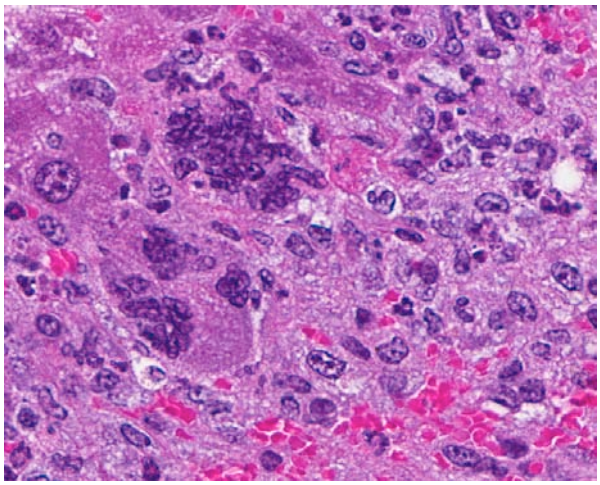

1-2. Liver, mouse. Closer view of multinucleated giant cells (viral syncitia) are present, often at the periphery of necrotic foci. (HE 400X)

JPC Diagnosis: 1. Liver: Hepatitis, necrotizing, multifocal and random, with hepatic and endothelial viral syncitia, and capsular fibrosis.
2. Pancreas: Dochitis, necrotizing, diffuse, minimal.

Conference Comment: The mouse strains most susceptible to the polytropic strain of mouse hepatitis virus (MHV) are C57BL, DBA/2, nude mice, SCID mice, and BALB/c. C3H is a partially susceptible strain, and A/J and SLJ mice are resistant. All strains are susceptible to the enterotropic strains. Tumor necrosis factor (TNF) -/- and transgenic mice persistently infected with MHV can transmit infection for months and infect susceptible mice and immunocompetent sentinel mice.[5] Co-infection of MHV with bacteria (i.e. *Helicobacter hepaticus*) decreases the severity of acute lesions but exacerbates hepatitis and meningitis in chronic infections.[3]

Despite the name "mouse hepatitis virus", polytropic MHV is not always hepatotropic. In addition to hepatic necrosis, common gross lesions include lymphoid tissue involution, ascites, hemorrhagic peritoneal exudate, necrotizing enterocolitis, thickened bowel segments in weanlings and adults, and mucosal proliferation or hyperplasia of the ascending colon and ileocecal junction in older mice. Microscopic lesions seen in other organs include intraepithelial eosinophilic intracytoplasmic viral inclusion bodies, necrotizing enterocolitis, segmental to diffuse villus blunting and atrophy at the ileocecal junction and ascending colon, and necrosis and syncytial giant cells of the splenic red pulp, lymphoid tissue, and hematopoietic tissues. In mice susceptible to neurotropic effects, there is necrotizing meningoencephalitis with spongiosis,

demyelination, and syncytial giant cells in the central nervous system.[5]

The differential diagnosis in mice for hepatitis and enteritis include:

a) Tyzzer's disease caused by *Clostridium piliformis* with intracytoplasmic bacilli and no giant cells
b) salmonellosis
c) mouse pox caused by ectromelia virus, an orthopoxvirus characterized by splenic necrosis ("tiger striping") and skin lesions with intracytoplasmic eosinophilic viral inclusion bodies
d) epizootic diarrhea of infant mice (EDIM) caused by a rotavirus with less severe disease in neonatal mice with epithelial vacuolar degeneration in the ileum and jejunum, and epithelial eosinophilic intracytoplasmic viral inclusion bodies and no multinucleated giant cells or endothelial changes
e) reovirus-3, an orthoreovirus which causes foci of hepatic necrosis, CNS lesions, myocardial necrosis and pulmonary hemorrhage
f) adenovirus, which presents with intranuclear viral inclusion bodies
g) *Helicobacter hepaticus,* which causes proliferative colitis and rectal prolapse.[3,5]

Contributor: Charles River
251 Ballardvale St.
Wilmington, MA 01887
www.criver.com

References:

1. Baker DG. Natural pathogens of laboratory animals, their effects on research. Washington, DC: ASM Press; 2003:29-31.
2. Compton SR, Ball-Goodrich LJ, Johnson LK, et al. Pathogenesis of enterotropic mouse hepatitis virus in immunocompetent and immunodeficient mice. *Comp Med*. 2004;54:681-689.
3. Compton SR, Ball-Goodrich LJ, Zeiss CJ,et al. Pathogenesis of mouse hepatitis virus infection in gamma interferon-deficient mice is modulated by co-infection with *Helicobacter hepaticus*. *Comp Med*. 2003;53:197-206.
4. Maronpot RR. *Pathology of the Mouse*. Vienna, IL: Cache River Press; 1999:96-97.
5. Percy DH, Barthold SW. *Pathology of Laboratory Rodents and Rabbits*. 3rd ed. Oxford, UK: Blackwell Publishing; 2007:17-62.
6. Pritchett-Corning KR, Cosentino J, Clifford, CB. Contemporary prevalence of infectious agents in laboratory mice and rats. *Lab Anim*. 2009;43:165-173.
7. Pullium JK, Homberger FR, Benjamin KA, et al. Confirmed persistent mouse hepatitis virus infection and transmission by mice with a targeted null mutation of tumor necrosis factor to sentinel mice, using short term exposure. *Comp Med*. 2003;53:439-443.
8. Rehg JE, Blackman MA, Toth LA. Persistent transmission of mouse hepatitis virus by transgenic mice. *Comp Med*. 2001;51:369-374.

CASE II: 42100-A (JPC 4001557).

Signalment: 5-month-old female Sprague-Dawley rat (*Rattus norvegicus*).

History: Tissues are from three rats that were part of a group of 60 rats receiving a trial diet that contained a single protein source. Rats within the group did not gain weight as rapidly as expected.

Gross Pathology: Rats were in a poor state of nutrition and weighed less than would be predicted for their age. Examination of the urinary system revealed pitted kidneys with white streaks within the cortex.

Laboratory Results: A pure growth of *Escherichia coli* was cultured from a sample of kidney from one of the rats.

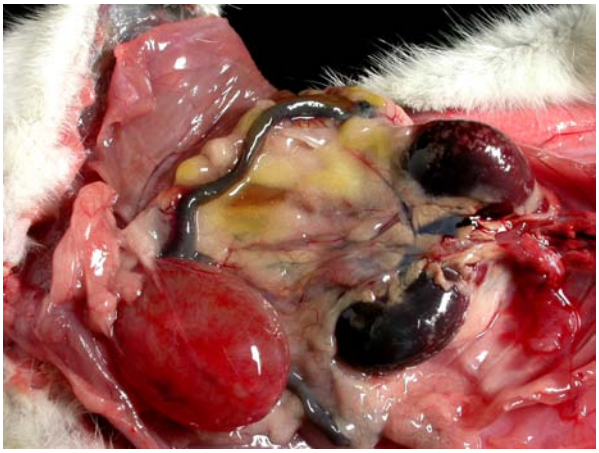

2-1. Kidney, rat. The kidneys are pitted with white streaks. Photograph courtesy of Institute of Veterinary, Animal, and Biomedical Sciences, Massey University, www.massey.ac.nz

Contributor's Histopathologic Description: Lesion severity is variable within the sections. The predominant lesion is visible within the renal pelvis. Here, mild to marked dilation of the pelvis is visible. Inflammation is visible surrounding the pelvis. This inflammation consists predominantly of lymphocytes and plasma cells with some sections also containing significant numbers of neutrophils. Small foci of mineralization are visible surrounding the pelvis in some sections. The transitional epithelium within the renal pelvis has undergone squamous metaplasia. Inflammation and necrosis is visible extending from the renal pelvis into the cortex. Tubules that are dilated by neutrophils are visible within the sections. Areas of fibrosis indicate previous episodes of nephritis within the cortex.

Contributor's Morphologic Diagnosis: Kidney. Pyelonephritis, moderate, subacute, neutrophilic, with marked squamous metaplasia of the transitional epithelium.

Contributor's Comment: The high mortality within the group of rats receiving this experimental diet suggested a dietary toxin or deficiency. In addition to the renal pelvis, squamous metaplasia of the transitional epithelium was also visible within the ureters and bladder suggesting vitamin A deficiency. Subsequent analysis revealed that the experimental diet that these rats were receiving contained an inadequate concentration of vitamin A. Overall within the 60 rats, 27% had visible uroliths and 5% had nephroliths. Bilateral pyelonephritis was detected histologically in 43% of rats and unilateral pyelonephritis in 25%.

Vitamin A regulates epithelial cell growth and differentiation, enables production of visual pigment, is necessary for normal function of the immune system, and influences skeletal development.[8] When rats are fed diets that contain no vitamin A, the most commonly reported clinical signs of deficiency are weight loss, corneal keratinization and ulceration, respiratory or skin disease, and salivary gland enlargement.[1] An 80% mortality rate due to inanition or bacterial infection of the skin or respiratory tract is expected after 15 weeks.[1] In the present case, the rats received some vitamin A, albeit in inadequate quantities. The restriction of the lesions to the transitional epithelium in these rats suggests that the transitional epithelium is the most susceptible to squamous metaplasia due to moderate vitamin deficiency.[6] The squamous metaplasia of the transitional epithelium then predisposed to the development of ascending bacterial infections and urolith and nephrolith formation.

While squamous metaplasia of the transitional epithelium lining the renal pelvis can occur secondary to bacterial infection, the metaplasia visible within the present case was considered an excessive reaction to an ascending bacterial pyelonephritis.

JPC Diagnosis: Kidney: Pyelonephritis, neutrophilic and lymphohistiocytic, diffuse, marked, with urothelial squamous metaplasia and coccobacilli.

Conference Comment: Vitamin A is one of four fat soluble vitamins, along with vitamins D, E and K, and has multiple functions. Vitamin A as retinoic acid functions in morphogenesis during embryonic development, maintenance of epithelial cells, bone growth, reproduction, immunostimulation, and may also have antioxidant effects.[3]

Vitamin A deficiency leads to impaired epithelial differentiation through an unknown mechanism, and leads to reduction in mucus-secreting cells, squamous metaplasia of the respiratory and genitourinary

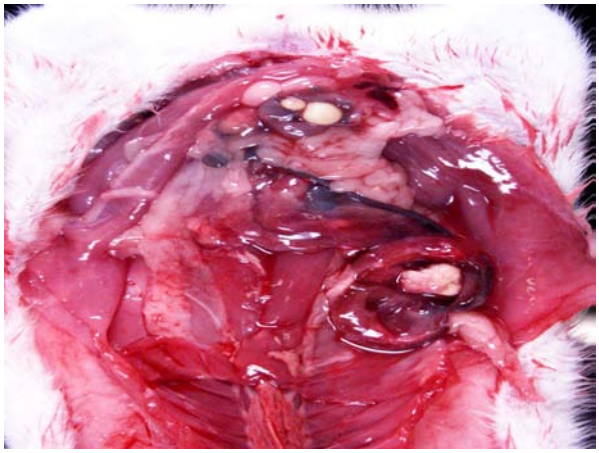

2-2, 2-3, 2-4. Kidneys, urinary bladder, rat. Nephroliths and uroliths were present in 5 and 27%, respectively, of examined rats. Photographs courtesy of Institute of Veterinary, Animal, and Biomedical Sciences, Massey University, www.massey.ac.nz

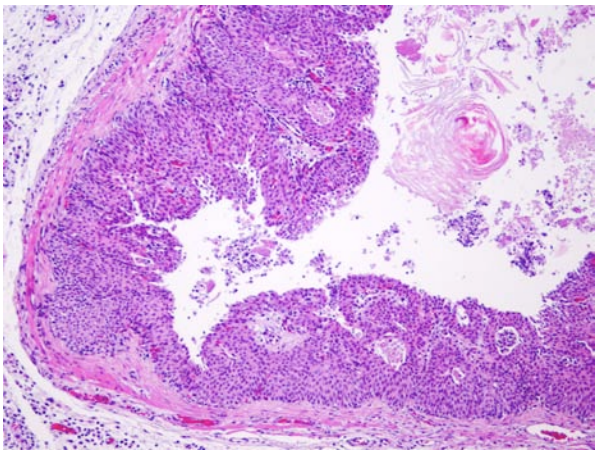

2-5, 2-6. Ureter, urinary bladder, rat. Urothelium is hyperplastic, piling up several layers deep, and the superficial layers are composed of flattened squamous epithelium (squamous metaplasia). The ureter (1-5) contains abundant keratin debris and sloughed epithelium. Photographs courtesy of Institute of Veterinary, Animal, and Biomedical Sciences, Massey University, www.massey.ac.nz

epithelium, and hyperkeratosis.[4] Hypovitaminosis A also leads to retarded osteoclastic resorption of endosteal bone, and lesions are varied depending on species affected, stage of growth, and severity of the deficiency.[7] Vitamin A deficiency also leads to the arrest of spermatogenesis at the spermatid phase in all species, especially in cattle, rats, and chickens, and causes abnormal estrous cycles, congenital anomalies, and fetal resorption. Hypovitaminosis A affects immune function, as vitamin A is thought to stimulate T-cells directly through 14-hydroxyretinol. During infection, synthesis of the negative acute phase protein, retinol-binding protein, is down-regulated, decreasing availability of vitamin A.[4]

In dogs, vitamin A deficiency results in hyperkeratosis of sebaceous gland ducts; vitamin A-responsive dermatosis in cocker spaniels is characterized by marked follicular keratosis of the chest and abdomen.[2] In male calves, vitamin A deficiency results in stenosis of the optic foramen and atrophy of the optic nerve,

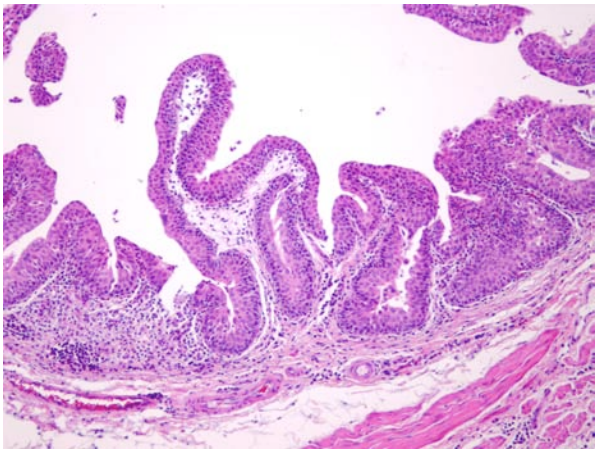

leading to blindness. Squamous metaplasia of the parotid gland is a pathognomonic lesion of hypovitaminosis A in cattle.[9] In guinea pigs and rats, vitamin A deficiency results in inadequate differentiation and organization of odontoblasts,

leading to irregular dentin formation and enamel hypoplasia.[5]

Contributor: Institute of Veterinary, Animal, and Biomedical Sciences
Massey University
Private Bag 11 222
Palmerston North 4410
New Zealand
www.massey.ac.nz

References:

1. Beaver DL. Vitamin A deficiency in the germ-free rat. *Am J Pathol*. 1961;38:335-357.
2. Hargis AM, Ginn PA. The integument. In: McGavin MD, Zachary JF, eds. *Pathologic Basis of Veterinary Disease*. 4th ed. vol. 1. St. Louis, MO: Elsevier; 2012:1066.
3. Jones TC, Hunt RD, King NW. Nutritional deficiencies. In: *Veterinary Pathology*. 6th ed. Baltimore, MD: Maple Valley Press;1997:781-783.
4. Meyers RK, McGavin MD, Zachary JF. Cellular adaptations, injury, and death: morphologic, biochemical, and genetic bases. In: McGavin MD, Zachary JF, eds. *Pathologic Basis of Veterinary Disease*. 4th ed. vol. 1. St. Louis, MO: Elsevier; 2012:29-30.
5. McDowell EM, Shores RL, Spangler EF, et al. Anomalous growth of rat incisor teeth during chronic intermittent vitamin A deficiency. *J Nutr*. 1987;117(7): 1265-74.
6. Munday JS, McKinnon H, Aberdein D, et al. Cystitis, pyelonephritis, and urolithiasis in rats accidentally fed a diet deficient in vitamin A. *J Am Assoc Lab Anim Sci*. 2009;48:790-794.
7. Thompson K. Bones and joints. In: Maxie MG, ed. *Jubb, Kennedy and Palmer's Pathology of Domestic Animals*. 5th ed. vol. 1. Philadelphia, PA: Saunders Elsevier; 2007:55-56.
8. Weber F. Biochemical mechanisms of vitamin A action. *Proc Nutr Soc.* 1983;42:31-41.
9. Zachary JF. Nervous system. In: McGavin MD, Zachary JF, eds. *Pathologic Basis of Veterinary Disease*. 4th ed. vol. 1. St. Louis, MO: Elsevier; 2012:865.

CASE III: S111/11 (JPC 4003457).

Signalment: 6-week-old male BALB/c mouse (*Mus musculus*).

History: The mouse was infected by intracerebral inoculation with a lethal dose of rabies virus (genotype 1).

Gross Pathology: No gross lesions were observed.

Laboratory Results: Further laboratory investigations were not performed.

Contributor's Histopathologic Description: Cerebrum: Within the gray matter of the cortex, thalamus, hippocampus and hypothalamus regions (these sections were submitted to the conference) there is low to moderate numbers of neurons with shrunken cell bodies, and hypereosinophilic cytoplasm frequently accompanied by karryorhexis or karyolysis (neuronal degeneration and necrosis). Occasionally in these cells, but significantly more often in normal appearing neurons, especially within the hippocampus, there are one to several intracytoplasmic, pale eosinophilic inclusion bodies up to 7 µm in diameter (Negri bodies). Some affected neurons are surrounded by lymphocytes and glial cells (neuronophagia). Focally distributed throughout the neuropil, aggregates of glial cells and lymphocytes are present (glial nodules). Perivascularly, there is a slight lymphocytic and histiocytic infiltration (perivascular cuffing) and few lymphocytes and histiocytes are found in submeningeal regions. In some sections, ventricles contain low amounts of lymphocytes and histiocytes.

Contributor's Morphologic Diagnosis: Encephalitis, nonsuppurative, minimal, with neuronal degeneration and necrosis and neuronal eosinophilic intracytoplasmic inclusion bodies, mouse, etiology consistent with rabies virus infection.

Contributor's Comment: Rabies virus (RV) belongs to the genus *Lyssavirus* in the *Rhabdoviridae* family of the order *Mononegavirales*. The characterization of the rabies virus isolates based on monoclonal antibodies grouped the rabies-associated viruses into four serogroups, with classical rabies forming serogroup 1, the African lyssaviruses forming serogroup 2 (Lagos bat virus), serogroup 3 (Mokola virus), and serogroup 4 (Duvenhage virus). DNA sequencing was used to further distinguish the members of each serogroup, which in turn became genotypes (see table).[21] The European bat lyssaviruses were classified into two groups (EBLV-1 and EBLV-2) and designated genotypes 5 and 6.[14] A further genotype has been identified in Australia, Australian bat lyssavirus.[11]

The genome of RV comprises five genes encoding the viral proteins nucleoprotein, phosphoprotein, matrix protein, glycoprotein and the viral RNA polymerase. The replication of RV proceeds in the presence of the host immune response, including the antiviral type I

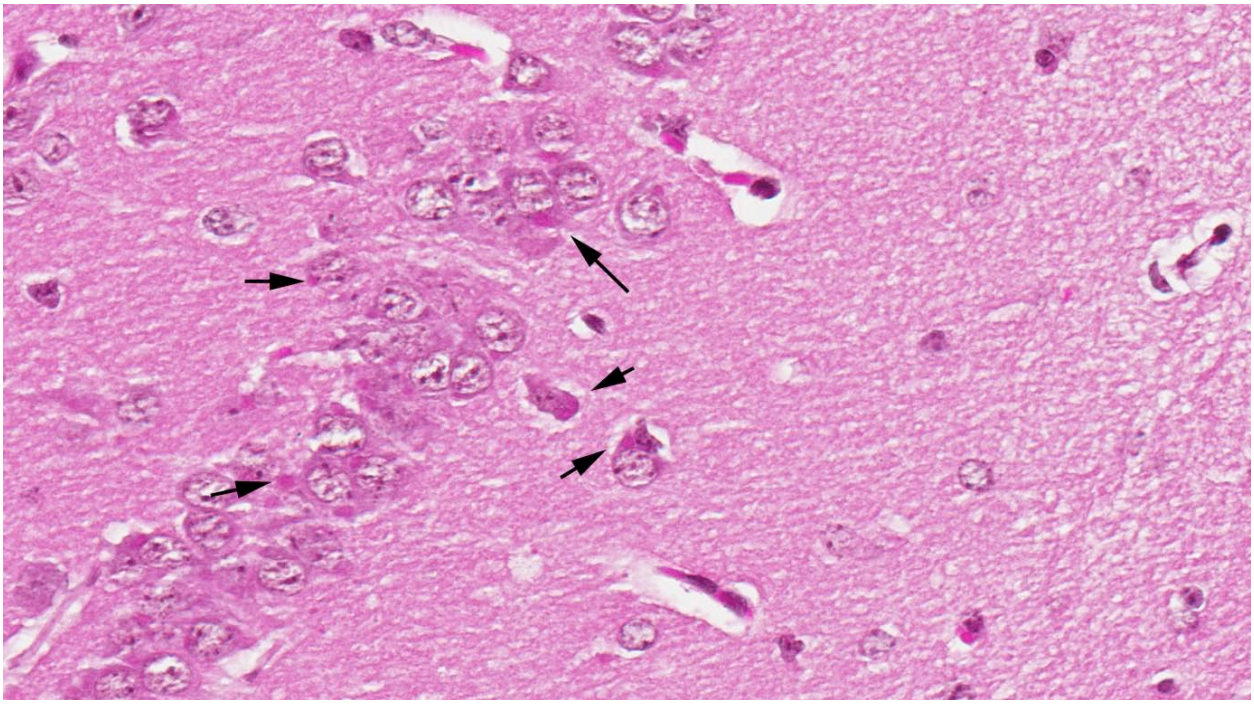

3-1. Brain, hippocampus, mouse. Many neurons contain 2-7 micron bright eosinophilic intracytoplasmic inclusion bodies (Negri bodies). (HE 400X)

interferon (IFN) system. RV is known for its IFN-sensitivity and therefore must encode mechanisms that prevent IFN expression.[5] It is hypothesized that the viral phosphoprotein is involved in this mechanism.[1]

Rabies occurs in more than 150 countries and territories worldwide. Dogs are the source of infection in all of the estimated 55,000 human rabies deaths annually in Asia and Africa. Bats are the source of most human rabies deaths in the United States of America and Canada. Bat rabies has also recently emerged as a public health threat in Australia, Latin America and Western Europe. Infections due to contact to rabid foxes, raccoons, skunks, jackals, mongooses and other wild carnivore are very rare. Human-to-human transmission by bite has never been confirmed.[23]

RV is the causative agent of the classical rabies and is responsible for the vast majority of all human rabies cases. The transmission occurs via the bite of rabid animals shedding virus within their saliva, or direct contact of infectious material (i.e. saliva, cerebrospinal liquid, nerve tissue) to mucous membranes or skin lesions. The virus cannot penetrate intact skin. Rabies virus replicates in striated muscle cells or infects nerve cells, followed by a retrograde transport of virions to the central nervous system (CNS). Within the CNS, virus replication induces pathologic effects on nerve cell physiology. The anterograde transport of virus to secretory tissues of salivary glands leads to viral shedding via saliva.[24]

In animals, RV infection brings out neurological signs which might differ slightly depending on the species and the time point infected. The incubation period for rabies is typically 1–3 months, but may vary from <1 week to >1 year.[23] After this so-called prodromal stage, the onset of clinical symptoms follows, which lasts for about 1-3 days with aggressiveness, daytime activities in nocturnal animals or abnormalities in appetite. Potentially, the prodromal stage is followed by the excitative phase with severe agitation and aggressiveness. Further, in the paralytic phase, the infected animals are unable to swallow, leading to a typical sign of foaming saliva around the mouth. A complete paralysis occurs and is followed by death.[24]

Many neurotropic viruses use apoptosis as a mechanism of neuropathogenicity.[16] The induction of apoptosis by rabies virus has been a controversial topic, but increasing evidence indicates that pathogenic rabies virus strains do not induce apoptosis.[8]

In natural rabies, pyknotic chromatolytic neurons are seen throughout the CNS most frequently in the brainstem, and periaqueductal gray matter, cervical spinal cord, thalamus and less frequently the cerebral cortex.[4] In general, these degenerated neurons do not harbor Negri bodies but are positive for viral antigen and may be accompanied by inflammatory reaction.[6] As in other viral encephalitides, neuronophagia and glial nodules are seen often in areas where neuronal degeneration and inflammatory cell infiltration are conspicuous. Topographic dissociation between location of inflammatory reactions and of Negri body has been reported in an autopsy study of 49 cases. Inflammatory changes were most frequently found in medulla, pons and spinal cord followed by thalamus and less frequently in cerebellum and hippocampus. Negri body bearing neurons were rare where inflammation was dense.[10] Perivascular infiltrates are composed of lymphocytes and monocytes intermingled with small numbers of granulocytes and plasma cells, depending on the stage and severity of infection.[7]

Two different mechanisms have been proposed for the transport of rabies virus through the axon to the cell body: transport of either the rabies virus capsid alone or transport of the whole virion. A recent study showed that the whole virion is transported to the cell body in an endosomal vesicle, although the exact mechanism by which this occurs remains unclear.[12] The rabies virus glycoprotein mediates the entry of the virion into the vesicle. However, as the rabies virus glycoprotein is inside the vesicle, it should not be able to interact directly with a specific transporter complex. Based on these observations, it is speculated that entry into the vesicle determines the direction and provides the driving force of rabies virus transport. This indicates that the nature of the vesicle formed dictates the transport method that follows.[19]

In cases of human rabies, the patients die with absence of protective antibodies. The immune privileged status of the CNS and the blood–brain barrier might explain the delayed development of a protective immune response and the poor survival rate.[10] Remarkably, there is one report of a human survivor of rabies. The patient had detectable antibody and the treatment applied was aimed to allow the humoral immune response to develop. High IgG titres developed and might have contributed to the survival of this patient.[24]

The influence of the immune privileged status of the CNS on the antibody response is controversial. In contrast to RV, Herpes viruses and Borna disease virus can infect the brain, but are effectively controlled by the immune system. Several other factors are discussed, as for example that the infectious dose transmitted with a bite is too small to trigger immune responses and further enable the virus to infect sensory nerves. A final explanation for the lack of antibody could result from immunosuppression induced by the virus. It is known that the viral phosphoprotein inhibits interferon response. However, RV infection is

associated with the increase in gene transcripts for interferon-inducible genes. It is speculated that interferon inhibition is transitory and provides a short delay in the host response.[10]

Table: Current classification of the Lyssavirus genus, host species and geographical distribution.[11]

[a] Species from which the virus is predominantly isolated.
[b] Single isolations have been made.

Virus and Genotype (I-VII)	**Host[a]**	**Geographical distribution**
Classical rabies virus (RABV), I	Numerous chiropteran and carnivoran species	Worldwide
Lagos bat virus (LBV), II	*Epomophorus wahlbergi* (Wahleberg's epauletted fruit bat)	Africa
Mokola virus (MOKV), III	Unknown	Africa
Duvenhage virus (DUVV), IV	*Miniopterus* species (?)	Southern Africa
European bat lyssavirus type 1 (EBLV-1), V	*Eptesicus serotinus* (Serotine bat)	Europe
European bat lyssavirus type 2 (EBLV-2), VI	*Myotis daubentonii* (Daubenton's bat)	Western Europe
Australian bat lyssavirus (ABLV), VII	Australian mega- and microchiropteran species	Australia
Aravan	*Myotis blythi* (lesser mouse-eared bat)[b]	Kyrgistan
Khujand	*Myotis mystacinus* (whiskered bat)[b]	Kyrgistan
Irkut	*Murina leucogaster* (greater tube-nosed bat)[b]	Eastern Siberia
West Caucasian bat virus (WCBV)	*Miniopterus schreibersi* (common bent-winged bat)[b]	Western Caucasus Mountains

JPC Diagnosis: Brain, cerebrum: Neuronal necrosis, with minimal lymphoplasmacytic perivasculitis and numerous neuronal intracytoplasmic viral inclusion (Negri) bodies.

Conference Comment: The contributor provided a very thorough overview of rabies virus. Following invasion and replication in rhabdomyocytes, virions enter the extracellular space of the neuromuscular junction and neurotendinal sensory stretch receptors, and enter the neurons via the acetylcholine receptor at the neural synapses. Once in the central nervous system, the virus concentrates in the limbic system and generally spares the neocortex, which is the cause of the furious stage of infection. Once in the central nervous system, virions can bud from the neuronal cell body and process plasma membranes and directly infect neighboring neurons. Negri bodies are found in greatest concentration in large neurons, such as in the pyramidal cells of the hippocampus, ganglionic neurons of the pontine nuclei, and cerebellar Purkinje cells. Negri bodies represent the accumulation of rabies virus nucleocapsids in cells due to the defective assembly of virions. Negri bodies are found in large numbers in salivary epithelial cells of carnivores, and the virus can be detected in chromaffin cells of the adrenal medulla, basal epithelial cells of the nasal mucosa, cornea, epidermis, and external root sheath of hair follicles. Infection of these sites is by peripheral nerves.[2]

Australian bat lyssavirus, mentioned by the contributor, is a virus closely related to rabies that was discovered in Australia in 1996. It occurs in various species of flying foxes and occasionally in other species of bats and is responsible for a few human fatalities. Lesions are similar to rabies and consist of nonsuppurative meningoencephalomyelitis and ganglioneuritis with Negri bodies.[6]

Pseudo-Negri bodies, which may be confused with rabies and are a reason that rabies diagnosis should not be based solely on the presence of Negri bodies, are found in cats, skunks, and dogs and are nonspecific, 1.5 µm, homogenous inclusions in the pyramidal cells of the hippocampus. They present in cats as nonspecific inclusions in the lateral geniculate neurons; in dogs as cytoplasmic lamellar bodies in the thalamic neurons and Purkinje cells; in aged sheep and cattle as nonspecific 1 µm, brightly eosinophilic, angulated inclusions in the large neurons of the medulla and spinal cord; in Japanese brown beef cattle; in mice as hippocampal inclusions; and in woodchucks as inclusions in the brainstem.[3,15,17,18,20,22]

Contributor: Friedrich-Loeffler-Institut
Federal Research Institute for Animal Health
17493 Greifswald-Insel Riems, Germany
(www.fli.bund.de)

References:

1. Brzozka K, Finke S, Conzelmann KK. Identification of the rabies virus alpha/beta interferon antagonist: Phosphoprotein P interferes with phosphorylation of interferon regulatory factor 3. *J Virol.* 2005;79(12): 7673-7681.

2. Cheville NF. Cytopathology of viral diseases. In: *Ultrastructural Pathology, the Comparative Cellular Basis of Disease*. 2nd ed. Ames, IA: Wiley-Blackwell; 2009:367-8.

3. Coetzer JAW, Tustin RCSwanepoel R. Rabies. In: Coetzer JAW, Tustin RC, eds. *Infectious Diseases of Livestock*. 2nd ed. vol. 2. Cape Town, South Africa: Oxford University Press; 2004:1123–1182.

4**.** Dupont JR, Earle KM. Human Rabies Encephalitis - a Study of 49 Fatal Cases with a Review of Literature. *Neurology.* 1965;15(11):1023-7.

5. Finke S, Conzelmann KK. Replication strategies of rabies virus. *Virus Res.* Aug 2005;111(2):120-131.

6. Fraser GC, et al. Encephalitis caused by a Lyssavirus in fruit bats in Australia. *Emerg Infect Dis.* 1996;2(4): 327-31.

7. Iwasaki Y, Liu DS, Yamamoto T, et al. On the Replication and Spread of Rabies Virus in the Human Central Nervous-System. *J Neuropath Exp Neur.* 1985;44(2):185-195.

8. Iwasaki Y, Sako K, Tsunoda I, et al. Phenotypes of Mononuclear Cell Infiltrates in Human Central-Nervous-System. *Acta Neuropathol.* 1993;85(6): 653-657.

9. Jackson AC, Rossiter JP. Apoptosis plays an important role in experimental rabies virus infection. *J Virol.* 1997;71(7):5603-5607.

10. Johnson N, Cunningham AF, Fooks AR. The immune response to rabies virus infection and vaccination. *Vaccine.* 2010;28(23):3896-3901.

11. Johnson N, Vos A, Freuling C, et al. Human rabies due to lyssavirus infection of bat origin. *Vet Microbiol.* 2010;142(3-4):151-159.

12. Klingen Y, Conzelmann KK, Finke S. Double-labeled rabies virus: Live tracking of enveloped virus transport. *J Virol.* 2008;82(1):237-245.

13. Marston DA, McElhinney LM, Johnson N, et al. Comparative analysis of the full genome sequence of European bat lyssavirus type 1 and type 2 with other lyssaviruses and evidence for a conserved transcription termination and polyadenylation motif in the G-L 3 ' non-translated region. *J Gen Virol.* 2007;88:1302-1314.

14. Maxie MG, Youssef S. Nervous system. In: Maxie MG, ed. *Jubb, Kennedy, and Palmer's Pathology of Domestic Animals*., 5th ed. vol. 1. Philadelphia, PA: Elsevier, 2007:283-457.

15. Mori I, Nishiyama Y, Yokochi T, et al. Virus-induced neuronal apoptosis as pathological and protective responses of the host. *Rev Med Virol.* 2004;14(4):209-216.

16. Nietfeld JC, Rakich PM, Tyler DE, et al. Rabies-like inclusions in dogs. *J Vet Diagn Invest*. 1989;4:333–338.

17. Pierce V, Snyder RL, McGrath JT. Intracytoplasmic neuronal inclusions in Woodchuck brain stem. *J Wild Dis*. 1990;26(1):62-66.

18. Schnell MJ, McGettigan JP, Wirblich C, et al. The cell biology of rabies virus: using stealth to reach the brain. *Nat Rev Microbiol.* 2010;8(1):51-61.

19. Summers B, Cummings JF, De Lanhunta A. Inflammatory diseases of the central nervous system. In: Summers B, Cummings JF, De Lanhunta A, eds. *Veterinary Neuropathology*. St. Louis, MO: Mosby; 1995:95-188.

20. Tordo N, Poch O, Ermine A, et al. Completion of the rabies virus genome sequence determination - Highly conserved domains among the L (Polymerase) proteins of unsegmented negative-strand Rna viruses. *Virology.* 1988;165(2):565-576.

21. Whitfield SG, et al. A comparative study of the fluorescent antibody test for rabies diagnosis in fresh and formalin-fixed brain tissue specimens. *J Virol Methods*. 2001;95:145–151.

22. WHO Rabies Feact Sheet No. 99. *http://www.who.int/mediacenter/factsheets/fs099/en/*. September 2010.

23. WHO Rabies Bulletin. *http://www.who-rabies-bulletin.org/About_Rabies/Transmission_Pathogenesis.aspx.*

24. Willoughby RE, Tieves KS, Hoffman GM, et al. Brief report - Survival after treatment of rabies with induction of coma. *New Engl J Med.* 2005;352(24): 2508-2514.

CASE IV: VS11 (JPC 4003034).

Signalment: 8-year-old male Rhesus macaque (*Macaca mulatta*).

History: Clinical History: This monkey developed intermittent antibiotic unresponsive hematuria, and ultrasonography showed a rounded, misshapen right kidney with a loss of architecture in the renal pelvis. ACT scan revealed a mass occupying the caudal 2/3 of the kidney and proximal ureter, consistent with a neoplasm. Unilateral nephrectomy was performed and the specimen was submitted as a biopsy.

Experimental History: This monkey received a single 7.55 Gy dose of whole-body irradiation at 3 years of age.

Gross Pathology: The entire right kidney, with attached capsule and 4.5cm segment of ureter was submitted in 10% neutral buffered formalin. An irregularly-shaped, 3.8x3x2cm firm, tan mass with scattered hemorrhages on cut surface replaced the caudal two-thirds of the kidney. A 5mm diameter x 4mm nodule protruded from the surface, underneath the capsule. The renal capsule was easily removed except for a 3mm diameter area, where it was firmly attached. The ureter measured 5mm in diameter where it exited the renal pelvis and was of normal diameter at the distal end of the specimen.

Laboratory Results:
Blood Chemistry:
BUN 13 mg/dL (13-27 mg/dL)
Creatinine 1.5 mg/dL (0.8-1.5 mg/dL)

Urinalysis:
Specific Gravity 1.007
Blood 80 cells/mL
Protein: 2+ (100 mg/dL)
Bacteria: none
WBC: 6-10/HPF
RBC: 30-50/HPF

Contributor's Histopathologic Description: An infiltrative neoplasm, irregularly dissected by tracts of mature collagenous connective tissue, distends the proximal ureteral lumen, effaces the adjacent renal parenchyma (more prominent in some sections) and compresses normal renal cortical tissue. The neoplasm is composed of fronds of collagenous connective tissue lined by single to multiple layers of epithelial cells which have oval, 15x10 micron nuclei with finely stippled basophilic chromatin and single nucleoli. The cytoplasm is eosinophilic, sometimes with clear vacuoles, and cell borders are indistinct. Mitotic figures are rare, with up to only 1 per five 40X fields. Small accumulations of granular to clumped deeply basophilic material (mineral) are scattered throughout. Rafts of neoplastic cells are present in blood vessels at the margins in some sections. Lymphoplasmacytic infiltrates are scattered throughout the neoplasm. Immunohistochemical staining for uroplakin III is negative. An internal positive control is provided by normal urothelium of the ureter. The parenchyma adjacent to the renal cortex is atrophied, with loss of tubules and glomeruli, and interstitial lymphoplasmacytic inflammation. Glomeruli are often small, occasionally segmented and some are surrounded by variably thick fibrous connective tissue. Cystic structures, lined by flattened epithelium, are filled with pale pink amorphous material. Occasional renal tubular epithelial cells have undergone karyolysis, and others have abundant eosinophilic cytoplasm containing brown granular pigment. Sporadically, epithelial cells are present in the tubular lumina. Interstitial fibrous connective tissue is prominent in areas where tubules are less numerous.

4-1, 4-2. Renal papillary carcinoma, Rhesus macaque. An irregular, firm, tan mass with scattered hemorrhages replaces the caudal kidney. Photographs courtesy of Wake Forest University Health Sciences, Animal Resources Program, http://www.wfubmc.edu/schoolofmedicine./

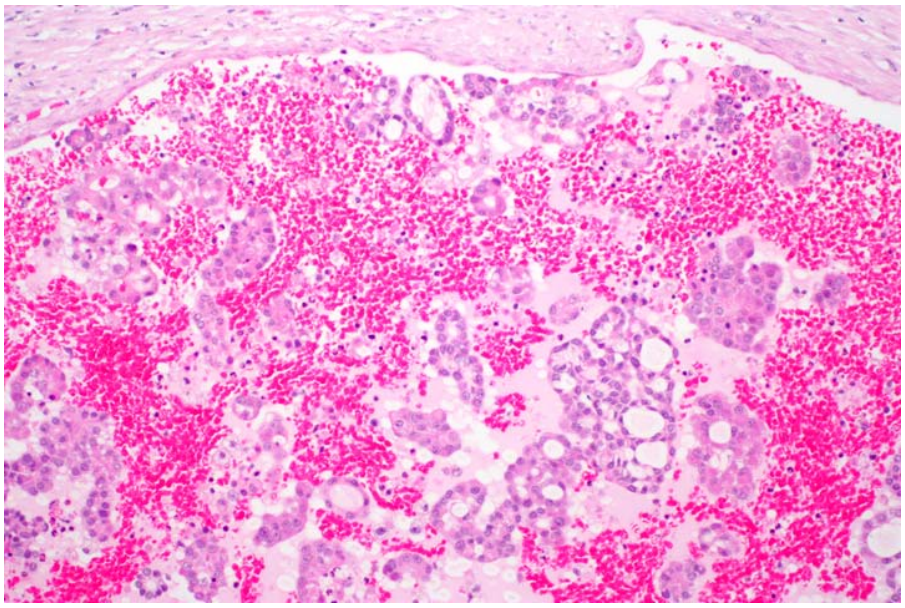

4-3. Renal papillary carcinoma, Rhesus macaque. A renal blood vessel contains numerous rafts of neoplastic epithelial cells. Photograph courtesy of Wake Forest University Health Sciences, Animal Resources Program, http://www.wfubmc.edu/schoolofmedicine.

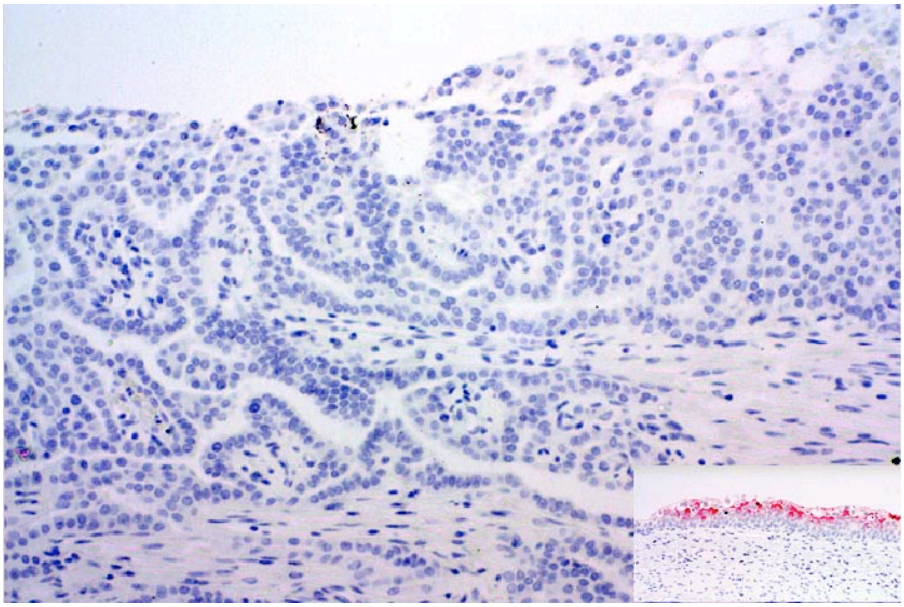

4-4. Renal papillary carcinoma, Rhesus macaque. Neoplastic cells are negative for uroplakin III. An internal positive control is provided by normal urothelium of the ureter (inset). Photograph courtesy of Wake Forest University Health Sciences, Animal Resources Program, http://www.wfubmc.edu/schoolofmedicine

Contributor's Morphologic Diagnosis: 1. Papillary carcinoma, kidney and ureter with vascular invasion. 2. Glomerulonephropathy, diffuse, subacute to chronic, mild, with interstitial fibrosis, glomerular atrophy, tubular loss and cyst formation.

Contributor's Comment: This submission provides a good example of what are considered to be radiation-induced lesions in the kidney. The kidney is one of the most radiosensitive organs[16] and is prone to secondary malignancies[2,3,5,13], as well as degenerative changes leading to renal dysfunction[6,16] following irradiation. Fifty percent of rhesus macaques that received whole body irradiation developed malignant neoplasms, 80% of which were renal carcinomas.[2,5] Humans undergoing radiation treatment for neoplasia have increased risk for developing renal neoplasms.[13] Although primary renal tumors are rare, greater than 65% in dogs[11], and more than 85% in humans are carcinomas[1], with the main differential diagnosis being urothelial (transitional cell) carcinomas. Primary tumors of the ureter are rare and often occur concurrently with neoplasms of the renal pelvis or urinary bladder[1,4,11]. Abnormalities were not detected in the urinary bladder during the CT scan or visible during the nephrectomy surgery in this animal. This combined with negative uroplakin III staining makes an urothelial carcinoma less likely. However, urothelial carcinomas in humans may not stain for uroplakin III, particularly those with invasive or metastatic behaviors.[15] In humans, renal carcinomas are further characterized based on morphology.[14,15]

Although mild, the nephropathy is likely secondary to irradiation. Irradiation-induced nephropathy is a significant long-term complication in rhesus macaques and humans.[6,16] The changes in rhesus macaques, 6-8 years after a single dose of irradiation (7.2-8.5 Gy) include glomerulopathy, ectatic capillaries, glomerulosclerosis, and periglomerular fibrosis.[16] About 25% of human patients receiving comparable doses of radiation (7-7.5 Gy) develop renal dysfunction.[6]

JPC Diagnosis: 1. Kidney: Renal papillary carcinoma.
2. Kidney: Glomerulonephropathy characterized by interstitial fibrosis, tubular degeneration and regeneration, proteinosis, and lymphoplasmacytic interstitial nephritis.

Conference Comment: Primary renal neoplasms are relatively uncommon in animals and humans; however, renal adenocarcinoma is the most common primary neoplasm affecting the kidneys of dogs, cats, cattle and horses, and occurrence is sporadic in sheep and pigs. The origin is most likely proximal convoluted tubular epithelial cells. Small, well-circumscribed neoplasms with no evidence of capsular invasion or metastasis are generally considered to be benign. Well-differentiated carcinomas may be very difficult to differentiate from adenomas, with cellular atypia, a high mitotic rate, local or vascular invasion, necrosis, and size (>2 cm) used as criteria for malignancy. Renal adenocarcinomas are reported more often in middle-aged male dogs with no breed predilection. In dogs, 50-60% of renal epithelial neoplasms metastasize, compared with 5% in the cow and 70% in the horse.[9,10,12]

Some renal adenocarcinomas in dogs have elevated expression of COX-2, suggesting COX-2 mediated prostaglandins may play a role in the modulation of neoplastic cell growth.[7] A notable paraneoplastic syndrome and common clinical pathology finding is secondary absolute polycythemia due to secretion of erythropoietin or erythropoietin-like peptide by the tumor.[12]

Grossly, renal adenocarcinomas appear as large (>2 cm), spherical to ovoid, well-demarcated masses that are usually unilateral and occupy one pole of the kidney. They usually arise in the cortex and compress adjacent renal parenchyma, and may occupy 80% or more of the kidney. They often present as light yellow to gray lobulated masses with areas of necrosis and hemorrhage. Common sites of metastasis are the lungs, regional lymph nodes, liver, and occasionally the skin. Invasion into the renal vein and posterior vena cava may can occur. Multiple and bilateral renal neoplasms, without evidence of metastasis to other organs, are considered to be of multicentric origin.[9,10,12]

Histologically, these neoplasms are often described by the predominant histologic type and further sub-classified by the predominant cytologic type, although there is no prognostic significance to histologic or cytologic type. Histologic types include papillary, tubular, and solid, and a mixture of all three patterns may be present in any one tumor. The tubular variant is most common in domestic animals, and often, the solid variant is usually poorly differentiated. There are several cytologic types, such as chromophobic, eosinophilic, and clear cell (with vacuolated cytoplasm).[9,10,12] The clear cell variant is more often seen in laboratory animals and they tend to be solid rather than tubular. Electron micrographs, may demonstrate abundant monoparticulate glycogen often within phago-lysosomes and few mitochondria or endoplasmic reticulum.[10] Uromodulin (Tamm-Horsfall glycoprotein), a unique protein produced by the kidney, is useful as an immunohistochemical marker.[9]

Differential diagnoses include oncocytoma, nephroblastoma and transitional cell carcinoma.[9,10,12]

Contributor: Wake Forest University School of Medicine
Department of Pathology/Comparative Medicine
NRC Building, E Floor
Medical Center Boulevard
Winston Salem, NC 27157-1040
http://www.wfubmc.edu/schoolOfMedicine/schoolOfMedicine_default.aspx?id=26651

References:
1. Alpers CE. The Kidney. In: Robbins and Cotran Pathologic Basis of Diseases. 8th ed. Philadelphia, PA: Saunders Elsevier; 2010:905-967.
2. Broerse JJ, Bartstra RW, van Bekkum DW, et al The carcinogenic risk of high dose total body irradiation in non-human primates. *Radiotherapy and Oncology*. 2000;54:247-253.
3. Broerse JJ, van Bekkum DW, Zurcher C. Radiation carcinogenesis in experimental animals. *Experientia*. 1989;45:60-69.
4. Epstein JI. The Lower Urinary Tract and Male Genital System. In: *Robbins and Cotran Pathologic Basis of Diseases*. 8th ed. Philadelphia, PA: Saunders Elsevier; 2010:971-1004.
5. Hollander CF, Zurcher C, Broerse JJ. Tumorigenesis in High-Dose Total Body Irradiated Rhesus Monkeys – A Life Span Study. *Toxicologic Pathol*. 2003;31(2): 209-213.
6. Kal HB, van Kempen-Harteveld ML. Renal Dysfunction after Total Body Irradiation: Dose-effect Relationship. *Int J Radiation Oncology Biol Phys*. 2006;64(4):1228-1232.
7. Khan KNM, Stanfield KM, Trajkovic D, et al. Expression of cyclooxygenase-2 in canine renal cell carcinomas. *Vet Pathol*. 2001;38:116-119.
8. Lingaas F, et al. A mutation in the canine BHD gene is associated with hereditary multifocal renal cystadenocarcinoma and nodular dermatofibrosis in the German shepherd dog. *Hum Mol Genet.* 2003;12(23): 3043-53.
9. Maxie MG, Newman SJ. Urinary system. In: Maxie MG, ed. *Jubb, Kennedy, and Palmer's Pathology of Domestic Animals*. 5th ed. vol 2. New York, NY: Elsevier Limited; 2007:498-501.

10. Meuten D. Tumors of the urinary system. In: Meuten D, ed. *Tumors in Domestic Animals*. 4th ed. Ames, IA: Iowa State Press; 2002: 509-518.
11. Meuton, DJ. Tumors of the urinary system. In: Meuten DJ, ed. *Tumors of Domestic Animals*. 4th ed. Ames, IA: Iowa State Press; 2002:380-392.
12. Newman SJ, Confer AW, Panciera RJ. Urinary system. In: McGavin MD, Zachary JF, eds. *Pathologic Basis of Veterinary Disease*. 4th ed. St. Louis, MO: Mosby; 2007:640-1.
13. Suit H, Goldberg S, Niemierko A, et al. Secondary carcinogenesis in patients treated with radiation: a review of data on radiation-induced cancers in human, non-human primate, canine and rodent subjects. *Radiat Res*. 2007;167:12-42.
14.Tickoo SK, Reuter VE. Differential diagnosis of renal tumors with papillary architecture. *Adv Anat Pathol.* 2011;18:120-132.
15.Truong LD, Shen SS. Immunohistochemical diagnosis of renal neoplasms. *Arch Pathol Lab Med.* 2011;135:92-109.
16. van Kleff EM, Zurcher C, Oussoren YG, et al. Long-term effects of total-body irradiation on the kidney of Rhesus monkeys. *Int J Radiat Biol*. 2000;76 (5):641-648.

Joint Pathology Center
Veterinary Pathology Services

WEDNESDAY SLIDE CONFERENCE 2011-2012

Conference 13

18 January 2012

CASE I: E1726/10 (JPC 3164890).

Signalment: 13-year-old male neutered domestic shorthair cat (*Felis catus*).

History: The animal was presented to the veterinarian with a mass of about 1.5 cm in diameter in the skin at the left lateral neck. The owner noticed the mass one month prior to presentation. Pruritus had not been noticed and the cat did not show additional tumors or other diseases. Metastases were not detected and following resection of the mass no relapse has occurred within two months.

Gross Pathology: The tissue sample submitted for histopathological examination had an extension of 2.5 x 1.5 x 1.0 cm consisting of skin and subcutis. In the center there was a round, superficially rough area of approximately 1.0 cm in diameter with alopecia. The affected skin displayed a slightly thickened, irregular epidermis.

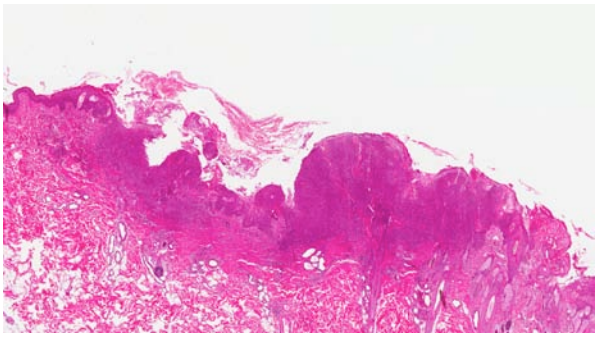

1-1. Haired skin, cat. The epidermis is focally and markedly thickened by a poorly demarcated, moderately cellular, unencapsulated, verrucous, infiltrative neoplasm. (HE 4X)

Contributor's Histopathologic Description: Haired skin: Multifocally, there are areas of mild to severe thickening of epidermis and follicular infundibular epithelium. In most areas, the basement membrane is intact with neoplastic cells confined to the epidermis. Multifocally overlying affected areas, there is a mild parakeratotic hyperkeratosis. In the unaffected areas there is a mild orthokeratotic hyperkeratosis.

In the thickened epithelial areas the normal germinal layer of the epidermis is replaced by multiple layers of neoplastic keratinocytes. The stratum granulosum and stratum corneum are mostly unaffected. Neoplastic cells have an increased size (about 30-50 µm in diameter), a polygonal shape and a small to moderate amount of homogenous to finely granular eosinophilic cytoplasm. Distinct cell borders and prominent intercellular bridging are present. Nuclei are large, round to oval, centrally placed, and vesicular with finely stippled chromatin and one to two prominent round magenta nucleoli. There is a mild to moderate anisocytosis and anisokaryosis. The number of mitotic figures range from 0 to 4 per high power field. Multifocally, dark basophilic round structures are present distributed within the neoplastic cells, interpreted as apoptotic bodies. In some areas the

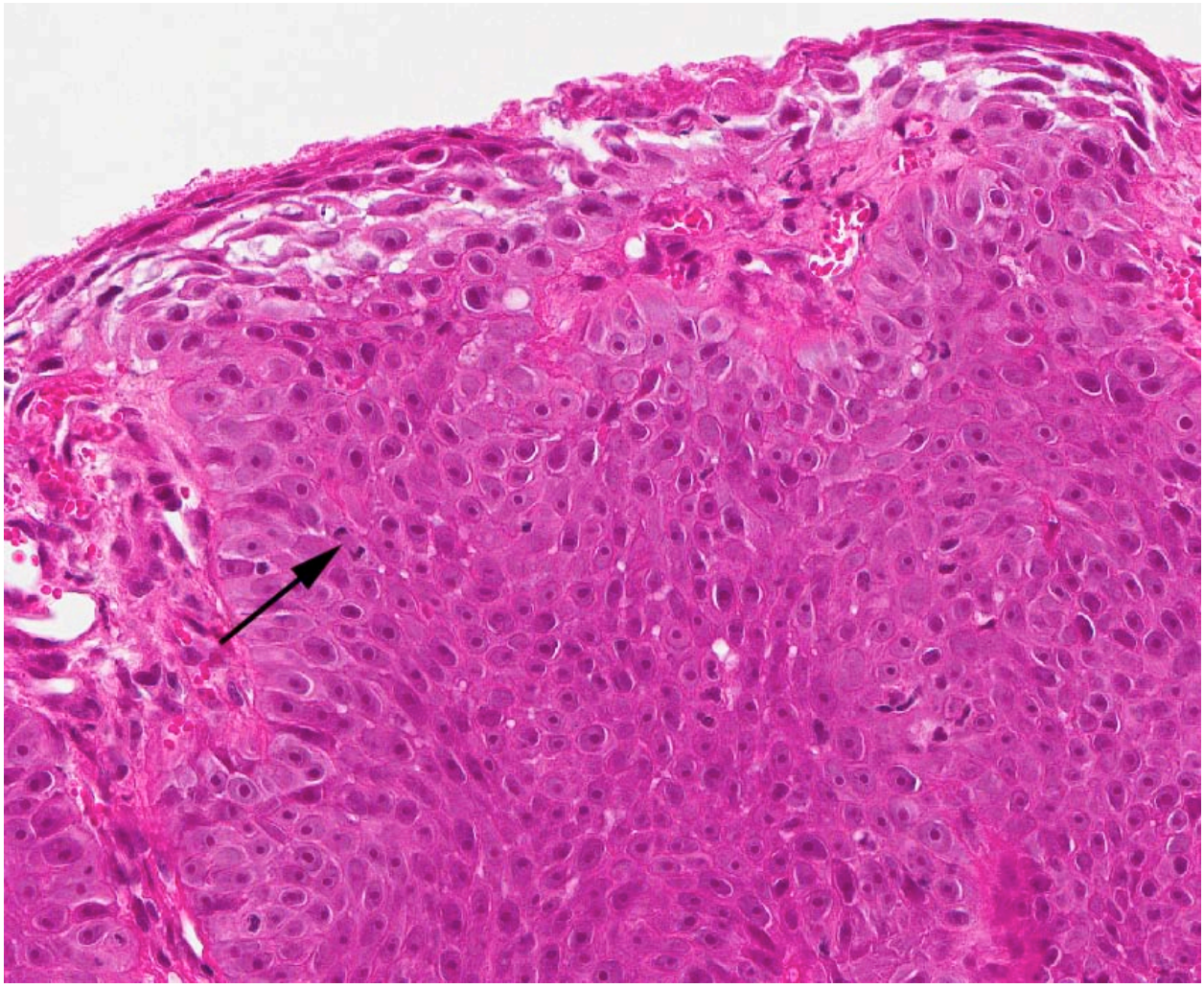

1-2. Haired skin, cat. Bowens disease characterized by markedly dysplastic keratinocytes without apparent maturation at all levels of the epidermis, as well as a mitotic figure (arrow). (HE 240X)

above described neoplastic cells penetrate the basement membrane and invade the underlying dermis, forming small nests or cords. There is multifocal erosion and focal ulceration of the epidermis, associated with hemorrhage and mild to moderate infiltration of neutrophils. In the dermis a mild, perivascular infiltration of neutrophils, lymphocytes and macrophages is present and few mast cells are observed. Multifocally there is moderate fibrosis of the dermis. No p53-positive tumor cells were detected by immunohistochemistry using a monoclonal anti-p53-antibody.

Contributor's Morphologic Diagnosis: Skin, squamous cell carcinoma in situ and focal transition to squamous cell carcinoma with dermatitis, suppurative and erosive to ulcerative, moderate, acute, diffuse.

Contributor's Comment: The morphologic findings are compatible with a multicentric squamous cell carcinoma (MSCCa) in situ, which shows transition to squamous cell carcinoma. Multicentric squamous cell carcinoma in situ, also referred to as Bowenoid in situ carcinoma (BISC) or Bowen-like disease, is an uncommon premalignant lesion in middle-aged to old cats and rarely reported in dogs.[6,8,17]

Grossly, irregular, slightly elevated to heavily-crusted plaques and verrucous or papillary lesions up to 5.0 cm in diameter are found on haired, pigmented or non-pigmented skin at any site of the body. Usually, multiple lesions occur, but also solitary MSCCa in situ are seen infrequently.[1,6,8] Lesions are reported to be chronic, not painful, and only mild pruritus is noted.[1] There is neither a casual relationship to sunlight exposure nor a breed or sex predilection.[6,7,8]

Histologically, the neoplastic keratinocytes are confined to the epidermal and follicular infundibular epithelium with the basement membrane remaining intact.[1,6] Some authors differentiate between an irregular nonhyperkeratotic and a verrucous

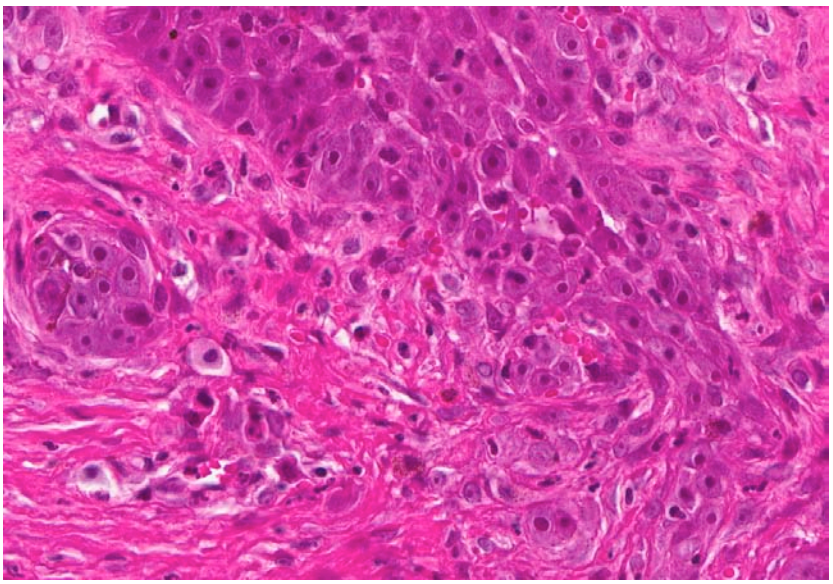

1-3. Haired skin, cat. Multifocally, at the deep margin, neoplastic keratinocytes breach the basement membrane, infiltrating the subjacent dermis as individual and small groups of cells.

hyperkeratotic type depending on the character and degree of epidermal thickening and hyperkeratosis.[1] According to this classification, the present case would belong to the non-hyperkeratotic type due to severe acanthosis of the epidermis and follicular infundibular epithelium with a mildly undulating surface and mild orthokeratotic hyperkeratosis, not showing verrucous surface contours, epithelial spires and pit-like invaginations filled with keratin as it is described for the verrucous hyperkeratotic type.[1]

Several studies suspect that papillomavirus infection may be associated with feline MSCCa in situ. In two studies, papillomavirus-antigen was detected in 11% and 48% of MSCCa in situ, respectively, using immunohistochemistry (IHC).[2,13] Additionally, it has been hypothesized that feline viral plaque, in which a high proportion of papillomavirus-antigen was detected by immunostaining, could be a precursor lesion of MSCCa in situ.[16]

One study found 11 out of 18 cases positive for papillomavirus L1 gene in PCR-analysis, suggesting that this method may be more sensitive than IHC.[11] The authors admit that the failure to demonstrate papillomaviral DNA in every lesion may suggest that MSCCa in situ is not caused by papillomavirus infection. However, they also state that the 7 negative cases may have been previously but transiently infected with papillomavirus, which may have caused cellular transformation.[11] Furthermore, a close relationship to human papillomaviruses was discovered, which led to the hypothesis of interspecies virus transmission.[11] Subsequently, multiple papillomaviruses (namely *Felis domesticus*-papillomavirus type 1, type 2 and a novel papillomavirus) from a swab of feline viral plaques and non-lesional skin were amplified, suggesting that papillomavirus can infect the epidermis without causing appreciable disease as well.[12]

In one report, infestation with *Demodex cati*, a normal resident of the skin in cats, was found in lesional sites of MSCCa in situ in 4 cats. Local cutaneous immunodeficiency due to epithelial dysplasia has been hypothesized as a predisposing factor for focal multiplication of mites.[9] In some cases, it is proposed that immunosuppression due to FIV or FELV infection may be a possible predisposition.[9,12]

For differential diagnosis, difficulty in distinguishing between the two basic types of squamous cell carcinoma in situ in cats have to be considered: MSCCa in situ and actinic keratosis (also named solar keratosis).[2] Actinic keratosis usually occurs as solitary lesion in white animals or in locations of unpigmented skin (like pinna, planum nasale, dorsal muzzle and eyelids).[2] Its histological appearance is less hyperplastic and hair follicles are less deeply affected than in MSCCa in situ.[2] Nevertheless, an accurate classification by clinical and histological findings is sometimes difficult.[2,8] Therefore, immunohistochemical detection of papillomavirus-antigen, which could be indicative of MSCCa in situ, and of p53-protein, which is frequently accumulated after UV-induced mutation of the p53 gene in actinic keratosis could be performed to arrive at the diagnosis.[2]

Similar to the present case, 17% to 25% of feline cases MSCCa in situ become locally invasive through the basement membrane and then have to be classified as squamous cell carcinomas, the most common malignant neoplasm of the feline skin.[1,7,8] These lesions, belonging to the well differentiated squamous cell carcinomas, occasionally still show "bowenoid" features like dorsoventrally elongated nuclei, that are tilted in one direction ("windblown" pattern) or bizarre multilobulated nuclei with smudgy chromatin.[8]

It has to be kept in mind that the described squamous cell carcinoma may also have developed due to UV-light induced mutations of tumor suppressor genes, unrelated to the diagnosed MSCCa in situ.[8]

Other skin tumors should be considered as additional differential diagnoses. Basal cell carcinomas and basosquamous carcinomas, which arise from basal

cells, are usually located in the dermis. However, they can be associated with the epidermis and are defined by other characteristics: in basal cell carcinomas, extensive proliferation of stromal fibroblasts and horizontal orientation of the tumor silhouette are frequently found. The appearance of bimorphic histologic features, showing basaloid cells peripherally and centrally abrupt keratinisation is indicative for basosquamous carcinomas.[7,8]

JPC Diagnosis: 1. Haired skin: Squamous cell carcinoma.
2. Haired skin: Bowenoid in situ carcinoma.

Conference Comment: Bowenoid in situ carcinoma (BISC) differ from solar-induced squamous cell carcinoma (SCC) in that they can occur in darkly pigmented skin or non-sun-exposed haired skin, extend along the outer root sheath and follow the hair follicles, and lack evidence of solar elastosis, such as linear bands of degenerated basophilic elastin accumulation arranged parallel to the skin surface. BISC is frequently associated with papillomavirus. With time, these slow growing tumors may break through the basement membrane and are then classified as a traditional SCC, as is seen in the present case. Occasionally, koilocytes and other cytopathic effects of the papillomavirus can still be observed, but usually other evidence of papillomavirus infection, such as immunohistochemical positivity, is lacking.[6,10]

SCC is typically locally invasive and slow to metastasize; however, SCCs arising from internal sites such as the tonsil, stomach, and urinary bladder are more prone to metastasize, and metastasis is often to the lungs and regional lymph nodes. In cattle, SCC is common on eyelids, conjunctiva, and the vulva; in horses, it is common on the penis, prepuce, eyelid and conjunctiva, and is also found in the nonglandular stomach; in rodents and pigs, SCC is also common in the nonglandular stomach; in sheep and goats, the vulva in recently sheared sheep is a common site as well as the pinnae; in rabbits it is found in subungual tissues, the eyelid and extremities; and SCC can also occur at brand sites (especially freeze brands) in livestock.[3,4,5,14,15]

Contributor: University of Veterinary Medicine, Hannover
Department of Pathology
Buenteweg 17D-30559
Hannover, Germany
http://www.tiho-hannover.de/kliniken-institute/institute/institut-fuer-pathologie/

References:

1. Baer KE, Helton K. Multicentric squamous cell carcinomas in situ resembling Bowen`s disease in cats. *Vet Pathol.*1993;30:535-543.
2. Favrot C, Welle M, Heimann M, et al. Clinical, histologic and immunohistochemical analyses of feline squamous cell carcinoma in situ. *Vet Pathol*. 2009;46:25-33.
3. Foster RA. Female reproductive system and mammary gland. In: McGavin MD, Zachary JF, eds. *Pathologic Basis of Veterinary Disease*. 4th ed. vol. 1. St. Louis, MO: Elsevier; 2012:1078, 1118.
4. Foster RA. Male reproductive system. In: McGavin MD, Zachary JF, eds. *Pathologic Basis of Veterinary Disease*. 4th ed. vol. 1. St. Louis, MO: Elsevier; 2012:1149, 1178.
5. Gelberg HB. Alimentary system and the peritoneum, omentum, mesentery, and peritoneal cavity. In: McGavin MD, Zachary JF, eds. *Pathologic Basis of Veterinary Disease*. 4th ed. vol. 1. St. Louis, MO: Elsevier; 2012:328-9, 354.
6. Ginn PE, Mansell JEKL, Rakich PM. Skin and appendages. In: Maxie MG, ed. *Jubb, Kennedy, and Palmer´s Pathology of Domestic Animals.* 5th ed. Edinburgh, UK: Elsevier; 2007:752-753.
7. Goldschmidt MH, Dunstan RW, Stannard AA, et al. *Histological Classification of Epithelial and Melanocytic Tumors of the Skin in Domestic Animals*. Washington, DC: Armed Forces Institute of Pathology; 1998:18-21
8. Gross TL, Ihrke PJ, Walder EJ, et al. Skin Diseases of the Dog and Cat: Clinical and Histopathological Diagnosis, 2nd ed. Oxford, UK: Blackwell Science; 2005: 148-151, 575-581, 583-584, 591-594, 597-598.
9. Guaguère E, Olivry T, Deleverdier-Poujade A, et al. *Demodex cati* infestion in association with feline cutaneous squamous cell carcinoma in situ: a report of five cases. *Vet Dermatol.* 1999;10:61-67.
10. Hargis AM, Ginn PE. The integument. In: McGavin MD, Zachary JF, eds. *Pathologic Basis of Veterinary Disease*. 4th ed. vol. 1. St. Louis, MO: Elsevier; 2012:1013-27.
11. Munday JS, Kiupel M, French AF, et al. Detection of papillomaviral sequences in feline Bowenoid in situ carcinoma using consensus primers. *Vet Dermatol.* 2007;18:241-245.
12. Munday JS, Willis KA, Kiupel M, et al. Amplification of three different papillomaviral DNA-Sequences from a cat with viral plaques. *Vet Dermatol.* 2008;19:400-404.
13. Munday JS, Kiupel M. Papillomavirus-associated cutaneous neoplasia in mammals. *Vet Pathol.* 2010; 47:254-264.
14. Newman SJ. The urinary system. In: McGavin MD, Zachary JF, eds. *Pathologic Basis of Veterinary Disease*. 4th ed. vol. 1. St. Louis, MO: Elsevier; 2012:648.

15. Njaa BL, Wilcock BP. The ear and eye. In: McGavin MD, Zachary JF, eds. *Pathologic Basis of Veterinary Disease*. 4th ed. vol. 1. St. Louis, MO: Elsevier; 2012:1237-8.
16. Wilhelm S, Degorce-Rubiales F, Godson Dale, Favrot C. Clinical, histological and immunohistochemical study of feline viral plaques and bowenoid in situ carcinomas. *Vet Dermatol.* 2006;17: 424-431.
17. Yager JA, Wilcock BP. 16 Solid epidermal tumors (papilloma, cutaneous horn, keratoses, squamous cell carcinoma). In: *Color Atlas and Text of Surgical Pathology of the Dog and Cat*. London, UK: Wolfe Publishing; 1994:253-254

CASE II: B19851 (JPC 4002876).

Signalment: A four-year-old male cat (*Felis vulgaris)*.

History: A four-year-old male cat was presented with thickening and erythema of the inner surfaces of the left ear. The ear was painful and curled. The outer surfaces were unaffected. The left pinna was partially removed and submitted for histopathology.

Gross Pathology: Besides the thickened and curled left ear with erythema, there were no other grossly visible pathologic findings.

Contributor's Histopathologic Description: The lesion is centered around the pinnal cartilage. It consists of an inflammatory infiltration of mainly neutrophils and moderate numbers of macrophages, multinucleated giant cells (foreign body type), lymphocytes and plasma cells. Several neutrophils are invading the pinnal cartilage. The latter is irregularly lined, angularly deformed (wrinkled and curled over 180 degrees) and possesses a loss of basophilia (cartilage degeneration). Collagenous tissue surrounds the pinnal cartilage (perichondrial fibrosis). The dermis is edematous and diffusely infiltrated by neutrophils, lymphocytes and plasma cells. Perivascular accumulations of mononuclear and polymorphonuclear cells are present.

Contributor's Morphologic Diagnosis: Pinna: diffuse, chronic, suppurative to granulomatous chondritis with degeneration and deformation of the pinnal cartilage.

Contributor's Comment: Feline relapsing polychondritis is a very rare disease and only a few reports of cats with the disease are found in the literature.[2,3] There is no sex predilection for the disease, but predominantly young to middle aged cats are affected.[3] In humans, the disease is believed to be an immune-mediated disease of type II collagen, which is restricted to cartilage.[2,3]

Sometimes the disease is also called auricular chondritis, because the main gross lesions are ear swelling and discoloration, erythema, pain and curling of one or both ears. However, two case reports describe involvement of additional cartilaginous tissues as reported in people.[1,3]

Histologically, there is degeneration, loss of basophilic staining and necrosis of the ear cartilage. There is also infiltration of mononuclear and polymorphonuclear cells, and perichondrial and perivascular fibrocyte and capillary endothelial cell proliferation. The histological lesions observed in this case are similar to those reported in the cases described in the literature.

JPC Diagnosis: Ear, pinna: Cellulitis, chronic-active, diffuse, moderate with mild neutrophilic chondritis, cartilage degeneration, and granulation tissue.

Conference Comment: Conference participants discussed the comparative pathology of feline relapsing polychondritis and auricular chondritis of laboratory rodents, to which some strains of mice, and aged Sprague-Dawley, Wistar, and fawn-hooded rats are predisposed.[4]

In rats, trauma from cagemates or metal ear tags is suspected as the inciting cause of auricular chondritis, but the disease frequently occurs without history or evidence of trauma. Unlike the feline disease,

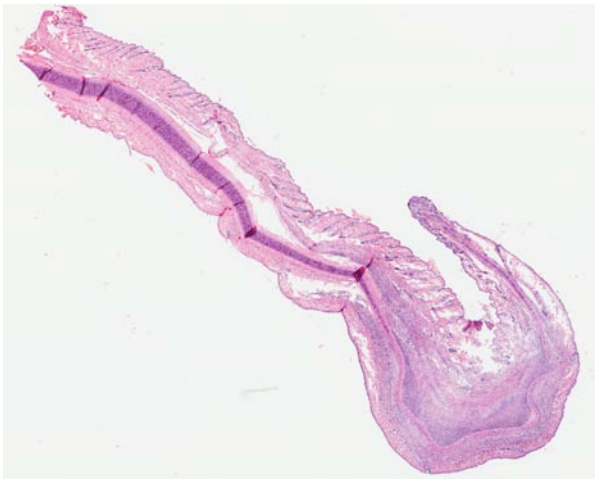

2-1. Ear pinna, cat. There is focally extensive inflammation centered on the pinnal cartilage, resulting in focal thickening and folding at the ear tip. (HE 4X)

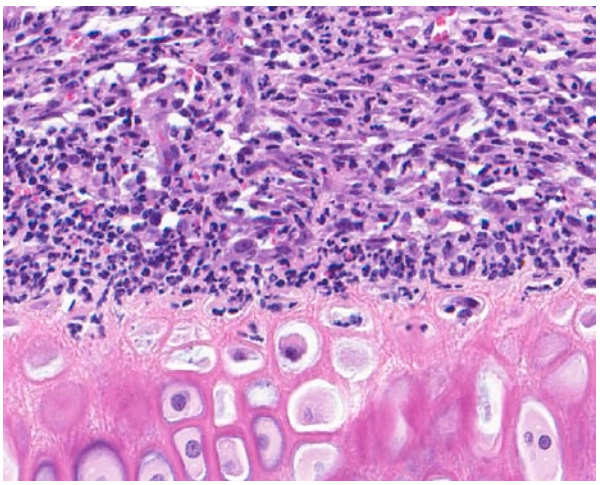

2-2. Ear pinna, cat. Area of granulation tissue with marked neutrophilic inflammation adjacent to the pinnal cartilage. Small numbers of neutrophils have breached the perichondrium and infiltrated the cartilage. (HE 200X)

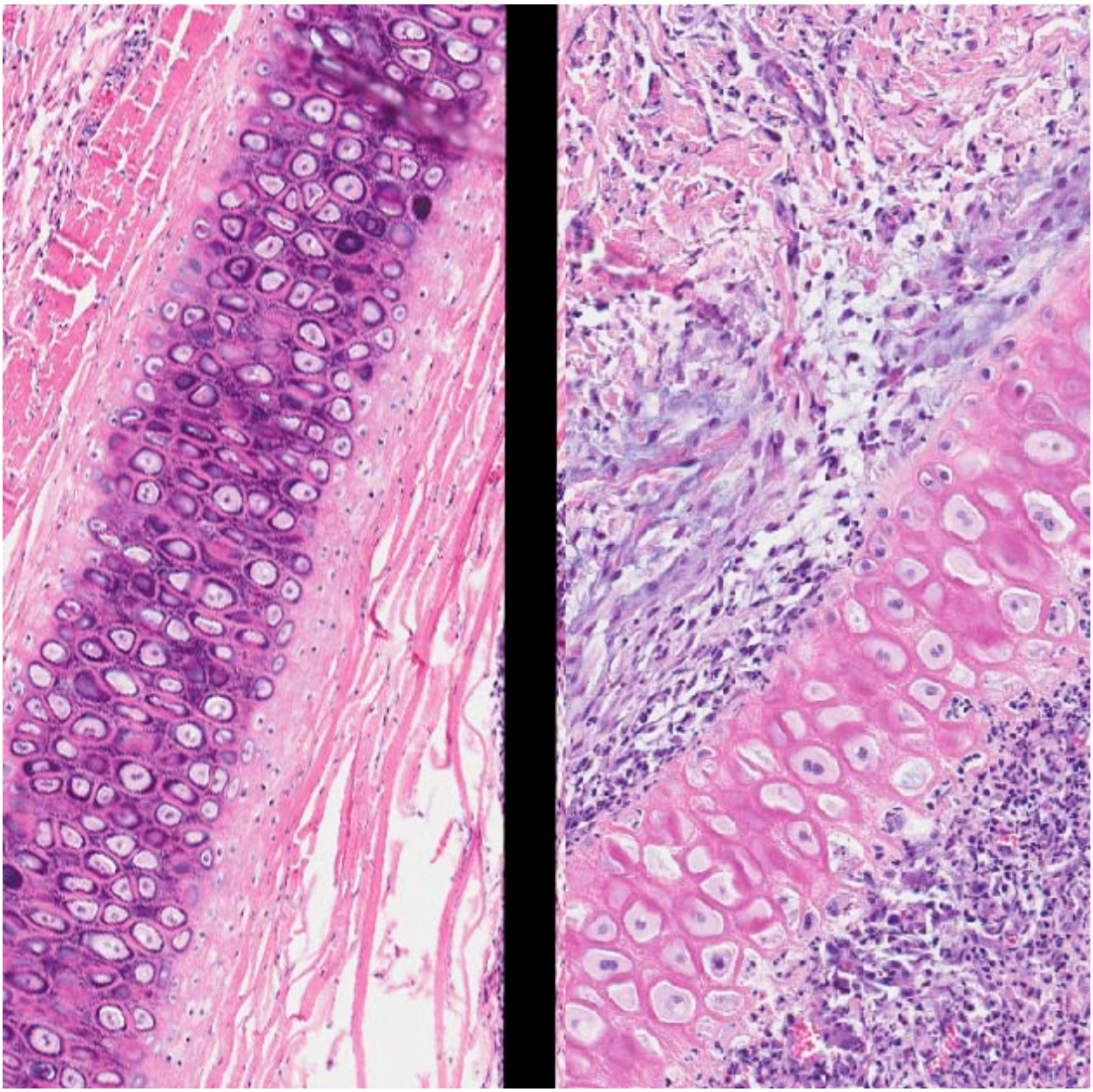

2-3. Ear pinna, cat. Mild degeneration of cartilage (right) in the area of the inflammation as evidenced by a pink discoloration due to a decreased amount of glycosaminoglycans in the matrix. (HE 120X, 140X)

auricular chondritis in rats is always bilateral, even when the metal ear tag is present in only one ear, and increases in incidence with age.[5] The disease presents grossly as firm, multinodular to diffuse thickening of pinnae, and bilateral lesions extend peripherally from the base of the pinnae. Occasionally, pinnae are uniformly thickened rather than having nodular lesions. There is degeneration and lysis of the auricular cartilage plate with granulomatous inflammation and proliferative immature cartilaginous nodules and fibrosis, and osseous metaplasia is characteristic in advanced lesions.[5]

Auricular chondritis in rats has been proposed as a model for relapsing polychondritis in humans, which involves several cartilage-containing tissues, including the ear.[5] In humans, relapsing polychondritis is associated with auricular chondritis, inflamed cartilage in other sites, and antibodies to type II collagen, IgG and C3 complement. Antibodies to type II collagen have not been demonstrated in the spontaneous auricular chondropathy of rats, and unlike relapsing polychondritis in humans, only the auricular cartilage is involved.[4,5]

In mice, it is speculated that metal ions from ear tags, such as copper and iron, incite an autoimmune process via activation of matrix metalloproteinases. These metal ions supply reactive oxygen species that induce inflammation and fibrosis, and oxidation of cartilage collagen renders the collagen fibrils more brittle and prone to mechanical fatigue. Tagged ears have increased amounts of metallothionein (MT-I and MT-II) and increased expression of Th1 cytokines, including interferon-γ, tumor necrosis factor-α, and interleukin-2; it is postulated that the lesion represents a delayed-type allergic contact dermatitis in response to the metal ions.[4] There are two proposed mechanisms for the fibrosis and osseous metaplasia seen in advanced lesions. In the first, cartilage degeneration, characterized by chondrolysis and splitting of the pinnal cartilage plate leads to perichondrial fibrous proliferation, which differentiates into fibroadipose tissue and progresses to fibrochondrous and/or osseochondrous tissue. In the second proposed mechanism, there is focal granulomatous inflammation without chondrolysis, and fibroblasts proliferate within the granulomatous inflammation and then differentiate into fibrochondrous tissue with subsequent chondrous and osseous differentiation.[5]

Contributor: University of Ghent
Laboratory of Veterinary Pathology
Faculty of Veterinary Medicine UGent
Salisburylaan 133
9820 Merelbeke
Belgium

References:

1. Baba T, Shimizu, A, Ohmuro T, et al. Auricular chondritis associated with systemic joint and cartilage inflammation in a cat. *J. Vet. Med. Sci*. 2009;1:79-82.
2. Delmage DA, Kelly DF. Auricular chondritis in a cat. *Journal of Small Animal Practice*. 2001;42:499-501.
3. Gerber B, Crottaz M, von Tscharner C, et al. Feline relapsing polychondritis: two cases and a review of literature. *Journal of Feline Medicine and Surgery*. 2002;4:189-194.
4. Kitagaki M, Hirota M. Auricular chondritis caused by metal ear tagging in C57BL/6 mice. *Vet Pathol.* 2007;44:458-466.
5. Kitagaki M, Suwa T, Yanagi M, et al. Auricular chondritis in young ear-tagged Crj:CD (SD)IGS rats. *Lab Anim Sci. 2003;*37(3): 249-253.

CASE III: S164/09 (JPC 3134629).

Signalment: 14-day-old male kitten Siberian cat (*Felis catus*).

History: This cat is one of two littermates which were both born with fully developed hair coat. Beginning on day 11, both kittens lost most of their fur of the trunk with only a few hairs remaining on the head, the feet and tail. Both kittens died unexpectedly after unspecific clinical symptoms and one was submitted for pathological examination.

Gross Pathology: At necropsy the kitten had alopecia affecting mainly the trunk. The skin appeared normal in the alopecic and haired areas. The liver was slightly enlarged, friable and of smudgy yellowish color. All other organs had signs of congestion.

Contributor's Histopathologic Description: Histologically, the principal lesion is an abnormal structure of hair shafts. Hair bulbs including the dermal papillae are prominent and appear unchanged. Most parts of the inferior segments of the hairs are also regularly formed. Failure of proper keratinization is present in the upper third of the follicle resulting in a collapse of the medullary cavity with attenuated hair shafts becoming compact, hyaline masses. Large numbers of hair shafts fail to penetrate the epidermis. Instead, twisted, coiled, or sometimes "S"-shaped hair shafts are found within the isthmus or infundibular parts of follicles. Infundibular openings are dilated containing masses of lamellar keratin. Adnexal glands presented no obvious changes and were interpreted to be within normal limits. However, conclusive evaluation without an appropriate age-matched control tissue was considered difficult.

Few mild lymphoplasmacytic infiltrates are present in the superficial and perifollicular dermis. The mostly bilayered epidermis is unremarkable with multifocal to segmental mild orthokeratotic hyperkeratosis.

Contributor's Morphologic Diagnosis: Haired skin: Trichomalacia (hair follicle dysplasia with defective hair shaft formation).

Contributor's Comment: Lesions are consistent with dysplastic hair shaft formation. Several kinds of follicular dystrophies have been described in humans, domestic and laboratory animals.

The main clinical feature, alopecia occurring at or shortly after birth, can be induced by changes in either quantity or quality of hair shafts. Congenital changes are based most frequently on inherited abnormal morphogenesis and therefore are termed hair follicle dysplasias. There are several kinds of dysplasias, depending to the differentiation level of affected cells (single differentiated cell or progenitor cell). Accordingly, changes in related tissues like cutaneous appendages, nails or claws and teeth may occur.

The hair follicle with its "product", the hair shaft, is a complex unit underlying tightly regulated cyclic changes.[6] Classification relies on differentiation between reduced hair follicle quantity and quality.[7]

Alterations in hair follicle quantity: Developmental reduction of hair placodes during organogenesis or defective morphogenesis with permanent loss of hair follicles can both lead to congenital alopecia. Delineation is often difficult because variable subsets of hair follicles are existent and are irregularly distributed over different body regions.

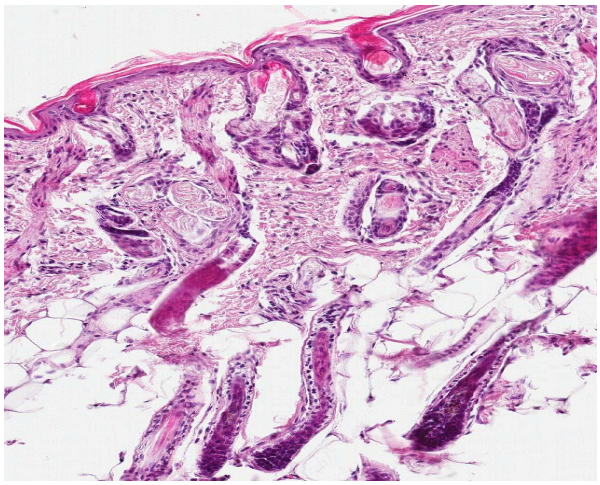

3-1. Haired skin, dog. Hair follicles exhbit dyslplasti at the level of the ostium, with dilation and abundant keratin debris. The hair bulbs are normal, and their placement within the subcutis suggests that this is a puppy. (HE 100X)

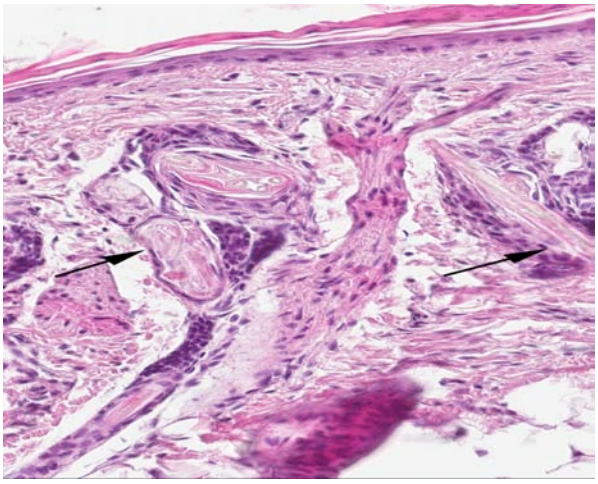

3.2. Haired skin, dog. At higher magnification, dysplastic follicles flank arrector pili muscles. The dilated follicles contain poorly formed, broken hair shafts or keratin debris, and the inner root sheath is disorganized, with some cells exhibiting cloudy swelling. (HE 200X)

Aplasia of hair follicles with dental dysplasia affects more than one tissue derived from the ectoderm, mostly apocrine glands. Several forms have been reported in humans, various breeds of dogs,[10] mice,[2] and cattle,[1] with only few of the underlying signaling pathway defects characterized yet.[2] Aplasia of hair follicles without dental dysplasia with a dominant autosomal inheritance has been described in pigs.[7]

Alterations in hair follicle quality: Structural changes leading to reduced, defective or absent hair shaft production can be subdivided into those resulting from morphological changes of the hair follicle itself or those where morphologically unchanged hair bulbs form defective hair shafts.

Especially in the dog, several breeds are affected with hairlessness resulting from hair follicle dysplasia with defects in hair follicle development, for example Mexican[5] or Peruvian hairless dogs and Chinese crested dogs.[11] In contrast to horses with only rare reports, diverse forms have been described in various breeds of cattle. Some of these have already been characterized as autosomal recessive or dominant, partly lethal traits.[7]

Hair follicle dysplasia without defects in hair follicle development (trichomalacia) is classically represented by nude mice amongst few others.[8] Beside few breeds of cats, (e.g. Sphinx breed) and dogs, 7 mainly in man, numerous forms of trichomalacia have been observed.[4]

A special form of dysplasia affects the neuroectodermally derived follicular melanocytes which also contribute to regular hair follicle development.[3] Histopathological changes are specific and identical in both syndromes with formation of enlarged melanin granules in melanocytes and later aggregation of perifollicular melanophages.[7] Depending on the affected breed and coat colors, color dilution alopecia and black hair follicular dysplasia have been differentiated.[13]

The case submitted here fulfills the relevant criteria for *hair follicle dysplasia without defects in hair follicle development (trichomalacia)* because of the unchanged appearance of hair follicles. Further changes in ectoderm-derived tissues, like apocrine glands or teeth, were not observed. The occurrence in both animals of the litter is suggestive of an inherited genetic defect. The queen had been mated to the identical sire before, without any abnormality in the offspring. Unfortunately the littermate was not available for pathological examination and confirmation of similar changes in hair shaft formation.

Death of this kitten was attributed to acute hepatic failure with severe hepatocellular degeneration and lipidosis (peripheral lipomobilization syndrome) based on the results of pathological examination of all other organ systems, including histology.

JPC Diagnosis: Haired skin: Trichomalacia, diffuse, moderate.

Conference Comment: The main abnormality in this case is the presence of abnormal hair shafts with no cuticle, cortex, or medulla along with malformed keratin fragments. Trichomalacia refers to degeneration of the hair shaft and is manifest grossly as alopecia with broken hair shafts in the presence of normal follicles.[12] In large animals, trichomalacia may be caused by certain nutritional deficiencies, such as copper, vitamin A, and folic acid; or by intoxication with hypervitaminosis A, D, or E, and with selenium and thalium toxicity.[9] Conference participants discussed psychogenic alopecia, but this is ruled out because the patient is a kitten and the lesion is diffuse instead of sparse.

Contributor: Freie Universitaet
Department of Veterinary Pathology
Berlin, Germany
http://www.vetmed.fu-berlin.de/einrichtungen/institute/we12/index.html

References:

1. Drogemuller C, Distl O, Leeb T. X-linked anhidrotic ectodermal dysplasia (ED1) in men, mice, and cattle. *Genet Sel Evol*. 2003;35(Suppl 1):S137-145.
2. Freire-Maia N, Lisboa-Costa T, Pagnan NAB. Ectodermal dysplasias: How many? *American Journal of Medical Genetics*. 2001;104:84-84.
3. Hume AN, Tarafder AK, Ramalho JS, et al. A Coiled-Coil Domain of Melanophilin Is Essential for Myosin Va Recruitment and Melanosome Transport in Melanocytes. *Mol Biol Cell*. 2006;17:4720-4735.
4. Itin PH, Fistarol SK. Hair shaft abnormalities--clues to diagnosis and treatment. *Dermatology*. 2005;211:63-71.
5. Kimura T, Ohshima S, Doi K. The Inheritance and Breeding Results of Hairless Descendants of Mexican-Hairless Dogs. *Laboratory Animals.* 1993;27:55-58.
6. Krause K, Foitzik K. Biology of the hair follicle: The basics. *Seminars in Cutaneous Medicine and Surgery*. 2006;25:2-10.
7. Mecklenburg L. An overview on congenital alopecia in domestic animals. *Vet Dermatol.* 2006;17:393-410.
8. Mecklenburg L, Tychsen B, Paus R. Learning from nudity: lessons from the nude phenotype. *Experimental Dermatology.* 2005;14:797-810.
9. Meckelburg L. Trichomalacia. In: Meckelburg L, Linek M, Tobin DJ, eds. *Hair Loss Disorders in Domestic Animals*. Ames, IA: Wiley-Blackwell; 2009:115-117.
10. Moura E, Cirio SM. Clinical and genetic aspects of X-linked ectodermal dysplasia in the dog -a review

including three new spontaneous cases. *Vet Dermatol*. 2004;15:269-277.
11. Sander P, Drogemuller C, Cadieu E, et al. Analysis of the canine EDAR gene and exclusion as a candidate for the hairless phenotype in the Chinese Crested dog. *Animal Genetics*. 2005;36:168-171.
12. Tieghi C, Miller WH Jr, Scott DW, et al. Medullary trichomalacia in 6 German shepherd dogs. *Can Vet J*. 2003;44(2):132-6.
13. Welle M, Philipp U, Rufenacht S, et al. MLPH Genotype--Melanin Phenotype Correlation in Dilute Dogs. *J Hered*. 2009;100(Suppl 1):75-9.

CASE IV: T10-7475 (JPC 4002870).

Signalment: Six-week-old male English setter dog (*Canis familiaris*).

History: Two of nine puppies in a litter of English setter dogs developed erythematous cutaneous lesions at the age of 2 weeks. Oral amoxicillin was given twice daily. After a week, the 2 puppies developed full body crusts, scabs, blistered footpads, and pustules on the lips and the eyelids. The puppies were still in a good body condition and nursing well. Other puppies in the litter were apparently healthy and doing well. Treatment was switched to cefadroxil antibiotic with low-dose prednisone added into the suspension. At 4 weeks of age, a total of 4 puppies were affected. Cefadroxil and prednisone were given to all 4 puppies with daily antimicrobial shampoos. The lesions worsened irrespective of treatment with anthelmintic, antibiotics, anti-fungal and anti-inflammatory drugs. There was some response to daily dosing of dexamethasone. Two severely affected puppies were hospitalized for more intensive care and diagnostic evaluation. Full thickness skin biopsy was taken from one of the puppies. Given the poor prognosis due to severity of the lesions and deteriorating health status, the 2 puppies were euthanized after 2 weeks of hospitalization (8 weeks of age) and necropsied.

Gross Pathology: Grossly, there were extensive skin erythema with alopecia on the face, body, and extremities. The tongues and oral mucosae were multifocally eroded and ulcerated.

Laboratory Results:
Skin scrapings were negative for mites. Heavy growths of *Staphylococcus intermedius* and beta *Streptococcus* sp. Group C and moderate *Rhizopus* sp. were obtained from culture on hair and scab. Tissues from the tongue, lymph node, spleen, skin, and small intestine from both euthanized puppies were positive for Canine parvovirus-2 (CPV-2) and negative for Canine distemper virus (CDV) and Canid herpesvirus 1 by **fluorescent antibody** test (FAT). Negative-staining electron microscopy detected parvovirus particles in the intestinal contents. The skin and small intestine were positive for CPV-2b and negative for CDV by polymerase chain reaction (PCR). The mucocutaneous junctions and small intestines stained positive for CPV by immunohistochemistry (IHC).

Contributor's Histopathologic Description: The epidermis of skin on the body, lips (mucocutaneous junction), ears, and footpads, from both puppies was mild to moderately hyperkeratotic (parakeratotic), irregularly acanthotic, multifocally necrotic, and occasionally covered with serocellular crusts. In all layers of the epidermis, there was scattered individual

4-1. 6-week-old male English setter puppy with full body crusts, scabs, blistered footpads, and pustules on the lips and the eyelids. Photograph courtesy of The University of Georgia, College of Veterinary Medicine, Department of Pathology, Tifton Veterinary Diagnostic and Investigational Laboratory, Tifton, GA 31793http://www.vet.uga.edu/dlab/tifton/index.php

keratinocyte apoptosis with lymphocyte satellitosis (varies from slide to slide). The individual cell apoptosis occasionally extended to the infundibular and upper sections of the hair follicles and associated sebaceous glands. Few basophilic to amphophilic intranuclear inclusions were present in the apoptotic basal cells and the overlying cells of stratum spinosum. Similar intranuclear inclusions were present in a few mast cells in the papillary dermis, the mucosal cells of the tongue, the small intestine crypt enterocytes, and the myocardiocytes of the heart in both puppies and in the mucosal cells of the oropharynx overlying the tonsil and in the epithelial cells of the esophageal glands in one of the puppies. The microscopic findings in the other tissues besides skin were typical of parvovirus infection. The findings in the other examined tissues were unremarkable.

Contributor's Morphologic Diagnosis: Epidermitis, and folliculitis, necrotizing, subacute with parakeratosis and intranuclear and intracytoplasmic inclusions.

Contributor's Comment: The gross and microscopic lesions are consistent with erythema multiforme (EM). Erythema multiforme is a cutaneous reaction of multifocal etiology seen uncommonly in dogs and rarely in cats.[3] In dogs, EM is most commonly idiopathic or reported in association with administration of antibiotics, anthelmintics and anti-inflammatory drugs, infections such as staphylococcal dermatitis, and folliculitis, and pseudomonal otitis externa, feed, and a commercial nutraceutical product.[4,6-8] It is also described in association with CPV-2 in a dog.[1] A group of chronic and persistent idiopathic EM is seen in older dogs ("old dog EM") without a history

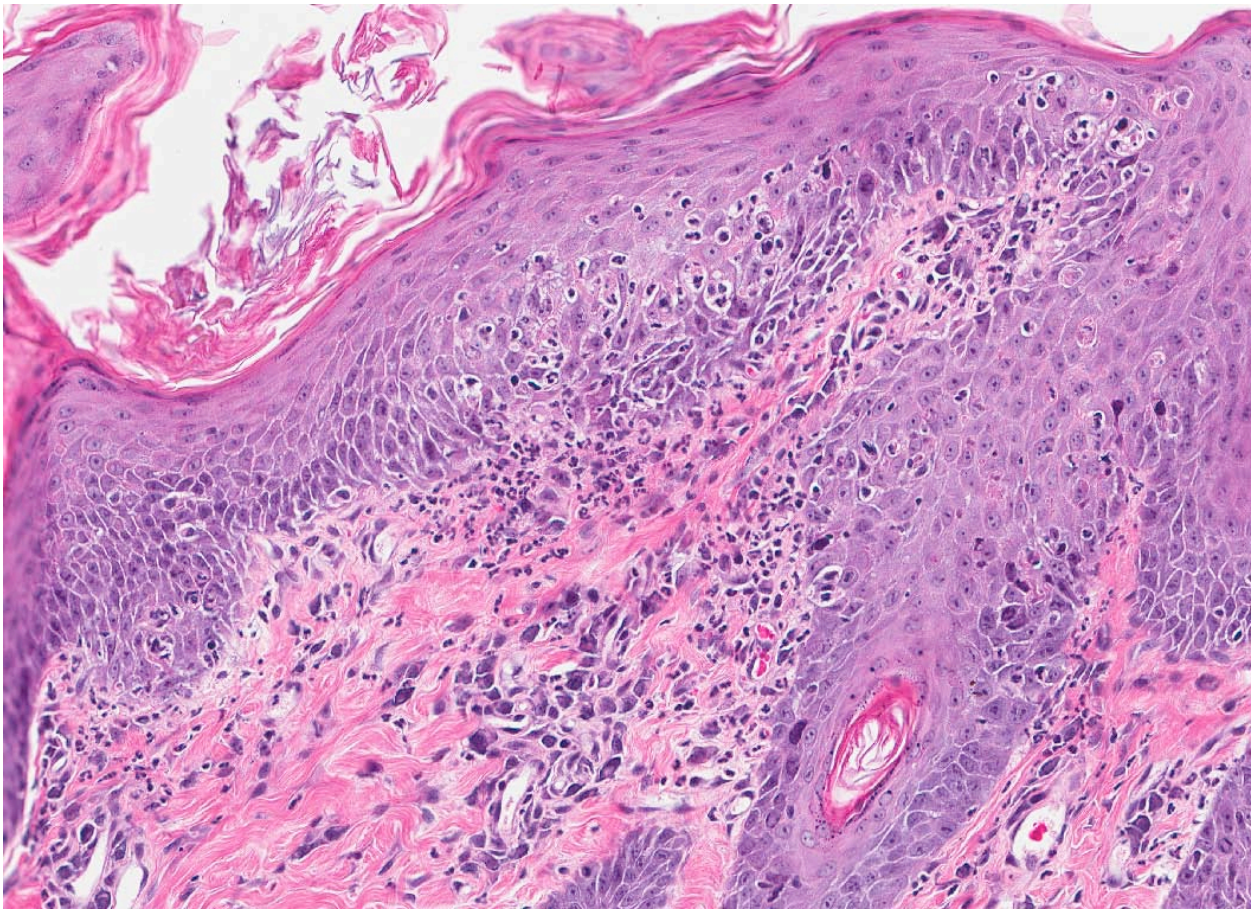

4-2. Haired skin, dog. Necrotizing dermatitis with marked neutrophilic infiltration of the epidermis. (HE 180X)

compatible with known triggers. Lesions are more exudative and proliferative, and predominantly involve the face and ears.[3] In humans, most cases were associated with drug administration and infections such as Herpes virus and *Mycoplasma pneumoniae*.[5]

Despite recognition of multiple etiologic and triggering causes, the pathogenesis of EM is not completely understood.[6,7] It is believed to be a host-specific T-cell mediated hypersensitivity reaction in which the immune response is directed against keratinocyte-associated antigens associated with the triggering causes.[3] In EM, cluster of differentiation (CD)44 was markedly up-regulated in keratinocytes and infiltrating cells and is involved in T-lymphocyte activation and site-specific extravasation of lymphocytes into tissues.[7] Keratinocyte apoptosis is probably produced by signals from intraepithelial CD8+ T lymphocytes.[8] Lymphocytes bind to the antigenically altered keratinocytes and trigger cell death via apoptosis. Keratinocyte apoptosis is principally seen in the basal cell layer in exfoliative cutaneous lupus erythematosus of the German shorthaired pointer dog, discoid lupus erythematous, and systemic lupus erythematosus. Keratinocyte apoptosis in EM, however, is seen at all levels of the epidermis.[3]

Erythema multiforme occurs in 2 forms that may overlap one another and to toxic epidermal necrolysis. Erythema multiforme minor is characterized chiefly by an acute onset of cutaneous erythematous macules and papules. In EM major (Stevens-Johnson syndrome), widespread mucosal lesions, extensive necrotizing and vesiculous skin lesions, and signs of systemic illness such as pain, lethargy, and pyrexia are present.[2] Based on this, the EM seen in the current cases was classified as EM major.

Because of the diversity of triggering factors associated with EM, recognition of the underlying cause for each individual case is important to propose the best treatment regimen. Age or sex predilection is not documented in dogs and cats. Extensive studies and documentation are needed to determine breed predilection to EM in dogs. Canine parvovirus infection was confirmed in several tissues and organs

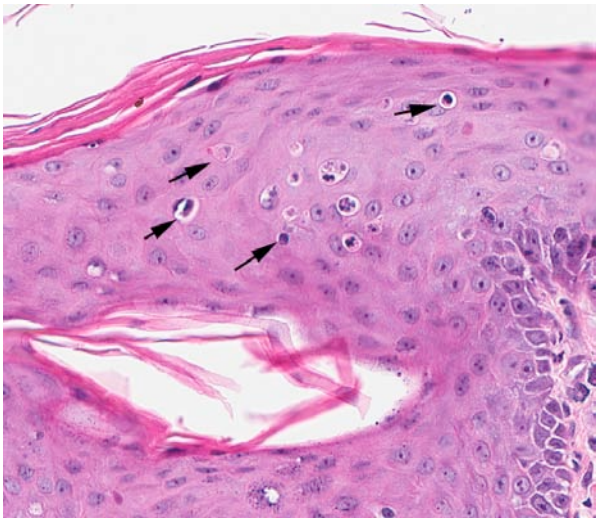

4-3. Haired skin, dog. Degenerating and necrotic keratinocytes within all layers of the epidermis. Adjacent to them are infiltrating neutrophils. (HE 400X)

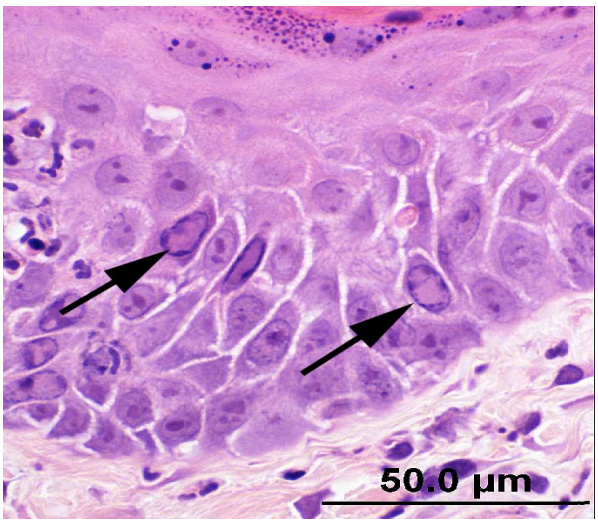

4-4. Haired skin, dog. Rhomboidal intranuclear viral inclusions within basal keratinocytes, characteristic of canine parvovirus-2 (arrows). Photograph courtesy of The University of Georgia, College of Veterinary Medicine, Department of Pathology, Tifton Veterinary Diagnostic and Investigational Laboratory, Tifton, GA 31793http://www.vet.uga.edu/dlab/tifton/index.phpv(HE 600X)

from the puppies by FAT, PCR, IHC, and electron microscopy. The EM observed in this litter of English setters was associated with systemic CPV-2b infection involving various tissues and organs.

JPC Diagnosis: Haired skin: Keratinocyte necrosis, multifocal, moderate, with neutrophilic epidermitis and folliculitis, marked perakeratosis, pustule formation, and viral intranuclear inclusion bodies.

Conference Comment: Conference participants debated that the multifocal single-cell death in the epidermal keratinocytes may be the result of the cytopathic effect of canine parvovirus, and not an indication of erythema multiforme (EM). Consideration is also given to toxic shock syndrome (TSS), in which early lesions resemble EM, although apoptotic keratinocytes are typically surrounded by neutrophils possibly due to the presence of bacterial toxins. Although the cause of skin lesions associated with TSS has not been determined, superantigen exotoxins which stimulate lymphocytes to release cytokines, including tumor necrosis factor-alpha may play a role.[2]

The puppies in this case started showing clinical signs when only 2 weeks old. Participants did not expect such young puppies to have developed an immune response directed against their own keratinocytes at such an early age. Also, conference participants felt that the keratinocyte satellitosis was predominantly neutrophilic and not lymphocytic. Additional features of EM that were not evident in our slide include a lymphohistiocytic infiltrate obscuring the dermoepidermal junction and around superficial blood vessels (interface dermatitis), subepidermal clefting and vesicle formation along the basement membrane, vacuolation of the basement membrane zone (hydropic degeneration), pigmentary incontinence, and, less commonly, severe dermal edema with vertical orientation of dermal collagen (gossamer collagen).[2,3]

The pathogenesis of EM is not fully understood, but is thought to be a host-specific T cell-mediated hypersensitivity reaction with a cellular immune response directed against various keratinocyte-associated antigens, including those associated with drugs, infections (viral, fungal, bacterial), neoplasia, various chemical contactants, foods and connective tissue disease. CD8+ T lymphocytes bind to antigenically altered keratinocytes (ICAM-1, MHC II, CD1a, and CD44 expression is upregulated) and trigger cell death via apoptosis. Apoptotic keratinocytes coalesce, leading to erosion, ulceration or hyperkeratosis. Studies support a combined type III and type IV immune reaction.[2,3]

Contributor: The University of Georgia, College of Veterinary Medicine
Department of Pathology
Tifton Veterinary Diagnostic & Investigation Laboratory
Tifton, GA 31793-1389
http://www.vet.uga.edu/dlab/tifton/index.php

References:

1. Favrot C, Olivry T, Dunston SM, et al. Parvovirus infection of keratinocytes as a cause of canine erythema multiforme. *Vet Pathol.* 2000;37:647–649.

2. Ginn PE, Mansell JEKL, Rakich, PM. The skin and appendages. In: Maxie MG , ed. *Jubb, Kennedy and Palmer's Pathology of Domestic Animals*. ,5th ed. vol. 1. New Yoryk, NY: Elsevier Saunders; 2007;656-7, 686.
3. Gross TL, Ihrke PJ, Walker EM, et al. In: Gross, Thelma Lee. Skin Disease of Dogs and Cats: Clinical and Histopathologic Diagnosis, 2nd ed. .Oxford, UK: Blackwell Science Ltd; 2005;52–68, 75-8.
4. Itoh T, Kojimoto A, Mikawa M, et al. Erythema multiforme possibly triggered by food substances in a dog. *J Vet Med Sci*. 2006;68:869–871.
5. Léauté-Labrèze C, Lamireau T, Chawki D, et al. Diagnosis, classification and management of erythema multiforme and Stevens-Johnson syndrome. *Arch Dis Child*. 2000;83:347–352.
6. Scott DW. Erythema multiforme in a dog caused by a commercial nutraceutical product. *J Vet Clin Sci*. 2008;1:16–21.
7. Scott DW, Miller WH. Erythema multiforme in dogs and cats: literature review and case material from the Cornell University College of Veterinary Medicine (1988–96). *Vet Dermatol*. 1999;10:297–309.
8. Scott DW, Miller WH, Griffin CE. Immune mediated disorders, erythema multiforme. In: Muller and Kirk's Small Animal Dermatology. 6th ed. Philadelphia, PA: Saunders; 2001;729–740.

Joint Pathology Center
Veterinary Pathology Services

WEDNESDAY SLIDE CONFERENCE 2011-2012

Conference 14

25 January 2012

CASE I: NADC MVP-2 (JPC 3065874).

Signalment: 5-month-old female white-tailed deer (*Odocoileus virginianus*).

History: Observed depressed, listless. Physical exam revealed fever (102.5 F), mild dehydration, normal auscultation of heart and lungs, no evidence of diarrhea. Treated with IV fluids, antibiotics and a non-steroidal anti-inflammatory drug. Deer died within 5 hours.

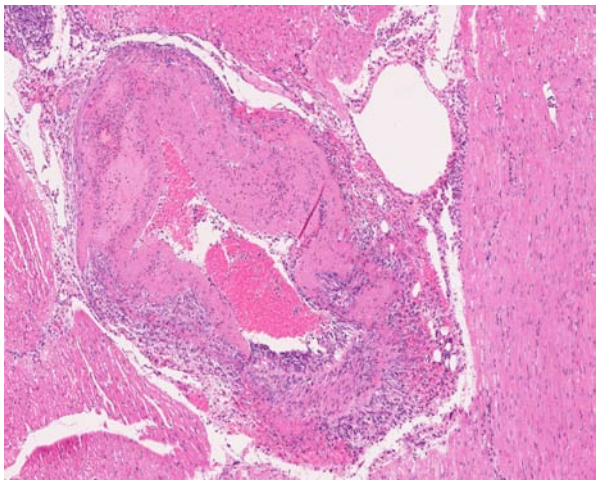

1-1. Heart, white-tailed deer. Necrotizing arteritis characterized by marked expansion of the wall by brightly eosinophilic protein, numerous inflammatory cells, and cellular debris (fibrinoid necrosis). (HE 67X)

Gross Pathology: The deer was of normal body condition with adequate deposits of body fat. There was crusty exudate around the eyes. Multifocal areas of hemorrhage were seen in the heart (epicardial and endocardial), lungs, kidney, adrenal glands, spleen, small and large intestines (mucosal and serosal surfaces) and along the mesenteric border, mesenteric lymph nodes and iliopsoas muscles. Multifocal ulcers were present in the pyloric region of the abomasum.

Laboratory Results:
PCR for OvHV-2: positive
PCR for EHV: negative
PCR for Bluetongue virus: negative
PCR for BVD: negative

Contributor's Histopathologic Description: Within the section of myocardium there is accentuation of medium to large arteries due to the infiltration of the vascular wall and perivascular spaces by inflammatory cells. Numerous lymphocytes and fewer neutrophils invade, and in some cases, efface the vessel wall. Fibrinoid degeneration and partially occluding fibrinocellular thrombi are present in the most severely affected vessels. Less affected vessels are characterized by large, rounded endothelial cells and intramural lymphocytes and neutrophils. Within the myocardium are multifocal areas of hemorrhage and scattered infiltrates of lymphocytes and macrophages.

Contributor's Morphologic Diagnosis: Myocardium: Arteritis and periarteritis, fibrinonecrotic,

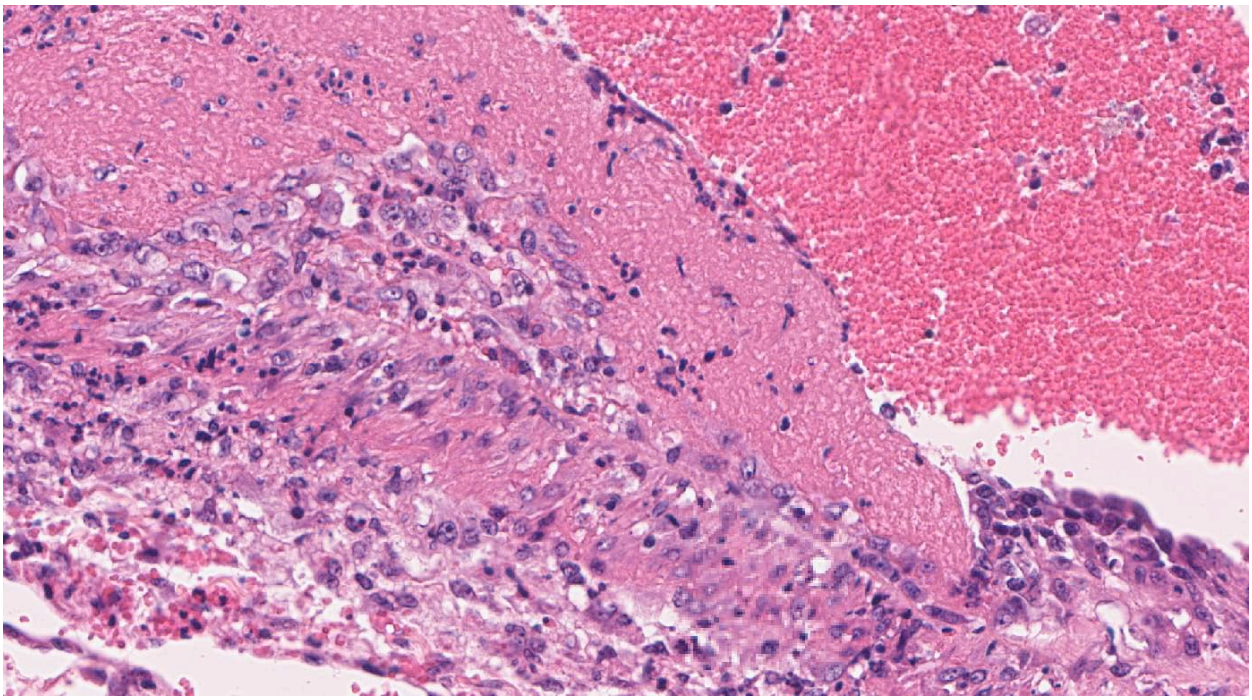

1-2. Heart, white-tailed deer. Higher magnification of affected myocardial artery with effacement of the muscular wall by abundant subintimal proein, neutrophils, macrophages, and cellular debris (fibrinoid necrosis). (HE 172X)

lymphocytic, multifocal, acute, moderate to severe, with fibrinoid degeneration, thrombosis and myocardial hemorrhage, white-tailed deer (*Odocoileus virginianus*).

Contributor's Comment: Malignant catarrhal fever (MCF) is the clinical manifestation of the infection of certain ruminant species with one of a group of pathogenic gammaherpesviruses known as MCF viruses. Most domestic cattle and numerous exotic species of ruminants are susceptible to clinical disease that may be sporadic or occasionally epidemic in nature. Clinical disease can range from peracute to chronic and has been reported in various species of cervidae including white-tailed deer, black-tailed deer, mule deer, reindeer, muntjac deer, sika deer, Shira's moose, Pere David's deer, swamp deer, rusa deer, and red deer.[1,2,4,6,7,13,14,15] The disease is characterized primarily by lymphoproliferation, mucosal inflammation and vasculitis. Historically, 2 MCF viruses have been associated with clinical disease, one endemic in wildebeest, known as alcephaline herpesvirus –1 (AIHV-1), and the other endemic in sheep, ovine herpesvirus-2 (OvHV-2) known as sheep-associated MCF (SA-MCF). Only AIHV-1 has been propagated in vitro and partially characterized. OvHV-2 is the major MCF virus worldwide. Recently, however, 2 additional members of the MCF virus group have been associated with clinical disease in deer. An MCF virus of unknown origin that causes clinical disease in white-tailed deer[8], and an MCF virus endemic in goats, provisionally known as caprine herpesvirus-2 (CpHV-2) has been associated with chronic alopecia in sika and white-tailed deer.[5,6] The literature on MCF contains descriptions of various manifestations of disease with diverse organ involvement. The variable nature of disease expression is thought to result from multiple regulatory genes in gammaherpesviruses acquired during evolution. Cell type as well as host species may alter the expression of these genes.[6]

Deer infected with OvHV-2 can have a variety of clinical signs. Typically, the affected animal is lethargic, febrile with diarrhea that is often watery or contains blood. Death usually occurs within 48 hours. Animals that live longer may have excessive watery to mucous discharge from the eyes, mouth and nose. Mucosal erosions or ulceration may be present in the nose, oral cavity or anywhere in the gastrointestinal tract. Corneal opacity may lead to blindness in one or both eyes. Compared to cattle, MCF in deer is usually an acute disease with animals showing few clinical signs before death. Lesions are more hemorrhagic and involve the viscera of the gastrointestinal tract. MCF in cattle is less acute and the severity of visceral lesions is decreased. Clinical signs in cattle are variable. Grossly, MCF in cattle produces enlarged lymph nodes, corneal edema, cutaneous crusts and hyperemia, oral hyperemia and ulceration, mucopurulent nasal discharge, and erosive or ulcerative lesions throughout the digestive system.

Deer acquire the infection through direct or indirect

contact with the reservoir species, most commonly sheep. Reservoir species remain infected with the virus but do not show any clinical signs. Research suggests that deer with MCF do not transmit the virus to other deer. Sheep between the ages of 6 and 9 months of age shed much more virus than do sheep of other ages and therefore are considered most dangerous to deer and other susceptible species.[9,10] Nasal secretions are the predominant vehicle by which virus is spread from sheep to other species.[9,10] There is some evidence that MCF viruses may be spread by aerosol over significant distances. Research on MCF in bison has documented transmission over distances of 2.5 to 3 miles, against prevailing winds and in the absence of common water sources suggesting that some mechanisms of transmission remain undefined.

Recent research suggests that some susceptible species may be latently infected with virus and that there may be recrudescence of disease during periods of stress. Much remains unknown concerning latent infections in susceptible species. The incubation period (time from infection to the manifestation of clinical disease) is unclear and can be quite variable, ranging from a few days to several months. In some species clinical signs have been seen as late as 8 months after exposure to infected sheep. In the present case deer were housed on a pasture that was within 50 yards of a pasture containing sheep. Lambing had occurred on the pasture approximately 6 months earlier. Six-month-old lambs were still present on the sheep pasture.

Differential diagnosis for diseases that cause ulceration and necrosis of the oral and gastrointestinal mucosa and hemorrhage in deer and other ruminants include epizootic hemorrhagic disease in deer, bluetongue, bovine virus diarrhea-mucosal disease, rinderpest, and vesicular diseases. Important vesicular diseases to consider are foot and mouth disease and vesicular stomatitis, which are grossly indistinguishable from one another.

JPC Diagnosis: Heart: Arteritis, necrotizing and proliferative, multifocal, severe, with thrombosis and mild multifocal myocarditis.

Conference Comment: Histologically, malignant catarrhal fever (MCF) typically presents as perivascular and intramural infiltrates of lymphocytes and lymphoblasts with accompanying fibrinoid necrotizing vasculitis, which is unique to this disease. Conference participants noted that this particular case was difficult, because the mononuclear cell infiltrate was not easily identifiable as lymphoblastic. For this reason, polyarteritis nodosa, a noninfectious proliferative and necrotizing vasculitis which occurs sporadically in all species of domestic animals, was also considered in the differential diagnosis.[11]

The most common sites for vascular lesions are the brain and leptomeninges, carotid rete, kidney, liver, adrenal capsule and medulla, salivary gland, and any section of skin or alimentary tract with gross lesions. Lymphocytic infiltrates are also present in the kidneys, periportal areas of the liver, gastrointestinal mucosa, dermis, meninges, and heart. Microscopic lesions seen in other areas are an active proliferation of lymphoblasts in lymph nodes, especially in T cell-dependent areas of interfollicular and paracortical zones; and lymphocytic uveitis with exudate from ciliary processes into the filtration angle, resulting in corneal opacity of the eye.[3,12,17]

In MCF, the virus is usually associated with lymphocytes in adults, and primary viral replication occurs in small and medium-sized lymphocytes. T-lymphocyte proliferation is likely secondary to infection of large granular lymphocytes, which have T-suppressor cells and natural killer cell activity. Viral infection and dysfunction of these cells causes lymphoproliferation, T-suppressor cell dysfunction, and necrosis. Thevasculitis is presumed to be immune-mediated, but demonstration of immunoglobulin and complement components has been inconsistent.[16]

Contributor: National Animal Disease Center
2300 Dayton Avenue
Ames, IA 50010
www.nadc.ars.usda.gov

References:

1. Beatson NS. Field observations of malignant catarrhal fever in red deer in New Zealand. *Biol of Deer Prod*. 1985;22:135-137.
2. Brown CC, Bloss LL. An epizootic of malignant catarrhal fever in a large captive herd of white-tailed deer (*Odocoileus virginianus*). *J Wildl Dis*. 1992;28(2): 301-305.
3. Gelberg HB. Alimentary system and the peritoneum, omentum, mesentery, and peritoneal cavity. In: McGavin MD, Zachary JF, eds. *Pathologic Basis of Veterinary Disease*. 4th ed. vol. 1. St. Louis, MO: Elsevier; 2012:1078, 1118.
4. Jessup DA. Malignant catarrhal fever in a free-ranging black-tailed deer (*Odocoileus hemionus columbianus*) in California. *J Wildl Dis*. 1985;21(2): 167-169.
5. Keel MK, Patterson JG, Noon TH, et al. Caprine herpesvirus-2 association with naturally occuring malignant catarrhal fever in captive sika deer (*Cervus nippon*). *J Vet Diagn Invest*. 2003;15:179-183.
6. Li H, Wunschmann A, Keller J, et al. Caprine hepesvirus-2-associated malignant catarrhal fever in white-tailed deer (*Odocoileus virginianus*). *J Vet Diagn Invest*. 2003;15:46-49.

7. Li H, Westover WC, Crawford TB. Sheep-associated malignant catarrhal fever in a petting zoo. *J Zoo Wildl Med*. 1999;30(3);408-412.
8. Li H, Dyer N, Keller J, et al. Newly recognized herpesvirus causing malignant catarrhal fever in white-tailed deer (*Odocoileus virginianus*). *J Clin Micro*. 2000;38(4):1313-1318.
9. Li H, Taus NS, Lewis GS, et al. Shedding of ovine herpsesvirus 2 in sheep nasal secretions: the predominant mode for transmission. *J Clin Microbiol*. 2004;42(12):5558-5564.
10. Li H, Hua Y, Snowder G, et al. Levels of ovine herpesvirus 2 DNA in nasal secretions and blood of sheep: implications for transmission. *Vet Microbiol*. 2001;79:301-310.
11. Maxie MG, Robinson WF. The cardiovascular system. In: Maxie MG, ed. *Jubb, Kennedy and Palmer's Pathology of Domestic Animals*. 5th ed. vol. 3, New York, NY: Elsevier Saunders; 2007:72-3.
12. Njaa BL, Wilcock BP. The ear and eye. In: McGavin MD, Zachary JF, eds. *Pathologic Basis of Veterinary Disease*. 4th ed. vol. 1. St. Louis, MO: Elsevier; 2012:1078, 1118.
13 Reid HW, Buxton D, McKelvey WA, et al. Malignant catarrhal fever in Pere David's deer. *Vet Rec*. 1987;121(12):276-277.
14. Tomkins NW, Jonsson NN, Young MP, et al. An outbreak of malignant catarrhal fever in young Rusa deer (*Cervus timorensis*). *Aust Vet J*. 1997;75(10): 722-723.
15. Williams ES, Thorne ET, Dawson HA. Malignant catarrhal fever in a Shira's moos (*Alces alces shirasi Nelson*). *J Wildl Dis*. 1984;20(3):230-232.
16. Zachary JF. Mechanisms of microbial infection. In: McGavin MD, Zachary JF, eds. *Pathologic Basis of Veterinary Disease*. 4th ed. vol. 1. St. Louis, MO: Elsevier; 2012:219.
17. Zachary JF. Nervous system. In: McGavin MD, Zachary JF, eds. *Pathologic Basis of Veterinary Disease*. 4th ed. vol. 1. St. Louis, MO: Elsevier; 2012:1078, 1118.

CASE II: 11-2389 (JPC 4002923).

Signalment: Juvenile elk (*Cervus canadensis*), sex not specified.

History: The calf was seen circling for 2 days near Yakima, WA. The animal was shot and the head and liver were submitted to the Washington Animal Disease Diagnostic Laboratory for histopathology.

Gross Pathology: **Brain:** On cut surface just off of midline in the left rostral diencephalon and extending into the left caudal brain stem, there were numerous 0.5–2.0 cm diameter yellow gelatinous masses. There were no gross lesions in the tongue, retropharyngeal lymph nodes, mandibular lymph nodes, tonsils, pharynx, nasal cavity, tympanic bullae or liver.

Laboratory Results: After DNA extraction from the sample, the entire internal transcribed spacer (ITS) region of the ribosomal RNA gene (comprising ITS1, 5.8S, and ITS2) was amplified by PCR using universal fungal primers. When this PCR amplicon was directly sequenced, the sequence most closely matched that of *Cryptococcus gattii* (also called *C. bacillisporus*) (100% sequence identity with GenBank acc # EF081162 (ATCC strain 32609) and others) when compared with sequences in GenBank. The ITS signature sequence from this isolate exactly matched that of *C. gattii* ITS type 4, which corresponds with PCR-fingerprint molecular type VGII.

Contributor's Histopathologic Description: **Brain:** Disrupting the gray and white matter of the left aspect of the diencephalon, mesencephalon, and brain stem were multifocal to coalescing expansile inflammatory nodules composed of central areas of necrosis surrounded by epithelioid macrophages, fewer lymphocytes and plasma cells, and scattered multinucleated giant cells. Within these foci there were numerous 5–18 µm diameter, round extracellular yeasts with a 1 µm thin wall, narrow-based budding, and a 2–8 µm thick, amphophilic, mucicarmine-positive mucinous capsule. There was spongiosis of the adjacent neuropil with few infiltrating lymphocytes and plasma cells. Occasionally, there was expansion of the Virchow-Robin space by small numbers of lymphocytes, plasma cells and occasional macrophages (perivascular cuffing). The leptomeninges overlying the cerebrum and brainstem were expanded by moderate numbers of lymphocytes, plasma cells, and macrophages associated with the same yeast bodies.

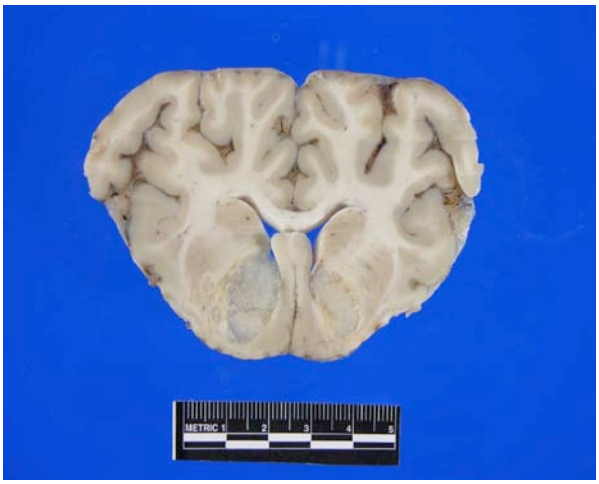

2-1. Cerebrum, calf. On cut surface just off of midline in the left rostral diencephalon and extending into the left caudal brain stem, there are numerous 0.5–2.0 cm diameter yellow gelatinous masses. Photograph courtesy of the Department of Veterinary Microbiology and Pathology and the Washington Animal Disease Diagnostic Laboratory, Pullman, WA 99164-7040 www.vetmed.wsu.edu

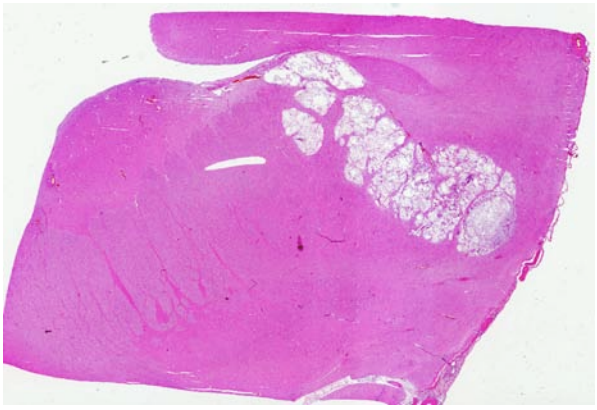

2-2. Cerebrum, calf. Focally extensive area of necrosis within the diencephalon containing numerous dimorphic yeasts and minimal inflammation. (HE 63X)

Sections of liver (not submitted) had mild centrilobular fatty degeneration of hepatocytes. No lesions were identified in other structures of the head.

Contributor's Morphologic Diagnosis: Meningoencephalitis, granulomatous, multifocal to coalescing, moderate, with many intralesional carminophilic yeasts (*Cryptococcus* sp.).

Contributor's Comment: Cryptococcosis is a localized to systemic fungal disease with worldwide distribution caused by a basidiomycete yeast-like fungus.[4] The two main species associated with disease in humans and animals are *Cryptococcus neoformans* and *C. gattii*, which vary in distribution, ecology and pathogenicity. Reproduction occurs primarily asexually, but the organism does possess the capability for sexual reproduction. Histologic lesions in animals caused by the two species are identical; differentiation must be done either by serotyping or at the molecular level.[1] Capsular serotypes B and C represent *C. gattii*; serotype A is *C. neoformans* var *grubii* and serotype D is *C. neoformans* var *neoformans*. Recently,

multilocus sequence typing (MLST) has separated *C. gattii* into 4 lineages, VGI – VGIV.[2]

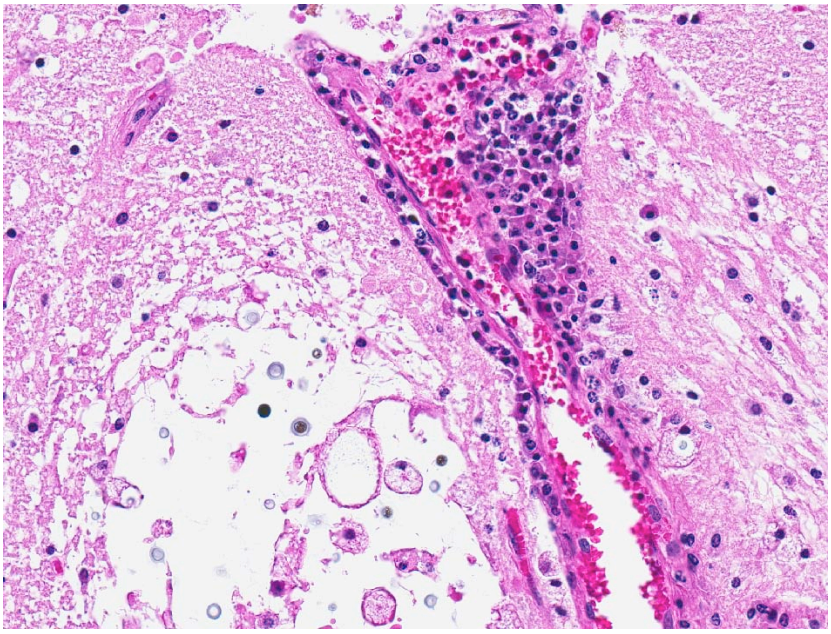

2-3. Cerebrum, calf. Higher magnification of necrotic area containing numerous 8-15µm dimorphic yeasts with a 2µm amphophilic cell wall. The yeasts are surrounded by a clear capsule. Within the area of necrosis, there are small numbers of large macrophages, some of which have engulfed yeasts. There is mild spongiosis of the adjacent neuropil and the lymphoplasmacytic cuffing of vessels. (HE 140X)

Cryptococcal disease is neither contagious nor zoonotic; animals and people acquire the infection by inhaling infectious particles from the environment. *C. neoformans* is found in soil and bird droppings, especially from pigeons.[4] *C. gattii* is found in association with eucalyptus trees and recently in the coastal Douglas fir and western hemlock forests of British Columbia and the Pacific Northwest US.[6] The infectious particle is likely the basidiospore, although dehydrated yeast bodies may also be infectious.[1] *C. neoformans* has emerged as an important secondary infection in people with HIV/AIDS; while *C. gattii* also causes disease in immunocompromised hosts, cryptococcosis in previously healthy individuals is more likely to be caused by *C. gattii*. Cryptococcosis in cats, the most common veterinary species affected, is rarely related to documented immunodeficiency.[4] Respiratory infections are the most common manifestation of disease, although systemic spread, especially to the brain, is not unusual. Some reports suggest that, in people, *C. gattii* infection is more likely to result in neurologic disease than is infection by *C. neoformans.*[1,5]

Cryptococcal virulence factors probably evolved as protection against ingestion by environmental amoeba; mammalian infection is likely accidental.[1] Those virulence factors include the ability to grow at temperatures above 30° C and the distinctive large, polysaccharide capsule which protects against phagocytosis and killing by neutrophils. Production of melanin by both pathogenic species protects the organisms against oxidative damage.

Although originally thought to be restricted to the eucalyptus forests of Australia, Southeast Asia and other tropical regions, *C. gattii* was identified in animal cases of cryptococcosis on Vancouver Island in 2000 and subsequently spread to people and animals in British Columbia, Washington and Oregon.[2] Retrospective studies suggested that *C. gattii* may have circulated in Southern California for much longer. The mechanism of the switch from tropical to temperate climates is unknown. However, most eucalyptus associated outbreaks in Australia are of molecular type

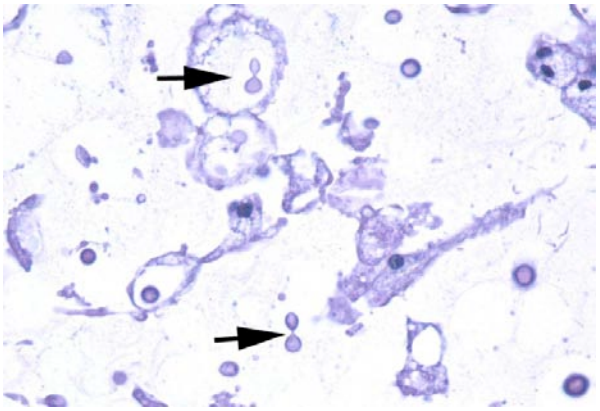

2-4. Cerebrum, calf. Cryptococcus gatti, exhibiting characteristic narrow-based budding. (HE 320X)

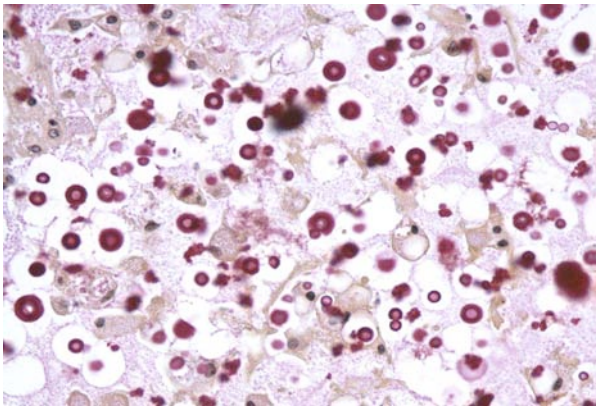

2-5. Cerebrum calf. Carminophilic 2-8 µm capsule surrounding C.gatti. (HE 320X)

VGI, whereas 90% of isolates from the Pacific Northwest are type VGIIa, and southern California isolates are type VGIII, the genotype commonly identified in Mexico. This suggests that different genotypes have different biogeoclimatic distributions.[5]

This case of neurologic cryptococcosis caused by *C. gattii* in a juvenile elk in Yakima County, WA represents further evidence of the spread of *C. gattii* infection within the Pacific Northwest region of the United States. A previous report of a case or cases of *C. gattii* infection in Yakima County provides no details.[5] There is limited information on *C. gattii* infection in wildlife. In 2006, a culture survey of wildlife species on Vancouver Island and lower mainland British Columbia found a 2% positive rate in nasal cavity swabs, a rate similar to that of sampled domesticated species.[6] Although no similar survey of wildlife in the Pacific Northwest is published, we would expect additional cases of *C. gattii* disease in wildlife in our area in the future.

JPC Diagnosis: Brain, dienchepalon: Meningoencephalitis, necrotizing and histiocytic, multifocal, severe, with numerous encapsulated yeasts, etiology consistent with *Cryptococcus gattii*.

Conference Comment: Conference participants discussed four important virulence factors, mentioned by the contributor. First is the mucopolysaccharide capsule, which prevents phagocytosis by alveolar macrophages, confers resistance to opsonization, impairs phagocytosis and leukocyte migration, activates complement and suppresses T-cell responses. Secondly, phenoloxidase, a laccase, produces the antioxidant melanin from diphenolic compounds, protecting the yeast from oxidative damage. Thirdly, serine protease cleaves fibronectin and other basement membrane proteins and may aid in tissue invasion. Fourth is the ability to grow at 37° C, a temperature at polysaccharide capsule expression is enhanced. Rabbits are naturally resistant to cryptococcosis, due to their higher normal body temperature of 39.5° C, which inhibits fungal replication and dissemination.[3]

Urease expression by *Cryptococcus* spp. appears to promote sequestration in microcapillaries, which is a critical step in dissemination to the brain. The organism's predilection for the central nervous system may be partially attributed to the lack of alternative pathway complement components in cerebrospinal fluid, which would otherwise bind to the carbohydrate capsule and enhance phagocytosis and killing by neutrophils.[3]

Protective immunity against *Cryptococcus* spp. requires a Th1 pattern of cytokine response, to include interleukin-12 (IL-12), IL-18, interferon gamma, tumor necrosis factor beta, granulocyte-macrophage colony stimulating factor, macrophage inflammatory protein-1, and monocyte chemoattractant protein-1. Humoral factors, such as opsonization by antibody and complement are important in clearance.[3]

Contributor: Washington Animal Disease Diagnostic Laboratory
Department of Veterinary Microbiology and Pathology
Washington State University
Pullman, WA 99164-7040
www.vetmed.wsu.edu

References:

1. Bovers M, Hagen F, Bockhout T. Diversity of *Cryptococcus neoformans-Cryptococcus gattii* species complex. *Rev Iberoam Micol*. 2008;25:S4-S12.
2. Byrnes III, EJ, Marr KA. The outbreak of *Cryptococcus gattii* in western North America: Epidemiology and clinical issues. *Curr Infect Dis Rep*. 2011;13:256-261.
3. Carroll SF, Guillot L, Qureshi ST. Mammalian model hosts of cryptococcal infection. *Comp Med*. 2007;57(1):9-17.
4. Caswell JL. Williams KJ. The respiratory system In: Maxie, MG ed. *Jubb, Kennedy and Palmer's Pathology of Domestic Animals*. 5th ed. Edinburgh, Scotland: Elsevier; 2007;642-643.
5. Datta K, Bartlett KH, Baer R, et al. Spread of *Cryptococcus gattii* into the Pacific Northwest region of the United States. *Emerging Infect Dis*. 2009;15:1185-1191.
6. Duncan C, Schwantje H, Stephen C, et al. *Cryptococcus gattii* in wildlife of Vancouver Island, Bristish, Columbia, Canada. *J Wildlife Dis*. 2006;42:175-178.

CASE III: 53364 AFIP (JPC 4002986).

Signalment: African jacana bird (*Actophilornis africanus)*, female 12+ years old, 251 g, wild- caught long-term captive.

History: A keeper found this bird dead near a stream in its exhibit. It had been moved from a nearby exhibit onto the current exhibit approximately 40 days prior. Following the move it had been eating well, and was approaching the keepers and taking food items at each feed-out.

Gross Pathology: At necropsy, this jacana was moderately autolyzed, and had adequate adipose stores and pectoral muscle mass. Multiple enlarged, firm interphalangeal joints were present on both feet. The nail was absent from the right first digit and the distal aspect was swollen to greater than 1 cm in diameter. The dorsolateral lung fields were mottled dark red. Approximately 50 petechial hemorrhages were present in the subepicardium of the heart and subserosal surface of the proventriculus. The spleen was diffusely swollen, soft, and dark pink-gray. Impression smears of the lung, spleen, and intestine yielded mixed inflammatory cells and large numbers of gram-positive rod bacteria which were often within inflammatory cells, particularly histiocytes.

Laboratory Results: Bacterial cultures of postmortem kidney samples preserved at -70 C yielded 3+ growth of *Erysipelothrix rhusiopathiae*, and 1+ growth each of *Escherichia coli* and *Enterococcus sp*.

Contributor's Histopathologic Description:
Kidney: Multifocally throughout the sections glomerular capillaries and small-caliber, thin-walled intertubular vessels are expanded by dense aggregates of tightly packed dark blue bacterial colonies which occasionally completely occlude vessel lumina. In these areas, the bacterial colonies are often observed to be contained within the cytoplasm of large irregular cells with eccentrically displaced nuclei. Medium and occasionally larger caliber veins and smaller arterioles contain moderately increased numbers of large blue-gray histiocytic cells. In some vessels these cells form small aggregates or dense sheets and contain small to large clusters of dark blue rod bacteria similar to those observed in the capillaries. In the most severely affected areas of some sections, occasional individual proximal tubules are lined by dissociated epithelial cells with hypereosinophilic hyalinized to clumped cytoplasm and pyknotic to fragmented nuclei (necrosis). Multifocally collecting ducts are mildly to markedly dilated and contain pale blue granular to fibrillar material admixed with amorphous basophilic debris. Low numbers of lymphocytes, heterophils, plasma cells and histiocytes are scattered throughout

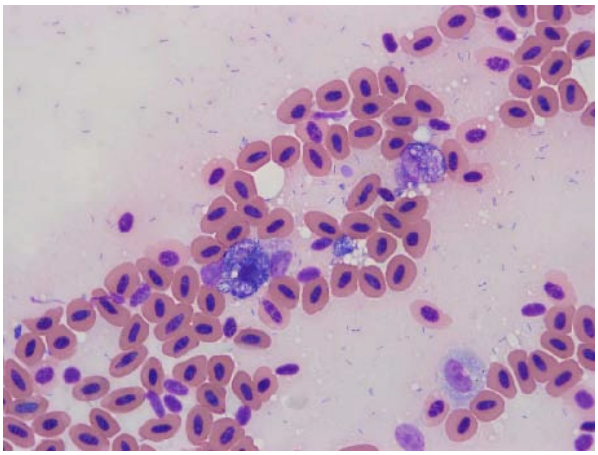

3-1. Lung, African jacana. Cytologic preparation showing several histiocytes distended by numerous phagocytosed bacilli. (Wright-Giemsa 1000X)

the sections. Rarely, random individual tubules are mineralized, and infrequently dark orange-brown granular material is present in the cytoplasm of tubular epithelium. The intracellular bacteria were strongly gram-positive with Goodpasture's Gram stain.

Other tissues: Large intracytoplasmic aggregates of bacteria similar to those in the kidney were present in phagocytic cells within vessels of most tissues. These were associated with hemorrhage and necrosis in the heart, spleen, and intestine. Histiocytosis was especially prominent in the spleen and was accompanied by a remarkably large number of intracellular bacteria. Multiple fibrinocellular thrombi were also present in the lung. Proliferative and ulcerative pododermatitis (bumblefoot) was confirmed and gram-positive and gram-negative rod bacteria, gram-positive coccoid bacteria and superficial fungal hyphae were present in the ulcerated areas. Supplemental digital images include a composite of affected heart in which a vessel contains histiocytes with intracytoplasmic gram-positive rod bacterial colonies.

Contributor's Morphologic Diagnosis: 1. Kidney: intravascular histiocytosis with intracellular gram-positive rod bacteria.
2. Kidney: mild to moderate multifocal acute tubular necrosis, mild multifocal granulocytic and lymphocytic interstitial nephritis, and moderate multifocal collecting duct ectasia with urate accumulation (not present in all sections).

Contributor's Comment: The bacterium *Erysipelothrix rhusiopathiae* is a cosmopolitan gram-positive, non-spore-forming, facultative anaerobe with numerous serotypes and variable virulence.[1,8,9] It has been documented to cause severe disease in a wide variety of animals including domestic and wild birds,

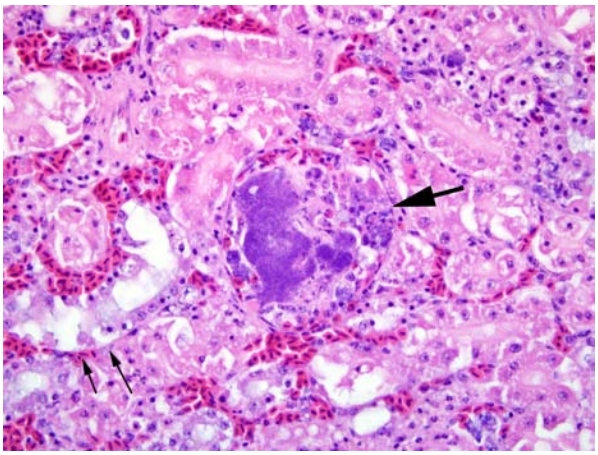

3.2. Kidney, African jacana. Necrotic glomerulus exhibiting a large intravascular bacterial embolus. There is a large aggregate of polymerized fibrin and necrotic debris within Bowman's capsule (large arrow). To the left of the glomerulus(small arrows), there is a tubule whose epithelium exhibits epithelial necrosis. (HE 400X)

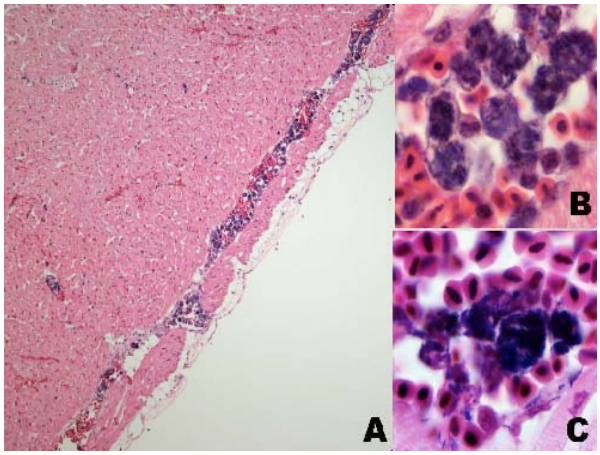

3.3 Heart, African jacana. Numerous vessels contain histiocytes distended by numerous phagocytosed bacilli (A – 100X, B- 400X.) The bacilli stain blue-black (gram-positive) on a Goodpasture's gram stain. (Gram, 1000X)

mammals ranging from whales to mice, and occasional reptiles. It is also a common commensal on aquatic and marine fishes and invertebrates.

Infection of livestock with *E. rhusiopathiae* results in significant financial losses, particularly in swine and turkey production units. *E. rhusiopathiae* is considered normal pharyngeal flora in up to 50% of swine and bacteria also cause significant disease, most commonly septicemia, polyarthritis, and endocarditis.[8] The septicemic form in swine often leads to disseminated intravascular coagulation with classic cutaneous manifestations characterized by diamond-shaped pink to purple raised foci commonly referred to as "diamond skin disease."[8] It causes a rapidly fatal septicemia in turkeys and other birds with inapparent to generalized petechiation in multiple organs and fibrinopurulent exudate on organ surfaces and joints.[1] In many cases there are limited histologic lesions, with colonies of intravascular bacteria with little or no inflammation as the primary feature.[3,11] While it may cause sporadic disease in a variety of wildlife, it is notable that *E. rhusiopathiae* has caused multiple significant mass mortality events involving hundreds of wild eared grebes in Nevada and brown pelicans in California, nearly an entire group of released captive raised kakapo in New Zealand, and one of 60 remaining Hawaiian 'Alala crows.[3,4,5,10]

Due to the ubiquitous nature of the bacteria, the potential for mass mortality events in birds, and the ability to infect individual birds of high value, *E. rhusiopathiae* should be considered as a potential cause of sudden death or sepsis in birds in zoological collections. The jacana in this case was wild caught in Tanzania and retained in the collection for approximately 12 years in multiple enclosures, most recently with a long-term mate, and had successfully raised several clutches of chicks. She had a history of proliferative pododermatitis lesions dating back to approximately 1 year after entering the collection. At necropsy the digital articular and skin lesions were chronic and proliferative, but also ulcerated and heavily colonized with opportunistic fungi and mixed bacteria. It hypothesized that infection in this case occurred via the skin wounds. An outbreak of *E. rhusiopathiae* affecting more than 300 chuckars was attributed to foot trauma caused by relocation from enclosures with solid flooring to wire-bottomed flooring.[2] Exposure to bedding material previously used by swine was the suspected source of the *E. rhusiopathiae* in the chukars. Disease in the jacana was suspected to have resulted from contamination of plantar skin wounds by bacteria in soil or enclosure bedding, water, mud, or other aquatic source associated with the stream. Bacteriologic surveys for potential sources were not evaluated in this case however, and dietary or other alternative sources including rodents or stray wildlife could not be ruled out.

JPC Diagnosis: Kidney: Glomerulitis and nephritis, necrotizing and histiocytic, multifocal, moderate, with numerous intravascular bacterial colonies.

Conference Comment: The degree of autolysis present in the sections hampers thorough interpretation of some of the pathologic tubular changes in this interesting case. Erysipelothricosis in birds often has such an acute course that the animal dies before many appreciable pathologic lesions occur.[7]

Erysipelothrix rhusiopathiae adheres to cells by producing neuraminidase, an enzyme that cleaves alpha glycosidic linkages in neuraminic acid, a reactive mucopolysaccharide in cell membranes. *Erysipelothrix rhusiopathiae* has hemagglutinating

activity that can result in complement-dependent hemolysis in severe acute disease. The hemagglutinating activity is believed due to the high neuraminidase activity in virulent strains.[6,10]

Acute to subacute systemic erysipelothricosis causes generalized septicemia and endothelial swelling of capillaries and venules, leading to adherence of monocytes to vascular walls and thus vascular fibrinoid necrosis, fibrin thrombosis, and invasion of vascular endothelium by bacteria. Chronic erysipelothricosis leads to polyarthritis, synovitis, fibrosis and articular cartilage destruction. Vegetative valvular endocarditis frequently occurs, resulting in vasculitis, myocardial infarcts, destruction of valve endocardium, and splenic and renal infarcts.[6,10]

Erysipelothrix rhusiopathiae is on a short list of gram positive bacilli important in veterinary medicine; others include *Actinomyces* spp., which are filamentous, *Corynebacterium* spp., and *Listeria monocytogenes*.

Contributor: Wildlife Disease Laboratories
San Diego Zoo Global
PO Box 120551
San Diego, CA 92112-0551
http://www.sandiegozoo.org/conservation/

References:

1. Bricker JM, Saif YM. Erysipelas. In: Calnek BW, ed. *Diseases of poultry*. 10th ed. Ames, IA: Iowa State University Press; 1997;302–313.
2. Butcher G, Panigrahy B. An Outbreak of Erysipelas in Chukars. *Avian Dis*. 1985;29(3):843-845.
3. Franson JC, Galbreath EJ, Wiemeyer SN, et al. Erysipelothrix rhusiopathiae Infection in a captive Bald Eagle (*Haliaeetus leucocephalus*). *J Zoo Wildl Med.* 1994;25(3):446-448.
4. Gartrell BD, Alley MR, Mack H, et al. Erysipelas in the critically endangered kakapo (*Strigops habroptilus*). *Avian Pathol.* 2005;34(5):383-7.
5. Jensen WI, Cotter SE. An outbreak of erysipelas in eared grebes (*Podiceps nigricollis). J Wildl Dis.* 1976;12(4):583-586.
6. Maxie MG, Robinson WF. Cardiovascular system. In: Maxie MG, ed. *Jubb, Kennedy, and Palmer's Pathology of Domestic Animals*. 5th ed. vol. 3. San Diego, CA: Academic Press; 2007;27-29.
7. Mazaheri A, Lierz M, Hafez HM. Investigations on the pathogenicity of Erysipelothrix rhusiopathiae in laying hens. *Avian Diseases*. 2005;49(4):574-576.
8. Qinning Wang Q, Chang B, Riley T. Review: Erysipelothrix rhusiopathiae *Vet Micro.* 2010;140:405–417.
9. Shibatani M, Suzuki T, Chujo M, et al. Disseminated intravascular coagulation in chickens inoculated with Erysipelothrix rhusiopathiae. *J Comp Pathol*. 1997;117 (2):147-156.
10. Thompson K. Bones and joints. In: Maxie MG, ed. *Jubb, Kennedy, and Palmer's Pathology of Domestic Animals*. 5th ed. vol. 1. San Diego, CA: Academic Press; 2007;163-164.
11. Work TM, A Donna Ball, B, Mark Wolcott. Erysipelas in a Free-ranging Hawaiian Crow (*Corvus hawaiiensis*) *Avian Dis.* 1999;43:338-341.

CASE IV: SP-10-6530 (JPC 4002892).

Signalment: 12-year-old male ring-tailed lemur (*Lemur catta*).

History: This captive ring-tailed lemur was housed in a Midwestern American zoo and first presented with labored breathing and was immobilized for a physical examination. It had significant respiratory effort under anesthesia. A large mass was observed on a thoracic radiograph, obscuring the heart shadow. The lemur recovered from anesthesia but continued to have labored breathing and lethargy. It was humanely euthanized.

Gross Pathology: A 9 x 7 x 9 cm gelatinous mass was present in the pleural cavity, replacing and displacing most normal lung parenchyma.

Laboratory Results: None performed.

Contributor's Histopathologic Description: The lung tissue is largely replaced in many sections by large thick-walled fibrous cavities with adjacent and intramural abundant lymphoplasmacytic nodular aggregates of macrophages, neutrophils, and eosinophils. The cavities are often lined by activated macrophages. Within many cavities are large, often multiple, viable and degenerate larval cestodes characterized by their segmented integument, calcareous corpuscles, a scolex with a rostellum bearing hooklets, and spinous tegument. Exogenous budding from the end opposite, the scolex is present in some slides. In the remaining lung, there were multifocal areas of parenchymal collapse of airways, peripheral emphysema, and pools of neutrophils, fibrin, and hemosiderin-laden macrophages in alveolar spaces and within capillaries. Many megakaryocytes were also circulating in the capillaries. Small nodular areas of lymphoplasmacytic inflammation are noted on the serosa of the intestine and on the diaphragm.

Contributor's Morphologic Diagnosis: Lung: Severe granulomatous and fibrous pleuropneumonia with intralesional larval cestodes (presumptive *Cysticercus longicollis,* the larval form of *Taenia crassiceps).*

Contributor's Comment: Larval cestodes often present as cysts, of which there are several forms: cysticercoids, cysticercus, coenurus, and hydatid cyst.[3] Of these, the presented case is a cysticercus based on the presence of only one scolex in each bladder (though bladder walls have degenerated in many of the fibrous cavities). Other key features to note are the thick tegument and the deeply basophilic calcareous corpuscles which are most numerous on the neck and scolex, but not in the bladder wall.[3]

Pulmonary, pleural, or peritoneal infection of lemurs by cysticerci has been well documented anecdotally and in the literature.[2,4] Based on these reports, one of which included molecular confirmation, and the similar morphology including rare budding seen in this case, the most likely etiology is *Cysticercus longicollis,* the larval form of *Taenia crassiceps,* though other *Taenia* sp. are possible.

Exposure to feces of the definitive host (typically wild canids, but also domestic cats and dogs) or consumption of infected secondary rodent hosts are possible modes of transmission to the lemur in this case. After ingestion by an aberrant host, it is not well-documented as to how the cysticerci migrate to the peritoneal or pleural cavities, but once there, these cases can be remarkably fulminating since the organism can proliferate by budding both endogenously and exogenously. Infection and rapid proliferation is associated particularly with

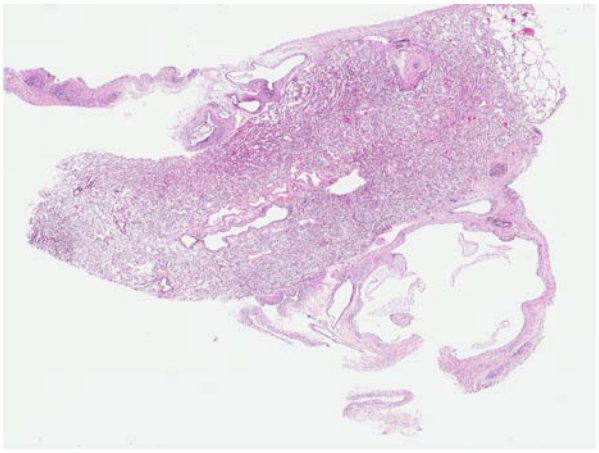

4-1. Lung, ring-tailed lemur. Lung parenchyma is replaced (lower left) by a large fibrous cyst contain cross sections of several cysticerci. (HE 40X)

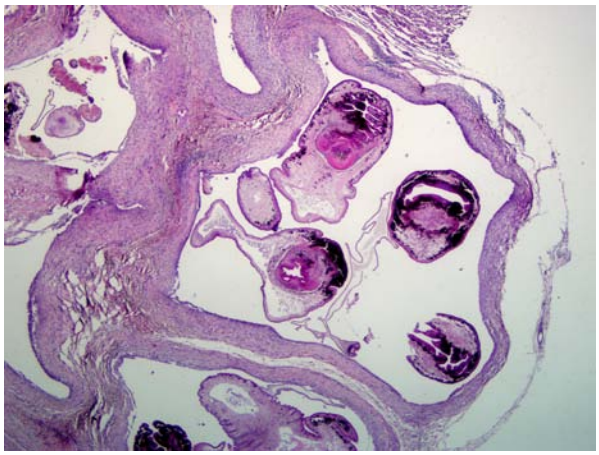

4-2. Lung, ring-tailed lemur. Within one of the fibrous cysts, there are several degenerating (mineralizing) cysticerci showing the scolex and invaginations of the thin bladder wall. (HE 100X)

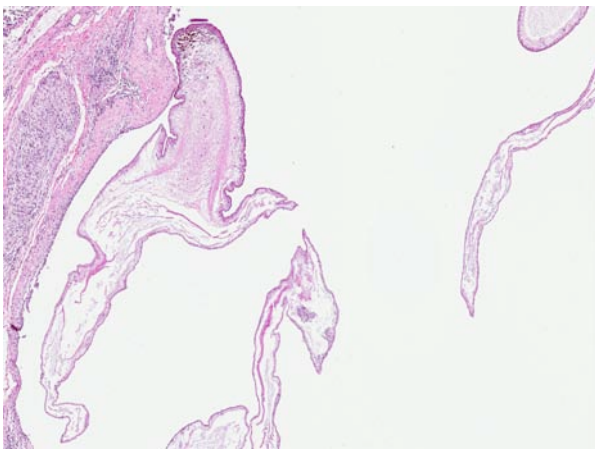

4-3. Lung, ring-tailed lemur. Cysticercus demonstrating evaginated scolex and bladder. (HE 200X)

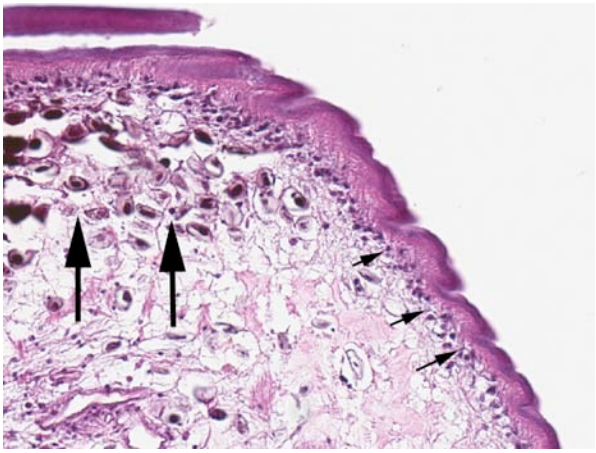

4.4. Lung, ring-tailed lemur. Tangential section through cysticercus demonstrating the serrated cuticle, spongy body cavity, somatic cell nuclei (small arrows), and numerous calcareous corpuscles (large arrows). (HE 320X)

immunosuppression. This disease is zoonotic, most recently associated with AIDS patients. There was no history or clinical pathology data to suggest this lemur is immunocompromised, but the perceived high frequency of cysticercosis in lemurs might indicate a predisposition in this exotic species which has presumably never been exposed to canid or felid parasites in their evolutionary history until very recently.

JPC Diagnosis: Lung: Cysticerci, multiple, with fibrosis and mild histiocytic and eosinophilic pneumonia.

Conference Comment: There is some variation among slides, and some participants may have received two sections of lung in which the histiocytic and eosinophilic pneumonia and bronchitis are a more prominent feature due to the presence of larval cysticerci in airways.

Other important cysticerci in veterinary species are included in the following chart[1]:

ADULT TAPEWORM	DEFINITIVE HOST	LARVAL FORM	INTERMEDIATE HOST	SITE
Taenia saginata	man	*Cysticercus bovis*	cattle	muscle
Taenia solium	man	*Cysticercus cellulosae*	pig, man	muscle
Taenia (*Multiceps*) *multiceps*	dog	*Coenurus cerebralis*	sheep, cattle	CNS
Taenia hydatigena	dog	*Cysticercus tenuicollis*	sheep, cattle, pig	peritoneum
Taenia ovis	dog	*Cysticercus ovis*	sheep	muscle
Taenia pisiformis	dog	*Cysticercus pisiformis*	rabbit	peritoneum, liver
Taenia serialis	dog	*Coenurus serialis*	rabbit	connective tissue
Taenia taeniaeformis	cat	*Cysticercus fasciolaris* (strobilocercus)	mouse, rat	liver
Taenia krabbei	dog	*Cysticercus tarandi*	reindeer	muscle
Taenia mustelae	wild felids		rodents	liver
Diphyllobothrium latum	bear, man		fish	muscle
Diphyllobothrium pacificum	seal, sea lion		marine birds	muscle

Contributor: Michigan State University
Department of Pathobiology and Diagnostic Investigation
Diagnostic Center for Population and Animal Health
4125 Beaumont Road
Lansing, Michigan 48910-8104
www.animalhealth.msu.edu

References:

1. Bowman DD, Lynn RC, Eberhard ML. *Georgi's Parasitology for Veterinarian*. 8th ed. St. Louis, MO: Saunders; 2003:130-153, 269, 275, 375-7.
2. Dyer NW, Greve JH. Severe Cysticercus longicollis cysticercosis in a black lemur (*Eulemur macaco macaco*). *J Vet Diagn Invest.* 1998;10:362-364.

3. Gardiner CH, Poynton SL. *An Atlas of Metazoan Parasites in Animal Tissues.* Washington, DC: Armed Forces Institute of Pathology; 2006.
4. Luzon M, de la Fuente-Lopez C, Martinez-Nevado E, et al. *Taenia crassiceps* cysticercosis in a ring-tailed lemur (*Lemur cata*). *J Zoo Wildl Med*. 2010;41:327-330.

Joint Pathology Center
Veterinary Pathology Services

WEDNESDAY SLIDE CONFERENCE 2011-2012

Conference 15

01 February 2012

CASE I: 11180095 (JPC 4003099).

Signalment: Cat (*Felis silvetris catus*), 12-year-old spayed female mix breed.

History: A 12-year-old mix breed cat was referred with a two-month history of persistent vomiting and loss of weight. At palpation an abdominal mass was detected. Ultrasound showed a heterogeneous and thickened gastric wall. Laparotomy revealed an intramural ulcerated mass close to the pyloric sphincter that was completely removed. The cat was still alive 5 months after surgical resection.

Gross Pathology: Gross examination of surgical biopsy showed a severely ulcerated mucosa with a diffuse and severe thickening of the gastric wall that appeared grayish.

Contributor's Histopathologic Description: The histological appearance of the gastric lesion consisted of an ulcerated and fibrinous exudative mass expanding and replacing the wall at the pyloric/fundic junction. The lesion affected the inner layers (*mucosa* and *tunica muscularis)* of the gastric wall and consisted of branching and anastomosing trabeculae of dense collagen separated by a densely cellular population of spindle-shaped cells (sclerosing fibroplasia). The trabecular collagen merged into

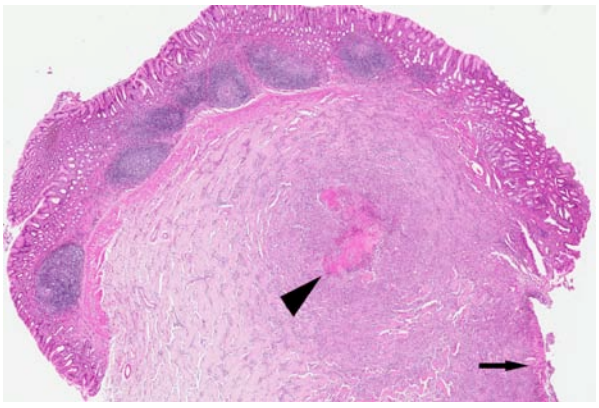

1-1. Stomach, cat. Section of stomach with lymphoid follicles in mucosa, lage area of mucosal ulceration (arrow), and large focus of Splendore-Hoeppli material in the muscular tunic. (*HE 6.3X)*

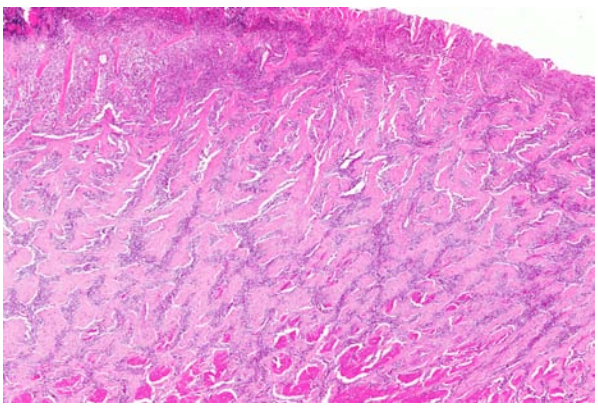

1-2. Stomach, cat. Retiform pattern of dense sclerosing fibroplasia effacing the ulcerated mucosa (top), submucosa, and muscular tunic (bottom). (*HE 24X)*

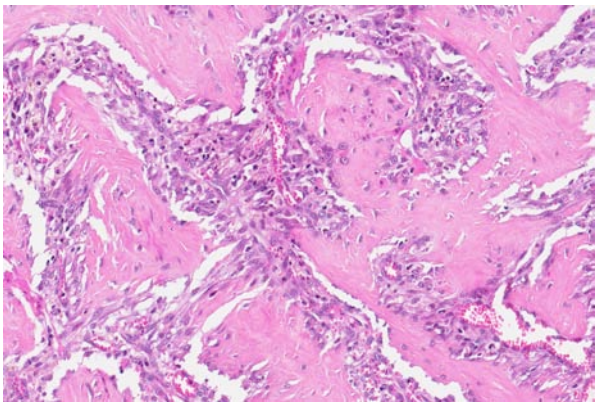

1-3. Stomach, cat. Higher magnifiacation of dense fibrous connective tissue separated by highly vascular granulation tissue. (HE 196X)

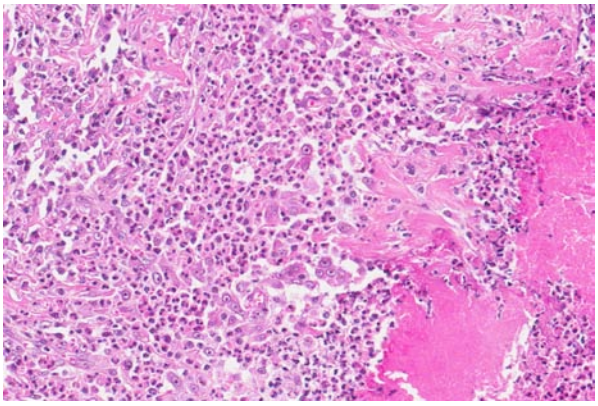

1-4. Stomach, cat. Scattered throughout the dense fibrous connective tissue are foci of large numbers of eosinophils and aggregates of brightly eosinophilic Splendore-Hoeppli material (at right). These areas also contain moderate numbers of macrophages and mast cells. (HE 6.3X)

typical granulation tissue at the periphery of the lesion. The fibroplasia contained variably dense infiltrates of eosinophils, mast cells, and fewer neutrophils, lymphocytes, and plasma cells. Multifocally there were necrotic foci with intralesional bacterial colonies and prominent eosinophils.

Contributor's Morphologic Diagnosis: Stomach: gastric eosinophilic sclerosing fibroplasia.

Contributor's Comment: We report a lesion in which eosinophilic inflammation is the predominant feature and which appears to be limited to the gastrointestinal tract. The presentation is typical of a feline gastrointestinal eosinophilic sclerosing fibroplasia as previously described.[1] Grossly, the lesion is an ulcerated mass at the pyloric sphincter or ileocecocolic junction which, due to the presence of dense sclerotic fibroplasias, can be clinically misdiagnosed as a neoplasm. Microscopically, the characteristic trabecular and anastomosing pattern of dense collagen which resembles osteoid, and the presence of numerous mast cells may lead to the incorrect diagnoses of osteosarcoma or sclerosing mast cell tumor. In the present case, bacteria were detected histologically at the center of necrotic foci enclosed in the submucosa. In a previous study of 25 cats[1] with similar eosinophilic sclerosing lesions, 15 had intralesional bacteria; Gram-negative rods were present in most of the lesions. On the contrary in Ozaki's *et al* study[6], gram-positive cocci (specifically, methicillin-resistant *Staphylococcus aureus*) were the most frequent. The significance is unknown. One hypothesis is to consider that bacterial organisms could initiate these lesions. However, the pyloric sphincter and ileocecocolic junction locations suggest that bacterial action could be combined with physical forces, such as mucosal foreign-body penetration. The reasons for the fibroplasia and eosinophilic response are not clear. Activated eosinophils can produce numerous mediators such as TGF-ß and IL-1 that can play a role in fibrosis by increasing extracellular matrix and fibroblast proliferation. The prominent eosinophilic infiltration in cats occurs as part of the feline eosinophilic granuloma complex or in response to a variety of stimuli, including parasites, viruses, bacteria, and fungi. *Toxoplasma gondii* was reported to cause eosinophilic fibrosing gastritis in cats.[5] An inherited eosinophilic dysregulation was also suspected in cats with eosinophilic granuloma complex, and in a recent study[1], hypereosinophilia was reported in 58% of tested cats, suggesting that genetically predisposed cats could develop eosinophilic inflammation in response to the penetration of bacteria into the gastro-intestinal wall secondary to mucosal foreign-body penetration.

JPC Diagnosis: Stomach: Necrosis, focally extensive, with marked fibrosis and eosinophilic and histiocytic inflammation.

Conference Comment: The etiopathogenesis of feline gastrointestinal eosinophilic sclerosing fibroplasia (ESF) remains controversial, with various hypotheses including sclerosing mast cell tumor (sMCT) and abcess-forming inflammatory granulation tissue with eosinophilic infiltration. It is also possible that ESF represents the common end point of any of a number of neoplastic or inflammatory processes; thus it is important to be aware of the potential differential diagnosis and diagnostic dilemmas presented by ESF.[1,2,3,4,7]

Conference participants agree with the contributor in this case and favor the diagnosis of feline gastrointestinal eosinophilic sclerosing fibroplasias (ESF), likely due to some previous inflammatory condition in the gastrointestinal tract. There is some significant slide variation, and some sections may not contain identifiable pylorus.

sMCT and ESF have several areas of major difference, including location, clinical pathology, clinical findings, survival time, and the presence of bacteria within the lesions. In sMCT, 76% of the lesions were located in the small intestine compared to only 16% for ESF. The majority of ESF cases are located mainly at the pyloric sphincter of the stomach as in this case (48%) or the ileocecocolic junction (24%). 58% of ESF had a peripheral eosinophilia, which was not reported in sMCT, and 100% of ESF had a palpable mass, compared to only 17% with sMCT. While both conditions showed spread to local lymph nodes, this only occurred in 28% of ESF cases as compared to 66% with sMCT, and there was metastasis to the liver in 66% of sMCT cases and no report of hepatic spread with ESF. Grossly, ESF presented as an ulcerated mass expanding the wall of the stomach or intestine and microabscesses or necrotic foci with cultured bacteria were present in 56% of cases and in all ileocecocolic and colonic cases, while sMCT presented as a marked transmural expansion of the small intestine by a firm, homogenous tan mass with abrupt mucosal ulceration in 58% of cases with no intralesional bacterial colonies and occasional surface colonies in ulcerated areas. The survival time with sMCT was much lower with an average of 92% of patients dead within 2 months of diagnosis compared to a variable survival time with ESF, depending on different circumstances, such as intestinal perforation or euthanasia, although cats treated with prednisone had a significantly higher survival time of up to 2 years.[1,2,3,4,7]

There are areas of similarity with these two conditions which gives rise to much of the controversy with these entities. In both conditions, there is a marked trabecular pattern of dense collagen, a heavy infiltrate of eosinophils, and the presence of mast cells (either the neoplastic component or an infiltrate of physiologic mast cells). Also, there is spread to local lymph nodes in both cases, which present as diffuse effacement of the lymph node architecture by dense collagenous trabeculae and multifocal microabscesses with ESF, and replacement of nodal architecture by neoplastic mast cells in sMCT. Both conditions have a fairly low mitotic rate, with 1 per 20 400x high power fields with sMCT and a variable number in ESF. Clinical signs were similar between each condition, which is expected, including similar rates of presentation for vomiting and weight loss.[1,2,3,4,7]

Contributor: Department of Pathology
Nantes-Atlantic National College of Veterinary Medicine
Food Science and Engineering
ONIRIS, Atlanpole – La Chantrerie
44 307 Nantes Cedex 03, France
www.oniris-nantes.fr

References:

1. Craig LE, Hardam EE, Hertzke DM, et al. Feline gastrointestinal eosinophilic sclerosing fibroplasia. *Vet Pathol.* 2009;1:63-70.
2. Gamble DA. Letter to the editor #2. *Vet Comp Oncol.* 2010;8:235-6.
3. Hasley CHC, Powers BE, Kamstock DA. Feline intestinal sclerosing mast cell tumour: 50 cases (1997-2008). *Vet Comp Oncol*. 2010;8:72-79.
4. Kamstock D, et al. Author's response. *Vet Comp Oncol.* 2010;8:236-242.
5. McConnell JF, Sparkes AH, Blunden AS, et al. Eosinophilic fibrosing gastritis and toxoplasmosis in a cat. *J Feline Med Surg.* 2007;9:82-87.
6. Ozaki K, Yamagami T, Nomura K, et al. Abscess-forming inflammatory granulation tissue with Gram-positive cocci and prominent eosinophil infiltration in cats: possible infection of methicillin-resistant Staphylococcus. *Vet Pathol*. 2003;40:283-7.
7. Schulman FY, Lipscomb TP. Letter to the editor. *Vet Comp Oncol.* 2010;8:234-5.

CASE II: 09-126 (JPC 3134341).

Signalment: Eight-year-old male golden retriever, *Canis familiaris.*

History: This dog presented in respiratory distress with a left sided systolic heart murmur and a lifelong history of generalized weakness, difficulty eating, and abnormal stance with hyperextended carpi, hock flexion, and abduction of all 4 paws. Frequent multiform ventricular premature complexes were noted during cardiology exam, as were periods of non-sustained ventricular tachycardia. This animal had survived previous bouts of both aspiration pneumonia and congestive heart failure and was treated for both based on echocardiographic and radiographic findings. The animal died during hospitalization.

Gross Pathology: The animal exhibited marked symmetrical atrophy of the masticatory, paravertebral, and proximal limb muscles resulting in pronounced bony prominences. The right middle and ventral aspects of both caudal lung lobes were red-purple, firm, and rubbery. Sections from the right middle lobe sank in 10% formalin. The heart exhibited marked dilation of both ventricles and atria and multifocal, white-tan streaks within the myocardium, especially within the interventricular septum near the apex. The muscular portions of the diaphragm were markedly thickened up to 1 cm in cross section. The proximal third of the stomach was displaced cranially into the thorax through a thick, fibrous, lax, tendinous portion of the diaphragm. The liver was enlarged and dark red with rounded margins.

Contributor's Histopathologic Description: Heart: The myocardium contains broad swaths of degenerating myofibers that contain abundant granular, basophilic material (mineral) and is multifocally replaced by coalescing bands of fibrous connective tissue with variable numbers of admixed fibroblasts and lesser amounts of mature adipose tissue. Myofibers in areas of mineralization are typically hypereosinophilic with flocculent to fragmented sarcoplasm and pyknotic nuclei (degeneration and necrosis). Small numbers of neutrophils and macrophages are occasionally present at the periphery of these mineralized areas.

Diaphragm: The diaphragm is markedly thickened. Myofiber numbers are diffusely and markedly reduced while remaining myofibers are individualized by marked fibrosis and adipose tissue deposition. Myofibers vary markedly in diameter and frequently exhibit loss of cross striations, hyalinization, and fragmentation (degeneration). Scattered myofibers contain abundant granular basophilic material (mineral) within the sarcoplasm.

Contributor's Morphologic Diagnosis: 1. Heart: myocardial mineralization and necrosis, multifocal to coalescing, moderate to marked, with moderate fibrosis.
2. Diaphragm: myocyte necrosis and loss, multifocal to coalescing, marked with marked fibrosis and fat replacement.

Contributor's Comment: The patient's widespread muscle necrosis with replacement by adipose tissue and fibrous connective tissue is consistent with Golden Retriever Muscular Dystrophy (GRMD), an animal

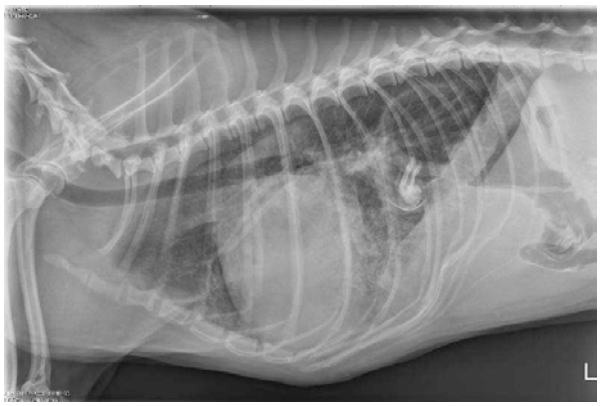

2-1. Lateral radiograph indicates generalized cardiomegaly with left atrial enlargment and an unstructured interstitial pattern that coalesces into a patchy alveolar pattern in caudoventral lung fields that is consistent with cardiogenic edema and/or pneumonia. The cranial half of the stomach is present within the thorax consistent with a hiatal hernia. Gas and a small amount of barium are present within the stomach. Photograph courtesy of the Department of Population Health and Pathobiology, College of Veterinary Medicine, North Carolina State University, 4700 Hillsborough Street, Raleigh, NC 27606 http://cvm.ncsu.edu/dphp/index.html

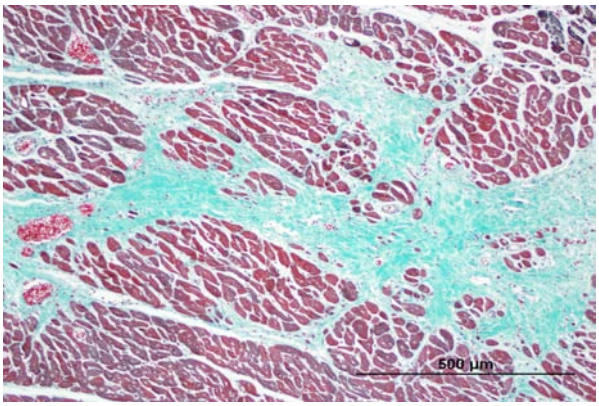

2-2. Heart, dog. Coalescing bands of fibrous connective tissue separate the cardiac myofibers. (Masson's Trichrome) Photograph courtesy of the Department of Population Health and Pathobiology, College of Veterinary Medicine, North Carolina State University, 4700 Hillsborough Street, Raleigh, NC 27606 http://cvm.ncsu.edu/dphp/index.html

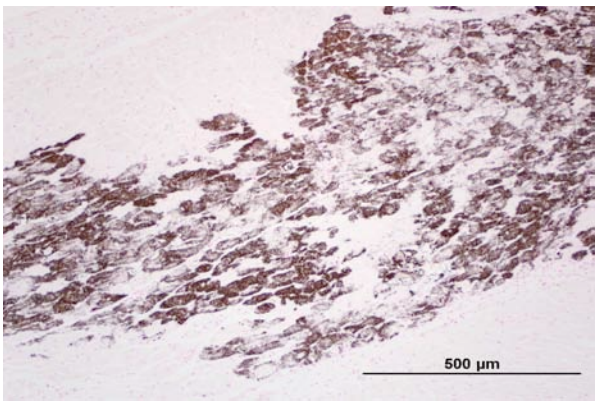

2-3. Heart, dog. Calcium deposition within broad swaths of myofibers is highlighted. (Von Kossa) Photograph courtesy of the Department of Population Health and Pathobiology, College of Veterinary Medicine, North Carolina State University, 4700 Hillsborough Street, Raleigh, NC 27606 http://cvm.ncsu.edu/dphp/index.html

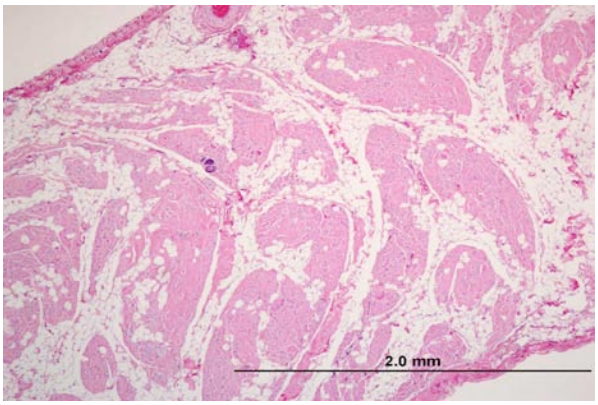

2-4. Diaphragm, dog. Myofiber numbers are markedly reduced. Remaining myofibers are individualized by marked fibrosis and adipose tissue deposition. A few myofibers contain abundant granular basophilic material (mineral) within the sarcoplasm. (HE) Photograph courtesy of the Department of Population Health and Pathobiology, College of Veterinary Medicine, North Carolina State University, 4700 Hillsborough Street, Raleigh, NC 27606 http://cvm.ncsu.edu/dphp/index.html

model for the human condition, Duchenne Muscular Dystrophy (DMD).[10-12] Both DMD and GRMD are the result of X-linked deficiencies in the cytoplasmic protein dystrophin. This protein is responsible for linking cytoplasmic actin to the transmembrane complexes of the sarcoglycans and dystroglycans, which interact with extracellular matrix components. Absence or dysfunction of dystrophin results in necrosis and regeneration of myocytes with progressive replacement by fibrous and adipose tissue. In young pups, death is thought to occur from respiratory failure following necrosis of diaphragmatic myofibers, while in older animals death frequently follows dysphagia and subsequent aspiration pneumonia or congestive heart failure.[11] This dog had evidence of aspiration pneumonia and congestive heart failure at necropsy. The role of the recent onset of ventricular arrhythmias in the animal's death was also considered. In young men with DMD, death from a combination of pneumonia and cardiovascular decompensation is common.[3]

X-linked dystrophin deficiencies have been identified in cats and a variety of dog breeds, including Irish Terrier, Samoyed, Rottweiler, Dalmation, Shetland Sheepdog, Labrador Retriever, Brittany Spaniel, Rat Terrier, Belgian Groenendael Shepherd, Schnauzer, and Spitz, but are best studied in the *mdx* mouse, German Shorthair Pointer, and Golden Retriever.[11] This particular patient was a member of the breeding colony at the National Center for Canine Models of Duchenne muscular dystrophy (NCDMD) at the University of North Carolina-Chapel Hill. As the murine models fail to show severe clinical signs or cardiac lesions comparable to those observed in humans, these canine models fill an important niche in therapeutic studies.[5,12]

Muscular dystrophies have been identified in people resulting from deficiencies or alterations of more than 30 different proteins[10] and may be X-linked, autosomal recessive, or autosomal dominant.[8] Many of these deficiencies have not yet been observed in veterinary species outside of the laboratory. Examples of spontaneous muscular dystrophies that have been identified in animals are summarized in Table 1. Other references contain a more extensive list of murine musculodystrophy models.[2,10]

Table 1. Spontaneous muscular dystrophies in veterinary species[modified from 8]

Deficient Protein (Human Disease Name)	Protein Location	Species
Laminin α_2 (Congential muscular dystrophy type 1A) (RC)	Extracellular Matrix	Dog[8] Cat[4,6,8] *dy/dy* mouse[8,9]
α-, β-, γ-, or δ-sarcoglycan (Limb-girdle muscular dystrophy types 2C-F)	Transmembrane	Dog[1,10] Cat[7] BIO14.6 hamster[10]
Dysferlin (Limb-girdle muscular dystrophy type 2B)	Transmembrane	SJL-*Dysf* mouse[9]
Dystrophin (Duchenne muscular dystrophy, Becker muscular dystrophy)	Cytoskeleton	Dog Cat *mdx* mouse[8,11]

2-5. Diaphragm, dog. Higher magnification shows marked fibrosis separating myocytes of variable diameter. (HE) Photograph courtesy of the Department of Population Health and Pathobiology, College of Veterinary Medicine, North Carolina State University, 4700 Hillsborough Street, Raleigh, NC 27606 http://cvm.ncsu.edu/dphp/index.html

JPC Diagnosis: 1. Heart, myocardium: Degeneration, necrosis, and loss, multifocal, with myocardial fibrosis and mineralization.
2. Diaphragm: Myofiber atrophy and loss, diffuse, moderate with myocyte atrophy and marked fatty infiltration.

Conference Comment: Dystrophin-dependent muscular dystrophy is confirmed immunohistochemically by the absence of dystrophin staining, or by Western blot analysis. Although muscle atrophy is the usual course in dystrophin-dependent muscular dystrophy, marked muscular hypertrophy of unknown cause is seen in mice, cats, and rat terrier dogs. Clinical pathology changes include a marked increase in serum creatinine kinase (CK) and aspartate aminotransferase (AST) in neonates; these continue to rise until 6 months of age. Serum CK and AST levels in older dogs are elevated to a lesser extent. Clinical signs of neuromuscular weakness progress until 8-12 months of age before stabilizing. Affected dogs exhibit a stiff-legged gait, thickened muscles at the base of the tongue, excessive drooling, abdominal breathing, and ribcage deformities due to contracture of the diaphragm. In some breeds, such as the rat terrier, there is paradoxical muscle hypertrophy of the thighs, neck, and shoulders. Female carriers are clinically normal but have elevated serum CK and AST.[13]

Gross lesions include severe degeneration indicated by pale streaks in the diaphragm, trapezius and sartorius muscles. In chronic cases, the diaphragm is thickened, contracted, and fibrotic. In the heart, the left ventricular wall and right side of the interventricular septum are most severely affected by necrosis, mineralization, and fibrosis. Common histologic findings not seen in this case are the presence of swollen and dark-staining fibers ("large dark fibers"), which represent the earliest stages of degeneration. Muscle fiber necrosis is due to the influx of calcium through defects in the sarcolemma. The basal lamina of necrotic fibers is preserved, leaving an empty sarcolemmal tube capable of fully regenerating the myofibers.[13]

Other common examples of muscular dystrophy in veterinary species include X-linked muscular dystrophy in mixed-breed cats, which have similar clinical, gross, and histologic findings to those seen in dogs. Cats with muscular dystrophy are also prone to develop malignant hyperthermia associated with restraint or general anesthesia. Unlike the canine condition, cardiac involvement in cats is not common. Merino sheep have an autosomal recessive muscular dystrophy, and skeletal muscle of affected sheep expresses normal dystrophin. The major gross feature is the replacement of the intermedius, soleus, anconeus, and medial head of the triceps with mature adipose tissue. This disorder only affects type 1 muscle fibers, with initial lesions of type 1 fiber hypertrophy followed by myofibril loss and formation of sarcoplasmic masses at the center or periphery of the cell. Some fibers develop peripheral annular fibrils known as "ringbinden". This condition is a result of loss of alpha-actinin and desmin proliferation, which forms the sarcoplasmic masses. It is important to distinguish true muscular dystrophies, which are inherited progressive myopathies, from other muscle disorders such as secondary nutritional degenerative myopathies.[13]

There are four categories of reaction to muscle injury. Focal monophasic reactions result from an isolated single event; multifocal monophasic reactions result from a single injurious event that causes widespread lesions in the same phase of injury; focal polyphasic reactions are due to repeated mechanical injury at the same location; and multifocal polyphasic reactions are the result of continuous injury over a prolonged period of time such that lesions are widespread and exhibit various pathologic changes ranging from degeneration to necrosis to regeneration.[13] This case is an example of a multifocal polyphasic (multiphasic) muscle lesion.

Contributor: North Carolina State University
Department of Population Health and Pathobiology
College of Veterinary Medicine
4700 Hillsborough Street
Raleigh, NC 27606
http://cvm.ncsu.edu/dphp/index.html

References:

1. Deitz K, Morrison JA, Kline K, et al. Sarcoglycan-deficient muscular dystrophy in a Boston terrier. *J Vet Intern Med*. 2008;22:476-480.
2. Durbeej M, Campbell KP. Muscular dystrophies involving the dystrophin-glycoprotein comples: an overview of current mouse models. *Curr Opin Genet Dev*. 2002;12:349-61.
3. Emery AE. The muscular dystrophies. *Lancet*. 2002;359:687-695.
4. Gaschecn F, Jaggy A, Jones B. Congenital diseases of feline muscle and neuromuscular junction. *J Feline Med Surg*. 2004;6:355-366.
5. Khurana TS, Davies KE. Pharmacological strategies for muscular dystrophy. *Nature Reviews: Drug Discovery*. 2003;2:379-390.
6. Poncelet L, Resibois A, Engvall E, et al. Laminin α2 deficiency-associated muscular dystrophy in a Maine coon cat. *J Small Anim Pract*. 2003;44:550-552.
7. Salvadori C, Vattemi G, Lombardo R, et al. Muscular dystrophy with reduced β-sarcoglycan in a cat. *J Comp Path*. 2009;140:278-282.
8. Shelton GD, Engvall E. Muscular dystrophies and other inherited myopathies. *Vet Clin North Am Small Anim Pract*. 2002;32:103-124.
9. Shelton GD, Engvall E. Canine and feline models of human inherited muscle disease. *Neuromuscul Disord*. 2005;15:127-138.
10. Vainzof M, Ayub-Guerrieri D, Onofre PC, et al. Animal models for genetic neuromuscular diseases. *J Mol Neurosci.* 2008;34:241-248.
11. Valentine BA, McGavin MD. Skeletal muscle. In: McGavin MD, Zachary JF, eds. *Pathologic Basis of Veterinary Disease*. 4th ed. St. Louis, MO: Elsevier; 2007:1026-1029, 1035-1037.
12. Valentine BA, Winand NJ, Pradhan D, et al. Canine X-linked muscular dystrophy as an animal model of Duchenne muscular dystrophy: a review. *Am J Med Genet*. 1992;42:352-356.
13. Van Vleet JF, Valentine BA. Muscle and tendon. In: Maxie MG, ed. *Jubb, Kennedy and Palmer's Pathology of Domestic Animals*. Vol. 1. 5th ed. Philadelphia, PA: Elsevier; 2007:198-9, 210-16.

CASE III: 09-565-3 (JPC 3136038).

Signalment: Adult merino sheep of unidentified gender, (*Ovis orientalis aries*) ovine.

History: This animal was one of multiple affected animals from a flock in Narrogin, Western Australia, submitted in March 2009. The animals had been turned out onto a lupin and wheat paddock (presumptive stubble) approximately six weeks previously (January 2009). Multiple animals were displaying signs of marked lethargy and weakness. Ten sheep were recumbent and unable to rise and were subsequently euthanized.

Gross Pathology: A post mortem examination was conducted on one of the affected animals in the field by the local veterinarian, who subsequently submitted both fresh liver and formalin fixed tissues to the Western Australian Department of Agriculture and Food for examination. The veterinarian reported extremely dry ruminal contents (suggesting dehydration) and the presence of peritoneal and pleural "proteinaceous" effusions. The liver was reportedly small with a yellow tinge and the kidneys appeared very dark.

Laboratory Results: Aerobic and anaerobic culture performed on the samples of fresh liver yielded no growth.

Contributor's Histopathologic Description: The hepatic architecture is diffusely disrupted by increased fibrous tissue surrounding portal triads, with fine septa ramifying outwards, distorting the lobular architecture and dissecting the hepatic plates resulting in isolation of small clusters of hepatocytes with occasional individualisation. Numerous hepatocytes appear swollen with moderate to marked anisocytosis and there are numerous mitotic figures, many of which appear abnormal, often arrested in metaphase. There are occasional scattered shrunken hypereosinophilic hepatocytes with condensed nuclei, consistent with apoptosis. Mild, diffuse bile duct proliferation is also apparent. Low numbers of lymphocytes, macrophages and neutrophils are present, particularly periportally. Modest numbers of canaliculi contain bile plugs. Also scattered throughout the hepatic parenchyma are

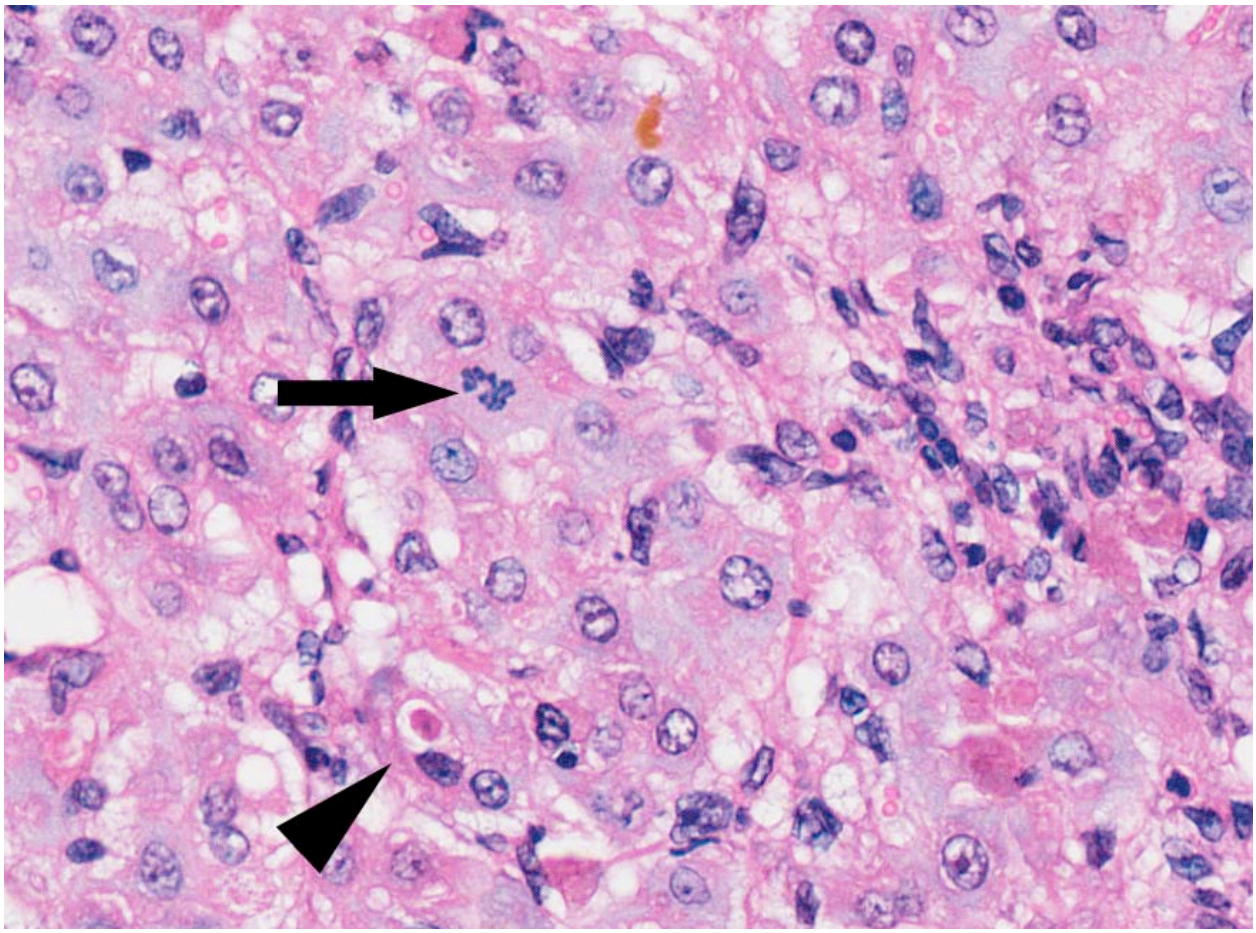

3-1. Liver, sheep. Marked disruption of hepatocellular architecture with nodulear regeneration, bile plugs, necrotic, rounded up hepatocytes (arrowhead), and mitotic figure (arrow), changes consistent with phomopsin toxicosis in the small ruminant. (HE 350X)

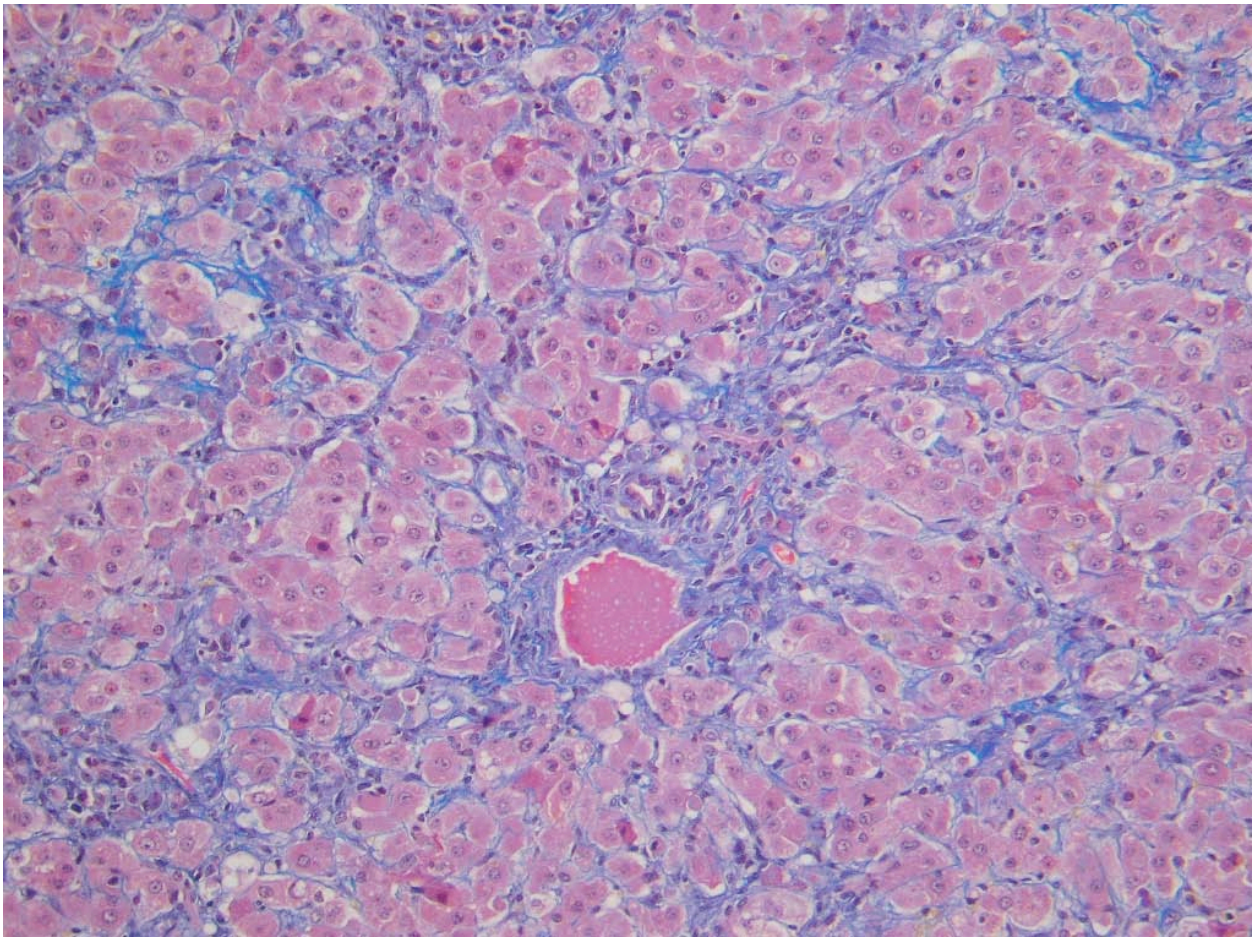

3.2. Liver, sheep. A Masson's trichrome stain demonstrates the amount of fibrous connective tissue within the section, which is difficult to appreciate on the HE stain. Photograph courtesy of the Department of Anatomic Pathology, Murdoch University School of Veterinary and Biomedical Sciences, Faculty of Health Sciences. South Street, Western Australia, Australia, 6150. http://www.vetbiomed.murdoch.edu.au/ in conjunction with the Department of Agriculture and Food, Government of Western Australia, South Perth, Western Australia, Australia, 6951. http://www.agric.wa.gov.au/PC_92812.html

occasional cells (hepatocytes and Kupffer cells +/- macrophages) with faint intracytoplasmic yellow-golden brown granular pigment. Shikata's Orcein and Schmorl's stains demonstrated this pigment to be a mix of copper and lipofuscin (+/- ceroid), respectively. A Perl's Prussian blue also demonstrated the presence of a minimal amount of iron.

Contributor's Morphologic Diagnosis: Liver: Moderate, diffuse, chronic hepatocellular dysplasia and dissecting portal fibrosis, with mild cholestasis, biliary hyperplasia and intracytoplasmic pigment accumulation.

Contributor's Comment: The history, clinical signs, reported necropsy findings and histopathological changes observed in the liver of this sheep are consistent with the syndrome of chronic phomopsin poisoning, which is also widely referred to as lupinosis. Lupinosis is a mycotoxicosis seen in animals ingesting lupin stubble or seed (*Lupinus* spp.) infected with the fungus *Diaporthe toxica* (anamorph *Phomopsis* sp.). *Diaporthe woodii* (anamorph *Phomopsis leptostromiformis*) was originally (and incorrectly) thought to be the source of the causative toxins.[6,11] *Diaporthe toxica* is parasitic on green lupins, and grows saprophytically on the dead host,[2,9] and produces a number of different toxins, the best known of which are the phomopsins A, B & C.[8] These compounds are hexapeptides, and appear to act predominately on the hepatic parenchyma, where they bind to tubulin and inhibit microtubule polymerization leading to progressive loss of microtubules. This in turn disrupts mitosis, resulting in mitotic arrest in metaphase and commonly fatty infiltration.[1] It is important to note that this disease is a distinct entity from the disease known as lupine poisoning, which causes acute neurological signs and results from the ingestion of lupines containing quinolizidine alkaloids.[7,9] Lupinosis most commonly occurs in sheep, but also occurs in cattle, and, rarely, in horses and pigs.[4,7] Outbreaks of the disease are most common in countries where lupins are eaten as a dead standing crop or grazed as stubble, a situation most often seen in

Australia. Lupinosis occurs occasionally, but not commonly, in South Africa and New Zealand.[4]

Clinically, a variety of clinical syndromes are observed, dependent on the species involved, the dose of toxin and the duration of exposure.[2,6,8] In sheep, acute lupinosis occurs when animals graze highly toxic stubbles over a short period. Clinical signs include anorexia, lethargy, weakness and jaundice. Rarely, hepatic encephalopathy or photosensitization is observed. Clinical signs are typically seen within two days of introduction to stubble. Most animals within a flock are affected and deaths occur within three or four days.[7] Chronic lupinosis occurs following the ingestion of low doses of toxins over a prolonged period. Variable numbers of sheep within a flock are affected and animals are typically weak and in poor body condition. Jaundice may or may not be apparent, and those sheep that are jaundiced are commonly anemic. Mortality rates are low. The disease course may also be subacute and intermediate in severity, and it is this form of the disease that is most commonly observed in Australia.[8] A toxin-related nutritional myopathy has also been reported in association with lupinosis, which may or may not respond to supplementation with vitamin E or selenium.[8] Experimental phomopsin toxicity has been shown to reduce reproductive performance also.[7]

On gross examination, livers from acutely affected sheep are enlarged and frequently discolored yellow or tan, with histological examination revealing variable degrees of hydropic change and an increased rate of hepatocyte loss (from widespread apoptosis). The degree of fatty change is variable and depends largely on the nutritional status of the animal. As the disease course progresses, increased, but ineffective mitotic activity becomes evident with the presence of numerous arrested mitoses. Progressive hepatic fibrosis occurs and there is accumulation of complex granular pigment within macrophages in the affected tissue, and may include any combination of copper, ferric iron, ceroid or lipofuscin. Variable degrees of portal hyperplasia may also be present.[6,9] Some of these changes, including hepatic fibrosis and biliary hyperplasia, can also be observed in other hepatotoxicities including pyrrolizidine alkaloid and aflatoxicosis. As in phomopsin toxicity, these toxins inhibit normal mitosis, and DNA replication frequently continues resulting in the production of greatly enlarged hepatocytes (megalocytosis). In Australia, sheep grazing lupin stubble may also be concurrently exposed to plants containing pyrrolizidine alkaloids such as heliotrope (*Heliotropium europaeum*), which may result in additive or synergistic hepatotoxity.[2]

Lupinosis has been largely eliminated in Australia by the breeding of *Phomopsis*-resistant lupins, and is seen now in years with late finishes and/or increased summer rainfall.

JPC Diagnosis: Liver: Hepatocellular degeneration and necrosis, diffuse, moderate, with fibrosis, intracanalicular cholestasis, Ito cell hyperplasia, and prominent hepatocellular mitotic activity.

Conference Comment: A few other noteworthy histologic features in this case include a decrease in the lobule size and a decrease in the distance separating central and portal areas, reflecting hepatocyte necrosis and atrophy. Other potential toxic causes for this lesion would include aflatoxin, which may present with more hepatic regeneration, bridging portal fibrosis, biliary hyperplasia and hemorrhagic necrosis, with maintenance of hepatic trabeculae; sporidesmin, a mycotoxin which targets biliary epithelium and causes necrosis; microcystin, a toxin of blue-green algae, which causes disassociation of centrilobular hepatocytes and submassive hepatic necrosis and hemorrhage; and pyrrolizidine alkaloids, which also cause bridging fibrosis, biliary hyperplasia, and megalocytosis.[9] Sheep appear to have increased resistance to pyrrolizidine alkaloid intoxication compared with other species.

The contributor mentioned the possibility of photosensitization in acute phomopsin toxicosis. Photosensitization appears as erythema, dermal edema, vesicle or bullae formation, exudation and extensive epidermal necrosis. There are three types of photosensitization. Type I, or primary photosensitization, occurs from ingestion of a plant or drug containing photoreactive substances, which are deposited in the skin. Type II photosensitization occurs in animals with a genetic inability to metabolize heme pigments, which results in a buildup of the photoreactive hematoporphyrin pigments, such as uroporphyrin I, coproporphyrin I, and protoporphyrin III. Type III, or hepatogenous photosensitization, occurs with an abnormal buildup of phylloerythrin, which is a degradation product of chlorophyll, because of a damaged or immature liver. The photosensitization in this case is type III and is secondary to cholestasis.[3] In cattle, phomopsin toxicity causes anorexia and ketosis in pregnant or lactating cows, and chronic exposure leads to fibrotic hepatitis with nodular regeneration (cirrhosis).[9]

The toxic principles of true lupinosis (not to be confused with phomopsin toxicosis) are quinolizidine alkaloids, which causes nicotinic effects such as salivation, ataxia, seizures, and dyspnea, and the alkaloid anagyrine, which causes arthrogryposis in calves and lambs following *in utero* exposure.[5,10]

Contributor: Murdoch University
Department of Anatomic Pathology
School of Veterinary and Biomedical Sciences
Faculty of Health Sciences
South Street
Western Australia, Australia, 6150
http://www.vetbiomed.murdoch.edu.au/
in conjunction with the Department of Agriculture and Food
Government of Western Australia
South Perth
Western Australia, Australia, 6951
http://www.agric.wa.gov.au/PC_92812.html

References:

1. Allen JG. Recent advances with cultivated lupins with emphasis on toxicological aspects. In: James LF, Keeler RF, Bailey EM, Cheeke PR, Hegarty MP, eds. *Poisonous Plants: Proceedings of the Third International Symposium*. Ames, IA: Iowa State University Press; 1992:229-233.
2. Cheeke PR. Toxins in protein supplements and grain legumes. In: *Natural Toxicants in Feeds, Forages, and Poisonous Plants*. 2nd ed. 1998;163–193.
3. Ginn PE, Mansell JEKL, Rakich PM. Skin and appendages. In: Maxie MG, ed. *Jubb, Kennedy and Palmer's Pathology of Domestic Animals*. Vol. 1. 5th ed. Philadelphia, PA: Elsevier; 2007:623-6.
4. Kellerman TS, Coetzer JAW, Naudé TW. *Plant Poisonings and Mycotoxicoses of Livestock in Southern Africa.* Cape Town, South Africa: Oxford University Press; 1988;27-29.
5. Maxie MG, Youssef S. Nervous system. In: Maxie MG, ed. *Jubb, Kennedy and Palmer's Pathology of Domestic Animals*. Vol. 1. 5th ed. Philadelphia, PA: Elsevier; 2007:247.
6. Peterson JE, Jago MV, Payne AL, et al. The toxicity of phomopsin for sheep. *Aust Vet J.* 1987;64:293–298.
7. Radostits OM, Gay CC, Done SH, et al. *Diseases associated with toxins in plants, fungi, cyanobacteria, plant-associated bacteria, and venoms in ticks and vertebrate animals*. 10th ed. Philadelphia, PA: Saunders; 2007;1906–1908.
8. Seawright AA. Mycotoxins and mycotoxicoses. In: *Animal Health in Australia: Chemical and Plant Poisons*. Vol. 2. 2nd ed. Canberra, Australia: Australian Government Publishing Service;1989;173-177.
9. Stalker MJ, Hayes MA. Liver and biliary system. In: Maxie MG, ed. *Jubb, Kennedy and Palmer's Pathology of Domestic Animals*. Vol. 2. 5th ed. Philadelphia, PA: Elsevier; 2007:370-376.
10. Thompson K. Bones and joints. In: Maxie MG, ed. *Jubb, Kennedy and Palmer's Pathology of Domestic Animals*. Vol. 1. 5th ed. Philadelphia, PA: Elsevier; 2007:61.
11. Williamson PM, Highet AS, Gams W, et al. *Diaporthe toxica* sp. nov., the cause of lupinosis in sheep. *Mycol Res.* 1994;98:1364–1368.

CASE IV: NCAH 2011-1 (JPC 4003053).

Signalment: Adult female beef ox, (*Bos taurus*).

History: Gross lesions were identified during the postmortem inspection of the carcass at slaughter. Lymph node samples were submitted for laboratory evaluation through the United States Department of Agriculture (USDA), Bovine Tuberculosis Eradication Program. Due to the gross lesions, the carcass was condemned (not used for human consumption).

Gross Pathology: The carcass was in normal body condition. The left parotid lymph node, and to a lesser degree the adjacent lymph nodes of the head, contained irregularly shaped areas which were discolored green. On cut surface, patchy areas of green extended into both the cortex and medulla. The facial musculature adjacent to the parotid lymph node, the tracheobronchial lymph nodes, and mediastinal lymph nodes were also multifocally green.

Contributor's Histopathologic Description: Lymph node: Large coalescing aggregates of macrophages and epitheloid macrophages with abundant eosinophilic cytoplasm expand the cortical and medullary sinuses. Numerous algal cells with low numbers of eosinophils, multinucleate giant cells, lymphocytes and plasma cells are intermixed with the macrophages. The algal cells are round, 7 to 15 microns in diameter, have a thin refractile cell wall, single basophilic round nucleus and amphophilic to eosinophilic granular cytoplasm. Low numbers of larger algal cells (sporangia) are filled with 2 to 6 daughter cells (sporangiospores or endospores). Intact algal cells and empty cell walls with no internal structures (degenerate algal cells) are both free in the sinuses and within macrophages. Within the cortex, there are few lymphoid follicles.

Contributor's Morphologic Diagnosis: Lymph Node: Lymphadenitis, granulomatous, severe, diffuse, chronic, with large numbers of algal organisms consistent with green algae.

Contributor's Comment: Algal infections are uncommon opportunistic pathogens of domestic and wild mammals and humans.[1] Culture is frequently required to make a definitive etiologic diagnosis, but even with culture, the precise genus and species of green algal infections have not always been clearly identified.[1] *Chlorella* spp. are commonly cited as the etiology of green algal infections, but it is important to note that not all green algal infections are due to *Chlorella* spp.[3,6]

Green algal infections have been described most commonly in sheep and in cattle, with individual case reports in a dog, man and several species of wild mammals.[1,4,5] The algae are found commonly throughout the world and infections have been associated with stagnant water or pasture irrigated with raw sewage.[5] Disease varies from subclinical with a localized lymphadenitis to severe clinical disease and systemic lesions.[1,2,5] Underlying immunosuppression or an overwhelming infectious dose are possible predisposing factors to causing disease by this ubiquitous organism.[5] Our case is consistent with one of the largest reports (a group of 8 cattle cases) in which green algae induced lymphadenitis was identified through postmortem slaughter inspection.[6] Green algal infections are also identified several times a year in cattle by the USDA Food Safety Inspection Service pathology laboratory, which receives samples from federally inspected slaughter facilities (S Hafner, personal communication).

Based on the lesion and organism morphology on HE stained slides, the primary differential diagnoses

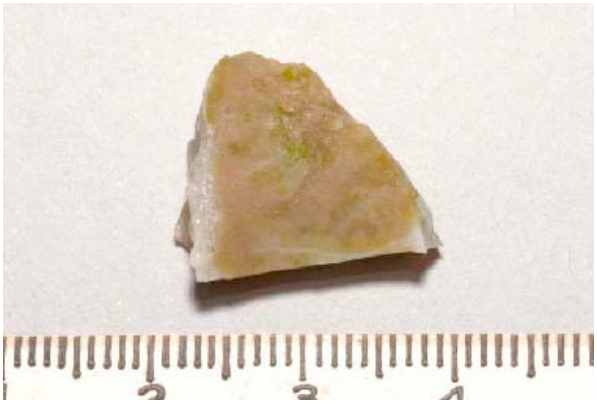

4-1. Lymph node, ox. The left parotid lymph node, and to a lesser degree the adjacent lymph nodes of the head contained irregularly shaped areas which were discolored green. Photograph courtesy of the National Centers for Animal Health, 1920 Dayton Avenue, Ames, IA 50010. http://www.aphis.usda.gov/animal_health/lab_info_services/about_nvsl.shtml

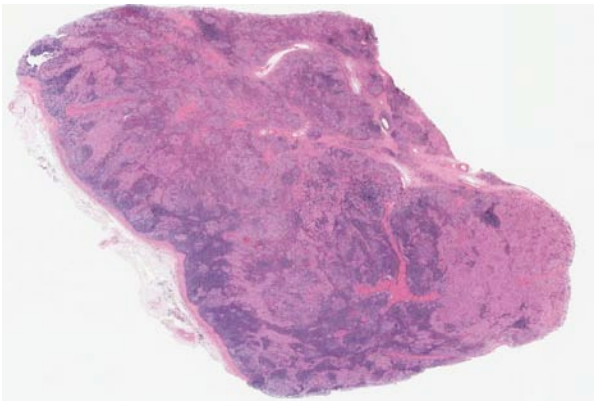

4-2. Lymph node, ox. The normal nodal architecture is effaced by multifocal to coalescing areas of granulomatous inflammation. (HE 6X)

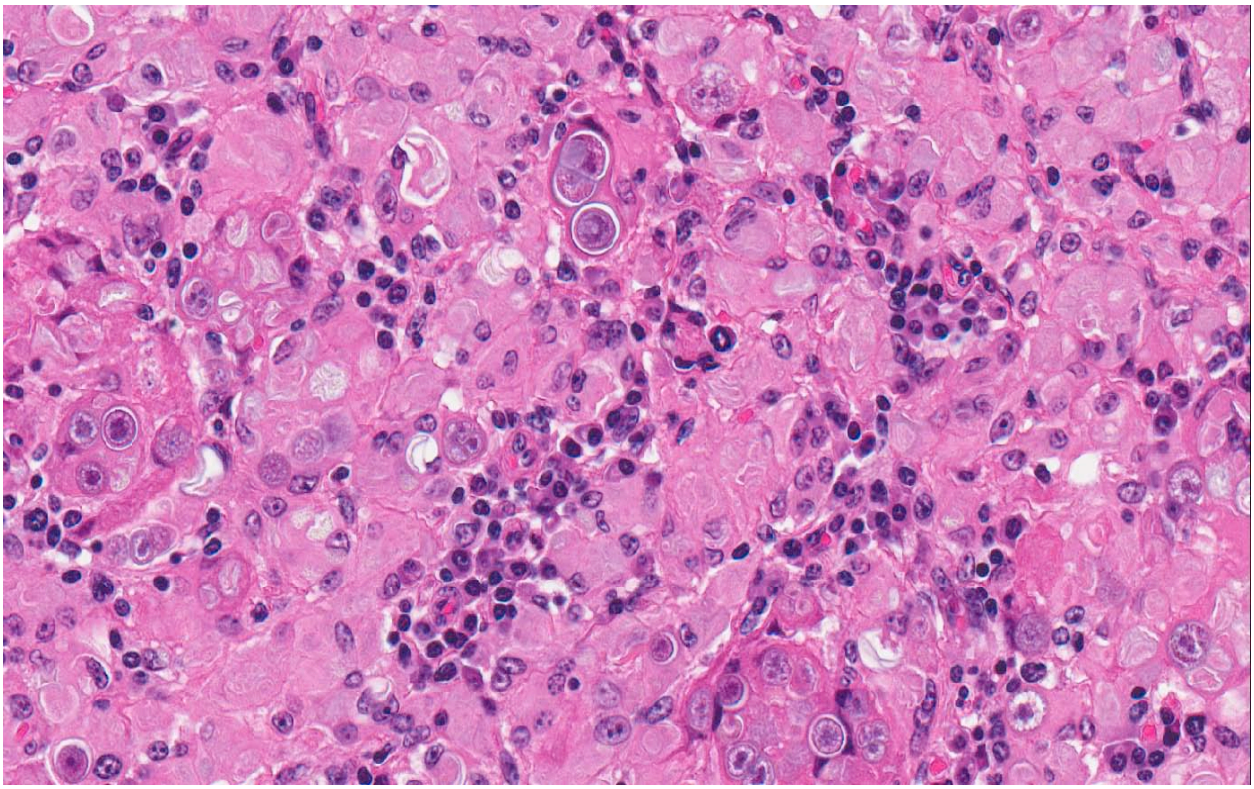

4-3. Lymph node, ox. Epithelioid macrophages and multinucleate giant cell macrophages contain numerous Chlorella algal cells, as well as multinucleated endosporulating sporangia (small arrows), and degenerate forms consisting primarily of a collapsed cell wall (large arrow). (HE 400X)

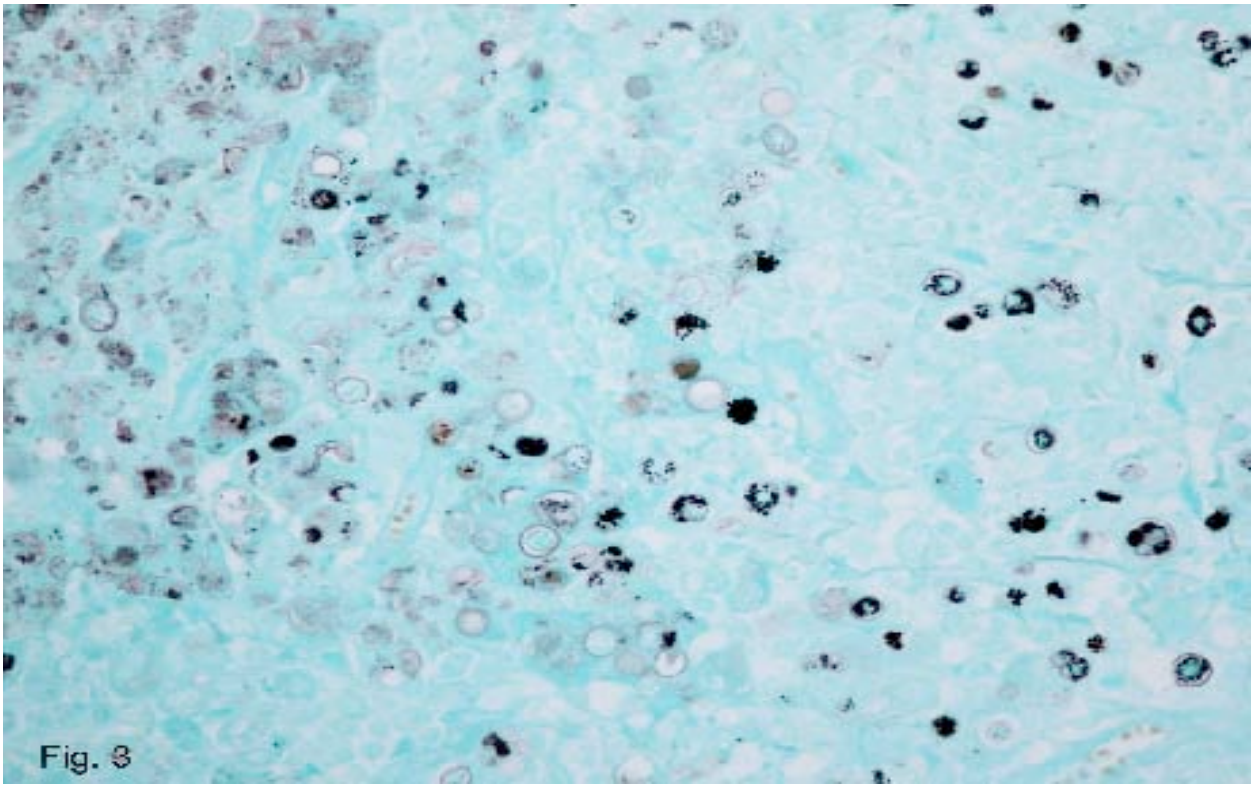

4-4. Lymph node, ox. The large silver-positive granules are helpful in differentiating Chlorella from Prototheca, according to Chandler. (Gomori Methenamine Silver). Photograph courtesy of the National Centers for Animal Health, 1920 Dayton Avenue, Ames, IA 50010.

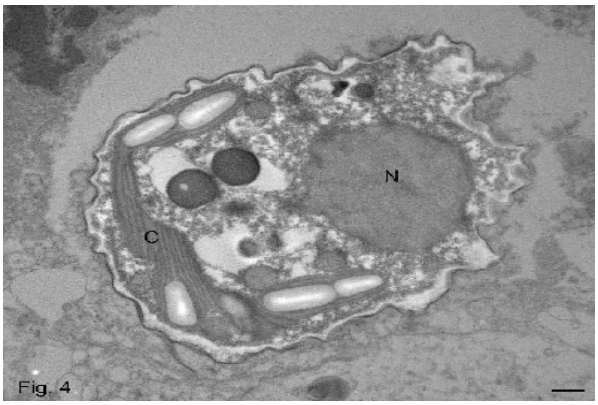

4-5. Lymph node, ox. Transmission electron micrograph. Single algal cell with round nucleus (N) and a large chloroplast (C). Lead citrate and uranyl acetate. Bar = 500 nm. Photograph courtesy of the National Centers for Animal Health, 1920 Dayton Avenue, Ames, IA 50010.

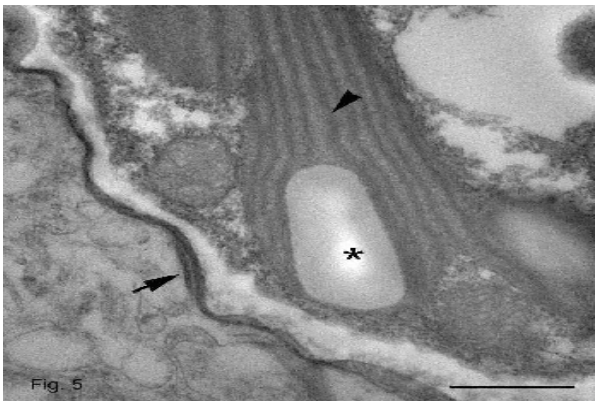

4-6. Lymph node, ox. Transmission electron micrograph. Within the chloroplast is a starch granule (asterisk) and thylakoids (arrowhead). The thylakoids form parallel stacks termed grana. Cell wall (arrow). Lead citrate and uranyl acetate. Bar = 500 nm. Photograph courtesy of the National Centers for Animal Health, 1920 Dayton Avenue, Ames, IA 50010. http://www.aphis.usda.gov/animal_health/lab_info_services/about_nvsl.shtml

include various types of green algae and *Prototheca* spp. Protothecosis occurs more commonly than disease by green algae and *Prototheca* spp. are achlorous, which is a key criteria for differentiating green algae from *Prototheca* spp.[1,5] Chandler et. al.[1] uses three criteria for differentiating *Chlorella* (a type of green algae) from *Prototheca* spp. and for making a presumptive diagnosis. In chlorellosis there are: 1) grossly visible green discoloration of the tissues due to the presence of chlorophyll in the algae, 2) spherical algal cells, with an average diameter of 9 microns that exhibit endosporulation, and 3) algal cells that have abundant large cytoplasmic granules that are strongly positive with PAS, GF, and GMS stains.[1] Other methods used to differentiate the two include impression smears of fresh tissue and transmission electron microscopy, both of which are based on the presence of numerous chlorophyll/chloroplasts.[1,5] It is important to remember that the green color of the *Chlorella* algae is lost during tissue fixation and processing.[1]

JPC Diagnosis: Lymph node: Lymphadenitis, granulomatous, diffuse, moderate to marked with numerous intrahistiocytic and extracellular endosporulating algae and moderate plasmacytosis.

Conference Comment: The contributor provided an excellent discussion of *Chlorella* spp. and the associated pathology. Conference participants discussed the differences between *Chlorella* and *Prototheca*, and the difficulties in differentiating the two entities by standard histologic methods.

In addition to *Chlorella* and *Prototheca,* other pathogens that reproduce asexually by endosporulation include *Rhinosporidium seeberi* and *Coccidioides immitis*.

Contributor: National Centers for Animal Health
National Animal Disease Center
Bacterial Diseases of Livestock Unit
1920 Dayton Ave
Ames, IA 50010

References:

1. Chandler FW, Kaplan W, Ajello L. Protothecosis and infections caused by morphologically similar green algae. In: Color Atlas and Text of the Histopathology of Mycotic Diseases. Chicago, IL: Year Book Medical Publishers; 1980;96-100.
2. Cordy DR. Chlorellosis in a lamb. *Vet Pathol*. 1973;10:171-176.
3. Haenichen T, Facher E, Wanner G, et al. Cutaneous chlorellosis in a gazelle (*Gazella dorcas*). *Vet Pathol*. 2002;39:386-389.
4. Quigley RR, Knowles KE, Johnson GC. Disseminated chlorellosis in a dog. *Vet Pathol*. 2009;46:439-443.
5. Ramirez-Romero R, Rodriguez-Tovar LE, Nevarez-Garza AM, et al. Chlorella infection in a sheep in Mexico and minireview of published reports from humans and domestic animals. *Mycopathologia*. 2010;169:461-466.
6. Rogers RJ, Connole MD, Norton J, et al. Lymphadenitis of cattle due to infection with green algae. *J Comp Path*. 1980;90:1-9.

Joint Pathology Center
Veterinary Pathology Services

WEDNESDAY SLIDE CONFERENCE 2011-2012

Conference 16

29 February 2012

CASE I: 09.6781/09.1998 (JPC 3135245).

Signalment: Age unknown (adult) male silver carp (*Hypophthalmichthys molitrix*).

History: Abnormal growth noted in both eyes over a period of several months; left eye enucleated 2 months prior to enucleation of the right eye.

Gross Pathology: A 1cm diameter homogenous, soft white-tan mass occupies the vitreous, posterior and part of the anterior chamber in both globes, obscuring the lenticular and iridial structures.

Contributor's Histopathologic Description: 109.001998 Left eye: Six sections of the globe are examined (slides A-C). There is a densely cellular, poorly circumscribed population of neoplastic cells filling the anterior and posterior chambers and vitreous. Neoplastic cells are dimorphic: the first population is spindloid with a small amount of fibrillar eosinophilic cytoplasm, a large oval nucleus with finely stippled chromatin and infrequent visible nucleoli. Mitotic figures average six per ten high power fields. The second neoplastic cell population is composed of well differentiated neurons, and this population is scattered throughout the fibroblastic

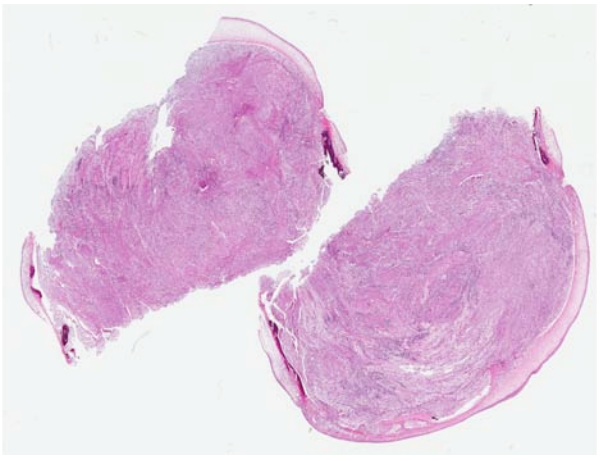

1-1. Globe, silver carp: The anterior chamber and vitreous, sclera, uvea, choroid, and even the cornea is infiltrated by a densely cellular neoplasm composed of broad streams and bundles. (HE 40X)

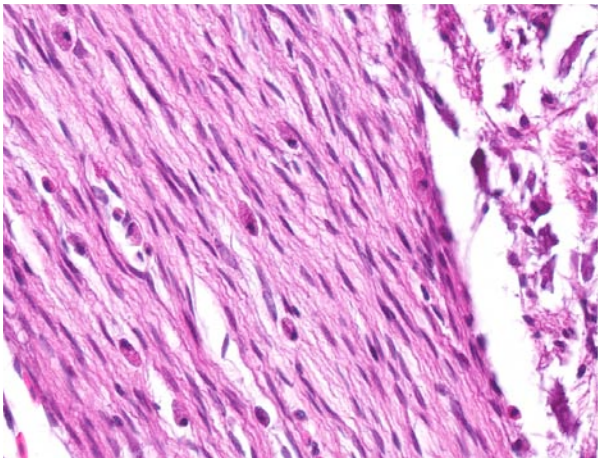

1-2. Globe, silver carp: Bland spindle cells are the primary cell population; mitoses are rare. (HE 400X)

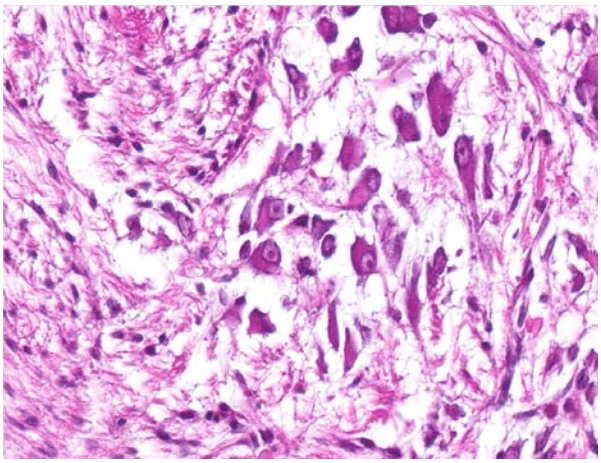

1-3. Globe, silver carp: A second neoplastic cell type are large polygonal cells resembling neurons. (HE 400X)

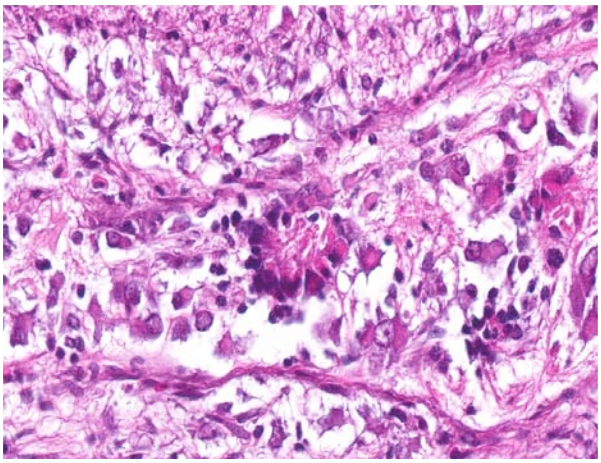

1-4. Globe, silver carp: Small triangular cells with apical nuclei form prominent rosettes (neuroblasts). (HE 400X)

neoplastic cell population. Neoplastic cells are arranged in thick interlacing fascicles and are infiltrated by a diffuse population of heterophils and macrophages. Neoplastic cells dissect through the stroma of the cornea and sclera.

109.006781 Right eye: One section of completely excised tissue is examined. The architecture of the iris, ciliary body and lens is diffusely effaced by a poorly circumscribed population of neoplastic cells that fills the vitreous body and protrudes into the anterior chamber. Neoplastic cells are dimorphic: the first population is spindloid with tapered cell borders, a moderate amount of fibrillar eosinophilic cytoplasm and a large elongate nucleus with stippled chromatin. These neoplastic cells are arranged in thick interlacing fascicles. Interspersed within this population of neoplastic spindle cells, there is a subpopulation of polyhedral to stellate neoplastic cells with abundant eosinophilic cytoplasm, a large eccentric nucleus with a fine chromatin pattern and prominent eosinophilic nucleolus. Mitotic figures average three per ten high power fields for all neoplastic cell types. Neoplastic cells invade the lens capsule and disrupt the lens, and there is moderate histiocytic and lymphoplasmacytic inflammation surrounding the lens fragments.

Contributor's Morphologic Diagnosis: Left and right globes: Ganglioneuroma.

Contributor's Comment: A diagnosis of ganglioneuroma is made based on the presence of the well differentiated neuronal and spindle neoplastic cell populations within the mass. Reported tumors of nerve cell origin within the peripheral nervous system of fish are rare and include schwannomas, neurilemmomas, retinoblastomas and ganglioneuromas. Ganglioneuromas are associated with spinal ganglia in both marine and freshwater species, and are typically reported within body cavities[6] and in association with gill filaments and the root of the tail fin.[1] These tumors are soft, pale and whitish and sometimes lobulated. The histologic features of this tumor include a classic single or grouped neoplastic ganglion cell with prominent vesicular chromatin and eosinophilic nucleoli, separated by interlacing fascicles of spindle neoplastic cells. Unlike retinoblastomas, ganglioneuromas do not exhibit rosette formation, and unlike schwannomas, they contain neuronally differentiated cells. Neoplasms of the retina in fish have been reported in association with exposure to methylazoxymethanol experimentally.[2,5] The species in which this tumor more frequently occurs include cats, pigs, cattle, dogs and horses, as well as reports of cockatiels and rats. The bilateral origin of the tumor in this case suggests an underlying genetic predisposition, which may be analogous to that of retinoblastomas.

Immunohistochemical staining with GFAP and vimentin was performed. Few foci of cellular processes within the spindloid cell population in the neoplasm were positive for GFAP, and there was positive internal control staining within the optic nerve. Vimentin staining, however, was negative for neuronal and spindle cells and there was no positive internal control staining within the optic nerve or elsewhere in the tissue.

JPC Diagnosis: Eye, globe: Ganglioneuroblastoma.

Conference Comment: The differential diagnoses proposed by conference participants included neuroblastoma, ganglioneuroma, and ganglioneuroblastoma. Neuroblastomas are derived from neural crest cells, may metastasize, and common sites include the adrenal medulla and sympathetic ganglia. Ganglioneuromas may arise from primitive neuroepithelial cells which exhibit neuronal differentiation and usually exhibit a benign behavior.

Common sites include the neuraxis, autonomic and cranial nerve ganglia, and adrenal medulla.

Conference participants felt that there were three distinct cell populations in this particular neoplasm, including the spindle cells, ganglion cells, and neuroblast cells with carrot-shaped nuclei that formed scattered rosettes. For this reason, we favor a diagnosis of ganglioneuroblastoma. Ganglioneuroblastomas exhibit histologic features of Conference participants also felt this neoplasm was malignant due to its locally invasive nature.

Additional differential diagnoses considered for this neoplasm include medulloepithelioma, melanoma, and retinoblastoma. Retinoblastomas present with numerous neuroblasts arranged in rosettes and can be easily confused with medulloepitheliomas in fish, except they are generally not as invasive and do not form heteroplastic elements such as undifferentiated mesenchymal cells, bone, or cartilage.[7]

There was some variation among sections due to the submission of both eyes, and some conference participants had evidence of retinal detachment and atrophy, as well as a lenticular cataract with Morgagnian globules in the lens. There were also areas of woven bone surrounding some sections of the cornea, and conference participants hypothesized that this could represent osseous metaplasia from the neoplasm or from exposed lens fibers.

S-100, neurofilament protein (NFP), synaptophysin, chromagranin A, and glial fibrillary acidic protein (GFAP) immunohistochemical stains were performed on this case, but all were non-contributory, which is likely due to the fact that the immunohistochemical stains at the Joint Pathology Center laboratory are not optimized for piscine tissues.

Contributor: Tufts Cummings School of Veterinary Medicine
Department of Pathology
Hospital for Large Animals
200 Westboro Road
North Grafton, MA 01536
www.tufts.edu/vet

References:

1. Gill BS. On the occurrence of ganglioneuroma and cysts of Henneguya ophiocephali Chakravarty 1938 in a fish. *J of Wildlife Dis*. 1975;11:314-317.
2. Hawkins WE, Overstreet RM, Fournie JW, et al. Development of aquarium fish models for environmental carcinogenesis: tumor induction in seven species. *J Appl Toxicol*. 1985;5:261-264.
3. Hawkins WE, Fournie JW, Overstreet RM, et al. Intraocular neoplasms induced by methylazoxymethanol acetate in Japanses medaka (Oryzias latipes.) *J Natnl Cancer Inst*. 1986;76:453-65.
4. Maxie MG, Youssef S. Nervous system. In: Maxie MG, ed. *Jubb, Kennedy, and Palmer's Pathology of Domestic Animals*. 5th ed. Philadelphia, PA: Elsevier; 2007:372, 453-455.
5. Porter BF, Storts RW, Payne HR, et al. Colonic ganglioneuromatosis in a horse. *Vet Pathol*. 2007;44:207-210.
6. Roberts RJ. In: Fish Pathology, 2nd ed. London, England: Bailliere Tindall, 1989:169.
7. Roberts RJ. Neoplasia of teleosts. In: Roberts RJ, ed. *Fish Pathology*. 3rd ed. Edinburgh, Scotland: Saunders; 2003:166-7.

CASE II: A10-42431 (JPC 3167832).

Signalment: Sex undetermined juvenile Moorish idol (*Zanclus cornutus*).

History: The body of an approximately 6cm juvenile Moorish idol was received in formalin. The fish was one of a group of recently shipped animals under observation and treatment in quarantine prior to display in a public aquarium. Constant low level mortalities had occurred from the time of arrival.

Gross Pathology: Reported gross findings varied among individuals and included lethargy, emaciation, abdominal distension, and intestines severely distended by thick yellow contents.

Laboratory Results: Intestinal mucosal scrapings were reported to contain numerous signet ring-like structures with multiple internal spheres.

Contributor's Histopathologic Description: Intestine: Multiple intestinal segments are characterized by plicae irregularly expanded by variable, mild to moderate, mixed populations of lymphocytes, plasma cells, and macrophages containing granular to refractile debris. Within affected areas, the normal mucosal architecture is altered by a combination of mild epithelial hypertrophy, hyperplasia, and pseudostratification, with compression and distortion of individual cells resulting from the presence of large numbers of approximately 20 µm, ovoid, intraepithelial parasitic bodies. Individual bodies (pansporoblasts) are defined by a thin pale eosinophilic limiting membrane and compressed peripheral nucleus, surrounding a vacuolated space typically containing 4-8 ovoid, 5 x 8 µm structures (sporoblasts and accessory cells). The round to ovoid internal structures have moderate amounts of slightly vacuolated pale eosinophilic cytoplasm and possess 1 or 2 central, condensed, basophilic nuclei, often with a prominent nucleolus. Similar structures are present within luminal debris. Occasional lifting of the epithelium from the basement membrane is evident in some areas and pockets of refractile debris are scattered throughout the epithelium.

Contributor's Morphologic Diagnosis: Intestine: Enteritis, segmental, subacute to chronic, moderate, with numerous intralesional myxozoal pansporoblasts.

Contributor's Comment: Microscopic findings are consistent with widespread intestinal infection by the myxozoan parasite *Enteromyxm* (*Myxidium*) *leei*. *Enteromyxm leei* causes severe enteritis and losses, particularly in sea bream and sea bass mariculture in the Mediterranean area.[6,8] The parasite exhibits an unusually low degree of host specificity and infections have been transmitted to over 25 marine fish species in

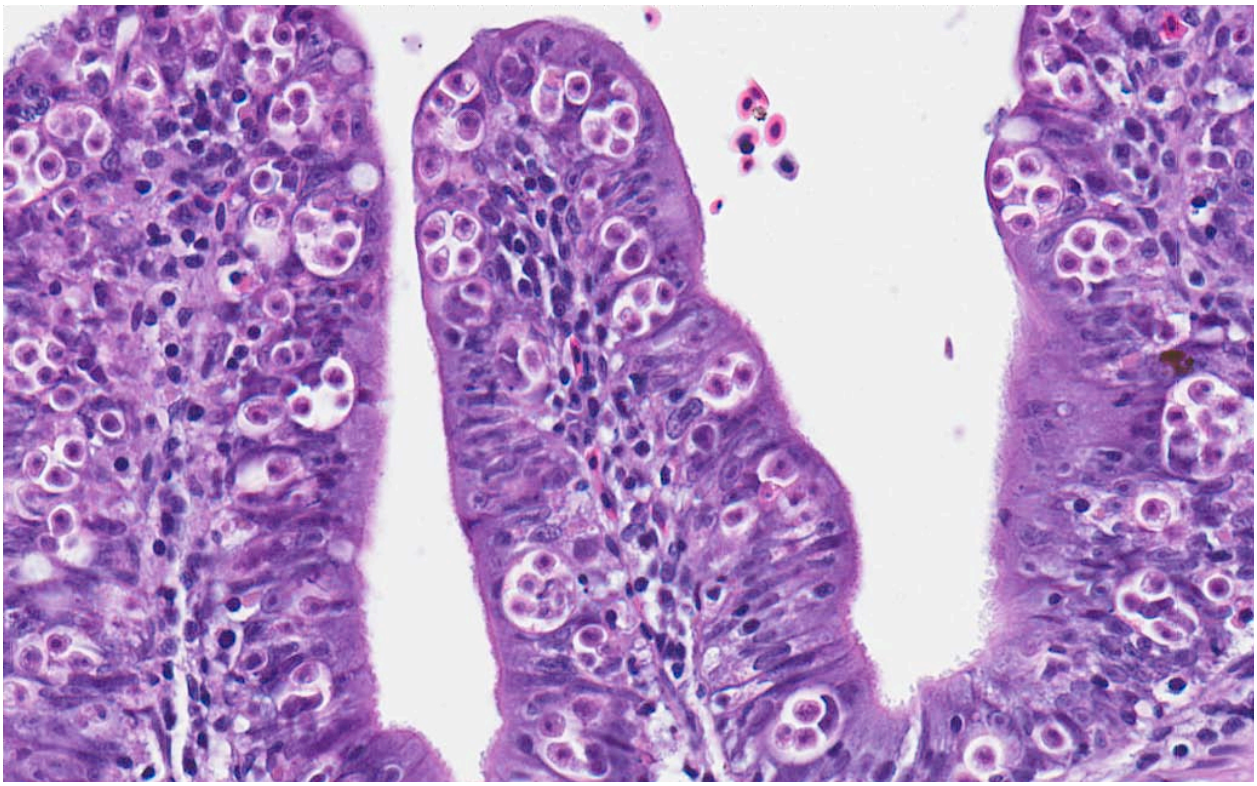

2-1. Intestine, Moorish idol: Approximately half of the intestinal epithelial cells contain myxosporidian pansporoblasts. (HE 400X)

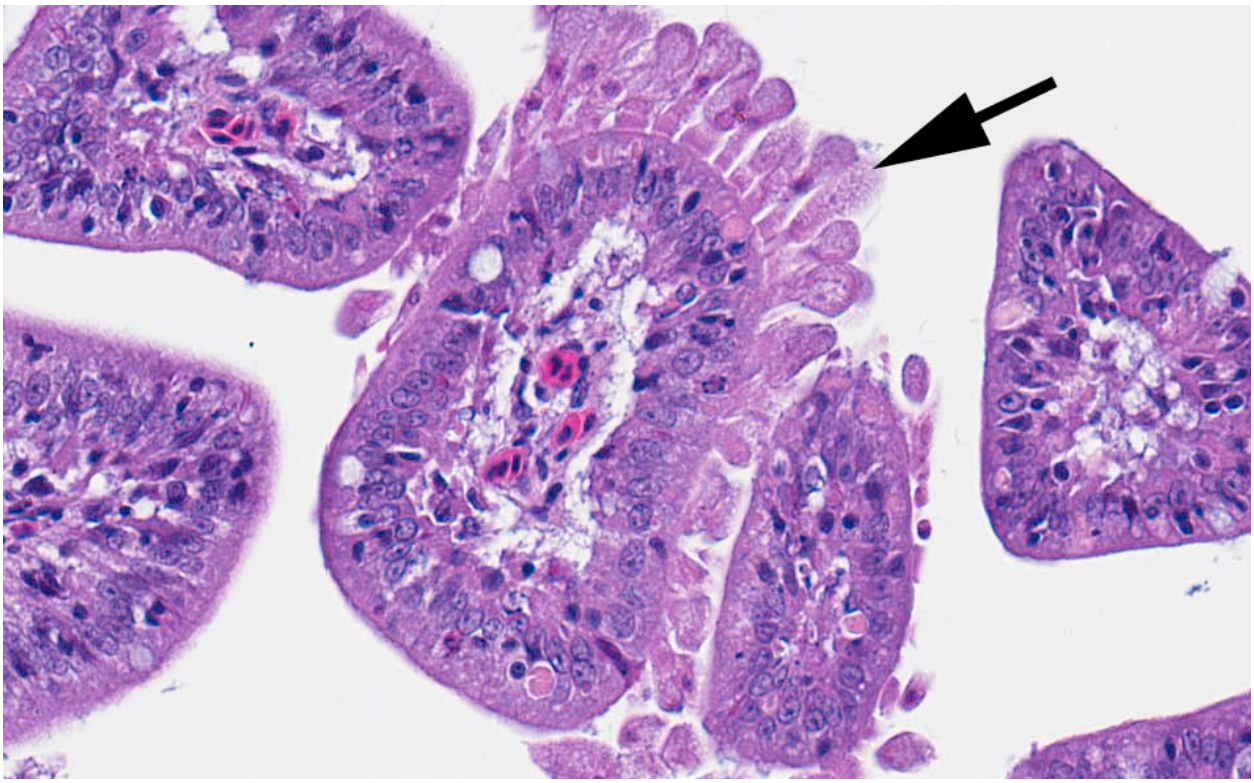

2-2. Intestine, Moorish idol: In an adjacent section of intestine, a florid carpet of ciliates multifocally cover the intestinal villi. (HE 400X)

a public aquarium.[8] An alternate host or actinosporean form of the parasite has not been identified and direct transmission has been demonstrated by cohabitation, exposure to contaminated effluent, and by the feeding of infected tissue.[4] Gross signs may include emaciation, darkening, lethargy, abdominal distension, pale soft liver, enlarged gallbladder, and a thickened and hemorrhagic intestinal wall.[6,8] Lesions occur throughout the intestine from the pyloric ceca to rectum, and occasionally in the gallbladder and intrahepatic bile ducts.[1,6,8] Development occurs between epithelial cells near the basement membrane. Pansporoblasts, up to 40 µm, consist of an enveloping pericyte or primary cell surrounding a clear space housing two developing sporoblasts and two or more accompanying accessory cells.[1] Although Giemsa, Gram, and acid-fast stains were performed, mature spores were not identified. Mature spores, when present, are arcuate, average 6.9 x 14.7 µm, and have two elongate polar capsules tapering to their distal ends.[3]

Myxozoans are important metazoan parasites of freshwater and marine fish closely related to the Cnidaria. This large group of obligate parasites includes over 1350 species in 52 genera, involving intracellular and intercellular histozoic representatives, as well as many coelozoic forms. Life cycles are complex and not fully understood for many species, although at least 25 are known to involve an invertebrate (oligochaete, polychaete, or bryozoan) alternative host. Taxonomy is largely based on the morphology of myxospores, characterized by multiple cells arranged in 1-7 spore valves, 1-2 amoeboid sporoplasms, and 2-7 nematocyst-like polar capsules with coiled extrudable polar filaments.[2,7]

Additional findings present in some sections include plasmodia of a coelozoic myxozoan associated with mild bile duct ectasia, epithelial attenuation, and periductular fibrosis. Some intestinal sections also include a focal area with large numbers of elongate structures with abundant finely granular to vacuolated cytoplasm, one to rarely two small nuclei, and a broad base of attachment to the mucosal epithelium. The nature of this organism is unknown, but possibly represents a developmental stage of another myxozoan.

JPC Diagnosis: Intestine: Enteritis, histiocytic and lymphocytic, segmental, moderate to marked, with mucosal hypertrophy and hyperplasia and numerous intracytoplasmic myxosporidian pansporoblasts.

Conference Comment: Conference participants discussed the usual mode of transmission for this myxozoan. Direct fish-to-fish transmission can occur through the ingestion of exfoliated infected intestinal epithelium.[5] The intestinal epithelium contains

autophagic vacuoles, a common finding in fish with gastrointestinal disturbances. Conference participants also discussed the presence of exocrine pancreatic atrophy, lack of coelomic adipose tissue, and atrophy and loss of the dorsal skeletal muscle, all of which are consistent with the reported gross findings and indicate cachexia. Participants attributed areas of myodegeneration in the dorsal skeletal muscle to possible capture myopathy.

Contributor: University of Georgia
Department of Pathology
College of Veterinary Medicine
501 DW Brooks Drive
Athens, GA 30602
www.vet.uga.edu/VPP

References:

1. Alvarez-Pellitero P, Palenzuela O, Sitja-Bobadila A. Histopathology and cellular response in *Enteromyxm leei* (Myxozoa) infections of *Diplodus puntazzo* (Teleostei). *Parasitology International*. 2008;57:110-120.
2. Bruno DW, Nowak B, Elliott DG. Guide to the identification of fish protozoans and metazoan parasites in stained tissue sections. *Diseases of Aquatic Organisms*. 2006;70:1-36.
3. Diamant A, Lom J, I Dykova. Myxidium leei n. sp., a pathogenic myxosporean of cultured sea bream Sparus aurata. *Diseases of Aquatic Organisms*. 1994;20:137-141.
4. Diamant A. Fish-to-fish transmission of a marine myxosporean. *Diseases of Aquatic Organisms*. 1997;30:99-105.
5. Fesit SW, Longshaw M. Phylum myxozoa. In: Woo PTK, ed. *Fish Diseases and Disorders.* 2nd ed. Vol 1. Cambridge, MA: CABI; 2006:271.
6. Fleurance R, Sauvegrain, Marques A, et al. Histopathological changes caused by Enteromyxm leei infection in farmed sea bream. *Sparus aurata*. 2008;219-228.
7. Kent ML, et al. Recent advances in or knowledge of the myxozoa. *The Journal of Eukaryotic Microbiology*. 2001;48:395-413.
8. Padrós F, Palenzuela O, Hispano C, et al. *Diseases of Aquatic Organisms*. 2001;47:57-62.

CASE III: 63048 (JPC 4002871).

Signalment: Approximately 9-year-old male mudpuppy (*Necturus maculosus*).

History: Keepers reported this mudpuppy, a collection animal at the Maryland Zoo in Baltimore, to the veterinary staff for acute coelomic distention and floating upside-down. On physical exam, the animal was dull but responsive, and had gained approximately 250g since its most recent weight check. Ultrasound exam revealed a large amount of free fluid within the coelomic cavity, while the heart, liver, and intestines all appeared to be within expected limits. The coelomic fluid had low specific gravity, 1.009, and cytologic examination of a concentrated sample showed many lymphocytes and presumptive granulocytes, as well as a single, septate, branching fungal hypha. Treatment was initiated, including twice daily coelomocentesis, ceftazidime (20mg/kg q72h), and once daily baths in intraconazole and Wright-Whitaker solution. On the fourth day of treatment, the animal was found moribund and floating upside-down. Shortly thereafter, the heartbeat could not be detected by Doppler.

Gross Pathology: On necropsy, there were multiple variably-sized areas of light red discoloration on the skin of the ventrum and around the cloaca (livor mortis). The musculature of the body wall was diffusely gelatinous on palpation (edema). Approximately 10mL of colorless, slightly turbid fluid was present within the coelomic cavity. The liver was predominantly brownish black with subtle, multifocal, light tan mottling of the capsular surface. The testes and kidneys appeared mottled light tan to dark brown. All other major organs were grossly unremarkable.

Laboratory Results: Fungal culture of the coelomic fluid yielded 2+ *Exophiala* species. Further speciation was not provided. There was no growth on aerobic bacterial culture.

Contributor's Histopathologic Description: Kidney: Multifocally infiltrating the interstitium and tubules is an inflammatory cell population consisting primarily of cells with large, multilobulated nuclei (neutrophils) and fewer cells with large, round to reniform nuclei (macrophages). Admixed with the inflammatory cells are variable amounts of fibrin, necrotic cellular debris, extravasated red blood cells (hemorrhage), and numerous slender, 5-7 µm diameter, septate fungal hyphae characterized by light brown pigment and acute angle dichotomous branching. Tubules are occasionally dilated and contain low numbers of red blood cells and viable and degenerating leukocytes.

Liver: The periportal areas are infiltrated by moderate numbers of macrophages and scattered neutrophils, admixed with occasional fragments of pigmented fungal hyphae. Portal areas consistently contain four or more bile ductules (biliary hyperplasia). There are moderate numbers of clustered and individual melanomacrophages scattered throughout the hepatic parenchyma.

** Some slides also contain sections of testes, which display inflammation and necrosis similar to that observed in the kidney sections.

Contributor's Morphologic Diagnosis: 1. Kidney: Tubulointerstitial nephritis, neutrophilic and histiocytic, multifocal, subacute, severe, with necrosis, and intralesional pigmented fungal hyphae.
2. Liver: Hepatitis, periportal, histiocytic and neutrophilic, multifocal, subacute, moderate, with

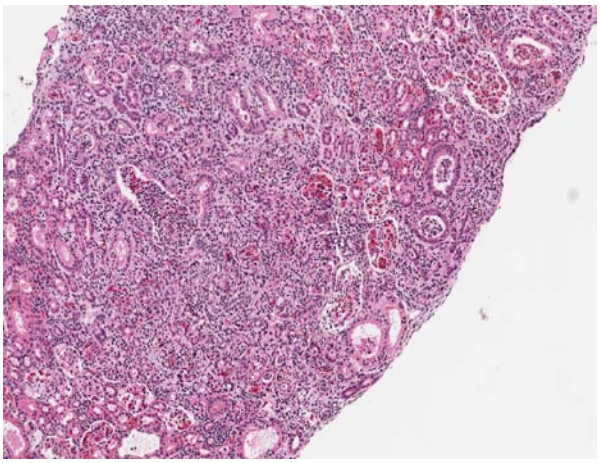

3-1. Kidney, mudpuppy: The renal interstitium is markedly expanded by large numbers of neutrophils and histiocytes, effacing normal renal tubular structure. (HE 120X)

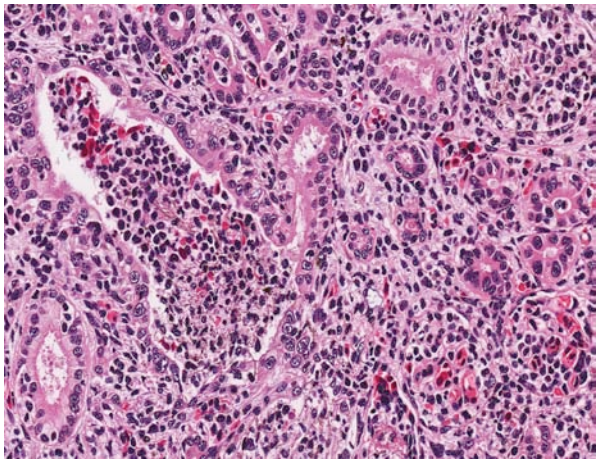

3-2. Kidney, mudpuppy: Numerous neutrophils, sloughed epithelial cells, and fewer histiocytes markedly distend renal tubules. (HE 240X)

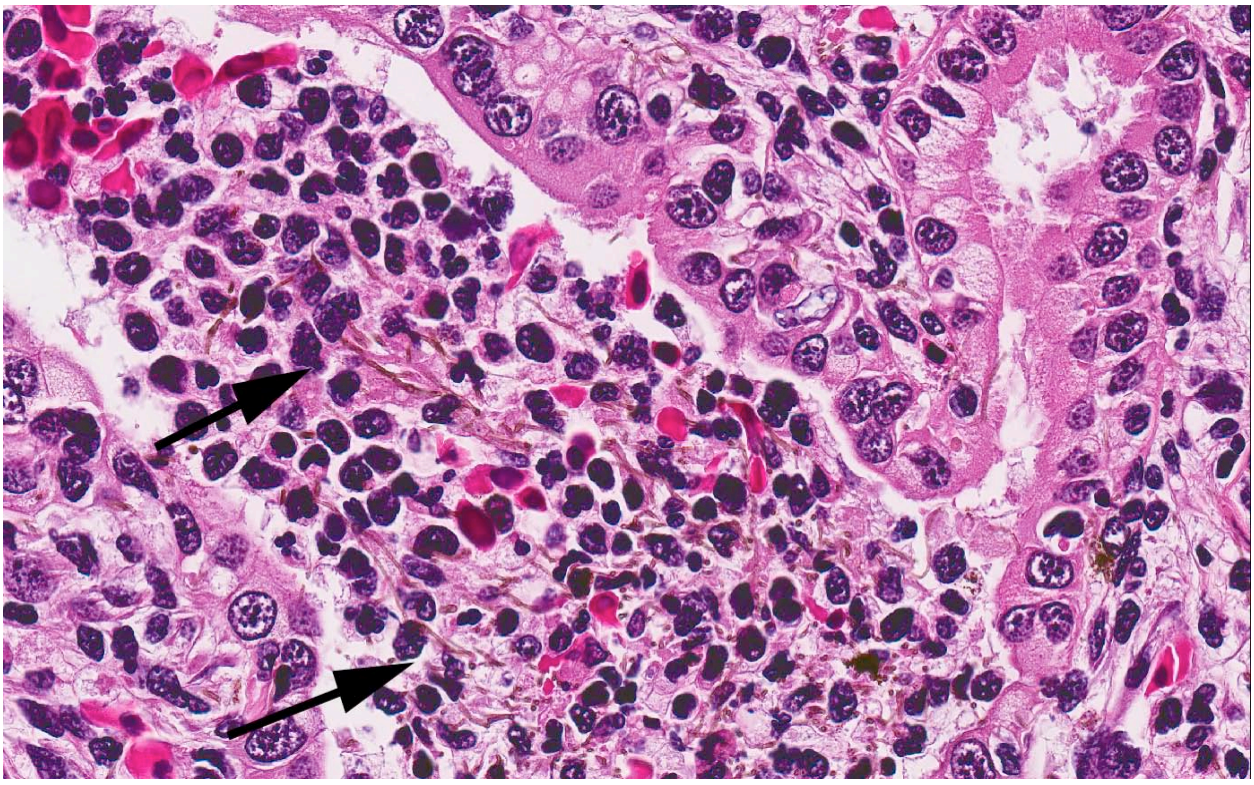

3-3. Kidney, mudpuppy: A higher magnification of this tubule reveals numerous pigmented fungal hyphae (arrows). Rare fungal hyphae are present within these areas. (HE 400X)

biliary hyperplasia, and intralesional pigmented fungal hyphae.

Contributor's Comment: Death of this mudpuppy was attributed to phaeohyphomycosis, a condition characterized by the presence in tissues of pigmented, or dematiaceous, hyphae, pseudohyphae, yeasts, or any combination of these forms.[12] Phaeohyphomycosis, which can be caused by over one hundred different types of pigmented fungi, encompasses a wide spectrum of opportunistic mycoses in humans and domestic animals, reports of which range from superficial cutaneous infection to fatal encephalitis.[1,2,5,6,12] Similarly, in amphibians, the disease may be limited to ulcerative or granulomatous lesions of the skin, or be disseminated systemically.[4] The term "phaeohyphomycosis" should not be confused with "chromoblastomycosis", which refers specifically to a localized cutaneous or subcutaneous pigmented fungal infection characterized by the presence of rounded sclerotic bodies.[12]

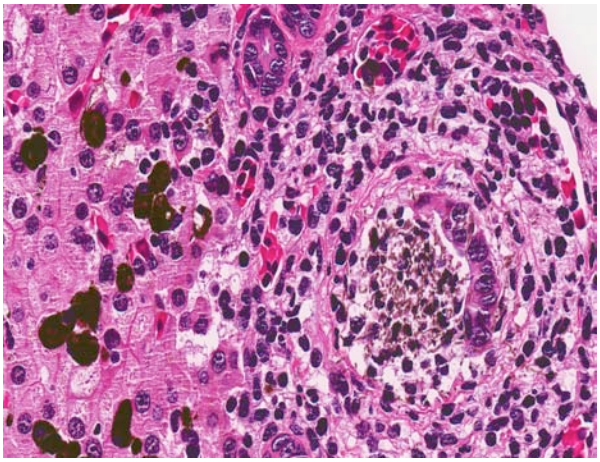

3-4. Liver, mudpuppy: Multifocally, pyogranulomas (right) are scattered thoughout the section. Fungal hyphae are present within pyogranulomas; in this case they are present within a degenerating biliary ductule. At left, numerous melanomacrophages are scattered throughout the hepatic parenchyma. (HE 400X)

Fungal culture of the mudpuppy's coelomic fluid yielded growth of a black mold morphologically consistent with an *Exophiala* species. As with other dematiaceous fungi, *Exophiala* is widely distributed in soil, decaying vegetation, and water. Species of *Exophiala* are notoriously difficult to classify and identify due to their complicated life cycles and morphologic plasticity, and recently molecular diagnostic tools have become important in defining the taxonomy of the group.[13,14] It has been reported as an emerging opportunistic pathogen in both immunocompetent and immune suppressed people,[14] including solid organ transplant recipients.[3,11] *Exophiala* species are significant pathogens in a

variety of fresh and saltwater fish including salmon,[8] flounder,[10] and sea dragons.[13]

Infection with dematiaceous fungi is typically initiated by introduction of the agent via an abrasive or penetrating wound, or by inhalation of fungal elements from the environment.[12] In this case, the presence a large mat of interwoven fungal hyphae within the central air space of one lung, and the lack of visible external wounds, were compatible with inhalation being the route of entry.

JPC Diagnosis: 1. Kidney: Nephritis, tubulointerstitial, pyogranulomatous, diffuse, moderate, with numerous pigmented fungal hyphae.
2. Liver: Hepatitis, pyogranulomatous, multifocal, mild to moderate, with rare pigmented fungal hyphae.

Conference Comment: Dematiaceous fungal hyphae are septate, 2-8 µm wide, and have non-parallel pigmented walls and random dilated, round, thick walled segments up to 25 µm in diameter that resemble chlamydospores or chlamydoconidium. Fungi grow in tissue as yeast, pseudohyphae and hyphae and may be extracellular and intracellular. Organisms that cause chromoblastomycosis, a condition mentioned by the contributor, are pigmented, but do not form hyphae in tissue, and their division by septation is distinctive. Additionally, they form large 4-15 µm, round, thick and dark-walled yeast-like cells, known as sclerotic bodies or muriform cells.[9]

There was some slide variation, and some sections had large hyphal mats within the ureter. This feature, along with the unusual and striking amount of inflammation within Bowman's space, interpreted as reflux tubulitis, led conference participants to consider an ascending infection.

Contributor: Johns Hopkins University School of Medicine
Department of Molecular and Comparative Pathobiology
733 N Broadway, Suite 840
Baltimore, MD 21205
http://www.hopkinsmedicine.org/mcp

References:

1. Anor S, Sturges BK, Lafranco L, et al. Systemic phaeohyphomycosis (Cladophialophora bantiana) in a dog – clinical diagnosis with stereotactic computed tomographic-guided brain biopsy. *Journal of Veterinary Internal Medicine*. 2001;15:257-61.
2. Bouljihad M, Lindeman CJ, Hayden DW. Pyogranulomatous meningoencephalitis associated with dematiaceous fungal (*Cladophialophora bantiana*) infection in a domestic cat. *Journal of Veterinary Diagnostic Investigation*. 2002;14:70-72.
3. Fothergill, AW. Identification of dematiaceous fungi and their role in human disease. *Clinical Infectious Disease.* 1996; 22(Suppl2):S179-84.
4. Genovese LM, Whitebread TJ, Campbell CK. Cutaneous nodular phaeohyphomycosis in five horses associated with *Alternaria alternata* infection. *Veterinary Record*. 2001;148:55-56.
5. Herrae P, Rees C, Dunstan R. Invasive phaeohyphomycosis caused by *Curvularia* species in a dog. *Veterinary Pathology*. 2001;38:456-59.
6. Jones TC, Hunt RD, King NW. Diseases caused by fungi. In: Jones TC, Hunt RD, King NW, eds. *Veterinary Pathology*. 6th ed. Baltimore, MD: Williams and Wilkins. 1997:530.
7. Kurata P, Munchan C, Wada S, et al. Novel Exophiala infection involving ulcerative skin lesions in Japanese flounder Paralicthys olivaceous. *Fish Pathology*. 2008;43(1):35-44.
8. Lief MH, Caplivsky D, Bottone EJ, et al. *Exophiala jeanselmei* infection in sold organ transplant recipients: report of two cases and review of the literature. *Transplant Infectious Disease*. 2011;13:73-79.
9. Nyaoke A, et al. Disseminated phaeohyphomycosis in weedy seadragons (*Phyllopteryx taeniolatus*) and leafy seadragons (*Phycodurus Eques*) caused by species of *Exophiala,* including a novel species. *Journal of Veterinary Diagnostic Investigation*. 2009;21:69-79.
10. Otis EJ, Wolke, RE. Infection of Exophiala salmonis in Atlantic Salmon (*Salmo salar* L.). *Journal of Wildlife Diseases*. 1985;21(1):61-64.
11. Pena-Penabad C, Duran MT, Yebra MT, et al. Chromomycosis due to Exophiala janeselmie in a renal transplant recipient. *European Journal of Dermatology.* 2003;13(3):305-7.
12. Schell WA, Salkin IF, McGinnis MR. Bipolaris, Exophiala, Scedosporium, Sporothrix, and other dematiaceous fungi. In: Murray PR, Barron EJ, Jorgensen JH, Pfaller MA, Yolken RH, eds. *Manual of Clinical Microbiology.* 8th ed. Washington, DC: ASM Press. 2003:1820-29.
13. Taylor SK. Mycoses. In: Wright KM, Whitaker BR, eds. *Amphibian Medicine and Captive Husbandry.* Malibar, FL: Krieger Publishing Company. 2001:187-188.
14. Zeng JS, De Hoog GS. Exophiala spinifera and its allies: diagnostics from morphology to DNA barcoding. *Medical Mycology*. 2008;46:193-208.

CASE IV: 07-2329-3 (JPC 4003032).

Signalment: Young fry (age not specified: estimated at 2 months), male and female (several fry submitted) brook trout (*Salvelinus fontinalis*).

History: Sudden and rapid increase in mortality in brook trout fry. The water temperature had risen from 10°C to 13-14°C in the past few weeks. No clinical signs were reported by the owner. Fingerlings were not affected. Over 90% of the fry died within a few days.

Gross Pathology: None (fry were sent opened and formalin-fixed).

Laboratory Results: After the initial presumptive diagnosis was given, fresh fry from the same tanks were sent to a fish virology laboratory. Infectious Pancreatic Necrosis Virus (IPNV) was isolated in high titers.

Contributor's Histopathologic Description: Submitted slides are parasagittal sections from 4 fry (which were needed to show the lesions), so there is significant variation among slides. Depending on the sections, lesions vary from necrosis of single or small clusters of cells to massive coagulative necrosis of exocrine pancreatic epithelium. There are mild to moderate associated degenerative changes in the adjacent adipose tissue. Inflammation is essentially absent. In some sections, there is also occasional single cell necrosis of hepatocytes and/or pyloric cecal epithelium ("McKnight cells"). In a few sections, there is rare degeneration and necrosis of myocytes.

Contributor's Morphologic Diagnosis: Acute, multifocal exocrine pancreatic necrosis.

Contributor's Comment: Based on the case history, microscopic lesions and isolation of IPNV in high titers, Infectious Pancreatic Necrosis (IPN) was diagnosed. IPN is caused by an *Aquabirnavirus*, family *Birnaviridae*, a double-stranded RNA virus.[6] IPVN has a worldwide distribution; it is a major cause of mortality and economic loss in young freshwater-farmed salmonids, and in juvenile salmon transferred from fresh to sea water.[4,6] IPVN is a pathogen of salmonids, but has also been isolated in healthy individuals from many other fish species and aquatic invertebrates.[4]

IPN is a highly contagious disease of usually acute onset that only affects young fish (<6 months), especially fry; older fish can be infected but are chronic carriers.[4] It can present, as in our case, as a

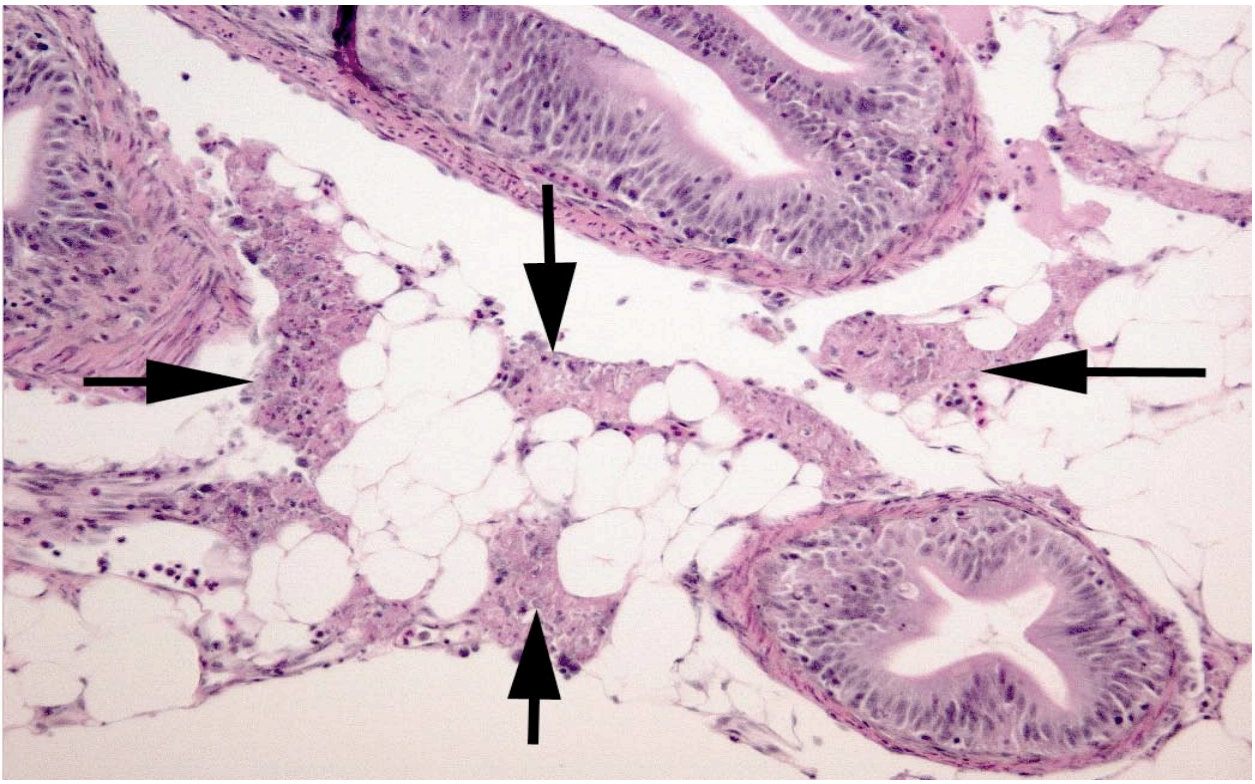

4-1. Exocrine pancreas, brook trout. There is diffuse necrosis of exocrine pancreatic epithelium with no inflammation and mild degenerative changes in the adjacent adipose tissue. Cross sections of normal pyloric ceca are also present (HE 100X). Image courtesy of the University of Montreal, Faculty of Veterinary Medicine, Montreal, Canada (http://www.medvet.umontreal.ca)

sudden and rapid increase in mortality with minimal clinical signs. When present, clinical signs include dorsal darkening, trailing white feces, abdominal distension, exophtalmos, hemorrhages on the ventrum, pale gills and corkscrew spiral swimming.[4] Mortality is variable, but it is most rapid and severe at temperatures between 10-14°C[4]; it can approach 100%. There is no treatment, but fasting and lowering water temperature can diminish the mortality. IPVN infection is often limited to a carrier state; infection is lifelong in carriers and in fish that survive the disease. Many of these fish chronically shed the virus. IPVN can be transmitted vertically and horizontally. It has marked tropism for the exocrine pancreatic epithelium, but IPVN has been demonstrated in kidney, liver and occasionally in other organs in post-smolt Atlantic salmon (*Salmo salar* L.).[1] Findings of an *in vitro* study showed that IPNV induced apoptosis followed by postapoptotic necrosis in fish embryonic cells.[2] *In vivo*, IPNV has been shown to induce apoptosis in hepatocytes of post-smolt Atlantic salmon[6]; in the exocrine pancreatic epithelium, apoptosis has not been demonstrated.

Gross lesions in fry, when present, include pale viscera with a few petechiae, and a mucoid plug in the GI tract.[4] The most characteristic microscopic lesion of IPN is, as its name implies, exocrine pancreatic necrosis[3,5,6], with or without secondary degenerative changes in the adjacent adipose tissue. Other lesions that can be observed are apoptosis of pyloric cecal epithelium ("McKnight cells"), hepatocyte single cell necrosis/apoptosis, focal myocyte degeneration/ necrosis and, in severe cases, necrosis of renal tubular and interstitial cells.[4,5] Hepatic lesions have been shown to play a major role in IPN in post-smolt Atlantic salmon.[5] A presumptive diagnosis can be established by histopathology but must be confirmed by virological methods (e.g. virus isolation; RT-PCR). Virus isolation in itself is not confirmatory as IPNV can be demonstrated in clinically healthy/carrier fish; thus, a high titer should be present to establish a definitive diagnosis.[4] Immunohistochemistry can also be used, and has the advantage of antigen localization. Other viruses can cause exocrine pancreatic necrosis in salmonids; the main differential diagnoses for the lesions in our case are sleeping disease in rainbow trout (*Oncorhynchus mykiss*) and pancreas disease in salmon, both caused by closely related alphaviruses (*Togaviridae*).[8] However, in both cases the skeletal and cardiac muscles are also main targets, with significant necrosis, and pancreatic involvement is minimal in sleeping disease.[8]

JPC Diagnosis: 1. Exocrine pancreas: Necrosis, multifocal to coalescing.
2. Intestine: Enteritis, necrotizing, multifocal, mild.

Conference Comment: IPN is mainly a disease of first-feeding salmonid fry, although it has been found in many other fish species, as noted by the contributor. The reason for this selective species susceptibility is unknown. The main target tissues of IPN virus in salmonids are the mucosal epithelial cells lining the gastrointestinal tract and the interstitial cells and macrophages of the kidney. Some species, such as the brook trout, harbor the virus in leukocytes and kidney stem cells; whereas others such as halibut and turbot have affected cells in the intestine, liver, and kidney. Apoptosis is an early and primary mechanism of cell death associated with IPN, as seen in the McKnight cells of the intestinal epithelium, occurring within two hours of infection and well before more extensive necrosis occurs later in the disease.[7]

Conference participants considered the pyknosis and loss of cellular detail in some sections of liver to be autolysis. Conference participants also discussed the epithelial lifting in the secondary lamellae of the gills, which is likely an artifact of formalin fixation rather than edema.

Contributor: University of Montreal
Faculty of Veterinary Medicine
3200, Sicotte, St-Hyacinthe
Quebec, Canada, J2S 2M2
http://www.medvet.umontreal.ca

References:

1. Ellis AE, Cavaco A, Petrie A, et al. Histology, immunocytochemistry and qRT-PCR analysis of Atlantic salmon, Salmo salar L., post-smolts following infection with infectious pancreatic necrosis virus (IPNV). *J Fish Dis*. 2010;33(10):803-18.
2. Hong JR, Lin TL, Hsu YL, et al. Apoptosis precedes necrosis of fish cell line with infectious pancreatic necrosis virus infection. *Virology*. 1998;250(1):76-84.
3. Lumsden JS. Gastrointestinal tract, swimbladder, pancreas and peritoneum. In: *Systemic Pathology of Fish: A Text and Atlas of Normal Tissues in Teleosts and Their Responses in Disease*. 2nd ed. London, UK: Scotian Press; 2006:168:199.
4. Noga, EJ. Infectious pancreatic necrosis (problem 75). In: *Fish Disease: Diagnosis and Treatment*. 1st ed. Ames, Iowa: Iowa State University Press; 2000;208-211.
5. Noguera PA, Bruno DW. Liver involvement in post-smolt Atlantic salmon, Salmo salar L., infected with infectious pancreatic necrosis virus (IPNV): a retrospective histopathological study. *J Fish Dis*. 2010;33(10):819-32.
6. Santi N, Sandtrø A, Sindre H, et al. Infectious pancreatic necrosis virus induces apoptosis in vitro and in vivo independent of VP5 expression. *Virology*. 2005;342(1):13-25.

7. Smail DA, Munro ALS. The virology of teleosts. In: Roberts RJ, ed. *Fish Pathology*. 3rd ed. Edinburgh, Scotland: Saunders; 2003:211-5.
8. Turnbull J. Musculoskeletal system. In: *Systemic Pathology of Fish: A Text and Atlas of Normal Tissues in Teleosts and Their Responses in Disease*. 2nd ed. London, UK: Scotian Press; 2006:288-320.

Joint Pathology Center
Veterinary Pathology Services

WEDNESDAY SLIDE CONFERENCE 2011-2012

Conference 17

07 March 2012

CASE I: GUVS1 (JPC 3032071).

Signalment: 2-year 5-month-old, female, domestic shorthair cat, feline (*Felis domesticus*).

History: This young adult cat lived in a rural area in northern Scotland, United Kingdom, and had a history of hunting small birds. In January 2006, it became dull and anorexic for 24 hours. The cat showed signs of distress and abdominal discomfort, and vomited yellow material. It developed seizures and died 36 hours after the onset of clinical signs. An in-contact cat was unaffected.

Gross Pathology: At postmortem examination, the cat had dilatation and thickening of several 1cm long segments of the jejunum and a 3cm long segment of the ileum.

Laboratory Results: Bacteriology: *Salmonella enterica* serovar typhimurium, phage type DT40, was recovered in profuse growth from the small intestine.

Virology: Intestinal contents were negative for feline parvovirus by the polymerase chain reaction.

Contributor's Histopathologic Description: Intestine (Ileum and caecum). The mucosa of the

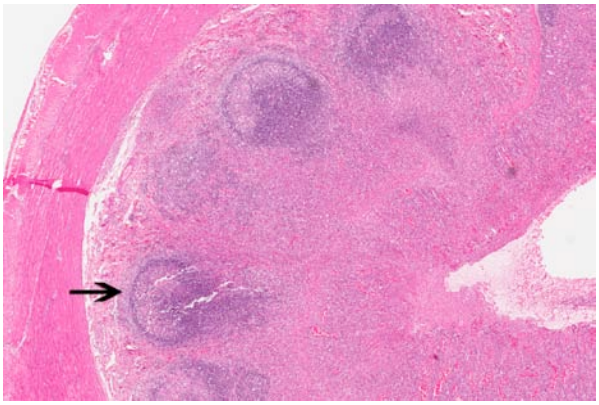

1-1. Small intestine (ileum), cat: The mucosa is diffusely and mildly thickened, with transmucosal necrosis affecting both intestinal villi and crypts. The necrosis extends down through the muscularis mucosa into underlying Peyer's patches (arrow). (HE 20X)

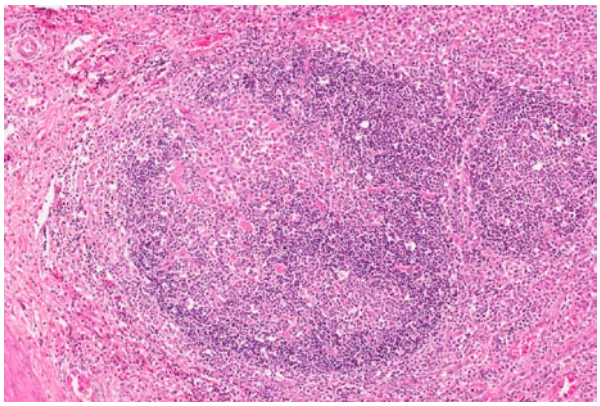

1-2. Small intestine (ileum), cat: There is marked depletion of Peyer's patches. (HE 80X)

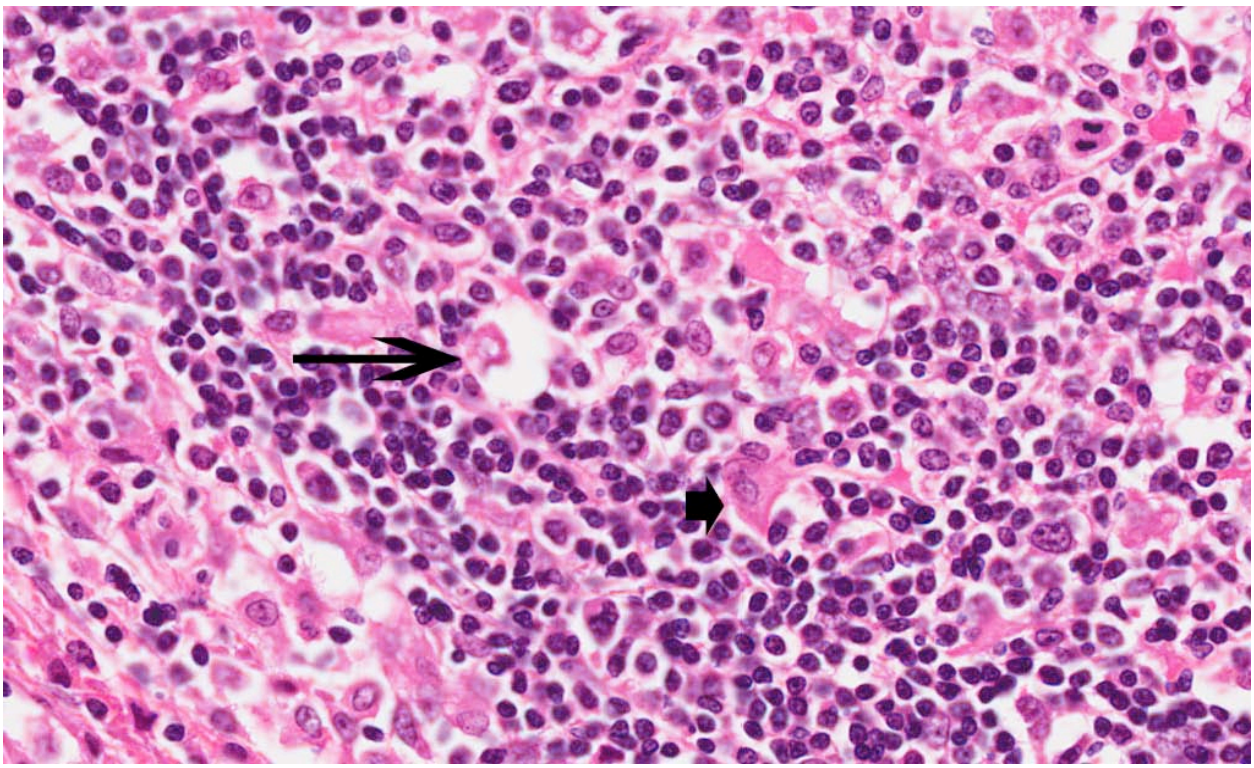

1-3. Small intestine (ileum), cat: Depleted Peyer's patches contain tingible body macrophages (arrow), histiocytes, neutrophils, and rare multinucleate syncytia (arrow head). (HE 400X)

ileum is eroded and there is necrosis, with exudation of neutrophils and necrotic cellular debris into the intestinal lumen. Destruction of villi and crypts is evident. The intestinal lamina propria is extensively infiltrated with neutrophils and sheets of macrophages, producing a pyogranulomatous inflammatory reaction. Bacteria are present on the luminal surface of the mucosa and also infiltrate the lamina propria. Less severe changes are present in the caecum.

Lymph node. The subcapsular, intertrabecular and medullary sinuses of the ileocaecal lymph node are infiltrated with macrophages and lesser numbers of neutrophils, producing a pyogranulomatous inflammatory reaction, and there is focal necrosis in some areas.

Contributor's Morphologic Diagnosis: Intestine: Enteritis, segmental, severe, necrotising, pyogranulomatous, with bacterial colonisation and invasion, consistent with enteric salmonellosis (*Salmonella enterica* serovar typhimurium, phage type DT40), domestic shorthair, feline Ileocaecal lymph node: Lymphadenitis, moderate, multifocal, locally extensive, pyogranulomatous, consistent with salmonellosis.

Contributor's Comment: The clinical signs and pathological findings in this cat were consistent with fatal enteric salmonellosis. The isolate of *Salmonella enterica* serovar *typhimurium* obtained from the affected cat was phage typed as the definitive type (DT) 40. This strain is associated with wild birds, particularly finches (family *Fringillidae*), in North America, Europe and Scandinavia.[2,4,5,8] The cat had a history of hunting wild birds, which represents the likely source of infection.

An outbreak of gastroenteritis due to *S. typhimurium* DT40 in cats and humans in central Sweden in 1999 was associated with infection and mortality in wild birds, notably common redpolls (*Carduelis flammea*) and Eurasian siskins (*Carduelis spinus*).[8] In the United Kingdom, *S. typhimurium* DT40 has been isolated from European greenfinches (*Carduelis chloris*), house sparrows (*Passer domesticus*), chaffinches (*Fringilla coelebs*) and European goldfinches (*Carduelis carduelis*), in decreasing order of frequency, as well as occasionally from other species of birds.[4] *S. typhimurium* DT40 has also been associated with epizootics of mortality in wild birds from winter 1997 to summer 1998 in eastern North America, including the Canadian Atlantic maritime provinces of New Brunswick, Novia Scotia, Prince Edward Island, Newfoundland and Labrador.[2] The species most commonly affected in North America were common redpolls (*Carduelis flammea*), pine siskins (*Carduelis pinus*), purple finches (*Carpodacus purpureus*),

evening grosbeaks (*Coccothraustes vespertinus*) and American goldfinches (*Carduelis tristis*), in decreasing order of frequency. *S. typhimurium* DT40 is considered to be an avian-adapted strain with a relatively narrow host range and a wide geographical distribution.[5] Wild bird strains of *S. typhimurium* (DT2, DT40, DT41, DT56 variant, DT99 and DT195) have been isolated at relatively low frequency from domestic livestock in the United Kingdom, but appear to be uncommon in humans, cats or dogs.[4]

The most common source of infection with *S. typhimurium* in cats is from the consumption of raw meat.[6] Healthy cats, as well as sick cats without enteric disease, may carry *S. typhimurium*, which is a potential zoonosis, although the reported prevalence of infection varies widely.[7,9] Cats may also be a source of antimicrobial resistant *S. typhimurium.*[9] The isolate of *S. typhimurium* DT40 from the cat reported here was resistant to streptomycin and sulphafurazole, but sensitive to ampicillin, clavulanate-potentiated amoxicillin, enrofloxacin, chloramphenicol, furazolidone, neomycin, oxytetracycline, and trimethoprim-sulphonamide, so was not considered to be a multi-drug resistant strain.

JPC Diagnosis: 1. Ileum: Enteritis, necrotizing and pyogranulomatous, diffuse, moderate to severe, with marked lymphoid necrosis and crypt regeneration.
2. Lymph node: Lymphadenitis, necrotizing and pyogranulomatous, diffuse, moderate to severe, with marked lymphoid necrosis.

Conference Comment: Lymphoid necrosis of the Peyer's patches and lymph node is a prominent feature in this case, and is consistent with the pathogenesis of *Salmonella*, which invade M cells in the Peyer's patches and epithelium of the distal small intestine, cecum, upper colon, and tonsils. Virulence factors include fimbriae (pilar adhesins), which are important for colonization and receptor mediated endocytosis; flagella which enhance movement and facilitate attachment; enterotoxins that produce secretory diarrhea by blocking closure of chloride channels; and bacterial wall lipopolysaccharides (endotoxins) that cause membrane injury and cell death. These endotoxins are composed of an O-specific side chain which is unique to each bacterial species, and a Lipid A core which activates mononuclear phagocytes and induces the production of tumor necrosis factor (TNF) and interleukin-1 (IL-1). This, in turn, induces endothelial cells to produce IL-6 and IL-8 and induce adhesion molecules, thus participating in leukocyte recruitment. Once adhered to macrophages, the bacteria inject bacterial proteins by a type III secretion system. S*almonella* sp. also induce apoptosis of macrophages by a type I secretory system which activates caspase-1. The resulting pattern of injury includes acute coagulative necrosis of enterocytes and vasculitis with thrombosis in the lamina propria, resulting in button ulcers, and the bacteria can migrate via the portal vein to the liver, causing paratyphoid nodules.[3,10]

Some conference participants interpreted multinucleated giant cell macrophages in the Peyer's patches as syncitial cells, which can be found feline parvovirus, a primary differential for this case. Also known as feline panleukopenia virus, feline parvovirus, like all parvoviruses, lack polymerase enzymes and are dependent on host cell DNA polymerase II, which are produced during S and early G2 phases, for replication. The resultant effects of parvovirus infection are thus greatest in tissues with a high mitotic rate, such as hematopoietic cells and dividing cells of intestinal crypts.[10]

Another differential is *Francisella tularensis*, the causative agent for tularemia. Tularemia, a gram negative intracellular coccobacillus, is passed by several types of ticks and causes necrosis of the liver, spleen, lymph nodes, lung, and bone marrow due to thrombosis, or less commonly caseating granulomas or hemorrhagic enteritis with ulceration over Peyer's patches in cats.[1]

Contributor: University of Glasgow Veterinary School
Division of Pathological Sciences
Institute of Comparative Medicine
Glasgow G61 1QH, Scotland, United Kingdom
http://www.gla.ac.uk/faculties/vet

References:

1. Cullen JM, Brown DL. Hepatobiliary system and exocrine pancreas. In: Zachary JF, McGavin MD, eds. *Pathologic Basis of Veterinary* Disease. 5th ed. St. Louis, MO: Elsevier; 2012:432-3.
2. Daoust PY, Busby DG, Ferns L, et al. Salmonellosis in songbirds in the Canadian Atlantic provinces during winter-summer 1997-98. *Can Vet J*. 2000;41(1):54-59.
3. Gelberg HB. Alimentary system and the peritoneum, omentum, mesentery, and peritoneal cavity. In: Zachary JF, McGavin MD, eds. *Pathologic Basis of Veterinary* Disease. 5th ed. St. Louis, MO: Elsevier; 2012:357, 376-7.
4. Pennycott TW, Park A, Mather HA. Isolation of different serovars of *Salmonella enterica* from wild birds in Great Britain between 1995 and 2003. *Vet Rec*. 2006;158(24):817-820.
5. Rabsch W, Andrews HL, Kingsley RA, et al. *Salmonella enterica* serotype Typhimurium and its host-adapted variants. *Infect Immun*. 2002;70(5): 2249-2255.

6. Stiver SL, Frazier KS, Mauel MJ, et al. Septicemic salmonellosis in two cats fed a raw-meat diet. *J Am Anim Hosp Assoc*. 2003;39(6):538-542.
7. Spain CV, Scarlett JM, Wade SE, et al. Prevalence of enteric zoonotic agents in cats less than 1 year old in central New York State. *J Vet Intern Med.* 2001;15(1): 33-38.
8. Tauni MA, Osterlund A. Outbreak of Salmonella typhimurium in cats and humans associated with infection in wild birds. *J Small Anim Pract*. 2000;41 (8):339-341.
9. Van Immerseel F, Pasmans F, De Buck J, et al. Cats as a risk for transmission of antimicrobial drug-resistant *Salmonella*. *Emerg Infect Dis*. 2004;10(12): 2169-2174.
10. Zachary JF. Mechanisms of microbial infections. In: Zachary JF, McGavin MD, eds. *Pathologic Basis of Veterinary* Disease. 5th ed. St. Louis, MO: Elsevier; 2012:169-70, 204-6.

CASE II: 3263-07 (JPC 3065887).

Signalment: 7-year-old, neutered, male, cat (*Felis domesticus*).

History: The animal presented with tachypnea and staggering one hour prior to death.

Gross Pathology: **Brain:** The animal had blood around the mouth and nostrils. The lung lobes had multiple, sometimes extensive, red to pink, often firm foci, and the cut surfaces exuded bloody froth. The right atrium contained a 14.5cm slender nematode, which was identified upon microscopic examination as *Dirofilaria immitis*. The heart weighed 17.15g and was within normal limits for size and shape.

Contributor's Histopathologic Description: There is severe villous intimal proliferation involving large and medium diameter arteries, which is near-occlusive in some instances. Slender and broad villous-like projections, consisting of stalks of collagen covered by prominent endothelial cells, extend into the lumens of affected arteries. Eosinophils in small to large numbers are dispersed singly or in loose aggregates, accompanied by lesser numbers of macrophages throughout the expanded tunica intima and are also present in the tunica adventitia and in adjacent alveolar septae. There is mild to moderate hypertrophy and hyperplasia of smooth muscle of the tunica media of some arteries in the section, with cytoplasmic vacuolation of few myofibers. In some sections of the large arteries, there are deposits of deeply eosinophilic, beaded material, considered to be necrotic remnants of nematodes, which are surrounded by macrophages and multinucleate giant cells. There is diffuse interstitial congestion, focal hemorrhages, patchy alveolar edema, hyperplasia of bronchial submucosal glands, and smooth muscle hypertrophy and hyperplasia of terminal bronchioles and alveolar ducts.

Contributor's Morphologic Diagnosis: Lung: Endarteritis, proliferative and eosinophilic, diffuse, chronic, severe, with medial hypertrophy and hyperplasia, hemorrhage, edema, smooth muscle hyperplasia and hyperplasia of the bronchial submucosal glands.

Heart: Nematode, intraluminal in right atrium, identified as *Dirofilaria immitis*.

Contributor's Comment: The histologic lesions in the pulmonary arteries are consistent with the endarteritis reported in feline dirofilariasis caused by *Dirofilaria immitis* (heartworm), which is

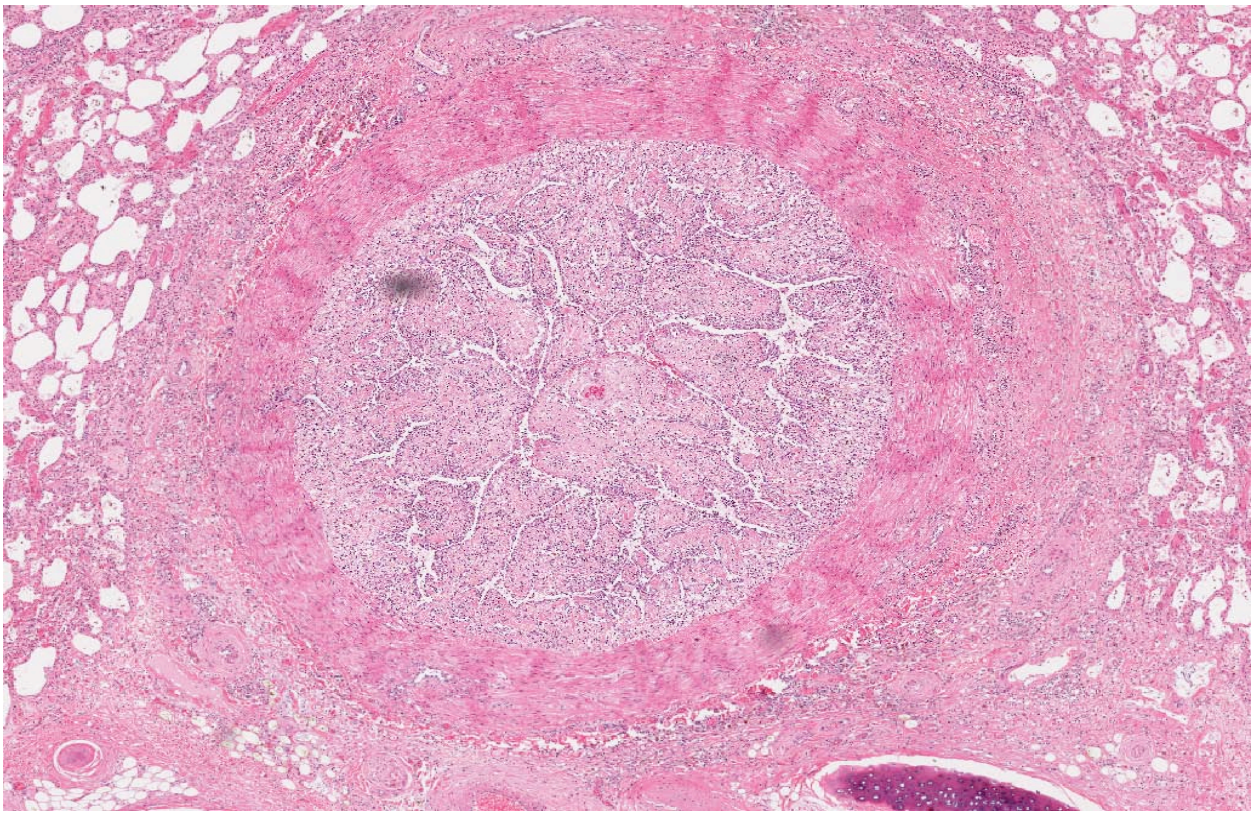

2-1. Lung, cat: Diffusely, the tunica intima of the pulmonary arteries and large caliber arterioles is thrown into prominent villar folds, which often occlude the lumen. (HE 20X)

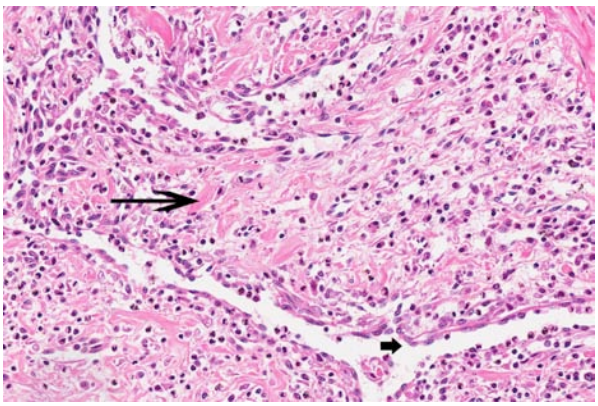

2-2. Lung, cat: Villar folds are composed of a loosely arranged core of mature collagen (arrow) and lined by 1-3 layers of mild to markedly hypertrophic endothelium (arrowhead). The villar folds are infiltrated by low to moderate numbers of viable eosinophils, and fewer neutrophils, histiocytes, and lymphocytes. (HE 200X)

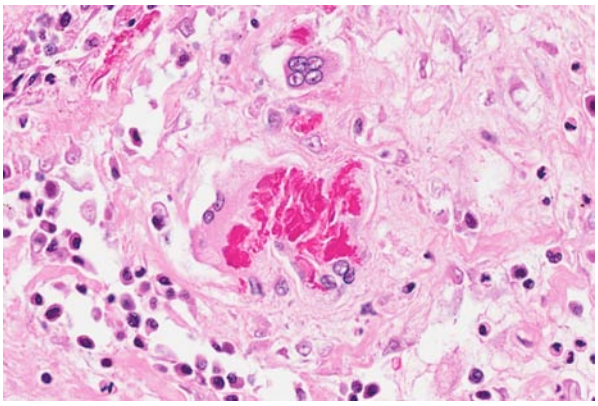

2-3. Lung, cat: Villar folds contain variable amounts of brightly eosinophilic granular material (Splendore-Hoeppli), which in some sections is engulfed by epithelioid macrophages. (HE 400X)

characterized by villous proliferation of the intima together with medial hypertrophy and hyperplasia.[9]
Two representative samples of the lung tissue were submitted. In one section, there is marked proliferative endarteritis together with granulomatous inflammation consisting of a thin layer of macrophages and multinucleate giant cells surrounding the deeply eosinophilic beaded to granular remnants of the parasite. Remnants of the parasite are noted in the adventitia of an affected vessel in the other section.

The marked villous endarteritis in dirofilariasis is reportedly attributable to the presence of live worms in the affected arteries and is of diagnostic importance.[2] In some cases of dirofilariasis, proliferation of intima results in occlusion of pulmonary arteries.[1] A characteristic lesion of canine dirofilariasis is medial hypertrophy of pulmonary arteries, which can be observed in cats, and has been considered a result of *D.immitis*-mediated stimulation of medial smooth muscle.[9] In cats, medial hypertrophy is often associated with *Aelurostrongylus abstrusus* and *Toxocara cati* infections[7,11,12], which can confound interpretation of these changes caused by *Dirofilaria* infections.[13]

Heartworm (HW) disease is primarily a pulmonary vascular disease caused by the filarial organism, *Dirofilaria immitis*. Mosquitoes, e.g. *Aedes* spp., *Anopheles* spp., and *Culex* spp. are the obligate hosts of the first, second and early third stages of *D. immitis*. These mosquitoes can transmit heartworms to numerous wild and companion animal species. The infective stage of the parasite develops within the malpighian tubules of the mosquito in 13 days, after which time it migrates to the proboscis or cephalic spaces of head and escapes into the new host when the mosquito feeds. The L3 larvae molt to L4s in 2-3 days. They remain in subcutaneous tissue for about 60 days, after which develop into L5 larvae. At the L5 stage, larvae migrate to the pulmonary arteries (predilection site). Microfilariae are produced about 6-7 months post-infection by gravid females. If *D. immitis* develops to maturity in hosts other than dogs, microfilaraemia is generally low or absent.[8] Both natural and experimental infections have shown that cats are considerably less susceptible to heartworm disease than dogs.[13] The infective stage (L3) of the parasite when experimentally inoculated into cats caused disease in only 25% of animals, whereas about 44-90% dogs were infected. The prepatent period too was found to be longer, e.g. 8 months or longer, in cats compared to 6 months in dogs.[5,13]

D.immitis occurs in the right ventricles or pulmonary vessels. Right-sided heart failure secondary to pulmonary hypertension is uncommon in cats.[4] Most often in cats, cases have a brief history of dyspnea followed by sudden death. These are the result of thromboembolism or acute right-side cardiopulmonary failure.[9] The pulmonary arterial change in heartworm disease of cats can be more severe than that observed in dogs. Eosinophilia appear to be more common in cats.[3,13]

Heartworm is enzootic in dogs in the United States.[10] On the other hand, heartworm disease of cats is rare and is mostly detected at the time of necropsy.[13] Diagnosis of heartworm disease in cats can be difficult because of the transient nature of infection and the low numbers of microfilariae seen in circulation[5,13], as well as shorter lifespan of the adult worm in the cat.[5,13] Angiography and serology have been used to detect heartworm infections, especially in cats due to low levels of microfilaremia.[6] ELISA is commonly employed for measurement of anti-*D.immitis* antibody to adult worms.[6]

JPC Diagnosis: Lung, arteries and arterioles: Endarteritis, villar and eosinophilic, diffuse, severe, with mild smooth muscle hyperplasia and Splendore-Hoeppli material.

Conference Comment: The contributor provided an excellent overview of feline pulmonary dirofilariasis. Domestic felids, ferrets, and California sea lions are dead-end hosts, and are not a source of transmission due to the absence of microfilaremia.[8]

There was some slide variation, and eosinophilic granulomas with Splendore-Hoeppli material were present in some sections. Conference participants felt this was the origin of the deeply eosinophilic conglomerations present in some sections. Other considerations were necrotic nematode debris, as suggested by the contributor, or conglomerations of fibrin and hemoglobin. Conference participants also noticed the presence of hemosiderosis, and attributed this to heart failure.

Contributor: University of Connecticut
Department of Pathobiology and Veterinary Science
61 N. Eagleville Road, U-3089
Storrs, CT 06269
http://www.patho.uconn.edu

References:

1. Abbott PK. Feline dirofilariasis in Papula. *Aust Vet J*. 1966;42:247-249.
2. Adcock JL. Pulmonary arterial lesions in canine dirofilariasis. *Am J Vet Res*. 1961;22:655-662.
3. Calvert CA, Mandell CP. Diagnosis and management of feline heartworm disease. *J Am Vet Med Assoc*. 1982;180:550-552.
4. Dillon R. Feline dirofilariasis. *Vet Clin North Am Small Anim Pract*. 1984;14:1185-1199.
5. Donahoe JM. Experimental infection of cats with Dirofilaria immitis. *J Parasitol.* 1975;61:599-605.
6. Green BJ, Lord PF, Grieve RB. Occult feline Dirofilariasis confirmed by angiography and serology. *J Am Anim Hosp Assoc.* 1982;19:847-854.
7. Hamilton JM. Pulmonary arterial disease of the cat. *J Comp Pathol*. 1966;76:133-145.
8. Maxie MG, Robinson WF. Cardiovascular system. In: Maxie MG, ed. *Jubb, Kennedy, and Palmer's Pathology of Domestic Animals*. 5th ed. vol. 3, Philadelphia, PA: Elsevier Saunders; 2007:87-9.
9. McCracken MD, Patton S. Pulmonary arterial changes in feline dirofilariasis. *Vet Pathol*. 1993;30:64-69.
10. Patton S, McCracken MD. Prevalence of *Dirofilaris Immitis* in cats and dogs in eastern Tennessee. *J Vet Diagn Invest.* 1991;3:79-80.
11. Swerczek TW, Nielsen SW, Helmboldt CF. Ascariasis causing pulmonary arterial hyperplasia in cats. *Res Vet Sci*. 1970;11:103-104.
12. Van Vleet JF, Ferrans VJ. Cardiovascular system, Arterial Diseases, and growth disturbances. In: Thomson RG, ed. *Thompson's Special Veterinary Pathology*. Philadelphia, PA: B.C. Decker; 1988:333.
13. Wong MM, Pedersen NC, Cullen J. Dirofilariasis in cats. *J Am Anim Hosp Assoc*. 1982;19:855-864.

CASE III: 09L-0417 (JPC 3133673).

Signalment: 7-year-old, male, English bull terrier, C*anis lupus familiaris*, canine.

History: The animal was submitted for post mortem examination after being found dead. Poisoning was suspected.

Gross Pathology: Necropsy was performed approximately 20 hours after estimated time of death. The animal was moderately obese, weighing 37.9 kg. Both kidneys were diffusely pale, showing a dry cut surface with white multifocal pinpoint subcapsular and cortical areas. Both parathyroids were moderately enlarged. The ribs and skull exhibited moderate demineralisation. A moderate left cardiac concentric hypertrophy was observed. In the left adrenal gland, severe cortical compression atrophy due to a medullary, pale cream soft mass was seen. Age-related changes, consisting of mild bilateral nodular endocardosis of atrio-ventricular valves, moderate erosive coxarthrosis and mild nodular hepatic and prostatic hyperplasia were present.

Contributor's Histopathologic Description: Kidneys: Glomeruli are variably-sized and mostly hypocellular containing a high amount of eosinophilic, acellular and amorphous material (amyloid, Congo/ Sirius red positive) and exhibit mesangial atrophy. Under UV light, the amyloid, in the Congo red stained sections, shows orange fluorescence (as described by Linke).[8] Congophilia is lost in sections pretreated with potassium permanganate confirming the amyloid to be of secondary origin. Amyloid is also seen in renal tubules, within the lumen of a pelvic artery (amyloid cast), and in the renal pelvis. Glomeruli also contain to lesser extent deposition of fibrous tissue and diffusely moderate to severely thickened Bowman capsules (Masson's Trichrome stain positive). Mild to moderate, multifocal lymphoplasmacytic infiltration (variable within provided slides) and tubular mineralization (calcification) are present. Renal tubules often contain protein casts.

Arteries/arterioles: Moderate to severe deposition of amyloid and fibrosis are also seen in the intima and media of arteries and arterioles in the liver, left ventricle and septum.

Left adrenal gland: Adrenal medulla is densely cellular with cells arranged in packets and nests and supported by a moderately fine fibrovascular stroma that occasionally thickens and dissects the parenchyma, leading to a disarranged lobular pattern. The mass is composed of round to polygonal cells exhibiting mild to moderate anisocytosis and anisokaryosis. The cytoplasm of neoplastic cells is finely granular, eosinophilic and most often poorly demarcated. Nuclei are round to oval, hyperchromatic, with finely stippled chromatin and most frequently, no nucleoli. Mitotic figures are rare. Neoplastic cells are synaptophysin positive (neuroendocrine origin) and are found intravascularly within adjacent mesentery and extending directly from the adrenal gland into an adjacent large artery (phrenicoabdominal artery?), subcapsularly and supracapsularly (infiltrative growth pattern). Scattered binucleated cells, haemosiderophages and cytomegaly are observed. Occasional vascular degeneration with mineralization (calcification) is seen in the adrenal cortex. Due to the medullary mass, a moderate to severe, diffuse cortical atrophy is present. Transition between adrenal medulla and cortex is multifocally poorly demarcated and in scattered areas a rim of fibrous tissue separates the two regions (pseudocapsule formation).

Contributor's Morphologic Diagnosis: 1- Kidney, severe diffuse glomerular, intratubular and pelvic amyloidosis, mild to moderate diffuse

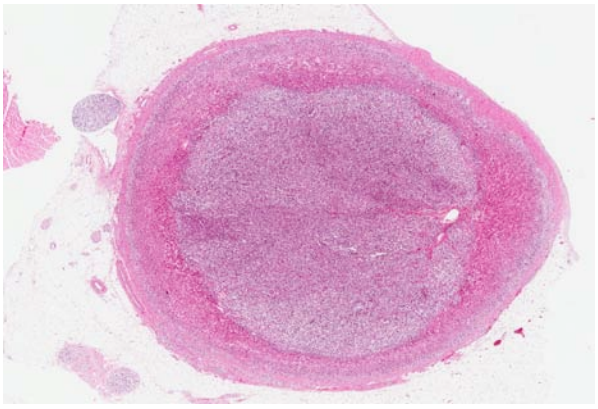

3-1. Adrenal gland, dog: The adrenal medulla is expanded by a well-demarcated neoplasm which compresses the overlying cortex. (HE 7X)

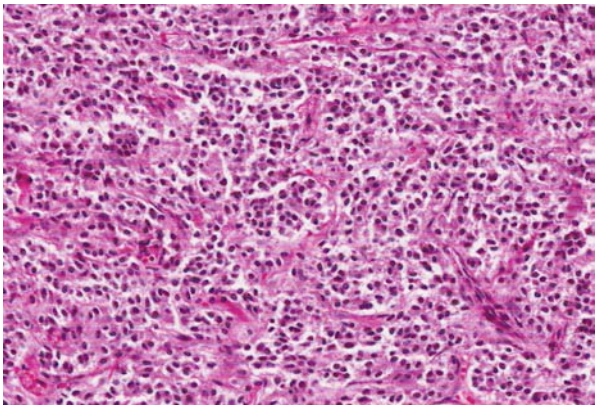

3-2. Adrenal gland, dog: Neoplastic cells are arranged in nests and packets and possess moderate amounts of finely granular, eosinophilic to brown cytoplasm. (HE 200X)

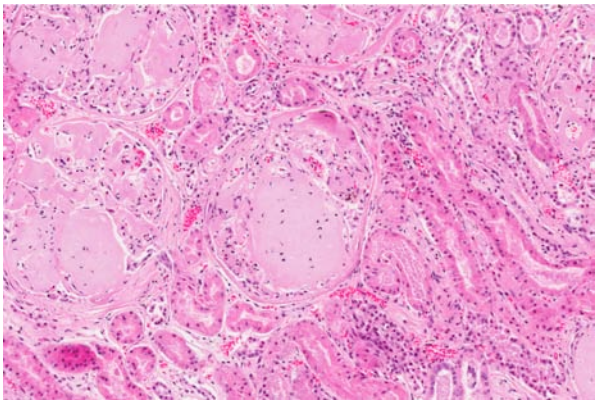

3-3. Kidney, dog: Diffusely, glomerular tufts are segmentally to globally expanded by large amounts of amorphous, finely fibrillar to waxy, lightly eosinophilic material (amyloid). (HE 200X)

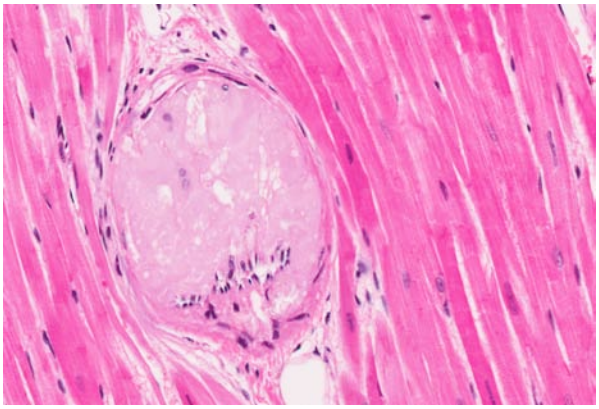

3-4. Heart, dog: Multifocally, the walls of large- and medium-caliber arteries are expanded by an accumulation of an amorphous eosinophilic proteinaceous material (amyloid). (HE 20X)

glomerulosclerosis and interstitial lymphoplasmacytic nephritis with focal calcification.
2- Kidney, liver and heart, moderate to severe multifocal amyloid angiopathy and arterio/arteriolosclerosis.
3- Adrenal, malignant pheochromocytoma with consecutive moderate to severe diffuse adrenal cortical atrophy.

Contributor's Comment: Amyloidosis consists of extracellular deposition of protein fibrils in beta-pleated sheets which are resistant to proteolytic cleavage and insoluble. The most frequent secondary changes associated with its presence include pressure atrophy, chronic renal failure and hepatic rupture. Secondary amyloidosis occurs when there is a long term rise in acute phase proteins, to be more precise in serum amyloid A, seen in chronic inflammation or neoplasia.[10,11,20] Studies have indicated its value as a prognostic marker for tumours and existence of metastases, in both humans [4,15] and animals.[20] Some authors attribute a tumourigenesis role to SAA based on the fact that different binding sites to extracellular matrix (ECM) components have been found in its structure.[10] The ECM provides tecidular structure, controls cell binding and so they propose that SAA possibly interacts with the ECM in a way that inhibits cellular adhesion and so promotes metastases.[10] In human medicine, it has been observed to coexist frequently with neuroendocrine tumours.[21] In humans, amyloid precursor like protein 1 has been reported to be more frequently expressed in neuroendocrine tumours of the small intestine.[1] In the latter studies it was also observed that in intestinal carcinomas, amyloid precursor proteins co-localised with synaptophysin, leading to the hypothesis that they would be transported to the cell membrane by synaptic microvesicles and affect tumour cell adhesion and invasiveness.[1] It has also been described that epinephrine increases the release of acute phase proteins.[7] Amyloid deposition is most commonly seen in the spleen, liver, enteric mucosa and arterial walls.[5,12]

The included table shows the main types of amyloid found in animals.

Type of amyloid	**Aetiology**	**Structures or organs mostly affected**	**Species and breeds most frequently affected**
Primary (AL) or Immunoglobin derived - Localized or generalized	Immunoglobin λ or κ in plasma cells dyscrasias from B cell monoclonal proliferation 25 types identified	Spleen, heart, tongue, Kidneys, nerves and joints (atypical distribution)	Uncommon Most frequent in dogs, horses and cats
Secondary or reactive systemic amyloidosis	AA (amyloid associated) serum protein (an acute phase reactant and the major HDL apoliprotein) produced by hepatocytes after cytokine stimuli (mainly IL6) [5,10]	Kidneys, arteries, spleen, liver, enteric mucosa, joints (gallinae)	Dogs, cattle, horses and cats Less frequently: swine and goats
Familial		Peripheral nerves, kidneys, heart, liver	Cats: Abyssinian, Siamese, Oriental Dogs: Beagles, Sharpei, Gray collies, English foxhound. Cattle: Holstein (with bovine leukocyte adhesion deficiency)
Apoliprotein A1 derived	Apoliprotein A1	Pulmonary arteries	Dogs
Islet amyloid polypeptide derived amyloid	Islet amyloid polypeptide Non-insulin dependent	Pancreas	Cats

Pheochromocytomas are tumours of chromaffin cells and are the most frequent tumours observed in the adrenal medulla.[2] Even though chromaffin cells produce catecolamines (epi/norepinephrine), in animals, clinical signs from their overproduction are rarely observed with a pheochromocytoma. When present, these symptoms consist mostly in tachycardia, cardiac hypertrophy and arterial sclerosis. In the rat, epinephrine has also been referred to act as a stimulant of interleukin release and secondary acute phase reactant.[7] Pheochromocytoma pathogenesis is unclear and has been associated in rats with chronic progressive glomerulopathy.[2,14,16] Genetic factors, pituitary tumours, hyperthyroidism, autonomic nervous system stimulation, hypercalcaemia, vitamin D_3 and diets rich in calcium, retinoids or sugars have also been implicated.[2,14,16,23] Interaction between the kidney and the adrenal gland include renalase, which is produced in the glomeruli and proximal tubules and induces metabolisation of catecholamines, thus leading to a decrease in the blood pressure.[3,7,19] There is a reduction in renalase synthesis in uraemic and end stage renal disease patients.[3,8,19] The renalase gene is also expressed in the heart, skeletal muscle and liver.[8]

In animals, hypertension is most commonly of secondary nature and associated with chronic renal failure. However, the reverse can happen, where renal changes can also be due to reduction in renal perfusion secondary to hypertension.[13]

Arteriolosclerosis includes various pressure-induced vascular changes and can be either mainly hyaline or hypertrophic. In the uraemic dog, the arterial and arteriolar lesions consist of deposition of subendothelial fibrin, internal elastic lamina dystrophy, necrosis of smooth muscle, mineralization and occasionally neutrophilic infiltration.[13] All of these changes were seen in this case together with the amyloid angiopathy, leading to the hypothesis that together with glomerulosclerosis, arteriolosclerosis was a more predominant feature that worsened and no longer is presented as blatant lesions.

Secondary hyperparathyroidism is seen in chronic renal failure and leads to osseous resorption in an attempt to increase the calcium levels. This mechanism changes the Ca:Ph ratio and as a consequence dystrophic calcification occurs.

The conditions seen in this case and their severity and distribution suggest that they are aetiologically related. Below, based on the above provided information, a hypothetical graphical simplifying attempt of the relationship between the present conditions is provided.

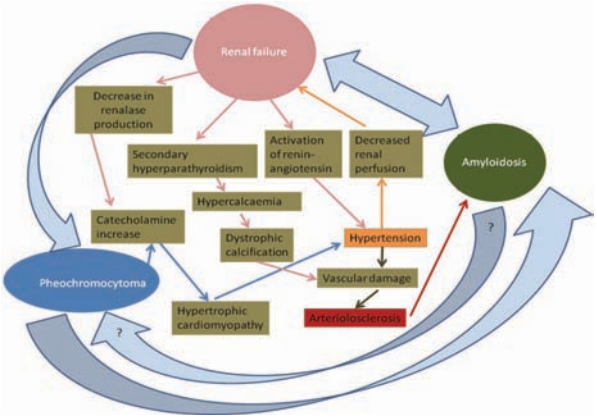

JPC Diagnosis: 1. Adrenal gland: Malignant pheochromocytoma.
2. Kidney: Amyloid, glomerular, segmental to global, diffuse, moderate, with multifocal lymphoplasmacytic interstitial nephritis.
3. Heart, mural arteries: Arteriosclerosis, hyaline, multifocal, mild (hyalinosis), with cardiac myofiber loss and fibrosis.

Conference Comment: The contributor provides an excellent description of amyloidosis, and our comment will only elaborate on some other details of this important pathologic condition in animal species.

Primary amyloidosis is rare in animals and may be encountered in the horse in the nasal vestibule and rostral parts of the nasal septum and turbinates. Secondary amyloidosis is far more common due to a reactive change caused by the synthesis of serum amyloid A (SAA) in the liver in response to IL-1, IL-6, and TNF in chronic inflammation. Cheetahs and Siberian tigers develop renal medullary interstitial amyloidosis in response to gastritis. Familial amyloidosis is usually autosomal recessive, and autosomal dominant in Abyssinian cats, which along with the Chinese Shar Pei develop amyloid in the kidneys, and Siamese cats develop amyloid in the liver. Localized amyloidosis can be deposited in the pancreas of cats and non-human primates with type II diabetes mellitus. Chickens can develop amyloid arthropathy associated with *Enterococcus faecalis*, and common sites of amyloid in geese and swans are the spleen and kidneys. In dogs, *Hepatozoon americanum* and *Ehrlichia canis* have been associated with renal amyloidosis and glomerulopathy, and excess dietary vitamin A has been associated with renal amyloidosis in cats.[12,13,19,20,22]

Renal amyloidosis may be presumptively diagnosed from a urine protein: creatinine of greater than 18. A ratio of less than 0.5 is considered normal, 1-3 indicates tubular disease, and greater than 3 indicates glomerular disease. Ultrastructurally, amyloid appears

as non-branching fibrils of 0.7-1.0 μm diameter that form single to laterally-aggregated bundles or interlocking mesh-like ribbons that lack periodicity.[6]

A differential diagnosis for the mural thickening of coronary arteries in this case is hyalinosis, a relatively common finding in the older dog. Hypertrophic hyalinization (hyalinosis) generally occurs in the intramural coronary and small meningeal and cerebral arteries of old dogs. There is generally no clinical significance in the CNS lesions, but this may result in multifocal intramural myocardial infarction. If valvular endocardiosis is present, these two lesions may lead to congestive heart failure. The mural deposits are most often fibrin or glycosaminoglycans (GAGs). Amyloid, as seen in this case[13] is far less common in hyalinosis.

Vascular invasion in the adrenal gland was not present on all slides.

Contributor: University of Liverpool
Department of Veterinary Pathology
Veterinary Science Building
Crown Street
Liverpool
L69 7ZJ
United Kingdom

References:

1. Arvidsson Y, Andersson E, Bergstrom A, et al. Amyloid precursor-like protein 1 is differentially upregulated in neuroendocrine tumours of the gastrointestinal tract. *Endocr Relat Cancer*. 2008;15:569-581.
2. Capen C. Endocrine glands. In: Maxie MG, ed. *Pathology of Domestic Animals*. Philadelphia, PA: Saunders Elsevier; 2007:419-422.
3. Desir GV. Renalase deficiency in chronic kidney disease, and its contribution to hypertension and cardiovascular disease. *Curr Opin Nephrol Hypertens*. 2008;17:181-185.
4. Findeisen P, Zapatka M, Peccerella T, et al. Serum amyloid A as a prognostic marker in melanoma identified by proteomic profiling. *J Clin Oncol*. 2009;27:2199-2208.
5. Gruys E. Protein folding pathology in domestic animals. *J Zhejiang Univ Sci*. 2004;5:1226-1238.
24. Gueft B, Ghidoni JJ. The Site of Formation and Ultrastructure of Amyloid. *Am J Pathol*. 1963;43(5): 837–854.
6. Kahl M, Schade R. Catecholaminergic modulation of rat acute phase reactants. *Agents Actions*. 1991;32:98-99.
7. Li G, Xu J, Wang P, et al. Catecholamines regulate the activity, secretion, and synthesis of renalase. *Circulation*. 2008;117:1277-1282.
8. Linke RP. Highly sensitive diagnosis of amyloid and various amyloid syndromes using Congo red fluorescence. *Virchows Arch*. 2000;436:439-448.
9. Malle E, Sodin-Semrl S, Kovacevic A. Serum amyloid A: an acute-phase protein involved in tumour pathogenesis. *Cell Mol Life Sci*. 2009;66:9-26.
10. Maxie MG. Urinary system. In: Maxie MG, ed. *Pathology of Domestic Animals*. 5th ed. Philadelphia, PA: Saunders Elsevier; 2007:463-465.
11. Maxie MG. Urinary system. In: Maxie MG, ed. *Pathology of Domestic Animals*, 5th ed. Philadelphia, PA: Saunders Elsevier; 2007:463-465.
12. Maxie MG. Cardiovascular system. In: Maxie MG, ed. *Pathology of Domestic Animals*. 5th ed. Philadelphia, PA: Saunders Elsevier; 2007:59-60.
13. Newman SJ. The urinary system. In: Zachary JF, McGavin MD, eds. *Pathologic Basis of Veterinary Disease*. St. Louis, MO: Elsevier; 2012:627-628,640.
14. Nyska A, Haseman JK, Hailey JR, et al. The association between severe nephropathy and pheochromocytoma in the male F344 rat -- the National Toxicology Program experience. *Toxicol Pathol.* 1999;27:456-462.
15. Ramankulov A, Lein M, Johannsen M, et al. Serum amyloid A as indicator of distant metastases but not as early tumor marker in patients with renal cell carcinoma. *Cancer Lett*. 2008;269:85-92.
16. Rosol TJ, Yarrington JT, Latendresse J, et al. Adrenal gland: structure, function, and mechanisms of toxicity. *Toxicol Pathol*. 2001;29:41-48.
17. Schiffrin EL, Lipman ML, Mann JF. Chronic kidney disease: effects on the cardiovascular system. *Circulation.* 2007;116:85-97.
18. Snyder PW. Diseases of immunity. In: Zachary JF, McGavin MD, eds. *Pathologic Basis of Veterinary Disease*. St. Louis, MO: Elsevier; 2012:284-288.
19. Stalker MJ. Liver and biliary system. In: Maxie MG, ed. *Pathology of Domestic Animals*. 5th ed. Philadelphia, PA: Saunders Elsevier, 2007;315-316.
20. Steinhoff MM, Wells SA, Jr., DeSchryver-Kecskemeti K. Stromal amyloid in pheochromocytomas. *Hum Pathol.* 1992;23:33-36.
21. Tecles F, Caldin M, Zanella A, et al. Serum acute phase protein concentrations in female dogs with mammary tumors. *J Vet Diagn Invest*. 2009;21:214-219.
22. Terio KA, O'Brien T, Lamberski N, et al. Amyloidosis in black-footed cats (*Felis nigripes*). *Vet Pathol*. 2008;43(3):393-400.
23. Tischler AS, Powers JF, Alroy J. Animal models of pheochromocytoma. *Histol Histopathol*. 2004;19:883-895.

CASE IV: V10-1558 (JPC 4001079).

Signalment: 7-year-old male castrated Siamese cross, feline (*Felis catus*).

History: The cat presented with a mass on the left iris of unknown duration. An aspiration of the iris was diagnosed as a plasmacytoma. Chemotherapy was attempted with no response. The left eye was enucleated and submitted for histopathological diagnosis.

Gross Pathology: There was a 1cm mass expanding the ventral iris.

Laboratory Results: Neoplastic cells are immunohistochemically positive for S-100 and melan-A.

Contributor's Histopathologic Description: Eye (left), anterior uvea: Diffusely expanding the iris, ciliary body, irido-corneal angle, and infiltrating into the adjacent sclera and uvea, and protruding into the anterior chamber is an unencapsulated, highly cellular, poorly demarcated neoplasm arranged in closely packed sheets, streams and bundles, and vague packets separated by a thin fibrovascular stroma. Neoplastic cells exhibit two morphologic forms. The first is a pleomorphic round cell with distinct cell borders, abundant granular eosinophilic to clear cytoplasm, and 1-2 large round to irregular often peripheralized nuclei with coarsely stippled chromatin and 1-3, large, occasionally irregular, magenta nucleoli. Anisocytosis and anisokaryosis is marked. The second form of neoplastic cell consists of spindle cells with indistinct cell borders, a moderate amount of eosinophilic cytoplasm, a round to oval nucleus with fine to coarsely stippled chromatin and 1-2 nucleoli. Anisocytosis and anisokaryosis is moderate. The mitotic rate in both morphologic populations is highly variable and reached up to 8 mitotic figures per high power field. Rarely, melanin pigment is identified within the cytoplasm of neoplastic cells.

Contributor's Morphologic Diagnosis: Eye, iris, left: Melanoma, diffuse, Siamese cross (*Felis catus*), feline.

Contributor's Comment: The cat in this case was interesting in that it presented with a visible, white nodule protruding into the anterior chamber. An aspiration of that mass consisted of multiple individualized round cells with abundant clear to pale blue cytoplasm, and 1-2 small round eccentrically placed nuclei. The mass was initially diagnosed as a potential plasmacytoma with a recommendation for removal and confirmation due to the rarity of that particular type of tumor. There is only a single case report by Michau et.al. in 2003 diagnosing an intraocular extramedullary plasmacytoma in a cat.[5]

4-1. Eye, cat: Clinical picture of a neoplasm within the anterior chamber.

The differential diagnosis for the gross presentation included nodular iris melanoma and a uveal cyst. On histopathologic examination, the neoplastic melanocytes diffusely infiltrated iridial stroma, ciliary body, and irido-corneal drainage angle and protruded into the anterior chamber resulting in the grossly visible nodule. Melanocytic tumors are the most common primary intraocular neoplasms in cats,[2,7] with intraocular sarcomas and ciliary epithelial neoplasms also occurring with lesser frequency.[3]

Diffuse iris melanoma generally begins as an asymmetrical abnormal pigmentation of the iris that may be clinically noted several years prior to the development of neoplasia.[2] This area of pigmentation may remain static or progress to nodular iridial irregularities and diffusely infiltrate the sclera, ciliary body, and posterior segment.[2] Neoplastic cells originate from melanocytes that line the anterior border of the iris.[9] Rarely, atypical melanomas, not associated with diffuse iris melanoma, may arise multifocally within the limbus or choroid. Little is known about their origin, behavior, and prognosis.[2,4]

Three morphologically distinct neoplastic cells are often found in feline diffuse iris melanoma. These different morphologic cell types may occur in any combination within diffuse iris melanoma, and no prognostic significance has yet been attached to these various combinations.[2,9]

1) **Pleomorphic round cells** (most common type) consist of cells with abundant eosinophilic cytoplasm and a primarily centralized round nucleus. These cells may occasionally exhibit cytomegaly, cytoplasmic invaginations forming pseudo-inclusions, and variable amounts of pigmentation.

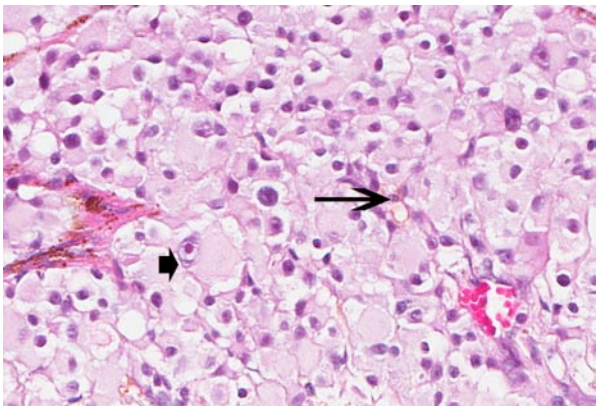

4-2. Eye, cat: Neoplastic cell are arranged in nest and packets and rarely contain a small amount of a brown granular pigment (melanin) (arrow). (HE 400X)

4-3. Eye, cat: There is diffuse atrophy of the inner (ganglion, plexiform, nuclear) layers of the retina (arrow), likely as a result of closure of the drainage angle and increase intraocular pressure. (HE 200X)

2) **Spindle cells** (2nd most common).
3) **Balloon cells** consist of cells with abundant eosinophilic to clear cytoplasm with a high cytoplasm to nuclear ratio and a small often centralized round nucleus. No prognostic significance has been associated with the morphologic type of neoplastic cells.

Poorly differentiated intraocular melanomas may exhibit a wide variety of morphoglogic and pigmentation characteristics. This often results in a struggle to develop a definitive morphologic diagnosis on H&E alone. Common immunohistochemical stains include HMSA-5, S-100, and tyrosinase.[1]

Feline diffuse iris melanomas are considered more likely to metastasize than canine uveal melanomas, but due to the slow progression of the tumor, the overall risk that an animal will die from the melanoma is less than 20%.[9] In cats, metastasis associated with diffuse iris melanomas has been documented affecting lungs, lymph nodes, skeletal system and abdominal viscera.[6] Predictors of metastasis include scleral invasion, invasion into posterior iris epithelium, and overall tumor size.[9]

Retroviral antigen has been identified in both intraocular sarcoma and diffuse iris melanoma.[1,3,8] In a retrospective study by Stiles et. al. in 1999, 3 of 36 intraocular melanomas tested positive for FeLV-FeSV DNA by nested PCR.[7] Another retrospective study in 2002 by Cullen et. al. failed to find viral DNA sequences in the intraocular melanomas examined in 10 cats.[3]

JPC Diagnosis: Eye, ciliary body, iris, choroid: Diffuse melanoma.

Conference Comment: Conference participants discussed the presence of ganglion cell layer and inner nuclear layer atrophy likely due to occlusion of the drainage angle by the neoplasm. Occlusion prohibits adequate drainage resulting in an increase in intraocular pressure (IOP) and subsequent development of closed angle secondary glaucoma.[6,10] Histologic findings characteristic of glaucoma are cupping of the optic disk (pathognomonic when present), dilated axonal sheaths, and axonal degeneration and loss. Progressive retinal changes include atrophy of the afferent nerve fiber layer and ganglion cell layer resulting in accentuation of Muller cells, thinning of the inner plexiform and nuclear layers and eventual blending together of the inner and outer nuclear layers, with the retina eventually being reduced to a thin glial scar with few outer nuclear layer remnants and melanophages from the retinal pigment epithelium. Diffuse iridal melanomas are the most common cause of secondary glaucoma in cats. Both increased IOP and degenerative structural changes must be present to warrant a diagnosis of glaucoma[6,10]; however, since IOP was not reported for this cat, and the eye was still visual according to the contributor, the cause of the retinal atrophy can only be speculated.

The contributor mentions uveal cysts, or pigmented uveal nodules, as a gross differential diagnsosis. Uveal cysts are fluid-filled cysts which may be congenital or arise secondary to trauma or inflammation. They are non-neoplastic, non-progressive and considered an incidental finding.

Contributor: Air Force Research Laboratory
2509 Kennedy Circle, Building 125
Brooks City Base, TX 78235

References:

1. Cullen CL, Haines DM, Jackson ML, et al. Lack of detection of feline leukemia and feline sarcoma viruses in diffuse iris melanomas of cats by immunohistochemistry and polymerase chain reaction. *J Vet Diagn Invest*. 2002;14:340-343.

2. Dubielzig RR. Tumors of the eye. In: Meuten DJ, ed. *Tumors in Domestic Animals*. 4th ed. Ames, IA; Iowa State Press; 2002:744-749.
3. Grahn BH, Peiffer RL, Cullen CL, et al. Classification of feline intraocular neoplasms based on morphology, histochemical staining, and immunohistochemical labeling. *Vet Ophthalmol*. 2006;9:395-403.
4. Harris BP, Dubielzig RR. Atypical primary ocular melanoma in cats. *Vet Ophthal*. 1999;2:121-124.
5. Michau TM, Proulx DR, Rushton SD, et al. Intraocular extramedullary plasmacytoma in a cat. *Vet Opthalmol.* 2003;6:177-181.
6. Njaa BL, Wilcock BP. The eye and ear. In: Zachary JF, McGavin MD, eds. *Pathologic Basis of Veterinary* Disease. 5th ed. St. Louis, MO: Elsevier; 2012:1215-20, 1228-9.
7. Planellas M, Pastor J, Torres MD, et al. Unusual presentation of a metastatic uveal melanoma in a cat. *Vet Ophthalmol*. 2010;13:391-394.
8. Stiles J, Bienzle D, Render JA, et al. Use of nested polymerase chain reaction (PCR) for detection of retroviruses from formalin-fixed, paraffin-embedded uveal melanomas in cats. *Vet Ophthalmol*. 1999;2:113-116.
9. Wilcock B, Dubielzig RR, Render JA. Histological Classification of Ocular and Otic Tumors of Domestic Animals. 2nd Series, Vol. IX. Washington, DC: Armed Forces Institute of Pathology, Washington, DC; 2002:18-19, 24-25.
10. Wilcock, BP. Eye and ear. In: Maxie MG, ed. *Jubb, Kennedy, and Palmer's Pathology of Domestic Animals*. 5th ed. vol. 1, Philadelphia, PA: Elsevier Saunders; 2007:514-5, 538-42.

Joint Pathology Center
Veterinary Pathology Services

WEDNESDAY SLIDE CONFERENCE 2011-2012

Conference 18

14 March 2012

CASE I: AFIP (JPC 4001563).

Signalment: Female 4-year-old cynomolgus monkey (*Macaca fascicularis*).

History: This monkey was a control animal in a 4-week oral gavage toxicity study with an experimental compound. It exhibited no clinical signs while on the study and was euthanized at the scheduled terminal sacrifice. The lesion was found incidentally during routine histopathologic evaluation of tissues.

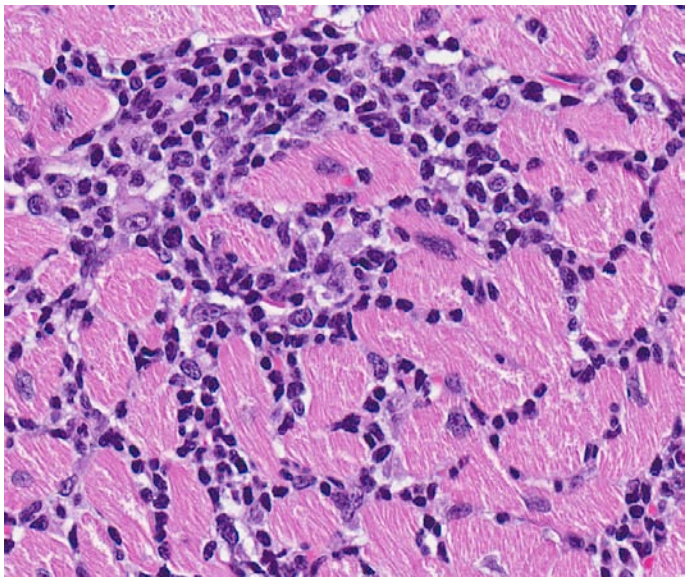

1-1. Heart, cynomolgus monkey: Numerous lymphocytes, macrophages, and lesser numbers of neutrophils and plasma cells infiltrate the myocardium and replace cardiomyocytes. (HE 320X)

Gross Pathology: Necropsy findings included a discolored duodenum, liver cyst, small pancreas, and an abnormally shaped spleen.

Laboratory Results: Three days prior to euthanasia, electrocardiography revealed multiple premature ventricular complexes, including periods of ventricular bigeminy and paroxysmal ventricular tachycardia.

Contributor's Histopathologic Description: Heart: There are moderate infiltrates of lymphocytes, plasma cells, macrophages, and rare neutrophils predominantly within the myocardium, and to a lesser extent affecting the endocardium and minimally affecting the epicardium. Inflammatory cell infiltrates and mild edema expand the interstitium and separate cardiac myofibers. Scattered myofibers exhibit degeneration characterized by variation in fiber size, hypereosinophilia, loss of cross striations, fragmentation, and nuclear hypertrophy. Rare myofibers contain protozoal pseudocysts. Pseudocysts are irregularly shaped, approximately 30 microns in length, and contain myriad amastigotes. Amastigotes are spherical, basophilic, approximately 2 microns in diameter, and have a darkly basophilic kinetoplast.

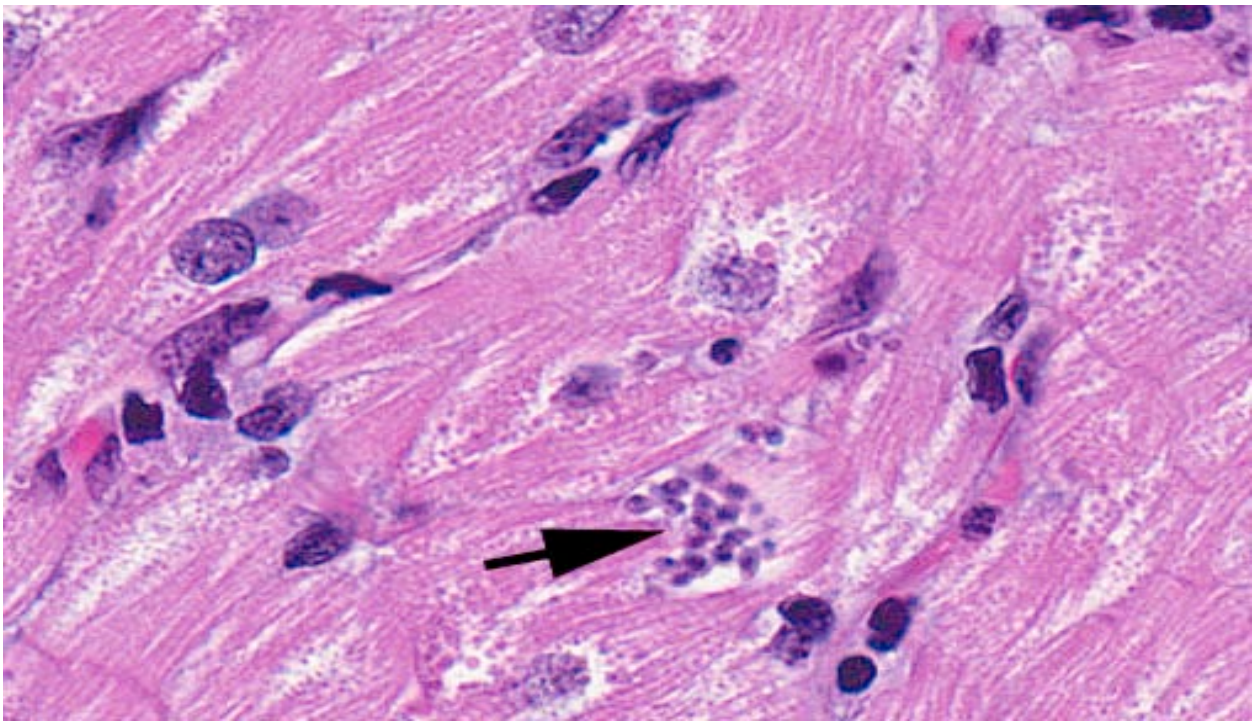

1-2. Heart, cynomolgus monkey: Amastigotes of Trypanosoma cruzi are present within the cytoplasm of rare cardiomyocytes. (HE 400X)

Contributor's Morphologic Diagnosis: Heart: Moderate, chronic, multifocal to coalescing lymphoplasmacytic and histiocytic myocarditis and endocarditis with myofiber degeneration and protozoal pseudocysts containing amastigotes (*Trypanosoma cruzi*).

Contributor's Comment: *Trypanosoma cruzi* is the causative organism of Chagas' disease. *Trypanosoma*, along with *Leishmania*, belongs to the subphylum *Sarcomastigophora.* *T. cruzi* is a hemoflagellate protozoan that is endemic in South America, Central America, Mexico, and in the southern United States. Natural reservoirs include opossums, armadillos, rodents, dogs, cats, pigs, raccoons, and monkeys.[1,4]

Insects serve as the vector for most *Trypanosoma* species. *Trypanosoma cruzi* resides in the hindgut of reduviid bugs.[1,3] At night these bloodsucking insects emerge to feed upon sleeping hosts. They usually target the face, and because of this are also known as "kissing bugs". Once fed the insects will often defecate, depositing infective organisms onto the skin. Trypanosomes gain entry through a wound in the skin or by crossing mucous membranes.[3] While circulating in the body, they are in a form known as trypomastigotes. Most species of *Trypanosoma* exist solely in this form, which is also the reproductive stage. *T. cruzi* is unique among trypanosomes in that it also forms a tissue pseudocyst containing amastigotes[3], and this is the form that undergoes multiplication in this species.[1] Amastigotes can then differentiate into trypomastigotes, which rupture out from their cysts and can either invade another cell or circulate within the blood to infect another intermediate host. Amastigotes are most commonly found in cardiac and skeletal muscle, but can also occur in reticuloendothelial, neural, and glial cells.[1,4]

T. cruzi infection in primates often results in nonspecific clinical signs including edema, anemia, hepatosplenomegaly, and lymphadenitis. The most severe sequela of infection is myocarditis. Myocarditis can result in dilated cardiomyopathy, arrhythmias, and eventually death.[7] Myocarditis is likely the result of a variety of factors, including a reaction to degenerating parasites as well as an autoimmune component caused by a release of proteins from degenerating myofibers.[6,8]

This case is unusual in that it occurred in a monkey originally from Asia, where *T. cruzi* is not found. This particular monkey originated from China and was shipped to a holding facility in Texas, where it was held indoors in quarantine for approximately 2 ½ months. Following quarantine, the monkey was placed in a single-sex corn crib style outdoor housing unit for 11 months. This is most likely where the animal became infected. The clinical history of this monkey while at the holding facility was unremarkable. A few cases of *T. cruzi* in animals housed at this facility have occurred, and human cases are not uncommon in the surrounding area.

JPC Diagnosis: Heart: Pancarditis, lymphoplasmacytic, and histiocytic, multifocal, mild to moderate, with myocardiocyte degeneration and necrosis and rare intracytoplasmic protozoal amastigotes.

Conference Comment: In most cases of cardiac *T. cruzi* infection,, granulomatous myocarditis with myocyte degeneration and necrosis is most severe in the right atrium and ventricle, while chronic disease, such as in this case, presents as lymphoplasmacytic myocarditis concentrated in the apex of the heart with fewer organisms. In addition to the organs listed by the contributor, *T. cruzi* amastigotes have been found within germinal cells in the testicle of dogs surrounded by an intense lymphoplasmacytic interstitial orchitis.[4]

Two proteins on the surface of *T. cruzi* are involved in its entry into macrophages and other host cells. Trans-sialidase removes host cell sialic residues and transfers them to a parasite surface protein (Ssp-3), which binds to host cells. Penetrin binds extracellular matrix proteins, heparin, heparin sulfate, and collagen and mediates parasite invasion into host cells. Intramacrophage survival is due to rapid movement from lysosomes to the cytosol, which is mediated by neuraminidase which removes sialic acids from host proteins and destabilizes the lysosomes, and hemolysins, in which lysosomal acid pH stimulates release and the formation of pores in lysosomal membranes.[2]

Protozoal pseudocysts were difficult to find, and were often located in myofibers unaffected by the inflammatory response. Due to the low numbers of observable parasites and atypical host, several viral etiologies were also considered in the differential diagnosis including picornaviridae, such as encephalomyocarditis virus or Coxsackie B virus, and morbillivirus (measles), adenovirus, and betaherpesvirus (cytomegalovirus).[5]

Contributor: Covance Laboratories, Inc.
3301 Kinsman Boulevard
Madison, WI 53704
www.covance.com

References:

1. Bowman DD. *Georgis' Parasitology for Veterinarians*. 7th ed. Philadelphia, PA: W.B. Saunders Company; 1999.
2. de Souza W, de Carvalho TMU, Barrias ES. Review on Trypanosoma cruzi: Host Cell Interaction. *Int J Cell Biol*. 2010;2010:295394.
3. Gardiner CH, Fayer R, Dubey JP. *An Atlas of Protozoan Parasites in Animal Tissues*. 2nd ed. Washington, DC: Armed Forces Institute of Pathology; 1998.
4. Jones TC, Hunt RD, King NW. *Veterinary Pathology*. 6th ed. Baltimore, MD: Wiliams & Wilkins; 1997.
5. Masek-Hammerman K, et al. Epizootic Myocarditis Associated with Encephalomyocarditis Virus in a Group of Rhesus Macaques (Macaca mulatta). *Vet Pathol*. 2012;49(2):386-92.
6. McAdam AJ, Sharpe AH. Infectious diseases. In: Kumar V, Abbas AK, Fausto N, eds. *Robbins and Cotran Pathologic Basis of Disease*. 7th ed. Philadelphia, PA: Elsevier Saunders; 2005:405-406.
7. Toft JD, Eberhard ML. Parasitic diseases. In: Bennett TB, Abee CR, Henrickson R, eds. *Nonhuman Primates in Biomedical Research Diseases*. San Diego, CA: Academic Press; 1998:115-116.
8. Valli VEO. Hematopoietic system. In: Maxie MG, ed. *Jubb, Kennedy and Palmer's Pathology of Domestic Animals*. 5th ed. vol. 3. Philadelphia, PA: Elsevier Ltd; 2007:254.

CASE II: G7979 (JPC 3136262).

Signalment: 10-year-old intact female rhesus monkey (*Macaca mulatta*), nonhuman primate.

History: The animal belonged to a breeding group of rhesus monkeys housed in an indoor-outdoor facility with free access to a large outdoor enclosure. This monkey was found dead without prior signs of illness.

Gross Pathology: Gross pathologic findings were limited to the abdominal cavity. Severe hepatomegaly was demonstrable, with fibrous transformation of the liver tissue affecting nearly all lobes and the gallbladder. Multiple cysts of different sizes were distributed throughout the fibrous hepatic tissue. The cysts had a diameter up to 5 cm that were filled with gelatinous to liquid material and contained hydatid sand. A generalized subacute peritonitis was a concomitant finding. The mesenteric lymph nodes appeared enlarged. Similar multiloculated cysts were present in the pancreas.

Contributor's Histopathologic Description: Histopathologic examination revealed metacestodal tissue in all liver samples. The liver parenchyma was destroyed by infiltrative growing cysts of different sizes which were surrounded by a fibrous hyaline membrane. Most cysts appeared empty. Single cysts contained protoscolices, arrays of hooklets and brood capsules. Calcareous corpuscles were present in the vicinity of the germinal layer. The cysts were surrounded by chronic inflammatory cell infiltration with foreign body-type giant cells.

Immunohistochemistry: *Echinococcus multilocularis:* positive.

Contributor's Morphologic Diagnosis: Liver: hepatitis, granulomatous, chronic, multifocal, severe, with metacestodes consistent with *Echinococcus multilocularis,* rhesus monkey (*Macaca mulatta*), non-human primate.

Contributor's Comment: *Echinococcus* belongs to the phylum of *Platyhelminthes*, the class of *Cestodea* and subclass of *Eucestodia*. The genus of *Echinococcus* is subordinated to the order of *Cyclophyllidea* and the family of *Taeniidae*. Echinococcosis is a zoonotic disease, caused by adult or larval stages of cestodes which belong to the genus *Echinococcus*. Up to now, four species of *Echinococcus* are known: *E. granulosus*, *E. multilocularis*, *E. oligarthrus* and *E. vogeli*. The life of the parasites shows a cyclic structure.

The alveolar echinococcosis (AE) is an infectious disease which is caused by the second larval stage (metacestode) of the fox tapeworm. The adult parasite lives in the gastrointestinal tract of foxes of the genera *Vulpes* and *Alopex*, which are the definitive hosts. The eggs, including the first larval stage (oncosphere), get

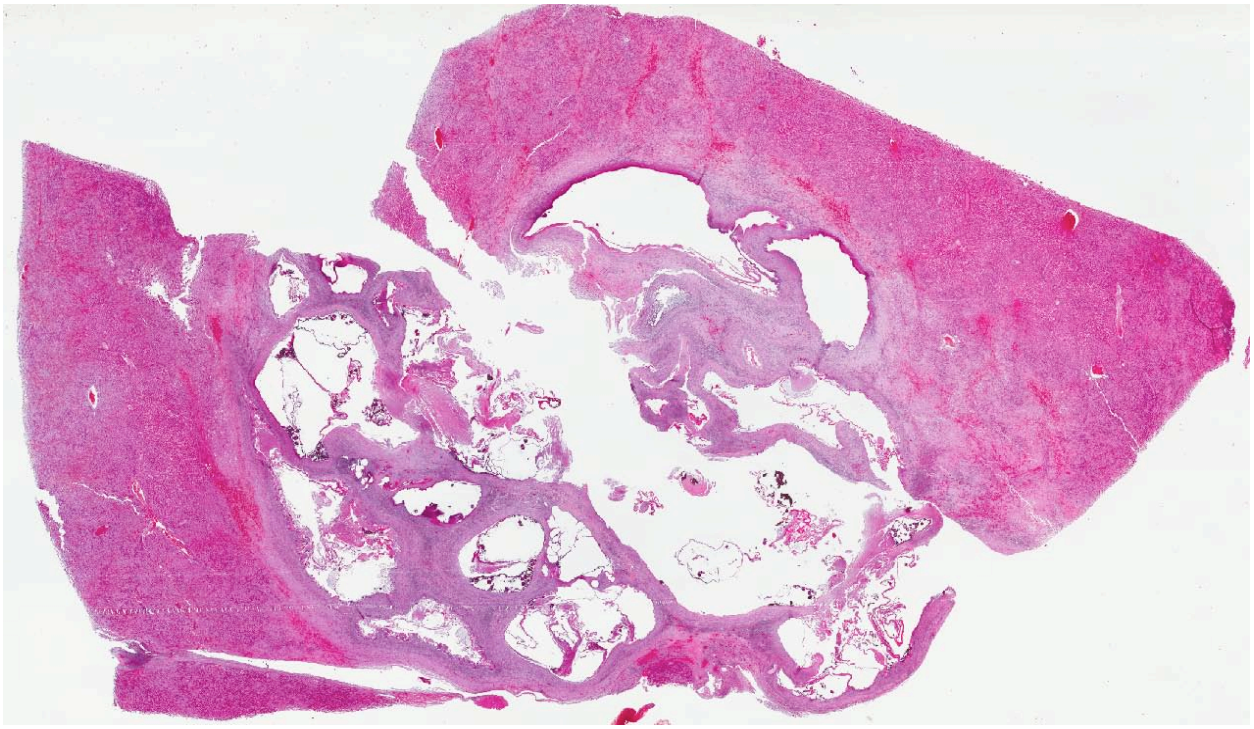

2-1. Liver, rhesus macaque: Hepatic parenchyma has been replaced by expanding and proliferating brood capsules of Echinococcus multlocularis. The cysts are surrounded by a fibrous capsule, and multifocal lymphocytic inflammation. (HE 10X)

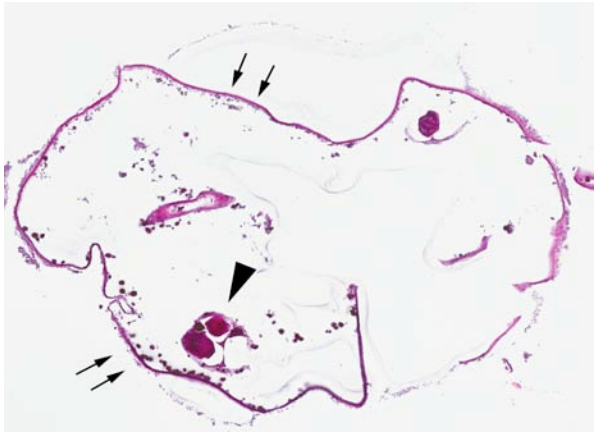

2-2. Liver, rhesus macaque: Brood capsules contain single to multiple strobilicerci, with a bladder (arrows) and protoscolex (arrowhead). (HE 200X)

outside with the feces and are ingested by intermediate hosts, which typically are rodents of the family *Arvicolidae*. In the intermediate host, the oncosphere penetrates the intestinal wall and enters the blood system. Via the blood stream, the oncosphere reaches different organs, especially the liver. Once the oncosphere has reached the liver it starts to develop into the metacestode stage. In contrast to *E. granulosus* with the development of a unilocular cyst, the typical cyst of *E. multilocularis* shows a multilocular structure. The cyst with brood capsules and protoscolices may disturb the functions of the liver, depending on its size and location. The development of protoscolices can take several months. There may be several thousand protoscolices within a cyst. If protoscolices are ingested by a definitive host, they develop to the sexually mature adult tapeworm, approximately four to six weeks after infection. Thus, the cycle is closed.[5]

All mammals (including man and nonhuman primates) in which metacestodes develop may be an intermediate host, but it is important to distinguish between a real intermediate host, which plays a role in the perpetuation of the cycle, and an accidental intermediate host like this monkey, which is a dead end for the parasite.

Many monkey species are susceptible to infection with *E. Multilocularis.*[1,2,6,7] In recently described small outbreaks, only a few species were affected (five *M. fascicularis* and two *Gorilla gorilla*[7] or 12 *M. fuscata*[8]). A larger outbreak at the German Primate Center affected three different Old World monkey species simultaneously in a period of 12 years.[9] In this largest reported outbreak, cynomolgus monkeys are the species at risk. As previously reported, the percentage of infected cynomolgus monkeys among colonies of captive primates was conspicuously high (> 50%).[3]

Since the 1990s, *E. multilocularis* infection is spreading geographically and increasing infection rates of red foxes have been noted in Eastern and Western European countries.[4] In Northern Germany, Denmark and Poland, prevalence rates in foxes are usually < 5%, but focal areas of higher prevalence exist. Animals in zoological gardens and in institutional colonies in the northern hemisphere are at risk and alveolar echinococcosis must be considered as an emerging disease. Certain species of non-human primates are very susceptible to alveolar echinococcosis and may thus indicate previously unknown areas of high transmission.

JPC Diagnosis: 1. Liver: Hydatid cyst, multiloculated, with hepatocellular loss and fibrosis, and mild granulomatous hepatitis.
2. Liver: Amyloidosis, diffuse, moderate.

Conference Comment: Amyloid, confirmed by Congo red staining, diffusely expands the space of Disse throughout the liver adjacent to the hydatid cysts. Secondary amyloidosis is frequently the major complication of several chronic inflammatory diseases. The incidence of AA amyloidosis is relatively high in cases with granulomatous diseases of known etiology such as tuberculosis, leprosy and osteomyelitis. Metazoan parasite-induced amyloidosis has also been reported in rodent filariasis, human schistosomiasis, and rodent and non-human primate alveolar hydatidosis. Hydatid cysts trigger a massive influx of leukocytes at the focus of infection.[1] Elaboration of cytokines in chronic inflammation stimulates increased positive acute phase proteins, such as serum amyloid A (SAA). Regulation of synthesis of acute phase proteins is largely modulated by cytokines such as IL-6, IL-1, TNF-alpha, IFN-gamma, and TGF-beta, and has been shown to influence the serum concentration of acute phase proteins. SAA is the most sensitive acute phase protein, and serum levels of SAA have been used both in diagnosis and monitoring of inflammatory and infectious diseases. Amyloidosis is thought to be due to either the defective degradation of SAA or the production of abnormal SAA that is resistant to degradation.[10]

Contributor: German Primate Center
Department of Infectious Pathology
Kellnerweg 4
37077 Göttingen, Germany
www@dpz.eu

References:

1. Bacciarini LN, Gottstein B, Pagan O, et al. Hepatic alveolar echinococcosis in cynomolgus monkeys (*Macaca fascicularis*). *Vet Pathol.*2004; 41:229-234.
2. Brack M, Tackmann K, Conraths FJ, et al. Alveolar hydatidosis (*Echinococcus multilocularis*) in a captive

rhesus monkey (*Macaca mulatta*) in Germany. *Trop Med Int Health*. 1997;2(8):754-759.
3. Deplazes P, Eckert J. Veterinary aspects of alveolar echinococcosis-a zoonosis of public health significance. *Vet Parasitol*.2001;98(1-3):65-87.
4. Eckert J, Conraths FJ, Tackmann K. Echinococcosis: an emerging or re-emerging zoonosis? *Int J Parasitol.* 2000;30(12-13):1283-1294.
5. Meyers WM, Neafie, RC, Marty AM, et al. Hydatidosis. In: Pathology of Infectious diseases, Vol. I Helminthiasis. Washington, DC:Armed Forces Institute of Pathology, 2000:145-164.
6. Rehmann P, Grone A, Lawrenz A, et al. *Echinococcus multilocularis* in two lowland gorillas (*Gorilla g. gorilla)*. *J Comp Pathol*. 2003;129:85-88.
7. Rehmann P, Grone A, Gottstein B, et al. Alveolar echinococcosis in the zoological garden Basle. *Schweiz Arch Tierheilkd.* 2005;147(11):498-502.
8. Sato C, Kawase S, Yano S, et al. Outbreak of larval *Echinococcus multilocularis* infection in Japanese monkey (*Macaca fuscata*) in a zoo, Hokkaido: western blotting patterns in the infected monkeys. *J Vet Med Sci*. 2005;67:133-135.
9. Tappe D, Brehm K, Frosch M, et al. *Echinococcus multilocularis* infection of several Old World monkey species in a breeding enclosure. *Am J Trop Med Hyg*. 2007;77(3):504-506.
10. Zachary JF. Mechanisms of microbial infections. In: Zachary JF, McGavin MD, eds. *Pathologic Basis of Veterinary Disease*. 5th ed. St. Louis, MO: Elsevier; 2012:287-8.

CASE III: AP10-5169 (JPC 4004526).

Signalment: 3-year-old male pigtail macaque (*Macaca nemestrina*) non-human primate.

History: The monkey received a total dose of 1200cGy total body irradiation on 9/18 and 9/19/2010. Antibiotic prophylaxis was instituted immediately. Cell infusion was performed on 9/20, during which the monkey had an anaphylactic episode, and was given Benadryl and recovered. Multiple whole blood transfusions were given between then and the time of death. Two weeks post-radiation, the monkey started doing poorly and showed signs of edema, petechiae, and watery diarrhea. Five days later, the monkey became hypothermic and died the next day while under light sedation with ketamine.

Gross Pathology: Multifocal cutaneous petechiae; subcutaneous edema; diarrhea staining in the perianal region; mild hydrothorax; hydropericardium 10 ml; mild ascites; diffuse collapsed/atelectatic lungs due to hydrothorax; marked diffuse edema of the stomach and intestinal wall.

Laboratory Results: Hypoproteinemia, pancytopenia.

Histopathologic Description: Stomach: Diffusely the mucosa is mildly thickened by a combination of necrosis, hemorrhage and innumerable small protozoans which surround, separate, and occasionally replace necrotic gastric glands. Glandular mucosa is multifocally and transmucosally necrotic – glandular epithelium is shrunken, with karyolytic or pyknotic nuclei. Often glands are lined with attenuated epithelium, with dilated lumens which contain sloughed epithelial cells, cellular debris, and protein. Glands are often separated with a combination of hemorrhage, edema, and cellular debris. Innumerable 4-6 µm pyriform protozoans with flocculent basophilic cytoplasm and a single round basophilic nucleus are present within the lamina propria, numerous gastric glands, and transmigrate the muscularis mucosa into the submucosa, where they often fill dilated lymphatics and are present in variable concentrations throughout the surrounding submucosa (where they are occasionally phagocytosed by macrophages). The submucosa is markedly expanded by edema, and multifocally, there is marked perivascular hemorrhage. The walls of affected arterioles are often expanded by brightly eosinophilic protein and cellular debris (necrotizing vasculitis). Protozoans are also present within the interstitium and lymphatics of the muscularis and serosa, but rarely associated with significant inflammation.

Contributor's Morphologic Diagnosis: Stomach; mucosa, lamina propria: Diffuse, severe edema and hemorrhage with myriads of extracellular/interstitial and intravascular/intralymphatic protozoa. (trichomonad gastritis)

Jejunum; mucosa, lamina propria: Diffuse, severe edema and hemorrhage with myriads of extracellular/ interstitial and intravascular/intralymphatic protozoa.

Bone marrow; sternum, femur, and tibia: Myeloid hypoplasia, severe, radiation-induced.

Contributor's Comment: Histopathology revealed a severe infection of the stomach and intestines by protozoal organisms; these organisms originated in the lumen and infiltrated through the mucosa into the submucosa and muscular layers, and were also present within blood and possibly lymphatic vessels. This caused marked disruption of the gastric and intestinal walls and was likely the cause of the severe protein loss indicated in the clinical chemistry finding of

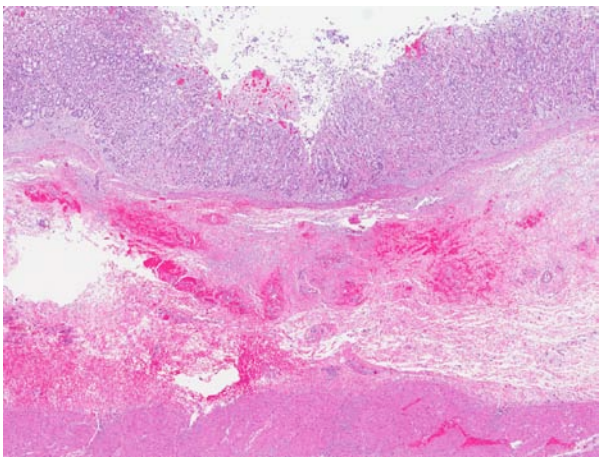

3-1. Stomach, pigtailed macaque: There is diffuse necrosis of the gastric mucosa, and necrosis mixed with hemorrhage and edema within the underlying mucosa. (HE 10X)

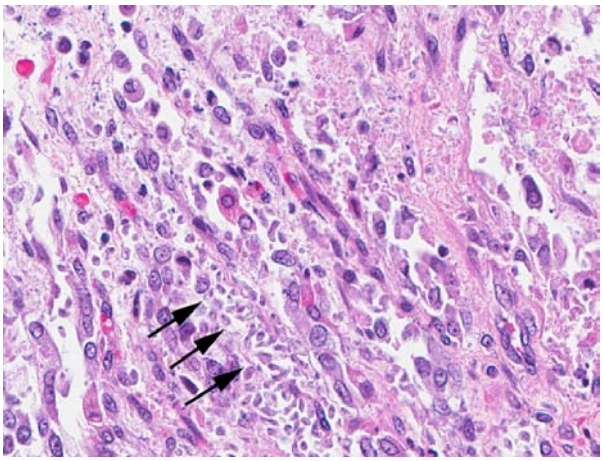

3-2. Stomach, pigtailed macaque: Numerous pyriform trichomonads are present within areas of necrosis within the gastric mucosa. (HE 400X)

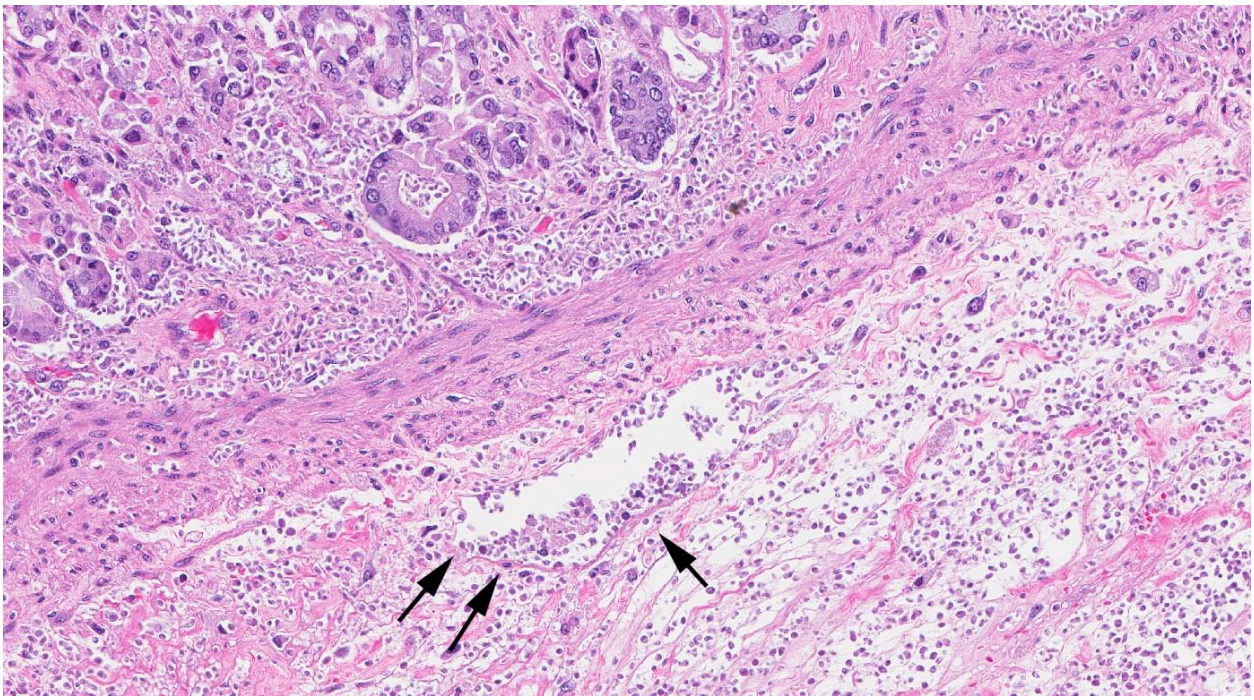

3-3. Stomach, pigtailed macaque: Innumerable trichomonads are present within the deep mucosa (including gastric glands), the muscularis mucosae, and the edematous submucosa, including a dilated lymphatic vessel (arrows). (HE 400X)

hypoproteinemia. Hypoproteinemia causes decreased osmotic pressure and loss of fluid from vessels, resulting in interstitial edema and accumulation of fluid in the body cavities. The size and morphology of the protozoal organism is consistent with a trichomonad. Trichomonads are anaerobic flagellated protozoa that are commensal organisms in many species of mammals and birds and, with some exceptions, are considered nonpathogenic. In monkeys, trichomonads may be present in the lumen or within crypts of the gastrointestinal tract but rarely elicit an inflammatory response or other pathologic changes, but have been reported as a cause of gastritis in SIV-infected macaques.[1] It is likely in the present case that the radiation induced hydrochloria and damage to the gastric and intestinal epithelium, resulting in breaks of the mucosal barrier and allowing entry and colonization of the protozoa and that the radiation-induced bone marrow immunosuppression rendered the monkey incapable of eliminating the infection. The protozoan was confirmed to be a trichomonad by electron microscopy.

JPC Diagnosis: Stomach: Gastritis, necrotizing, multifocal to coalescing, moderate to severe, with marked submucosal edema, necrotizing vasculitis, and innumerable protozoan trophozoites.

Conference Comment: Conference participants discussed the histologic changes that are likely attributed to the ablative dose of radiation received by the macaque including the profound lack of inflammation present in relation to the protozoal infection. Non-human primates with simian immunodeficiency virus (SIV) can also be similarly affected, but there is usually accompanying neutrophilic inflammation.[1] The mucosal necrosis is also likely due to the direct effects of radiation providing a route of entry for the normally commensal organism. Radiation injury in the stomach results in parietal cell death, hypochlorhydria, and the increased pH would lead to breakdown of the mucosal barrier and is another route of entry for the protozoa, as well as increased survivability of the parasite within the stomach. The marked submucosal edema is likely due to several factors, including lymphatic obstruction by the protozoa and decreased oncotic pressure due to hypoproteinemia from maldigestion and malabsorption as well as loss from diarrhea.

Contributor: St. Jude Children's Research Hospital
Pathology Department
262 Danny Thomas Place
Memphis, TN 38105

References:

1. Kondova I, Simon MA, Klumpp SA, et al. Trichomonad gastritis in rhesus macaques (Macaca mulatta) infected with simian immunodeficiency virus. *Vet Pathol.* 2005;42(1):19-29.

CASE IV: 2010-46 (JPC 3166452).

Signalment: Twenty-three-month-old male Wistar Transgenic, *Rattus norvegicus*.

History: This rat was noted to have a swollen testicle on 3/9/2010. Physical examination revealed a quiet but responsive animal with mild ocular porphyrin staining and a swollen discolored scrotum. Only one testicle was found in the scrotum on palpation. The rat was a sentinel animal and was not previously used in research studies. The animal was submitted to necropsy for complete postmortem evaluation on the day after examination.

Gross Pathology: Gross examination revealed pale mottled lungs, an enlarged spleen covered by white material and a mottled liver with a roughened surface. Multiple areas of yellow-brown pigmentation were in the omentum and the mesentery. The right testicle was in the scrotum. The left testicle was in the abdomen. Both testicles were cystic with multiple cysts containing a thick, yellow-tinged fluid.

Contributor's Histopathologic Description: The normal architecture of the testicle is effaced by large sheets of neoplastic cells separated by thin septa and multifocal variably sized cystic spaces which contain eosinophilic material with cysts lined by flattened to cuboidal epithelial cells. The neoplastic cells are polyhedral to cuboidal and have acidophilic, often vacuolated, cytoplasm with small round to oval nuclei. At the periphery occasional seminiferous tubules are observed. These tubules are lined by one layer of cuboidal cells and rare giant cells with minimal evidence of normal spermatogenesis. The surface of the tunica vaginalis has multifocal papillary projections which consist of proliferative cuboidal epithelioid cells overlying a fibrovascular core. Similar neoplastic cell proliferation is associated with the tunica vaginalis of the epididymis.

Contributor's Morphologic Diagnosis: 1. Interstitial cell tumor, left testicle.
2. Mesothelioma, left testicle.
3. Diffuse severe testicular atrophy and degeneration with cyst formation.

Contributor's Comment: The incidence and types of primary testicular neoplasms vary between the different stocks and strains of rats. For neoplasms of gonadal stromal origin, interstitial cell (Leydig cell) tumors occur most frequently in older male rats with incident rates approaching 90% in the Fischer 344 (F344) strain[1] and 11% in the Wistar stock[5]. Interstitial cell tumors are uncommon in the Sprague-Dawley stock.[1] Leydig cells are found adjacent to the seminiferous tubules in the testicle and produce testosterone in the presence of luteinizing hormone (LH). When Leydig cells are stimulated by the pituitary hormone LH, the cells may grow uncontrollably and form a Leydig cell tumor.[6] These tumors are usually benign[1], however, they may be hormonally active and have been associated with concurrent hypercalcemia.[4,6] This neoplasm usually has a nodular growth pattern. In larger neoplasms, testicular architecture may be completely effaced.[1] Mesotheliomas are tumors arising from the serosal membranes of the coelomic cavities. The tunica vaginalis propria testis is one of these cavities, which is formed by an outpouching of the abdominal peritoneum. Mesothelioma occurs most frequently in the pleural or peritoneal cavity, but in rare cases these tumors can also arise from the mesothelial cell lining of the tunica vaginalis testis of the testes and epididymis.[1] Mesotheliomas are occasionally encountered in laboratory rats with a higher incidence (2.3%) in the F344 strain.[3] Spontaneous

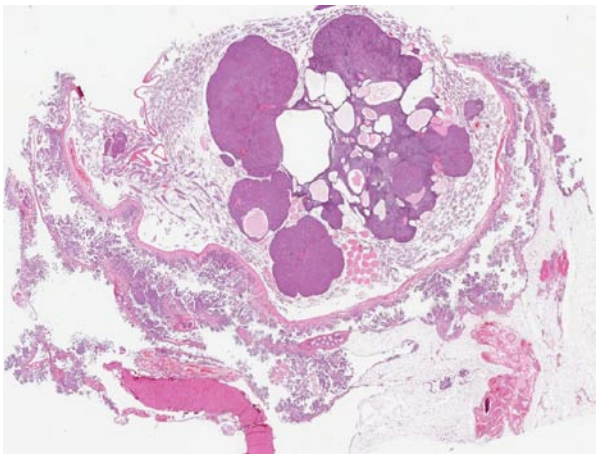

4-1. Testis, Wistar rat: Enlarged testis containing a densely cellular interstitial cell tumor, and a mesothelioma expanding the vaginal tunics. (HE 6.3X)

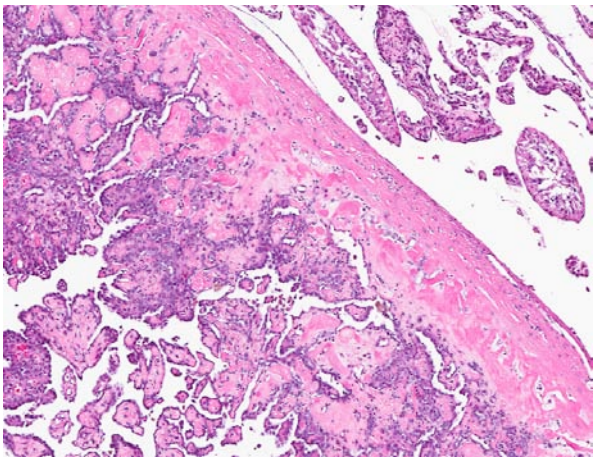

4-2. Testis, Wistar rat: Mesothelioma proliferating along the vaginal tunic (left), atrophic seminiferous tubules of the testis (right). (HE 180X)

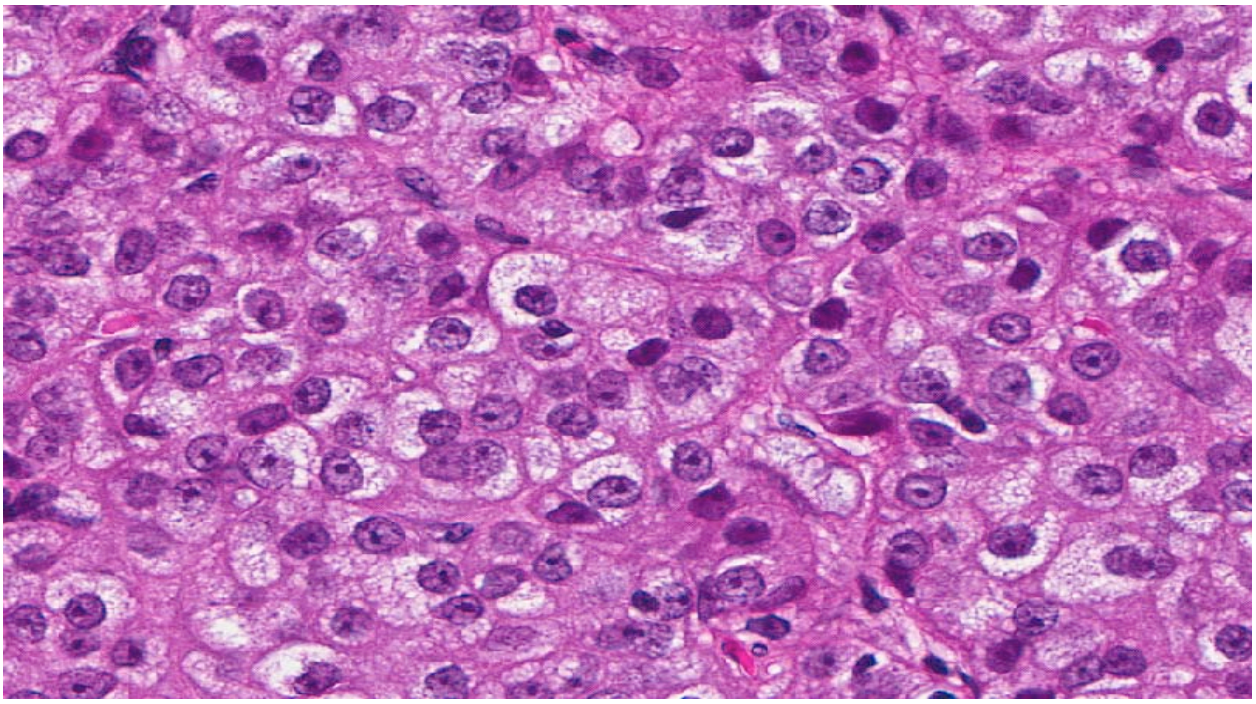

4-3. Testis, Wistar rat: Nests and packets of vacuolated neoplastic cells within the interstitial cell tumor inside the testis proper. (HE 320X)

mesotheliomas have not been reported in the Wistar rat. To the authors' knowledge, this is the first reported case of concomitant interstitial cell tumor and mesothelioma in the testicle of a Wistar rat.

JPC Diagnosis: 1. Testis: Interstitial cell tumor.
2. Testis, vaginal tunics: Mesothelioma.

Conference Comment: Interstitial cell tumors, common in rats and rabbits, often exhibit hemorrhage, necrosis, and mineralization; none of which are features of this case. Typically, interstitial cell tumors demonstrate immunoreactivity for inhibin, and mesotheliomas demonstrate immunoreactivity for vimentin and cytokeratin. Ultrastructurally, interstitial cell tumors contain lipid droplets, lipofuscin, abundant smooth endoplasmic reticulum, desmosomes, and characteristic tubulovesicular mitochondrial cristae; whereas, other testicular and epididymal cells have lamellar mitochondrial cristae. Ultrastructural features of mesothelioma include a microvillous cell membrane, junctional complexes, pinocytotic vesicles, and a distinct basal lamina. Microfilaments are often abundant and may be difficult to differentiate from endothelial cells.[2]

Conference participants discussed the atrophy of the seminiferous tubules and lack of sperm in the epididymis; likely due to elevated temperature associated with the intrabdominal location.

Contributor: Emory University
Yerkes National Research Center
Department of Pathology and Laboratory Medicine
Atlanta, GA

References:

1. Boorman GA, Everitt, JI. Neoplastic Disease. In: Suckow MA, Weisbroth SH, Franklin CL, eds. *The Laboratory Rat.* 2nd ed., Amsterdam, Netherlands: Elsevier Academic Press; 2006: 479-511.
6. Carlson G, Sibley RK. Electron microscopy of testicular and paratesticular neoplasms. In: Russo J, Sommers SC, eds. *Tumor Diagnosis by Electron Microscopy*. vol. 2, Philadelphia, PA: Field and Wood Medical Publishers, Inc.; 1988:140-153, 159.
3. Goodman DG, Ward JM, Squire RA, et al Neoplastic and nonneoplastic lesions in aging F344 rats. *Toxicol. Appl. Pharmacol.* 1979;48:237-248..
2. Percy DH, Barthold SW. In: *Pathology of Laboratory Rodents and Rabbits.* 3rded. Blackwell, Ames, IA: 2007:174-177.
5. Poteracki J, Walsh K.M. Spontaneous Neoplasms in Control Wistar Rats: A Comparison of Reviews. *Toxicological Sciences*. 1998;45:1-8.
4. Troyer H, Sowers JR, Babich E. Leydig cell tumor induced hypercalcemia in the Fischer rat. *Am. J. Patho*. 1982;108:284-290.

Joint Pathology Center
Veterinary Pathology Services

WEDNESDAY SLIDE CONFERENCE 2011-2012

Conference 19

21 March 2012

CASE I: UKLDDC7501 (JPC 2985450).

Signalment: 1-year-old male domestic shorthair, *Felis domesticus*, feline.

History: The cat presented with a 1-month history of ataxia, head tilt, and aggression towards other animals and people. Prior to death, the cat was capable of eating and drinking.

Gross Pathology: The animal presented in good body condition and postmortem preservation. The only significant gross finding was a 1.2 cm in diameter well demarcated light brown mass in the rostral portion of the left cerebral hemisphere.

Laboratory Results: Pathogenic bacteria, viruses, and fungi were not isolated from the brain, lungs, liver, kidneys, or intestines.

Contributor's Histopathologic Description: Located within the cerebral neuropil is an expansile, well demarcated area consisting of large numbers of neutrophils, macrophages, and lymphocytes, small amounts of fibrous connective tissue, and variably sized areas of necrosis. Intermixed throughout the

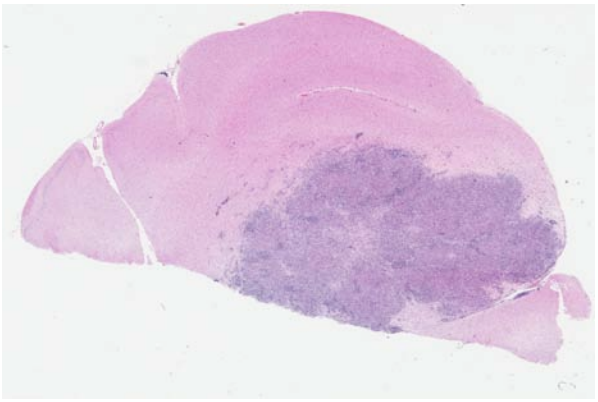

1-1. Cerebrum, cat: Multifocally within the cerebrum, there are large areas of necrosis with a prominent cellular infiltrate. (HE 4X)

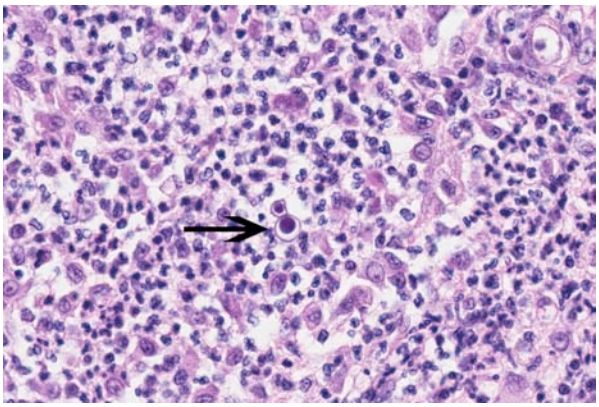

1-2. Cerebrum, cat: Within areas of necrosis, the neuropil is infiltrated and replaced by large numbers of neutrophils and macrophages, centered on 12-18 µm diameter yeasts which demonstrate occasional broad-based budding (arrow). (HE 40X)

lesion are low numbers of 7-2 micrometer round to oval yeast bodies which have thick cell walls, moderate amounts of poorly staining cytoplasm, and round 3-15 micrometer homologous staining nuclei. Some of the yeast bodies display broad based budding. Multiple blood vessels in the neuropil adjacent to the lesion are surrounded by low to moderate numbers of lymphocytes and macrophages. The overlying meninges contain low to moderate numbers of lymphocytes, macrophages and neutrophils, and small amounts of fibrillar acidophilic proteinaceous material.

Contributor's Morphologic Diagnosis: Severe chronic focal necrotizing pyogranulomatous encephalitis with intralesional yeast. Moderate chronic multifocal meningoencephalitis.

Contributor's Comment: Blastomycosis was diagnosed based on the morphological characteristics of the yeast. Blastomycosis is most-frequently reported in canids and humans, though cases in other domesticated and non-domesticated species are occasionally seen.[6] The dimorphic fungi are not commonly isolated from the environment, but are thought to survive in manure and in soil containing decaying vegetation and high moisture content.[1] Disease is thought to be initiated by inhalation of *B. dermatitidis* conidia. At body temperatures, conidia transform to the yeast phase which may disseminate and elicit pyogranulomatous inflammatory responses in the lungs, bones, liver, spleen, lymph nodes, skin, eyes, urogenital tract, and brain.[2,4,7] This case is remarkable as the cat presented with neurologic signs accompanied with a distinct cerebral lesion suggestive of neoplasia. Lesions consistent with *B. dermatitidis* were not seen in other organs or tissues.

JPC Diagnosis: Cerebrum: Meningoencephalitis, pyogranulomatous, multifocal, severe, with lymphocytic perivascular cuffing and budding yeasts.

Conference Comment: The three clinical forms of blastomycosis are primary pulmonary infection, most common in domestic animals, disseminated disease, as in this case, and local cutaneous infection secondary to direct tissue inoculation, which is rare. *B. dermatitidis* has several virulence factors. Blastomyces Adhesion 1 (BAD-1) is a surface protein which mediates adhesion to host cells and modulates immune response, and alpha-glucan protects against killing by macrophages. The adhesion molecules bind to CD14 and complement receptor 3 (CR3) on macrophages and induces activation; however, *Blastomyces* is not readily phagocytized. *Blastomyces* initially causes a neutrophilic response, but with the onset of cell mediated immunity, a granulomatous response predominates. Differential diagnosis for this case includes *Cryptococcus* spp., which often cause a gelatinous toruloma in the brain, and *Aspergillus* spp., which often causes severe necrotizing vasculitis.[3,5]

Contributor: University of Kentucky
Department of Veterinary Science
Livestock Disease Diagnostic Center
http://fp1.ca.uky.edu/lddc

References:

1. Quinn PJ, Carter ME, Markey B, Carter GP. Mycology. In: *Veterinary Clinical Microbiology*. 1999. Edinburgh. Mosby; 1994:367 -380.
2. Baumgardner DJ,Laundre B. Studies on the molecular ecology of Blastomyces dermititidis. *Mycopathol*. 2000;152 5 1-58.
3. Hendrix DVH, Rohrbach BW, Bochsler PN, et al. Comparison of histologic lesions of endophthalmitis induced Blastomyces dermititidis untreated and treated dogs: 36 cases (1986-2001). *J Am Vet Med Assoc*. 2004;224(8):1317-1322.
4. Breider MA, Walker TL, Legendre AM, et al. Blastomycosis in cats: Five cases (1979-1986). *J Am Vet Med Assoc*. 1988;193(5):570-572.
5. van Ee RT and Wright B. Ocular changes in a cat with disseminated blastomycosis. *J Am Vet Med Assoc.* 1985;137(6): 629-631.
6. Caswell JL, Williams KJ. Respiratory System. In: Maxie MG, ed. *Jubb, Kennedy, and Palmer's Pathology of Domestic Animals.* Vol 2, 5th ed. Philadelphia, PA: Elsevier Saunders; 2007:640-4.
7. Lopez A. Respiratory system, mediastinum, and pleurae. In: McGavin MD, Zachary JF, eds. *Pathologic Basis of Veterinary Disease*. 5th ed. St. Louis, MO: Mosby; 2011:526.

CASE II: V07-14306 (JPC 3106650).

Signalment: One-year-old female Border collie (*Canis familiaris*).

History: This dog experienced chronic diarrhea that was often hemorrhagic, coupled with wasting. She was treated with various agents for giardiasis. She responded to treatment but then the diarrhea/wasting recurred. The dog was not brought in for further treatment. She was presented to the veterinarian several weeks later, and was extremely emaciated and anorexic, with severe, watery diarrhea. Euthanasia was elected rather than further treatment. Another dog (11-months-old) in the household and had similar symptoms.

Gross Pathology: This young female Border collie was extremely thin, with no subcutaneous or internal body fat present. Terminal weight was 19.2 lbs. There was fecal pasting around the anus. The portal vein was markedly distended caudal to the liver and readily visible as it coursed caudad. The liver had a greenish tinge to the serosal surface and an accentuated lobular pattern, and was very firm on palpation. The heart was enlarged and rounded, with a developing double apex, and both ventricular walls were thin. The small intestine was distended with gas, and contents had a foul odor. There were aggregates of yellowish-brown mucoid material attached to mucosal surfaces in a random distribution.

Laboratory Results: Parasitology - fecal samples from both dogs were positive for *Heterobilharzia americana* trematode eggs on fecal sedimentation test (Dr. Jack Malone, Louisiana State University, performed assay).

Contributor's Histopathologic Description: Liver sections had severe and striking periportal fibrosis coupled with a mixed inflammatory infiltrate. Numerous trematode eggs were seen in portal regions; these had commonly induced a fibrotic response. Mixed inflammatory infiltrates composed of lymphocytes, plasma cells, and occasional eosinophils were seen, primarily in portal triads. There were also copious aggregates of brownish-black pigment granules deposited throughout the liver, most common in the portal triads. The small intestine (multiple sections) had copious numbers of trematode eggs embedded in the mucosa, submucosa, and extending into the muscularis in some areas (i.e., transmural distribution); these were surrounded by varying amounts of reactive fibroplasia and mixed inflammatory infiltrate forming microgranulomas.

Contributor's Morphologic Diagnosis: Liver: hepatitis, chronic, portal, nonsuppurative due to *Heterobilharzia americana*.
Small intestine: Enteritis, chronic, nonsuppurative, transmural, due to *Heterobilharzia americana*.

Contributor's Comment: This was a case of disseminated trematode infection due to *Heterobilharzia americana*, a schistosome trematode found in the southern US. Primary hosts include rabbits, raccoons and bobcats, all of which occur in the San Juan River Valley of northwestern New Mexico (i.e., "four corners" region of US). The fluke has essentially the same life cycle as *Fasciola hepatica* (also present in this area), and uses the same lymnaeid snail as part of its indirect life cycle.

In addition to the lesions in the tissues submitted, there were disseminated granulomas surrounding eggs in the pancreas, lung, lymph node, and kidney; the small intestine and liver were most severely affected. The trematode is in the family Shistosomatidae; these parasites are of relatively low importance in North America. In addition to this trematode in dogs, there is a dermatitis of humans (i.e., "swimmer's itch") that is

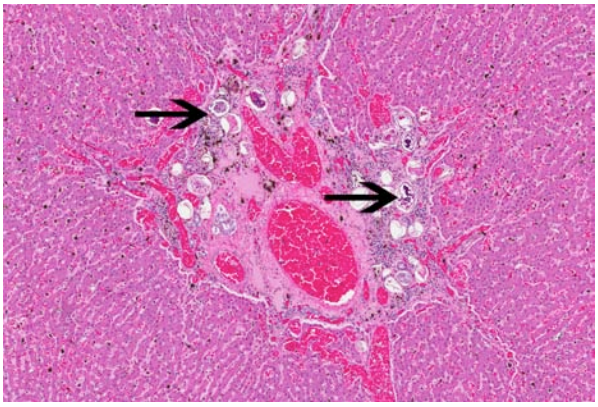

2-1. Liver, dog: Multifocally, portal areas are expanded by fibrous connective tissue and numerous clear spaces containing trematode eggs (arrows). (HE 4X)

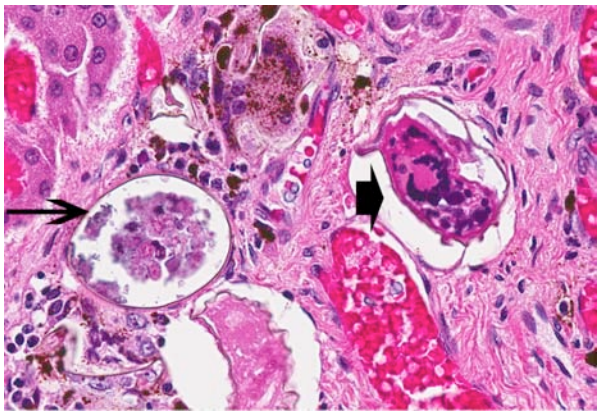

2-2. Liver, dog: Eggs are irregularly oval, up to 110 µm in diameter , and are non-operculated, with a 2 µm thick brown shell (arrow) and contain a developing miracidium (arrowhead). (HE 40X)

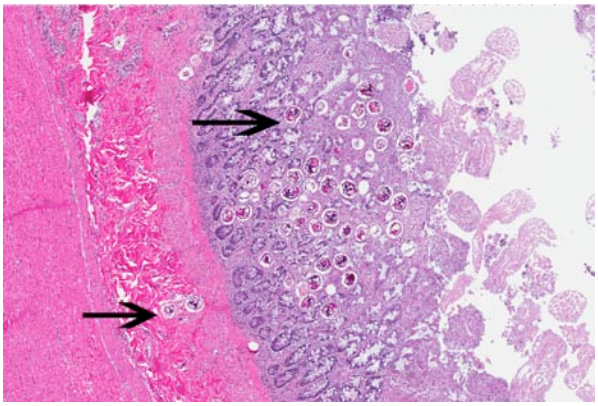

2-3. Small intestine, dog: The lamina propria and submucosa contain numerous trematode eggs (arrows). (HE 4X)

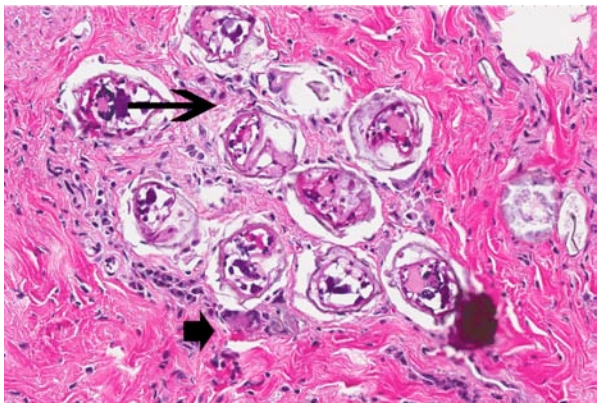

2-4. Small intestine, dog: Within the submucosa, eggs are often surrounded and occasionally engulfed by epithelioid macrophages (arrow) and occasional multinucleate giant cell macrophages (arrowhead). (HE 20X)

caused by a cercariae of wild waterfowl (*Trichobilharzia*, *Austrobilharzia*, and *Bilharziella*).[1]

The miracidium hatches very soon after the egg comes in contact with water, and then enters a freshwater snail (*Lymnaea cubensis*), in which cercariae develop in daughter sporocysts. Activity by these snails is dependent upon ambient temperatures between ranges of 10°C-29°C.[4] If the ambient temperatures are within this range, development in the snail is completed within 30 days. Upon emergence from the snail, the cercariae penetrate the skin of the host (i.e., dog, rabbit, raccoon, bobcat, or nutria), and migrate by way of the lungs to the liver. After a period of development in the liver, mature males and females make their way to the mesenteric vein and mate. Theseadults do not reproduce in mammalian hosts, but may live there for 4-10 years producing thousands of eggs during that time.[6] Eggs laid in the terminal branches of the mesenteric veins passively work through the bowel wall via a mechanism of proteolytic enzymes that are emitted through an ultramicroscopic pore in the eggshell. They then progress to the gut lumen and escape in the feces. If feces are deposited in water, the process starts over again. The eggs evoke a granulomatous reaction that eventually prevents their egress, and favors their carriage to other organs with consequent production of widely disseminated granulomas.

It is of interest that fluke infestations, which are most often associated as problems in animals in a wet climate, can occur in a "high desert" climate and geographical environment such as the American Southwest. In the area involved, there is both flood irrigation and excessive water runoff situations during a summer wet or "monsoon" season. During these times, the necessary elements for this infection (as well as fascioliasis in cattle) are present, especially along the river bottoms or "bosque" zones. Of further interest is the involvement of the lymnaeid snail that is "double dipping" in trematode infections in several species with two different trematode parasites.

JPC Diagnosis: 1. Liver: Hepatitis, portal, granulomatous, diffuse, moderate, with numerous trematode eggs and nodular hemosiderosis.
2. Small intestine: Enteritis, granulomatous, multifocal, moderate, with numerous mucosal and submucosal trematode eggs and intravascular adult schistosomes.

Conference Comment: As mentioned by the contributor, cercariae penetrate the skin and leave seldom seen petechiae with a marked leukocytic inflammatory response to the parasite. The cercariae develop into schistosomula and migrate through dermal vessels to the lungs, where a heavy parasite load can result in pneumonia. After migration to the liver, hepatic cirrhosis can result following healing of the granulomatous response to the eggs, leading to liver failure and gastrointestinal malabsorption. Common laboratory abnormalities reflect hepatic failure, widespread granulomatous disease, and parasitism, and include hypoalbuminemia, hyperglobulinemia, hypercalcemia, azotemia, anemia, and eosinophilia. Anemia reflects both enteric blood loss and chronic inflammatory disease. A reported sequel to schistosomiasis is membranoproliferative glomerulonephritis, due to the accumulation of antigen-antibody complexes within the glomerular capillary wall, which stimulates an inflammatory cascade leading to varying degrees of glomerular cell proliferation and basement membrane thickening. Clinical pathology abnormalities common in cases of glomerulonephritis include renal proteinuria, hypoalbuminemia, azotemia, and anemia.[2,3]

Diarrhea is a typical clinical finding attributed to rupture of enteric mucosal vessels and a type I hypersensitivity reaction that results in enteric

ganglionitis. Small granulomas, called pseudotubercles, form in deeper tissues in chronic disease when endophebitis precludes escape of the eggs into the intestinal lumen, as discussed by the contributor. Pseudotubercles are initially primarily eosinophilic and later progress to traditional granulomas. With chronicity, degenerate eggs often mineralize or become coated with Splendore-Hoeppli material. Adult schistosomes elicit eosinophilic endophlebitis, intimal proliferation, and thrombosis in mesenteric and portal veins, as demonstrated in this case. Adults feed on erythrocytes and regurgitate hematin pigment, which was also evident in this case.[5] Due to slide variation, not all sections of small intestine featured adult schistosomes in mesenteric vessels.

Contributor: NMDAA/Veterinary Diagnostic Services
700 Camino de Salud NE
Albuquerque, NM 87106
http://nmdaweb.nmsu.edu/animal-and-plant-protection/veterinary-diaqnostic-services

References:

1. Bowman DD.Georgi's' parasitology for veterinarians. 6th ed. Philadelphia, PA: WB Saunders Co; 1995:128-129.
2. Fabrick C, Bugbee A, Fosgate G. Clinical features and outcome of Heterobilharzia americana infection in dogs. *J Vet Intern Med*. 2010;;24(1):140-4.
3. Flowers JR, et al. Heterobilharzia americana infection in a dog. *J Am Vet Med Assoc*. 2002;220(2): 193-6, 183.
4. Goff WL, Ronald WC. Certain aspects of the biology and life cycle of Heterobilhazia americana in east central Texas. ln: *Am J Vet Res*. 1981;V42(10) 1775-1781.
5. Maxie MG, Robinson WF. Cardiovascular system. In: Maxie MG, ed. *Jubb, Kennedy, and Palmer's Pathology of Domestic Animals*. Vol 3. 5th ed. Philadelphia, PA: Elsevier Saunders; 2007:95-7.
6. Slaughter JC, Billups LH, Acor GK. Canine heterobilharziasis. *Compendium Small Animals*1988;10, (5) 606-611.

CASE III: A10-536 (JPC 4001074).

Signalment: 4.5-year-old male rhesus macaque (*Macaca mulatta*).

History: This rhesus macaque was inoculated with SIVmac251 as part of an experimental single-cycle SIV vaccination trial and had undergone routine phlebotomies. Twenty months post inoculation, the animal developed chronic weight loss (25% weight loss over four months.) The animal was also reported to have anorexia and chronic diarrhea. On clinical examination, the animal was in poor body condition and was observed to have pale mucous membranes as well as a large palpable abdominal mass. Due to suspicion of progression to simian acquired immune deficiency syndrome, the animal was humanely euthanized.

Gross Pathology: A large, roughly oval, firm, encapsulated mass was adhered to the serosal surface of the mid-distal colon. On cut surface, the mass was friable, with interlacing patterns of pale tan to white. The mucosa of the colon was thickened and pale with an irregular cobblestone appearance. The mucosa of the duodenum and most of the jejunum was also thickened with prominent lacteals. The right lung lobes were atelectatic with multifocal to coalescing white fibrotic areas and firm white raised nodules on the tissue margins. A large thrombus partially obstructed a pulmonary artery. The left lung lobes were red and diffusely edematous. There were no gross lesions noted on examination of the central nervous system.

Contributor's Histopathologic Description: Colon: Replacing and disrupting the muscular layers and submucosa of the colon is a large region of liquefactive necrosis that is characterized by innumerable degenerative neutrophils, large numbers of macrophages, fewer plasma cells, and lymphocytes admixed with fibrin, cellular and karyorhectic debris (necrosis). Interspersed with the inflammation and necrosis are marked numbers of 2-3 µm, pale basophilic, round to oval, protozoal organisms that have apically oriented nuclei. Large numbers of viable and non-viable organisms are also noted within macrophages. Numerous colonic crypts also contain protozoal organisms similar to those described above. Inflammatory cells breach the colonic basement membrane in multiple places and to varying degrees separate and surround colonic crypts. Endothelial cells of the vasculature within the abscesses are plump, branched, and reactive. The serosa is proliferative and thickened with abundant fibroplasia, edema, and scattered numbers of inflammatory cells in similar proportions to those noted above. Submucosal lymphoid aggregates are often disrupted by the inflammation and there are several ectopic lymphoid follicles close to the serosa. There are small numbers

3-1. Colon, rhesus macaque: The colon is diffusely and transmurally thickened by a cellular infiltrate which traverses the muscularis mucosa and markedly expands the submucosa (arrow). (HE 0.9X)

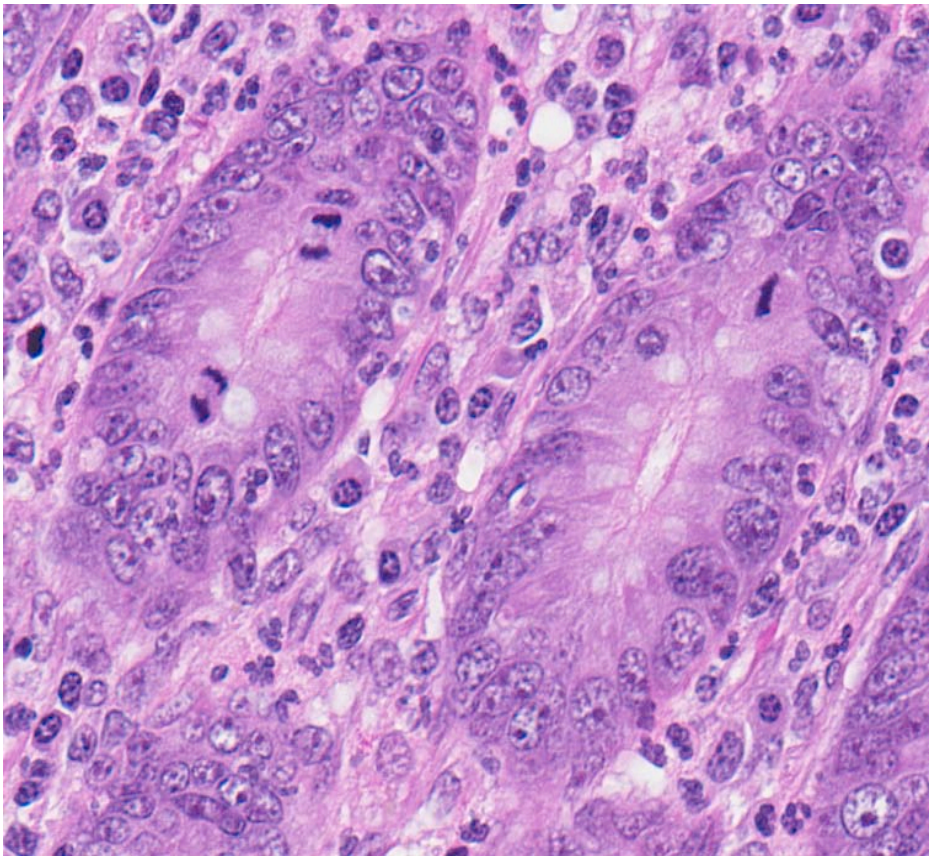

3-2. Colon, rhesus macaque: The colonic mucosa is multifocally hyperplastic, and contains numerous mitotic figures at all levels within the glands. (HE 400X)

of epithelial associated bacteria noted along the lumen surface of the colonic epithelium (*Brachyspira* sp.).

Contributor's Morphologic Diagnosis: Colon: Locally extensive, severe, chronic, necrosuppurative, and histiocytic abscessation with intralesional protozoal organisms consistent with *Spironucleus* spp.

Contributor's Comment: The genus *Spironucleus* is composed of flagellated protists of the phylum *Sarcomstigophora* and is closely related to other flagellates of the genera *Giardia* and *Hexamita*.[1,7] Being of the order *Diplomonadida*, this organism is bilaterally symmetrical with two karyomastigonts and flagella that are typically not appreciated using light microscopy.[1,7,8] It lacks an undulating membrane.[7] This genus inhabits the gastrointestinal tract of a variety of animal hosts including birds, fish, mice, and non-human primates.[1,5,10,12,13,14] *Spironucleus* can remain as a normal commensal in the intestine but also possesses the capacity to invade the intestinal epithelium and localize to other organ systems.[5,8] Following ingestion, *Spironucleus* transforms from a resistant non-motile cyst into a motile trophozoite (flagellated form).[1,7,14] Currently, the taxonomy of the closely related genera of flagellates is being elucidated through the use of small subunit ribosomal DNA (SSU rDNA) sequencing and *Spironucleus* can be broken out into three separate clades. The first and most primitive clade likely originated in marine environments. The second clade was isolated from freshwater Ide and Angelfish while the third clade was isolated from terrestrial animals.[1,8] The three clades are likely only distantly related to one another.

In fish, *Spironucleus salmonicida* causes significant mortality in farmed salmon.[10] *Spironucleus vortens* is a fresh water species that causes disease in the ornamental fish industry and is highly suspected to be one of the potential causative agents of hole-in-the-head disease in cichlids.[5,11]

In birds, *Spironucleus meleagridis* was first isolated from turkeys and described and named by McNeil, Hinsha and Kofoid in 1941 but was later found to infect many species of birds.[5,9,14] Infection with *Spironucleus meleagridis* is reported to cause infectious catarrhal enteritis in turkeys and other fowl including Chukar partridges and ring-necked pheasants and is also associated with significant morbidity and mortality.[5] Cysts of *S. meleagridis* are found most

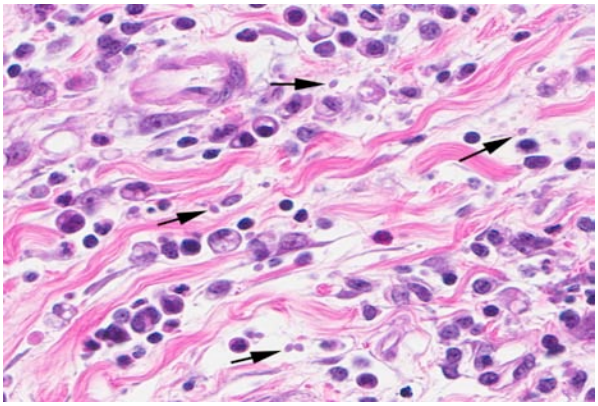

3-3. Colon, rhesus macaque: Innumerable 2-4 µm pyriform protozoa (arrows) are present throughout all layers of the colon, including the submucosa as demonstrated here. (HE 400X).

frequently in thick mucus and are less frequently found in feces. This mechanism may enhance transmission and survival of the organism in the environment.[14]

In laboratory rodents, *Spironucleus muris* (and potentially other *Spironucleus* species) is a commensal organism of the small intestine of rats, mice, and hamsters but can cause significant disease in immunocompromised animals (i.e., disease, environmental stress, very young animals). In severe outbreaks there can be up to 50% mortality particularly in young mice that clinically have depression, diarrhea, and weight loss. The organism primarily colonizes the duodenal crypts and may cause an acute or chronic form of disease.[12]

In non-human primates, a flagellated organism (*Octomitus pithici*) was described in the feces of nonhuman primates as early as 1929 by DaCunha and Muniz.[6] More recently, phylogenetic analysis was performed on an unknown diplomonad isolated from two rhesus macaques immunocompromised from simian acquired immune deficiency syndrome (SAIDS). The organism was most closely related to *Spironucleus meleagridis*. Further investigation and screening of both SIV infected and uninfected rhesus macaques revealed that the organism was prevalent in the colony and most likely a commensal organism in normal macaques. It is suspected that the organism invades the colonic mucosa in immunocompromised animals, striking the gastrointestinal associated lymphatic tissue and disseminating either to regional lymph nodes or systemically via the lymphatics or vasculature.[1] We suspect that in the present case, the abscess originated in a colonic lymph node following invasion from the colon. Lesions associated with *Spironucleus* were not seen in other tissues.

The bacteria noted along the epithelial border are consistent with *Brachyspira* sp. (*B. pilsicoli* is the most common). This is a common, often incidental finding in the large intestine of macaque species. The role that this bacterium plays in colonic inflammation is currently unknown; however, since it can be found in the colon of almost all macaque species, its role in causing disease is likely negligible.

JPC Diagnosis: Colon: Colitis, necrosuppurative, transmural, diffuse, severe, with innumerable protozoan trophozoites.

Conference Comment: Pathologic infection with commensal organisms or parasites that would otherwise be cleared by an immunocompetent animal is common in non-human primates with SIV, and often results in death. Because the lentivirus depletes CD4+ T cells, infected non-human primates commonly develop opportunistic infections with *Pneumocystis carinii*, *Mycobacterium avium-intracellulare* and *M. tuberculosis*, *Cryptosporidium* spp., cytomegalovirus (CMV), adenovirus, papovavirus (SV40), *Cryptococcus neoformans*, *Toxoplasma gondii*, *Candida albicans* and *Plasmodium*.[2,3]

In SIV-infected monkeys, lymphadenopathy and splenomegaly due to lymphoid hyperplasia is present in early stages of disease with lymphoid atrophy (depletion) in later stages, and thymic atrophy occurs in young animals. Histologically, there is giant cell (syncitial) interstitial pneumonia, granulomatous and giant cell lymphadenitis and splenitis, giant cell meningoencephalomyelitis, non-septic vegetative valvular endocarditis, glomerulosclerosis, and syncitial giant cells may also be present in lymph nodes, kidney, and the gastrointestinal tract.[2,3]

Other lentiviruses of veterinary importance include equine infectious anemia virus in horses, Maedi-visna virus which produces ovine progressive pneumonia in sheep, caprine arthritis-encephalitis virus in goats, feline immunodeficiency virus in wild and domestic felids, and bovine immunodeficiency-like virus in cattle.[4]

Contributor: New England Primate Research Center
Harvard Medical School
Division of Comparative Pathology
One Pine Hill Drive
Southborough, MA 01772
www.hms.harvard.edu/NEPRC

References:

1. Bailey C, Kramer J, Mejia A, et al. Systemic spironucleosis in 2 immunodeficient rhesus macaques (Macaca mulatta). *Vet Pathol*. 2010;47:488-494.
2. Barry P, Martinas M, Lerche M, et al. Virology research. In: Wolfe-Coote S, ed. *The Laboratory Primate*. San Diego, CA: Elsevier Academic Press; 2005:565-569.
3. Baskin GB. Pathology of nonhuman primates. In: *Pathology of Laboratory Animals* 49th conference. Washington, DC: Armed Forces Institute of Pathology, 2005.
4. Campbell RSF,Robinson WF. The comparative pathology of the lentiviruses. *J Comp Pathol*. 1998;119 (4):348-352.
5. Cooper GL, Charlton BR, Bickford AA, et al. Hexamita meleagridis (Spironucleus meleagridis) infection in chukar partridges associated with high mortality and intracellular trophozoites. *Avian Dis*. 2004;48:706-710.
6. da Cunah A MJ. Nota sobre os parasitas intstinaes do Macacus rhesus con a descripcao de uma nova especie de octomitus. *Mem Inst Oswaldo Cruz*. 1929;5:34-35.

7. Gardiner CH FR, Dubey JP. An Atlas of Protozoan Parasites in Animal Tissues. 2 ed. Washington, DC: Armed Forces Institute of Pathology;1998.
8. Jorgensen A, Sterud E. Phylogeny of spironucleus (eopharyngia: diplomonadida: hexamitinae). *Protist*. 2007;158:247-254.
9. McNeil E HW, Kofoid CA. Hexamita Meleagridis Sp. Nov. from the Turkey. *American Journal of Epidemiology.*1941;34 Section C(2):71-82.
10. Millet CO, Lloyd D, Williams C, et al. Effect of garlic and allium-derived products on the growth and metabolism of Spironucleus vortens. *Exp Parasitol*. 2011;127:490-499.
11. Paull GC. Spironucleus vortens, a possible cause of hole-in-the-head disease in cichlids. *Diseases of Aquatic Organisms*. 2001;45:197-202.
12. Percy DH. *Pathology of Laboratory Rodents and Rabbits.* 3rd ed. Ames, Iowa: Blackwell Publishing; 2007.
13. Wenrich D. A Species of Hexamita (Protozoa, Flagellata) from the Intestine of a Monkey (Macacus rhesus). *The Journal of Parasitology*. 1933;19:225-229.
14. Wood AM, Smith HV. Spironucleosis (Hexamitiasis, Hexamitosis) in the ring-necked pheasant (Phasianus colchicus): detection of cysts and description of Spironucleus meleagridis in stained smears. *Avian Dis*. 2005;49:138-143.

CASE IV: G8229 (JPC 4003619).

Signalment: 16-year-old male intact mandrill (*Mandrillus sphinx*) non-human primate.

History: The animal lived in a zoological garden as the alpha male of a mandrill group. At the age of ten years, the animal developed multifocal ulcerative and nodular pruritic lesions of the facial skin at the nasal mucocutaneous junctions as well as on the oral and nasal mucosa. The course of disease was undulating with periods of improvement alternating with phases of deterioration with expansion of the cutaneous and mucosal wounds associated with inappetence, apathy, and stridors. Skin biopsies taken one year after the onset of clinical signs revealed a granulomatous inflammation with evidence of fungal structures. Although the etiological agent could not be classified, an aspergillosis, a mucormycosis, and a trichophytosis were ruled out on the basis of the histomorphology of the fungal elements. During the course of disease, different sole and combined antimycotic therapeutic approaches were applied. However, permanent recovery could not be achieved. Due to worsening of the skin lesions, the development of new ulcers in the left gluteal region and increasing psychosocial stress within the group, the mandrill was finally euthanized for animal welfare reasons. The mandrill was serologically positive for simian immunodeficiency virus (SIV) and negative for simian t-cell leukemia virus (STLV) and herpes B.

Gross Pathology: At necropsy, the mandrill was in good nutritional condition. The skin on the bridge of the nose revealed a severe multifocal to confluent ulcerative dermatitis with marked, partly nodular thickening of the subcutis and superficial crust formation. The ulcerative lesions extended to the corners of the mouth and also involved the anterior nasal and oral mucosa. A focally extensive ulcerative and proliferative skin lesion (ca. 8 x 5 cm) was also present between the anus and the left ischial tuberosity. The mandibular and left inguinal lymph nodes were moderately enlarged.

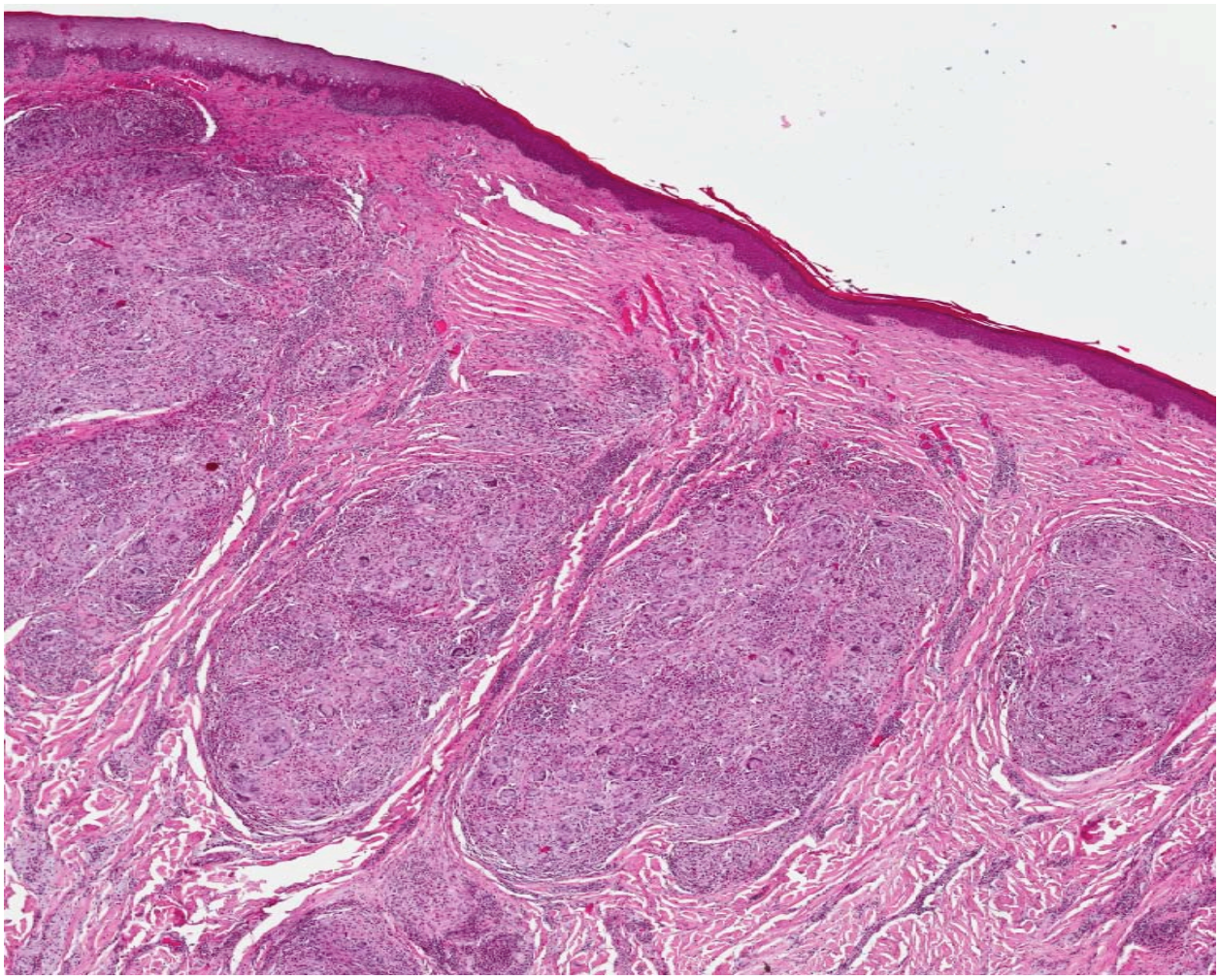

4-1. Glabrous skin (mucous membrane), mandrill: The submucosa is expanded by multiple coalescing, poorly-formed granulomas. (HE 4X)

Laboratory Results: Immunohistochemistry using a polyclonal anti-*Candida albicans*-antibody revealed a positive reaction of the fungal organisms. Fungal culture of the skin revealed fast-growing, light green yeast colonies on a chromogene medium. Microscopically, the colony material consisted of gram positive, narrow-budding, round yeasts with a size of 2-5 µm. On the species level, the isolated yeast was identified as *Candida albicans* using MALDI-TOF MS.[1] The etiology was confirmed by a PCR with *Candida albicans*-specific primers targeting the gene for the integrin like protein alpha INT1,[6] which was positive on the fungal culture material.

Contributor's Histopathologic Description: At microscopic examination, the dermis and subcutis of the nasal skin respectively the propria of the oral mucosa contained multifocal to coalescing nodular inflammatory foci beneath an extensively ulcerated squamous epithelium. The nodules were composed of abundant macrophages, eosinophils, multinucleated giant cells, viable and degenerate neutrophils, and fewer lymphocytes and plasma cells and were separated by strands of mature collagenous connective tissue. In addition, a few fibroblasts aligned along the periphery of the inflammatory cell infiltrates. Multinucleated giant cells were primarily Langhans type, with occasional foreign-body type, and contained up to 20 nuclei. There were multifocal slight hemorrhages. Multifocally within giant cells, but also located in the extracellular space, there were faintly stained fungal organisms represented by round, thick-walled, yeast-like bodies as well as short hyphae. The fungal elements were strongly positive with Grocott stain and with PAS reaction (Figure 2B). They were only weakly stained by Congo red. Hyphae were characterized by rare, irregular branching, infrequent septation, thin, non-pigmented walls, and occasional bulbous dilations. The yeast-like bodies measured between 5 and 10 µm, were sometimes surrounded by a clear halo and sporadically seemed to form pseudohyphae. There was no evidence of angioinvasion.

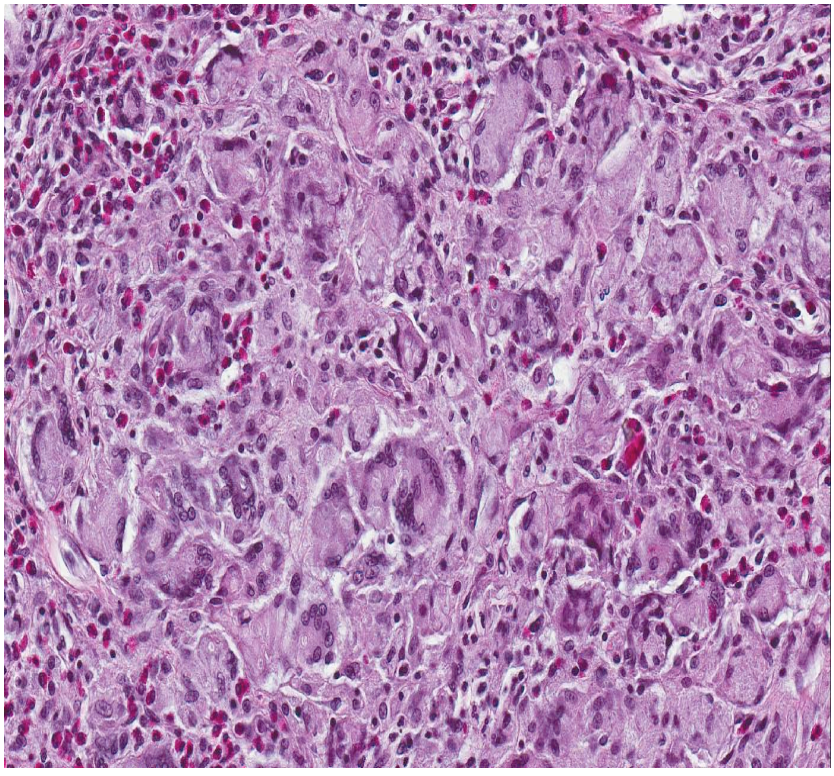

4-2. Glabrous skin (mucous membrane), mandrill: The granulomas are composed centrally of numerous epithelioid and multinucleated giant cell macrophages of the foreign body and Langhans types, admixed with moderate numbers of eosinophils, and neutrophils (HE 8.0X)

Contributor's Morphologic Diagnosis: Mucocutaneous junction: dermatitis/panniculitis and stomatitis, granulomatous and eosinophilic, chronic, multifocal to coalescing, marked, with multifocal ulceration, hemorrhages, and numerous intralesional fungal organisms (short hyphae and yeast-like bodies), mandrill, nonhuman primate.

Contributor's Comment: Candidiasis is caused by yeasts of the genus *Candida*, usually *C. albicans*, and is the most frequently occurring mycotic disease in nonhuman primates.[5] *Candida* spp. are ubiquitous dimorphic fungi that normally inhabit the alimentary and genital mucosa as well as the skin of mammalian animals and humans.[5,11] They represent opportunistic pathogens as disease generally only develops when the host resistance is lowered due to pre-existing disease (metabolic disorders, hematologic malignancies etc.), retrovirus infection, immunosuppressive drugs, or penetrating trauma or burns. Further risk factors include stress, cachexia, nutritional deficiencies, and immunologic defects.[5,9] *Candida* infections most often cause localized or systemic suppurative to necrotizing, ulcerative mucosal lesions with pseudomembrane formation, but they are also rarely associated with chronic deep cutaneous granulomatous lesions with evidence of giant cells.[5,6,12] In humans, chronic mucocutaneous candidiasis (CMC) is defined as the inability to clear fungal infections leading to persistent and recurring infections of skin and mucous membranes with yeasts, mostly *Candida albicans*. Although CMCs can arise from a variety of clinical

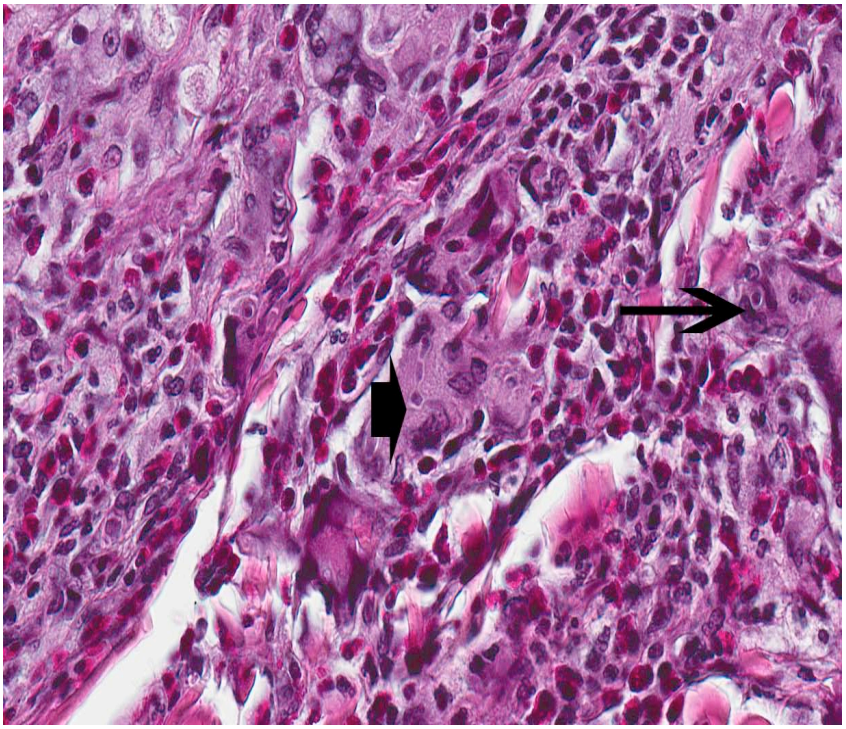

4-3. Glabrous skin (mucous membrane), mandrill: Primarily within the cytoplasm of macrophages, there are numerous oval, 2-6 µm yeasts (arrow) with a 1 µm cell wall and dense basophilic cytoplasm. Yeasts often line up to form pseudohyphae (arrowhead). (HE 40X)

conditions (HIV infection, steroid therapy etc.), they also may present as primary, hereditary immunodeficiencies due to impaired cell-mediated immunity against *Candida* species, mainly reflecting defects in the T_h17 response.[10]

Obvious predisposing immunosuppressive factors to facilitate tissue invasion of the opportunistic fungi could not be identified in the present case. As mandrills are natural and asymptomatic carriers of SIV, the SIV infection of the animal did probably not represent an immunocompromising factor.[8,14] However, it cannot be excluded that a possible immunosuppressive factor could have been social stress due to the mandrill's role as the alpha male of the group at a rather young age. The presence of a primary immunodeficiency with general increased susceptibility for mucocutaneous candidiasis is also not unlikely and might also explain the poor success of the antimycotic therapy.

Other common etiologies for fungal infections of the skin in nonhuman primates include dermatophytes (*Microsporum canis*, *Trichophyton mentagrophytes*), *Histoplasma capsulatum* var. *duboisii*, *Sporothrix schenckii*, and *Coccidioides immitis*. While dermatophytes usually cause a mild superficial inflammatory response with hyperkeratosis and alopecia, infections with *Histoplasma capsulatum* var. *duboisii*, *Sporothrix schenckii*, and *Coccidioides immitis* may lead to ulcerative and granulomatous dermatitis.[3,5,14] Further descriptions of cutaneous mycoses in nonhuman primates include cutaneous zygomycosis characterized by necrotizing dermatitis and panniculitis in two adult female rhesus monkeys following extensive fight wound trauma and a focal fungal granuloma in the skin of the nose caused by *Madurella mycetomatis* in a female adult mandrill.[2,13]

JPC Diagnosis: Mucous membrane: Stomatitis, granulomatous, multifocal to coalescing, severe, with ulceration and numerous intracellular yeasts, pseudohyphae, and hyphae.

Conference Comment: *Candida* persists in the oropharyngeal cavity in the yeast form by ligand-receptor interactions. Yeast ligands include mannose, C3d receptors, and mannoproteins; and host receptors include fibrinogen, fibronectin, thrombin, collagen, laminin, and vitronectin-binding proteins. *Candida* yeast mainly bind mannose receptors, while *Candida* hyphae primarily bind complement receptor 3 (CR3) and the Fc-gamma receptor. Binding induces the yeast form to switch to the invasive filamentous form, which proliferates at normal body temperatures.[15] *Candida* spp. produce a large number of functionally distinct adhesins that are important determinants of virulence; they also produce enzymes, including aspartyl proteinases, which degrade extracellular matrix proteins; catalases, which resist oxidative killing by phagocytic cells; and adenosine which blocks neutrophil oxygen radical production and degranulation.[4,16]

Candidiasis is mainly a disease of keratinized epithelium in young animals, especially pigs, calves, and foals and typically presents as a superficial infection that produces relatively mild lesions in skin and mucous membranes that grossly appear as white pseudomembranes which, when removed, reveal ulcerated or erythematous tissue underneath. In birds it is a common infection in the mouth, esophagus, crop, and proventriculus. In piglets, lesions present in the oral cavity ("thrush"), esophagus, and gastric squamous mucosa. In calves, lesions are present in the ventral sac of the rumen, omasum, or reticulum following prolonged antibiotic therapy, and in foals, gastroesophageal candidiasis involves the squamous

epithelium and is associated with ulceration adjacent to the margo plicatus.[4]

In adult ruminants, *Candida* is one of several angioinvasive fungi that can produce mycotic abomasitis or rumentits and subsequent fungal hepatitis. The feeding of a high carbohydrate diet increases volatile fatty acids and leads to the disruption of normal rumen flora and proliferation of *Streptococcus bovis*, with subsequent lactic acid production. Ruminal acidosis results in mucosal ulceration allowing fungal hyphae to penetrate the mucosa, invade the vasculature, cause thrombosis, infarction, and acute necrosis. Subsequent hematogenous or direct spread leads to dissemination via portal vasculature to the liver.[15]

Contributor: German Primate Center
Pathology Unit
Kellnerweg 4, 37077 Göttingen, Germany
www.dpz.eu

References:

1. Bader O, Weig M, Taverne-Ghadwal L, et al. Improved clinical laboratory identification of human pathogenic yeasts by matrix-assisted laser desorption ionization time-of-flight mass spectrometry. *Clinical Microbiology and Infection*, doi: 10.1111/j. 1469-0691.2010.03398.x. [Epub ahead of print], 2010.
2. Baskin GB, Chandler FW, Watson EA. Cutaneous zygomycosis in rhesus monkeys (*Macaca mulatta*). *Vet Pathol*. 1984;21:125-128 .
3. Bernstein JA, Didier PJ. Nonhuman primate dermatology: a literature review. *Vet Dermatol.* 2009;20:145-156.
4. Brown CC, Baker DC, Barker IK. Alimentary system. In: Maxie MG, ed. *Jubb, Kennedy and Palmer's Pathology of Domestic Animals.* 4th ed. Philadelphia, PA: Elsevier; 2007:230.
5. Gibson SV. Bacterial and mycotic diseases. In: Bennett BT, Abee CR, Henrickson R, eds. *Nonhuman Primates in Biomedical Research: Diseases*. San Diego: Academic Press, 1998:60-110.
6. Kirkpatrick CH. Chronic mucocutaneous candidiasis. *J Am Acad Dermatol*. 1994;31:S14-S17.
7. Lim YH, Lee DH. Rapid PCR method for detecting *Candida albicans* using primers derived from the integrin-like protein gene αINT1 of *Candida albicans*. *Journal of Microbiology*. 2000;38:105-108.
8. Liovat AS, Jacquelin B, Ploquin MJ, et al. African non human primates infected by SIV – Why don't they get sick? Lessons from studies on the early phase of non-pathogenic SIV infection. *Curr HIV Res*. 2009;7:39-50.
9. Migaki G, Schmidt RE, Toft JD, et al. Mycotic infections of the alimentary tract of nonhuman primates: a review. *Vet Pathol*. 1982;19:93-103.
10. Netea MG, Maródi L. Innate immune mechanisms for recognition and uptake of Candida species. *Trends Immunol.* 2010;31:346-353.
11. Samaranayake YH, Samaranayake LP. Experimental oral candidiasis in animal models. *Clin Microbiol Rev*. 2001;14:398-429 .
12. Slater DN, Harrington CI, Wylde P, et al. Systemic candidiasis: Diagnosis from cutaneous manifestations. *JRSM*. 1982;75:875-878.
13. Voracek T, Vielgrader H, Vogel B, et al. A case of fungal granuloma in a female mandrill *(Mandrillus sphinx*). *Proc Eur Assoc Zoo Wildl Vet,* 4th scientific meeting; 2002:501-502.
14. Wachtman LM and Mansfield KG: Opportunistic infections in immunologically compromised nonhuman primates. *ILAR J.* 2008;49:191-208.
15. Zachary JF. Mechanisms of microbial infections. In: McGavin MD, Zachary JF, eds. *Pathologic Basis of Veterinary Disease*. 5th ed. St. Louis, MO: Mosby; 2011:234-7.
16. Zöller M, et al. Mucocutaneous Candidiasis in a Mandrill (*Mandrillus sphinx*). *J Comp Pathol*. 2012 Jan 31. [Epub ahead of print]

Joint Pathology Center
Veterinary Pathology Services

WEDNESDAY SLIDE CONFERENCE 2011-2012

Conference 20

28 March 2012

CASE I: W139-11 (JPC 4006397).

Signalment: 5-year-old Thoroughbred mare horse, *Equus caballus*.

History: The horse presented to the University of Melbourne referral equine clinic with acute, severe, uncontrolled abdominal pain. On examination, the mare was distressed and had no gut sounds, pale pink mucous membranes and marked tachycardia (heart rate 100). A displacement of the large colon was suspected based on rectal findings and at exploratory laparotomy, volvulus of the left dorsal and ventral colon was corrected. There was no visible compromise of the bowel and the volvulus did not appear to fully explain the severity of pain. Subsequently, the mare exhibited signs of severe pain despite intense multimodal analgesia including nonsteroidal anti-inflammatories, alpha-2 agonists, lignocaine and ketamine constant rate infusions and morphine. The horse was euthanized

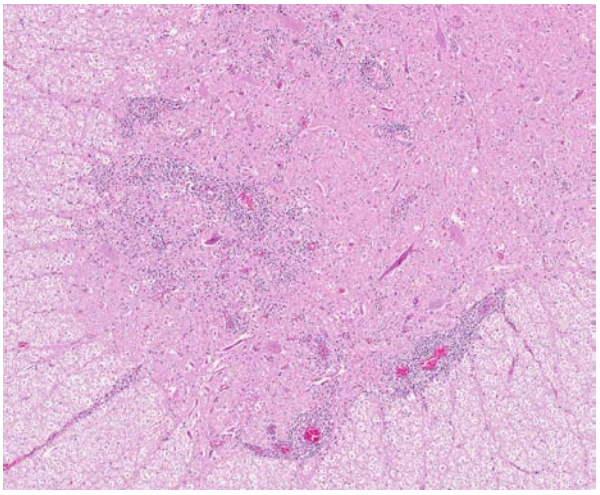

1-1. Spinal cord, horse: Diffusely, vessels within the gray matter are outlined by an accumulation of lymphocytes and plasma cells within the Virchow-Robins space. (HE 4X)

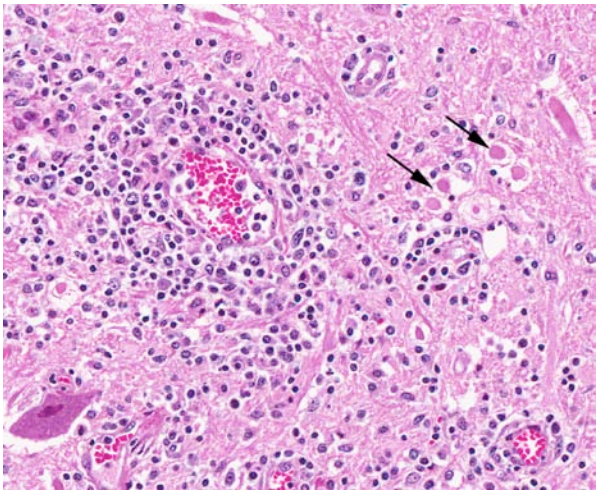

1-2. Spinal cord, horse: The inflammatory infiltrate, primarily lymphocytes, plasma cells, and histiocytes, extends in some areas outward from the perivascular space and infiltrates the surrounding neutrophils. Neuronal changes, however, are limited to a few spheroids (arrows). (HE 240X)

approximately 24 hours after initial presentation. Euthanasia was based on the severity and refractory nature of the pain, of unknown origin.

Gross Pathology: The animal was in lean, fit body condition, with moderate amounts of internal body fat. There was a surgical incision site on the ventral mid-line of caudal abdomen with associated subcutaneous edema. A small amount of fibrin was noted on and over the serosa of the ventral cecum. The brain and spinal cord were grossly within normal limits. The CSF collected was watery and colorless (within normal limits).

Laboratory Results:

Lactate:	13.8mmol/L	(<2)
Fibrinogen:	5.6 g/L	(2.0 – 4.0)
Total bilirubin:	68 µmol/L	(0 – 40)
AST:	457 U/L (150 – 400)	
CK:	3439 U/L	(50 – 400)
Total protein:	58 g/L	(58 – 76)

CSF fluid collected at post mortem was within normal limits, with low cellularity and only a few lymphocytes identified in cytospin preparations.

Formalin fixed sections of brain and spinal cord were positive for Murray Valley Encephalitis (MVE) using PCR, and were negative for EHV-1 using PCR.

Contributor's Histopathologic Description: Sections of brain and spinal cord showed widespread changes affecting mainly the grey matter, with lesions sparing the cerebral cortex, but involving midbrain, brain stem, and spinal grey matter especially in thoracic and lumbar regions, but without any significant change in the nerve roots, ganglia or peripheral nerves. The cerebellar cortex was also spared.

Lesions consisted of thick perivascular cuffs comprised predominantly of small lymphocytes, with lesser numbers of large lymphocytes, plasma cells, and macrophages. In some areas, inflammatory foci extended into the parenchyma, and were associated with neuronal necrosis, especially in the spinal cord. Lesions were intense in the lumbar grey matter. A careful search for protozoa or inclusion bodies failed to reveal any. Apart from a few small ring hemorrhages perivascularly in the brain stem, the lesions were devoid of hemorrhage.

Contributor's Morphologic Diagnosis: Brain and spinal cord: Severe chronic non-suppurative polioencephalomyelitis consistent with Murray Valley Encephalitis.

Contributor's Comment: The horse described had both histological evidence of encephalitis and a positive PCR result for Murray Valley Encephalitis virus. Although the PCR has not been validated for fixed tissue, the histological lesions along with the PCR result are highly suggestive for Murray Valley Encephalitis (MVE). Experience with previously confirmed cases of EHV-1 at this institution has often showed extensive hemorrhagic lesions of brain stem and spinal cord of horses, with minimal inflammation. Based on the clinical presentation, CNS pathology and the negative PCR reaction, this case is not consistent with EHV-1.

There have been two neurological syndromes seen in horses in south-eastern Australia in 2011, peaking in March and April (autumn/fall) associated with arboviral infections: central neurological and musculoskeletal clinical diseases, with some overlap in the lesser affected horses. Neurological signs have most commonly included: ataxia, depression, behavioral changes, tremor, hyperesthesia, muscle fasciculations, hypermetria and colic.[1] Musculoskeletal signs reported in horses that have shown no CNS signs include: listlessness, reluctance to walk, stiff gait, pyrexia and anorexia.[1]

Three viruses- Murray Valley Encephalitis (MVE) virus, Kunjin virus and Ross River Virus (RRV), have been associated with these two syndromes. MVE and Kunjin have been most commonly associated with the neurological syndrome and RRV with the musculoskeletal syndrome. Horse deaths have occurred associated with Murray Valley Encephalitis and Kunjin, but most (≥ 85%) of the horses affected have recovered with supportive treatment.[2] The included table shows serological / viral data from thirteen horses with post mortem evidence of encephalitis / encephalomyelitis (spinal cord often not submitted) seen by the Department of Primary Industries, Victoria:

Number of horses with histological evidence of encephalitis	MVE	Kunjin	Hendra
5*	+	-	-^
6**	-	+	-
1*	+	+	NA
1	-	-	NA

*, The diagnosis is based on demonstration of viral agent(s).
**, In 2 of the 6 horses the diagnosis was based on serology results; the presence of antibodies against Kunjin virus and absence of antibodies against MVE. Kunjin virus was detected by PCR and/or virus isolation in the other 4 horses.
^, One of the 5 horses was not tested.

NA, Not assessed.

Tests used:

- MVE: Antibody assays (Virus neutralization test (VNT) and ELISA) and Agent detection tests (direct PCR and/or virus isolation followed by PCR and sequencing)
- Kunjin: VNT, direct PCR with or without sequencing and/or virus isolation followed by PCR and sequencing
- Hendra: Eleven of the 14 horses were tested for Hendra by PCR. All 11 tested negative (see table).
- Ross River virus testing is pending on these cases.

The prevalence of all three arboviruses this year is related to very high rainfall experienced over the preceding spring, summer and autumn and the resultant increase in mosquito vectors. The increase in water may also have affected the distribution of water birds (the main reservoir hosts for MVE and Kunjin). In many parts of Victoria the 2010-2011 rainfall measurements have been more than double the long term mean for each area.[3] This is particularly significant as most of the state has been in drought for up to 14 years (depending on area), with rainfall in these years often being much lower than the mean.

MVEV and Kunjin are *Flaviviruses* present in northern Australia, Papua New Guinea and Indonesia,[4] with more widespread Australian distribution when the seasonal conditions are conducive. Kunjin is closely related to West Nile Virus.[8] The main vector in Australia is *Culex annulirostris* and the main hosts appear to be water birds, although antibodies have been found in many bird and mammalian species.[4] Usually humans are subclinically infected, but MVE can produce mild disease featuring fever, headache, nausea and vomiting and with Kunjin, a rash, swollen joints, muscle weakness and fatigue. Rarely, both viruses can cause severe disease of meningitis or encephalitis sometimes resulting in death.

RRV is an arbovirus (Alphavirus) which commonly causes human disease in Australia, with approximately 5000 notifications yearly.[4,6] Symptoms of infection in humans include joint pain, joint effusion, rash and pyrexia.[4,6] In horses, the virus is known to cause in the musculoskeletal system the symptoms described above. Macropods and other marsupials are suspected to be the main reservoir species.

Hendra virus has been included in testing to rule out the possibility of this rare, zoonotic disease, which is not an arbovirus. All tested horses have been negative. Horses with Hendra virus infection can have very similar signs to those discussed previosuly including depression, fever, neurological signs and colic.[5] Another common (but not always present) clinical presentation is respiratory disease.[5]

JPC Diagnosis: Spinal cord: Poliomyelitis, lymphohistiocytic, diffuse, severe, with marked neuronal degeneration.

Conference Comment: The differential diagnosis for lymphohistiocytic poliomyelitis in a horse should include Murray valley encephalitis virus (MVEV), West Nile virus (WNV), Kunjin virus, the alphaviruses (Eastern, Western, and Venezuelan encephalitis viruses), other Flaviviruses such as Japanese encephalitits virus and Dengue virus, Borna virus, and Rabies virus. The lack of Negri bodies usually seen with rabies, lack of Joest-Degen bodies usually seen with Borna virus, and lack of neutrophilic involvement usually seen with the alphaviruses and other flaviviruses makes these conditions less likely. Of these remaining candidate conditions, MVEV is the only one to produce disease with the severity seen in the present case. WNV produces mild to moderate lesions of nonsuppurative polioencephalomyelitis with multifocal gliosis and occasional neuronal necrosis, and primarily affects the gray matter of lower brainstem and thoracolumbar spinal cord. Kunjin virus is typically even less pathogenic than WNV.[7,9]

Contributor: University of Melbourne
Veterinary Science
250 Princes Hwy
Werribee
Victoria
Australia, 3030
www.vet.unimelb.edu.au

References:

1. http://www.vetboard.vic.gov.au/docs/Equine_arbovirus_update_20110323.ppd (30th May, 2011).
2. http://www.dpi.qld.gov.au/4790_20274.htm (30th May, 2011).
3. http://www.bom.gov.au/climate/data/ (30th May, 2011).
4. Carver S, Bestall A, Jardine A, et al. Influence of hosts on the ecology of arboviral transmission: Potential mechanisms influencing Dengue, Murray Valley encephalitis, and Ross River virus in Australia. *Vector Borne Zoonotic Dis*. 2009;9(1):51-64.
5. Field H, Schaaf K, Kung N, et al. Hendra virus outbreak with novel clinical features. *Australia. Emerg Infect Dis*. 2010;16(2):338-40.
6. Harley D, Sleigh A, Ritchie S. Ross River Virus Transmission, infection and disease: a cross disciplinary review. *Clin Microbiol Rev*. 2001;(4): 909-932.
7. Maxie MG, Youssef S. Nervous system. In: Maxie MG, ed. *Jubb, Kennedy and Palmer's Pathology of*

Domestic Animals. 5th ed. Vol 1. New York, NY: Elsevier Saunders; 2007:421-425.
8. Barthold SW, Bowen RA, Hedrick RP, et al. West nile virus. In: MacLachlan NJ, Dubovi EJ, eds. *Fenner's Veterinary Virology*. 4th Ed. London, UK, Academic Press; 2011:472.
9. Zachary JF. Nervous system. In: McGavin MD, Zachary JF, eds. *Pathologic Basis of Veterinary Disease*. 5th ed. St. Louis, MO: Mosby; 2011:805-6, 839-40.

CASE II: A08276724 (JPC 3103238).

Signalment: 1-year-old male Rocky Mountain Horse, *Equus caballus*.

History: This colt from northern Indiana was euthanized along with a 2-year-old filly, and presented for necropsy in September 2007, after two days of weakness, depression, and neurologic signs including head pressing. Both horses had been reared on the premises and had received no vaccinations.

Gross Pathology: Ascarids were in the small intestine. Verminous arteritis with serpiginous intimal tracts was noted in the cranial mesenteric artery.

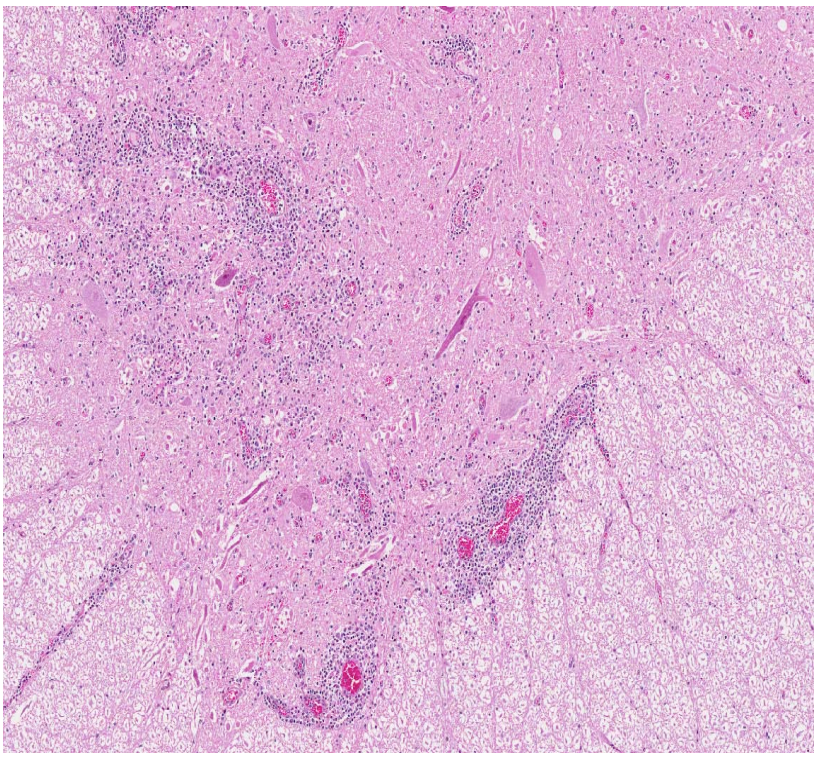

2-1. Cerebrum, horse: Multifocally, Virchow's Robins are expanded by a combination of neutrophils and histiocytes, with fewer macrophages. (HE 220X)

Cerebral leptomeninges were congested and wet. The lateral ventricles of the brain were slightly dilated.

Laboratory Results: Brain tissue from both horses was positive by PCR for Eastern equine encephalitis (EEE) virus, negative by fluorescent antibody test for rabies virus, and negative by RT-PCR for West Nile virus; EEE virus was also isolated in cell culture.

Contributor's Histopathologic Description: In this section of cerebrum, cortical gray matter is more severely affected than white matter by inflammatory changes and necrosis. Thin cuffs (1 or 2 cell layers) of lymphocytes, plasma cells, macrophages and neutrophils surround venules in the cerebral cortex. These perivascular cuffs are thicker (4 or 5 layers) in the cerebral white matter. The leptomeninges, especially in sulci, also have perivascular to diffuse infiltration by the same types of leukocytes. Some venules, especially in the cerebral cortex, have fibrinoid material in their walls or in surrounding tissue; a few have microscopic perivascular hemorrhage. There is widespread, predominantly neutrophilic infiltration of the cortical gray matter. Increased numbers of macroglia and microglia accompany the leukocytes. Focally, heavy neutrophil infiltration is noted in foci of parenchymal necrosis. Many neuronal soma are shrunken with intense cytoplasmic eosinophilia and pyknosis or karyolysis. Some of these dead neurons are surrounded by numerous neutrophils; others are not. A few are undergoing neuronophagia. Similar, but less severe neutrophilic inflammation is evident in the cerebral white matter.

Contributor's Morphologic Diagnosis: Cerebrum**,** neutrophilic poliomeningoencephalitis.

Contributor's Comment: Eastern equine encephalitis (EEE) was suspected because of the clinical signs in two young unvaccinated horses in late summer, so tissues were shipped to the National Veterinary Services Laboratories (NVSL) for diagnostic testing. Histologic changes of severe neutrophilic polioencephalitis supported the tentative diagnosis, which was confirmed by PCR and subsequent virus isolation in both horses. This colt proved to be the sentinel case in an EEE outbreak in northern Indiana. By late October 2007, 17 horses in 24 Indiana counties had tested positive for EEE. This outbreak was considered the widest dispersion of EEE in Indiana in the past 10-15 years. The fact that the first cases were not detected until September was attributed to dry weather in early and mid-summer followed by rainy weather in late summer to support the mosquito population. Horses are considered accidental hosts for EEE virus, which is maintained in birds and transmitted to horses, people and other animals by mosquito vectors.[1] After the development of viremia, the virus invades the brain hematogenously and replicates in neurons, glial cells and vessels. Histologic lesions target the cerebral cortex, sparing

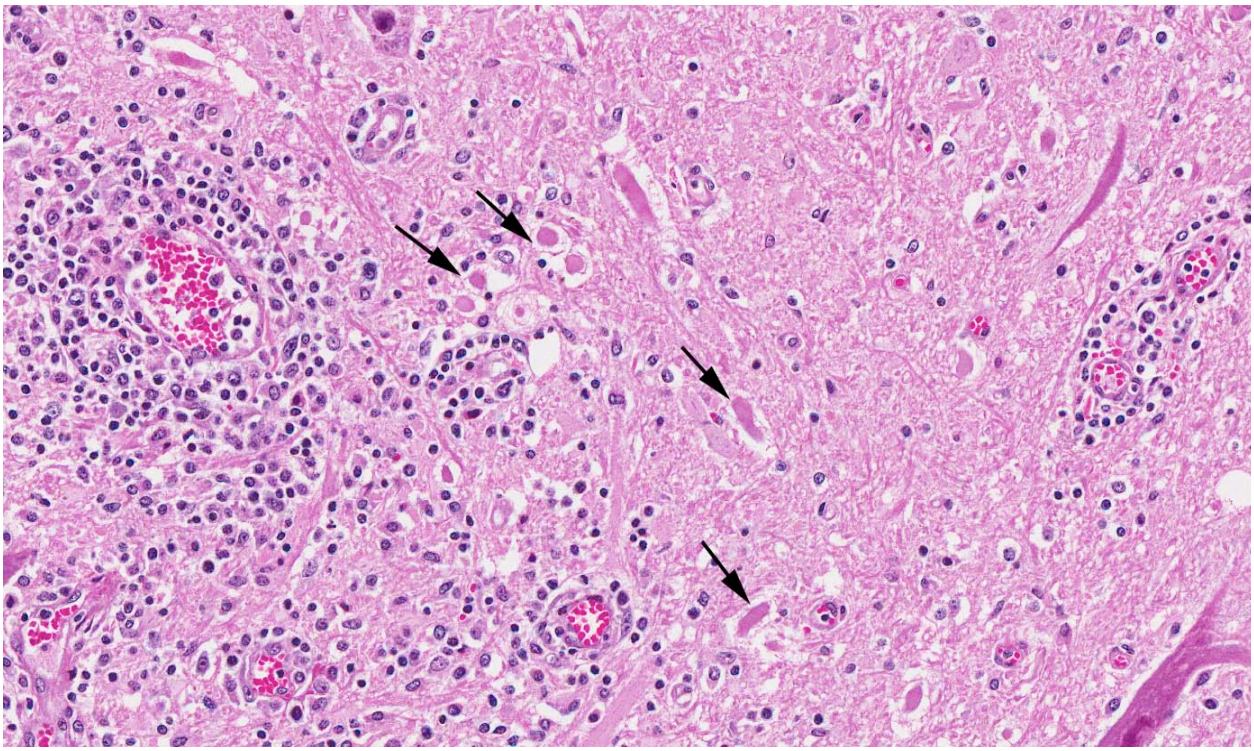

2-2. Cerebrum, horse: Foci of neutrophils admixed with cellular debris are scattered throughout the cerebrum. (HE 160X)

white matter and ganglia, resulting in neuronal degeneration and death, typically with prominent neutrophil infiltration, especially in acute fatal cases.

JPC Diagnosis: Spinal cord: Meningoencephalitis, neutrophilic and lymphocytic, diffuse, moderate, with neuronal necrosis and neuronophagia.

Conference Comment: In some sections, there is rare vasculitis and thrombosis, with large areas of hemorrhage and necrosis. In horses with Eastern equine encephalitis (EEE), gross lesions are asymmetrical in the gray matter and include congestion, hemorrhage, malacia, cerebral hyperemia, edema, petechiation and focal necrosis.[2] Gray matter lesions are more severe in the frontal, rhinencephalic, and occipital areas of the cerebral cortex, as well as the thalamus and hypothalamus, and the intensity of inflammation diminishes as lesions progress caudally. Eastern equine encephalitis virus may cause small intestinal lesions that include multifocal myonecrosis, lymphomonocytic myositis and focal mild perivascular lymphocytic infiltration in the submucosa. Pigs typically develop myocarditis from EEE virus, and Guinea pigs and white mice are highly susceptible.[1]

Other new-world alphaviruses in the Togaviridae family include Western equine encephalitis (WEE) virus and Venezuelan equine encephalitis (VEE) virus. The three basic phases of alphavirus encephalitis, common to EEE, WEE, and VEE, are virus replication in peripheral tissue and subsequent spread, neuroinvasion, and viral spread within the CNS with primary infection of neurons and fatal neurodegeneration.[2] Western equine encephalitis is typically the least virulent of the three viruses, although lesions and pathogenesis are similar to EEE and VEE. In horses, VEE often presents as a purely nonsuppurative encephalomyelitis, sometimes accompanied by myeloid depletion of the bone marrow and lymphocytolysis in the spleen and lymph nodes. Necrotizing vasculitis, thrombosis and cerebrocortical necrosis are particularly prominent in VEE, but are also reported in EEE, as demonstrated in this case.[3] VEE has been shown to enter the CNS directly via olfactory neuroepithelium to the olfactory bulbs.[2]

Contributor: Purdue University
Animal Disease Diagnostic Laboratory
Department of Comparative Pathobiology
406 S. University St.
West Lafayette, IN 47907
http://www.addl.purdue.edu/
http://www.vet.purdue.edu/cpb/

References:

1. Maxie MG, Youssef S. Nervous system. In: Maxie MG, ed. *Jubb, Kennedy and Palmer's Pathology of Domestic Animals.* 5th ed. Vol 1. New York, NY: Elsevier Saunders; 2007:423-425.

2. Steele KE, Twenhafel NA. REVIEW PAPER: pathology of animal models of alphavirus encephalitis. *Vet Pathol*. 2010;47(5):790-805.
3. Zachary JF. Nervous system. In: McGavin MD, Zachary JF, eds. *Pathologic Basis of Veterinary Disease*. 5th ed. St. Louis, MO: Mosby; 2011:839-40.

CASE III: D-09-8307 (JPC 3164937).

Signalment: Nine-year-old gelding Thoroughbred, *Equus caballus*, equine.

History: The owner complained that the horse seemed to be lame when riding in sand. Over the next 24 hours there was rapidly ascending paralysis. The horse was dog sitting and then became recumbent with complete loss of deep sensation to the rear limbs. Cerebral spinal fluid (CSF) was collected from the lumbar region and appeared to be blood. CSF collected from the thoracic region was cloudy. The owner opted for humane euthanasia and a post mortem examination was performed.

Gross Pathology: Hemorrhage at the lumbosacral region. No fracture was detected. No other significant findings. Sections of the spinal column were submitted to the Tai Lung Veterinary Laboratory for histological interpretation. These sections of the spinal cord were fixed in 10% neutral buffered formalin, processed, sectioned and stained with haematoxylin and eosin (H&E).

Pathologist's findings: On trimming of the spinal cord sections submitted for histological examination, the segment from lumbar vertebra 1 to lumbar vertebra 4 was visibly compressed with a 15 mm x 4 mm dorsal protrusion.

Laboratory Results: Cytology Examination results:
Cerebrospinal fluid (lumbosacral – per submitting veterinarian): Field was entirely composed of red blood cells and marked numbers of neutrophils and macrophages.
CSF for culture – No significant findings
PCR for Japanese Encephalitis – Negative
PCR for West Nile Virus – Negative
Virology – Rabies:
Negri Bodies – Negative
Immunofluorescent Test - Negative

Contributor's Histopathologic Description: Spinal cord: One cross section and one longitudinal section from the area of lumbar vertebra four (L4) are examined. L4-L6 represents the most devastatingly affected segment with large areas of gray matter loss (cavitation). In both the dorsal and the ventral gray column there is severe hemorrhage, neuronal necrosis, spheroids, high protein perivascular edema and an inflammatory cell infiltrate consisting of neutrophils, macrophages and fewer lymphocytes. Blood vessels radiating from the gray matter into the surrounding white matter are surrounded by perivascular edema and hemorrhage. Multifocally, in the white matter there are swollen, eosinophilic axons (spheroids) and Wallerian degeneration characterized by the presence of gitter cells in dilated myelin sheaths. White matter changes also include vascular diapedesis and perivascular cuffs composed of neutrophils, macrophages and lymphocytes. There are multifocal areas of hemorrhage seen in the white matter and the meninges. Multifocally, vascular fibrinoid necrosis is also evident.

Contributor's Morphologic Diagnosis: Spinal cord, lumbar: Myelopathy, necrotizing, ischemic, extensive, severe, acute, neutrophilic and histiocytic with massive hemorrhage and Wallerian degeneration, Thoroughbred, equine.

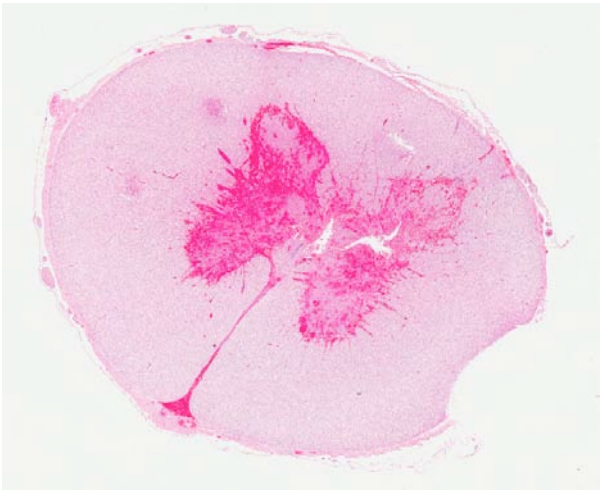

3-1. Spinal cord, horse: Extensive hemorrhage outlines the gray matter. (HE 5X)

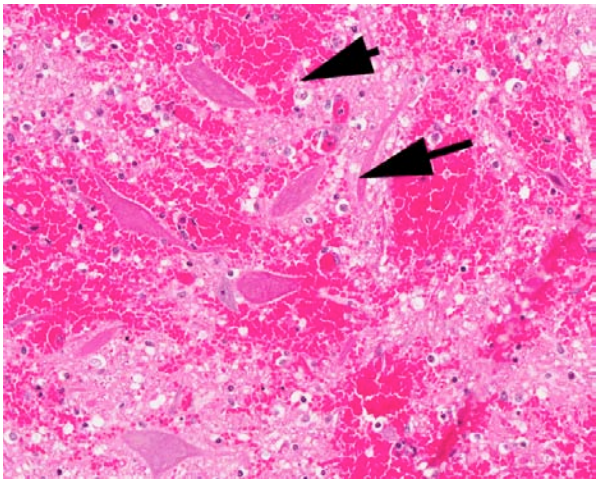

3-2. Spinal cord, horse: In areas of hemorrhage, neurons exhibit degenerative signs such as swelling, hypereosinophilia, and loss of Nissl substance (arrows). (HE 150X)

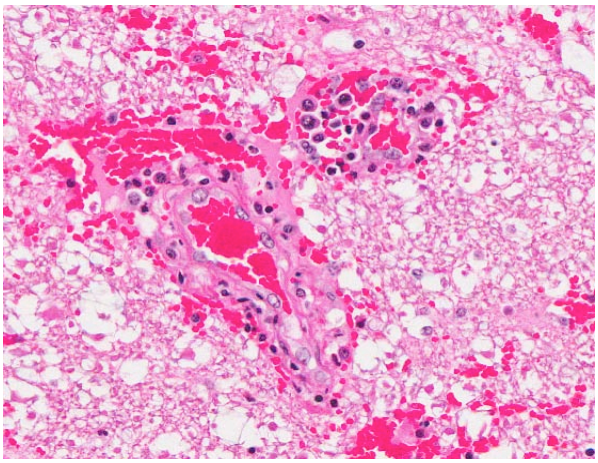

3-3. Spinal cord, horse: Scattered throughout the hemorrhagic gray matter, vessel walls are often expended by fibrin, infiltrating neutrophils and histiocytes, and cellular debris (fibrinoid vasculitis). (HE 188X)

3-4. Spinal cord, lumbar. Severe hemorrhage and cavitation.

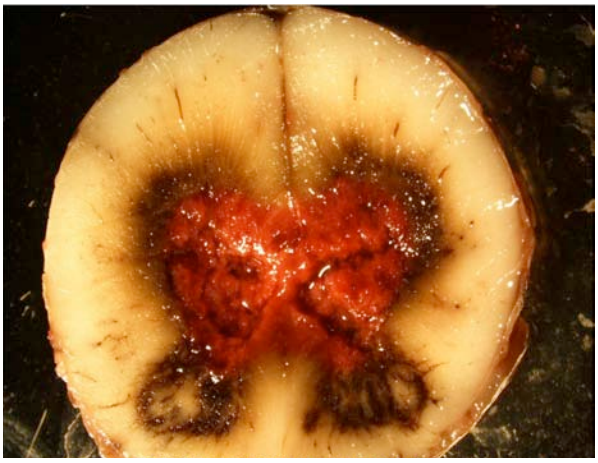

3-5. Spinal cord, lumbar. Liquefactive necrosis of the gray matter.

Contributor's Comment: The most likely cause of the devastating changes seen in the spinal column and considering the rapid onset of clinical signs, aggressive progression of paralysis and the protrusion of the spinal column seen grossly is trauma. There was neither history of degenerative disk disease nor evidence of fibrocartilaginous emboli but these scenarios were considered due to the sudden onset of clinical signs and the ischemia evident histologically.[1] However, in the literature it is thought that the cervical spinal cord is the area primarily affected by fibrocartilaginous emboli in the horse.[4]

Despite there being no evidence of vertebral fracture during post mortem examination, acute compression of the spinal column and resultant ischemia would account for the changes seen histologically. It has been reported that direct injuries to the spinal cord can occur without obvious injury to the vertebrae with devastating effects.[2]

Grey matter with its high metabolic rate and dependence on oxygen is much more sensitive than white matter to ischemic changes.[5] This would explain why the gray matter in this case is so much more severely affected than the white matter.

Acute, traumatic spinal cord injury generally occurs by primary and secondary mechanisms. The primary event is the mechanical injury to the tissue, which may include compression. The secondary mechanism consists of the interruption in vascular supply and perfusion.[5]

The gray matter is composed primarily of cell bodies and dendrites of nerve cells. Neurons are the most sensitive to injury out of all the cells in the central nervous system as they have limited energy stores. They are dependent on an intact blood flow to supply oxygen and nutrients, particularly glucose. Neurons are dependent on a continuous supply of oxygen to remain viable and if the supply is interrupted, vulnerable neurons will degenerate. It is reported that the more rapid the onset of ischemia, the more severe the lesion tends to be. The severe hemorrhage seen primarily in the gray matter is consistent with damage to the capillary framework which tends to be more concentrated in the gray matter than in the white matter. There are also fewer anastomoses in the vessels that supply the white matter.[6]

It is thought that the tendency for spinal cord tissue to become soft and suffer liquefactive necrosis is due to the abundance of lipids and enzymes and a lack of fibrous connective tissue in the CNS.[6]

JPC Diagnosis: Lumbar spinal cord, gray matter: Hemorrhage and necrosis, diffuse, severe.

Conference Comment: Although not reported in the history, conference participants considered post-anesthesia hemorrhagic myelopathy as a possible ruleout in this case. When horses are anesthetized and laid in dorsal recumbency, compression of the azygous vein can result in venous infarction and ischemic necrosis, and poliomyelomalacia of the caudal spinal cord is the most common histopathological finding.[3] Another possible cause is fumonisin B1 toxicity from the consumption of corn contaminated with the saprophytic fungus *Fusarium verticillioides*, which typically causes edema and necrosis of the cerebral white matter, but chiefly cause gray matter necrosis in the brain stem and spinal cord.[2] Also considered was purpura hemorrhagica, which causes vasculitis, vascular necrosis and hemorrhage secondary to antigen-antibody complexes; or endotoxemia, although accompanying inflammation would be expected.[6]

Contributor: Tai Lung Veterinary Laboratory
Agriculture, Fisheries and Conservation Department
Lin Tong Mei, Sheung Shui
New Territories, Hong Kong SAR
www.afcd.gov.hk

References:

1. Fuentealba IC, Weeks BR, Martin MT, et al. Spinal cord ischemic necrosis due to fibrocartilaginous embolism in a horse. *Journal of Veterinary Diagnostic Investigation*. 1991;3:176-179.
2. Maxie MG, Youssef S. Nervous system. In: Maxie MG, ed. *Jubb, Kennedy and Palmer's Pathology of Domestic Animals*. 5th ed. Vol 1. New York, NY: Elsevier Saunders; 2007: 343-345, 358-9.
3. Ragle C, et al. Development of equine post anaesthetic myelopathy: Thirty cases (1979-2010). *Equine Vet Ed*. 23(12); 2011:630-5.
4. Sebastian MM, Giles RC. Fibrocartilaginous embolic myelopathy in a horse. *Journal of Veterinary Medicine*. 2004;51:341-343.
5. Summers BA, Cummings JF, de Lahunta A. Injuries to the central nervous system. In: *Veterinary Neuropathology*. Mosby, St. Louis, MO, Mosby: 195;189-193.
6. Zachary JF. Nervous system. In: McGavin MD, Zachary JF, eds. *Pathologic Basis of Veterinary Disease*. 5th ed. St. Louis, MO: Mosby; 2011:851-852, 860-861, 892, 899-900.

CASE IV: AFIP 2 (JPC 4003090).

Signalment: Third trimester fetus, male Arabian horse.

History: The dam aborted the fetus approximately 2 months before the expected foaling date.

Gross Pathology: The liver is markedly friable, and the subcapsular surface is stippled yellow and red. Within the thymus is a moderate amount of white to yellow opaque material.

Laboratory Results: Fluorescent antibody testing for equine herpesvirus-1on liver tissue was positive. Additional ancillary test results were as follows: bacterial culture of the stomach contents did not isolate organisms; bacterial culture of the thymus isolated few *Staphylococcus xylosus* and *Acinetobacter lwoffii*, interpreted as contaminants; serology for *Leptospira* spp. and equine viral arteritis virus was negative.

Contributor's Histopathologic Description: Scattered randomly throughout the liver are numerous small foci of coagulative necrosis infiltrated by numerous macrophages, lymphocytes, and plasma cells. Within hepatocytes adjacent to the areas of necrosis are variable numbers of large, eosinophilic, intranuclear inclusion bodies that marginate the chromatin to the periphery. Within the portal triads are numerous mononuclear cells consistent with hematopoietic precursor cells. Immunostaining for equine herpesvirus demonstrates marked positive immunoreactivity within inflammatory cells and necrotic cellular debris in the areas of hepatocellular necrosis.

Within the spleen, white pulp is markedly expanded by karyorrhectic cellular debris, and few intact lymphocytes remain.

The thymic medulla contains a moderate amount of necrotic debris and is infiltrated by numerous eosinophils. Rarely, thymic reticular cells contain a single, large, eosinophilic intranuclear inclusion body. Within the lung, alveolar septa contain variable amounts of necrotic cellular debris. (Thymus and lung were not submitted)

Contributor's Morphologic Diagnosis: Liver: Severe, acute, random, necrotizing hepatitis with hepatocellular intranuclear inclusion bodies.
Spleen: Marked lymphoid necrosis.
Thymus (not submitted): Moderate to marked lymphoid necrosis.
Lung (not submitted): Mild, multifocal, necrotizing interstitial pneumonia.

Contributor's Comment: Herpesviral abortion occurs in horses, cattle, goats, pigs, dogs, and cats.[9] In horses, herpesviral abortion is most commonly attributed to equine herpesvirus-1, an alphaherpesvirus that causes abortion, neonatal disease, respiratory disease, or neurologic disease in horses.[7,9] Most horses are infected with equine herpesvirus as young animals, as the virus is widespread.[7] Equine herpesvirus 1 can cause abortion as a result of initial infection with the virus or as a result of recrudescence of latent virus within the dam.[7] Most equine herpesvirus abortions occur in the third trimester of pregnancy, as was the case in the submitted fetus.[5,7]

This fetus demonstrated the classic histologic lesions of equine herpesvirus abortion including multifocal necrotizing hepatitis, splenic and thymic necrosis, and

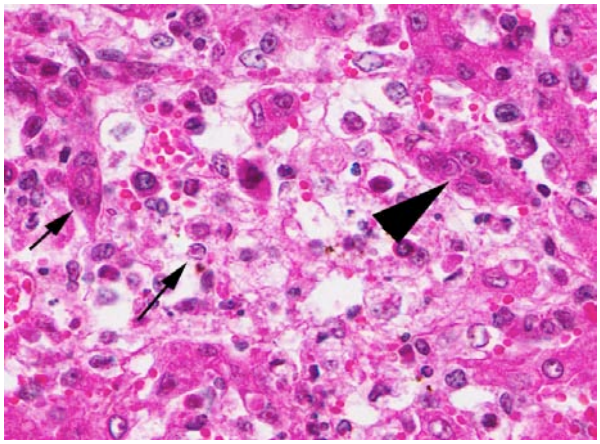

4-1. Liver, foal: Small areas of necrosis are scattered throughout the liver and hepatocytes at the periphery contain small eosinophilic herpesviral inclusions which marginate the chromatin (arrows). A muntinucleated viral synctytium with inclusions within multiple nuclei is also present (arrowhead). (HE 400X)

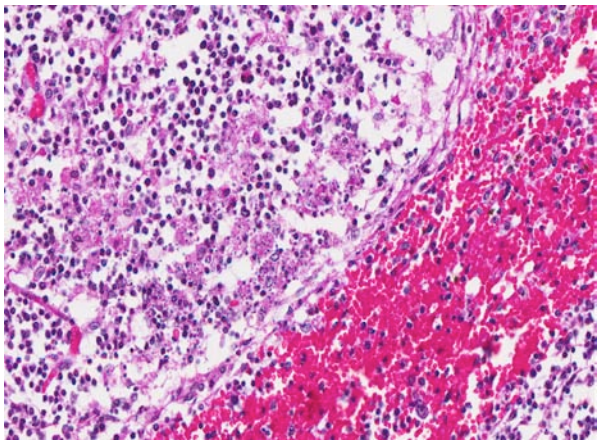

4-2. Spleen, foal: Splenic white pulp is markedly depleted, and expanded with abundant cellular debris. (HE 400X)

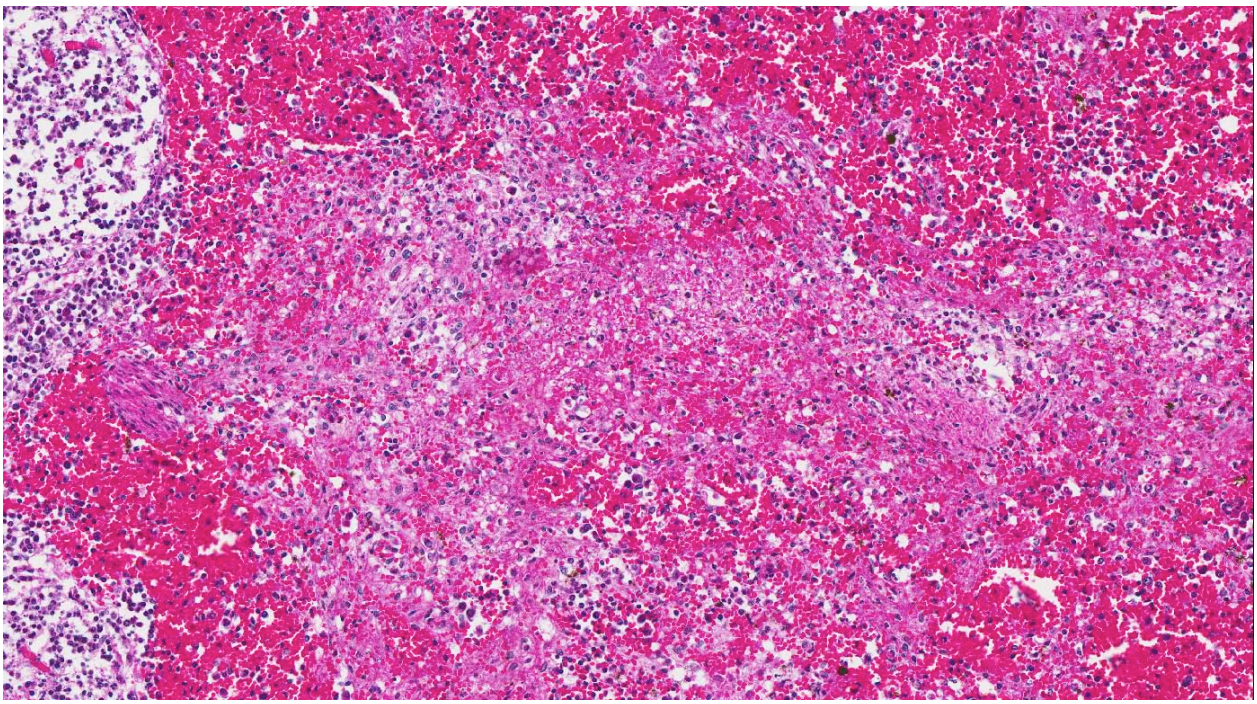

4-3. Spleen, foal: There are rare foci of red pulp necrosis scattered throughout the parenchyma. (HE 400X)

interstitial pneumonia.[7] Adrenal gland necrosis is also reported to occur.[9] The florid hepatic necrosis with intranuclear inclusion bodies is somewhat atypical, as in most cases of equine herpesviral hepatitis, inclusion bodies are rare.[7] Inclusion bodies are most commonly identified in the bronchiolar and alveolar epithelium, reticular cells of the spleen and thymus, and, less often, in hepatocytes.

Gross examination of this fetus revealed a friable liver, and foci of hepatic necrosis were not seen grossly. In addition, white to yellow fluid seen grossly in the thymus likely corresponded to necrotic cellular debris identified microscopically. Additional gross lesions that may occur in equine herpesviral abortions include pulmonary edema, bronchiolar fibrin casts, splenic petechiation, and renal cortical hemorrhage.[7] These lesions were not identified in this fetus.

Upon infection with equine herpesvirus 1, primary viral infection occurs within the upper respiratory tract, resulting in viremia. Viremia enables spread of the virus to the gravid uterus with infection of uterine endothelial cells. In the uterus, the virus may induce vasculitis and infarction of microcotyledons with subsequent spread to the feto-placental unit.[5,9] Uterine endothelial cells are more susceptible to infection in late pregnancy, leading to the increased risk of abortion in the third trimester.[5]

Though this fetus was aborted, occasionally foals will be born infected with the virus. In these cases, foals typically die with an interstitial pneumonia, and they may develop focal necrosis of intestinal crypt epithelium with intranuclear inclusion bodies in crypt epithelium.[7]

In this case, histopathologic changes were highly suggestive of equine herpesvirus infection. Immunohistochemistry was performed for confirmation. In addition to histopathology and immunohistochemistry, other methods of equine herpesvirus 1 diagnosis include virus culture and isolation and polymerase chain reaction.[5,7]

JPC Diagnosis: 1. Liver: Hepatitis, necrotizing, multifocal and random, moderate, with lymphohistiocytic pericholangitis and hepatocellular, endothelial, and biliary viral syncytia and intranuclear inclusion bodies.
2. Spleen, white pulp: Lymphoid necrosis, diffuse, severe, with random red pulp necrosis, fibrin, and intrahistiocytic intranuclear viral inclusion bodies.

Conference Comment: Equine herpesvirus 1 (EHV1) proliferates rapidly in nasal, pharyngeal, and tonsillar mucosa, and infects primarily T-lymphocytes, resulting in viremia and subsequent endothelial infection in numerous sites including the lungs, uterus, and CNS. This results in vasculitis, thrombosis, and ischemic necrosis. With damage of maternal uterine endothelial cells following viral infection, there is thrombosis, inflammation, and perivascular edema which leads to infarction of the endometrium and separation of

maternal and fetal placental layers. Viral infection of fetal endothelium and other cells in many organs leads to abortion or birth of weak foals that die soon after pneumonia. Infection in older foals, usually greater than 1 year-old, is typically a self-limiting upper respiratory disease.[1,2,3,4,5,7]

Viral replication occurs in the nucleus, and the viral envelope is acquired by budding through the inner layer of nuclear membrane. Positively charged residues in EHV1, glycoprotein B and glycoprotein C, bind to heparan sulfate moieties of host cells, and equine major histocompatibility complex (MHC) I acts as a functional receptor for glycoprotein D (gD), facilitating entry and infection of the cell.[6]

This case was atypical because portal hepatitis and edema of the capsule and the space of Disse were the prominent features instead of necrosis. Another unusual feature was the abundance of syncytial cells within hepatocytes, biliary epithelium, and endothelial cells.

Other causes of equine abortion include equine herpesvirus 4, which occurs sporadically and is considered a milder pathogen then EHV1 and which generally causes lesions only in the endometrium and not the fetus; equine viral arteritis, an Arterivirus that causes fetal autolysis and myocardial arteritis; *Streptococcus zooepidemicus*, which causes fetal autolysis and fibrinonecrotic placentitis around the cervical star; *Leptospira* sp., which also causes fetal interstitial nephritis; nocardioform abortion due to *Crossiella equi* occurring in late gestation, which causes necrotizing placentitis involving the base of the uterine horns; and *Salmonella* sp., most commonly *S. typhimurium* and rarely *S. abortus-equi*; causing maternal septicemia and fibrinonecrotic placentitis. Other bacteria such as *E. coli*, *Streptococcus equi*, *Staphylococcus aureus*, *Pseudomonas aeruginosa*, *Actinobacillus equuli*, and *Klebsiella pneumoniae*, as well as late gestational fungal infection by *Aspergillus fumigates*, *Mucor* sp., *Candida* sp., and *Histoplasma capsulatum* can cause abortion due to necrotizing placentitis.[7] Mare reproductive loss syndrome, associated with the eastern tent caterpillar (ETC) and possibly the result of non-beta-hemolytic *Streptococcus* and *Actinobacillus* spp. infection or a toxin related to the ETC, is another potential cause of equine abortion.[8]

Contributor: Oklahoma State University
Department of Veterinary Pathobiology
Room 250 McElroy Hall
Stillwater, OK 74078
http://www.cvhs.okstate.edu

References:

1. Caswell JL, Williams KJ. Respiratory system. In: Maxie MG, ed. *Jubb, Kennedy, and Palmer's Pathology of Domestic Animals.* Vol. 2. 5th ed. Philadelphia, PA: Elsevier Saunders; 2007:640-4.
2. Del Piero F, Wilkins PA, Timoney PJ, et al. Fatal Nonneurological EHV-1 Infection in a Yearling Filly. *Vet Pathol*. 2001:38;474–474.
3. Foster RA. Female reproductive system and mammary gland. In: McGavin MD, Zachery JF, eds. *Pathologic Basis of Veterinary Disease.* 5th ed. St. Louis, MO: Elsevier Mosby; 2012:1111.
4. Lopez A. Respiratory system, mediastinum, and pleurae. In: McGavin MD, Zachery JF, eds. *Pathologic Basis of Veterinary Disease.* 5th ed. St. Louis, MO: Elsevier Mosby; 2012:505-6.
5. Lunn DP, Davis-Poynter N, Flaminio MJBF, et al. Equine herpesvirus-1 consensus statement. *J Vet Intern Med*. 2009:23;250-61.
6. Sasaki M, Hasebe R, Makino Y. Equine major histocompatibility complex class I molecules act as entry receptors that bind to equine herpesvirus-1 glycoprotein D. *Genes Cells*. 2011;16(4):343-357.
7. Schlafer DH, Miller RB. Female genital system. In: Maxie MG, ed. *Jubb, Kennedy, and Palmer's Pathology of Domestic Animals*. Vol. 3. 5th ed. St. Louis, MO: Elsevier Limited; 2007:495, 506-8, 522-3, 532-534.
8. Sebastian MM, et al. REVIEW paper: mare reproductive loss syndrome. *Vet Pathol*. 2008;45(5): 710-22.
9. Smith KC. Herpesviral abortion in domestic animals. *Vet J*. 1997;153:253-268.

Joint Pathology Center
Veterinary Pathology Services

WEDNESDAY SLIDE CONFERENCE 2011-2012

Conference 21

11 April 2012

CASE I: 12874-04 (JPC 3133955).

Signalment: 13-week-old male white domestic turkeys (*Melagris gallopavo*).

History: Several animals were submitted after lesions of the skin on the head were observed. 100 birds were dead and 300 displayed signs out of 13,000 birds.

Gross Pathology: Four of five turkeys had necrosis and edema of areas of skin on the head, and/or snood, and/or wattles.

Laboratory Results: *Pasteurella multocida* was isolated from skin lesions.

Contributor's Histopathologic Description: Specimens of skin, largely without feather follicles, came from the wattles of several birds. The microscopic lesions are a mixture of infarction and inflammation. Several areas of acute necrosis of the epidermis and dermis are mixed with areas of severe heterophilic infiltration, edema, fibrin, epidermal necrosis, ulceration and numerous bacterial colonies. A small region of early fibroblast proliferation,

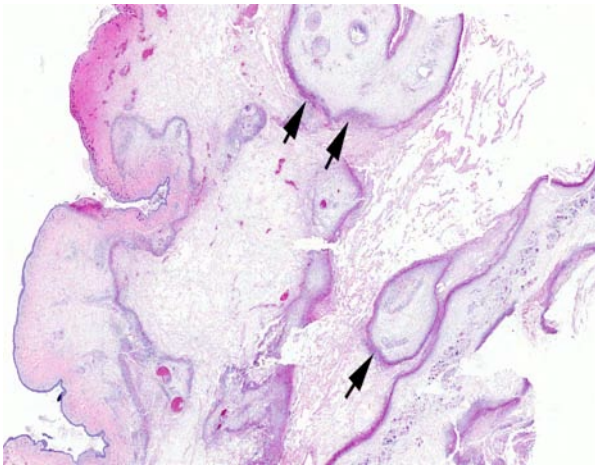

1-1. Non-feathered skin, turkey: There are multiple well-demarcated areas of infarction within the dermis and subcutis, outlined by a dense band of inflammatory cells and cellular debris. Intervening areas are markedly expanded by edema. (HE 9X)

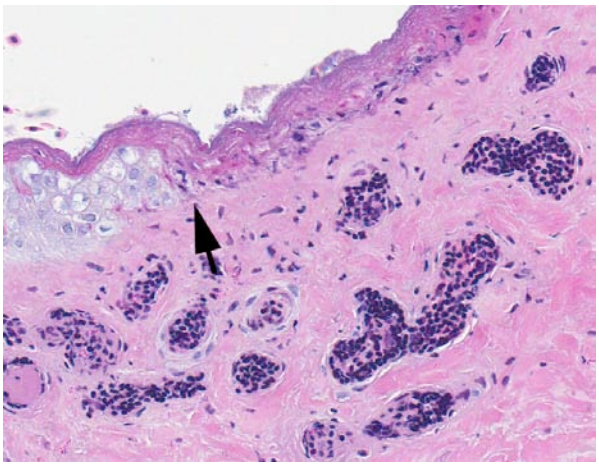

1-2. Non-feathered skin, turkey: Areas of epidermal necrosis at the edges of infarcts are very well demarcated (arrow). (400X)

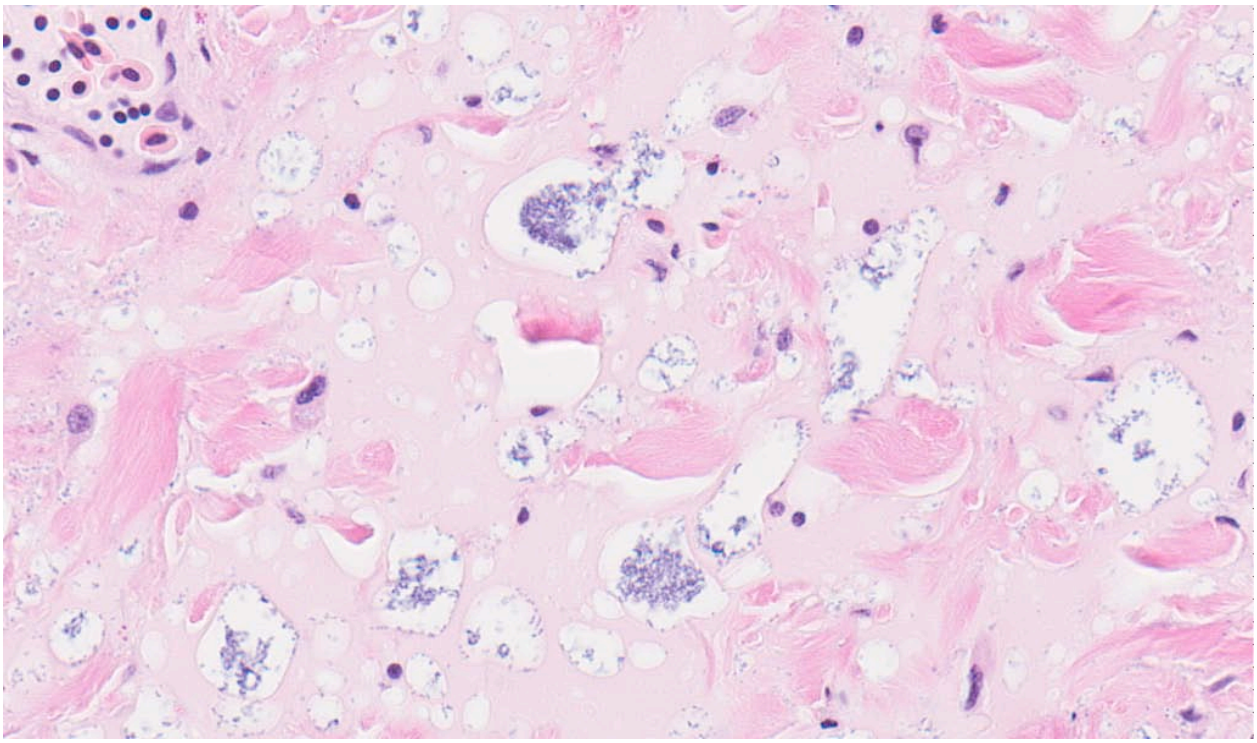

1-3. Non-feathered skin, turkey: The deep dermis contains numerous colonies of 2-4 µm rod-shaped bacilli. (HE 400X)

capillary proliferation and predominantly histiocytic inflammation occurs in some sections. No gross or histologic lesions were observed in internal organs, and affected skin was the only site of *Pasteurella* isolation and visceral tissues was unaffected.

Several ascarids were found in one cross section of jejunum (not shown).

Contributor's Morphologic Diagnosis: Severe necrotizing dermatofasciitis, with focal infarcts, and bacterial colonies.

Contributor's Comment: *Pasteurella multocida* is the etiology of severe necrotizing dermatitis in turkeys that can affect the skin of the carcass as well as of the face.[1] Outbreaks can be recurrent and cutaneous lesions may predominate over systemic infection in affected flocks.[2] Lesions of internal organs are uncommon although septicemia has resulted from experimental infection via scarification.

It is suspected that dermal manifestations such as this are a result of generalized Schwartzman reaction, and occur in the context of subclinical or previous infection. In turkey poults sensitized to *P. multocida* LPS, inflammation was observed in turkeys challenged with epidermal LPS, whereas inflammation and vasculitis resulted when intradermal and intravenous injections were given.[3]

Pasteurella multocida produces a spectrum of disease in turkeys. Lesions may be minimal in the peracute cases. Consolidation of the lungs, often extensive, is the most common manifestation of acute infection, with fibrinous exudates in the coelomic cavity. *Erysipelas* and colibacillosis are the major differential etiologies. Because surviving birds become carriers, depopulation may be necessary to stop recurrence.[4]

Serotyping of the *Pasteurella* isolate, conducted at NVSL, revealed that it was different from the organism previously used for vaccines and also differed from previous pathogenic isolates from this particular facility.

JPC Diagnosis: Unfeathered skin: Dermatitis and cellulitis, necrotizing and heterophilic, diffuse, severe, with numerous intracellular and extracellular bacilli and multifocal skeletal muscle necrosis and mineralization.

Conference Comment: In the moderator's experience, this is an unusual presentation of fowl cholera in a turkey, and is more typical of chronic fowl cholera in male broiler chickens, which develop caseous necrosis of the subcutaneous tissues of the wattle. Female broilers or breeders typically present with acute egg yolk peritonitis, and chronic cases in female turkeys and chickens produce caseous to fibrinonecrotic salpingitis. Fowl cholera in turkeys usually presents with a triad of lesions that include

fibrinous pericarditis, splenic necrosis, and fibrinonecrotic pneumonia and air sacculitis, and occasionally multifocal necrotizing hepatitis or fibrinocaseous arthritis. Infections are generally acquired from oculonasal secretions which contaminate drinkers, and the reservoir in poultry is pigs, cats, and raccoons. The differential diagnosis includes *Erysipelothrix rhusiopathiae*, which is the best option and causes cutaneous hemorrhage and infarction with thrombosis and cyanosis, "paintbrush" hemorrhages, systemic hemorrhage and necrosis, and splenomegaly; as well as colibacillosis caused by *E. coli*, or frostbite with secondary bacterial infection.[4]

Contributor: University of Missouri
Veterinary medical Diagnostic Lab
1100 East Rollins Street
Columbia, MO 65211
http://www.cvm.missouri.edu/vpbio/index.html

References:

1. Glass SE, Panigrahy B. Dermal necrosis caused by Pasteurella multocida infection in turkeys. *Avian Diseases*. 1990;34:491-494.
2. Frame DD, Clark FD, Smart RA. Recurrent outbreaks of a cutaneous form of *Pasteurella multocida* infection in turkeys. *Avian Diseases*. 1994;38:390-392.
3. Mendes S, Carmichael KP, Nunnally JC, et al. Lesions resulting from attempted Shwartzman reaction in turkey poults inoculated with Pasteurella multocida lipopolysaccharide. *Avian Diseases.* 1994;38:790-796.
4. Charlton BR, et al. Avian Disease Manual. 6th edition. American Association of Avian Pathologists. 2006:77, 81, 84-7.

CASE II: N09-168 (JPC 3166501).

Signalment: Fourteen male and female sexually immature five to six-week-old bobwhite quail (*Colinus virginianus*).

History: These birds were a representative sampling of a flock with a reported history of spiked mortality, depression and respiratory distress. On physical exam quails had ruffled feathers, white watery diarrhea, and a few were non-ambulatory and in lateral recumbency.

Gross Pathology: All birds were in poor body condition as determined by prominent keel bones and inadequate musculature. Eight of the fourteen birds were alive. All live birds and five of six dead birds were necropsied. Four of the 13 birds had cloudy air sacs interpreted as mild airsacculitis. The lumen of two ceca and one ileum had a whitish-yellow caseous cores. The mucosal and serosal surfaces of the intestinal tracts of five birds were dark red(congestion and hemorrhage). There were multiple depressed areas (ulcerations) in the duodenum of two birds and the ileum of a third bird. Mucosal scrapings from the intestines of multiple birds revealed numerous thin-walled, circular protozoa (*Eimeria* spp.) within enterocytes.

Contributor's Histopathologic Description: In some sections, the small intestinal mucosa is replaced by large, well-demarcated bands of abundant eosinophilic cellular debris with loss of differential staining and cells with pyknotic nuclei and eosinophilic, vacuolated cytoplasm. In some sections, these necrotic bands extend into the submucosa and muscularis. The mucosa and submucosa in less severely affected sections contain numerous plasma cells, moderate lymphocytes, and few extravasated erythrocytes. The muscularis is expanded by increased clear spacing and ectatic lymphatics (edema), and blood vessels are engorged with blood. Moderate to numerous rod-shaped basophilic structures (bacteria) are randomly distributed throughout the mucosa. Randomly distributed throughout intestinal villi, affecting up to 30% of enterocytes, there are numerous coccidia at variable stages of development (sporozoites, schizonts containing merozoites, and gamonts).

Contributor's Morphologic Diagnosis: Intestine: Enteritis, necrotizing, diffuse, severe, subacute with intralesional coccidia.

Intestine: Enteritis, necrotizing and ulcerative, diffuse, severe, acute with intralesional bacteria.

Contributor's Comment: *Clostridium colinum*, first named and described in 1974, has been established as the causative agent of ulcerative enteritis.[1,2] *C. colinum* is an anaerobic, gram-positive, spore-forming, fastidious, bacterial rod that affects multiple gallinaceous species, particularly captive game birds, young poults, and young chickens.[3] *Colinus virginianus*, the bobwhite quail, is the most susceptible

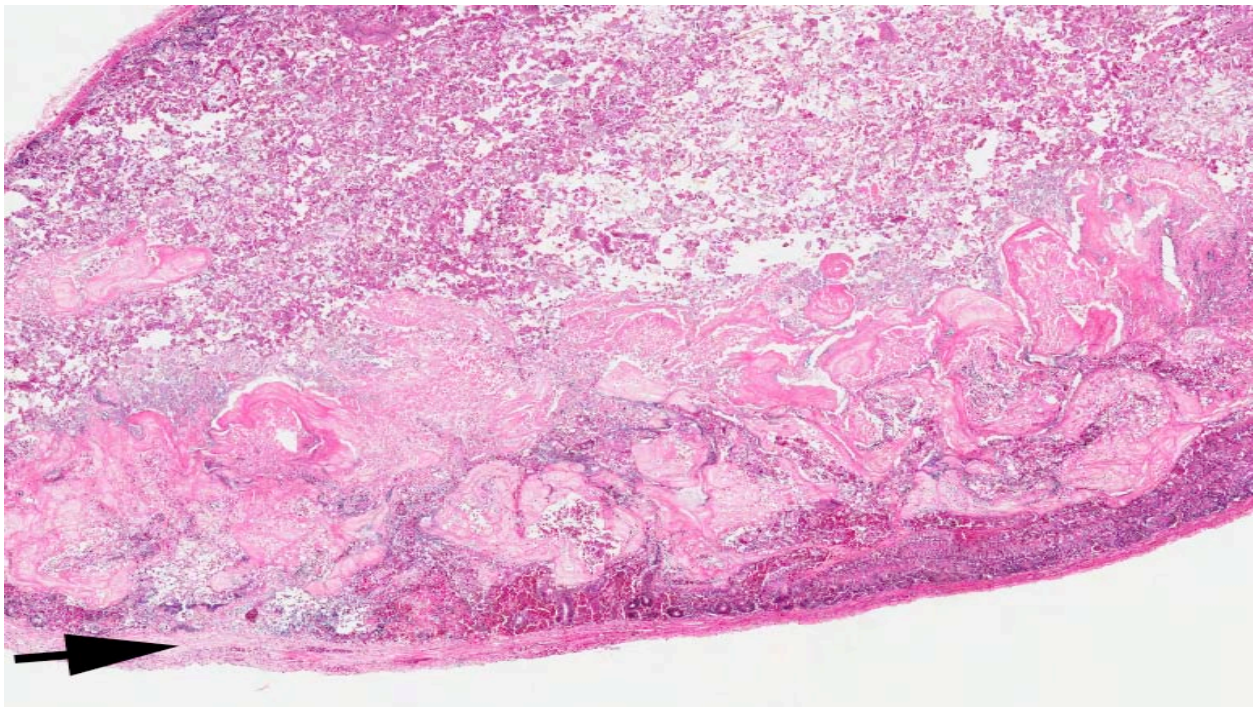

2-1. Small intestine, bobwhite quail: There is multifocal to coalescing areas of mucosal necrosis, which is focally transmural at one point (arrow). (HE 15X)

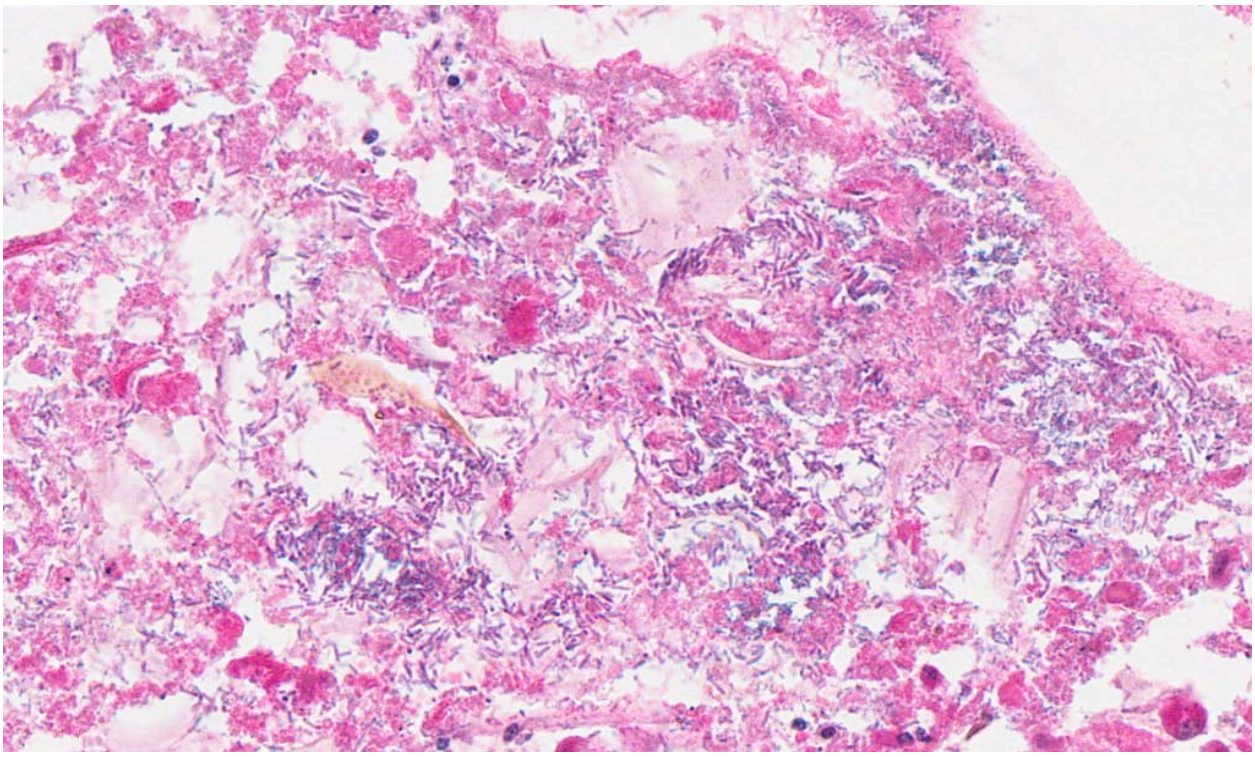

2-2. Small intestine, bobwhite quail: Robust, rod-shaped, 1x4 µm bacilli (C. colinum) abound within necrotic mucosal tissue. (400X)

species while *Coturnix coturnix japonica*, the Japanese quail, is resistant.[1,3] *C. colinum* produces spores that persist in the environment for years and is transmitted from the droppings of acutely ill or recovered carrier birds.[2,3] The typical clinical presentation can range from classic signs of depression (ruffled feathers, listlessness, drooped wings) to acute death. In quail, mortality can reach 100% in days.[3]

Fecal smears and histopathologic tissue sections were positive for abundant protozoal organisms consistent with coccidia of the genus *Eimeria*. Eimeriosis is thought to be a major predisposing factor for the development of ulcerative enteritis.[3] Often it is not possible to determine whether mortality can be attributed to the Eimeriosis or the Clostridial infection.[3] Attempts to culture the *C. colium* in this case were not successful but the presence of gram positive bacterial rods on histopathologic evaluation along with the classic deep and coalescing intestinal ulcers are sufficient for a presumptive diagnosis of ulcerative enteritis.

In some southern states, quail hunting is a $30 million a year or greater industry. As the industry continues to grow in popularity, increasing numbers of small scale brood-rearing/hunting operations have appeared.[4] With the rise of these operations, increased incidences of quail disease outbreaks can be expected. Ulcerative enteritis is a quail disease that is common and potentially devastating to new and unprepared quail operations.

JPC Diagnosis: Small intestine: Enteritis, fibrinonecrotizing, transmural, multifocal to coalescing, severe, with numerous robust bacilli and rare coccidia.

Conference Comment: Ulcerative enteritis, or "quail disease", often causes up to 100% mortality in quail and usually occurs in young birds. Additional histologic lesions include centrilobular or diffuse pinpoint coagulative hepatic necrosis with abundant bacteria and variable splenic necrosis. The intestinal necrosis is often severe enough to penetrate the intestine and cause peritonitis.[3] The differential diagnosis for ulcerative enteritis includes coccidiosis, which is often seen with quail disease but does not cause focal hepatic necrosis or splenomegaly; *Histomonas meleagridis*, a flagellated amoeboid protozoan which produces similar caseous cecal cores and targetoid hepatic necrosis and can look grossly similar; and *Hetarakis gallinarum*, a cecal worm which also produces cecal and hepatic necrosis.

There was some slide variation, and some sections were of small intestine with transmural, well-demarcated coagulative necrosis bordered by bacilli, which demonstrated the histologic effects of the diffusion of clostridial toxin into tissue. Other sections

included pancreas which exhibited variable vacuolation of the exocrine epithelial cells, which was interpreted as autolysis by conference participants. Most conference participants found it difficult to identify the coccidia, and discussed the role of coccidians, as well as ascarid migration, hemorrhagic enteritis in turkeys caused by avian adenovirus type 2, and severe salmonellosis, as a predisposing factor for necrotic enteritis of chickens and turkeys caused by *Clostridium perfringens* type A or C, which does not affect quail. Necrotic enteritis mostly affects broiler chickens, and grossly presents with necrotic intestinal mucosa with a pseudomembrane. In the moderator's experience, eimeriosis is not necessary as a predisposing factor for ulcerative enteritis.[3]

Contributor: Tuskegee University School of Veterinary Medicine
Department of Pathobiology
Tuskegee Institute, AL 36088
www.nadc.ars.usda.gov

References:

1. Berkhoff H. *Clostridium colinum* sp. nov., nom. rev., the Causitive Agent of Ulcerative Enteritis (Quail Disease) in Quail, Chickens, and Pheasants. *International Journal of Systematic Bacteriology*. 1985;35 (2)::155-159.
2. Brown J, Dawe D. Antibiotic Treatment of Ulcerative Enteritis of Bobwhite Quail. *Journal of Wildlife Diseases*. 1970; Vol 6. January..
3. Charlton BR, et al. *Avian Disease Manual*. 6th edition. American Association of Avian Pathologists. 2006:102-3, 120-121.
4. Flanders A, McKissick J. Economic Impacts of Alabama Quail Hunting. 2008.
5. The University of Georgia. Center for Agribusiness and Economic Development College of Agricultural and Environmental Sciences. Center Report: CR-08-21.

CASE III: AFIP 2010 #1 (JPC 3167238).

Signalment: Adult male chicken, *Gallus domesticus.*

History: This chicken was a member of a backyard flock. The chickens of this flock demonstrated difficulty breathing, coughing with the expectoration of plugs of mucus, swelling of the tissues of the head, and chalky droppings. There was mortality.

Gross Pathology: The bird had mild pectoral muscle atrophy. Petechiae were present along the length of the tracheal mucosa, which was covered by watery mucus containing yellow debris.

Laboratory Results: Immunohistochemistry for Infectious Laryngotracheitis Virus antigen: positive in trachea and air sac.

Contributor's Histopathologic Description: Trachea: The luminal surface of the mucosa is covered by a thick pseudomembrane comprised of fibrin and protein which are admixed with large numbers of heterophils with erythrocytes, macrophages, lymphocytes, plasma cells, scattered necrotic epithelial cells and occasional syncytial cells with eosinophilic intranuclear inclusion bodies. There is diffuse and marked erosion of the respiratory epithelium with focal ulcerations, and the mucosa is occasionally lined by attenuated epithelial cells, few of which form syncytia and have amphophilic to eosinophilic intranuclear inclusion bodies and marginated chromatin. The lamina propria and, to a lesser extent, the submucosa are diffusely infiltrated by moderate to large numbers of macrophages, lymphocytes plasma cells and heterophils. There is congestion of blood vessels in the lamina propria and submucosa.

Cranial Air Sac (not present on every slide): The air sac is folded and its connective tissue stroma is markedly expanded by edema, fibrin, karyorrhectic debris, and an infiltrate of heterophils, histiocytes and lymphocytes, with congestion and foci of hemorrhage. Along the luminal surface is an exudate of degenerate heterophils, detached and necrotic epithelial cells, protein and fibrin, and rafts of syncytial cells. Syncytial cells have as many as seventeen nuclei, which frequently possess eosinophilic intranuclear inclusion bodies and marginated chromatin.

Contributor's Morphologic Diagnosis: Trachea. Marked, diffuse, fibrinonecrotizing and heterophilic, tracheitis with pseudomembrane formation, epithelial syncytia and intranuclear inclusion bodies, etiology consistent with Gallid herpesvirus-1.
Air Sac. Marked, diffuse, fibrinoheterophilic and exudative air sacculitis, with epithelial syncytia and intranuclear inclusion bodies, etiology consistent with Gallid herpesvirus-1.

Contributor's Comment: Gallid herpesvirus 1 (GaHV-1) is the sole member of the Iltovirus genus within the alphaherpesvirinae subfamily and the cause of avian laryngotracheitis, or "LT" as it is known in the poultry industry. The virus naturally infects chicken and pheasants, and it circulates widely in the field and worldwide. Young turkeys can be experimentally infected, producing mild clinical signs. The virus has a narrow tropism that is limited to the upper and lower respiratory epithelia as well as the conjunctival epithelium. GaHV-1 has also been detected in feather

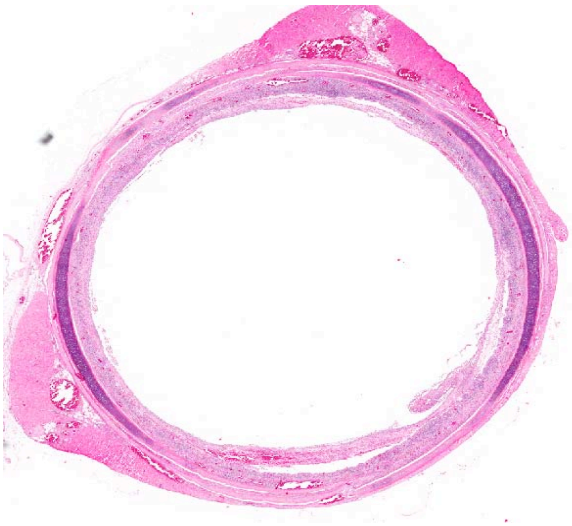

3-1. Trachea, chicken: The tracheal mucosa is circumferentially necrotic and replaced by a pseudomembrane composed of fibrin, hemorrhage and inflammatory cells. (HE 8X)

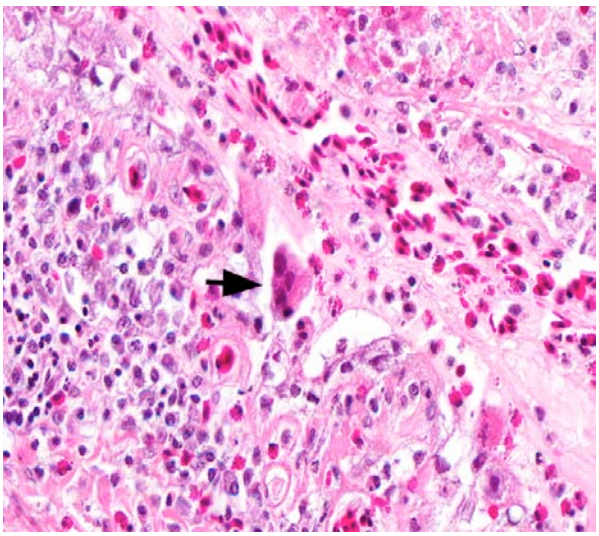

3-2. Trachea, chicken: Remaining epithelial cells occasionally form syncytia which contain round, eosinophilic intranuclear inclusion bodies which peripheralize nuclear chromatin (arrow). (HE 400X)

shafts.[2] There is no evidence of a viremic phase, but it can be transported to the trigeminal ganglion. Like other alphaherpesviruses, GaHV-1 can remain latent and can be reactivated several months later, for instance, after relocation of chickens or the onset of laying.[6] Vaccination of layer chickens (well before onset of production) is commonly practiced in areas of intensive poultry production if there is endemic disease. The epidemiology of the disease is complicated by the variable virulence of field strains, clinically inapparent carriers and circulation of vaccine strains.[6,7] Strains that are closely related genetically to vaccine strains have been isolated from outbreaks and have produced severe respiratory signs in experimentally inoculated chickens.[5] This phenomenon is a recognized problem for the poultry industry and has been termed "vaccinal laryngotracheitis"[5].

Although histopathology is not the most sensitive method available for recognizing the presence of the virus compared to molecular methods.[6], infectious laryngotracheitis is diagnosable by histopathology, as the virus causes fusion and desquamation of epithelial cells (syncytial cells) with basophilic to eosinophilic intranuclear inclusions.

JPC Diagnosis: Trachea and air sac: Tracheitis and air sacculitis, fibrinonecrotic and heterophilic, circumferential, severe, with occasional epithelial syncitia and numerous intranuclear viral inclusion bodies.

Conference Comment: Gross lesions with Gallid herpesvirus 1 (GaHV-1) include severe laryngotracheitis with necrosis, hemorrhage, ulceration and occlusive pseudomembranous or caseous plugs in the trachea. In milder forms there is sinusitis, conjunctivitis, congestion of mucous membranes and seromucoid discharge. The lungs and air sacs are rarely affected, although syncytia and intranuclear viral inclusion bodies are readily apparent in the section of air sac in this case.[1,4] The differential diagnosis for GaHV-1 includes:

- Newcastle disease, a Paramyxovirus that causes high mortality, although the surface epithelium is seldom lost
- Fowl pox, which has intracytoplasmic viral inclusion bodies (Bollinger bodies), no syncytial cells, epithelial proliferation, and similar caseous exudates which can plug the trachea
- Infectious bronchitis caused by a Coronavirus which presents with no viral inclusion bodies and readily affects the lower respiratory tract
- Avian influenza, an Orthomyxovirus with similar lesions and a lack of viral inclusion bodies
- *Mycoplasma gallisepticum* which causes severe air sacculitis, has no pseudomembranes and has a lack of extensive epithelial necrosis
- Infectious coryza caused by *Avibacterium paragallinarum* which causes facial edema and usually involves the lower respiratory tract and other organs
- *Trichomonas gallinae*, the cause of frounce in raptors and canker in columbids, which presents with caseous material in the trachea and esophagus
- Vitamin A deficiency which presents with hyperkeratotic lesions primarily in the mouth and tongue[1]

Contributor: University of Connecticut
Department of Pathobiology and Veterinary Science, U-3089
61 North Eagleville Road
Storrs, CT 06269-3089
http://www.patho.uconn.edu/

References:

1. Charlton BR, et al. Avian Disease Manual. 6th edition. American Association of Avian Pathologists. 2006:15, 43, 46, 52, 55, 90, 93, 154, 165.
2. Davidson I, Nagar S, Ribshtein I, et al. Detection of wild and vaccine-type avian infectious laryngotracheitis virus in clinical samples and feather shafts of commercial chickens. *Avian Dis*. 2009;53(4): 618-23.
3. Dufour-Zavala L. Epizootiology of infectious laryngotracheitis and presentation of an industry control program, *Avian Dis*.2008;52:1-7.
4. Guy JS, Garcia M. Laryngotracheitis. In: Saif YM, ed. *Diseases of Poultry*. Ames, IA: Blackwell Publishing; 2008:137-52.
5. Oldoni I, Rodriguez-Avila A, Riblet SM, et al. Pathogenicity and growth characteristics of selected infectious laryngotracheitis virus strains from the United States. *Avian Pathol*.2009;38:47-53.
6. Guy JS, Garcia M. Laryngotracheitis. In: *Diseases of Poultry.* 12th ed. Ames, IA: Blackwell Publishing Professional; 2008:137-144.
7. Kirpatrick NC, Mahmoudian A, Colson CA, et al. Relationship between mortality, clinical signs and tracheal pathology in infectious laryngotracheitis. *Avian Pathol*.2006;35:449-53.

CASE IV: 62555 (JPC 4002939).

Signalment: Adult male American Singer Canary (*Serinus canaria*), Avian.

History: An adult male American Singer Canary presented for scaly proliferation of unknown duration on both legs. The bird was singly housed since acquired on 5/7/2010, and was periodically treated with topical Scalex (0.03% pyrethrin and 0.3% piperonyl butoxide) following the manifestation of lesions. Given the severity and progression of the lesions despite treatment, the animal was euthanized.

Gross Pathology: On external examination of the hind limbs, the skin was markedly thickened and contained many frond-like keratinized projections (hyperkeratosis). Dried blood was present on the left foot, and all toenails were severely overgrown. No fractures were palpated, and the remainder of the exam was unremarkable.

Contributor's Histopathologic Description: Legs and feet including skin, underlying bone and musculature: Diffusely there is marked orthokeratotic hyperkeratosis of the overlying stratum corneum, with proliferation of anastomosing parallel plates radiating from the epidermis and creating a complexity of keratinized tunnels. Within these anastomosing tunnels and adjacent to the epidermis, are multiple cross and oblique sections of parasitic arthropods that are approximately 100 to 250 µm in diameter. Characteristic features of these arthropods include a spiny, chitinous exoskeleton, highly chitinized segmented appendages, striated skeletal muscle, distinct reproductive and digestive tracts, yolk glands, and occasional observation of mouthparts. Scattered throughout the anastomosing tunnels are numerous, 20-40 µm, spherical to ovoid developing ova. Rare, granular to amorphous, pigmented material is also present within these tunnels, depicted as mite excrement. Mild, multifocal acanthosis is noted within the underlying epidermis with prominent, rarely anastomosing rete pegs. The dermis is multifocally and markedly infiltrated with large numbers of inflammatory cells consisting predominantly of macrophages, and fewer lymphocytes and plasma cells. The inflammation multifocally extends into the underlying subcutis.

Contributor's Morphologic Diagnosis: Skin (feet and lower legs), dermatitis, proliferative, diffuse, chronic active, marked, with marked orthokeratotic hyperkeratosis, mild acanthosis, marked histiocytic lymphoplasmacytic dermatitis, intracorneal parasitic arthropods, and developing ova.

Contributor's Comment: *Knemidokoptes* is a common ectoparasitic burrowing mite that causes proliferative skin lesions in a variety of avian species. First described in budgerigars, over 15 *Knemidokoptes* spp. have now been reported[3] in a variety of avian species including galliforms (chickens, turkeys, etc.), passerines (canaries, finches, robins, etc), psittacines (budgerigars, parrots, cockatiels, parakeets, etc), and anseriforms (ducks, geese). Additionally, infection has been identified in both free-ranging and captive bird species, with lower prevalence in wild birds.[7] Mainka et al. reported that approximately 0.05-3% of wild passerines examined in Hong Kong were infected with *Knemidokoptes* mites.[7] Despite these findings, additional studies have suggested that the prevalence of subclinical infection in both captive and wild birds may be largely undocumented.[9] These findings suggest that *Knemidokoptes* spp. may serve as an opportunistic pathogen and manifest with stress or

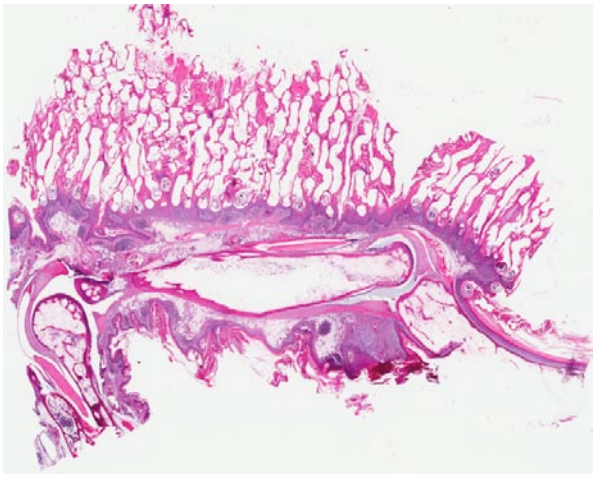

4-1. Cross section of phalanx, canary: At subgross inspection, there is profound orthokeratotic hyperkeratosis (top) with moderate epidermal hyperplasia. Longitudinal section of the bones of the phalanx is seen at the bottom of the section. (HE 7X)

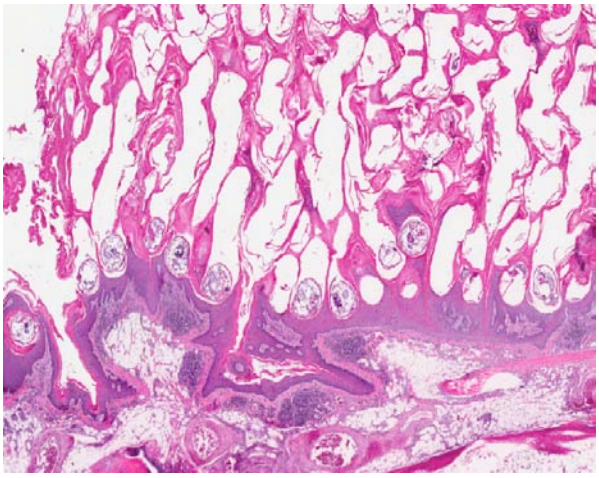

4-2. Cross section of phalanx, canary: Tortuous clear spaces within the keratin scale (mite tunnels) contain cross sections of adult mites. (HE 20X)

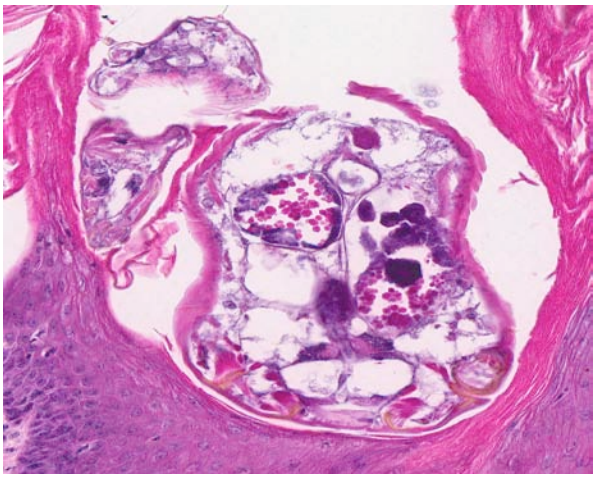

4-3. Cross section of phalanx, canary: Cross sections of adult mites within the keratin scale contain a brown serrated chitinous cuticle, jointed appendages with skeletal muscle, gonads, and a rudimentary nervous system. (HE 192X)

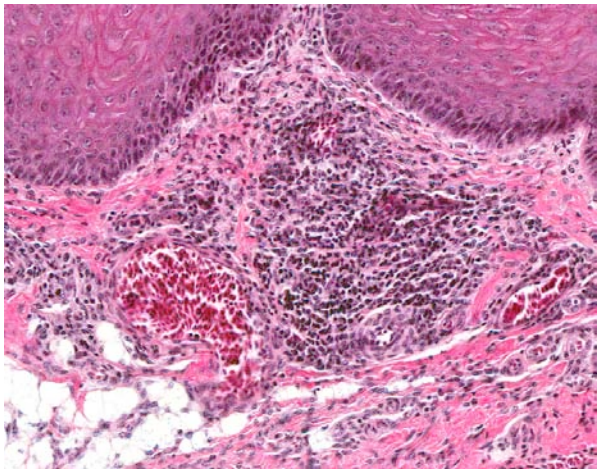

4-4. Cross section of phalanx, canary: Dermal vessels are frequently surrounded by a cellular infiltrate composed predominantly of lymphocytes with fewer plasma cells and histiocytes. (HE 2X)

secondary to other predisposing conditions, however this has not been confirmed.

Knemidokoptes spp. are often referred to as scaly leg, tassel leg, or scaly face mites due to the mite's predilection sites and characteristic lesions. Infected birds generally present with slowly progressive, proliferative, crusting lesions on unfeathered regions of the body, particularly the legs, feet, cere, and periocular regions.[1,3] Proliferative lesions can also be observed in feathered parts of the body[8], but are less common and may be associated with chronicity or vary by mite species. Left untreated, severe infections may progress to thickened, frond-like keratinized protuberances that can reduce flexibility, cause lameness, and inability to perch.[3] Additional gross lesions include necrosis of the digits[12], restriction secondary to leg bands, and overgrown nails. Hyperplastic lesions surrounding the cere may obstruct the nasal openings. Generally, pruritis is not observed, with the exception of *K. gallinae*, which causes an intense irritation, feather plucking, and self-mutilation.[1,6] Diagnosis can be made by skin scraping[10], tape preparations[8], or histopathology. As the *Knemidokoptes* spp. life cycle takes place entirely on the host, transmission generally occurs as a result of direct or indirect contact from an infected to an uninfected host.[3,6] Histopathologic lesions include severe, diffuse hyperkeratosis with the formation of tunnels in the stratum corneum and intracorneal mites.[9,10] Characteristic features of the mites include a spiny, chitinous exoskeleton, striated epidermis, uninterrupted dorsal striations, segmented appendages, striated skeletal muscle, and distinct reproductive and digestive tracts.[1,6] Female adults are generally 0.5 mm in length and contain short legs that lack pretarsi[1]; males are smaller, contain longer legs that include pretarsi, thus making them morphologically similar to *Sarcoptes* spp.[1] Finally, underlying dermal inflammation consisting of histiocytes, lymphocytes, plasma cells, and heterophils is also commonly observed.[9]

Common species of *Knemidocoptes* that produce lesions in avian include *K. jamaicensis*, the scaly leg mite of passerines, particularly canaries and finches, but has been observed in other species.[5,9] *K. mutans* is observed on the legs, combs and wattles of gallinaceous birds.[6] *K. gallinae*, the depluming mite, causes severe irritation and self mutilation in chickens secondary to burrowing, resulting in decreased egg production and weight loss.[6] Finally, *K. pilae* causes "scaly face mange" in pisittacine birds.[11] Secondary lesions include beak overgrowth and deformity, with consequential dysphagia and grooming impairment.

JPC Diagnosis: Feathered skin: Orthokeratotic hyperkeratosis, diffuse, severe, with numerous intracorneal adult mites and eggs, epidermal hyperplasia, and marked lymphoplasmacytic perivascular dermatitis.

Conference Comment: This case provides an excellent example of mites in tissue section. The cuticle, mouth parts, striated muscles, thickened cuticle at their point of attachment, and eggs inside and outside of the female mites are well demonstrated. Although the diagnosis is readily evident histologically, the differential diagnosis for the gross finding of scaly hyperkeratotic encrustations on the featherless areas of the face and legs include dermatophytosis, the dry version of fowl pox, and cutaneous papilloma virus causing papillomas on the feet of European goldfinches.[2,4]

Other mites which typically affect caged layers (but do not result in severe hyperkeratosis like *Knemidocoptes* spp.) include *Dermanyssus gallinae*, the red mite which feeds on host blood and causes anemia and mortality in heavy infestations and has also been reported to transmit fowl cholera and spirochetosis; and *Ornithonyssus sylviarum*, the northern fowl mite which can transmit fowl pox and Newcastle disease. Grossly, both mites appear as red or black specks on the feathers and skin.[2]

Contributor: Johns Hopkins University School of Medicine
Department of Molecular and Comparative Pathobiology
733 N. Broadway St., Suite 811
Baltimore, MD 21205
http://www.hopkinsmedicine.org/mcp/index.html

References:

1. Bowman DD. Georgis' Parasitology for Veterinarians. 6th ed. Philadelphia, PA: W.B. Saunders Co.; 1999:61-64.
2. Charlton BR, et al. Avian Disease Manual. 6th edition. American Association of Avian Pathologists. 2006:43, 130, 141.
3. Dabert J, Mihalca AD, Sándor D. The first report of *Knemidocoptes intermedius* Fain et Macfarlane, 1967 (Acari: Astigmata) in naturally infected European birds. *Parasitol Res*, web: n. pag, 2011 Apr 19.
4. Dorrestein GM. Passerines. In: Ritchie BW, Harrison GJ, Harrison LR, eds. *Avian medicine: principles and application*. Lake Worth, FL: Wingers Pub; 2004:884.
5. Latta SC, O'Connor BM. Patterns of Knemidokoptes jamaicensis (Acari: Knemidokoptidae) infestations among eight new avian hosts in the Dominican Republic. *J Med Entomol*. 2001;38:437-440.
6. Loomis EC. External Parasites. In: Hofstad MS, Barnes JH, Calned BW, Reid WM, Yoder HW, eds. Diseases of Poultry. 8th ed. Ames, Iowa: Iowa State University Press;1984;606-608.
7. Mainka SA, Melville DS, Galsworthy A, et al. Knemidocoptes sp. On wild passerines at the Mai Po Nature Reserve, Hong Kong. *J Wildl Dis*. 1994;30:254-6..
8. Miller DS, Taton-Allen GF, Campbell TW. Knemidokoptes in a Swainson's Hawk, Buteo swainsoni. *J Zoo Wildl Med*. 2004;35:400-402.
9. Pence DB, Cole RA, Brugger KE, et al. Epizootic Podoknemidokoptiasis in American Robins. *J Wildl Dis*. 1999;35:1-7.
10. Schmidt RE, Reavill DR, Phalen DN. Gastrointstinal system and pancreas. In: *Pathology of Pet and Aviary Birds*. Ames, Iowa: Iowa State Press; 2003:43.
11. Toparlak M, Tüzer E, Gargili A, Gülanber A. Therapy of Knemidocoptic mange in Budgerigars with spot-on application of moxidectin. Tr. *J. of Veterinary Animal Sciences*. 1999;23:173-174..
12. Morishita TY, Johnson G, Johnson G, et al.Scaly-leg mite infestation associated with digit necrosis in Bantam Chickens (Gallus domesticus). *J Avian Med Surg*. 2005;19:230-233.

Joint Pathology Center
Veterinary Pathology Services

WEDNESDAY SLIDE CONFERENCE 2011-2012

Conference 22

18 April 2012

CASE I: 0801727 (JPC 3121674).

Signalment: Mouse (*Mus musculus*) heterozygous F1 p53(+/-) transgenic (C3H/HeNTac female inbred x C57BL/6-Trp53tml Brd het N12 male inbred F_1) approx 45 weeks age female.

History: Mouse survived to terminal sacrifice in a 39-week study, with no clinical abnormalities noted.

Gross Pathology: The brain had a mass. No lesion was recorded grossly in the nasal cavities.

Contributor's Histopathologic Description: The nasal submucosa is greatly expanded by nests of tumor cells sometimes forming rosettes along a basement membrane. The rosettes in some cases have a distinct lumen; others contain fibrillar cytoplasmic processes suggestive of microvilli. Nests of cells also extend under the olfactory and respiratory epithelium and in

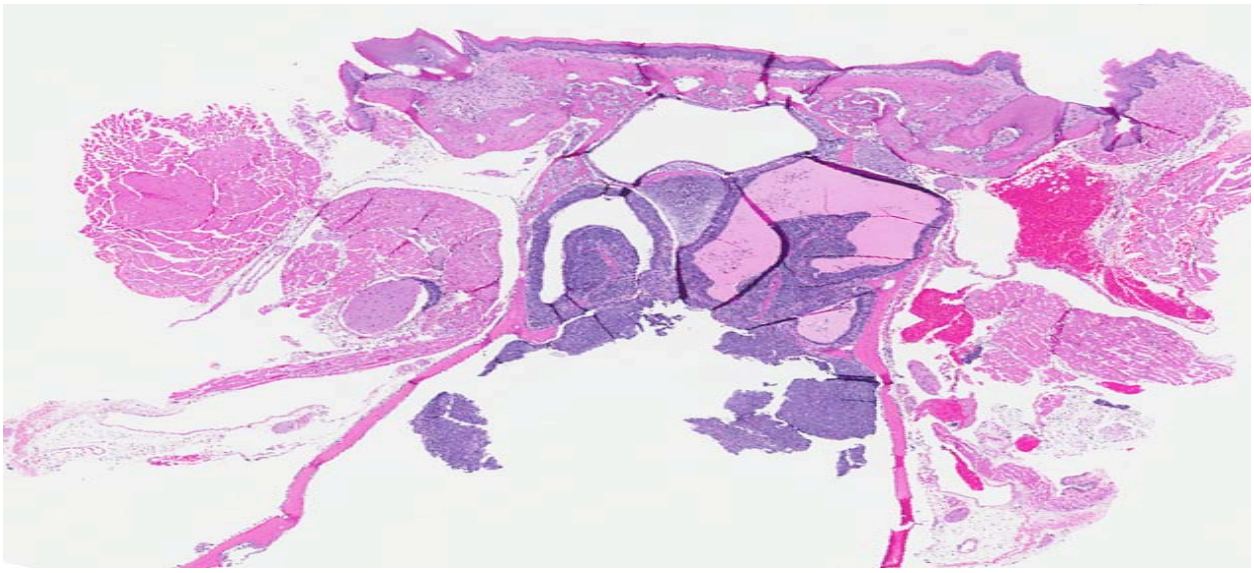

1-1. Nasal cavity, turbinate bones, mouse: Filling the nasal cavity and infiltrating the nasal septum and turbinates is an unencapsulated, densely cellular neoplasm. (HE 4X)

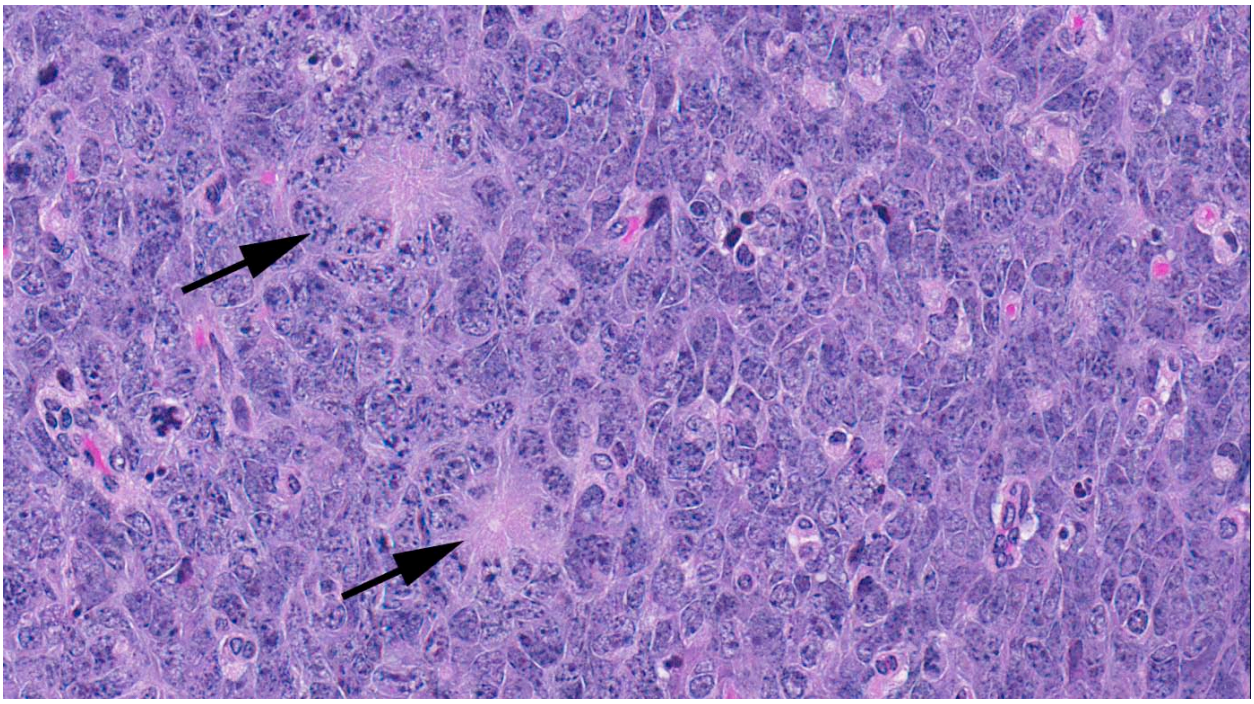

1-2. Nasal cavity, turbinate bones, mouse: Neoplastic cells are polygonal and arranged in nests and packets, with a mitotic rate of up to 8 per 400X field. Multifocally, neoplastic cells are arranged in true rosettes (arrows). (HE 400X)

between Steno's and Bowman's glands along the turbinates and nasal septum. Tumor cells and nests extend through the cribriform plate into the olfactory bulb, across the nasal septum, and into the maxilla and periodontal space. Many tumor cells do not appear to rest upon a basement membrane. In several areas tumor cells appear contiguous with olfactory epithelium and then extend beneath it. There is scant fibrovascular stroma.

Tumor cells are pleomorphic: those in rosettes tend to be elongate to triangular, with a wider base and scant cytoplasm; apical processes are sometimes present. The nuclei are basal, round to ellipsoid, with coarsely clumped chromatin or multiple nucleoli. There is a second population of tumor cells that is smaller and rounder, with very scant cytoplasm and multiple nucleoli; these are most often outside of the rosettes. The mitotic index is high (up to 25 mitotic figures per 0.238 mm^2 high power field).

Adjacent to the main tumor mass, the architecture of many submucosal (Bowman's) glands is disorganized, with loss of cellular polarity and no apparent lumen. In some areas the cells are piled into more than one layer or even extend away from the basement membrane. These cells are enlarged and basophilic, with nuclei containing multiple nucleoli or coarsely clumped chromatin. Although not nearly as common as in the main tumor mass, mitotic figures are not rare in these glands.

Cells in the overlying epithelium range from normal to containing eosinophilic granules, pyknotic nuclei or nuclear remnants, and lacking microvilli. There are intact neutrophils and nuclear remnants within the eosinophilic material (fluid) within the nasal cavities.

Contributor's Morphologic Diagnosis: Neuroepithelial carcinoma (Esthesioneuroblastoma).

Contributor's Comment: The study pathologist received the brain sections before the nasal sections (since the latter required time to decalcify) and made a tentative diagnosis of ependymoma (based upon the rosettes), although the tumor morphology was not a "good fit". On receipt of the nasal sections it became obvious the lesion in the brain was an extension of a nasal esthesioneuroblastoma. This case illustrates the importance of keeping in mind esthesioneuroblastoma (and other tumors of nasal origin) as a differential for large brain tumors that may appear to originate in the rostral brain.

This tumor in the nasal sections is a good example of an esthesioneuroblastoma[1], with occasional true rosettes (Flexner-Wintersteiner rosettes) and more common pseudorosettes (Homer-Wright rosettes). This is an exceedingly rare tumor in mice, as in all mammals[2], and is likely present here in part because the strain is heterozygous for p53 gene knockout. The diagnosis in the brain was made more difficult as there the tumor adopted a solid sheet-type architecture, with

only rare rosettes, a situation apparently typical of esthesioneuroblastomas in animals other than humans.[2]

JPC Diagnosis: Olfactory bulb and nasal turbinates: Esthesioneuroblastoma.

Conference Comment: Esthesioneuroblastomas, or olfactory neuroblastomas (ONB), arise from olfactory neuroepithelium, residual neural crest cells, or local components of the dispersed neuroendocrine system and are most often reported in dogs and cats. The olfactory epithelium contains three cell types, which can be histologically identified in the tumor: basal cells, olfactory neurosensory cells, and supporting sustentacular cells. They arise in the ethmoturbinate region and may penetrate the cribriform plate and infiltrate the cerebral cortex. ONBs may be confused with lymphoma or undifferentiated carcinoma if important diagnostic features such as palisades around blood vessels and rosette or pseudorosette formation are not present. ONBs are positive for synaptophysin, chromogranin, CD56, neuron specific enolase (NSE), neural fibrillary protein (NFP) and S-100 protein.[4]

Ultrastructural features include cytoplasmic membrane-bound dense core neurosecretory granules which contain neurotubules and neurofilaments. Olfactory differentiation with olfactory vesicles and microvilli or apical cilia on apical borders may be seen in Flexner-Wintersteiner rosettes. The fibrillary stroma corresponds to the immature nerve processes, and Schwann-like cells are uncommonly encountered.[4,5]

The differential diagnosis of ONB includes the group of "small round blue cell" malignant neoplasms that can occur in the sinonasal tract, such as sinonasal undifferentiated carcinoma, extranodal NK/T cell lymphoma, rhabdomyosarcoma, Ewing/primitive neuroectodermal tumor (PNET), mucosal melanoma and neuroendocrine carcinomas (NEC).[4] Other tumors considered in the differential diagnosis are paraganglioma, extramedullary plasmacytoma, pituitary adenoma, extracranial meningioma, mesenchymal chondrosarcoma, and granulocytic sarcoma. In cats, feline leukemia virus has been identified in association with olfactory neuroblastoma, but a causal role has not been established.[3]

Contributor: Toxicology Battelle Columbus
505 King Avenue
Columbus, OH 43201
www.battelle.org

References:

1. Maronpot RR. *Pathology of the Mouse*. Vienna. IL: Cache River Press; 1999.
2. Reznik GK, Schuller HM, Stinson SF. Tumors of the nasal cavities. *IARC Sci Publ*. 1994;(111):305-24.
3. Schrenzel MD, Higgins RJ, Hinrichs SH, et al. Type C retroviral expression in spontaneous feline olfactory neuroblastomas. *Acta Neuropathol*. 1990;80(5):547-53.
4. Thompson LD. Olfactory neuroblastoma. *Head Neck Pathol*. 2009;3(3):252-9.
5. Wippold FJ II, Perry A. Neuropathology for the neuroradiologist: rosettes and pseudorosettes. *AJNR Am J Neuroradiol*. 2006;27(3):488-92.

CASE II: 2010 628 (JPC 4003044).

Signalment: 9-year-old, female, intact Kuhl's black-eared marmoset (*Callithrix kuhlii*).

History: Euthanized due to progressive lethargy with weight loss and diarrhea.

Gross Pathology: The animal was in markedly thin body condition at the time of death. The small and large intestines were distended with gas, and the contents were diffusely sparse, pasty and tan to slightly green. The intestinal wall varied segmentally from thin and flaccid to irregularly thickened and corrugated. The mesenteric and colonic lymph nodes were uniformly enlarged.

Contributor's Histopathologic Description: Pancreas: The lobular architecture of the exocrine pancreas is distorted by confluent deposits of mature collagenous connective tissue that separate, infiltrate and accentuate the preexistent lobular architecture and expand the periductal connective tissue stroma. There is diffuse atrophy of the exocrine secretory acini and many of the interlobular ducts are ectatic and contain one or more cross- and oblique sections of spirurid nematodes that measure up to 150 µm in diameter. Intraductular spirurids are characterized by a 10-15 µm thick cuticle with sharp spicules, polymyarian-coelomyarian somatic musculature, prominent lateral cords, each containing an excretory canal. The intestinal tract is composed of cuboidal to columnar uninucleated cells that are often finely vacuolated and exhibit a prominent eosinophilic brush border. Female nematodes have uteri containing thick-shelled, 50 µm x 25 µm, embryonated eggs and males display ductus deferens with intralumenal spermatozoa. Associated with the nematodes are intralumenal aggregates of eosinophils, macrophages and fewer neutrophils. Overall, the pancreatic lobules are composed of small groups of disorganized acini with lightly eosinophilic, vacuolated cytoplasm, abundant intralobular duct profiles and increased exocrine to endocrine tissue ratio (exocrine pancreatic atrophy) as well as low number of lymphocytes and plasma cells. Isolated pancreatic lobules have low to moderate numbers of interstitial and intralumenal neutrophils (not present in all sections).

Arterioles, pancreaticoduodenal ligament: The walls of arterioles are multifocally expanded by irregular plaques of mineralized to hyalinized connective tissue that efface the tunica media, interrupt the elastic lamina, elevate the endothelium and impinge on the vascular lumina (arteriosclerosis).

Duodenum: Multifocally throughout the mucosa, villi are blunted and fused, enterocytes are attenuated and crypts are lined by hyperplastic epithelial cells. Expanding the lamina propria in the villous tips and effacing multiple glands in the submucosa is a lightly eosinophilic, acellular matrix (amyloid) that is mildly infiltrated by low numbers of neutrophils and contains karyorrhectic debris. Moderate numbers of lymphocytes, plasma cells and neutrophils are scattered throughout the muscularis mucosa.

Special stains:
Congo Red: Congophilic, birefringent (green under polarized light) material, consistent with amyloid, was abundant in the tips of duodenal villi and around

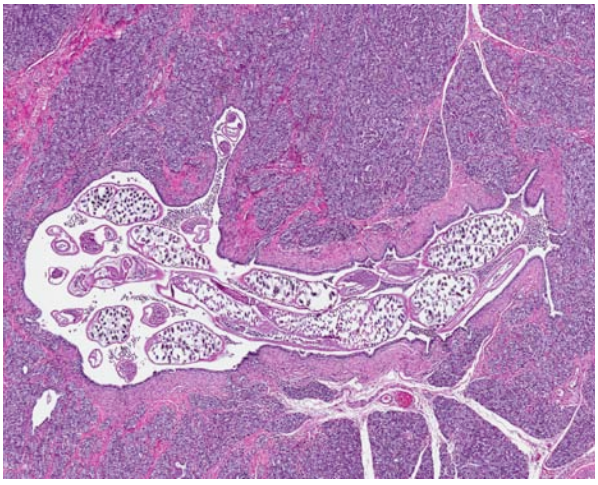

2-1. Pancreas, marmoset: Throughout the section, pancreatic ducts are ectatic and contain cross sections of expanded by the presence of numerous adult spirurid nematodes. (HE 35X)

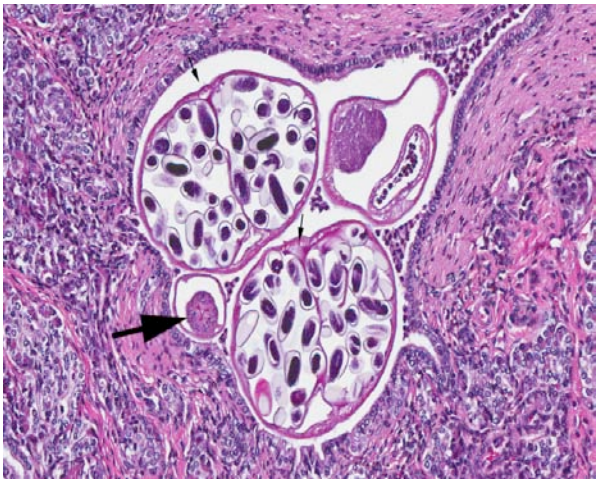

2-2. Pancreas, marmoset: Adult nematodes have a 5µm thick, smooth cuticle, a pseudocoelom, lateral cords (small arrows), a prominent triradiate esophagus (arrow), and numerous larvated eggs within the uterus. The surrounding pancreatic exocrine tissue (representative of the entire pancreas) is diffusely atrophic, characterized by smaller cell size, loss of zymogen granules, and a subjective increase in interlobular fibrous connective tissue. (HE 144X)

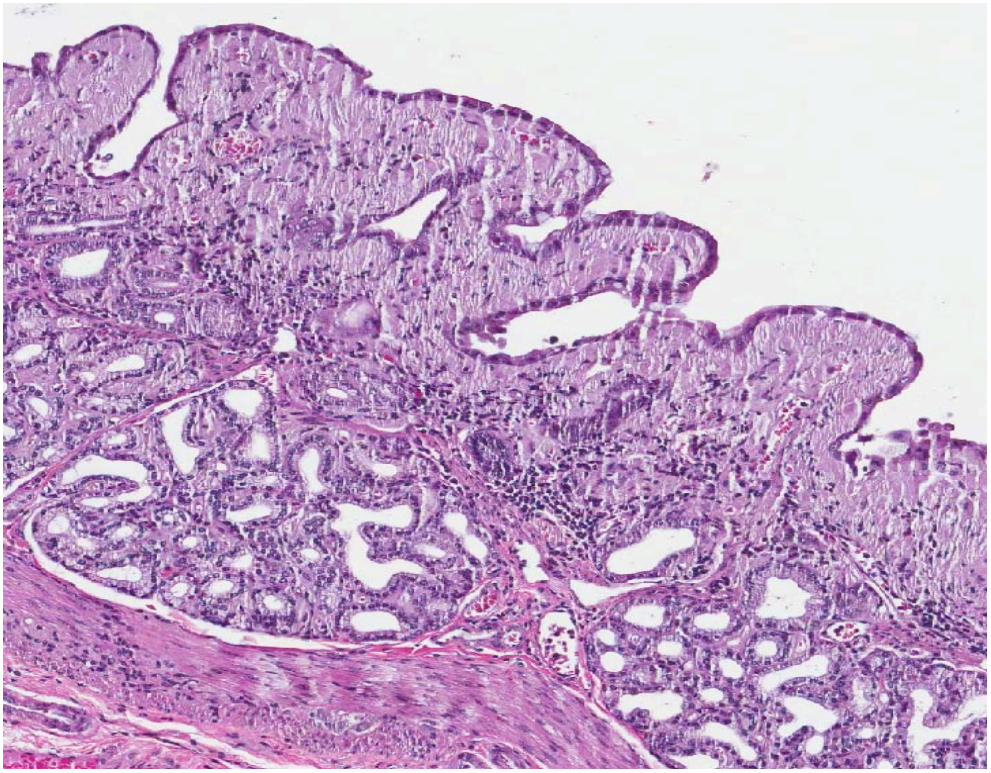

2-3. Duodenum, marmoset: Villi are diffusely blunted and fused, and their lamina propria is effaced by a homogenous amphophilic material (amyloid). (HE 100X)

Brunner's glands. Amyloid deposits were also present in the liver, kidney and spleen.

Contributor's Morphologic Diagnosis: Pancreas:
1) Atrophy, acinar cell, chronic, severe with dissecting and periductular fibrosis, lymphoplasmacytic and eosinophilic infiltrates, ductular ectasia and intralumenal nematodes (morphology consistent with *Spirurid* spp.).
2) Pancreatitis, neutrophilic, subacute, mild (not present in all sections).

Duodenum:
1) Amyloidosis, mucosal and interstitial, multifocal, severe with villous blunting, atrophy and fusion, attenuation of enterocytes, crypt hyperplasia, gland loss.
2) Enteritis, lymphoplasmacytic to neutrophilic, chronic, generalized, mild.

Arterioles (mesenteric, not present in all sections):
Medial arteriosclerosis, hyaline-type, chronic, multifocal, mild with mineralization.

Contributor's Comment: Nematodes in the pancreatic ducts were associated with lobular atrophy, periductular fibrosis and mild inflammation. The nematodes exhibit morphologic features consistent with *Trichospirura leptostoma*, a spirurid that inhabits the pancreatic duct of certain species of calltrichids (members of the New World primate family, *Callitrichidae*) including marmosets, tamarins, squirrel monkeys and owl monkeys.[1] Transmission occurs through ingestion of the intermediate host, the common cockroach. Trichospiruriasis is usually considered asymptomatic in marmosets; however, chronic wasting syndrome and exocrine pancreatic insufficiency have been associated with a heavy parasitic burden.[2] Morphologically, the severity of pancreatic lesions are associated with parasite load and progress from pancreatitis to pancreatic fibrosis with atrophy of exocrine pancreatic tissue and, rarely, to obstructive cholestasis.[1,3]

Unique histomorphological features of *T. leptostoma* include their location in interlobular pancreatic ducts, small cross-sectional diameter, long muscular esophagus, excretory pores in the lateral cords and primitive somatic musculature.[4] Based on the changes in the section presented, trichospiruriasis likely contributed to pancreatic insufficiency and secondary malnutrition.

A complicating disease in this animal that is also exceedingly common in captive calltrichids is chronic inflammatory bowel disease (IBD) characterized by diffuse, mucosal atrophy, lymphoplasmacytic inflammation and areas of mucosal ulceration. Typically, callitrichid IBD is most severe in the colon, but lesions were diffuse in this case and were complicated by intestinal amyloidosis. This condition is presently enigmatic, but multiple contributory factors have been implicated including various bacterial infections (*Helicobacter sp.*, *Campylobacter jejuni*, and enteropathogenic *Escherichia coli*), immune dysfunction, genetic predisposition and stress.[5,6,7,8] Cotton top-tamarins (*Saguinus oedipus*) have been previously used as a primate model of colitis-

associated colonic carcinogenesis because of the high propensity for spontaneous colitis that often progresses to adenocarcinomas in this species.[9]

Chronic systemic inflammation caused by the parasitic infestation and enterocolitis likely induced systemic AA amyloidosis due to elevated levels of the SAA amyloidogenic precursor molecule. In addition to the intestinal tract, amyloidosis was also present in the liver, spleen and kidneys. Ingestion of 'amyloid enhancing factors' and hereditary predisposition have been implicated as contributory to the development of systemic AA amyloidosis in colonies of captive marmosets.[10]

JPC Diagnosis: 1. Pancreas, exocrine tissue: Atrophy, diffuse, severe.
2. Pancreatic ducts: Numerous male and female adult spirurid nematodes with mild intraductal neutrophilic exudates.
3. Duodenum, mucosa: Amyloid, diffuse, moderate with marked villar blunting and fusion.
4. Mesentery, adipose tissue: Atrophy, diffuse, severe.
5. Large muscular artery: Mineralization, medial, mural, multifocal, marked.

Conference Comment: Although marmosets are popular as a laboratory primate species for a number of reasons, in captivity the animals are very susceptible to a not fully understood condition known as wasting marmoset syndrome (WMS). WMS is characterized by failure to thrive and generalized weakness which often progresses to death. Characteristics commonly associated with WMS are poor weight gain, weight loss, muscle atrophy, alopecia, diarrhea, and colitis. Histologic features include thin, atrophic intestinal mucosa and chronic lymphoplasmacytic enteritis usually in the distal jejunum and ileum. Other lesions include ulcerative typhlocolitis and bone fragility due to decreased intestinal vitamin D absorbtion. WMS is perhaps the most important and poorly understood disease syndrome of callitrichids.[14,15,16]

The etiology of WMS is not known; however, malnutrition, alterations in intestinal microflora, parasitic infestations, and malabsorption have been suggested as the possible primary or contributing causes. Conference participants discussed several possible underlying etiologies, such as pancreatic spirurid infestation as in this case; bile duct fibrosis and obstruction by fluke migration; and immune-mediated enteropathic disease due to antibodies to gliadin, a glycoprotein found in wheat and other cereals, which is common in humans with celiac disease. In the moderator's experience, pancreatic trichospirurids are often incidental and associated with no pathologic effects. Conference participants attributed the prominent fibrous connective tissue separating and surrounding exocrine pancreatic lobules as due to pancreatic atrophy from WMS and not fibrosis from the trichospirurids, and the loss of exocrine pancreatic zymogen granules as due to depletion.[14,15,16]

The predominant clinical pathologic alterations in marmosets with WMS include mild macrocytic normochromic anemia, thrombocytosis, hypoproteinemia, hypoalbuminemia, and elevated alkaline phosphatase levels due to colonic inflammation. Most of these changes have been attributed to protein-calorie malnutrition and muscle wasting. Thrombocytosis in these marmosets probably represents a nonspecific response of the bone marrow to the chronic wasting and enteric inflammation. Thrombocytosis is mediated by cytokines released during chronic inflammation, and include thrombopoietin (TPO) and interleukin 6 (IL-6), which is commonly increased in inflammatory conditions.[1]

Contributor: Wildlife Conservation Society
Global Health Program - Pathology and Disease Investigation
2300 Southern Blvd
Bronx, NY 10460
http://www.wcs.org

References:
1. Toft JD. The pathoparasitology of the alimentary tract and pancreas of nonhuman primates: a review. *Vet Pathol*. 1982;19:(Suppl)44-92.
2. Ludlage E, Mansfield K. Clinical care and diseases of the common marmoset (Callithrix jacchus). *Comp Med*. 2003;53:369-382.
3. Hawkins JV, Clapp NK, Carson RL, et al. Diagnosis and treatment of Trichospirura leptostoma infection in common marmosets (Callithrix jacchus). *Contemp Top Lab Anim Sci*. 1997;36:52-55.
4. Smith WN, Chitwood MB. Trichospirura leptostoma gen. et sp. n. (Nematoda: Thelazioidea) from the Pancreatic Ducts of the White-Eared Marmoset Callithrix jacchus. *J Parasitol*. 1967;53:1270-1272.
5. Saunders KE, Shen Z, Dewhirst FE, et al. Novel intestinal Helicobacter species isolated from cotton-top tamarins (Saguinus oedipus) with chronic colitis. J. Clin. Microbiol. 1999;37:146–151.
6. Won YS, Vandamme P, Yoon JH, et al. Helicobacter callitrichis sp. nov., a novel Helicobacter species isolated from the feces of the common marmoset (Callithrix jacchus). *FEMS Microbiol Lett*. 2007;271:239-244.
7. Wood JD, Peck OC, Tefend KS, et al. Evidence that colitis is initiated by environmental stress and sustained by fecal factors in the cotton-top tamarin (Saguinus oedipus). *Dig Dis Sci.* 2000;45:385-93.
8. Mansfield KG, Lin KC, Xia D, et al. Enteropathogenic Escherichia coli and ulcerative

colitis in cotton-top tamarins (Saguinus oedipus). *J Infect Dis*. 2001;184:803–807.
9. Kanneganti M, Mino-Kenudson M, Mizoguchi E. Animal Models of Colitis-Associated Carcinogenesis. *J Biomed and Biotech*. 2011:Article ID 342637.
10. Ludlage E, Murphy CL, Davern SM, et al. Systemic AA Amyloidosis in the Common Marmoset. *Vet Pathol*. 2005;42:117-124.
11. Lewis SM, Hotchkiss CE, Ullrey DE. Nutrition and Nutritional Diseases. In: Wolfe-Coote S, ed. *The Laboratory Primate*. London, UK: Elsevier Academic Press; 2005;195.
12. April M, Keith JC. Cardiovascular and lymphoreticular systems. In: Bennett BT, Abee CR, Henrickson R, eds. *Nonhuman Primates in Biomedical Research: Diseases*. San Diego, CA: Academic Press; 1998;256.
13. Logan AC, Khan KN. Clinical pathologic changes in two marmosets with wasting syndrome. *Tox Pathol*. 1996;24(6):707-9.
14. Gore MA, Brandes F, Kaup FJ, et al. Callitrichid nutrition and food sensitivity. *J Med Primatol*. 2001;30 (3):179-84.
15. Sousa MB, Leão AC, Coutinho JF, et al. Histopathology findings in common marmosets (Callithrix jacchus Linnaeus, 1758) with chronic weight loss associated with bile tract obstruction by infestation with Platynosomum (Loos, 1907). *Primates*. 2008;49(4):283-7.
16. Schroeder C, Osman AA, Roggenbuck D, et al. IgA-gliadin antibodies, IgA-containing circulating immune complexes, and IgA glomerular deposits in wasting marmoset syndrome. *Nephrol Dial Transplant*. 1999;14(8):1875-80.

CASE III: 11-0394 (JPC 4004300).

Signalment: Adult male African green monkey (*Cercopithecus aethiops*).

History: This single-housed nonhuman primate was on a research protocol but had not been exposed to an agent. The monkey had not been eating well for several days. One morning, caretakers noted the monkey had dark tarry feces and respiratory difficulty. Moist rales were auscultated bilaterally. Radiographs were taken and showed a gas-filled stomach and intestines and a cloudy hemithorax. Rule outs were gastric dilatation and intestinal intussusception. The monkey was treated by passing an orogastric tube to relieve the gas and giving IV fluids, furosemide, and enrofloxacin. Barium was also administered via the orogastric tube for further radiographs. The animal was found dead in the cage a couple of hours after treatment began.

Gross Pathology: The monkey was in thin body condition (body condition score of 2/5) with small amounts of subcutaneous and abdominal fat and severe dehydration. There was a self-bite wound on the left lateral aspect of the cranial tongue. The nasal passages were mildly edematous and there was a small amount of clear mucus present. There was focally extensive subcutaneous and muscular bruising over the right cranial skull and mild subcutaneous edema of the ventral neck. The lungs were non-collapsed and consolidated with extensive multifocal to coalescing dark red to pale firm areas and multifocal pleural adhesions to the thoracic wall and the diaphragm. The pericardium was moderately thickened. The liver was diffusely dark and congested with multifocal pitting over all lobes. The gallbladder was markedly distended by clotted blood, fibrin, and bile. The stomach was moderately distended by white fluid (barium) and gas. The upper half of the small intestine contained a moderate amount of barium-stained digesta and the lower half contained a moderate amount of dark green fluid digesta. The cecum contained abundant dark green soft material. The colon was empty except for a small amount of gas. There were no significant gross findings in any of the other organs observed.

Laboratory Results: *Bordetella bronchiseptica* was cultured from the lung.

Contributor's Histopathologic Description: Diffusely affecting the section of lung, bronchi, bronchioles, and alveoli are filled by an exudate composed of abundant fibrin, neutrophils that are often degenerate, hemorrhage, and eosinophilic proteinaceous edema fluid and fewer macrophages. Normal tissue architecture is disrupted and displace by

3-1. Viscera in situ, African green monkey: The lungs fail to collapse (note the rib impressions in dorsal lung fields) and have multifocal areas of consolidation. Photograph courtesy of Comparative Research Pathology Branch, US Army Medical Research Institute of Chemical Defense, http://usamricd.apgea.army.mil.

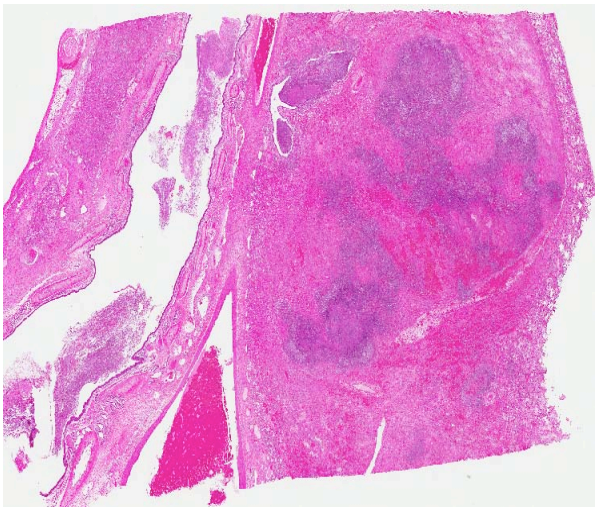

3-2. Lung, African green monkey: 60% of the section, adjacent to a large airway, is effaced by coalescing areas of lytic necrosis. (HE 40X)

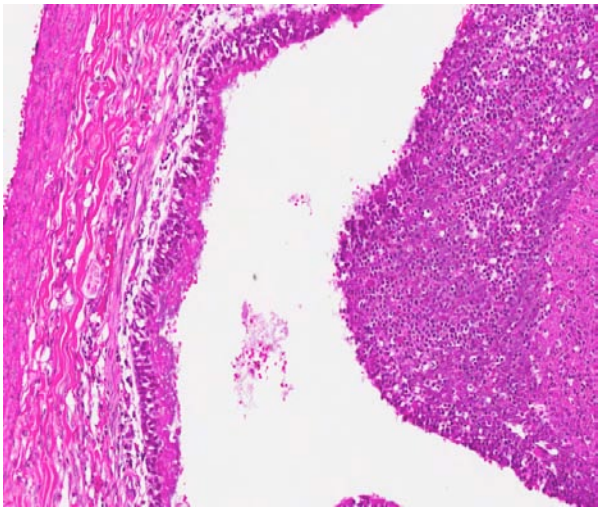

3-3. Lung, African green monkey: Airway lumina are filled by an exudate composed of inflammatory cells, hemorrhage and fibrin. Multifocally, bronchiolar epithelium is mildly hyperplastic, and cilia have a peculiar amphophilic appearance. (HE 100X)

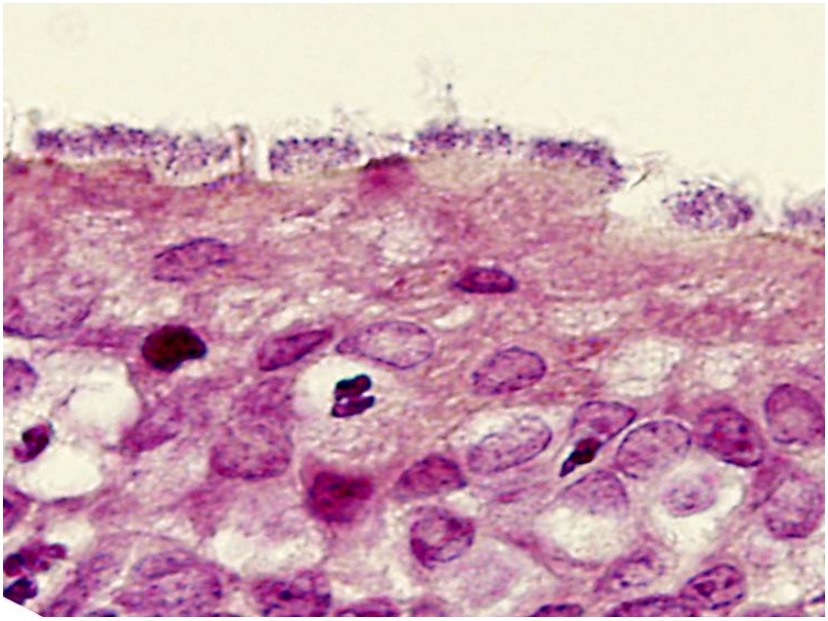

3-4. Lung, African green monkey: Interspersed between the cilia of the bronchiolar epithelium are numerous small, rod-shaped bacteria. (B&H, 1000X) Photograph courtesy of Comparative Research Pathology Branch, US Army Medical Research Institute of Chemical Defense, http://usamricd.apgea.army.mil.

distinct multifocal to coalescing abscesses composed of abundant necrotic debris, degenerate neutrophils, fibrin, and hemorrhage. Multifocally the bronchial and bronchiolar epithelium is hyperplastic. There is multifocal mild to moderate perivascular edema, fibrin, and hemorrhage with occasional neutrophils. The pleura is expanded multifocally by fibrin, hemorrhage, and hyperplastic mesothelial cells. Numerous cilia-associated gram-negative coccobacilli are noted with the Brown-Hopps stain.

Contributor's Morphologic Diagnosis: Lung: Bronchopneumonia, fibrinosuppurative and necrohemorrhagic, diffuse, severe, with fibrinous pleuritis and gram-negative cilia-associated coccobacilli.

Contributor's Comment: Other notable histopathologic findings in this animal included a severe hemorrhagic and fibrinosuppurative cholecystitis, a diffuse moderate subacute periportal hepatitis with bile stasis, a mild acute tracheitis, and numerous cecocolic oxyurids (pinworms) with minimal granulomatous typhlitis and colitis.

Bordetella bronchiseptica is a small gram-negative coccobacillus of the respiratory tract in numerous animal species. Along with other factors, it is the cause of nonprogressive atrophic rhinitis in pigs as well as bronchopneumonia and is considered the primary cause of infectious tracheobronchitis in dogs.[1] It is also considered a major cause of respiratory disease in guinea pigs.[2] *Bordetella bronchiseptica* is an occasional opportunistic respiratory pathogen causing suppurative bronchopneumonias in several other species including rabbits, rats, foals, cats, and sea otters.[1-3] In nonhuman primates, *Bordetella bronchiseptica* has been documented as a cause of pneumonia and upper respiratory infections in prosimians (bushbabies), new world primates

(marmosets and squirrel monkeys), and old world primates (African green monkeys and rhesus macaques).[4-5] Nonhuman primates can be naturally infected with *Bordetella pertussis* and develop whooping cough-like disease also.[5]

Bordetella is transmitted by aerosolization or fomites and the bacteria adhere to the ciliated epithelium of the upper respiratory tract. Interspecies transmission can occur. The bacteria evade the immune defenses via several virulence factors (hemolysin, lipooligosaccharide, and tracheal cytotoxin) and replicate among the cilia. Ciliostasis with decreased mucociliary clearance and host cell death occurs.[1] Bronchopneumonia typically occurs in animals with weakened pulmonary defenses due to age, stress, viruses or other infectious agents, or other predisposing factors.[5] Once the defenses are breached, the bacteria can enter the lung and the inflammatory process begins centered on the bronchioles, then spreads upward into the bronchi and downward into the alveoli. The inflammatory exudate collects in the airways and tends to spread centrifugally and exudate can be coughed up and aspirated into other lobules, continuing the process. The cytokines released from pulmonary injury cause rapid recruitment of neutrophils and alveolar macrophages and cause increased vascular permeability resulting in leakage of edema fluid, fibrin, and sometimes hemorrhage.[6]

Other ruleouts considered at necropsy for the bronchopneumonia in this case included *Streptococcus pneumoniae* or other *Streptococcus* spp, *Klebsiella pneumoniae*, *Mycoplasma* spp, *Pasteurella* spp, and viruses such as influenza, measles, and cytomegalovirus. An interesting finding in this animal was the hemorrhagic and fibrinosuppurative cholecystitis, which is typically associated with gram-negative agents like *Salmonella* or *E. coli*. It is possible the cholecystitis was caused by the *Bordetella* infection but since cultures were not taken of the gallbladder, this cannot be definitively proven.

JPC Diagnosis: Lung: Pneumonia, bronchointerstitial, fibrinosuppurative and necrotizing, diffuse, severe, with hemorrhage and numerous cilia-associated coccobacilli.

Conference Comment: The typical gross appearance of pulmonary bordetellosis in primates is a purulent bronchopneumonia with severe pulmonary consolidation and fibrinopurulent pleuritis and pericarditis. Other reported gross findings include mucopurulent exudate within the nares, nasal passages, trachea and often tympanic bullae; middle ear infection; and meningitis.[5]

As mentioned by the contributor, *Bordetella* spp. have several important virulence factors. Adenylate cyclase toxin, known as hemolysin, is a member of the RTX (repeats in toxin) family of toxins and is secreted by the bacteria. The RTX domain forms ion-permeable pores in host cell membranes and allow the transfer of the adenylate cyclase domain. Increased cAMP production occurs after entry of the toxin into leukocytes, which greatly inhibits phagocytosis and the oxidative burst. Tracheal cytotoxin is secreted by the bacteria and stimulates host cells to secrete nitric oxide which induces ciliostasis and apoptosis of ciliated epithelial cells. Dermonecrotic toxin (DNT) is an intracellular toxin that is vasoconstrictive and cytotoxic and is released upon bacterial lysis; it shares structural and functional homology with cytotoxic necrotizing factor 1 (CNF1) of *E. coli*.

Filamentous Hemagglutinin (FHA), pertactin and fimbriae are adhesive proteins that allow attachment of the bacteria to ciliated epithelial cells. Lipooligosaccharide is a lipopolysaccharide with endotoxin activity found in the bacterial cell wall. The *Bordetella* virulence gene (Bvg) operon regulates the expression of most of these virulence factors.[1,6]

Although *Bordetella* is usually a co-pathogen in pigs, cattle, dogs and cats, it is the primary agent in several important veterinary diseases. *Bordetella bronchiseptica,* as a primary agent, can cause severe pneumonia in guinea pigs.[2] *B. avium* is the primary agent of turkey coryza. *B. avium* can also infect several species of fowl, psittacines, ratites, finches and domestic songbirds, and in cockatiels it has been associated with lockjaw syndrome, which is a respiratory disease with temporomandibular rigidity.[8] *B. hinzii*, a commensal organism in the upper respiratory tract of poultry and an opportunistic pathogen in immunocompromised humans, has been identified as the causative agent of rhinitis, tracheitis, and bronchopneumonia in a rabbit and a B6 mouse.[7]

Contributor: US Army Medical Research Institute of Chemical Defense
Comparative Pathology Branch
Research Support Division
3100 Ricketts Point Rd.
Aberdeen Proving Ground, MD 21010-5400
http://usamricd.apgea.army.mil/

References:

1. Caswell JL, Williams KJ. Respiratory system. In: Maxie MG, ed. *Jubb, Kennedy, and Palmer's Pathology of Domestic Animals*. 5th ed. Vol. 2. New York, NY: Elsevier; 2007:589-590, 632, 638-639, 650.
2. Percy DH, Barthold SW. *Pathology of Laboratory Rodents and Rabbits*. 3rd ed. Ames, IA: Blackwell Publishing; 2007:141-142, 226-228, 267-268.

3. Staveley CM, Register KB, Miller MA, et al. Molecular and antigenic characterization of *Bordetella bronchiseptica* isolated from a wild southern sea otter (*Enhydra lutris nereis*) with severe suppurative bronchopneumonia. *J Vet Diagn Invest*. 2003;15:570-574.
4. Gibson SV. Bacterial and mycotic diseases. In: Bennett BT, Abee CR, Henrickson R, eds. *Nonhuman Primates in Biomedical Research Diseases*. San Diego, CA: Academic Press; 1998:75-76.
5. Osborn KG, Lowenstine LJ. Respiratory diseases. In: Bennett BT, Abee CR, Henrickson R, eds. *Nonhuman Primates in Biomedical Research Diseases*. San Diego, CA: Academic Press; 1998:294-295.
6. López A. Respiratory system, mediastinum, and pleurae. In: McGavin MD, Zachary JF, eds. *Pathologic Basis of Veterinary Disease*. 5th ed. St. Louis, MO: Elsevier; 2012:458-9, 472-3, 480, 499, 520-1, 524-5.
7. Hayashimoto N, Yasuda M, Goto K, et al. Study of a Bordetella hinzii isolate from a laboratory mouse. *Comp Med*. 2008;58(5):440-6.
8. Charlton BR, et al. *Avian Disease Manual*. 6th ed. American Association of Avian Pathologists. 2006:71-3.

CASE IV: CVD 11-4 (JPC 4006049).

Signalment: Eight year-old female baboon (*Papio* sp.).

History: Multiple ulcerated skin lesions were noted on the limbs, tail, and sex skin of an 8 year-old female baboon from the Southwest National Primate Research Center at the Texas Biomedical Research Institute. Impression smears were taken and submitted for cytology. The animal was euthanized following the identification of organisms and evidence of extensive infection.

Gross Pathology: The animal was thin with decreased body fat. Multiple irregular-shaped, slightly raised, firm and frequently ulcerated skin lesions were present on all four limbs, feet, sex skin, and the tail, ranging in size from <0.5 cm to >4 cm. On section the dermis was expanded by pink-tan nodules.

Contributor's Histopathologic Description: Skin: There is a focally extensive area of epidermal ulceration, hemorrhage and in some sections, overlying serocellular crust. The remaining epidermis is mildly to moderately thickened (acanthosis). The dermis is markedly expanded by granulation tissue and coalescing nodular aggregates of mixed inflammatory cells consisting of variable numbers of neutrophils, plump macrophages, multinucleated giant cells and fewer lymphocytes and eosinophils. Within the cytoplasm of many of the macrophages and multinucleated giant cells are numerous round to oval, pale staining organisms (yeast), which are 8-15 microns in diameter, with a clear, refractile, ~1-2 micron-thick cell wall, a 1-2 micron, basophilic nucleus, and rare narrow-based budding, morphologically consistent with *Histoplasma capsulatum* var. *duboisii*. Lymphohistiocytic perivascular cuffs are present at the periphery of the lesion.

Contributor's Morphologic Diagnosis: Haired skin: Dermatitis, granulomatous, nodular, multifocal, moderate, with ulceration, hemorrhage, epidermal hyperplasia, and numerous intrahistiocytic yeasts, baboon (*Papio* sp.), nonhuman primate.

Contributor's Comment: African histoplasmosis is a chronic progressive fungal infection endemic in Western and Central Africa and caused by *Histoplasma capsulatum* var. *duboisii*. Natural infection is rare and has been reported only in baboons and humans. In 1988, the first reported animal case in the United States was diagnosed in an adult red baboon at the Southwest Foundation for Biomedical Research (currently the Texas Biomedical Research Institute) in San Antonio, Texas. Imported from Senegal, this animal was in the United States for approximately 2 years prior to diagnosis.[2] In 1991 this same research institute experienced an epizootic of *H. capsulatum* var. *duboisii* involving over 20 cases in both wild-caught and native-born baboons.[3]

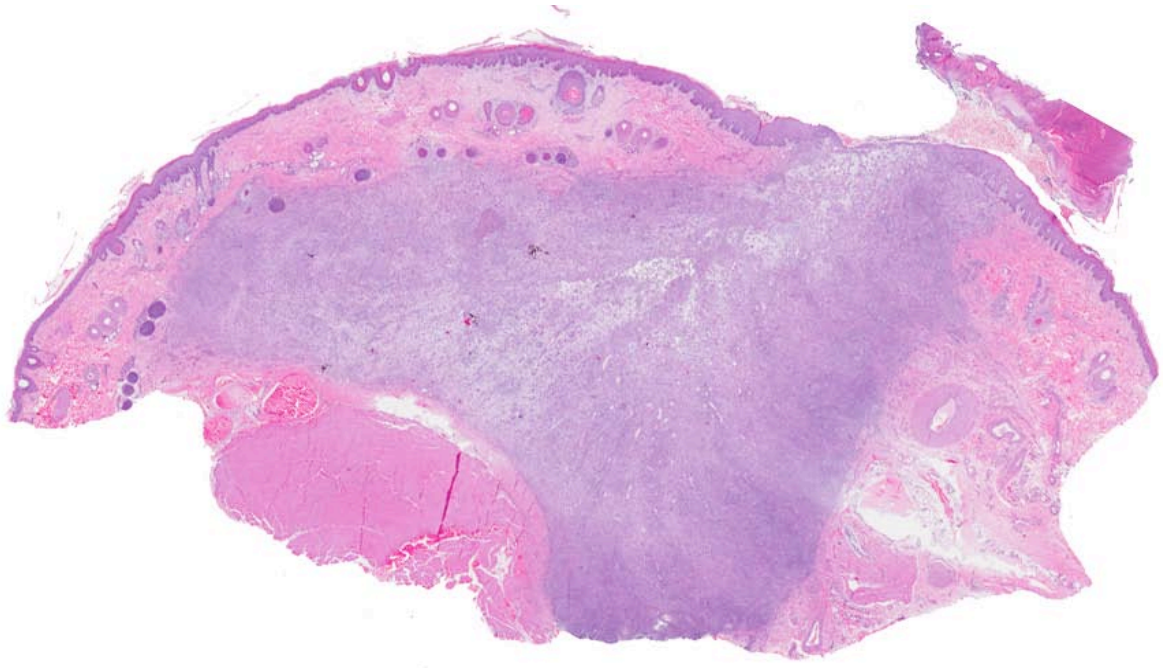

4-1. Glabrous skin, baboon: Within the superficial and deep dermis, there is a well-demarcated area of dense cellular infiltration. (HE 50X)

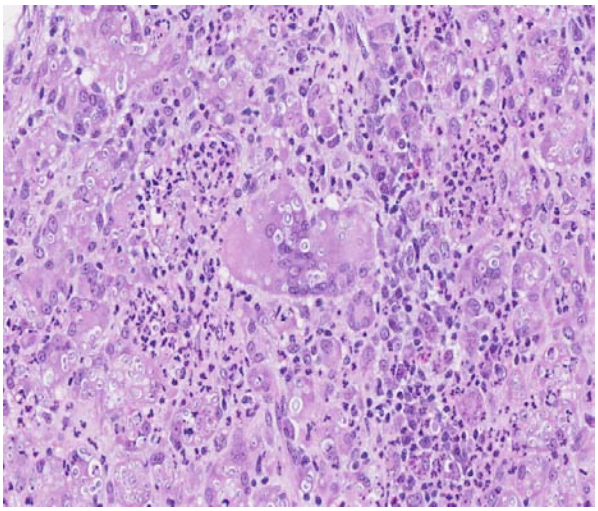

4-2. Glabrous skin, baboon: The cellular infiltrate is composed of numerous epithelioid and multinucleated giant cell macrophages admixed with numerous neutrophils. The macrophages often contain one to multiple 5-8 µm round to oval yeasts. (HE 200X)

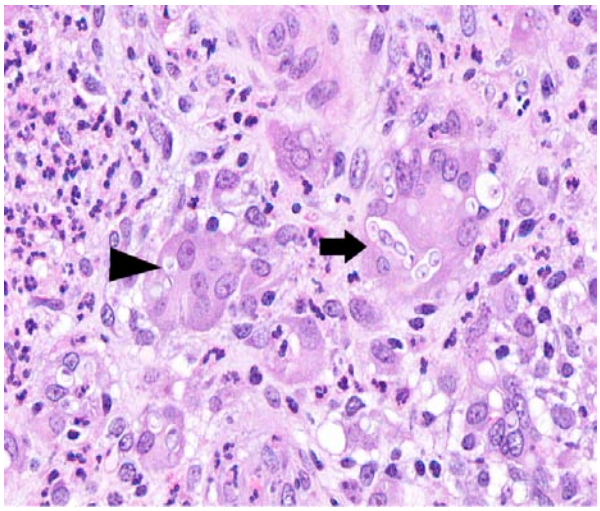

4-3. Poorly-haired skin, baboon: Within macrophages and giant cells, yeasts often form small chains (arrow) and exhibit narrow-based budding (arrowhead). (HE 400X)

Although the ecology and pathogenesis of infection remain unclear, soil is believed to be the natural reservoir of *H. capsulatum* var. *duboisii,* with inhalation, ingestion, and possibly dermal contact the most likely methods of transmission. Inhalation and ingestion of the organism are thought to initially infect the lung or intestinal tract, with subsequent hematogenous spread to the skin, for which the organism appears to have a predilection. Infected animals may remain asymptomatic for a year or more before clinical symptoms become apparent.[3,4]

Grossly, the lesions are typically nodular, ulcerated and/or exudative and commonly found on the face, ears, digits, tail, scrotum and buttocks.[3,4] Draining regional lymph nodes may become enlarged. Osteomyelitis caused by *H. capsulatum* var. *duboisii* has been reported, presumably by extension from skin to subjacent bone. Lesions have also been reported in nasal turbinates and testis.

Although *Histoplasma capsulatum* var. *duboisii*. stains well with Gomori's methenamine silver or Gridley's fungal stains, identification can usually be made from standard histology sections by its unique morphologic appearance which often includes organization in pairs and short chains, combined with the characteristic granulomatous inflammation.[6] The organism can be easily distinguished from the more common *Histoplasma capsulatum* var. *capsulatum* which presents as small oval yeast only 2-4 m in diameter. *Blastomyces dermatitidis* is similar in size and shape to *H. capsulatum* var. *duboisii*, but can be differentiated by its broad-based budding and lack of chain formation. *Cryptococcus neoformans* typically incites much less inflammation in tissues compared with *H. capsulatum* var. *duboisii,* and morphologically the yeast phase is slightly smaller with a thin cell wall and a wide, clear, unstained capsule that stains positive with mucicarmine. The immature or non-endosporulating spherules of *Coccidioides immitis* can be similar in shape but are often slightly larger (5-25 m) than *H. capsulatum* var. *duboisii*; and are accompanied by the presence of larger mature spherules containing endospores.[5,6]

The disease in humans is rare and generally limited to people in or from Africa. Epidemiologic data reveal the organism's predilection for lymph nodes, skin and bone. In humans, pulmonary involvement is more common in HIV-negative individuals while the incidence of disseminated disease is increased in HIV-positive patients.[5] It is unclear what role immunosuppression plays in the risk of infection. The reported incidence of disease remains very low despite the high incidence of HIV infection in endemic regions, and is much lower compared with reports of opportunistic infections with *Histoplasma capsulatum* var. *capsulatum* from the same areas.[5]

JPC Diagnosis: Glaborous skin: Dermatitis, pyogranulomatous, focally extensive, severe, with numerous intracytoplasmic yeasts.

Conference Comment: This is an excellent example of African histoplasmosis in a baboon and the contributor provides a thorough overview of the disease. Conference participants discussed the list of rule outs mentioned by the contributor, as well as *Lacazia loboi* and cutaneous *Paracoccidioides brasiliensis*, which have similar morphology. Lobo's disease has only been reported in humans and dolphins and is characterized morphologically by 10 m in diameter yeast which bud to form chains that resemble

a string of pearls. Cutaneous paracoccidiomycosis is characterized by pyogranulomatous inflammation and multibudding yeast mother cells approximately 60 m in diameter with a 1 m thick refractile cell wall surrounded by 2-10 m spherical daughter cells.[1,4]

Contributor: Covance Laboratories, Inc
Nonclinical Safety Assessment - Pathology - MC 19
3301 Kinsman Blvd
Madison, WI 53704-2523
http://www.covance.com/products/nonclinical/toxicology/risk-assessment/index.php

References:

1. Brummer E, Castaneda E, Restrepo A. Paracoccidioidomycosis: an update. *Clin Microbiol Rev*. 1993;6(2):89-117.

2. Butler TM, Gleiser CA, Bernal JC, et al. Case of disseminated African histoplasmosis in a baboon. *J Med Primatol*. 1988;17(3):153-161.

3. Butler TM, Hubbard GB. An epizootic of *Histoplasma duboisii* (African histoplasmosis) in an American baboon colony. *Lab Anim Sci.* 1991;41(5): 407-410.

4. Durden WN, St Leger J, Stolen M, et al. Lacaziosis in bottlenose dolphins (*Tursiops truncatus*) in the Indian River Lagoon, Florida, USA. *J Wildl Dis.* 2009;45:849-856.

5. Loulergue P, Bastides F, Baudouin V, et al. Literature review and case histories of Histoplasma capsulatum var. duboisii infections in HIV-infected patients. *Emerg Infect Dis*. 2007;13(11):1647-1652.

6. Migaki G, Hubbard GB, Butler TM. *Histoplasma capsulatum* var. *duboisii* infection, baboon. In: Jones TC, Mohr U, Hunt RD, eds. Nonhuman Primates II: Monographs on Pathology of Laboratory Animals. New York, NY: Springer-Verlag; 1993.

Joint Pathology Center
Veterinary Pathology Services

WEDNESDAY SLIDE CONFERENCE 2011-2012

Conference 23

02 May 2012

CASE I: S788/08 (JPC 3102484).

Signalment: 1.2-year-old female common squirrel monkey, *Saimiri sciureus*, New World monkey.

History: The animal showed severe dyspnea, apathy, hypothermia and mucous nasal discharge. In the oral cavity a mucous exudate and multifocal moderate gingival erosions were observed. The animal's condition worsened gradually and it died spontaneously.

Gross Pathology: At necropsy the body was in a moderate nutritional condition. In the oral cavity multifocal gingival ulcerations of 1 to 2 mm in diameter were observed. The lung showed severe congestion, moderate alveolar edema and multifocal hemorrhages of 2 to 4 mm in diameter. The spleen was moderately enlarged. The liver displayed moderate diffuse lipidosis. On the left shoulder (at the level of the supraspinatus muscle) a subcutaneous hemorrhage, 2 x 2 cm, was observed.

Laboratory Results:
Radiological findings: mild multifocal radiodense areas in the thoracic cavity.
Using an antibody against human Herpes simplex virus type 1, a strong positive reaction (Herpes simplex virus infection) was observed in tissue sections of the oral mucosa and liver.
Ultrastructurally, in hepatocytes intranuclear herpesviral nucleocapsids were observed.

Contributor's Histopathologic Description: The liver had a regular architecture. There were irregularly distributed, sublobular foci of coagulation necroses. Hepatocytes adjacent to the necrotic areas displayed cytoplasmic vacuoles of variable size interpreted as fatty degeneration. Furthermore, in some perilesional hepatocytes large eosinophilic intranuclear inclusion bodies causing chromatin margination and clumping were observed. The liver also displayed a mild to moderate, acute congestion.

Contributor's Morphologic Diagnosis: Liver: multifocal moderate acute coagulation necrosis with eosinophilic intranuclear inclusion bodies, and multifocal moderate hepatic lipidosis.

Contributor's Comment: In the submitted liver tissue, the main lesion consists of multifocal coagulation necrosis, and eosinophilic intranuclear inclusion bodies in adjacent hepatocytes.

Upon histological examination of other tissues, a severe multifocal ulcerative to necrotizing gingivitis with hydropic degeneration of epithelial cells, multinucleated giant cells (syncytia), eosinophilic intranuclear inclusion bodies, and a moderate necrotizing vasculitis was observed. The cerebellum showed a moderate subacute multifocal necrotizing inflammation with eosinophilic intranuclear inclusion bodies in neurons. The small intestine displayed a subacute multifocal moderate necrotizing enteritis with multinucleated cells (syncytia) and intranuclear

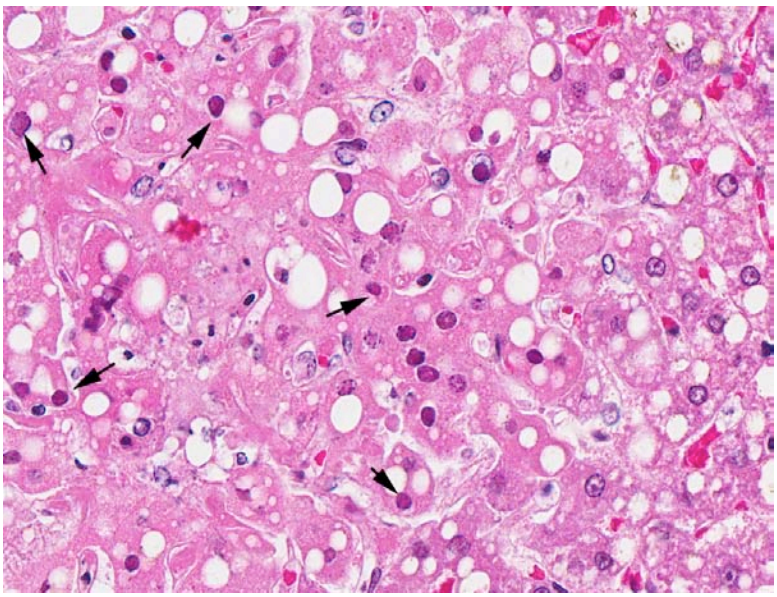

1-1. Liver, squirrel monkey: At the edges of the scattered foci of necrosis, degenerating hepatocytes contain a large magenta intranuclear viral inclusion that peripheralizes the chromatin. (HE 400X)

eosinophilic inclusion bodies in enterocytes. In the spiral ganglion of the ear, numerous eosinophilic intranuclear inclusion bodies were observed. The lymphoid tissues showed a severe lymphocytic depletion. In the nasal cavity a mild subacute diffuse purulent inflammation was present. In the lung, a mild multifocal subacute histiocytic pneumonia, moderate fibrin-rich alveolar edema, severe multifocal hemorrhages and severe congestion were found.
The detection of syncytia and eosinophilic intranuclear inclusion bodies as well as the ultrastructural demonstration of herpesviral nucleocapsids indicates a systemic herpesviral infection. Using immunohistochemistry an infection with human Herpes virus type 1 (HHV-1; Herpes simplex virus 1) was confirmed. Based on the ulcerative to necrotizing lesions, syncytia formation and the detection of eosinophilic intranuclear inclusion bodies in the mouth of the affected animal, an oral route of infection should be considered.

Herpesviruses are a family of large DNA viruses which infect humans, mammals, vertebrates and invertebrates.[1,9] The virions are 200-250 nm in diameter, consist of a linear double-stranded DNA genome of 120-240 kbp packaged in an icosahedral capsid approximately 125 nm in diameter, embedded in a matrix containing many viral proteins, itself wrapped in a lipid membrane containing several glycoproteins.[2,9] The family Herpesviridae is divided in three subfamilies Alpha-, Beta- and Gammaherpesvirinae on the basis of their genomic attributes.[2,9]

Nonhuman primates are primary hosts of a number of alpha- and gammaherpesviruses, whereas some host specific herpesviruses (e.g. Herpesvirus ateles, Herpesvirus saimiri, Rhesus rhadinovirus) were described.[2,8,11] In their natural hosts these viruses cause mild or inapparent infections, but they generally are associated with severe infections when interspecies transmission occurs.[3,4,10] The ability of herpesviruses to cross interspecies barriers is responsible for a major zoonotic risk of these pathogens.[5,8] Hence, the human herpesviruses are transmissible from humans to primates; however, spontaneous infections in monkeys appear to be rare.[5,8] In Old World primates, HHV-1 infections remain localized at the mucocutaneous tissues and the virus-host relationship is comparable to that of humans.[6,8] In contrast, New World monkeys and prosimians are more susceptible to infection and systemic disease.[5] In spontaneously infected owl monkeys, (*Aotus trivirgatus*), tree shrews (*Tupaia glis*), common marmosets (*Callithrix jacchus*), black-tufted-ear marmosets (*Callithrix penicillata*) and lemurs, a severe disease leading to death occurs in most cases.[8] In most mentioned species, erosions and ulcers of the oral mucous membranes and mucocutaneous junction of the lips, and focal necrosis and hemorrhage and eosinophilic intranuclear inclusion bodies were observed.[5,8] The source of the herpesvirus infection in nonhuman primates seems to be, in most cases, the close contact with persons shedding virions.[8] Close contact is also necessary for the transmission of the infection, hence most cases of herpesvirus infections in nonhuman primates occur in animals kept by private persons.[8] Therefore, the use of appropriate protective measures for humans handling nonhuman primates should greatly reduce the risk of infection.

JPC Diagnosis: 1. Liver: Hepatitis, necrotizing, multifocal and random, mild, with hepatocellular intranuclear viral inclusion bodies.
2. Liver, hepatocytes: Lipidosis, micro- and macrovesicular, diffuse, moderate.

Conference Comment: Herpes simplex (*Herpesvirus hominis*) has two distinct subtypes. Herpes simplex type 1 (HSV-1) causes oral lesions and encephalitis in adult humans, and HSV-2 causes genital lesions in adult humans and systemic disease in human infants. Both types produce the same fatal disease in New World monkeys.

Discussion during the conference was focused on developing a plausible differential diagnosis for these lesions in both New and Old World monkeys: Macaqacine herpesvirus (herpesvirus B), which causes fatal encephalomyelitis in man, produces similar lesions as seen in this case of necrotizing hepatitis as well as hemorrhagic necrosis in the lung, brain, and lymphoid organs. *Herpesvirus tamarinus* (herpesvirus T), which is asymptomatically carried by squirrel monkeys, and herpes simplex both cause identical necrotizing lesions in other New World monkeys such as aotus monkeys, marmosets, and tamarins. Virus isolation or immunohistochemical staining is necessary to differentiate them. Simian varicella virus causes similar necrotizing lesions with herpetic viral inclusions and syncitial cells of vesicular rash and encephalitis, pneumonia, and hepatitis in African green monkeys and other Old World monkeys.[7]

Contributor: University of Veterinary Medicine, Hannover
Department of Pathology
Bünteweg 17
D-30559, Hannover
Germany
http://www.tiho-hannover.de/
http://www.tiho-hannover.de/einricht/patho/index.htm

References:

1. Batista FM, Arzul I, Pepin JF, et al. Detection of ostreid herpesvirus 1 DNA by PCR in bivalve molluscs: a critical review. *J. Virol. Methods*. 2007;139 (1):1-11.
2. Davison AJ, Trus BL, Cheng N, et al. A novel class of herpesvirus with bivalve hosts. *J Gen Virol*. 2005;86,41-53.
3. Fickenscher H, Fleckenstein B. Herpesvirus saimiri. *Philos. Trans. R . Soc. Lond. B Biol. Sci*. 2001;356 (1408):545-567.
4. Hall KT, Giles MS, Goodwin DJ, et al. Characterization of the herpesvirus saimiri ORF73 gene product. *J. Gen. Virol*. 2000;81(Pt 11):2653-2658.
5. Juan-Sallés C, Ramos-Vara JA, Prats N, et al. Spontaneous herpes simplex virus infection in common marmosets (Callithrix jacchus). *J. Vet. Diagn. Invest*. 1997;9(3):341-345.
6. Kik MJ, Bos JH, Groen J, et al. Herpes simplex infection in a juvenile orangutan (Pongo pygmaeus pygmaeus). *J. Zoo. Wildl. Med*. 2005;36(1):131-4.
7. Mansfield K, King N. Viral diseases. In: Bennett BT, Abee CR, Henrickson R, eds. *Nonhuman Primates in Biomedical Research, Diseases*. San Diego, CA: Academic Press; 1998:5-12.
8. Mätz-Rensing K, Jentsch KD, Rensing S, et al. Fatal Herpes simplex infection in a group of common marmosets (Callithrix jacchus). *Vet Pathol*. 2003;40(4): 405-411.
9. McGeoch DJ, Dolan A, Ralph AC. Toward a comprehensive phylogeny for mammalian and avian herpesviruses. *J. Virol*. 2000;74(22):10401-1046.
10. Rootman DS, Haruta Y, Hill JM. Reactivation of HSV-1 in primates by transcorneal iontophoresis of adrenergic agents. *Invest Ophthalmol. Vis. Sci*. 1990;31 (3):597-600.
11. Schäfer A, Lengenfelder D, Grillhösl C, et al. The latency-associated nuclear antigen homolog of herpesvirus saimiri inhibits lytic virus replication. *J. Virol*. 2003;77(10):5911-5925.

CASE II: G7740 (JPC 3105937).

Signalment: 2-month-old intact female red-handed tamarin (*Saguinus midas*), nonhuman primate.

History: The animal belonged to a group of tamarins (*Saguinus midas*) on exhibit at a German Zoo. The group was established with one breeding couple. Reproduction has been successful and the female has given birth to 20 children. Out of these, two were born dead and six infants died within the first three month after birth. The group lived in an indoor-outdoor enclosure. The tamarin was one of two offspring of the year 2007. The other offspring was found dead 12 days earlier with similar symptoms. The parents remained clinically healthy. This monkey was euthanized due to a poor prognosis.

Gross Pathology: The tamarin was in a poor body condition. There was little content in stomach and intestinal tract. The great parenchymas were free of macroscopically conspicuous alterations. The brain was hyperemic with scattered foci of malacia.

Contributor's Histopathologic Description: Histopathologic examination revealed granulomas in brain, heart and liver. The granulomas occurred in all parts of the brain and were frequently found adjacent to small blood vessels. They consisted of macrophages, lymphocytes and few granulocytes. Protozoan organisms were found within the granulomas. They occurred free or within pseudocysts. Individual ovoid organisms measured 2.5 x 1.5 µm, pseudocysts were about 60 – 120 mm in diameter and contained numerous individual organisms. The lesions were followed by non-suppurative meningitis. Organisms were demonstrable within the meninges. The morphology of these organisms was consistent with microsporidia. Organisms of this type were also detected in other histologically unchanged organs. Pseudocysts and spores were gram positive and Giemsa positive single organisms in the pseudocysts reacted acid fast.

Immunohistochemistry: *Encephalitozoon cuniculi:* positive, provided by Prof. Pospischil, University Zürich, Switzerland

Immunohistochemistry for Toxoplasma gondii: negative

Contributor's Morphologic Diagnosis: CNS: encephalitis, granulomatous, subacute, multifocal, severe, with myriad intralesional and free laying protozoa, etiology consistent with *Encephalitozoon*

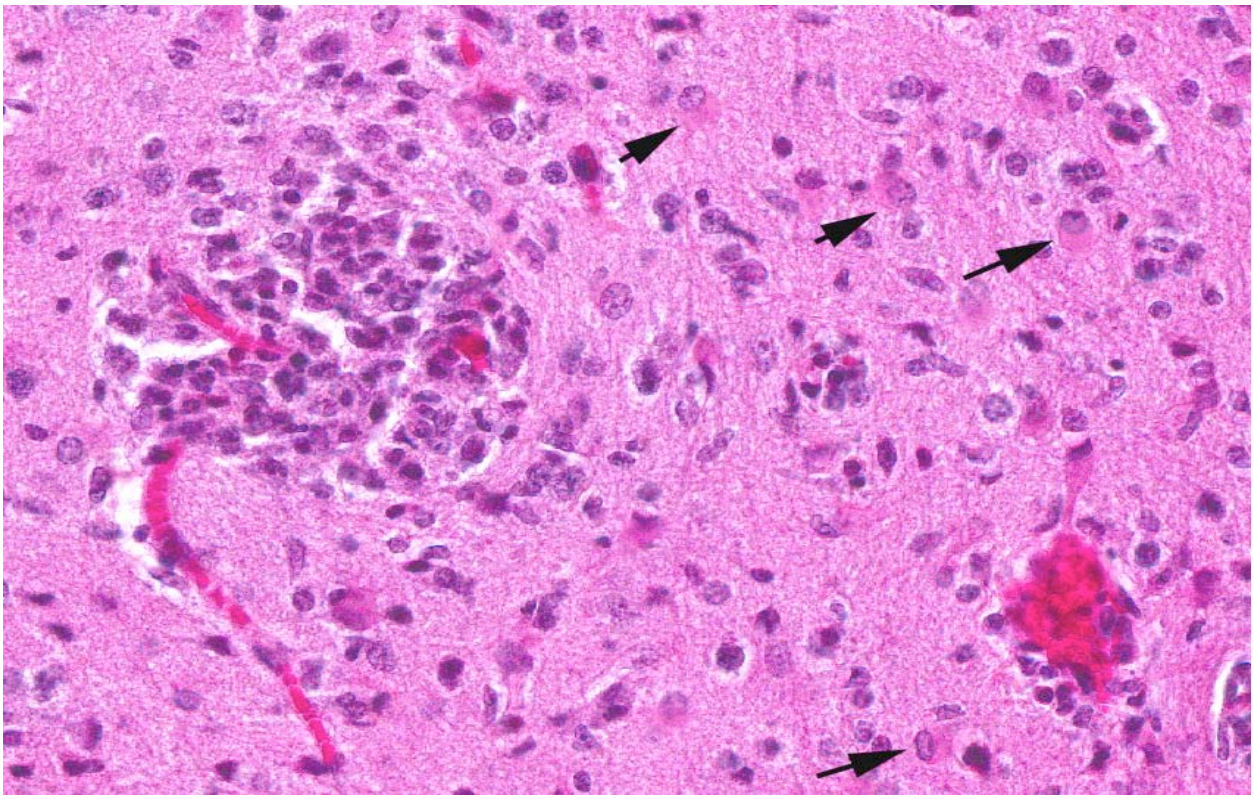

2-1. Cerebrum, tamarin: The gray matter contains numerous foci of necrosis which are filled with moderate numbers of histiocytes, often in perivascular areas. The adjacent neuropil exhibits gliosis, including numerous gemistocytic astrocytes (arrows). (HE 400X)

cuniculi, tamarin (*Saguinus midas*), nonhuman primate.

Contributor's Comment: Encephalitozoonosis is caused by *Encephalitozoon cuniculi*, an obligate intracellular protozoan parasite of the family *Pleistophoridae* and the phylum *Microspora*. *E. cuniculi* is a small oval parasite that measures 2.5 x 1.5 µm. The organism is characterized by a coiled polar filament in the mature spore stage. Ruptured mature spores release the organisms into the surrounding environment and infect other cells. The parasite is able to infect a variety of cell types but there is a predilection for macrophages, cells of the central nervous system and renal tubular epithelium. Spores are passed out with the urine.

Infections may be acquired horizontally or vertically. Infection of mammals most often occurs by ingestion or inhalation of contaminated urine or feces shed by the infected host. Transplacental transmission has also been described.

Microsporidia of the genus *Encephalitozoon* are well recognized pathogens in a wide range of hosts. *E. cuniculi* and other members of the microsporidial parasites have been regaining interest as opportunistic pathogens for individuals with a compromised immune system.

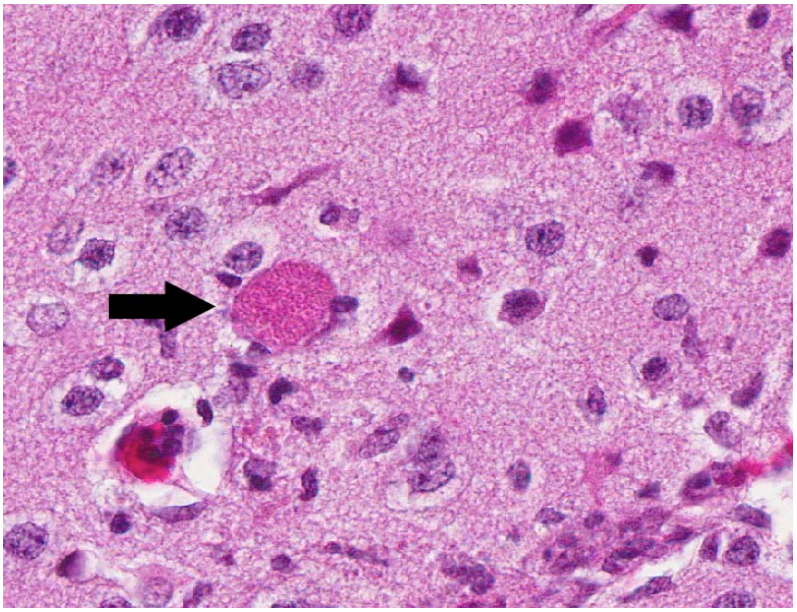

2-2. Cerebrum, tamarin: Throughout the neuropil are large, poorly-staining 60-140 µm pseudocysts containing numerous microsporidians, consistent with Encephalitozoon cuniculi. (HE 400X)

E. cuniculi is known for its widespread occurrence in rabbits and is an important opportunistic pathogen in HIV-infected immunocompromised humans. To date, three different *Encephalitozoon* species are identified. The different strains have different host preferences and were designated according to their main host as 'rabbit strain', 'mouse strain' and 'dog strain'. Furthermore, the three strains differ in their geographic distribution. The rabbit strain has a worldwide distribution, the mouse strain occurs in Europe only, and the dog strain has been identified in America and South Africa only.

Natural *E. cuniculi* infection may occur in nonhuman primates. Most reported cases involved different New World monkey species, mainly infant squirrel monkeys.[1,2,8] Furthermore, *E. cuniculi* was detected in emperor tamarins[3] and cotton top tamarins.[5] Clinically, signs of infected monkeys are usually absent or the animal develops nonspecific clinical disorders prior to death. The occurrence of latent infections is possible. Infections may be associated with stillbirths, abortions and perinatal deaths. *Encephalitozoon* infection in a colony can be diagnosed clinically by serologic investigation.[6]

Diagnosis can be made by finding the parasites and the typical associated lesions during histopathologic examination of the tissue or by demonstrating the agent in the urine. *E. cuniculi* must be differentiated from *Toxoplasma gondii* in histological sections. Staining properties of the organism and the nature of the inflammatory response can help to differentiate it from other infections. *E. cuniculi* stains poorly with hematoxylin and eosin, but stains well with Giemsa, Gram, periodic acid-Schiff (PAS) and Ziehl-Nielson. *Encephalitozoon* is gram-positive and variably acid fast, which is consistent with microsporidia and distinct from protozoa such as *Toxoplasma* or *Neospora*. *Toxoplasma* does not stain with a gram-stain. Furthermore, *Toxoplasma* cysts are smaller than *Encephalitozoon* pseudocysts, and individual *Toxoplasma* organisms are larger and crescent shaped, while *Encephalitozoon* is smaller and ovoid.[2]

Electron microscopy can reveal the presence of the typical parasitophorous vacuoles as well as the distinctive polar filaments. The polar filament may be coiled up to six times around the inner wall of the spore or may be extruded. Immunological or molecular techniques are best suited to distinguish between different protozoan species and strains.

JPC Diagnosis: Brain: Meningoencephalitis, granulomatous, multifocal, marked, with gliosis and numerous microsporidian pseudocysts.

Conference Comment: *Encephalitozoon* exhibits selective parasitism of vascular endothelium, especially in the brain and kidney, as well as renal tubular epithelium. Spores, which are the infective stage, usually obtain entry through the digestive tract, and the sporoplasm, which contains the genetic material, is either released and engulfed by macrophages or injected into endothelial cells through the extruded polar filament. Asexual replication occurs to form numerous proliferative meronts, which differentiate into sporoblasts and then sporonts. A dense spore wall is produced over the plasma membrane, which thickens and allows spore organelles to form. Spores are then packaged within a parasitophorous vacuole, which enlarges and causes host cell rupture. There is release of spores into the extracellular spaces, which then can infect adjacent cells, or enter the vascular system or the renal tubular lumen to be passed in the urine.[4,7]

Typical gross lesions in nonhuman primates include granulomatous meningoencephalitis and vasculitis, nonsuppurative interstitial nephritis and pneumonia, and granulomatous placentitis. A "classic" gross lesion in the rabbit is multifocal irregularly depressed pits in the kidneys with indistinct linear pale gray-white streaks on cut surface. In severe cases, hydrocephalus, thrombosis of meningeal blood vessels, and focal encephalomalacia can occur.[2,4,7] In the dwarf rabbit, which is especially susceptible, *E. cuniculi* has been associated with phacoclastic uveitis and cataract formation, in addition to meningoencephalomyelitis and radiculoneuritis.[4]

In addition to the electron microscopy findings of a parasitophorous vacuole and coiled polar filament mentioned by the contributor, a corrugated proteinaceous electron dense exospore, a chitinous radiolucent endospore, an anchoring disc at the anterior pole, and an electron lucent posterior vacuole are present.[7]

Contributor: German Primate Center
Department of Infectious Pathology
Kellnerweg 4
37077 Göttingen
Germany
http://dpz.eu

References:

1. Asakura T, Nakamura S, Ohta M, et al. Genetically unique microsporidian *Encephalitozoon cuniculi* strain type III isolated from squirrel monkeys. *Parasitol. Intern*. 2006;55:159 -162.
2. Baskin G. *Enzephalitozoon cuniculi* infection, squirrel monkey. In: TC Jones TC, Mohr U, Hunt RD, eds. *Nonhuman Primates II*. 1993;193-196.
3. Guscetti F, Mathis A, Hatt J-M, et al. Overt fatal and chronic subclinical *Encephalitozoon cuniculi* microsporidiosis in a colony of captive emperor tamarins (*Saguinus imperator*). *J. Med. Primatol*. 2003;32:111-119.
4. Percy DH, Barthold SW. Pathology of Laboratory Rodents and Rabbits. 3rd ed. Ames, IA: Blackwell Publishing; 2007;290-4.
5. Reetz J, Wiedemann M, Aue A, et al. Disseminated lethal *Encephalitozon cuniculi* (genotype III) infections in cotton-top tamarins (*Oedipomidas oedipus*) – a case report. *Parasitol. Intern*. 2004;53:29–34.
6. Shadduck JA, Baskin G. Serologic evidence of *Encephalitozoon cuniculi* infection in a colony of squirrel monkeys. *Lab. Anim. Sci*. 1989;39:328–330.
7. Wasson K, Peper RL. Mammalian microsporidiosis. *Vet Pathol.* 2000;37(2):113-28.
8. Zeman DH, Baskin G. Encephalitozoonosis in squirrel monkeys (*Saimiri sciureus*). *Vet Pathol*. 1985;22:24–31.

CASE III: 10A089 (JPC 4002933).

Signalment: 8.74-year-old female Indian Rhesus macaque (*Macaca mulatta),* nonhuman primate.

History: This animal was part of a routine SHIV study, at the end of which it was euthanized for tissue collection. Clinically normal animal, incidental finding at necropsy.

Gross Pathology: A 5.5 X 4.5 X 3 cm, irregularly round, whitish, sessile, expansile, soft mass, with bosselated but smooth external surface and no adhesions to the adjacent structures, is identified on the right ovary. The cut surface is light tan-to-beige, smooth and relatively soft, with a few irregularly-shaped, non-intercommunicating cyst-like structures. The left ovary along with the rest of genital tract is grossly normal. All other organs are within normal limits.

Contributor's Histopathologic Description: Right ovary: About 98% of the ovarian parenchyma is completely effaced and replaced by an unencapsulated, infiltrative, and densely to sparsely cellular neoplasm, compressing preexisting ovarian stroma and pre-antral and antral follicles present in the periphery between the neoplasm and ovarian tunica albuginea , and sparing the oviduct (not present in all slides). Neoplastic cells are arranged in sheets, islands, nests, strands, and cords of round-to-polygonal cells (germ cells) separated by fine fibrovascular stroma, which is expanded in many areas by varied amount of slightly eosinophilic lacy-to-amorphous material (secretory protein/edema). Neoplastic cells have distinct to indistinct cell borders, minimal-to-abundant eosinophilic granular cytoplasm, large round, centrally located, and vesicular nuclei with finely stippled chromatin and a single magenta nucleolus. Multifocally, neoplastic cells surround numerous variably-sized cyst-like spaces that are usually filled with proteinaceous fluid and occasionally contain small amount of lacy material admixed with a few neoplastic cells, lymphocytes, neutrophils and cellular debris and tend to form binucleated-to-multinucleated cells with up to 5 nuclei. Mitotic figures are common (average 3-4 per HPF), some of which are atypical, and there is marked anisocytosis and anisokaryosis. Interspersed among neoplastic cells are multifocal accumulations of lymphocytic infiltrate, clusters of interstitial gland cells with large vacuolated cytoplasm, variably distinct borders, and central-to-eccentric nucleus, scattered single cell necrosis, low numbers of plasma cells and neutrophils, and occasional eosinophils. Variably-sized masses of neoplastic cells are present within lymphatic vessels, and there are focal areas at the periphery of the mass where neoplastic cells tend to breach the adjacent tunica albuginea. Edema and some mineralized foci are also noted.

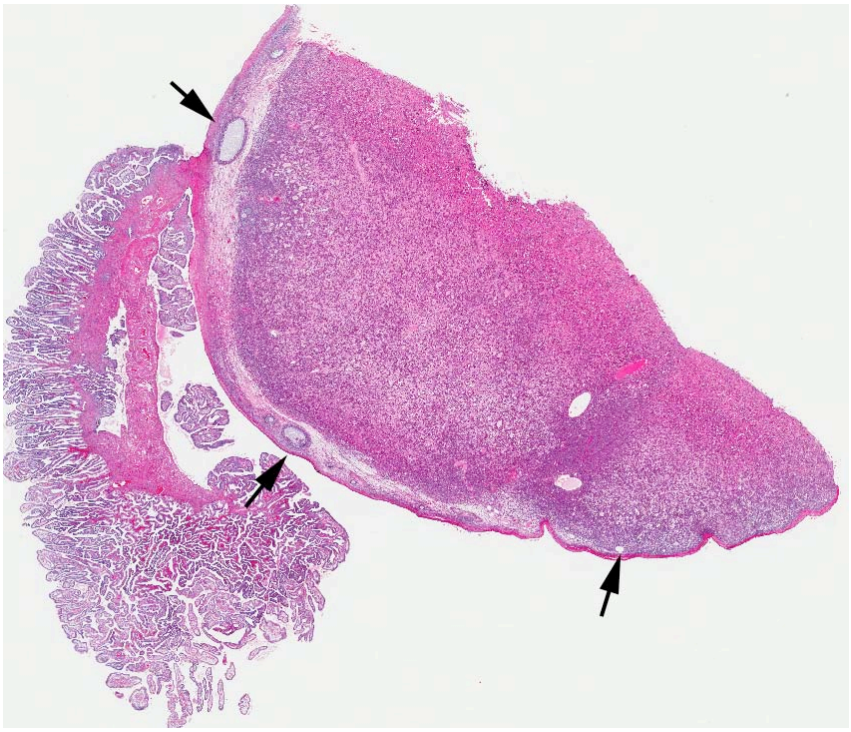

3-1. Ovary and fimbria, rhesus monkey: The majority of the ovary is replaced by an infiltrative neoplasm (dysgerminoma). Several remaining follicles are present at the edge of the ovary (arrows). (HE 4X)

Immunohistochemistry:
- Vimentin, multifocally weakly positive.
- Cytokeratin, negative.
- Alpha-fetoprotein, negative.
- CD3, negative for neoplastic cells; positive for lymphocytic infiltrate.

Contributor's Morphologic Diagnosis: Right ovary: dysgerminoma, rhesus monkey *(Macaca mulatta).*

Contributor's Comment: An incidental finding of unilateral ovarian dysgerminoma in a rhesus monkey *(macaca mulatta)* is examined histologically and immunohistochemically. To our knowledge there is only one documented report of ovarian dysgerminoma in a rhesus monkey.[6] Ovarian dysgerminomas and seminomas, their testicular analogue, are germ cell tumors that arise from primordial germ cells of the ovary

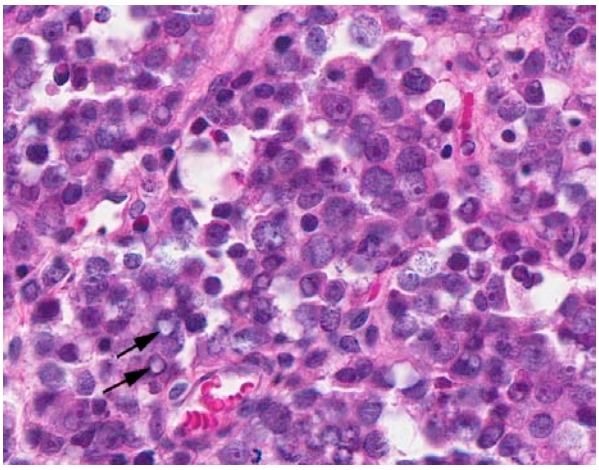

3-2. Ovary, rhesus monkey: The neoplasm is composed of germ cells with large nuclei, prominent nuclei, and often, clear cytoplasmic invaginations into the nucleus (arrows). (HE 400X)

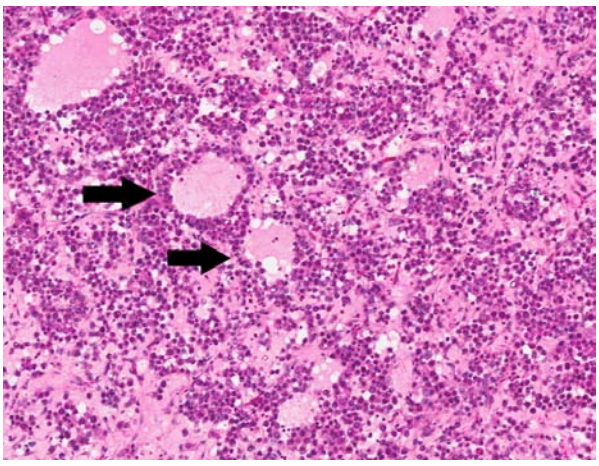

3-3. Ovary, rhesus monkey: Centrally, there is marked edema, apoptosis, and necrosis with dropout (arrows) separate neoplastic cells and cause a bit of diagnostic confusion if only this portion of the slide was viewed. (HE 100X)

and the testis. In female domestic animals, germ cell tumors are limited to germinoma and teratomas, whereas in women and female laboratory animals other ovarian germ cell neoplasms also include: embryonal carcinoma, choriocarcinoma, and endodermal sinus tumor.[7] Although rare, ovarian dysgerminomas are reported in a variety of mammals and non-mammalian species, including humans (girls and women)[9]; non-human primates[6]; domestic animals[7]; and wildlife, avian, amphibian and reptilian species and fishes.[11] Macroscopically, microscopically and immunohistochemically changes observed in this case are basically similar to those previously reported in other mammals and lower vertebrates.[11,4] Grossly, the neoplasm is usually unilateral but may be bilateral, relatively soft, with smooth external surface, and may have cystic structures on cut surface. Histologically, the neoplasm is usually diffusely densely cellular with focal cystic and mineralized areas and high mitotic index, and neoplastic cells are round to polygonal with granular cytoplasm. Interestingly in this case, the neoplasm is relatively less densely cellular but contains abundant amount of extracellular proteinaceous material consistent with accumulation of protein secretion and/or edema. Although not prominent in this case, some neoplastic germ cells express vimentin in perinuclear pattern, but no expression of cytokeratin, alpha-fetoprotein, or CD3 can be detected by immunohistochemistry. On histopathological examination, differential diagnosis should include any round cell neoplasm, especially lymphosarcoma. In general, ovarian dysgerminomas are considered to be nonfunctional in all species; however, they can be hormonally active.[2]

More recently, stem cell markers such as OCT3/4, SOX2, and growth differentiation factor 3 (GDF3) have been reported to be expressed variably in germ cell tumors.[4] Unfortunately, these markers expression could not be investigated in this case. The exact cause of dysgerminomas has not been determined, but more recent molecular studies[3] have implicated loss of function with potential tumor suppressor gene *TRC8/RNF-139* as a possible cause in humans. This would shed some light on the molecular pathways involved in the pathogenesis of this neoplastic condition, which remains to be determined.

JPC Diagnosis: Ovary and oviduct: Dysgerminoma.

Conference Comment: Dysgerminomas are considered potentially malignant, although they metastasize in only 10-20% of cases. Ovarian dysgerminomas are considered to arise from the follicular oocytes or testicular homologues within the ovary, in addition to primordial germ cells. The neoplastic cells share ultrastructural similarity to normal fetal oogonia. These neoplasms typically exhibit cytoplasmic and membranous immunoreactivity for placental alkaline phosphatase (PLAP), which is also positive in other malignant germ cell tumors, and is mainly useful in differentiating it from non-germ cell tumors such as clear cell carcinoma, malignant lymphoma, and granulosa cell tumor. Dysgerminomas also show membrane staining for CD117 (c-kit), which helps to differentiate them from embryonal carcinomas and yolk sac neoplasms. The stem cell-related protein Oct-4 mentioned by the contributor is also positive in embryonal carcinomas, although it is highly sensitive for dysgerminoma. However, podoplanin, which exhibits strong cytoplasmic immunoreactivity for dysgerminoma, can be used to rule out embryonal carcinoma, in which it is negative. The oncofetal glycoprotein alpha-fetoprotein mentioned by the contributor as negative for dysgerminoma is a positive marker for yolk sac

tumors. Many of these immunohistochemical markers are not widely available for veterinary diagnostics; therefore, CD117 may be the most useful and available marker to definitively prove dysgerminoma.[10]

Dysgerminomas have been reported in related maned wolves (*Crysocyon brachyurus*), which may have a genetic predisposition to these neoplasms, as well as in mountain chicken frogs (*Leptodactylus fallax*). In horses, dysgerminoma has been reported as a cause of hypertrophic osteopathy, which is more commonly associated with concurrent thoracic disease.[1,5,8]

Contributor: Tulane National Primate Research Center
Division of Comparative Pathology
18703 Three Rivers Road
Covington, LA 70433-8915

References:

1. Chandra AM, Woodard JC, Merritt AM. Dysgerminoma in an Arabian filly. *Vet Pathol*. 1998;35 (4):308-11.
2. Gelberg HB, McEntee K. Feline Ovarian Neoplasm. *Vet Pathol*. 1985;22:577-576.
3. Gimelli S, Beri S, Drabkin HA, et al. The tumor suppressor gene *TRC8/RNF139* is disrupted by a constitutional balanced translocation (8;22) (q24.13;q11.21) in a young girl with dysgerminoma. *Molecular Cancer*. 2009;8:52.
4. Goplan A, Dhall D, Olgac S, et al. Testicular mixed germ cell tumors: a morphological and immunohistochemical study using stem cell markers, OCT3/4, SOX2 and GDF3, with emphasis on morphologically difficult-to-classify areas. *Modern Pathology.* 2009;22:1066-1074.
5. Fitzgerald SD, Duncan AE, Tabaka C. Ovarian dysgerminomas in two mountain chicken frogs (*Leptodactylus fallax*). *J Zoo Wildlife Med.* 2007;38(1): 150-153.
6. Holmberg CA, Sesline D, Osburn, B. Dysgerminoma in a Rhesus Monkey: Morhologic and Biological Features. *J. Med. Primatol*. 1978;7:53-58.
7. Maclachnan NJ, Kennedy PC. Tumors of the genital systems. In: Meuten D, ed. Tumors in Domestic Animals. 4th ed. Ames, IA; Blackwell Publishing: 2002;547-557.
8. Munson L, Montali RJ. High prevalence of ovarian tumors in maned wolves (*Chrysocyon brachyurus*) at the National Zoological Park. *J Zoo Wildlife Med*. 1991;22(1):125-129.
9. Pectasides D, Pectasides E, Kassanos D. Germ cell tumors of the ovary. *Cancer Treat. Rev*. 2008;34(5): 427-41.
10. Rabban JT, Soslow RA, Zaloudek CZ. Immunohistology of the female genital tract. In: Dabbs DJ, ed. *Diagnostic Immunohistochemistry, Theranostic and Genomic Applications*. 3rd ed. Philadelphia, PA: Saunders-Elsevier; 2010:737-8.
11. Strunk A, Imai DM, Osofsky A, et al. Dysgerminoma in an eastern rosella *(Platycercus eximius exemius)*. *Avian Diseases*. 2011;55:133-138.

CASE IV: 070347-7 (JPC 4006378).

Signalment: Adult male African green monkey (*Chlorocebus aethiops*).

History: These monkeys were part of a study characterizing pathologic changes associated with aerosolized tularemia. Theses monkeys received an average inhaled dose of 729 colony-forming units of *Francisella tularensis (F. tularensis*) and died or were euthanatized between days 7 and 11 postinfection. Clinical changes were evident by 48 hours postinfection, and key physiologic abnormalities included increases in body temperature, heart rate, peak cardiac pressure, and mean blood pressure.[15]

Gross Pathology: Prominent gross changes in all cases included numerous pinpoint to 1-cm, well-demarcated, necrotic foci present consistently in the lungs, mediastinal lymph nodes, and spleen but also seen in the heart, mediastinum, diaphragm, liver, urinary bladder, urethra, and mesentery. The lungs, mediastinal lymph nodes, and spleen were most severely affected, with as much as 50% of the tissue replaced by necrotic foci.

Laboratory Results: Immunohistochemical labeling demonstrated strong *F. tularensis* immunoreactivity in the cytoplasm of multiple cell types but was especially prominent within macrophages of the tonsil; mandibular, mediastinal, mesenteric, axillary, and inguinal lymph nodes; and in alveolar macrophages. Strong *F. tularensis* immunoreactivity was also observed in the following cell types: pleural mesothelial cells; respiratory epithelial cells of the larynx, trachea, bronchi, and bronchioles; epicardial cells; degenerating hepatocytes; reticuloendothelial cells and macrophages in the spleen; glomerular mesangial cells and/or endothelial cells; a variety of cell types in the bone marrow; cortical cells of the adrenal gland; the epithelium of the urinary bladder and urethra; and neutrophils and macrophages infiltrating multiple tissues. In addition, granular or amorphous extracellular antigen was evident in areas of necrosis or pyogranulomatous inflammation in multiple tissues.[15]

Electron microscopy was performed on the lung of one African green monkey (AGM). Organisms were readily identified within membrane-bound vacuoles within the cytoplasm of alveolar macrophages adjacent to the nucleus. The bacteria varied in shape but were generally oval or elongate and measured 0.4 to 0.5 mm in width. Bacteria contained a thin cell wall, a pale central cytoplasm, and a darker rim of cytoplasm near the cell wall. An outer membrane was present in some organisms and appeared as an irregular or wavy membrane loosely surrounding the organism. Many cells containing internal bacilli were seen in various stages of degeneration characterized by swollen irregular mitochondria with faded or absent internal cristae, cytoplasmic vacuoles, enlarged membrane-bound vacuoles with indistinct borders (with or without bacteria), disrupted smooth and rough endoplasmic reticulum, disrupted Golgi apparatus, and disrupted cell membranes. Because severe degeneration and necrosis often hindered recognition of these small bacteria, we used immunoelectron microscopy to distinguish organisms. The identification of *F. tularensis* was made with confidence when the bacterial cell wall contained black

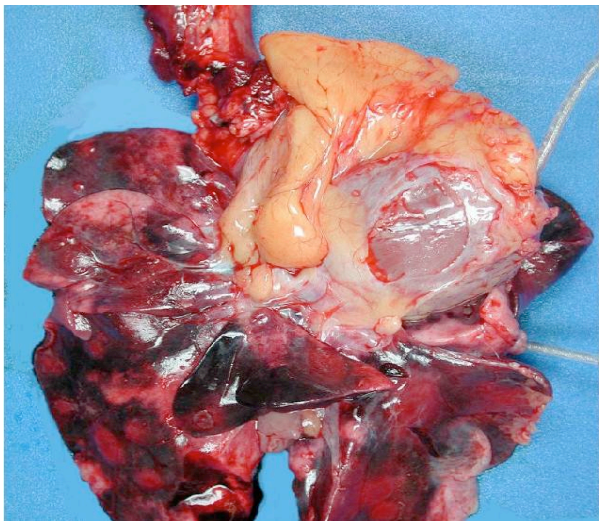

4-1. Lung, African green monkey: Up to fifty percent of the lung is replaced by foci of necrosis and suppuration. (Photo courtesy of the Division of Pathology, United States Army Medical Research Institute of Infectious Diseases (USAMRIID), Frederick, Maryland.)

4-2. Lung, African green monkey: The spleen contains numerous 0.1 to 0.2 cm diameter, raised, white lesions. Splenic borders are rounded, indicating marked congestion. (Photo courtesy of the Division of Pathology, United States Army Medical Research Institute of Infectious Diseases (USAMRIID), Frederick, Maryland.)

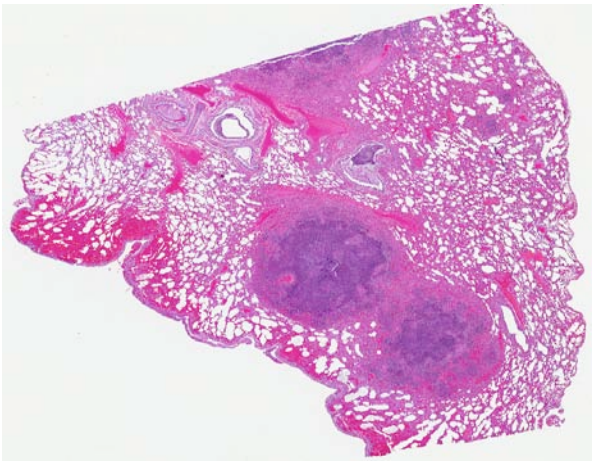

4-3. Lung, African green monkey: Large areas of necrosis efface airways and extend into surrounding tissue. (HE 40X)

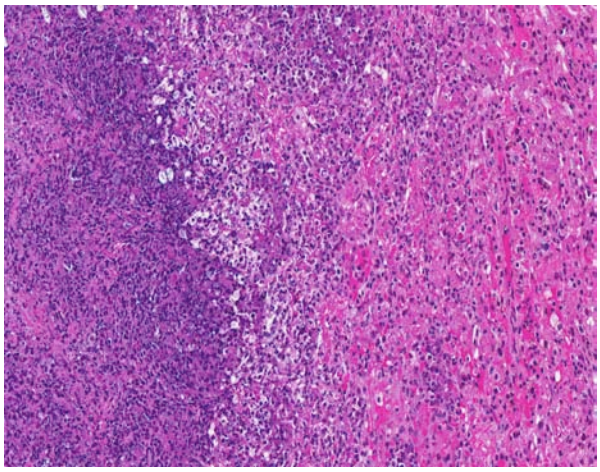

4-4. Lung, African green monkey: Foci of lytic necrosis (left) transition to consolidated pulmonary parenchyma (right). (HE 400X)

grains of gold particles that were evenly distributed over the entire bacterium.[15]

Contributor's Histopathologic Description: Histologic changes in all tissues consisted of well delineated foci of necrosis and neutrophilic and histiocytic inflammation, with varying amounts of hemorrhage, edema, fibrin, and vasculitis. Some lesions were immature pyogranulomas.

Contributor's Morphologic Diagnosis: Lung: Bronchopneumonia, necrotizing, multifocal, marked, with hemorrhage, edema, necrohemorrhagic pleuritis, multifocal necrotizing vasculitis, and rare thrombi.

Contributor's Comment: *Francisella tularensis* is a small pleomorphic gram-negative coccobacillus and is the causative agent of tularemia, also known as "rabbit-fever." Tularemia is a sporadic zoonotic disease in humans, and most cases in the USA are concentrated in south central and western states, primarily in rural areas of Arkansas, Missouri, and Oklahoma.[2] An enzootic life cycle of *F. tularensis* exists among wildlife, particularly involving rabbits, hares, and rodents. Humans may become infected through arthropod bites, through intact skin by handling infected animal carcasses, by ingesting contaminated food or water, or by inhaling contaminated aerosols.[7] *F. tularensis* is a highly virulent bacterium, with as few as 10 organisms constituting an infectious dose, and it can survive for long periods in the environment.[7,12] Most naturally acquired human cases can be successfully treated if it is diagnosed early and the patient is maintained on antibiotics for extended periods.[5]

Tularemia has been placed on the Centers for Disease Control and Prevention list of Class A biothreat agents. In natural cases, pneumonic tularemia is often a consequence of inhalation of bacteria. In a biowarfare or bioterrorism event involving *F. tularensis*, it is very likely that the bacteria would be disseminated via aerosolization, resulting in a high incidence of pneumonic tularemia.[7] Pneumonic tularemia presents some particular challenges relative to other forms (ulceroglandular, glandular, oculoglandular, oropharyngeal, typhoidal, and septic) of the disease. For instance, the antibiotic regimens most applicable for the treatment or postexposure prophylaxis of pneumonic tularemia, especially in a mass casualty event, are not completely certain. Also, vaccines that protect against ingestional or transdermal infection may not protect against high doses of inhaled bacteria.[10] Further, the correlates of immune protection against aerosolized *F. tularensis* have not been established with certainty. Therefore, appropriate animal models of aerosolized tularemia are required to develop the necessary medical countermeasures.[15]

The monkeys in this study exhibited a number of similarities to human tularemia, in particular with regard to the pneumonic form of disease. The key pathologic features of inhalational tularemia in these monkeys were numerous and widespread necrotizing pyogranulomatous lesions that especially targeted the lungs and lymphoid tissues. Bacteria were present in many cell types but were most readily present in alveolar macrophages, as well as macrophages in other tissues. Ultrastructural features included the presence of bacteria within cytoplasmic vacuoles that were located adjacent to the nucleus (*Francisella*-containing vacuoles),[4] as well as degenerative changes in infected cells. In addition, all five AGMs in our study had significant pleuritis associated with the lung lesions, representing another feature in common with the human counterpart, and one also shared by the rhesus macaque model.[7,8] Likewise, our finding that most lesions were characterized by necrosis combined with

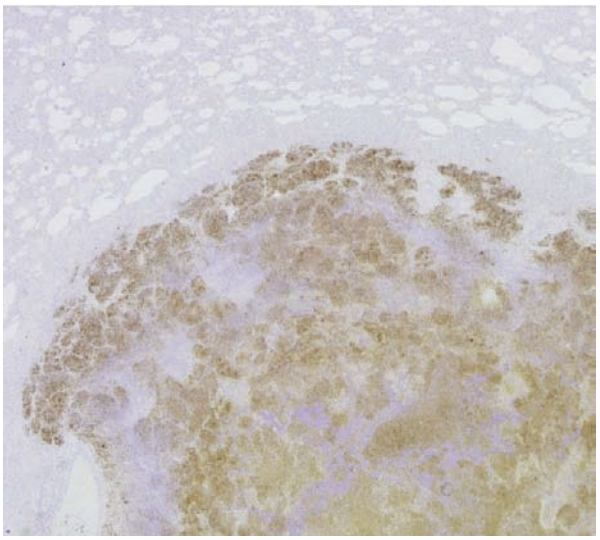

4-5. Lung, African green monkey: Alveolar macrophages and neutrophils exhibit marked immunoreactivity for F. tularensis.

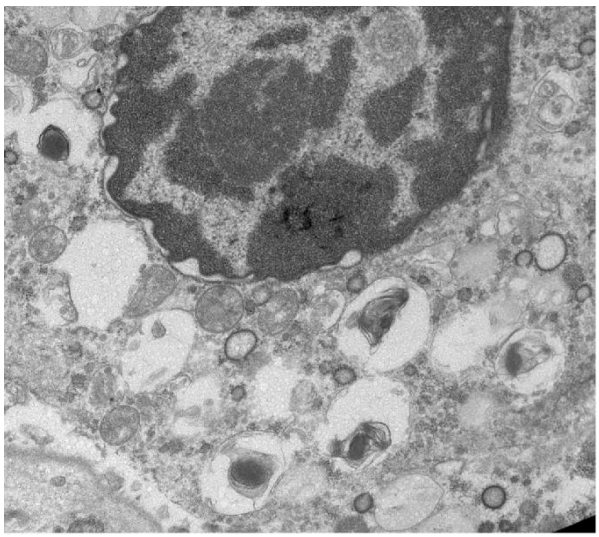

4-6. Lung, African green monkey: Electron micrograph of an alveolar macrophage with several intracytoplasmic vacuoles containing F. tularensis bacteria. The wavy, lamellated cell membranes are characteristic of this bacterium when phagocytosed.

neutrophilic and histiocytic inflammation progressing to form immature pyogranulomas is consistent with histologic findings in most forms of human tularemia, except the typhoidal form.[15]

Two differences between the disease in AGMs and that in humans were noted. We did not observe granulomas associated with epithelioid macrophages and multinucleated giant cells in the target organs of AGMs. It is possible that the monkeys in this study succumbed to disease before such lesions had sufficient time to fully develop. Another exception is that the kidney is a reported target of human tularemia, yet none of our cases displayed gross or histologic changes in the kidney. We did observe, however, that most kidneys had positive immunohistochemistry labeling (for bacterial antigen) within glomerular mesangial and/or endothelial cells. The importance of positive staining in the absence of pathologic changes in the tissue is unclear. One report did describe histologic changes in the renal glomeruli of rhesus macaques.[8] It is uncertain if the renal lesions provide a significant contribution to the pathogenesis in human tularemia in the face of the significant bacterial burden and lesions in the pulmonary and lymphoid systems, as well as other key organs.[15]

Our finding that *F. tularensis* was found in abundance in macrophages in the lungs, lymphoid tissues, and other tissues is a feature of the disease in AGMs with potentially critical significance to understanding the human condition. The ability of *F. tularensis* to infect macrophages, evade the immune system by preventing phagolysosome fusion, and then replicate in these cells is considered a key aspect of its pathogenesis.[3] Infected macrophages also appear to be important in the pathogenesis of tularemia in that they secrete both proinflammatory and anti-inflammatory cytokines,[13] although a full understanding of the host and pathogen factors that operate within infected macrophages is lacking. Nonetheless, the AGM may provide a useful experimental model for investigating the nature of host-pathogen interactions in macrophages, as well as other aspects involved in the pathogenesis of tularemia.[15]

There are limited numbers of documented reports of experimental aerosolized tularemia in rhesus macaques, mostly dating back to the 1960s. These reports describe acute bronchiolitis progressing to bronchopneumonia, lymphadenitis, splenitis, and hepatitis with neutrophilic and histiocytic inflammation with intrahistiocytic bacteria.[6,8,14,17] Such features are similar to those seen in the AGMs of our study. Rhesus macaques have become increasingly expensive and limited in supply in recent years, which limits their usefulness as a model of tularemia. The most recent report of tularemia in nonhuman primates documents an epizootic of tularemia in a group of cynomolgus macaques (*Macaca fascicularis*) that contracted oropharyngeal tularemia by ingesting contaminated food and water. The tularemic lesions were present in the oral mucosa, tongue, lungs, liver, spleen, and lymph nodes consistent with ingestional human tularemia.[11] Therefore, the AGM model of inhalational tularemia we describe appears to share important features of the human condition and thus should provide a useful nonhuman primate model for future research. It is essential to continue to characterize the clinical and pathologic changes that occur in animal models of tularemia, as well as the

molecular mechanisms involved in this disease. Future experimental studies to develop early preventive regimens, early diagnostic procedures (identifying target organs for sampling), and clinical algorithms to optimize treatment efficacy will depend on reliable animal models that consistently mimic human disease. Likewise, relevant animal models will also be necessary to investigate avenues of altering pathogen and host factors, to include novel antibiotic therapies, immunomodulators, or inflammatory inhibitors. In that light, the AGMs reported here displayed consistent gross and histologic lesions after exposure to aerosolized *F. tularensis* with important parallels to human tularemia. This species of nonhuman primate may serve as a suitable and reliable animal model for further studies with *F. tularensis.*[15]

JPC Diagnosis: Lung: Bronchopneumonia, necrosuppurative, multifocal, severe, with fibrinous pleuritis.

Conference Comment: There are three strains that cause tularemia: *Francisella tularensis var tularensis*, the most virulent and commonly isolated form, *F. tularensis var holoarctica*, and *F. tularensis var mediasiatica*. Naturally acquired tularemia is rare in nonhuman primates, although a few recent outbreaks in New World monkeys have been reported in the United States and Europe. Typical gross findings include pyogranulomatous pneumonia and enteritis; necrosuppurative glossitis and gingivitis; and necrotizing splenitis, lymphadenitis, and hepatitis. Tularemia is difficult to differentiate from other causes of gram negative sepsis and often causes lesions indistinguishable from those of *Yersinia pseudotuberculosis*, a top differential diagnosis for this case; however, unlike *F. tularensis, Y. pseudotuberculosis* often forms large botryoid colonies of extracellular coccobacilli.[11,15,16]

Contributor: USAMRIID
Pathology Division
Attn: MCMR-UIP
1425 Porter Street
Fort Detrick, MD 21702

References:

1. Baskerville A, Hambleton P, Dowsett AB. The pathology of untreated and antibiotic-treated experimental tularaemia in monkeys. *Br J Exp Pathol*. 1978;59(6):615–623.
2. Boyce JM. Recent trends in the epidemiology of tularemia in the United States. *J Infect Dis.* 1975;131 (2):197–199.
3. Butchar JP, Rajaram MVS, Ganesan LP, et al. Francisella tularensis induces IL-23 production in human monocytes. *J Immunol.* 2007;178:4445–4454.
4. Checroun C, Wehrly TD, Fischer ER, et al. Autophagy-mediated reentry of *Francisella tularensis* into the endocytic compartment after cytoplasmic replication. *Proc Natl Acad Sci USA.* 2007;103(39): 14578–14583.
5. Cross JT, Penn RL. *Francisella tularensis* (tularemia). In: Mandell GL, Bennett JE, Dolin R, eds. Principles and Practice of Infectious Diseases. 5th ed. Philadelphia, PA: Churchhill Livingstone; 1999:2393–2401
6. Day WC, Berendt RF. Experimental tularemia in *Macaca mulatta*: relationship of aerosol particle size to the infectivity of airborne *Pasterurella tularensis*. *Infect Immun*. 1972;5(1):77–82.
7. Dennis DT, Inglesby TV, Henderson DA, et al. Tularemia as a biological weapon: medical and public health management. *JAMA*. 2001;285(21):2763–2773.
8. Hall WC, Kovatch RM, Schricker RL. Tularaemic pneumonia: pathogenesis of the aerosol-induced disease in monkeys. *J Pathol.* 1973;110:193–201.
9. Hartings JM, Roy CJ. The automated bioaerosol exposure system: preclinical platform development and a respiratory dosimetry application with nonhuman primates. *J Pharmacol Toxicol Methods.* 2004;49:39–55.
10. Hepburn MJ, Friedlander AM, Dembek ZF. Tularemia. In: Textbooks of Military Medicine, Aspects of Biological Warfare. Fort Sam Houston, TX: Borden Institute, Office of the Surgeon General, United States Army Medical Department Center and School; 2007:167-184.
11. Mätz-Rensing K, Floto A, Schrod A, et al. Epizootic of tularemia in an outdoor housed group of cynomolgus monkeys (Macaca fascicularis). *Vet Pathol.* 2007;44(3):327–334.
12. Nayar GP, Crawshaw GJ, Neufeld JL. Tularemia in a group of nonhuman primates. *J Am Vet Med Assoc.* 1979;175(9):962–963.
13. Rajaram MV, Ganesan LP, Parsa KV, et al. Akt/ PKB modulates macrophage inflammatory response to *Francisella* infection and confers a survival advantage in mice. *J Immunol*. 2006;177:6317–6324.
14. Schricker RL, Eigelsbach HT, Mitten JQ, et al. Pathogenesis of tularemia in monkeys aerogenically exposed to *Francisella tularensis* 425. *Infect Immun*. 1972;5(5):734–744.
15. Twenhafel NA, Alves DA, Purcell BK. Pathology of inhalational *Francisella tularnesis* spp. Tularnesis SCHU S4 infection in African green monkeys (*Chlorocebus aethiops*). *Vet Pathol*. 2009;46:698-706.
16. Valli VEO. Hematopoietic system. In: Maxie MG, ed. *Jubb, Kennedy, and Palmer's Pathology of Domestic Animals*. 5th ed. vol 3. Philadelphia, PA: Elsevier; 2007:297-9.
17. White JD, Rooney JR, Prickett PA, et al. Pathogenesis of experimental respiratory tularemia in monkeys. *J Infect Dis.* 1964;114:277–283.

Joint Pathology Center
Veterinary Pathology Services

WEDNESDAY SLIDE CONFERENCE 2011-2012

Conference 24

09 May 2012

CASE I: 0S10400 (JPC 4002913).

Signalment: 12 week-old male (castrated) and female commercial cross (for meat production) pigs, *Sus scrofa domestica.*

History: Porcine reproductive and respiratory syndrome virus (PRRSv) negative herd.
Historical mortality; 2% in the nursery phase of production (3-13 weeks of age).
40% mortality from weeks 9-12 in the nursery with no response to antimicrobial therapy.

Clinical signs included sudden death, seizure like activity, lameness with joint enlargement, and weakness with muscle fasciculations.

Gross Pathology: Swollen joints with increased synovial fluid, swollen chondro-costal junctions, multiple fracture calluses on ribs, rib bones were soft and rubbery and bent 20-30 degrees before breaking.

Laboratory Results: Serum Chemistry

Serum calcium	Result	Units
Pig 1	4.1	mg/dl
Pig 2	4.8	mg/dl
Pig 3	4.9	mg/dl
Pig 4	5.3	mg/dl
Pig 5	4.6	mg/dl
Pig 6	5.9	mg/dl
Pig 7	4.7	mg/dl
Pig 8	5.1	mg/dl
Pig 9	5.9	mg/dl
Pig 10	4.7	mg/dl

Serum Vitamin D
Vitamin D analysis in serum from 10 pigs reveals no detectable (<2.0 ng/ml) amount of 25-hydroxy vitamin D3.

Normal reference range for serum vitamin D	
Age of animal	*25-OH-D3 (ng/ml)*
Neonate	5-15
10 days	8-23
Finishing pigs	30-35
Mature	35-70
At Parturition	35-100

Bone analysis

Identification	Bone Ash	Bone density	Bone Calcium	Bone Phosphorus
Pig 1	0.26	1.29 g/ml	32%	16%
Pig 2	0.33	1.2 g/ml	36%	18%
Pig 3	0.37	1.27 g/ml	38%	18%
Pig 4	0.29	1.08 g/ml	34%	18%
Pig 5	0.33	1.09 g/ml	40%	18%

Swine; rib bone, normal references	
Bone ash	58-62 %
Bone density	1.4-1.5 g/ml.
Bone ash Calcium	32-39%
Bone ash Phosphorus	13-22%

PCRs
Negative for SIV, *Mycoplasma hyopneumoniae*, and PRRS (lung)
Negative for *Erysipelothrix rhusiopathiae*, *Mycoplasma hyorhinis* (joint fluid)

Bacteriology
Lung, liver, spleen, and joint fluid; No significant growth

Contributor's Histopathologic Description: Rib bone, costochondral junction (slide Bd): Physeal cartilage is diffusely thickened and irregular resulting in flaring of the distal metaphysis. Hypertrophic chondrocytes are arranged in poorly organized columns and there are multiple islands of retained cartilage within the metaphysis. Long tongues of cartilage remain within the primary spongiosa that are often surrounded by variably thick seams of unmineralized osteoid which are lined by cuboidal osteoblasts. Chondrocytes within retained cores are variably degenerate and occasionally lost. There is disorganization of primary spongiosa with multifocal fractures and areas of hemorrhage and fibrin accumulation. Osteoclasts are often associated with secondary spongiosa, many of which are present within Howship's lacunae, and marrow spaces are often devoid of marrow elements and contain moderate numbers of mesenchymal cells and variable amounts of fibrous connective tissue. There is multifocal thinning of cortical bone with increased numbers of associated osteoclasts, and the periosteum is variably thickened.

Contributor's Morphologic Diagnosis: Rib bone, costochondral junction: Failure of endochondral ossification with hyperplasia of physeal cartilage and retention of cartilage cores (nutritional osteodystrophy; Rickets).

Contributor's Comment: Metabolic bone disease broadly categorizes disturbances related to bone formation and remodeling. Rickets and osteomalacia are metabolic bone diseases associated with flawed bone mineralization in growing and adult animals, respectively.[5] The pathogenesis is similar for these diseases and is linked to imbalances of phosphorus or vitamin D.[3] In some instances, there are inherited forms of rickets associated with vitamin D metabolism or renal function. However, most reported cases of rickets in production animal medicine are outright diet mixing errors. Swine are particularly sensitive to rickets development because of rapid growth and confined facilities.[5]

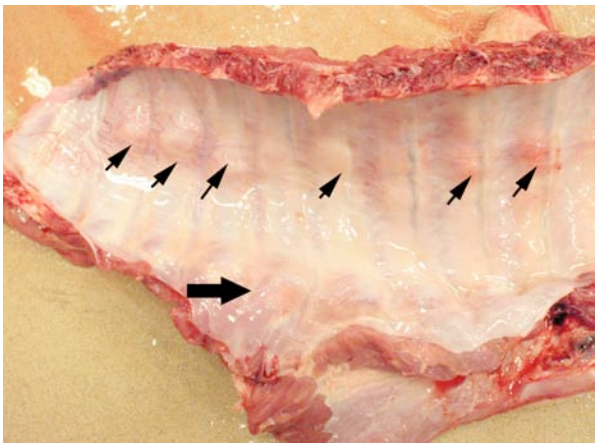

1-1. Pig, ribs: Multiple rib fractures (arrows) as well as an enlarged costochondral junction (large arrow) is present in this 12-week-old pig. Photo courtesy of: The Department of Veterinary Pathology, 2764 Veterinary Medicine, Iowa State University, Ames, Iowa 50011. http://vetmed.iastate.edu/vpath and http://vetmed.iastate.edu/vdpam/

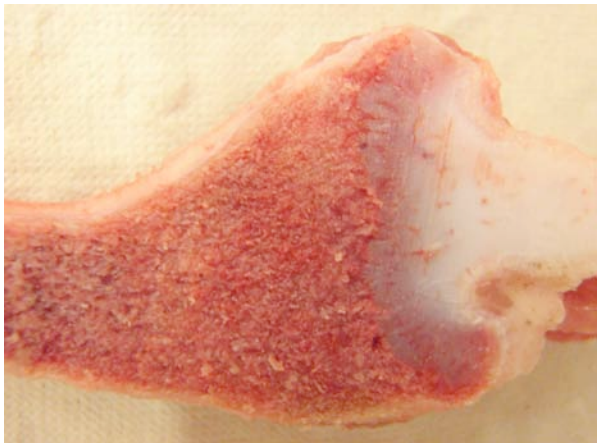

1-2. Pig, rib: Tangential section of the costochondral junction in a 12-week-old pig. The growth plate is expanded and scalloped in an irregular fashion. Photo courtesy of: The Department of Veterinary Pathology, 2764 Veterinary Medicine, Iowa State University, Ames, Iowa 50011. http://vetmed.iastate.edu/vpath and http://vetmed.iastate.edu/vdpam/

Swine rickets has not garnished much attention in the last few decades as most nutritional programs provide adequate phosphorus and vitamin D required for normal bone growth and homeostasis. However, current industry practice for diet composition in market swine is tailored for lean muscle mass growth, not bone formation. Variations in quality or quantity of feed ingredients can cause clinical signs and lesions compatible with rickets. This old and well characterized disease process can be easily overlooked and forgotten. Investigation of recent cases of metabolic bone disease/acute deaths with high

1-3. Pig, rib: Subgross image of the growth plate from the rib in Fig. 1-2. The irregular tongues of cartilage (arrows) are present. The metaphysis is flared, marrow spaces within the metaphysis are filled with collagen rather than marrow, and the cortex is markedly thinned. Artifactual dilation of subphyseal presence is marked. (HE 5X)

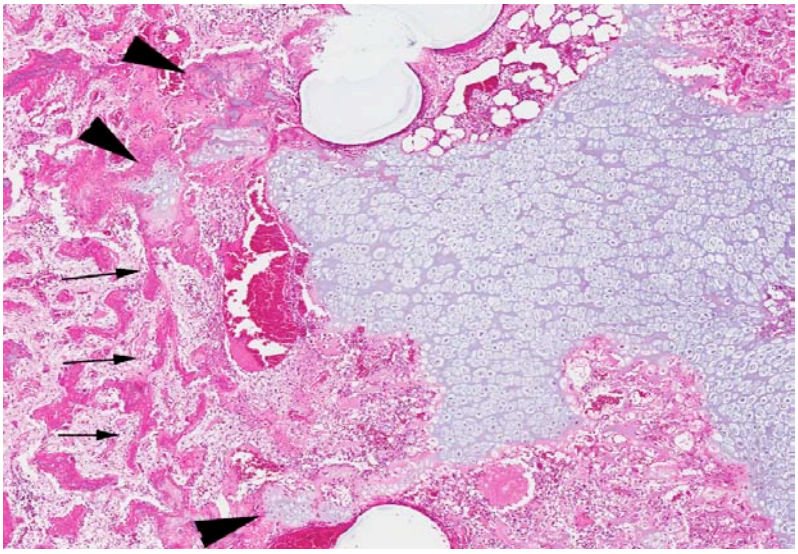

1-4. Pig, rib: Areas of unmineralized cartilage are present within the primary trabeculae (arrowheads). Secondary trabeculae are often oriented parallel to the growth plate (arrows). (HE 34X)

morbidity and mortality presented to the Iowa State University Veterinary Diagnostic Laboratory (VDL) ultimately led to the discovery of a feed with a base mix product inadequate in vitamin D_3 and recall of that product.

Vitamin D can be synthesized in the skin from 7-dehydrocholesterol following ultraviolet light exposure or be supplied in the diet. Dietary supplementation of vitamin D is considered a necessary practice for swine. Following skin conversion or small intestinal absorption, vitamin D is hydroxylated to 25(OH)D in the liver with biologically active vitamin D, 1,25(OH)D, produced thereafter in the kidney. The main activity of 1,25(OH) D is to regulate small intestinal calcium absorption along with lesser phosphorus absorption and inhibit parathyroid hormone.[4]

Lack of calcium absorption results in calcium mobilization from bone to maintain the finely regulated physiologic homeostasis of blood calcium concentration. The result of inadequate deposition or excess mobilization is metabolic bone disease.[3] If bone reserves of calcium are exhausted or delayed in release, hypocalcaemia can result in death.

Growing pigs with classic rickets will have weak bones that bend before they break. Enlarged growth plates can give the appearance of swollen joints.[1] Osteomalacia is usually seen in late finishing or adult swine since this is a condition of increased absorption of previously formed bone. Fractured femurs,

vertebrae, or ribs at load out or at slaughter occur with increased frequency when there is osteomalacia. Lactational osteoporosis has similar features but occurs in lactating or newly-weaned sows. These aforementioned clinical signs are classical for metabolic bone disease. However, there are atypical presentations that can result in sudden death without premonitory signs.[2]

Chronic nutrient imbalances can have acute clinical manifestations other than pathologic fractures or rubbery or weak bones. Somewhat more unusual is the rather abrupt onset of clinical signs associated with acute hypocalcemia. In clinical observations from recent cases, growing pigs unexpectedly develop one or more of the following clinical signs: tremors, tetany, seizure-like muscle fasciculations, weakness, lameness, painful gait with reluctancy to move, and bone fractures (macroscopic and/or microscopic). Often, the first clinical sign observed in affected animals in our cases was acute death. In a large population of pigs, many of these clinical signs may occur simultaneously.

Most common mechanisms of rickets in growing pigs are: inadequate dietary supplementation of vitamin D_3; inadequate absorption of phosphorus due to low phosphorus in diet, phosphorus unavailable as phytate, or inadequate phytase usage;imbalance of feed calcium to phosphorus ratio; and improper formulation of Ca:P ratio in diet (should be roughly 1.2:1).[2]

JPC Diagnosis: 1. Rib bone: Physeal chondrodystrophy with delayed endochondral ossification.
2. Rib bone: Fibrous osteodystrophy.
3. Rib bone: Cortical osteopenia.

Conference Comment: It is common for rickets to present with focally thickened physeal cartilage, as in this case, which represents pockets of disorganized retained hypertrophied chondrocytes within areas of normal endochondral ossification. This represents a timeline of variations of adequate and inadequate dietary vitamin D, and can look similar to osteochondrosis; however, rickets also presents with trabecular disruption, hemorrhage, and infractions.[1,5]

The moderator discussed the fact that in rickets, the physeal cartilage is not hyperplastic, indicating proliferation of chondrocytes, but rather a failure of resorption of normal chondrocytes, and they are thus considered retained. For this reason conference participants preferred the term of physeal chondrodystrophy. This presents as a failure of orderly maturation of physeal chondrocytes, disorganization of columns of chondrocytes, irregular retention of hypertrophied chondrocytes, rare mineralized

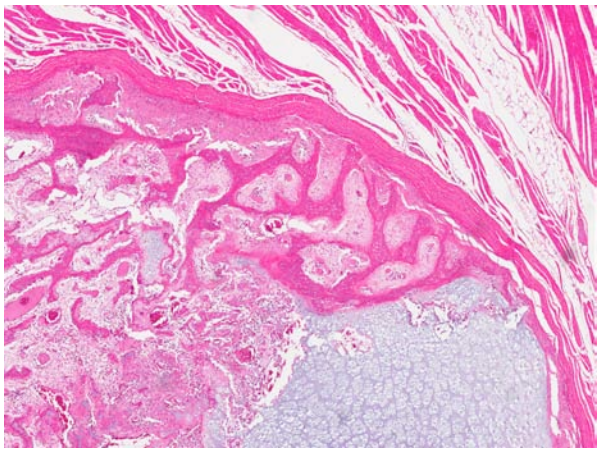

1-5. Pig, rib: The metaphyseal cortex is very thin (osteopenic) and bolstered by trabeculae of woven bone. (HE 34X)

longitudinal septa formation, disorganized and thickened primary and secondary trabeculae without normal mineralized longitudinal septa, and secondary and tertiary trabeculae lined by hypertrophied osteoblasts and many osteoclasts forming Howships lacunae. In mammals, failure of endochondral ossification occurs because blood vessels can only penetrate into the physis when there is apoptosis of chondrocytes and mineralization of the longitudinal septa, which does not occur properly due to decreased available serum ionized calcium.[1]

The presence of a flared metaphysis with course spicules of chondro-osseous tissue and fibrosis in the perichondrial groove and cutback zone is due to the presence of unmineralized bone matrix that cannot be bound by osteoclasts, which are only able to bind and resorb mineralized bone. This is the reason for the presence of prominent thickening along costal-chondral junctions, colloquially known as rachitic rosary.[1,5]

The cortex is composed mostly of woven bone with increased cortical porosity, and the cortical osteopenia is due to increased cortical lysis as a result of the attempt at calcium resorption. In the diaphysis, the marrow fibrosis and increased osteoclasts is mostly intracortical and endocortical, but there is some classic peritrabecular fibrous connective tissue. Conference participants interpreted this as fibrous osteodystrophy (FOD). FOD occurs along with rickets due to hypocalcemia from decreased resorption from bone and absorption from the intestines and resultant secondary hyperparathyroidism. In the early stages of FOD, fibrous proliferation can be subtle and the fibrous connective tissue begins and is oriented around bone spicules. This is in contrast to myelofibrosis, where fibrous connective tissue is oriented toward the middle of the marrow cavities.[1,5]

In addition to decreased dietary phosphorus or vitamin D, rickets in young animals or osteomalacia in adults can be the result of chronic fluorosis. It is also theoretically possible to be caused by low dietary calcium with normal dietary vitamin D.

Contributor: Iowa State University
Department of Veterinary Pathology
2764 Veterinary Medicine
Ames, Iowa 50011
http://vetmed.iastate.edu/vpath
http://vetmed.iastate.edu/vdpam/

References:

1. Carlson CS, Weisbrode SE. Bones, joints, tendons, and ligaments. In: McGavin MD, Zachary JF, eds. *Pathologic Basis of Veterinary Disease*. 5th ed. St. Louis, MO: Mosby; 2011:926-7, 948-50.
2. Crenshaw TD. Calcium, phosphorus, vitamin D and vitamin K. In: Lewis AJ, Southern LL, eds. *Swine Nutrition*. 2nd ed. Boca Raton, FL: CRC Press LLC; 2001:187-212.
3. Dittmer KE, Thompson KG. Vitamin D metabolism and rickets in domestic animals: a review. *Vet Pathol.* 2011;48:389-407.
4. Moe SM. Disorders involving calcium, phosphorus, and magnesium. *Prim Care*. 2008;35:215-2vi.
5. Thompson K. Bones and joints. In: Maxie MG, ed. *Jubb, Kennedy and Palmer's Pathology of Domestic Animals.* 5th ed. Vol 1. New York, NY: Elsevier Saunders; 2007:75-80.

CASE II: 10-1124 (JPC 4006473).

Signalment: 6-month-old intact female Yorkshire sow (*Sus scrofa domesticus*).

History: This case was part of a traumatic bone injury study involving a comminuted fracture of the femoral shaft with stabilization via surgical pinning. This particular animal developed a suppurative infection along the pins, but was maintained until the end of the study.

Gross Pathology: The mid femur was markedly swollen with a dense fibrous capsule surrounding the fractured bone, sequestrate and woven bone. Multifocal abscesses were noted tracking along the surgical pins.

Laboratory Results: *Staphlococcus aureus* was cultured from the open pin lesions; however, no bacteria was visualized in the submitted tissue samples.

Contributor's Histopathologic Description: Bone, femur (per contributor): Focally extensive, pre-existing cortical bone is discontinuous (fractured) and thinned with scalloped edges, and replaced by irregular trabeculae of woven bone in varying degrees of maturation. Multifocally, woven bone is contiguous with the remodeled cortical bone and intertwined trabeculae are perpendicular to the cortical bone (reactive bone). Both cortical bone and woven bone are frequently surrounded and bounded by disorganized islands of cartilage undergoing endochondral ossification (callus) composed of tightly packed chondrocytes in a basophilic matrix as well as densely packed fibroblasts and collagen fibers which diffusely fill and obscure the marrow cavities (myelophthisis). Diffusely, bone trabeculae are lined by plump reactive osteoblasts which are frequently in close apposition to the bone or in regions which are scalloped and discontinuous, and frequent multinucleated osteoclasts rest in resorption bays (Howship's lacunae). Multifocally deep to the reactive bone is a swath of loose fibrosis admixed with myriad neutrophils, fewer macrophages and lymphocytes, high numbers of plump reactive fibroblasts, eosinophilic cellular and karyorrhectic debris (necrosis), eosinophilic proteinaceous material (edema), fibrin, hemorrhage and moderate numbers of small caliber vessels with reactive endothelium (granulation tissue). Multifocally within this area there are frequent multinucleated osteoclasts which are either free or surround fragments of osteolysis. These are also often centered on sequestrae characterized by sharp angulated fragments of necrotic bone with empty lacunae. The larger sequestrae are surrounded by the previously described granulation tissue (involucrum).

Contributor's Morphologic Diagnosis: Bone, femur (per contributor): Osteomyelitis, necrotizing, neutrophilic, focally extensive, marked with cortical fracture, reactive bone, callus formation, myelophthisis and sequestrae, Yorkshire sow, *Sus scrofa domesticus.*

Contributor's Comment: Cases of acute osteomyelitis are most frequently associated with aerobic bacteria such as *Staphylococcus* sp. and *Streptococcus* sp. resulting from hematogenous spread

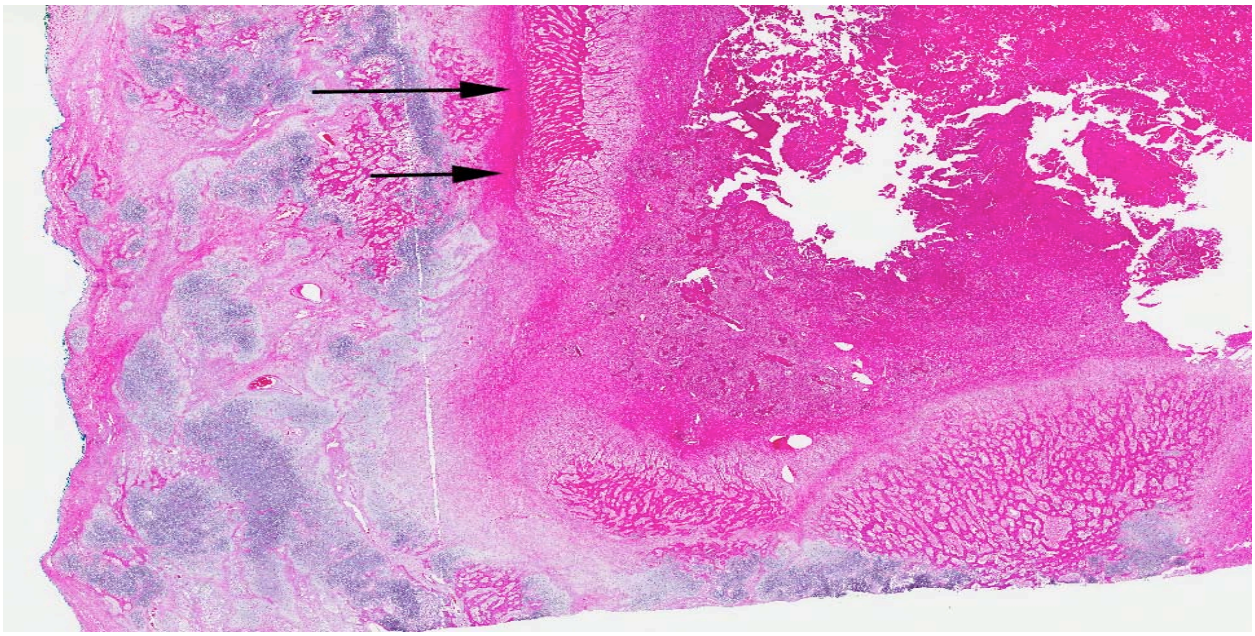

2-1. Pig, long bone: Subgross of callus formation following fracture. Numerous islands of chondroid metaplasia are present in the section. A fragment of osteopenic cortex is present (arrows) with marked periosteal and endosteal new bone growth. (HE 4X)

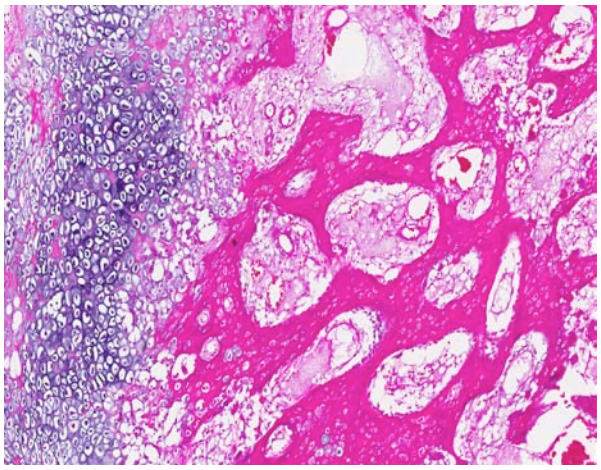

2-2. Pig, long bone: Scattered throughout the section, contiguous with trabeculae of woven bone at right (note the numerous haphazardly arranged lacunae characteristic of woven bone), are foci of chondroid metaplasia (left). Chondrocytes in these foci are also very numerous and haphazardly arranged. (HE 150X)

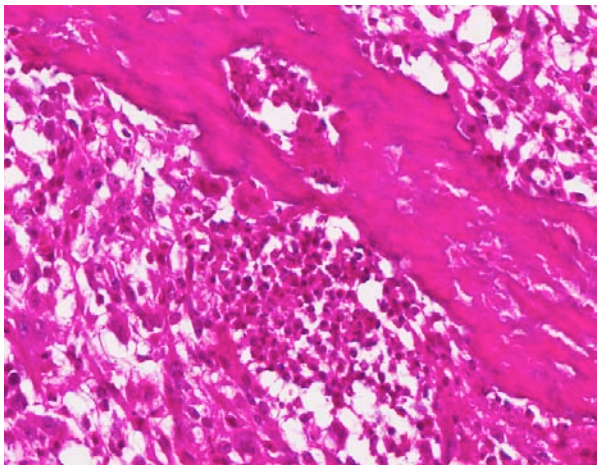

2-3. Pig, long bone: Fragments of necrotic, pre-existent lamellar trabecular bone are surrounded by numerous viable and degenerate neutrophils. (HE 340X)

in younger animals in which the physis is still open, or resulting from sepsis secondary to omphalitis. The veterinary literature describes less pathogenic agents such as *Fusobacterium necrophorum* or coliforms which can be opportunistic infections causing acute osteomyelitis.

In pigs, *Actinomyces pyogenes* is frequently isolated from osteomyelitic lesions as well as in cattle and sheep, while *Salmonella* sp. are commonly isolated from foals.

Additionally, anaerobic bacteria, such as *Peptostreptococcus anaerobicus* or *Bacteroides asaccharolyticus*, as well as mixed aerobic and anaerobic infections are also frequent causes of acute osteomyelitis.[1]

Bacteria such as *Staphylococcus aureus* or *Pseudomonas aeruginosa* contain fibronectin-binding surface proteins, which have the ability to interact with collagen, or the surface proteins contain binding sites that attach to sialoprotein, a noncollagenous bone matrix protein.[5]

Posttraumatic osteomyelitis usually represents a form of exogenous infection in which the bacteria are introduced through a traumatic wound as in this case, or through a surgical wound. Entrance of infection can occur following simple wounding in which the formation of hematomas under the skin may allow bacterial contamination and infection to develop. Such an infectious process may proceed without obviously apparent clinical signs. Posttraumatic osteomyelitis is frequently avascular as in this case, resulting from a nidus of necrotic bone and the probable inoculation of environmental or skin bacteria secondary to penetrating wounds, such as those caused by bullet, tooth or other foreign bodies.

As the fractured femur in this case was stabilized through open treatment of closed fractures, the posttraumatic or iatrogenic infection may have resulted from the placement of the pins or may have contaminated a sterile wound through that portal of entry. This pathogenesis represents the most common forms of osteomyelitis reported in small animals. When the skin is devitalized to the point that bacterial contamination is possible, infection of bone is an ever present danger.

Subsequent to inadequate treatment of acute osteomyelitis, the condition can obviously progress to become chronic and therefore represents an infection that is well established in bone and has been present for several weeks, months, or even years. Chronic infection can occur after bony union and structural stabilization has occurred or prior to union of the fracture. If the infection occurs before bone union, the treatment of the condition is made more difficult by the presence of the non-union or delayed union. An infected non-union is the worst possible treatment scenario in which the clinician is first required to allow for healing of the fracture and then to deal with the infection.[3]

JPC Diagnosis: Long bone: Osteomyelitis, suppurative, chronic, with medullary and periosteal new bone growth.

Conference Comment: There is marked variations in the slides submitted for this case. Lesions identified within the conference which were not present on all slides include callus formation, (either from the

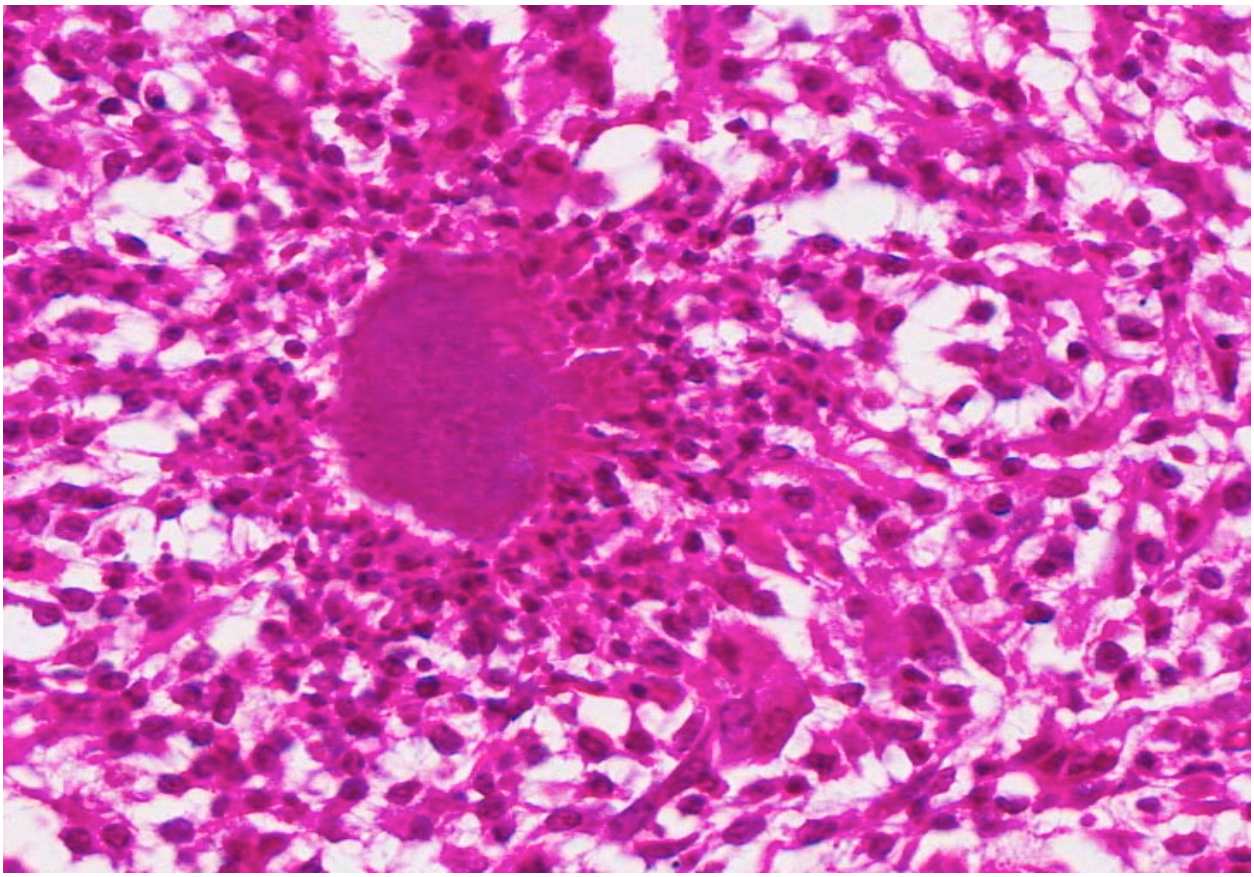

2-4. Pig, long bone: Scattered throughout the medullary cavity, colonies of bacteria enmeshed in protein are surrounded by large numbers of viable and degenerate neutrophils as well as fewer macrophages.

fracture repair or a pathologic fracture from the osteomyelitis), reactive periosteal changes without antecedent callus formation, extensive chondrous metaplasia, medullary osteosclerosis, and cortical osteopenia. Additionally, although the contributor did not find bacteria present histologically in the lesion, conference participants were able to find cocci bacteria within the area of suppuration.

It was difficult to determine the presence of a fracture from review of the submitted slides alone. Some slides had areas of very regular periosteal new bone growth arranged perpendicularly and radiating outwards from the periosteum with endosteal perpendicular reactive woven bone formation, with no callus formation. Other slides had very haphazard spicules of reactive woven bone and periosteum with extensive areas of disorganized cartilage, and this is likely the callus formed from the original fracture. Conference participants interpreted the islands of cartilage as chondrous metaplasia in reaction to decreased oxygen tension rather than endochondral ossification, which in the moderator's experience is generally minimal in a callus and occurs late in the process.

Ideal fracture repair begins with the formation of a hematoma from locally disrupted periosteum, blood vessels, and tissue. Macrophages, platelets, and the dead bone release various growth factors, including bone morphogenic proteins (BMPs), transforming growth factor-beta, platelet derived growth factors, which stimulate the proliferation of woven bone and is the initial scaffolding laid down to stabilize the area. Proliferating undifferentiated mesenchymal cells invade the area, which eventually undergo osseous or chondrous metaplasia to form the haphazard reactive woven bone and hyaline cartilage, and is termed the primary callus. The primary callus is eventually replaced by lamellar bone and may be remodeled by osteoclasts over a long period of time. If the fracture is unstable and there is excessive movement, the area instead forms mature fibrous tissue, which does not serve as a substrate for bone formation and becomes a nonunion. With time pseudoarthrosis can occur.[2]

In this case, we prefer the use of the term medullary osteosclerosis (a condition in which increased fibrous connective tissue fills spaces between spicules of woven bone) rather than myelophthisis (which is usually reserved to describe bone marrow suppression

secondary to marrow infiltration by malignant cells or local production of myelosuppressive cytokines).

The contributor mentioned the presence of sequestrum formation within the lesion. Conference participants interpreted the small fragments of necrotic bone as the result of surgical trauma from the initial surgery, not as an involucrum (a dense layer of fibrous connective tissue or reactive bone which walls off a focus of necrotic bone). An involucrum separates the sequestrum from its vascular supply and thus prohibits its resorption; however, in this case, the small fragments of dead bone appear to have access to a vascular supply and conference participants predicted that they should eventually be resorbed.[2]

In regards to the observed osteopenia, cortical bone normally compacts from the endocortical surface and progresses outward, (a finding not observed in this case). Conference participants discussed the potential reasons for this increased cortical porosity, such as osteoclastic resorption due to the elucidation of cytokines such as tumor necrosis factor (TNF), interleukin 1 (IL-1), IL-16, prostaglandin E_2 from the suppurative inflammation and triggering the expression of receptor activator for nuclear factor kappa B ligand (RANKL), also known as osteoclast differentiation factor (ODF), which stimulates osteoclasts upon binding their RANK receptors; or periosteal new bone growth in response to disuse osteopenia from the surgical implant, called stress shielding. In accordance with Wolff's Law, the reduction of stresses relative to normal would cause bone to adapt by reducing its mass, either by becoming more porous, called internal remodeling, or by getting thinner, called external remodeling.[2,4] Lesions of skeletal muscle, which were not present in all slides, include myofiber atrophy, edema, reactive fibrosis, or foci of coagulation necrosis and regeneration of skeletal muscle, and multifocal areas minimal lymphocytic inflammation.

Contributor: Armed Forces Radiobiology Research Institute
Veterinary Services Department
4301 Jones Bridge Road
Bethesda, MD 20814-4712
http://www.usuhs.mil/afrri/

References:

1. http://vetpath.wordpress.com/systemic-pathology/bone-pathology-steve-weisbrode-2/
2. Carlson CS, Weisbrode SE. Bones, joints, tendons, and ligaments. In: McGavin MD, Zachary JF, eds. *Pathologic Basis of Veterinary Disease*. 5th ed. St. Louis, MO: Mosby; 2011:921-3, 932, 951-2, 961-2.
3. Newton C, Nunamaker. Textbook of small animal orthopaedics. In:Nunamaker D, ed. *Osteomyelitis*. J.B. Lippincott Company. Online: http://cal.vet.upenn.edu/projects/saortho/chapter_37/37mast.htm
4. Thompson K. Bones and joints. In: Maxie MG, ed. *Jubb, Kennedy and Palmer's Pathology of Domestic Animals.* 5th ed. Vol 1. New York, NY: Elsevier Saunders; 2007:92-8.
5. Woodard JC. Outline of Veterinary Skeletal Pathology, Online: http://www.cldavis.org/woodard_bone/contents.htm

CASE III: 07/11 (JPC 4003387).

Signalment: 4-year-old female Leister cross, *Ovis aries*, ovine.

History: The ewe was presented to the clinic with severe dyspnea and weight loss. Respiratory signs of variable degree had been present during the last month, no fever was recorded. At clinical examination there was marked inspiratory and expiratory dyspnea with respiratory noise from the upper airways. The sheep was depressed and the temperature 39.1º C. A trial medical therapy with antibiotics and corticosteroids was unsuccessful in relieving clinical signs and the ewe was euthanized.

Gross Pathology: A space occupying mass was found in the caudal part of the nasal cavity, filling a large proportion of both the left and right side of the caudal nasal cavity. It markedly compressed the ethmoid bone and middle nasal concha on the left side, and was attached to the caudal region of the ethmoid bone. The mass was firm, pale and fibrous. When cutting through the mass there was a gritty sensation and marked resistance.

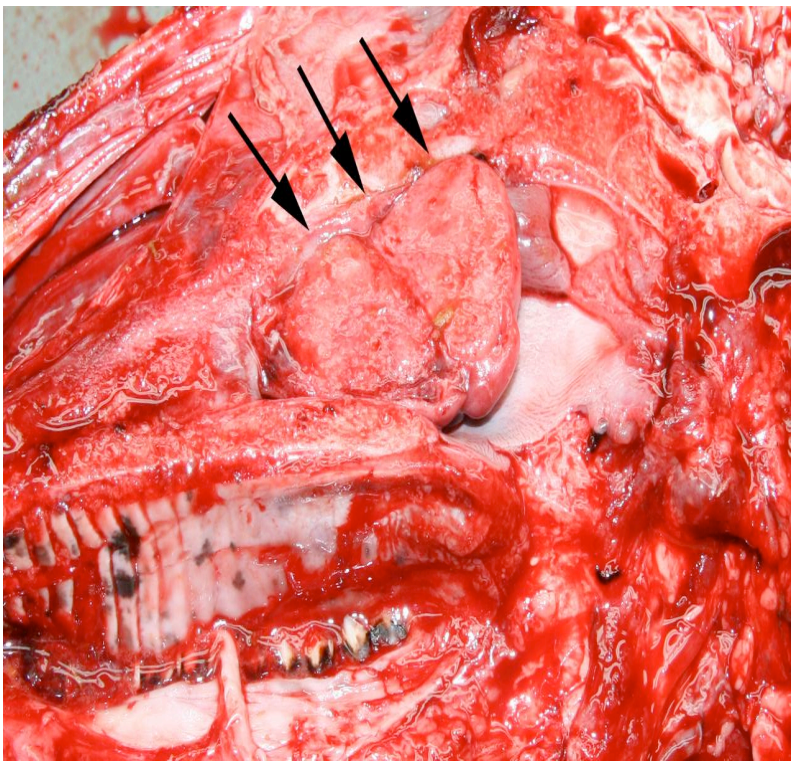

3-1. A space occupying mass was found in the caudal part of the nasal cavity, filling a large proportion of both the left and right side of the caudal nasal cavity. It markedly compressed the ethmoid bone and middle nasal concha on the left side, and was attached to the caudal region of the ethmoid bone. Photo courtesy of: Department of BVF, Division of Pathology, Pharmacology & Toxicology, SLU (Swedish University of Agricultural Sciences), Box 7028, SE-750 07 Uppsala, Sweden. http://www.bvf.slu.se/

Laboratory Results: Aerobic bacterial culture was performed and yielded no specific growth.

Contributor's Histopathologic Description: Nasal mucosa: In the lamina propria is a large expansile, partially encapsulated and demarcated mass composed of numerous spicules of woven bone separated by an abundant fibrous stroma. Osteoblasts outline bone spicules, although a transition from collagenous fibrous matrix to bone matrix is occasionally seen. In several places along bone margins osteoclasts are present, as well as adipose tissue. Within the stroma streams of plump and slender spindle shaped fibroblast-like cells and abundant collagenous extracellular matrix is seen. Dense collagen tissue is mixed with areas of myxoid matrix tissue. No mitotic figures were seen in examined sections. Moderate numbers of scattered as well as smaller multifocal accumulations inflammatory cells are present throughout the mass. Inflammatory cells consist of large numbers of plasma cells and smaller numbers of lymphocytes and neutrophils, and occasional eosinophils. Multifocally there are dense accumulations of inflammatory cells with a high proportion of neutrophils and these are sometimes centered on bone margins. Rarely fusifom microorganisms are found (not present in all slides). In the respiratory mucosa there is also subepithelial and periglandular diffuse moderate to marked infiltration of plasma cells and lymphocytes with smaller numbers of neutrophils. Extravasated erythrocytes are multifocally present.

Contributor's Morphologic Diagnosis: 1. Nasal cavity: Ossifying fibroma with plasmacytic and neutrophilic inflammation.
2. Nasal cavity: Rhinitis, lymphoplasmacytic and neutrophilic, chronic, moderate, diffuse.

Contributor's Comment: Benign lesions arising from membranous bone include ossifying fibroma, osteoma and fibrous dysplasia.[10] The morphologic features of the present case are most consistent with an ossifying fibroma. Ossifying fibromas show an intermediate morphologic architecture between osseous metaplasia of fibrous connective tissue, with predominate fibrovascular stroma separating poorly differentiated bone (as seen in fibrous dysplasia), and dense accumulations of well differentiated cancellous or compact bone with delicate intervening

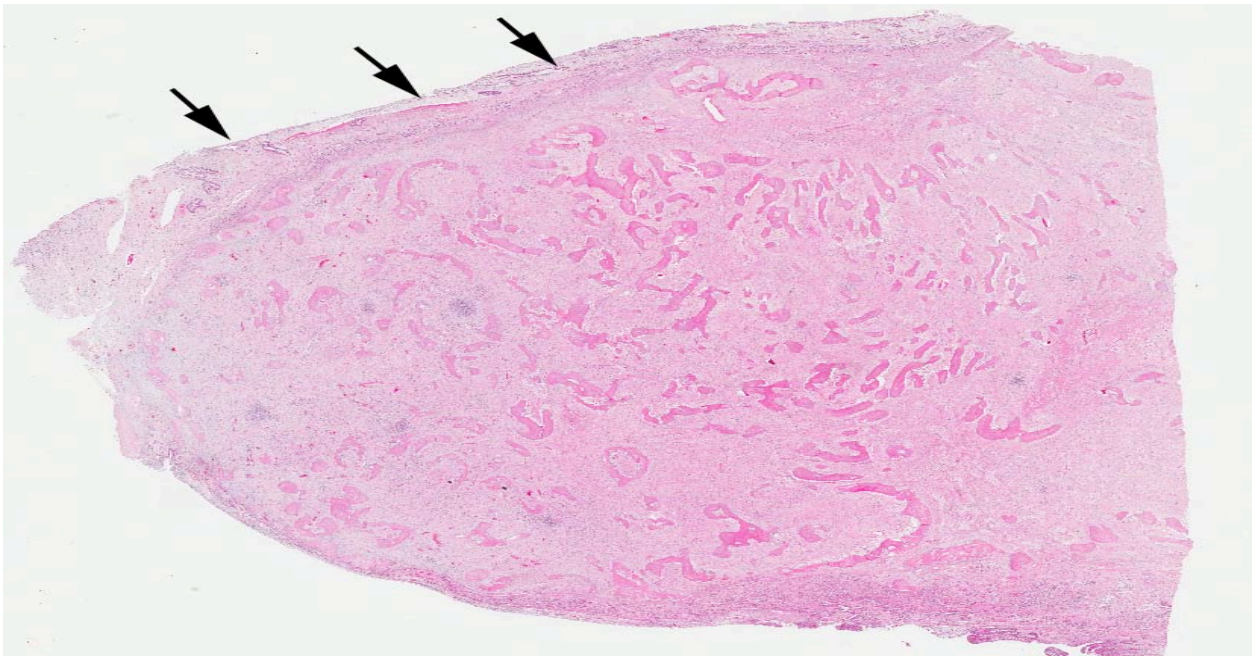

3-2. Nasal cavity, sheep: An expansile mass composed of spindle cells on a collagenous matrix with interspersed bony spicules expands the nasal mucosa. (HE 5X)

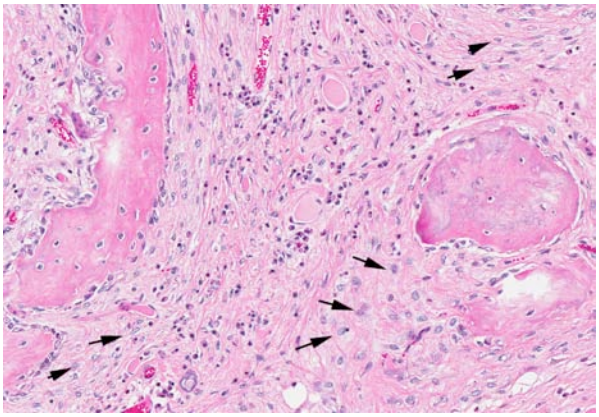

3-3. Nasal cavity, sheep. Within the mass, neoplastic spindle cells (arrows) on a loosely arranged fibrous stroma separate spicules of woven bone lined by a single layer of osteoblasts. (HE 150X)

fibrovascular tissue (as seen in osteoma).[10] However, osteomas may show features of both ossifying fibromas and fibrous dysplasia, and it has been suggested that osteomas could represent the end stage lesion of other processes.[10] Ossifying fibromas are rare in all species.[10] In sheep, ossifying fibroma has previously been reported in the mandible of a young adult.[8] Also involving the mandible, ossifying fibroma has been described in several cases of young horses.[4] Furthermore, osteoma of the nasal cavity and frontal bone has been described in a sheep, and recently myxomatous fibroma with presence of bone spicules rimmed by osteoblasts and fewer osteoclasts was described in bighorn sheep.[3,6] In addition, mucinous osteoma with features of ossifying fibroma has been reported in the nasal cavity of a horse.[7] In the present case, there was a marked inflammatory reaction within the mass and in the respiratory mucosa. The neoplasia may be related to chronic inflammation, although it is also possible that inflammation could arise secondary to disturbed airway function due to the presence of neoplasia. Chronic rhinitis is known to induce proliferative lesions including polypoid thickening of nasal mucosa, which may cause obstruction of the nasal passages.[2] Metaplastic ossification of connective tissue components incepted in inflamed nasal mucosa was discussed in the pathogenesis in an atypical osteoma in a bull.[9] Chronic rhinitis was also found in the ovine case of skull osteoma described by Pérez *et al*., who also described presence of inflammatory cells in the fibrous stoma in part of the neoplasm.[6]

JPC Diagnosis: Nasal cavity: Ossifying fibroma.

Conference Comment: Ossifying fibroma is an intraosseous lytic mass that destroys bone, and in early lesions is often intramedullary and does not produce a mass effect. Although considered benign, they are expansile and destroy adjacent normal bone. If this lesion was present in soft tissue it would be termed a fibroma with osseous metaplasia. This neoplasm differs from osteoma or exostoses, which arise from the periosteum and are proliferations of bone rather than fibrous tissue.[1,11]

Fibrous dysplasia looks and behaves in a very similar manner to ossifying fibroma, Fibrous dysplasia is also more common in young animals and is an important

differential diagnosis for this case. However, fibrous dysplasia does not have spicules and trabeculae of woven to lamellar bone lined by osteoblasts, which is a defining feature of ossifying fibroma, as in this case. Another distinguishing feature is that fibrous dysplasia typically has lamellar bony trabeculae concentrated centrally in the mass, with predominantly woven bone at the periphery.[1,5,11]

Fibrous osteodystrophy (FOD) was also discussed as a possibility, but in this case there is lamellar bone overlying woven bone in the spicules and trabeculae, and lamellar bone is usually not seen in FOD. Developing cortical bone occurs with woven bone laid down first which becomes compacted with overlying lamellar bone, and the lamellar bone present in this case likely represent preexisting bone. FOD also presents as a more fibroblast-rich lesion with less collagenous matrix as compared to ossifying fibroma, and is bilateral.[1,11]

Because of the areas of inflammation, osteoclasis, and fibrosis, conference participants discussed chronic osteomyelitis as a possibility in this case; however, in osteomyelitis there is a concentric orientation of the inflammation to the fibrous connective tissue or the reactive bone, and in this case there is relatively little inflammation compared to the amount of fibrous connective tissue.[1]

Contributor: SLU (Swedish University of Agricultural Sciences)
Department of BVF
Division of Pathology, Pharmacology & Toxicology
Box 7028, SE-750 07 Uppsala, Sweden
http://www.bvf.slu.se/

References:

1. Carlson CS, Weisbrode SE. Bones, joints, tendons, and ligaments. In: McGavin MD, Zachary JF, eds. *Pathologic Basis of Veterinary Disease*. 5th ed. St. Louis, MO: Mosby; 2011:951-2, 956-8.
2. Caswell JF, Williams KJ. Respiratory system. In: Maxie MG, ed. *Jubb, Kennedy, and Palmer's Pathology of Domestic Animals*. 5th ed. Philadelphia, PA: Saunders Elsevier; 2007:533-534.
3. Fox KA, Wootton SK, Quackenbush SL, et al. Paranasal sinus masses of Rocky Mountain bighorn sheep (*Ovis canadensis canadensis*). *Vet Pathol.* 2011;48:706-712.
4. Morse CC, Saik JE, Richardson DW, et al. Equine juvenile mandibular ossifying fibroma. *Vet Pathol*. 1988;24:415-421.
5. Nelson AM, Baker DC. Pedal osteosarcoma in a donkey. *Vet Pathol*. 1998;35(5):407-9.
6. Pérez V, Rúa P, Benavides J, et al. Osteoma in the skull of a sheep. *J Comp Pathol.* 2004;130:319-322.
7. Puff C, Ohnesorge B, Wagels R, et al. An unusual mucinous osteoma with features of an ossifying fibroma in the nasal cavity of a horse. *J Comp Pathol*. 2006;135:52-55.
8. Rogers AB, Gould DH. Ossifying fibroma in a sheep. *Small Ruminant Res*. 1998;28:193-197.
9. Rumbaugh GE, Pool RR, Wheat JD. Atypical osteoma of the nasal passage and paranasal sinus in a bull. *Cornell Veterinarian.* 1978;68:544-554.
10. Thompson KG, Pool RR. Tumors of bones. In: Meuten DJ, ed. *Tumors in Domestic Animals.* 4th ed. Ames, Iowa: Iowa State Press; 2002:248-255.
11. Thompson K. Bones and joints. In: Maxie MG, ed. *Jubb, Kennedy and Palmer's Pathology of Domestic Animals.* 5th ed. Vol 1. New York, NY: Elsevier Saunders; 2007:111-2.

CASE IV: 11/247 (JPC 4004158).

Signalment: 5 male and 1 female 22 day-old Ross 308 broiler chickens, *Gallus gallus domesticus.*

History: Six chickens were received for necropsy from a flock of 14000 individuals. The chickens showed signs of poor growth during the first 2 weeks, and on day 11 a new batch of feed was introduced. In the 3rd week the chickens weighed 40-50 grams less than normal. The feed intake was slightly increased. From day 18 signs of leg problems were observed in the flock, and tibiotarsal fractures were detected. On day 20, 40 chickens had fractures and 235 had been euthanized. From day 22, another new batch of feed was introduced. On day 27, an improvement in flock health had occurred and the remaining flock was slaughtered at normal time.

Gross Pathology: The six chickens had been euthanized and they weighed 482-654 grams. Four chickens had a unilateral fracture in the distal tibiotarsus, one chicken had a unilateral fracture in a femur, and in one chicken no fractures were detected. Surrounding the fractures there were moderate to large hemorrhages. Mineralization of bones was severely reduced in all six chickens. The hypertrophic zone of the growth plate in the proximal tibiotarsus was moderate to severely widened towards the metaphysis in all six chickens. Enlarged parathyroid gland was not detected macroscopically.

Contributor's Histopathologic Description: In the proximal tibiotarsus there is severe widening of the hypertrophic zone of the growth plate. The hypertrophic zone is dominated by wide cartilage columns consisting of large hypertrophic chondrocytes in an orderly fashion. These cartilage columns are either naked or lined by a very narrow zone of osteoid. Multifocally, the lining of the columns are ragged and scalloped, and in some areas with clusters of osteoclasts.

The thickness of the proliferating zone of the growth plate was considered normal. In the metaphysis, the cortical bone is severally thinned, and there is mild multifocal proliferation of fibroblasts subperiosteally. In some sections bacterial emboli are seen in medullary vessels.

Contributor's Morphologic Diagnosis: Proximal tibiotarsus: Failure of endochondral ossification, with retention of hypertrophic chondrocytes, severe, consistent with rickets.

Contributor's Comment: Rickets in chickens is characterized by severe fragility of long bones and bending of long bones due to poor mineralization, and it may be caused by an imbalance between calcium and phosphorus or vitamin D deficiency.[3] The histopathology of rickets differs depending on the cause of the disease.[3,9] A hypocalcemic form is characterized by accumulation of proliferating chondrocytes;[2] and chickens fed a diet low in calcium showed, by 2 weeks of age, a variably lengthened and disorganized proliferating zone and shortened cartilage columns of the hypertrophied zone.[7] A hypophosphatemic form is characterized by accumulation of hypertrophic chondrocytes in the metaphyseal zone.[4] Chickens fed a diet low in phosphorus showed, by 2 weeks of age, lengthening of the hypertrophic zone,[6] and a diet with excess calcium

4-1. Tibia, 22-day-old chicken. The proximal tibial metaphysis is filled by a large core of unmineralized cartilage. The hypertrophic zone of the growth plate in the proximal tibiotarsus was moderate to severely widened towards the metaphysis. Photo courtesy of The Norwegian School of Veterinary Science, PO box 8146 Dep., 0033 Oslo, Norway. www.vetinst.no

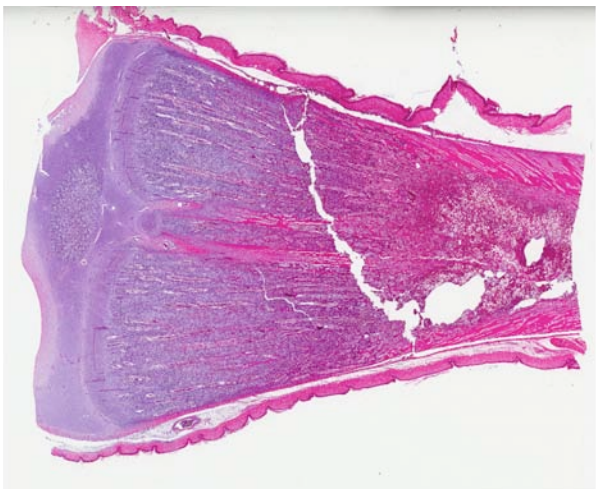

4-2. Tibia, 22-day-old chicken. Subgross histologic image of the tibia in image 4-1. (HE 4X)

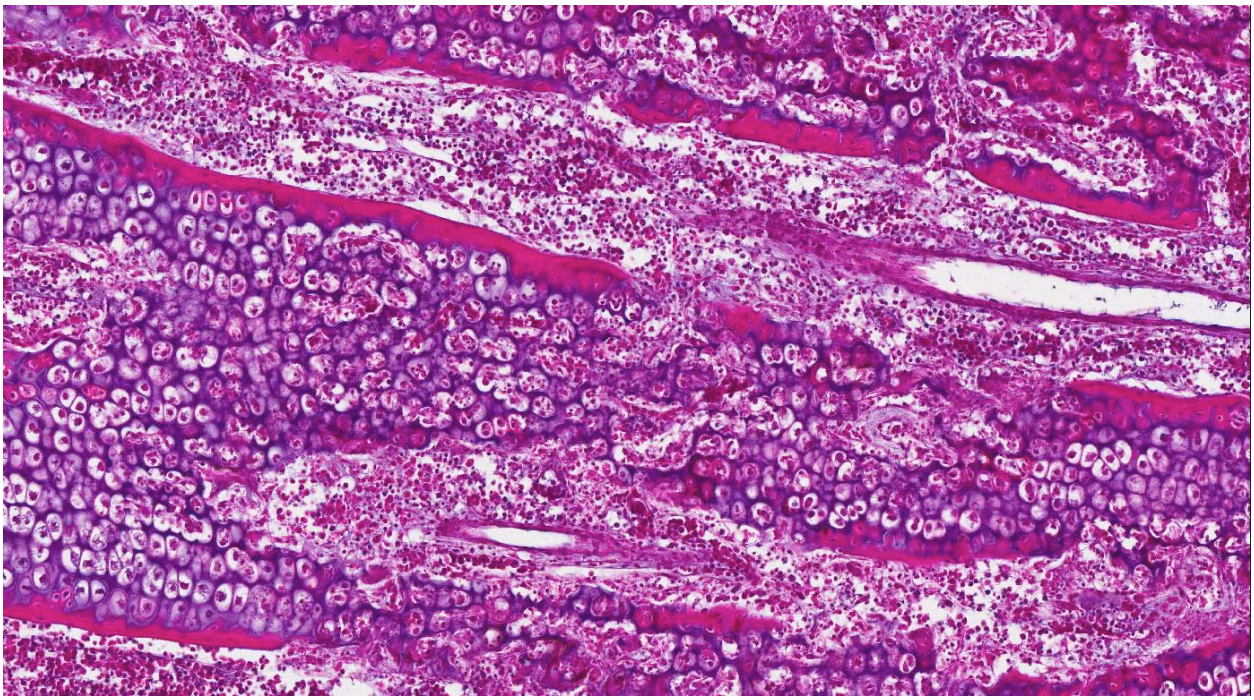

4-3. Tibia, 22-day-old chicken: Long trabeculae composed of unmineralized cartilage from the hypertrophic zone are lined by a wide osteoid seam. (HE 140X)

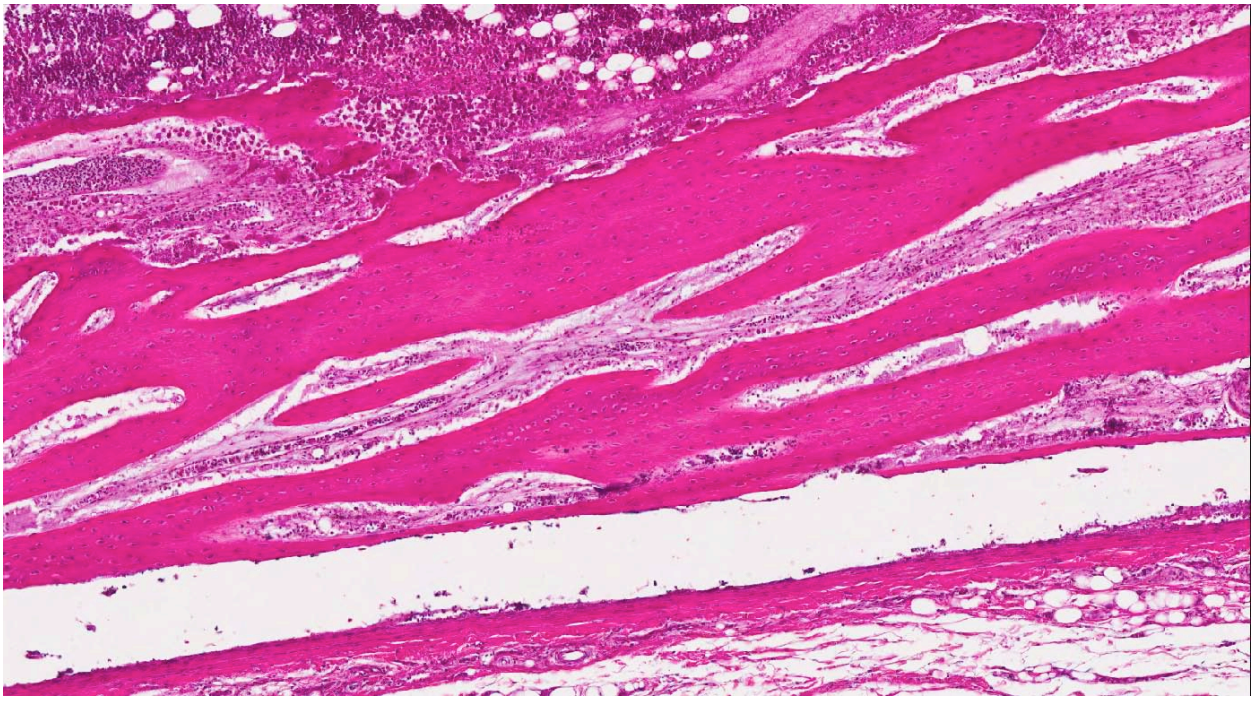

4-4. Tibia, 22-day-old chicken. The cortex is markedly thin and composed of woven bone. There are numerous osteoclasts within Howship's lacune on the endosteal surface, and abundant loose fibrous connective tissue within endocortical vascular spaces. (HE 200X)

caused similar lesions.[6] These two forms differ in histopathology from the rickets of vitamin D deficiency.[3] In vitamin D deficiency, the enlargement of the epiphyseal plate initially is due to widening of the proliferating and hypertrophic zones; as the deficiency progresses it may be primarily the former.[3] The extensive lengthening of the hypertrophic zone found in these chickens may indicate a hypophosphatemic rickets; however, preliminary analyses of the feed used for this flock showed

decreased levels of vitamin D_3, while calcium and phosphorus were within normal range.

JPC Diagnosis: 1. Proximal tibiotarsus: Physeal chondrodystrophy with marked elongation of the zone of hypertrophy, delayed endochondral ossification, and cortical osteopenia.
2. Proximal tibiotarsus: Fibrous osteodystrophy.

Conference Comment: Although the lesions may be most similar to hypophosphatemic rickets, the history and dietary analysis are convincing for hypovitaminosis D. Conference participants discussed the importance of relying on dietary analysis to determine the type of deficiency rather than fine variations in bone lesions.

Some slides have areas of poor tissue preservation or autolysis with colonies of coccoid bacteria and homogeneous, eosinophilic, acellular material filling medullary spaces. PTAH and Masson's trichrome histochemical stains were performed to determine if the acellular material is widespread fibrin exudation; however, PTAH did not stain fibrin, and conference participants considered serous atrophy of fat affecting the metaphysis and epiphysis as the more likely cause for the acellular material. The Masson's trichrome revealed perivascular fibrosis of vessels penetrating the growth plate, mild peritrabecular fibrosis in the metaphysis, endocortical fibrosis, fibrosis in the vascular spaces of the cortex, and minimal fibrosis in the epiphysis interpreted as fibrous osteodystrophy secondary to hypovitaminosis D, similar to case 1.[3]

Also similar to case 1 are the findings of cortical osteopenia with woven bone in the cortex and increased cortical porosity due either to delayed osteonization or increased cortical lysis. Rickets in avian species differs from that in mammals in that there is delayed onset of osteoid deposition, atrophy of osteoblasts on cartilage cores, and retention and minimal disorganization of hypertrophied chondrocytes in wide regular columns which often extend deep into the metaphysis. As mentioned by the contributor, the multifocal marked osteoclast hyperplasia of metaphyseal trabeculae and endocortical surfaces at the diaphysis was interpreted by conference participants as normal endocortical osteoclasis, or modeling of the endocortical surface of a rapidly growing bird.[1,3]

The primary differential diagnosis in this case is tibial dyschondroplasia (TD), a spontaneous lesion of rapidly growing birds which is characterized by a large mass of avascular cartilage in the tibiotarsal metaphysis with necrosis of the prehypertrophic zone of chondrocytes, and is similar to osteochondrosis in mammals. The lesions in TD are very similar to those of rickets, and are the result of failure of chondrocytes to fully differentiate and allow vascularization, mineralization, and resorption of cartilage matrix.[3,5,8]

Contributor: The Norwegian School of Veterinary Science
PO box 8146 Dep.
0033 Oslo
Norway

References:

1. Hedstrom OR, Cheville NF, Horst RL. Pathology of vitamin D deficiency in growing turkeys. *Vet Pathol*. 1986;23(4):485-98.
2. Jande SS, Dickson IR. Comparative histological study of the effects of high calcium diet and vitamin D supplements on epiphyseal plates of vitamin-D-deficient chicks. *Acta Anat* (Basel). 1980;108:463-468.
3. Klasing KC. Nutritional diseases. In: Saif YM, ed. *Diseases of Poultry*. 12th ed. Oxford, England: Blackwell Publishing; 2008:1121-1148.
4. Lacey DL, Huffer WE. Studies on the pathogenesis of avian rickets. I. Changes in epiphyseal and metaphyseal vessels in hypocalcemic and hypophosphatemic rickets. *Am J Pathol*. 1982;109:288-301.
5. Leach RM jr, Gay CV. Role of epiphyseal cartilage in endochondral bone formation. *J Nutr*. 1987;117(4): 784-90.
6. Long PH, Lee SR, Rowland GN, et al. Experimental rickets in broilers: gross, microscopic, and radiographic lesions. I. Phosphorus deficiency and calcium excess. *Avian Dis.* 1984;28:460-474.
7. Long PH, Lee SR, Rowland GN, et al. Experimental rickets in broilers: gross, microscopic, and radiographic lesions. II. Calcium deficiency. *Avian Dis.* 1984;28:921-932.
8. Orth MW, Cook ME. Avian tibial dyschondroplasia: a morphological and biochemical review of the growth plate lesion and its causes. *Vet Pathol*. 1994;31(4): 403-4.
9. Randall CJ. Nutritional deficiencies and metabolic disorders. In: Randall CJ, ed. *A Colour Atlas of Diseases and Disorders of the Domestic Fowl and Turkey*. 2nd ed. London, UK: Wolfe Publishing Ltd; 1991:109-124.

Joint Pathology Center
Veterinary Pathology Services

WEDNESDAY SLIDE CONFERENCE 2011-2012

Conference 25

16 May 2012

CASE I: N315/07 (JPC 3126927).

Signalment: Four-year-old female Belgian blue cross-breed, bovine *(Bos taurus)*.

History: Access to 'rough' grazing. Presented with stranguria and hematuria.

Gross Pathology: Ammoniacal smell on opening the peritoneal cavity in which a diffuse fibrin-rich exudate and approximately 60 liters of urine-containing fluid is present. There is perforation of the bladder wall approximately 4cm proximal to the urethral exit within an approximately 16cm diameter, soft red mass raised above the mucosal surface. A similar lesion extends along the ventral bladder wall towards the ureteral openings. The distal 30cm long segment of the esophagus is diffusely mottled red and pale with longitudinal sloughing of the mucosa (consistent with

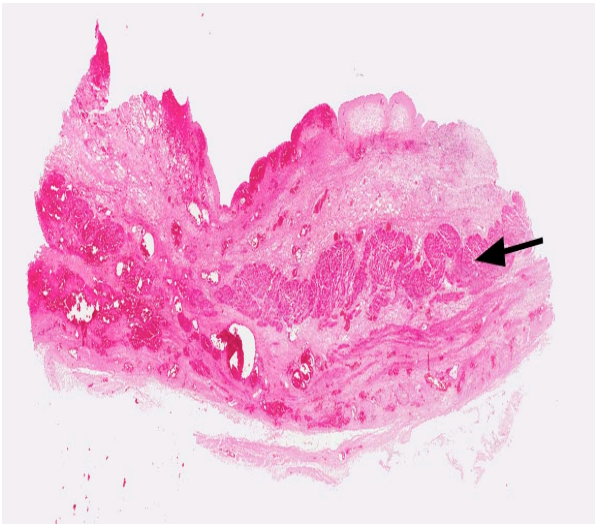

1-1 . Ox, urinary bladder: Marked transmural thickening of the wall of the urinary bladder by edema. The arrow marks the location of the muscular tunic. (HE 4X)

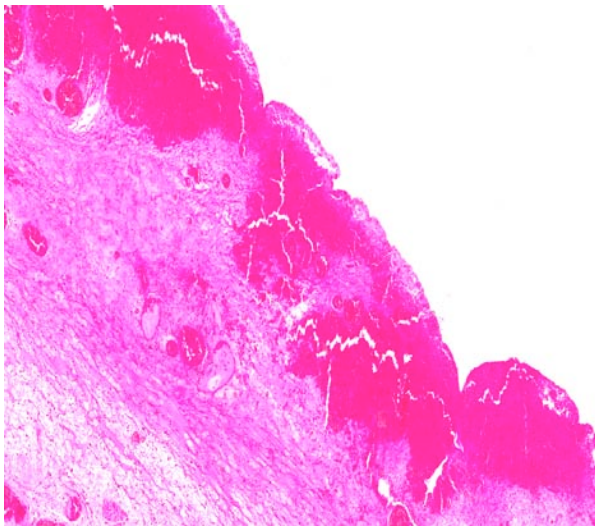

1-2. Ox, urinary bladder: There is total loss of the mucosal epithelium with suffusive hemorrhages within the submucosa, and marked edema beneath. Vessels throughout the section contain emigrating neutrophils, and occasional vasculitis is seen. (HE 160X)

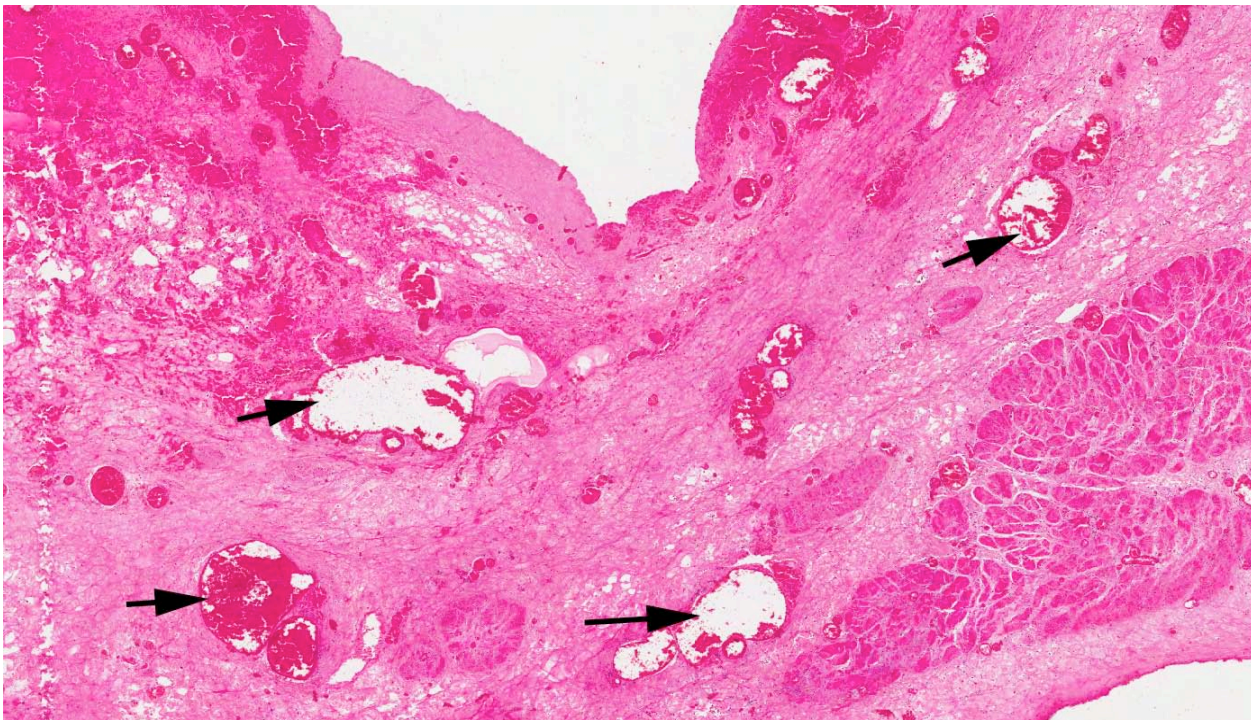

1-3. Ox, urinary bladder: The vessels in the submucosa are cavernous. (HE 10X)

persistent reflux resulting in extensive erosion/ulceration).

Contributor's Histopathologic Description: Sloughing of urothelium with an irregularly elevated exposed stromal surface containing abundant engorged, ectatic blood vessels of varying diameter lined by well-differentiated endothelial cells with adjacent stromal hemorrhage, fibrinous exudate and scattered leukocytes. These changes extend transmurally with evidence of vasculitis & thrombosis. Fibrinocellular exudate was noted on the serosal surface of the intestine (peritonitis).

Contributor's Morphologic Diagnosis: Bladder: Vascular congestion, ectasia, and hemorrhage, with attendant vasculitis, thrombosis and fibrinous exudation; diffuse; severe.

Contributor's Comment: The gross and histopathological changes in the bladder are consistent with bladder perforation and peritonitis secondary to hemangiomatous lesions in the bladder wall. Such lesions are associated with the long-term ingestion of bracken fern in cattle (Enzootic hematuria). This animal had been on rough grazing with access to such fern.

Enzootic hematuria occurs in mature cattle, is characterized by hematuria and anemia, and is associated with hemorrhages or neoplasms particularly of the bladder. The syndrome is attributed to the long-term ingestion of bracken fern (*Pteridium aquilinum* subsp. *Aquilinum*) and can be reproduced experimentally.[3,5] Bracken fern contains several toxins including a thiaminase, carcinogens (quercetin, shikimic acid, prunasin, ptaquiloside, ptaquiloside Z, aquilide A), and a "bleeding factor".[1] Administration of ptaquiloside to guinea pigs results in hemorrhagic cystitis suggesting that this is a significant toxin in the induction of hematuria.[5]

Cattle fed low levels of bracken fern develop microscopic, followed by macroscopic, hematuria. Microhematuria is usually associated with petechial or ecchymotic hemorrhages of the bladder mucosa with microscopic evidence of vascular ectasia and engorgement and these vessels are prone to hemorrhage. Nodular hemangiomatous lesions also develop.[3] Occasionally, macroscopic hematuria is associated with these non-neoplastic changes, but usually results from the development of tumors which ulcerate and hemorrhage into the bladder lumen.[3] Several types of epithelial and mesenchymal neoplasms may develop, and in over 50% of affected cattle, mixed epithelial–mesenchymal neoplasms develop. Papillomas, fibromas, and hemangiomas with carcinomas are most commonly found.[1,3,5]

JPC Diagnosis: Urinary bladder: Necrosis, transmural, diffuse, with marked hemorrhage, vascular ectasia, and necrotizing vasculitis.

Conference Comment: Conference participants discussed obstruction as a likely and more commonly encountered candidate condition for the lesion in this case, and possibly the cause of the histologic lesion. The expected neoplasia with hemorrhagic cystitis was not visible in the slide, and the grossly described masses may have caused an obstruction and the subsequent transmural hemorrhage and necrosis of the bladder wall, leading to the rupture.

This cow likely then had post-renal azotemia, and although serum was not available for analysis, conference participants considered the option of measuring the aqueous humor of the eye at necropsy to determine if the animal was azotemic, since creatinine is not protein-bound and diffuses freely in both the eye and the abdominal fluid. The urea nitrogen and creatinine of the abdominal fluid could be compared to that of the aqueous humor, and in the case of a ruptured urinary bladder, the concentrations in the abdominal fluid should approach double that of the serum or humor.[2,4]

Additional clinical pathology abnormalities expected in a cow with post-renal azotemia would be hyperphosphatemia, since azotemia is the primary cause of elevated phosphorous in veterinary medicine due to decreased excretion from decreased glomerular filtration rate, and hyponatremia and hypochloremia due to loss in the urine and diffusion along the concentration gradient. Although small animals often have metabolic acidosis associated with renal failure, cattle present with metabolic alkalosis due to rumen atony and subsequent acid sequestration. This is due to stasis of ruminal content, similar to that seen in cattle with displaced abomasum or ileus. Conference participants expected a high plasma total CO_2 and total bicarbonate (HCO_3^-) and respiratory compensation indicated by a high $_pCO_2$. Although hyperkalemia is expected with post-renal azotemia, the accompanying metabolic alkalosis in cattle drives potassium into cells in exchange for hydrogen following its concentration gradient to the extracellular space. An expected gross finding in this case would be bilateral hydronephrosis or hydroureter secondary to the obstruction.[2,3,4]

Contributor: UCD Veterinary Sciences Centre
UCD School of Agriculture, Food Science and Veterinary Medicine
University College Dublin
Belfield
Dublin 4, Ireland
www.ucd.ie

References:

1. Hopkins NCG. Aetiology of enzootic haematuria. *Vet Rec*. 1986;118:715–717.
2. Langston C. Acute uremia. In: Ettinger SJ, Feldman EC, eds. *Textbook of Veterinary Internal Medicine*. 7th ed. Vol 2. St. Louis, MO: Saunders Elsevier; 2010:1969-83.
3. Maxie MG, Newman SJ. The urinary system. In: Maxie MG, ed. *Jubb, Kennedy and Palmer's Pathology of Domestic Animals*. 5th ed. Vol. 2. Philadelphia, PA: Elsevier Saunders, 2007:518-520.
4. Tripathi NK, Gregory CR, Latimer KS. Urinary system. In: Latimer KS, ed. *Duncan and Prasse's Veterinary Laboratory Medicine: Clinical Pathology*. 5th ed. Ames, IA: Wiley-Blackwell; 2011:270-80.
5. Xu LR: Bracken poisoning and enzootic haematuria in cattle in China. *Res Vet Sci*. 1992;53:116–121.

CASE II: 11-4158 (JPC 4002911).

Signalment: 6-month-old male intact Shih Tsu mix dog *(Canis familiaris)*.

History: The puppy was presented to the veterinary teaching hospital 15-18 hours after ingesting up to 8 Midol tablets (500mg acetaminophen, 60mg caffeine, 15mg pyrilamine maleate per tablet). No decontamination had been attempted. The patient was treated with N-acetylcysteine and Denamarin, plus Norm-R fluids at ½ maintenance dose. The puppy exhibited signs of hepatic encephalopathy and was euthanized due to poor prognosis.

Gross Pathology: There was generalized mild icterus of subcutis and mucous membranes. The liver was diffusely pale tan to yellow with a distinct reticular pattern. At the time of necropsy, the urine was transparent yellow.

Laboratory Results: Presentation:
ALT = 261
AP = 239.
One day later:
ALT = 17, 090
AP = 578
Total bilirubin = 4.5
Urine was coffee colored.

Contributor's Histopathologic Description: Liver: Approximately 50% of the liver parenchyma was involved in acute degenerative to necrotizing changes. There was extensive coagulative necrosis of hepatocytes adjacent to all central veins and extending to the midzonal regions. Necrotic hepatocytes were rounded up and contained hypereosinophilic, fragmented cytoplasm. Scattered cells lacked nuclei, while others contained pyknotic to karyorrhectic nuclei. Sinusoids adjacent to central veins were filled with red blood cells (congestion).

Kidney: Widely scattered tubules within the cortex and medulla contained dark orange-brown globules (presumptive hemoglobin). There were similar pigment globules within the cytoplasm of widely scattered epithelial cells lining these tubules. Proximal convoluted tubular epithelium had scattered degenerate cells with hypereosinophilic cytoplasm and pyknotic nuclei. Regenerative epithelial cells were rare. The urinary spaces of several glomeruli were moderately dilated and filled with weakly eosinophilic protein fluid residue. There was similar protein fluid within numerous tubules within the cortex.

Within the stomach (not shown) were numerous lymphocytic nodules in the lamina propria, associated with large, silver positive, spiral bacteria (presumptive *Helicobacter* sp.) in the superficial mucus and glands.

Contributor's Morphologic Diagnosis: 1. Diffuse, acute, severe centrilobular hepatocellular necrosis.
2. Diffuse, mild to moderate hemoglobinuric nephrosis (presumptive).
3. Diffuse, moderate, chronic gastritis (tissue not submitted).

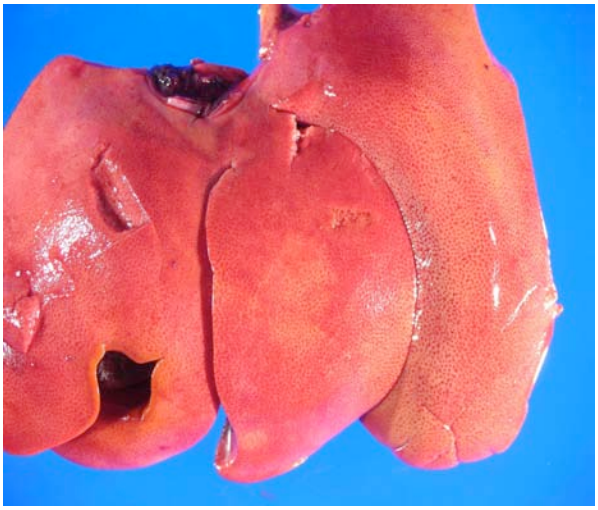

2-1. Dog, liver: The liver is yellow-tan with a distinct reticular pattern. The discoloration of the liver is the result of hepatocellular necrosis, the generalized icterus in the animal, and likely a bit of lipidosis as well. The reticular pattern is accentuated due to the strict centrilobular necrosis. (Photo courtesy of: Department of Veterinary Microbiology and Pathology, Washington State University, Pullman, WA 99164-7040 www.vetmed.wsu.edu)

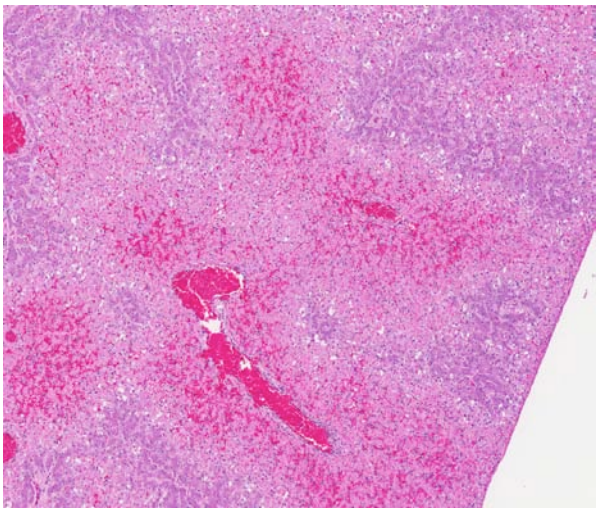

2-2. Dog, liver: A distinct centrilobular pattern of necrosis is seen. (HE 136X)

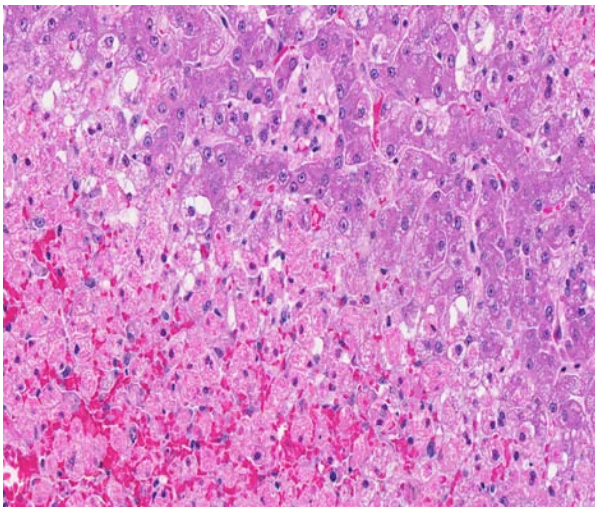

2-3. Dog, liver: Interface of necrotic centrilobular hepatocytes (lower left) and hepatocytes undergoing acute mild toxic degeneration, characterized by cytoplasmic accumulation of lipid. (HE 270X)

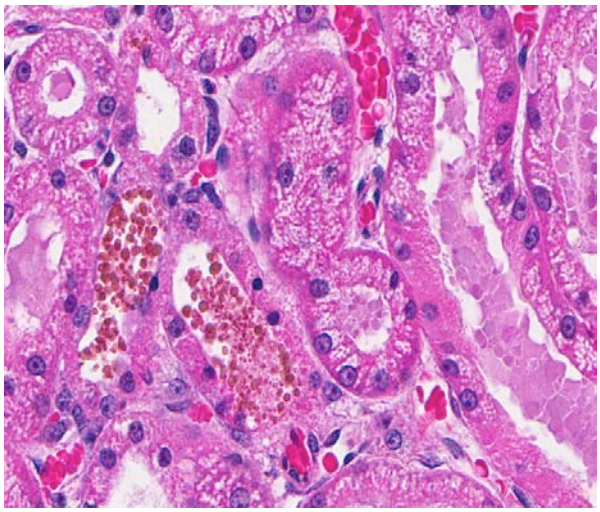

2-4. Dog, kidney: Vacuolar degeneration and necrosis of proximal convoluted tubules, with intraluminal hemoglobin casts. (HE 340X)

Contributor's Comment: The lesions in this puppy were compatible with acute acetaminophen intoxication. The toxic dose of acetaminophen in dogs ranges from 200-600mg/kg[6]; this 4kg puppy ingested up to 4grams in 8 Midol tablets. The recommended therapeutic dose in dogs is 15mg/kg every 8 hours. By contrast, cats are much more susceptible to toxicity and toxicosis has been seen with doses as low as 10mg/kg.

Acetaminophen (N-acetyl-p-aminophenol) is a widely used over-the-counter analgesic and antipyretic drug considered very safe in humans at therapeutic doses and having fewer gastrointestinal side effects than aspirin or ibuprofen.[4] Yet poisoning by acetaminophen accounts for approximately half of all cases of acute liver failure in people in the US and Britain. Poisoning in dogs and cats is usually associated with administration by well-intentioned by uninformed owners, or by accidental ingestion as in this case.[6]

The liver is a common target of toxicosis, especially from ingested toxins, due to several factors.[7] The liver is exposed to high concentrations of ingested compound via the portal circulation; exogenous and endogenous compounds concentrate in the liver by binding to transport proteins and enzymatic sites; and as the primary site of biotransformation of ingested compounds it is exposed to high concentrations of metabolites. Hepatic biotransformation of xenobiotics occurs in 2 phases: phase I involves metabolism generally by mixed function oxidases, and phase II involves detoxification of metabolites by conjugation with water, sulfate, glucuronate, glutathione and others. Toxicity occurs when metabolism into toxic metabolites overwhelms conjugation systems. As such the centrilobular hepatocytes (zone 3), with high concentrations of mixed function oxidases, are most susceptible to toxicity from compounds that are metabolized to toxic intermediates requiring conjugation. Acetaminophen is a classic example of such a compound.

Mechanisms of acetaminophen induced liver injury have been recently reviewed.[4] Although still under intense investigation, hepatotoxicity occurs in 5 primary steps: 1) metabolism into reactive metabolite by cytochrome P450 (CYP); 2) consumption of glutathione leading to excess reactive oxygen and nitrogen species; 3) increase oxidative stress resulting in alterations in calcium homeostasis and mitochondrial permeability; 4) loss of mitochondrial ability to synthesize ATP and 5) loss of ATP leading to necrosis.

At non-toxic doses, acetaminophen is metabolized by direct conjugation to glutathione and the non-toxic conjugates are excreted in urine and bile.[6] At toxic doses, glutathione is overwhelmed and metabolism is shunted to the CYP system, resulting in the toxic metabolite N-acetyl-p-benzoquinone imine (NAPQI). NAPQI requires glutathione for detoxification; with glutathione already severely depleted, NAPQI binds covalently to cellular proteins and enzymes, disrupting membranes and leading to oxidative stress. Depletion of glutathione also leads to increased reactive oxygen and nitrogen species. N-acetylcysteine, developed for treatment of acetaminophen toxicity, increases detoxification of NAPQI by direct conjugation and through increased glutathione synthesis. This compound, and S-adenosylmethionine (an intermediary in production of cell membranes and glutathione), have been used effectively in dogs and cats with acetaminophen toxicity.[6] Although uncoupling of mitochondrial permeability transition

with subsequent loss of ATP is considered the primary mechanism of acetaminophen induced hepatotoxicity, other mechanisms that have been explored are altered hepatic blood flow due to necrosis of sinusoidal endothelium, and the role of inflammation, chemokines and cytokines both in development of toxicity and in hepatic repair.[4]

Methemoglobin formation is the primary mechanism of toxicity in cats; hepatotoxicity occurs only at high doses. Cats are more susceptible to acetaminophen toxicity than dogs because of much lower levels of glucuronyltransferase.[6] In addition, feline red blood cells have more sulfhydryl groups than other species, making them highly susceptible to oxidative injury. In contrast, dogs develop methemoglobinemia only at higher toxic doses. Histologic lesions of hemoglobinuric nephrosis in this case, although mild, support the likelihood that this puppy ingested high enough doses of acetaminophen to produce metahemoglobinemia.

The other toxic principle in Midol tablets is caffeine, a methylxanthine in the same class of compounds with theobromine and theophylline.[2] Toxic doses for dogs range from 110-200mg/kg; the 4kg puppy ingested up to 480mg, making direct toxicity from caffeine a possible complication. Caffeine is also metabolized by the liver; hepatic damage from acetaminophen could have compromised caffeine metabolism and enhanced its toxicity in this case. Signs of caffeine toxicity are vomiting, tremors and seizures. There are no gross or histologic lesions related to toxicity, although it is possible that the terminal CNS signs in this dog may have been due to a combination of liver failure and caffeine toxicity.

JPC Diagnosis: 1. Liver: Necrosis, centrilobular, diffuse. 2. Kidney, proximal tubules: Degeneration and necrosis, multifocal, mild, with hemoglobin casts.

Conference Comment: Heinz bodies, which are foci of denatured globin apparent as a membranous inclusion in the erythrocyte, are expected to be present in a peripheral blood smear in this case due to the oxidative damage to erythrocytes from acetaminophen toxicity, and are an indicator of intravascular hemolysis. Heinz body formation results from oxidative damage that causes disulfide links between glutathione and globin chains, resulting in aggregation and precipitation of globin in the cell. Also, the predicted mean cell hemoglobin concentration (MCHC) would be increased due to artifact from measured Heinz bodies which would artificially increase the MCHC. Luna hemoglobin stain can be used to confirm the hemoglobin casts within the renal tubules.[3]

The serum hepatic chemistry changes in this case are typical of acetaminophen toxicosis, with normal hepatic enzymes on the first day and massive increases by the third day, which demonstrates the clinical importance of not ruling out hepatic necrosis even when hepatic enzymes are normal when first measured. The reason the alanine transaminase (ALT) is markedly increased and the alkaline phosphatase (AP) is relatively normal the day after presentation is ALT, in addition to aspartate aminotransferase (AST), is a leakage enzyme and increases with hepatic degeneration and necrosis, while AP is an inducible enzyme mainly useful in detecting cholestasis and originates from the biliary tree.[1]

Conference participants discussed how hemoglobinuric nephrosis is a misnomer, as hemoglobin is not directly nephrotoxic. Hemoglobin passes into the glomerular filtrate after haptoglobin saturation, resulting in formation of granular casts. The combination of ischemia and hypoxia due to anemia and hypotension, as well as tubular obstruction, and interstitial edema contribute to the tubular necrosis. Conference participants discussed the common causes of coffee colored urine in dogs, and cystitis with concurrent hematuria is the most likely source, with hemoglobinuria being next, and myoglobinuria being very rare.[5] Conference participants interpreted the eosinophilic fluid within Bowman's space as either autolysis or reflux from tubular necrosis.

Contributor: Washington State University
Department of Veterinary Microbiology and Pathology
Pullman, WA 99164-7040
www.vetmed.wsu.edu

References:

1. Bain PJ. Liver. In: Latimer KS, ed. *Duncan and Prasse's Veterinary Laboratory Medicine: Clinical Pathology*. 5th ed. Ames, IA: Wiley-Blackwell; 2011:213-23.
2. Carson TL. Methylxanthines. In: Peterson ME, Talcott PA, eds. Small Animal Toxicology, 2nd ed. St Louis, MO: Elsiever; 2006: 845-852.
3. Fry MM, McGavin MD. Bone marrow, blood cells, and the lymphatic system. In: McGavin MD, Zachary JF, eds. *Pathologic Basis of Veterinary Disease*. 5th ed. St. Louis, MO: Mosby; 2011:705-11.
4. Hinson JA, Roberts DW, James LP. Mechanisms of acetaminophen-induced liver necrosis. In: Utrecht J, ed. *Adverse Drug Reactions: Handbook of Experimental Pharmacology*. Berlin, Germany: Springer-Verlag; 2010:368-405.
5. Maxie MG, Newman SJ. Urinary system. In: Maxie MG, ed. *Jubb, Kennedy, and Palmer's Pathology of Domestic Animals*. 5th ed. Vol. 2. Philadelphia, PA: Saunders Elsevier; 2007:432-6.

6. Sellon RK. Acetaminophen. In: Peterson ME, Talcott PA, eds. *Small Animal Toxicology*. 2nd ed.St. Louis, MO: Elsiever; 2006: 550-557.
7. Stalker MJ, Hayes MA. Liver and biliary system. In: Maxie MG, ed. Jubb, Kennedy and Palmer's Pathology of Domestic Animals. 5th ed. Edinburgh, Scotland: Elsevier; 2007:364-367.

CASE III: 10-2049 (JPC 4004362).

Signalment: 10-month-old male castrated Scottish terrier dog (*Canis familiaris*).

History: The dog was diagnosed with a urinary tract infection 4 months prior to presentation, and was treated with antibiotics. The infection resolved but there was ongoing, waxing and waning hematuria. At the time of presentation, there had been a recent onset of polyuria and increased urgency to urinate. Contrast radiographs at the time of presentation revealed a filling defect in the urinary bladder. Ultrasound imaging showed a broad-based, heteroechoic mass arising near the trigone region of the bladder. A portion of the urinary bladder was surgically resected and submitted for histologic evaluation.

Gross Pathology: A segment of bladder wall approximately 2 x 3 cm was submitted for biopsy with an attached 2 x 4 x 3 cm, polypoid, soft, red-brown mass that protruded into the lumen of the bladder. Approximately 2 cm of ureter were also submitted.

Laboratory Results: CBC:
WBC 18,100/ul
Neutrophils 14,118/ul
Lymphocytes 543/ul
Monocytes 1,629/ul

Serum Chemistry:
Albumin 2.6 g/dl (N: 3.0-3.9)

Urinalysis:
Albumin 500 ug/dl (3+)
Blood 250/ul

Contributor's Histopathologic Description: Multiple histologic sections were examined with similar findings. Arising from the mucosal epithelium is a multilobular mass supported by a fibrovascular core. Lobules of the mass are composed of a background of neoplastic spindle cells with a myxomatous stroma admixed with frequent multi-nucleated, large, elongate or rounded cells with abundant, fibrillar, eosinophilic cytoplasm. The elongate cells occasionally have prominent cross-striations and are consistent with myogenic "strap cells." The multiple nuclei of the elongate and large round cells have peripheralized chromatin with 1-2 prominent nucleoli. The spindle cells in the background have indistinct cell borders with scant to moderate pale eosinophilic cytoplasm around a central oval nucleus. The nuclei have coarsely clumped to vesicular chromatin and often have 1-2 prominent nucleoli. There is marked anisocytosis and anisokaryosis. Mitotic figures are observed with 14 per 10 high power fields. Each lobule of the mass is supported by a fibrovascular core and is lined by transitional epithelium. The ureter has hyperplastic epithelium, and there appears to be a portion of a neoplastic lobule that is within the ureteral lumen, but not attached to the wall of the ureter.

Contributor's Morphologic Diagnosis: Urinary bladder: Botryoid rhabdomyosarcoma.

Contributor's Comment: Botryoid rhabdomyosarcomas are rare tumors in dogs that most frequently occur in the urinary bladder of young, large breed dogs. There are four categories of rhabdomyosarcomas that are recognized in people, including embryonal, botryoid, alveolar, and pleomorphic. Embryonal rhabdomyosarcomas are

3-1. Dog, urinary bladder: Ultrasound imaging of the bladder of a 10-month old Scottish terrier showed a broad-based, heteroechoic mass arising near the trigone region of the bladder.

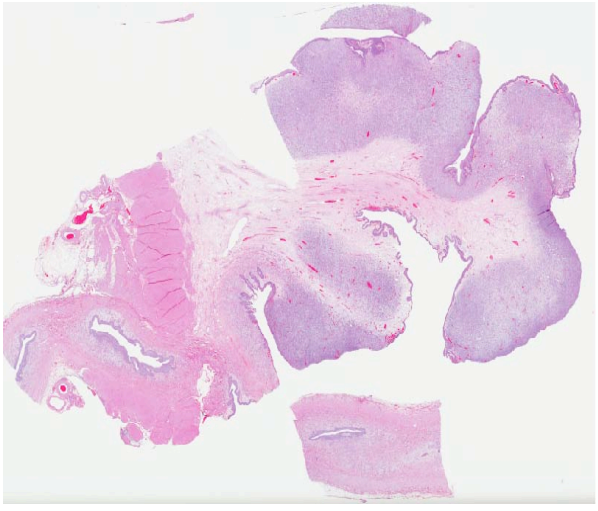

3-2. Dog, urinary bladder. A polpypoid mass elevates the overlying mucosa at right. The ureters enter the trigone at left. (HE 3.6X)

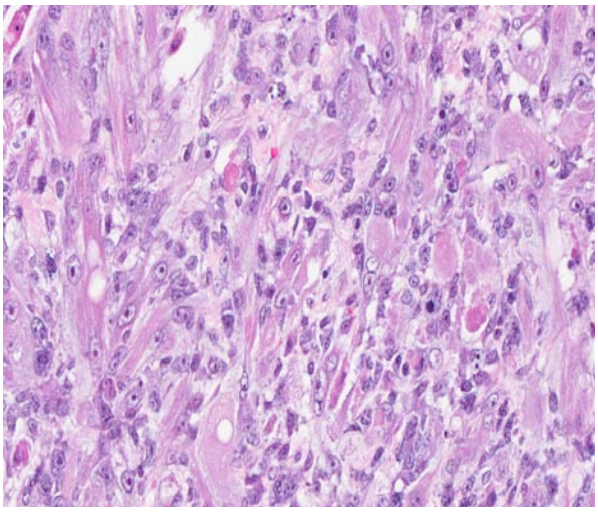

3-3. Dog, urinary bladder. The neoplasm is composed of long bundles and streams of pleomorphic spindle cells. Many of the neoplastic cells are elongate with abundant with abundant eosinophilic fibrillar cytoplasm, recapitulating skeletal muscle ("strap" cells). (HE 400X)

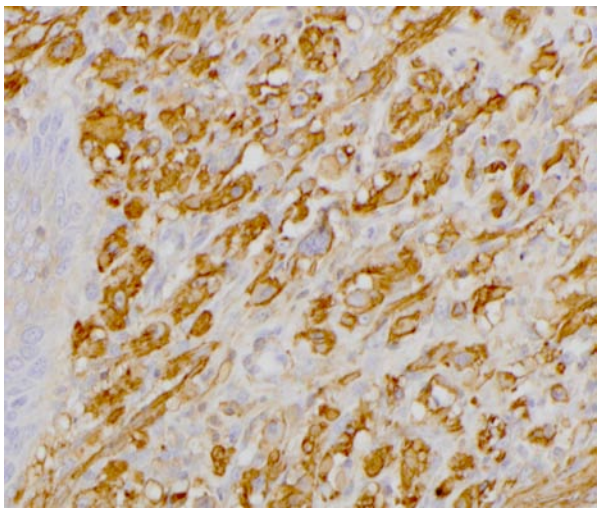

3-4. Dog urinary bladder. Neoplastic cells exhibit diffuse strong cytoplasmic positivity for muscle-specific actin. (MSA, 400X). (Photo courtesy of N.C. State University, College of Veterinary Medicine, Population Health and Pathobiology – Histology Lab, 1060 William Moore Dr., Raleigh, NC 27607. http://www.cvm.ncsu.edu/dphp/path/anatomicpath.html)

characterized by the presence of primitive myogenic cells that occur in two forms, either with large, well-differentiated rhabdomyoblasts on a background of smaller round cells, or a myotubular arrangement with spindle cells forming a myxoid arrangement and often with multinucleate cells and strap-like cells that may or may not have cross striations. Botryoid rhabdomyosarcomas are generally regarded as a variant of embryonal rhabdomyosarcoma with a histologic appearance consistent with the myotubular form, and a gross appearance of a polypoid, grape-like pattern, that often projects into the lumen. The presence of myogenic cells is diagnostic, and myogenic origin can be confirmed with a number of immunohistochemical markers including desmin, muscle-specific actin, and myoglobin. In addition, myogenin and MyoD can be used to identify specific stages of myogenesis.[7] PTAH stains can also be used to try to recognize cross-striations if they are present. In this case, the prominent multinucleated and strap-like cells are diagnostic. In addition, there is strong immunohistochemical staining for muscle specific actin.

Saint Bernards are often listed as being overrepresented in the occurrence of botryoid rhabdomyosarcomas based on a 1973 paper with a case series in which 4 of 7 dogs were Saint Bernards.[5] However, in a review of published cases of canine botryoid rhabdomyosarcomas, no additional cases in Saint Bernards have been described, and there have been at least three cases reported in golden retrievers.[1,7] Other breeds affected include Labrador retriever, Maltese, Newfoundland, Rottweiler, Basset hound, miniature poodle, and a great Dane.[1,5,6,8,9,10] In addition to occurring in the urinary bladder, a few case reports have described botryoid rhabdomyosarcomas in the genital tract as well,[1,9] and there is also a case report of an embryonal rhabdomyosarcoma in the oropharynx and temporal muscles of a young Bassett hound.[6]

Botryoid rhabdomyosarcomas typically have a poor prognosis. The metastatic rate is not well-reported as several cases are euthanized close to the time of initial diagnosis or there is a lack of follow-up in many cases. Out of 14 cases of genital or urinary tract botryoid rhabdomyosarcomas described in case reports, at least five of them had widespread metastases to multiple organs including liver, lungs, lymph nodes, heart, subcutaneous tissue, muscle, gingiva, adrenal gland, spleen, and kidney.[1,5,6,10]

JPC Diagnosis: Urinary bladder: Botryoid rhabdomyosarcoma.

Conference Comment: The contributor provided an excellent discussion of botryoid rhabdomyosarcoma and the associated pathology. Conference participants discussed the following common clinical sequella to this neoplasm. Urinary outflow obstruction is a common finding with these neoplasms, resulting in post-renal azotemia, hematuria, dysuria, and stranguria. The proteinuria and large amount of albumin in the urine can be attributed to the hematuria. Hypertrophic osteopathy is reported to occur concurrently with botryoid rhabdomyosarcoma, thought to be due to vascular or neurogenic stimuli which affect changes in the peripheral vascular supply, as seen with pulmonary masses. Poorly oxygenated

blood passes through arteriovenous shunts, producing local passive congestion and poor tissue oxygenation and stimulating proliferation connective tissue, including the periosteum and the synovial membrane. The affected animals are usually young and present bilaterally symmetrical, nonedematous soft tissue swellings affecting primarily the distal portions of all four limbs. The initial soft tissue swellings are soon accompanied by a diffuse periosteal new-bone formation, which may ultimately affect all the bones of the limbs, and the bone lesions resolve after tumor removal.[2,3,4]

Contributor: N.C. State University
College of Veterinary Medicine
Population Health and Pathobiology – Histology Lab
1060 William Moore Dr.
Raleigh, NC 27607
http://www.cvm.ncsu.edu/dphp/path/anatomicpath.html

References:

1. Bae IH, Kim Y, Pakhrin B, et al. Genitourinary rhabdomyosarcoma with systemic metastasis in a young dog. *Vet Pathol*. 2007;44:518-520..
2. Brodey R. Hypertrophic osteoarthropathy in the dog: A clinicopathologic study of 60 cases. *J Am Vet Med Assoc*. 1971;159:1242.
3. Cooper BJ, Valentine BA. Tumors of muscle. In: Meuten DJ, ed. *Tumors of Domestic Animals*. 4th ed. Ames, IA: Iowa State Press; 2002:354.
4. Halliwell WH, Ackeman N. Botryoid rhabdomyosarcoma of the urinary bladder and hyperosteoarthropathy in a young dog. *J Am Vet Med Assoc*. 1974;165:911.
5. Kelly DF. Rhabdomyosarcoma of the urinary bladder in dogs. *Vet Pathol.* 1973;10:375-384..
6. Kim DY, Hodgin EC, Cho DY, et al. Juvenile rhabdomyosarcomas in two dogs. *Vet Pathol*. 1996;33:447-450.
7. Kobayashi M, Sakai H, Hirata A, et al. Expression of myogenic regulating factors, Myogenin and MyoD, in two canine botryoid rhabdomyosarcomas. *Vet Pathol*. 2004;41:275-277.
8. Kuwamura M, Yoshida H, Yamate J, et al. Urinary bladder rhabdomyosarcoma (sarcoma botryoides) in a young Newfoundland dog. *J Vet Med Sci*. 1998;60:619-621.
9. Suzuki K, Nakatani K, Shibuya H, et al. Vaginal rhabdomyosarcoma in a dog. *Vet Pathol*. 2006;43:186-188.
10. Takiguchi M, Watanabe T, Okada H, et al. Rhabdomyosarcoma (botryoid sarcoma) of the urinary bladder in a Maltese. *J Small Anim Pract*. 2002;43:269-271.

CASE IV: N08-659 (JPC 3134301).

Signalment: 6-year-old castrated male bloodhound (*Canis familiaris*), canine.

History: Acute onset of renal failure. The dog died naturally.

Gross Pathology: Both kidneys had a slightly granular (irregular) surface and were light brown. The parietal pleura and intercostal muscles were diffusely mineralized. The endocardial surface of the left atrium was diffusely mineralized; smaller areas of mineralization were present in the pulmonary artery. The lungs were mottled pink to purple, were irregularly firm. Approximately 50% of randomly sampled lung sections sank in formalin.

Laboratory Results: Plasma Chemistry: (only relevant findings listed)

BUN	155 mg/dL	(9-24)
Creat	7.0 mg/dL	(0.6-1.6)
Tot Prot	6.3 mg/dL	(5.6-7.6)
Albumin	2.0 g/dL	(3.1-4.2)
Globulin	4.3 g/dL	(2.1-3.7)
A/G ratio	0.5	(0.9-1.9)
Calcium	8.9 mg/dL	(9.9-11.5)
Phos	25.4 mg/dL	(2.2-4.6)
Sodium	164 mEq/L	(146-153)
Chloride	128 mEq/L	(110-117)
Bicarb	12 mmol/L	(16-23)
Anion Gap	28.6	(16-24)

Urinalysis: (only relevant findings listed)

Specific gravity	1.013
pH	7.0
Protein	2+
WBC	2-6
RBC	25-30

Rare transitional and squamous epithelial cells; Rare cellular casts

Urine Leptospirosis PCR – negative

Blood Gases		
pH	7.051	(7.31-7.42)
Bicarb	13.6	(17-24)
Base excess	-17.3	(02)
PO2	64.9	(85-95)
PCO2	48.6	(29-42)

Contributor's Histopathologic Description: Lung: There is widespread marked mineralization of bronchial walls and alveolar septa. The bronchial epithelium is occasionally ulcerated. The bronchial lumens and alveoli contain varying combinations and concentrations of fibrin, neutrophils, macrophages and erythrocytes. In some areas large, plump fibroblasts are present. Several blood vessels contain haphazardly arranged fibrin and neutrophils. Mutifocally there is fibrin, intermixed with neutrophils and macrophages, on the pleural surface.

In the left atrium (not submitted) there is marked mineralization surrounded by degenerate neutrophils,

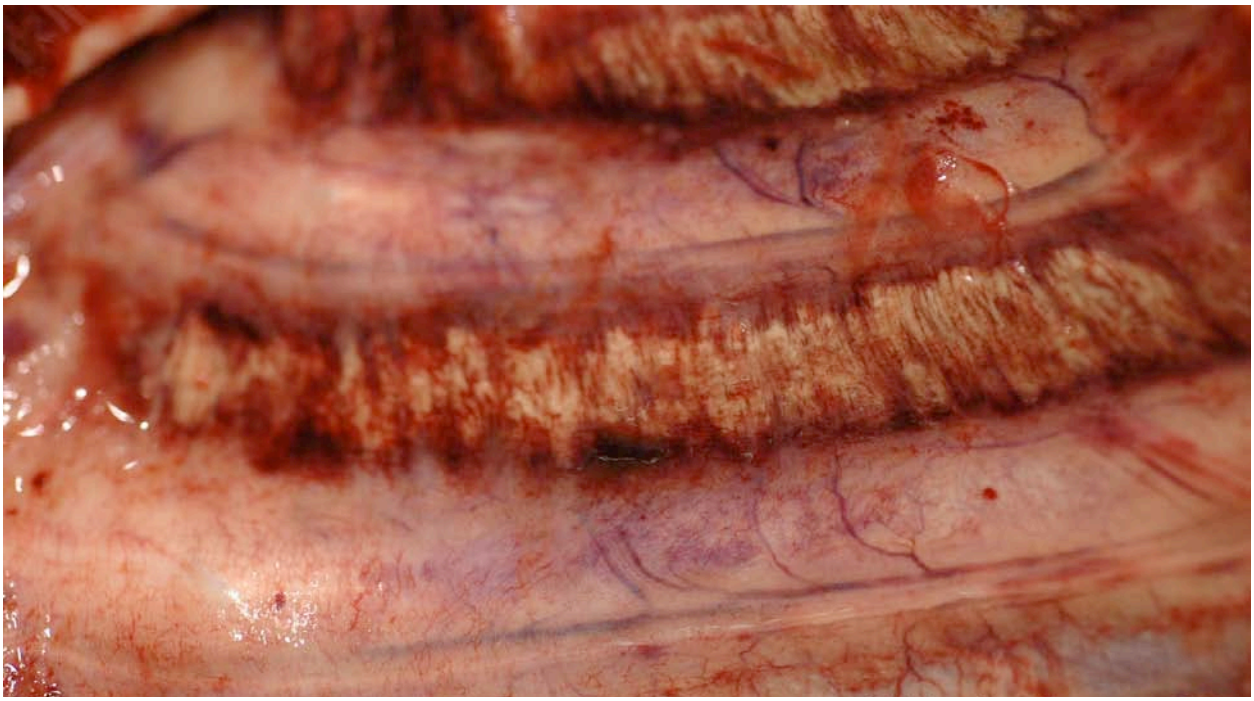

4-1. Dog. There is diffuse mineralization of the intercostal muscles and pleura. (Photo courtesy of: University of Tennessee, College of Veterinary Medicine, Department of Pathobiology, 2407 River Drive, Room A201, Knoxville, TN 37996-4542)

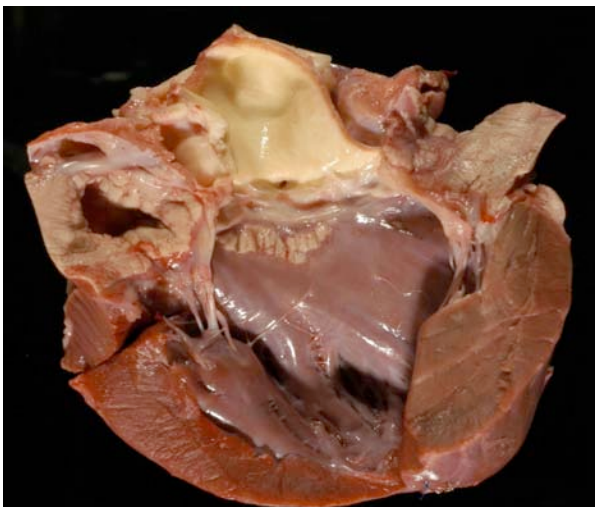

4-2. Dog. Heart. There is diffuse mineralization of the left atrium and focal mineralization of the left ventricle just below the aortic valve. (Photo courtesy of: University of Tennessee, College of Veterinary Medicine, Department of Pathobiology, 2407 River Drive, Room A201, Knoxville, TN 37996-4542)

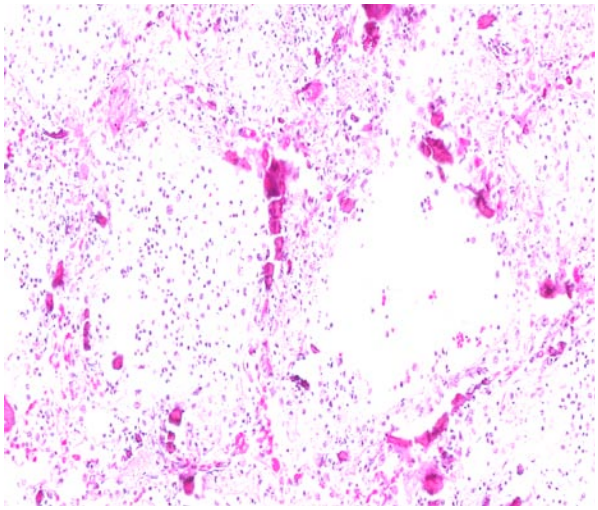

4-3. Dog, lung. Alveolar septa are markedly expanded by inflammatory cells, fibrin, cellular debris, and mineral. Alveolar spaces contain large numbers of neutrophils, alveolar macrophages, fibrin, and cellular debris. (HE 136X)

macrophages and karyorrhectic nuclear debris. The overlying endocardium is thickened. Similarly, the mesothelium lining the intercostal muscles (not submitted) is ulcerated and replaced by a sheet of fibrin. The underlying collagen is mineralized and surrounded by neutrophils, macrophages and karyorrhectic nuclear debris.

Contributor's Morphologic Diagnosis: Lung: Marked acute diffuse mineralization and fibrinosuppurative pneumonitis.

Contributor's Comment: The clinical presentation of uremic pneumonitis is consistent with adult respiratory distress syndrome (ARDS). Possible causes of ARDS include, but are not limited to: thermal or caustic injury, viral infections, ingested toxins, septicemia, disseminated intravascular coagulation, chronic left heart failure, pancreatitis, surfactant dysfunction, ventilator-induced injuries, adverse drug reactions, and uremia.[2]

Uremic pneumonitis results from diffuse alterations in alveolo-capillary permeability combined with complicating factors.[1] These additional factors include, but are not limited to: alterations in coagulability[1], fluid overload, pulmonary hypertension, decreased oncotic pressure, and metabolic acidosis-induced pulmonary vasoconstriction.[5] The intensity of the azotemia does not correlate with the presence of uremic pneumonitis.[1] One study examining the prevalence of uremic pneumonitis in humans that had died of glomerulonephritis found that uremic pneumonitis occurred exclusively in those patients that had rapidly progressive (and very inflammatory) mesangioproliferative glomerulonephritis.[1]

The uremia-associated damage to the alveolus and capillaries results in leakage of plasma into the alveoli and interstitium.[1] The resultant histologic lesions are characterized by diffuse alveolar capillary damage, protein-rich interstitial and intra-alveolar edema, atelectasis, alveolar hemorrhages and hyaline membranes.[5] Mineral is frequently deposited on the walls of the alveolar ducts and pulmonary arterioles.[9] This tissue damage ultimately results in recruitment of neutrophils and macrophages. In rats, proteolytic enzymes and oxidants derived from the increased numbers of macrophages in the interstitial spaces are believed to be responsible for the destruction of elastic fibers, collagen and proteoglycans in the alveoli. Similarly, increased numbers of neutrophils mediate destruction through elastase, cathepsins, collagenase, myeloperoxidase and other oxidants.[5] The resulting enzymatic and oxidative injuries exacerbate the uremia-associated damage to the alveolus and capillaries.

Cardiovascular lesions are also associated with uremia. Acute renal failure may result in fibrinoid vascular necrosis (arterial hyaline degeneration), while chronic renal failure produces hyperplastic arteriosclerosis. Mural endocarditis associated with uremia is typically confined to the left atrium and large elastic arteries, as was seen in this case. This lesion begins with deposition of glycosaminoglycans in the subendocardium/intima. This may progress to necrosis of the lining endothelium as well as the collagen, elastin and reticulin fibers with secondary inflammation. As in this case, concurrent mineralization can be marked.[8]

Nonrenal lesions of uremia are more likely to occur in cases of chronic renal failure than in cases of acute renal failure. Mineralization of the intercostal spaces, beneath the parietal pleura, as was seen in this case, is common. It is preceded by necrosis of the subpleural connective tissue with extension to the intercostal muscles and overlying parietal pleura. The pathogenesis of diffuse tissue mineralization in uremia is not completely clear. Uremic mineralization is likely a combination of dystrophic and metastatic mineralization. In dogs, renal failure is usually associated with hyperphosphatemia and hypocalcemia, as was seen in this dog. This may be complicated by concurrent renal secondary hyperparathyroidism.[9]

The increased anion gap in combination with decreased bicarbonate is consistent with a metabolic titration acidosis. The increased anion gap is likely due to the uremic acids. Additionally, the PCO2 is high (respiratory acidosis) and the PO2 is low (hypoxemia). The combination of these blood gas findings suggests decreased alveolar ventilation secondary to the marked uremic pneumonitis. This dog had both a metabolic and a respiratory acidosis.

Despite the acute onset of clinical signs of renal failure reported in this case, the renal lesions were chronic and consisted primarily of a lymphoplasmacytic interstitial nephritis with marked glomerulocystic change. The inciting cause of the renal failure in this dog is not known.

JPC Diagnosis: Lung: Alveolitis, chronic and necrotizing, focally extensive, severe, with marked mineratlization, hyaline membranes, emphysema, and fibrinous pleuritis.

Conference Comment: Even though there is hypocalcemia due to renal failure, there is still widespread soft tissue mineralization due to the drastic hyperphosphatemia. Mass law is the product of serum phosphorus and calcium, and soft tissue mineralization occurs when this exceeds 70.[3] In the moderator's experience, the most common location for uremic pneumonitis is in the first third or fourth portion of the dorsal diaphragmatic lobes, and not in cranioventral lobes.

Conference participants discussed the fact that this dog likely had glomerular disease as the inciting cause of chronic renal failure because of the proteinuria and serum hypoalbuminemia. Renal and hepatic disease are the two primary sources of hypoalbuminemia, and only renal disease will preserve globulins as in this case. The two primary glomerular lesions in dogs in chronic renal failure are glomerulonephritis and amyloidosis. Cystitis is the most common cause of proteinuria in dogs, but concurrent hypoalbuminemia does not occur as in this case. The proteinuria must be evaluated in light of the erythrocytes present, which in this case are minimal, because hematuria contributes protein through albumin, globulin, and hemoglobin. Additionally, the urine dilution must be taken into consideration; the urine is dilute in this case, and therefore the proteinuria is significant.[4,10,11,12]

Conference participants differentiated this as a case of chronic renal failure from acute renal failure for the following reasons: the presence of serum hypoalbuminemia, since albumin has a half-life of around 20 days; the presence of glomerular disease, as acute renal failure of glomerular origin is extremely rare; the presence of soft tissue mineralization[4,10,11,12], and the presence of non-regenerative anemia due to decreased erythropoietin production by the kidneys and uremia-induced erythrocyte fragility, since anemia is usually not present with acute renal failure.[6]

Conference participants discussed the azotemia as a mixture of pre-renal and renal origin, since the hypernatremia and hyperchloridemia point to dehydration and renal failure usually results in hyponatremia and hypochloridemia. Mixed metabolic and respiratory acidosis is present in this case, as mentioned by the contributor. In addition to the respiratory component being due to mineralization of pulmonary septa and decreased alveolar ventilation, pulmonary thrombosis is another likely cause, although this was not present in the slides.[4,10,11,12] This is due to the loss of antithrombin III from glomeruli, placing the dog in a hypercoagulable state. The most common locations for thrombosis are the lungs and the aortic quadrification.[7] Renal failure also usually produces vasculitis, especially in the midzonal region of vessels, and this is generally prominent in the lungs and gastrointestinal tract, although this was not present in this case.[4,11]

Contributor: University of Tennessee
College of Veterinary Medicine
Department of Pathobiology
2407 River Drive, Room A201
Knoxville, TN 37996-4542

References:

1. Bleyl U, Sander E, Schindler T. The pathology and biology of uremic pneumonitis. *Intensive Care Med*. 1981;7:193-202.
2. Caswell JL, Williams KJ. Respiratory system. In*: Jubb, Kennedy, and Palmer's Pathology of Domestic Animals*. 5th ed. Vol. 2. Edinburgh, Scotland: Saunders Elsevier; 2007:564-567.
3. Cortadellas O, Fernandez del Palacio MJ, Talavera J, et al. Calcium and phosphorus homeostasis in dogs with spontaneous chronic kidney disease at different stages of severity. *J Vet Intern Med.* 2010;24:73-79.

4. Dibartola SP. Clinical approach and laboratory evaluation of renal disease. In: Ettinger SJ, Feldman EC, eds. *Textbook of Veterinary Internal Medicine*. 7th ed. Vol 2. St. Louis, MO: Saunders Elsevier; 2010:1955-69.
5. Heidland A, Heine H, Heidbreder E, et al. Uremic pneumonitis: evidence for participation of proteolytic enzymes. *Contr Nephrol*. 1984;41:352-366.
6. King LB, Giger U, Diserens D, et al. Anemia in chronic kidney failure. *J Vet Intern Med*. 1992;6(5): 264-270.
7. Kuzi S, Segev G, Haruvi E, et al. Plasma antithrombin activity as a diagnostic and prognostic indicator in dogs: a retrospective study of 149 dogs. *J Vet Intern Med*. 2010;24(3):587-96.
8. Maxie MG, Robinson WF. Cardiovascular system. In: *Jubb, Kennedy, and Palmer's Pathology of Domestic Animals*. 5th ed. Vol. 3. Edinburgh, Scotland: Saunders Elsevier; 2007:30.
9. Maxie MG, Newman SJ. Urinary system. In: *Jubb, Kennedy, and Palmer's Pathology of Domestic Animals*. 5th ed. Vol. 2. Edinburgh, Scotland: Saunders Elsevier; 2007:432-436.
10. Polzin DJ. Chronic kidney disease. In: Bartges J, Polzin DJ, eds. *Nephrology and urology of small animals*. West Sussex, England: Wiley-Blackwell; 2011:433-471.
11. Polzin DJ. Chronic kidney disease. In: Ettinger SJ, Feldman EC, eds. *Textbook of Veterinary Internal Medicine*. 7th ed. Vol 2, St. Louis, MO: Saunders Elsevier; 2010:1990-2021.
12. Tripathi NK, Gregory CR, Latimer KS. Urinary system. In: Latimer KS, ed. *Duncan and Prasse's Veterinary Laboratory Medicine: Clinical Pathology*. 5th ed. Ames, IA: Wiley-Blackwell; 2011:270-80.